

THE UNIVERSITY OF HULL

**AERATION OF OILS IN THE PRESENCE OF BOTH EDIBLE AND  
NON-EDIBLE SURFACTANTS**

being a Thesis submitted for the Degree of Doctor of Philosophy in the  
University of Hull

by

Emma Jayne Garvey

BSc (University of Huddersfield)

November 2014

## **ACKNOWLEDGEMENTS**

I would like to thank my academic supervisor Prof. Bernard P. Binks for his excellent supervision and advice. I am grateful for all of the guidance he has given me.

I would also like to thank the Biotechnology and Biological Sciences Research Council (BBSRC) and the Nestlé Product Technology Centre York for financial support in sponsoring this project. I am also extremely grateful for all of the support, encouragement and advice I have received from my industrial supervisor Dr. Josélio Vieira.

I am also grateful to all in the Surfactant & Colloid Group for their support and friendship.

Finally, I would like to thank my family and all of my fantastic friends that have helped me and supported me throughout this time. I am lucky to have so many brilliant people around me that are always there when I need them and to ask for advice. I would be lost without you all.

## PRESENTATIONS

The work contained within this thesis has given rise to the following presentations:

1. Oral presentation: 'Whipping of oils', University of Hull Research Colloquia, 18<sup>th</sup> June 2014, Hull, UK.
2. Oral presentation: 'Whipped oils', Surfactant & Colloid Group seminar series, 3<sup>rd</sup> February 2014, University of Hull, Hull, UK.
3. Oral presentation: 'Whipping of oils', Nestlé Product Technology Centre student symposium, 2<sup>nd</sup> September 2013, York, UK.
4. Oral presentation: 'Foaming of oils', International Symposium on Food Rheology and Structure, 9<sup>th</sup> April 2012, Zurich, Switzerland.
5. Oral presentation: 'Foaming of oils', Surfactant & Colloid Group seminar series, 10<sup>th</sup> January 2012, University of Hull, Hull, UK.
6. Oral presentation: 'Foaming of oils', Nestlé Product Technology Centre student symposium, 12<sup>th</sup> September 2011, York, UK.
7. Poster presentation: 'Foaming of oils', University of Hull Research Colloquia, 9<sup>th</sup> July 2012, Hull, UK.

## ABSTRACT

Unlike aqueous foams, very little literature exists in the area of non-aqueous foams despite this being an important field industrially, e.g. in confectionary manufacture and in the oil industry. Since the air-oil surface tension is normally at least half that of the air-water surface tension, the driving force for the adsorption of surfactant at the air-oil surface is significantly lower. The foamability and foam stability of mixtures of surfactants in oil have been investigated in an effort to understand how to control the amount and stability of such foams. The surfactants studied include phospholipids, monoglycerides, diglycerides, fatty acids and alcohols in numerous oils.

Incorporation of gases of different types (including air, carbon dioxide and nitrous oxide) has been achieved using different methods. These include aeration by a thermostatted foaming column and the dissolving of gas into a system via a soda siphon. Temperature effects have also been investigated with aerations conducted at 25, 45 and 60 °C amongst other temperatures. The effect of the saturation of diglycerides has also been studied.

The solubility differences of the gases in oil no doubt influenced the process of disproportionation of bubbles, although drainage of oil and coalescence of bubbles occurs also. The foam half-life varied from minutes to months depending on the system composition. The effect of temperature was also found to influence the stability of the foam produced; in the case of compressed air as temperature increases foam stability decreases.

A whipped oil has also been produced with numerous two-component systems which has a stability of over 18 months. The formation of a gel was clearly important for the whipped oil production. Therefore the viscosity, solid content and solid surfactant size of the gel has been studied. It was clear through numerous investigations that temperature was crucial for foam formation and subsequent foam stability. Factors investigated were the effect of fatty acids and fatty alcohol chain length which highlighted the importance of the viscosity and solid content of a mixture prior to aeration for foam production. The basic behaviour of foams and previous relevant work in the area, along with results obtained are discussed in this thesis.

## CONTENTS

|          |   |           |
|----------|---|-----------|
| <b>1</b> | <b>INTRODUCTION</b>                                   | <b>1</b>  |
| 1.1      | Foam  | 1         |
| 1.1.1    | Structure   | 1         |
| 1.1.2    | Stabilisation methods                                 | 2         |
| 1.1.3    | Breakdown mechanisms                                  | 4         |
| 1.2      | Surfactants   | 6         |
| 1.2.1    | Structure   | 6         |
| 1.2.2    | Phase behaviour in oil                                | 7         |
| 1.3      | Review of relevant non-aqueous foams literature       | 9         |
| 1.3.1    | Early work  | 9         |
| 1.3.2    | Non-aqueous foams stabilised by edible surfactants    | 11        |
| 1.3.3    | Non-aqueous foams stabilised by particles             | 18        |
| 1.4      | Fat crystallisation                                   | 20        |
| 1.4.1    | Formation and structure                               | 20        |
| 1.4.2    | Relevant previous work on organogels                  | 24        |
| 1.4.2.1  | Effect of fatty acids and fatty alcohols on gelation  | 25        |
| 1.4.2.2  | Effect of monoglycerides and diglycerides on gelation | 29        |
| 1.5      | Aims and objectives                                   | 33        |
| 1.6      | Presentation of thesis                                | 33        |
| 1.7      | References  | 35        |
| <b>2</b> | <b>EXPERIMENTAL</b>                                   | <b>38</b> |
| 2.1      | Materials   | 38        |
| 2.1.1    | Oils  | 38        |

|          |  |    |
|----------|--|----|
| 2.1.2    | Surfactants  | 41 |
| 2.1.3    | Particles  | 45 |
| 2.1.4    | Additional edible ingredients  | 47 |
| 2.1.5    | Gases  | 47 |
| 2.2      | Methods  | 48 |
| 2.2.1    | Visual solubility determination of additive in oil   | 48 |
| 2.2.2    | Differential scanning calorimetry  | 49 |
| 2.2.3    | X-ray diffraction  | 49 |
| 2.2.4    | Optical microscopy   | 50 |
| 2.2.5    | Cryo-Scanning Electron Microscopy (SEM)  | 50 |
| 2.2.6    | Surface tension  | 50 |
| 2.2.7    | Contact angle determination  | 51 |
| 2.2.8    | Rheology   | 51 |
| 2.2.9    | Pulsed nuclear magnetic resonance  | 52 |
| 2.2.10   | Viscosity measurements   | 52 |
| 2.2.11   | Grinding mill  | 53 |
| 2.2.12   | Sonication   | 53 |
| 2.2.13   | Sample preparation of surfactant in oil mixtures for aeration via hand shaking or gas sparging | 53 |
| 2.2.14   | Aeration techniques  | 53 |
| 2.2.14.1 | Hand shaking   | 54 |
| 2.2.14.2 | Gas sparging   | 54 |
| 2.2.14.3 | Soda siphon  | 55 |
| 2.2.14.4 | Foaming column   | 56 |

|          |   |    |
|----------|---|----|
| 2.2.14.5 | Whipping technique  | 58 |
| 2.2.14.6 | Hobart mixer  | 59 |
| 2.2.15   | Concept samples   | 60 |
| 2.2.15.1 | Indulgent chocolate filling                                   | 60 |
| 2.2.15.2 | Extruded filling  | 61 |
| 2.2.15.3 | Biscuit filling   | 62 |
| 2.2.15.4 | Whipped spread  | 62 |
| 2.2.15.5 | Wafer filling   | 62 |
| 2.3      | References  | 63 |
| <b>3</b> | <b>PHOSPHOLIPIDS IN OIL</b>                                   | 64 |
| 3.1      | Introduction  | 64 |
| 3.2      | Initial foamability investigations                            | 64 |
| 3.2.1    | Surfactants   | 64 |
| 3.2.2    | Particles   | 65 |
| 3.3      | Characterisation of phospholipids in high oleic sunflower oil | 66 |
| 3.3.1    | Visual solubility determination                               | 66 |
| 3.3.2    | Microscopy  | 68 |
| 3.4      | Aeration  | 71 |
| 3.4.1    | Gas sparging  | 71 |
| 3.4.2    | Foaming column  | 75 |
| 3.4.2.1  | Epikuron 145 V in HOSO  | 75 |
| 3.4.2.2  | Epikuron 170 in HOSO  | 80 |
| 3.4.2.3  | Epikuron 130 P IP in HOSO                                     | 83 |
| 3.4.2.4  | Epikuron 200 in HOSO  | 87 |

|             |  |           |
|-------------|--|-----------|
| 3.4.2.5     | Comparison of Epikuron phospholipids   | 90        |
| 3.4.3       | Effect of aeration method  | 93        |
| 3.4.4       | Viscosity of phospholipid-oil dispersions  | 95        |
| 3.5         | Conclusions  | 97        |
| 3.6         | References   | 98        |
| <b>4</b>    | <b>SATURATED AND UNSATURATED MONO/DIGLYCERIDES IN<br/>HIGH OLEIC SUNFLOWER OIL</b> | <b>99</b> |
| 4.1         | Introduction   | 99        |
| 4.2         | Unsaturated mono/diglyceride in high oleic sunflower oil                           | 99        |
| 4.2.1       | Characterisation of surfactant in oil before aeration                              | 100       |
| 4.2.1.1     | Visual solubility determination  | 100       |
| 4.2.1.2     | Microscopy   | 102       |
| 4.2.2       | Aeration   | 105       |
| 4.2.2.1     | Foaming column   | 105       |
| 4.2.2.1.1   | Effect of concentration at 45 °C   | 105       |
| 4.2.2.1.2   | Effect of temperature  | 111       |
| 4.2.2.1.2.1 | Aeration at 25 °C  | 111       |
| 4.2.2.1.2.2 | Aeration at 60 °C  | 114       |
| 4.2.2.1.2.3 | Summary  | 114       |
| 4.2.2.1.3   | Effect of gas type   | 115       |
| 4.2.2.1.3.1 | CO <sub>2</sub>  | 115       |
| 4.2.2.1.3.2 | N <sub>2</sub> O   | 120       |
| 4.2.2.1.3.3 | Summary  | 122       |
| 4.2.2.2     | Soda siphon  | 123       |

|             |  |     |
|-------------|--|-----|
| 4.2.2.2.1   | Effect of concentration with CO <sub>2</sub> as gas    | 123 |
| 4.2.2.2.2   | Effect of temperature                                  | 128 |
| 4.2.2.2.2.1 | Aeration at 25 °C                                      | 128 |
| 4.2.2.2.2.2 | Aeration at 60 °C                                      | 133 |
| 4.2.2.2.2.3 | Summary  | 133 |
| 4.2.2.2.3   | Effect of gas type                                     | 134 |
| 4.2.2.2.3.1 | Summary  | 134 |
| 4.3         | Saturated mono/diglyceride in high oleic sunflower oil | 140 |
| 4.3.1       | Characterisation                                       | 140 |
| 4.3.1.1     | Differential scanning calorimetry                      | 140 |
| 4.3.2       | Aeration   | 144 |
| 4.3.2.1     | Sparged gas  | 144 |
| 4.3.2.1.2   | Aeration at 60 °C and 80 °C                            | 144 |
| 4.3.2.2     | Foaming column   | 147 |
| 4.3.2.2.1   | Aeration at 25 and 35 °C                               | 147 |
| 4.3.2.2.2   | Aeration at 60 °C                                      | 147 |
| 4.3.2.2.3   | Summary  | 153 |
| 4.3.2.3     | Whipping technique                                     | 154 |
| 4.3.2.3.1   | Effect of temperature increase                         | 157 |
| 4.4         | Conclusions  | 161 |
| 4.4.1       | Unsaturated mono/diglyceride                           | 161 |

|          |  |            |
|----------|--|------------|
| 4.4.2    | Saturated mono/diglyceride   | 162        |
| 4.5      | References   | 163        |
| <b>5</b> | <b>CHARACTERISATION OF GELS OF MYRISTIC ACID IN HIGH OLEIC SUNFLOWER OIL</b> | <b>164</b> |
| 5.1      | Introduction   | 164        |
| 5.2      | Solubility determination in HOSO   | 165        |
| 5.3      | Differential scanning calorimetry  | 167        |
| 5.3.1    | Effect of cooling rate   | 170        |
| 5.4      | XRD  | 173        |
| 5.5      | Microscopy   | 177        |
| 5.5.1    | Optical microscopy   | 177        |
| 5.5.2    | Cryogenic scanning electron microscopy                                       | 181        |
| 5.6      | Surface energy determination   | 183        |
| 5.7      | Rheology   | 184        |
| 5.7.1    | Effect of oscillation frequency  | 184        |
| 5.7.2    | Effect of temperature  | 187        |
| 5.7.3    | Viscosity  | 191        |
| 5.8      | Pulsed nuclear magnetic resonance  | 194        |
| 5.9      | Conclusions  | 196        |
| 5.10     | References   | 197        |
| <b>6</b> | <b>AERATION OF MIXTURES OF MYRISTIC ACID IN OIL</b>                          | <b>199</b> |
| 6.1      | Introduction   | 199        |
| 6.2      | Effect of myristic acid concentration  | 199        |
| 6.2.1    | Cryogenic scanning electron microscopy                                       | 210        |

|          |  |            |
|----------|--|------------|
| 6.3      | Effect of storage time   | 212        |
| 6.4      | Effect of storage and aeration temperature   | 214        |
| 6.4.1    | Effect of storage temperature on foam stability  | 214        |
| 6.4.2    | Effect of aeration temperature on foamability  | 218        |
| 6.5      | Effect of cooling rate   | 222        |
| 6.6      | Effect of oil type   | 228        |
| 6.6.1    | Vegetable oils   | 228        |
| 6.6.2    | Non-edible oils  | 240        |
| 6.6.2.1  | 5 wt.% myristic acid in ethylene glycol, eugenol, high oleic<br>sunflower oil and squalane   | 242        |
| 6.6.2.2  | 5 wt.% myristic acid in benzyl acetate, cyclohexane, 1-dodecanol,<br>glycerol, heptane, isopropyl myristate, toluene and tricaprylin | 247        |
| 6.7      | Effect of ground myristic acid in HOSO   | 252        |
| 6.8      | Conclusions  | 255        |
| 6.9      | References   | 256        |
| <b>7</b> | <b>INVESTIGATION OF STRUCTURING AGENTS IN OIL</b>  | <b>258</b> |
| 7.1      | Introduction   | 258        |
| 7.2      | Fully hydrogenated rapeseed oil rich in behenic acid in HOSO   | 258        |
| 7.3      | Cetostearyl alcohol  | 262        |
| 7.3.1    | HOSO   | 262        |
| 7.3.2    | Dodecane   | 265        |
| 7.4      | Dimodan HR kosher in HOSO  | 268        |
| 7.4.1    | Gel characterisation   | 268        |
| 7.4.1.1  | DSC  | 268        |

|           |  |     |
|-----------|--|-----|
| 7.4.1.2   | Optical microscopy                                 | 269 |
| 7.4.1.3   | Rheology   | 273 |
| 7.4.1.3.1 | Effect of frequency                                | 273 |
| 7.4.1.3.2 | Effect of temperature decrease from 90 °C to 10 °C | 276 |
| 7.4.1.3.3 | Effect of time                                     | 278 |
| 7.4.1.3.4 | Viscosity measurement                              | 280 |
| 7.4.1.4   | Pulsed nuclear magnetic resonance                  | 282 |
| 7.4.2     | Aeration   | 284 |
| 7.4.2.1   | Hobart mixer                                       | 284 |
| 7.4.2.1.2 | Rheology of foam                                   | 286 |
| 7.4.2.2   | Whipping technique                                 | 288 |
| 7.5       | Stearic acid in HOSO                               | 293 |
| 7.5.1     | Effect of temperature increase                     | 300 |
| 7.5.2     | Effect of whipping temperature                     | 304 |
| 7.6       | Fatty acids and fatty alcohols in HOSO             | 311 |
| 7.6.1     | Differential scanning calorimetry                  | 311 |
| 7.6.2     | Effect of fatty acid chain length in HOSO          | 314 |
| 7.6.3     | Effect of fatty alcohol chain length in HOSO       | 320 |
| 7.7       | Concept samples                                    | 327 |
| 7.7.1     | Indulgent chocolate filling                        | 327 |
| 7.7.1.1   | High oleic sunflower oil based filling             | 327 |
| 7.7.1.2   | Hazelnut oil based filling                         | 328 |
| 7.7.2     | Extruded filling                                   | 330 |
| 7.7.2.1   | High oleic sunflower oil based extruded filling    | 330 |

|          |   |            |
|----------|---|------------|
| 7.7.2.2  | Peanut oil based extruded filling             | 331        |
| 7.7.3    | Biscuit filling                               | 332        |
| 7.7.4    | Whipped spread                                | 333        |
| 7.7.5    | Wafer filling                                 | 334        |
| 7.8      | Conclusions                                   | 336        |
| 7.9      | References                                    | 337        |
| <b>8</b> | <b>SUMMARY OF CONCLUSIONS AND FUTURE WORK</b> | <b>338</b> |
| 8.1      | Conclusions                                   | 338        |
| 8.2      | Future work                                   | 339        |
|          | <b>APPENDIX</b>                               | <b>341</b> |

## LIST OF SYMBOLS

|                        |  |
|------------------------|--|
| A                      | Surface area ( $\text{m}^2$ )  |
| d                      | d-spacing ( $\text{\AA}$ )   |
| E                      | Gibbs elasticity ( $\text{mN m}^{-1}$ )  |
| G'                     | storage modulus (Pa)   |
| G''                    | loss modulus (Pa)  |
| M                      | molecular mass ( $\text{Kg mol}^{-1}$ )  |
| Mh                     | molecular mass of the hydrophilic section of a molecule ( $\text{Kg mol}^{-1}$ ) |
| R                      | gas constant ( $\text{J K}^{-1} \text{mol}^{-1}$ )                               |
| T                      | temperature (K)  |
| $t_{1/2}$              | foam half-life (min)   |
| $T_f$                  | temperature of fusion (K)  |
| $x_B$                  | mole fraction (mol)  |
| $\Delta_{\text{fus}}H$ | enthalpy of fusion ( $\text{KJ mol}^{-1}$ )                                      |
| $\lambda$              | wavelength (m)   |
| $\gamma$               | surface tension ( $\text{mN m}^{-1}$ )   |
| w                      | work done (N m)  |
| $\sigma$               | film tension ( $\text{mN m}^{-1}$ )  |
| $\eta$                 | viscosity (Pa s)   |

## LIST OF ABBREVIATIONS

|               |  |
|---------------|--|
| AAA           | triarachidonoyl-glycerol                             |
| BBB           | tribehenoyl-glycerol                                 |
| CBE           | cocoa butter equivalent                              |
| Cryo SEM      | cryogenic scanning electron microscopy               |
| DSC           | differential scanning calorimetry                    |
| FHR-B         | fully hydrogenated rapeseed oil rich in behenic acid |
| FHR-S         | fully hydrogenated rapeseed oil rich in stearic acid |
| G. C. LR 10   | Grindsted Citrem LR 10 Extra Kosher                  |
| G. C. N12 veg | Grindsted Citrem N12 veg                             |
| HLB           | hydrophile-lipophile balance                         |
| HOSO          | high oleic sunflower oil                             |
| HSA           | 12-hydroxystearic acid                               |
| LPG           | liquid petroleum gas                                 |
| OTFE          | oligomeric tetrafluoroethylene                       |
| PA            | phosphatidic acid                                    |
| PC            | phosphatidylcholine                                  |
| PDMS          | polydimethylsiloxane                                 |
| PE            | phosphatidylethanolamine                             |
| PI            | phosphatidylinositol                                 |
| pNMR          | pulsed nuclear magnetic resonance                    |
| PO-DAG        | palm oil diglyceride                                 |
| PSO           | palm super olein                                     |
| PTFE          | polytetrafluoroethylene                              |
| REA           | rincinelaidic acid                                   |
| SFO           | sal fat olein  |
| SEM           | scanning electron microscopy                         |
| SSS           | tristearoyl-glycerol                                 |
| TEAO          | triethanolammonium oleate                            |
| TIO           | glycerol tris (2-ethylhexanoic) ester                |
| XRD           | X-ray diffraction                                    |

# 1 INTRODUCTION

There is very little literature in the area of non-aqueous foams, therefore the purpose of this Ph.D is to further knowledge in the area. The area is of great importance to many industries such as the food, cosmetic and oil industry. Nestlé creates confectionary products, therefore the area of aeration is of significant importance particularly in creating new products and making the nutritional profile of current products better.

This chapter will consist of an introduction into foams including the structure of foams, the stabilisation methods and main breakdown mechanisms along with previous work in the area of non-aqueous foams. The chapter will also include an introduction into the area of fat crystallisation and previous work in the area of organogels.

## 1.1 Foam

A foam is a dispersion of gas in a continuous phase which can be liquid or solid;<sup>1</sup> in this thesis only liquid continuous phases are considered. The important factors involved in foam stability and the relevant literature in the area of non-aqueous foams will be discussed. The majority of the next section will consist of the behaviour of aqueous foams.

### 1.1.1 Structure

A foam can be stated as being 'dry' and also 'wet', the main difference being that in a dry foam the foam bubbles are polyhedral in shape with a liquid volume fraction of  $< 10\%$ <sup>2</sup>, whereas in a wet foam the foam bubbles are spherical in shape with a typical liquid volume fraction of 10 to 35 %<sup>3</sup>. A liquid volume fraction higher than 35 % is a dispersion of air in a liquid phase.

When a foam is formed the gas bubbles are initially spherical in shape which is due to the surface energy being at its lowest possible value. Surface tension is an important factor in the formation of foam. As can be seen in Figure 1.1 there are incomplete interactions at the interface between the gas and the liquid. These incomplete interactions create an energy surplus which is termed surface free energy. The surface free energy causes the formation of a spherical shaped bubble as the energy (surface area) is kept to a minimum in this shape. Surfactants can reduce the surface free energy

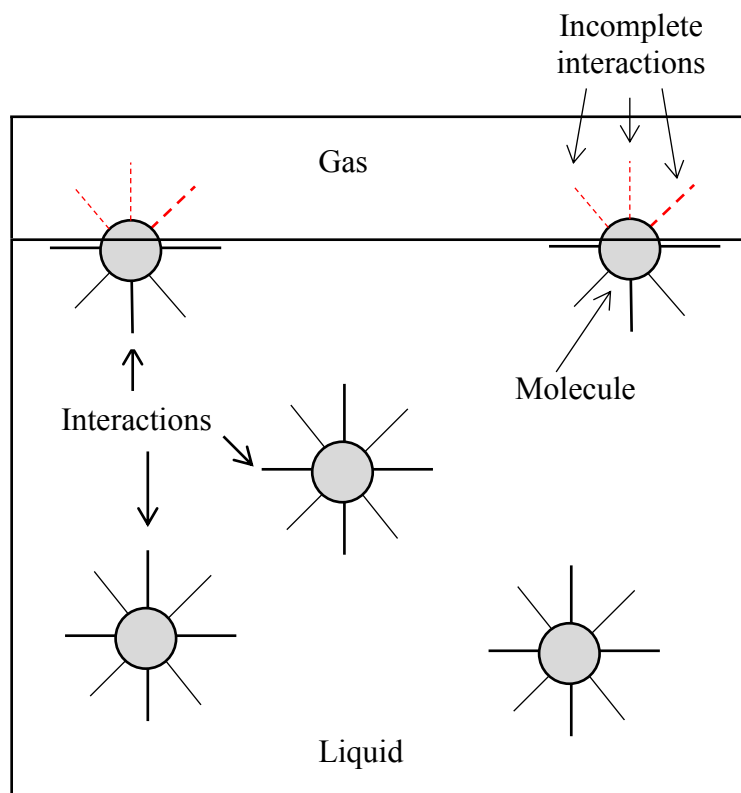
(work done) by interacting with molecules at the gas-liquid interface. The interaction then causes a hydrocarbon/fluorocarbon chain to be present at the gas-liquid interface. The equation for surface tension,  $\gamma$ , is shown below,

$$\gamma = \frac{dw}{dA} \quad (1.1)$$

where  $dw$  is the amount of work done and  $dA$  is the change in surface area.

Typical surface tension values for water, hydrocarbons and fluorocarbons are approximately  $72 \text{ mN m}^{-1}$ ,  $20\text{-}30 \text{ mN m}^{-1}$  and  $15 \text{ mN m}^{-1}$  respectively. As oil and hydrocarbons have a similar value it is less likely that a foam will be stabilised by a hydrocarbon-chained surfactant. However, this is not the case as shown by work conducted by Shrestha et al.<sup>4-7</sup> which will be discussed in detail.

**Figure 1.1.** Origin of surface tension.



### 1.1.2 Stabilisation methods

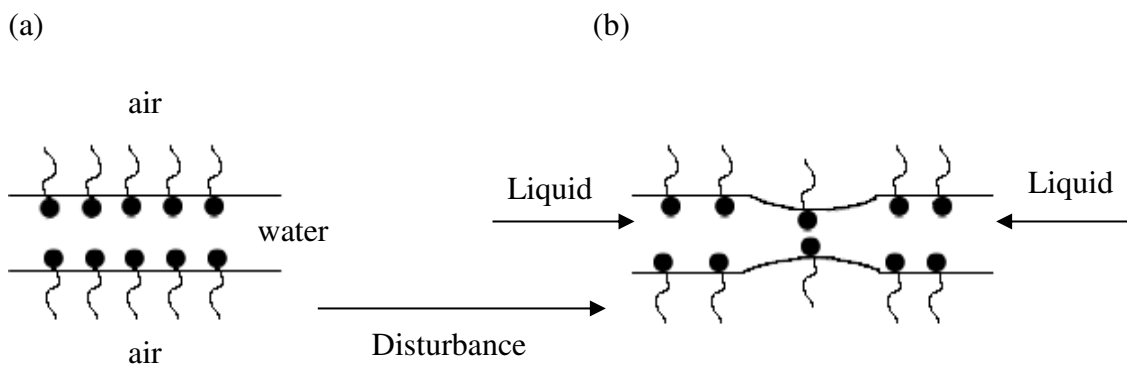
Surfactants, proteins and surface-active polymers (once added to a liquid phase with some method of aeration or agitation) are known to create a foam. The adsorption to the gas-liquid interface is thought to create a barrier which increases the film rigidity and

viscosity of the continuous phase, resulting in a decrease in the rate of coalescence, disproportionation and liquid drainage (these foam collapse procedures are discussed further in the breakdown mechanisms section).

The Gibbs-Marangoni effect is the ability of a foam to withstand external forces applied such as sudden expansion. If a foam is stretched, any given area of the interface will have a reduced coverage of surfactant, therefore the surface tension in this area will be higher in comparison to the rest of the foam film. This causes an immediate contraction of the film. The contraction creates movement of liquid from an area of relatively low surface tension to the higher surface tension area which continues until enough surfactant has adsorbed at the interface for there to no longer be a surface tension gradient (shown in Figure 1.2). The mechanism provides resistance to foam film rupture and it is this resistance that determines the elasticity,  $E$ , of the film.<sup>8</sup> The extent of the elasticity depends on the rate at which the surface tension reduces. If such resistance does not occur, then the foam will collapse due to the external force. Figure 1.2 shows the effect of a stretched foam film from before to during the film disturbance.<sup>9</sup> Equation 1.2 relates the surface elasticity to the surface tension and area where  $E$  is the Gibbs elasticity,  $d\sigma$  is the increase in film tension and  $d\ln A$  is the increase in surface area which has occurred.<sup>9</sup>

$$E = \frac{2d\sigma}{d\ln A} \quad (1.2)$$

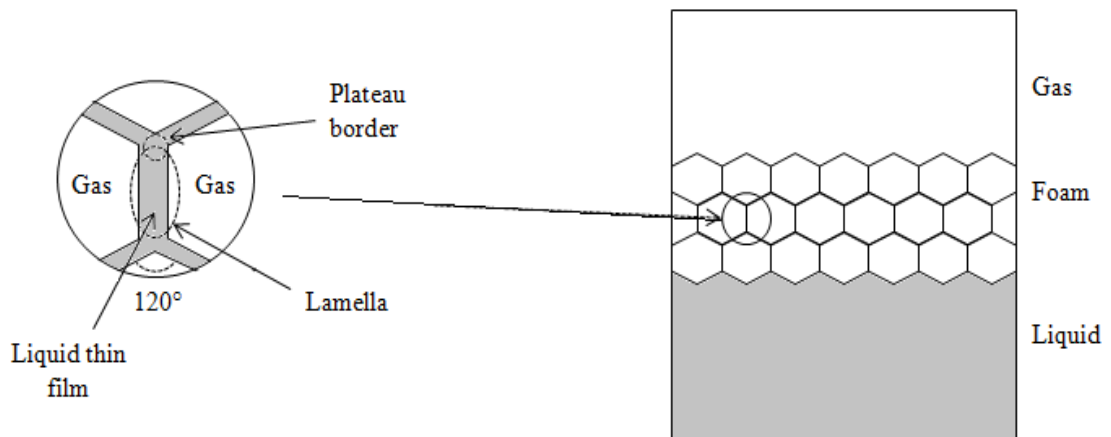
**Figure 1.2.** (a) A foam film before disturbance, (b) the Gibbs Marangoni effect after the film has been stretched.



### 1.1.3 Breakdown mechanisms

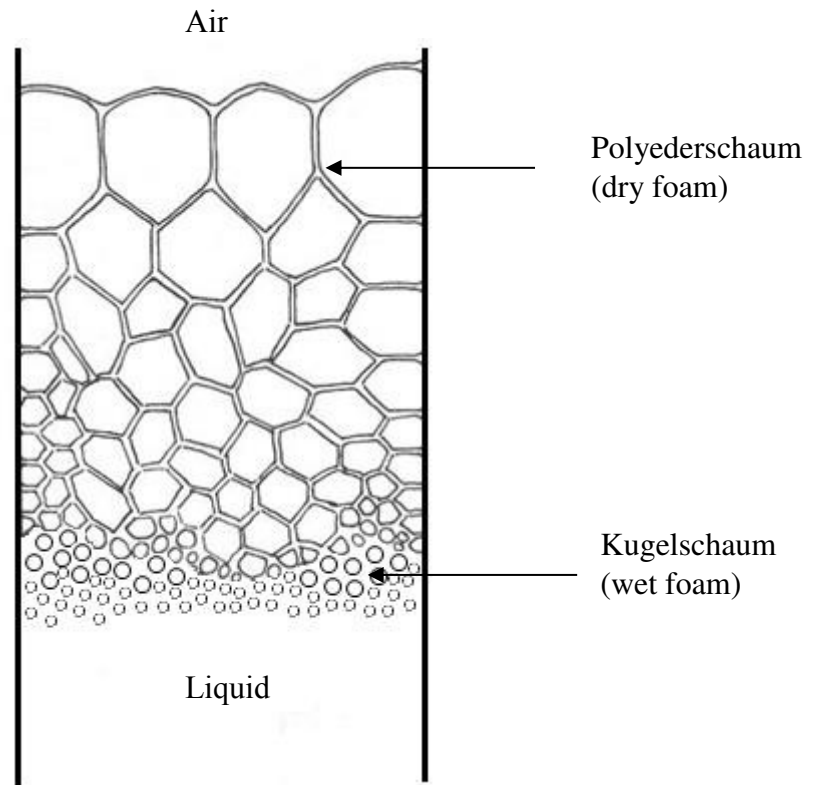
A foam collapses due to three main mechanisms, namely liquid drainage, coalescence and disproportionation, all of which involve structures in a foam called the lamella and the Plateau border (designated in Figure 1.3). In this figure it is indicated that the liquid film between bubbles is termed the lamella and the point at which the lamella meet (at  $120^\circ$ ) is known as a Plateau border.

**Figure 1.3.** The structure of a foam film.



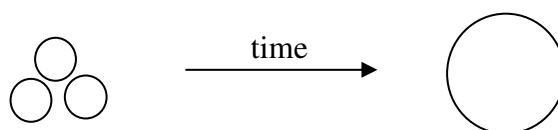
Liquid drainage occurs mainly due to gravity, however liquid drainage is also due (to a lesser extent) to the Plateau border having a lower pressure and shear stress than that of the lamella. The foam breakdown due to liquid drainage can be resisted by an increase in the viscosity of the continuous phase; the addition of surfactants can create this.<sup>10</sup> Figure 1.4 illustrates the effect of liquid drainage whereby bubbles known as polyederschaum (polyhedral in shape with a thin foam film at the top of a foam column) form from originally spherical bubbles with a thick foam lamella. Bubbles which are spherical in shape with a thick foam lamella are known as kugelschaum. The breakdown mechanism of liquid drainage generally occurs first, then coalescence and disproportionation, as the foam lamella is thinner due to liquid drainage resulting in less resistance to coalescence and disproportionation.

**Figure 1.4.** Image and terms used for the bubble shape change which occurs in a foam.



Coalescence is the merging of two or more bubbles as shown in Figure 1.5. Coalescence occurs because the merging of the bubbles creates a lower surface area. The resulting lower surface area requires less surfactant to be present at the air-liquid interface. To prevent this occurrence a higher concentration of surfactant may be required or a change in the surfactant type. The reduction of the rate of this breakdown mechanism and disproportionation as surfactant concentration increases is evident in the results and discussion section.

**Figure 1.5.** The merging of bubbles which occurs in coalescence.



Disproportionation is the movement of gas from small bubbles with a high internal pressure to larger bubbles with a lower internal pressure via the Plateau border. This

pressure is known as the Laplace pressure ( $\Delta p$ )<sup>10</sup> and is shown below in equation 1.3. It is clear from the equation that as the bubble radius increases, the pressure inside the bubble ( $\Delta p$ ) decreases. The rate of the breakdown mechanism can be reduced or possibly even halted by changing the gas type; this is because gases have different solubility in liquid continuous phases. An increase in the quantity of surfactant present can also reduce the rate of disproportionation, as surfactant can accumulate in the Plateau border creating a more viscous medium for the gas to pass through. The presence of liquid crystal multilayers of surfactants can also retard disproportionation.

$$\Delta p = \frac{2\gamma}{r} \quad (1.3)$$

where  $\gamma$  is the surface tension of the gas-liquid interface and  $r$  is the radius of the bubble.

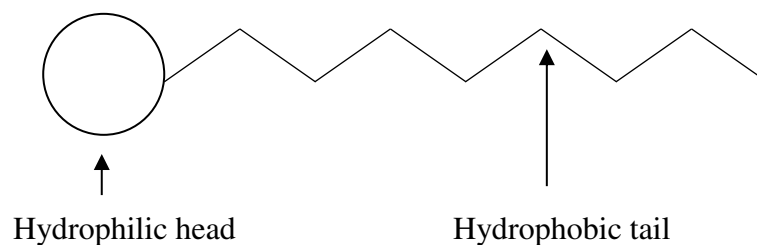
## 1.2 Surfactants

The basic structure and the phase behaviour of a surfactant in oil are to be described along with the relevance to the creation of non-aqueous foams.

### 1.2.1 Structure

A surfactant is a surface-active agent that has the ability to adsorb at an air-liquid surface; it consists of a hydrophilic head and a hydrophobic tail group as shown in Figure 1.6.

**Figure 1.6.** Structure of a typical surfactant.



The contribution of the hydrophilic head and hydrophobic tail can be described by the hydrophile-lipophile balance (HLB) number which is a quantitative measure. A

hydrophilic surfactant has a high HLB number, a hydrophobic surfactant has a low HLB number,

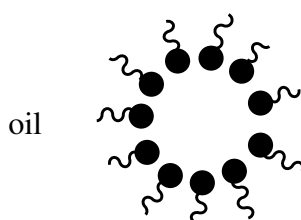
$$HLB = 20 \times \frac{M_h}{M} \quad (1.4)$$

where  $M_h$  is the molecular mass of the hydrophilic section of the molecule and  $M$  is the molecular mass of the whole molecule.<sup>11</sup>

Surfactants can aggregate to form various structures such as micelles, which in water are usually spherical in shape. The aggregation number is the number of monomers in the micelle. As the aggregation number increases, micelles will no longer be spherical and become rod or disc shaped.

Micelles are formed spontaneously and reversibly. The formation involves the hydrophobic tail groups arranging themselves into the most favourable position in the continuous phase. If the continuous phase is oil, a reverse micelle will be produced, an example of which is shown in Figure 1.7. The concentration at which a micelle is formed is the critical micelle concentration (cmc).

**Figure 1.7.** Structure of a reverse micelle.



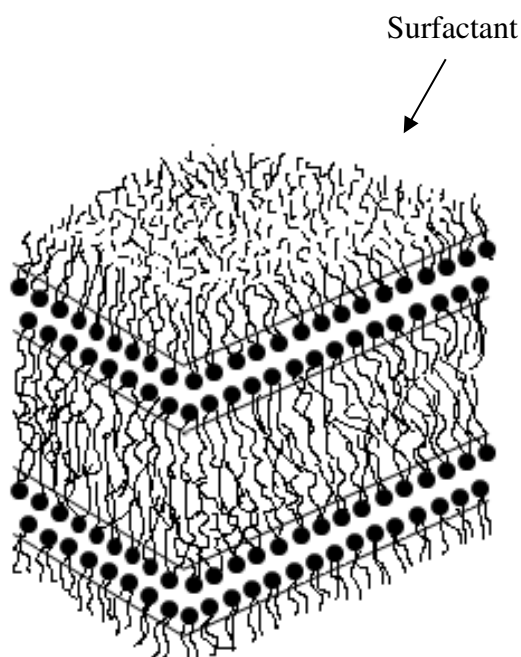
### 1.2.2 Phase behaviour in oil

A liquid crystal is when a phase is intermediate between a liquid and a solid. The liquid crystals can take many forms which are determined by curvature. It has been found through previous studies, that with the surfactant in the form of a lamellar liquid crystal non-aqueous foams can be formed.

A lamellar liquid crystal is a structure with zero curvature in which surfactant bilayer sheets are separated by a liquid. With an increase in the temperature the structure of a liquid crystal will be lost creating the formation of micelles as the surfactant becomes

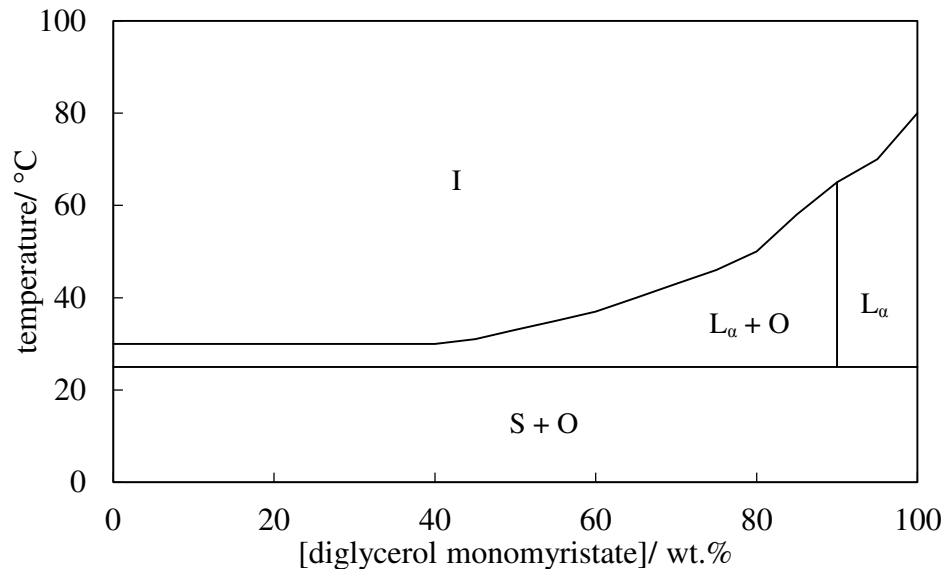
more soluble in the liquid. Figure 1.8 indicates how a lamellar liquid crystal is orientated. In oil the hydrophilic heads are inwards and the hydrophobic tails interact with the oil.

**Figure 1.8.** A lamellar liquid crystal in oil.



A typical phase diagram is shown in Figure 1.9 whereby the surfactant changes from solid, to a liquid crystal then to be dissolved in oil as temperature increases. As can be seen, as the surfactant concentration increases the temperature of formation of the lamellar liquid crystal remains constant but the temperature of transformation from a lamellar liquid crystal to an isotropic solution increases. The phase diagram (discovered with the use of small and wide angle x-ray scattering) is from work by Shrestha et al. for diglycerol monomyristate in squalene.<sup>12</sup>

**Figure 1.9.** Phase diagram of diglycerol monomyristate in squalene. S is solid, O is excess oil, I is an isotropic single phase and  $L_\alpha$  is a lamellar liquid crystal from ref. 12.



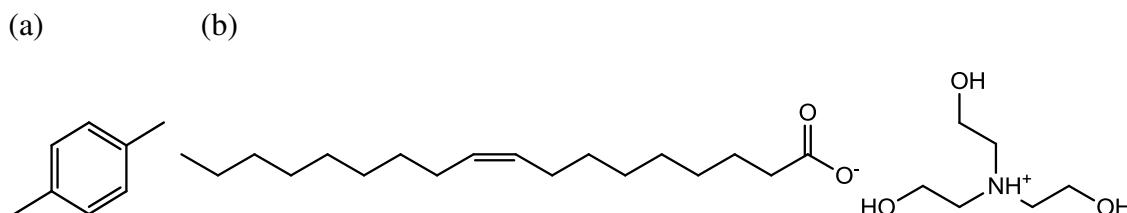
### 1.3 Review of relevant non-aqueous foams literature

As stated earlier in the chapter, there is very little literature in the area of non-aqueous foams. It is known that oil foams can be stabilised by surfactants,<sup>4-7</sup> particles<sup>13,14</sup> and a mixture of polymers and detergent particles.<sup>15</sup> Despite this, the stabilisation of oil foams specifically with the use of food-grade surfactants is sparse.

#### 1.3.1 Early work

Early work in the area of non-aqueous foams was conducted by Friberg et al.<sup>16</sup> It was found that a foam in a mixture of triethanolammonium oleate (TEAO) and p-xylene had excellent stability. The structure of TEAO and p-xylene are shown in Figure 1.10. TEAO with a concentration of 3-13 wt.% was added to p-xylene with the resulting foam having an increase in stability as the concentration increased. It was determined that the increase in stability was due to an increased presence of lamellar liquid crystals and the authors suggested that the liquid crystalline phase “adhered to the air surface.”

**Figure 1.10.** Structure of (a) p-xylene and (b) triethanolammonium oleate (TEAO).



It was recognised by Ross and Nishioka<sup>17</sup> that a foam can be produced at the solubility boundary of a substance in the continuous phase. Mixtures of various polymers including polymethylmethacrylate, chlorinated polypropylene and epoxy resin in 22 different solvents produced a foam. The foam was produced with N<sub>2</sub> gas which was input into the solution at 20 °C. 5 wt.% of the polymer was added to the solvent, unless saturation occurred with < 5 wt.% substrate, in which case, this quantity was used. It was found that foams were produced at the phase separation boundary; however, the foams produced were on the whole not stable for more than 10 seconds.

In 1981<sup>18</sup> it was found that the stability of a non-aqueous foam can vary with gas type. The gases used in the investigation were compressed air and natural gas (main component methane<sup>19</sup>). The aerated substance in this study was crude oil, with gas entering through the bottom of the vessel containing the oil. It was found that the average foam stability was longer with natural gas than with compressed air. The increased stability was suspected to be due to the movement of wax crystals in the crude oil to the gas-liquid interface which was enhanced by the natural gas. The effect of viscosity on the foam was also studied; it was observed that as the viscosity of the crude oil increased the foam stability also increased.

Ottewill et al.<sup>20</sup> found that as the concentration of surfactant-coated calcium carbonate nanoparticles in dodecane and ethyl benzene increased the foam stability also increased. The oil containing the particles was hand shaken for 10 seconds, then the foamability and foam stability was measured. It was also found that foams produced with the particles in ethyl benzene had a higher stability (with 60 wt.% particles stable for ~7

minutes) than foams produced with dodecane (with 60 wt.% particles stable for ~3 minutes).

Bergeron et al.<sup>21</sup> showed that fluorosurfactants have the ability to adsorb at an air-dodecane interface and stabilise the resulting foam produced with N<sub>2</sub> gas. The fluorosurfactants were FC-740 (a fluoroalkyl ester) and FS-2k (a fluorosilicone), both of which reduced the surface tension of dodecane. The reduction was from 25 mN m<sup>-1</sup> to 20.5 mN m<sup>-1</sup> with FC-740 and to 19 mN m<sup>-1</sup> with FS-2k. The critical micelle concentration (cmc) was observed to be approximately 0.4 wt.% for both of the surfactants (which is relatively low). It was thought that the surfactant adsorbed at the gas-liquid interface, creating repulsive forces that stabilised the foam films to collapse.

### 1.3.2 Non-aqueous foams stabilised by edible surfactants

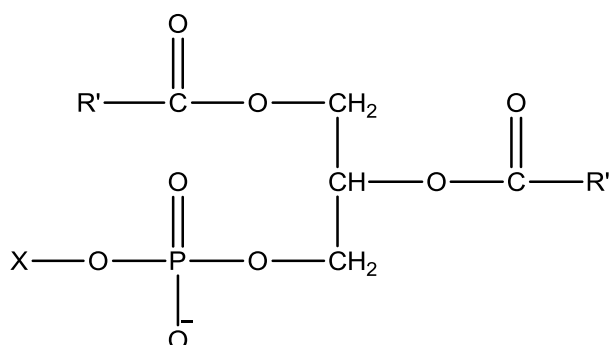
Mellema and Benjamins<sup>8</sup> studied the foamability of sunflower oil with eight commercial phospholipid surfactants. 100 mL of the oil with 0.3-0.5 wt.% surfactant was placed into a glass beaker and heated to 130 °C. Air was injected into the oil for 15 seconds below the air-oil surface. It was found that the foam stability at high temperatures was mainly determined by the rate of liquid drainage. Lecithin surfactants were used, which are a mixture of phospholipids. These phospholipids reduced the air-oil surface tension from 30 mN m<sup>-1</sup> to 27 mN m<sup>-1</sup>. The elasticity of the air-oil surface with different surfactants was measured by dynamic drop tensiometry. They found that the surfactant elasticity and foamability could be categorised into four groups.

- Group 1; ‘high elasticity’ with elasticity values of 50-30 mN m<sup>-1</sup>, foam production of ~50 mL.
- Group 2; ‘high-intermediate elasticity’ elasticity values of 9-40 mN m<sup>-1</sup>, foam production 0-25 mL.
- Group 3; ‘intermediate elasticity’ elasticity values 10-15 mN m<sup>-1</sup> with 20-25 mL foam production.
- Group 4; ‘minor elasticity’ with elasticity range of 0-5 mN m<sup>-1</sup>, producing 0-15 mL foam.

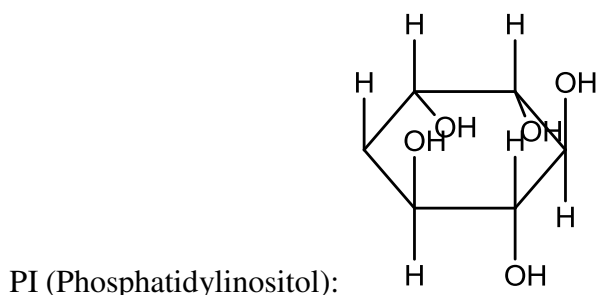
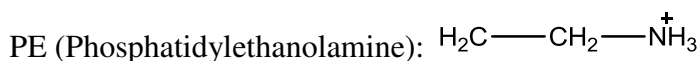
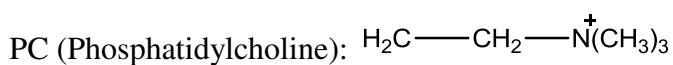
There was found to be a relation between the phospholipid content of the surfactant (as shown in Figure 1.11) and the groups they reside in. Surfactants in group 1 were typically rich in phosphatidylinositol and/or phosphatidyl-ethanolamine, group 2 had a

relatively large amount of lysophospholipids, groups 3 and 4 were rich in phosphatidylcholine. Lysophospholipid has 1 hydrophobic tail, creating a less mobile solute in the oil, therefore less solubility and less foam formation than group 1. Phosphatidylcholine was readily soluble in the sunflower oil, therefore the surfactants adsorb and desorb from the air-oil interface with ease creating minor elasticity and foamability.

**Figure 1.11.** Molecular structures of the main phospholipids present in the study.<sup>22</sup>



X is:



PA (Phosphatidic acid): H



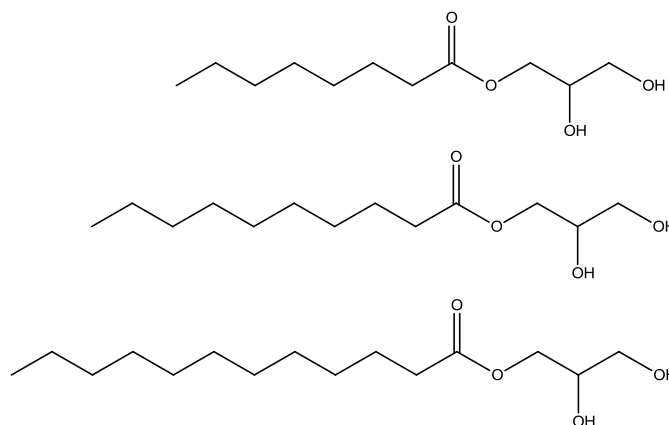
Shrestha et al.<sup>4</sup> have also studied monocaprylin, monocaprin and monolaurin (straight chain monoglycerides with respective chain lengths of C<sub>8</sub>, C<sub>10</sub> and C<sub>12</sub> as shown in Figure 1.12). 5 wt.% of the surfactant was studied in liquid paraffin, squalane and

squalene. Foams produced with monocaprylin were only stable for a maximum of two minutes in all three oils at 25 °C. Foam produced with monocaprin in squalene (170 mL) collapsed within three hours. In squalane and liquid paraffin 130-120 mL foam was initially produced, after 180 minutes approximately 90 mL foam remained and complete foam collapse occurred within approximately four hours. At 60 °C in liquid paraffin, 240 mL of foam was produced, but collapsed after 4 minutes. It was thought the reduced stability was due to the 'solid surfactant particles' melting, resulting in an isotropic solution.

Monolaurin produced foam in all three oils which was stable for up to 14 hours. The foam stability increased from squalene to squalane with liquid paraffin having intermediate stability. The liquid drainage of monolaurin was slower than that of monocaprin. The bubbles within the foam produced with monolaurin in squalane took up to 6 hours to become polyhedral and polydisperse, whereas bubbles within a foam produced with monocaprin were initially polyhedral and polydisperse at the top of the cylinder. As the concentration of monolaurin in squalane increased from 1 to 7 wt.% the foamability was similar, but the stability of the foam increased from 1 hour to over 14 hours.

It was clear from the study that more foam was produced with monolaurin than with monocaprin. It was suggested that the foamability and foam stability increased as the hydrocarbon chain length increased. It was also found in this study that the foams produced with squalane and liquid paraffin were more stable than foams produced with squalene. The structure of 5 wt.% monolaurin in the three oils was small needle/ rod-like shaped crystals. These crystals formed a complex network structure which created a viscous continuous phase where the crystals adsorbed at the bubble surface. Wide angle X-ray scattering analysis suggested that the crystals present were  $\beta$  crystals ( $\beta$  crystals are described in detail in Section 1.4). The presence of the monoglycerides was found not to have a significant effect on the surface tension of the oils used. The particle size of the monolaurin was found to decrease as the concentration increased; it was suggested that this property created a better packing at the gas-liquid interface, therefore creating an increase in foam stability.

**Figure 1.12.** Structure of monocaprylin, monocaprin and monolaurin.



In a further study by Shrestha et al.,<sup>5</sup> 5 wt.% diglycerol monomyristate and diglycerol monolaurate (Figure 1.13) were added to liquid paraffin, squalane, squalene and glycerol tris (2-ethylhexanoic) ester (TIO). The stability of the foams produced with diglycerol monolaurin in this paper was < 8 minutes, < 30 minutes, < 5 minutes and < 10 minutes, respectively. It is worth noting that with squalane only a few mL of foam was produced. In the oil systems with diglycerol monomyristate it was thought that either lamellar  $\beta$  crystals or a mixture of the micro-rods and the lamellar  $\beta$  crystals were responsible for the high stability.

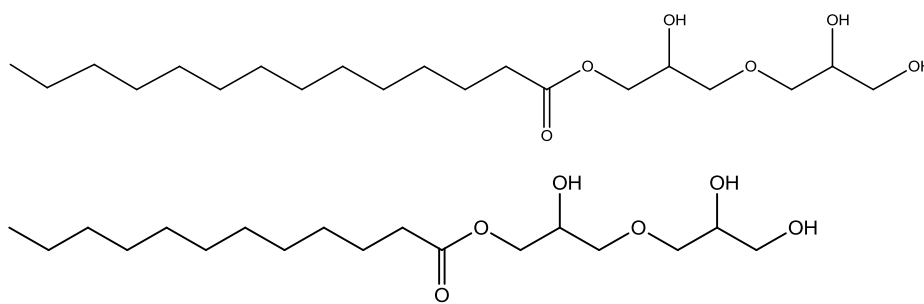
Aeration of the diglycerol monomyristate in the four oils was conducted at both 25 °C and 40 °C. A system of diglycerol monomyristate in liquid paraffin created highly stable foams at 25 °C, where the foam was stable for several days. Cavities within the bulk of the foam occurred 12 hours after formation, however, the original outer structure was retained for up to several days as the foam lamella had high rigidity. The stability of the foam was thought to be due to very small micro-rods of solids which may be lamellar  $\beta$ -phase or an alpha gel in combination with lamellar liquid crystals being present around the bubbles.

Foams produced with diglycerol monomyristate in squalene were highly stable, however the foam collapse of this system was hard to monitor. After 3-4 hours the foam became dry with breakage of the foam occurring randomly in the column. The foam did not move down the vessel under gravity to fill the void causing the recording of the foam volume/stability over time to be difficult, therefore the foam was stated as being stable for over 3 hours. The diglycerol monomyristate in glycerol tris (2-ethylhexanoic) ester produced a foam which was stable for < 90 minutes. A foam was not produced with diglycerol monomyristate in squalane. The micro-rods and liquid crystals in

diglycerol monomyristate in squalane were identified through optical microscopy as coagulated; this does not appear to occur with the surfactant in squalene and liquid paraffin. The overall foam stabilities were higher with diglycerol monomyristate in the oils than with diglycerol monolaurate.

Foams with diglycerol monomyristate in liquid paraffin and squalene were then produced at 40 °C with the foamability and foam stability compared to that of the foams produced at 25 °C. It was found that the temperature change did not have an effect on the foamability, however, the foam produced with both systems collapsed completely within 15 minutes at 40 °C.

**Figure 1.13.** Structure of diglycerol monomyristate (upper) and diglycerol monolaurate (lower).



The importance of the lamellar liquid crystal structure for non-aqueous foam stability has also been recognised by Shrestha et al.<sup>6</sup> In a study with diglycerol monolaurate in olive oil (see Table 1.1 for main fatty acid content), it was found that a foam could be produced with as little as 1 wt.% of the surfactant. As the surfactant concentration increased from 0-10 wt.% a maximum volume of foam (200 mL) was seen with 3-5 wt.% of the surfactant. With 1 wt.% of the surfactant, 25 mL of foam was produced, which then fully collapsed after 20 minutes. With 10 wt.% of the surfactant, 125 mL of foam was produced with a foam stability of more than 6 hours. It is clear that the foams produced with liquid paraffin, squalane, squalene and TIO had a significantly lower stability and foamability than that produced with olive oil. The appearance of the foam produced with 1 wt.% of the surfactant was found to be large, polydispersed polyhedral bubbles. Spherical, less polydispersed bubbles with a generally more viscous continuous phase were seen as the surfactant concentration increased. As the concentration increased the amount of drained liquid and the rate of liquid drainage decreased.

Although the stability of the foam increased as surfactant concentration increased, the surfactant concentration appeared to have a less significant effect on the foamability of the system. It was stated that the foam stability was thought to be due to the presence of lamellar liquid crystals creating rigidity at the air-liquid interface. The surface tension of the olive oil with and without surfactant was measured; the surface tension decreased from  $32.1 \text{ mN m}^{-1}$  to  $\sim 26.5 \text{ mN m}^{-1}$  as surfactant was added.

Shrestha et al.<sup>7</sup> have aerated diglycerol monomyristate in olive oil, finding that with 1 wt.% 60 mL of foam was produced; with 3, 5 and 10 wt.% 110-120 mL foam was produced. The foam created with 1 wt.% of the surfactant collapsed within approximately 20 minutes, with 10 wt.% the foam was stable for more than a month. The stability, therefore, is much greater than that observed with diglycerol monolaurate in olive oil, where with 10 wt.% of the surfactant present the foam was only stable for around 6 hours. The bubbles in the foam created with 5 wt.% of surfactant after 3 hours (when the liquid drainage appeared to have ceased) became polydisperse and polyhedral at the top of the foam column, but remained visually wet and spherical at the bottom of the foam column. With 10 wt.% of the surfactant present, the bubbles remained relatively spherical for several weeks, even after liquid drainage had subsided (which was after 24 hours). It was found through microscopy of the foam produced with 10 wt.% surfactant that small  $\alpha$ -solids surrounded the foam bubbles, which increased the viscosity of the continuous phase. The  $\alpha$ -solid particle size decreased as the surfactant concentration increased. The surface tension of the olive oil at  $25 \text{ }^\circ\text{C}$  decreased from  $32.1 \text{ mN m}^{-1}$  to  $24.2 \text{ mN m}^{-1}$  with 10 wt.% diglycerol monomyristate present, suggesting that the  $\alpha$ -solids adsorbed at the air-liquid interface. The liquid drainage of the systems decreased as the surfactant concentration increased.

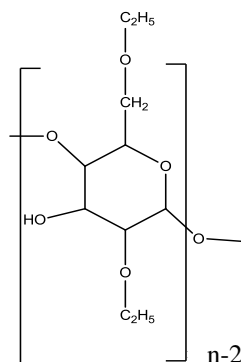
The studies into non-aqueous foams conducted by Shrestha et al.<sup>4-7</sup> involved a similar sample preparation for aeration, whereby the surfactant addition to the oil is at  $60\text{-}80 \text{ }^\circ\text{C}$  then mixed for up to 72 hours before aeration. The aeration technique was conducted at various temperatures with the use of liquid petroleum gas (LPG). The LPG (approximately 20 wt.%) was added to the mixture consisting of surfactant and oil in an air tight vessel. The mixture was then shaken with the initially dissolved LPG. The gas was then released through the nozzle, followed by any foam generated being poured into a measuring cylinder where the liquid drainage, foamability and foam stability was then monitored.

Murakami and Bismarck<sup>23</sup> produced non-aqueous foams with oligomers of tetrafluoroethylene (OTFE) particles in 17 oils with various chain lengths. The oils included straight chain hydrocarbons, esters, alcohols, silicone oil, a triglyceride and a fatty acid. After conducting wetting tests it was found that the wetting transition (particles go from non-wetted to wetted or vice versa) for the oils had an advancing contact angle of  $46 \pm 1^\circ$ . Milky non-aqueous foams (formed through hand shaking for 15 seconds) were produced at the wetting transition and the foams were stable for over 4 months. By measuring the viscosity of the oil it was found that foams from oils of low viscosity coalesced, whereas oils with high viscosity did not form bubbles. Microscopy of foams generated in silicone oil and ethyl benzoate with particles showed that the bubbles were spherical in shape and tens to hundreds of  $\mu\text{m}$ 's in size.

The ability of a fine powder of hydrophobic ethylcellulose polymer<sup>24</sup> with varying molecular weight of 77, 120, 158 and 220 Da has been investigated as an aid to aerate a cocoa butter equivalent (CBE) and rapeseed oil. Free soya lecithin (60 wt.% phospholipids) was also added to the studied system. The CBE is similar physically and chemically to cocoa butter but with a lower quantity of impurities. The CBE is 64 wt.% saturated fatty acids, 33 wt.% monounsaturated fatty acids and 3 % polyunsaturated fatty acids. The solid fat content was measured and decreased from 71 wt.% at 20 °C to 4 wt.% at 35 °C. Model chocolate was made by adding 0-0.2 wt.% ethylcellulose to 25 wt.% melted CBE and then stirring until a clear solution was formed, 0.4 wt.% lecithin and 0-0.2 wt.% sucrose was then added, followed by blending for approximately 2.5 hours.

The chocolate sample with only ethylcellulose (Figure 1.14) surfactant created a thick paste even after prolonged blending; with lecithin addition the viscosity reduced. It was found with the presence of ethylcellulose the sugar particles were more efficiently dispersed and less aggregated, therefore it was thought that the ethylcellulose co-adsorbs at the sugar surface together with lecithin. The interfacial tension measurements indicated that ethylcellulose formed a mixed interfacial film with the lecithin at the oil-air interface. It was found that if ethylcellulose was to be used with chocolate the presence of lecithin is essential.

**Figure 1.14.** Structure of ethylcellulose.<sup>25</sup>



Su-Jia et al.<sup>26</sup> have investigated the ability to create a foam with the addition of various phospholipids to cocoa butter. It was found that a foam could be produced and that the amount increased as the phosphatidylcholine content increased. It was also found that the foamability of the mixture increased as temperature was increased from 26 °C to 37 °C.

### 1.3.3 Non-aqueous foams stabilised by particles

Binks et al.<sup>15</sup> have also studied the effect of the phase separation boundary on the foamability of non-aqueous oils by investigating the effect of temperature on a base oil with polymers or detergent particles. The foaming procedure consisted of compressed air input via a Mott diffuser (average pore size 22 µm) into a measuring cylinder containing the investigated mixture. It was found that foam formation only occurred when the single-phase mixture was close to the phase separation boundary (solvent affinity for the solute was low). The phase separation boundary was indicated as the region where the mixture converted from turbid (additive not fully soluble in the solvent) to clear (additive soluble in the solvent). A relatively large amount of foam was produced with all of the additives from the 5 minutes of aeration at the phase separation boundary (up to 400 mL). It was found that the foam formed contained approximately 50 vol.% of the liquid which reduced to approximately 20 vol.%. The foam was then found to collapse (average foam stability was approximately 5 minutes), it was found that the foam did collapse during the aeration by coalescence. At least 1 wt.% of the solute was required to create a foam. The bubbles in the foam were polydisperse (diameter of a few mm) and spherical.

Work by Binks and Rocher<sup>13</sup> showed the possibility of creating a non-aqueous foam with the use of PTFE particles. The oils studied were perfluorohexane, n-heptane, polydimethylsiloxane (PDMS), toluene, sunflower oil, eugenol and benzyl acetate. The oil surface tension ranged from 11.9 mN m<sup>-1</sup> with perfluorohexane to 38.0 mN m<sup>-1</sup> with benzyl acetate. Particles were found to be wet and dispersed in perfluorohexane, n-heptane, PDMS and toluene which have surface tension values of 11.9, 20.1, 21.1 and 28.4 mN m<sup>-1</sup>, respectively. Sunflower oil, eugenol and benzyl acetate had surface tensions of 32.5, 36.4 and 38.0 mN m<sup>-1</sup> respectively, and created an air-in-oil foam. Particles in glycerol (63.4 mN m<sup>-1</sup>) and water (72.5 mN m<sup>-1</sup>) were non-wetted creating a liquid-in-air material.<sup>13</sup> Three agitation methods were used to create the material that was formed; namely a blender, rotor stator homogeniser and hand shaking. Air-in-oil foams were produced with sunflower oil, rapeseed oil, eugenol,  $\alpha$ -hexylcinnamaldehyde and benzyl acetate. Even with liquid drainage the bubbles remained stable for many days. The bubble size of the air-in-oil foams produced was approximately 100-300  $\mu$ m which decreased slightly with a decrease in surface tension from rapeseed oil < eugenol < benzyl acetate. Non-spherical bubbles were seen in eugenol; it is thought this was because of a dense, rigid layer of 'jammed' particles which prevented relaxation to a spherical shape.

In a further study by Binks et al.,<sup>14</sup> four types of polytetrafluoroethylene (PTFE) particles and oligomeric tetrafluoroethylene (OTFE) particles were used. The particles, which differed in size, shape and surface roughness, were added to 32 liquids, including vegetable oils and water which had a wide range of surface tension values. It was found that after agitation by three different methods, the behaviour of the fluoro particles in the liquids could be characterised. If the surface tension was less than 28.7 mN m<sup>-1</sup> then the particles dispersed in the continuous phase after agitation. With a surface tension of 33-45 mN m<sup>-1</sup> bubbles could be produced and above this tension particles were non-wetted. The difference in the fluoro particle size, shape and surface roughness did not have an effect on the overall behaviour in the liquids. The bubbles in the foams were 20-300  $\mu$ m in diameter and both spherical and non-spherical. Approximately 10 mL of foam was produced with 5 wt.% particles which was stable for many days. As the particle concentration of Ultraflon MP-8T in sunflower oil and eugenol increased from 0.5 to 10 wt.% the stability increased from many days to over 6 months, respectively. After hand shaking the particles in eugenol for 5 minutes it was found that the foamability increased from ~0.5 mL with 0.5 wt.% particles to ~3.5 mL foam with 10

wt.% particles. The foams produced in this system initially the drain oil within 5 minutes after agitation of the mixture, bubbles then cream upwards due to gravity. Particles not involved in stabilising the foam were seen to sediment.

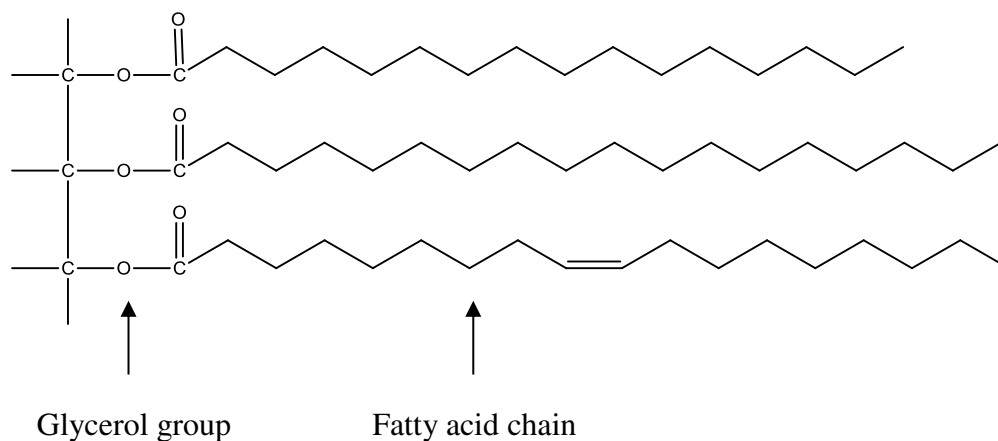
#### 1.4 Fat crystallisation

A fat is a multi-component mixture of triacylglycerols which are triesters of fatty acids with glycerol.<sup>27</sup> It can be seen in Chapter 6 that a gel-like structure is important for the formation of a whipped oil. Therefore the crystallisation of fats and the formation of gels with edible materials is to be discussed.

##### 1.4.1 Formation and structure

A triglyceride molecule (also known as a triacylglyceride) is a glycerol group bonded to three fatty acid chains. The fatty acids can vary in chain length as can the quantity of double bonds present, as shown in Figure 1.15.

**Figure 1.15.** A typical triglyceride structure.



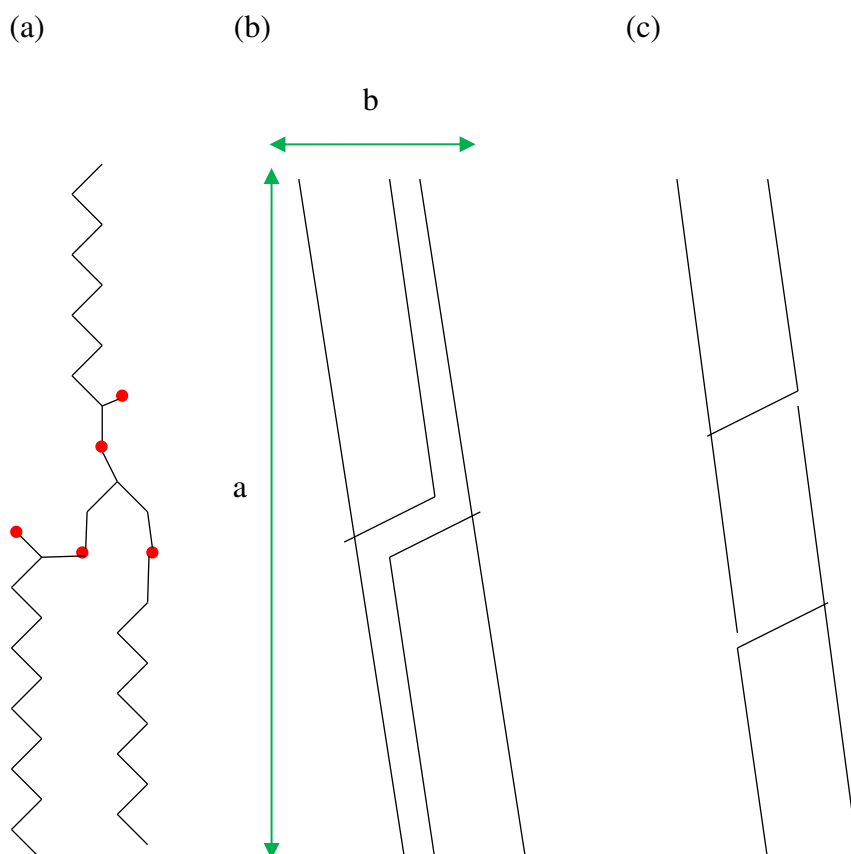
The attractive forces which are present between the triglyceride molecules determine the formation of a crystal structure known as fat crystals. Fat crystals can have various structures (polymorphs) which are of the same chemical compound but demonstrate different packing of the hydrocarbon chains and angle of tilt. The most prominent

polymorphs are  $\alpha$ ,  $\beta'$  and  $\beta$  shown in Figure 1.16 and Figure 1.17. The type of polymorph formed is dependent on the type of oil present, fatty acid distribution, oil purity and crystallisation conditions (e.g. temperature, rate of cooling).<sup>28</sup>

The  $\alpha$  form is the least stable polymorph, therefore it is formed and melted at a lower temperature than that of the  $\beta'$  form and the  $\beta$  form, where  $\beta$  is the most stable polymorph with highest melting temperature.<sup>27</sup> The stability of the crystals to an increase in temperature increases due to closer packing of the triglyceride.<sup>28</sup>

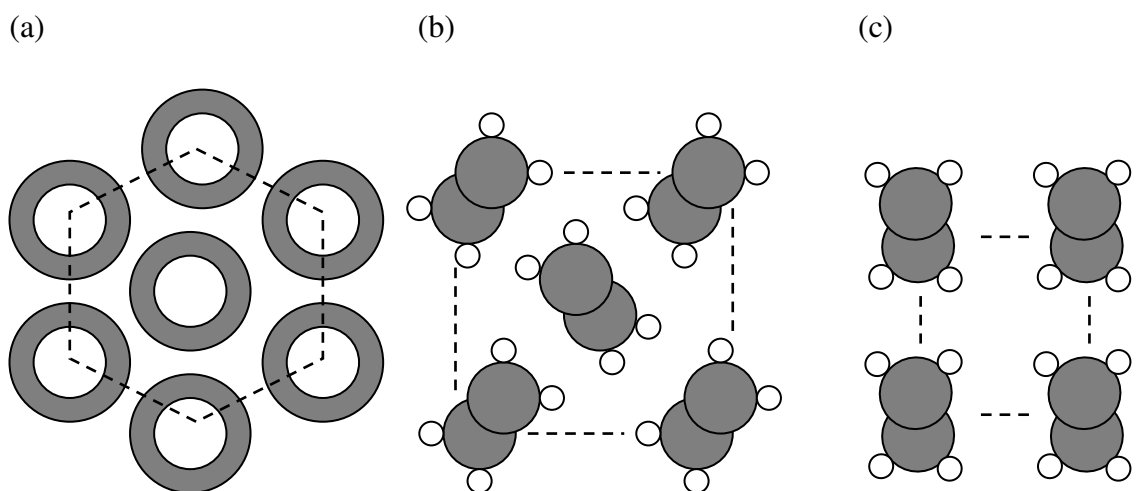
When a triglyceride crystallises, the chains align side by side to maximise the van der Waals interactions as shown in Figure 1.16. A characteristic that can aid to the identification of the polymorph present in a mixture is the long and short spacings. The long spacing 'a' is defined as the distance between the methyl groups at each end of the molecule, Figure 1.16 (b). Long spacings increase with increasing chain length and decrease with increasing tilt angles. The short spacing 'b' is the distance between the inter-chains, Figure 1.16 (b).

**Figure 1.16.** Structure of a triglyceride in a fat crystal. (a) is a unit cell of a triacylglycerol, (b) is a type 2 long axis and (c) is a type 3 long axis.



The  $\alpha$  form is known as metastable which means that the structure will transform into more stable forms such as  $\beta'$  and  $\beta$ , this can occur by melt-mediated transformation.<sup>27</sup> Melt-mediated transformation is the careful melting of the  $\alpha$  form which then recrystallises to the  $\beta'$  or  $\beta$  form with the necessary conditions. The melt-mediated transformation can occur due to a difference in the melting temperature of the polymorphic forms which is  $\alpha < \beta' < \beta$  as temperature increases. As the forms increase in melting temperature there is a change in shape from hexagonal (with randomly orientated chains which rotate about the long spacing axis), to orthorhombic (where the hydrocarbon chains are parallel) to triclinic (where the hydrocarbon chains are parallel and the crystal planes are perpendicular to the adjacent planes) as Figure 1.17 depicts. The orientation of ethylene groups is important as this can determine the packing of the triacylglycerol and therefore the stability and melting temperature of the crystal. Under the microscope the  $\alpha$  form produces a large amount of very tiny crystals, the  $\beta'$  form is usually a bulky shape/ spherulite and the  $\beta$  form is usually needle-shaped.<sup>30</sup>

**Figure 1.17.** Packing arrangement, from above, of ethylene groups within long fatty acid chains of triacylglycerols. (a) hexagonal (typical structure for  $\alpha$ ), (b) orthorhombic (typical structure for  $\beta'$ ) and (c) triclinic (typical structure for  $\beta$ ).<sup>28</sup>



The type of fat crystal formed can be very important for the final product achieved. This is especially the case for chocolate, as the crystal form is important for the breaking of the chocolate, taste and texture in the mouth. A technique called tempering is used to achieve the ideal, required crystal form. Tempering is the process conducted to acquire

the favoured polymorph and comprises of careful heating, then cooling with, at times, a further heating procedure. The knowledge of which polymorphs are present and the melting temperatures of the polymorphs are essential. It is known that if a triglyceride has the same fatty acid chains then the  $\alpha$ ,  $\beta'$  and  $\beta$  will have similar formation and melting temperatures.<sup>31</sup> If the fatty acid chains are vastly different then the formation and melting temperatures will be very different.

A fat crystal gel (often referred to as an organogel) can be formed in a mixture of fat crystals and oil due to hydrogen bonding and van der Waals forces between the glycerol chains. A gel is defined as a two-phase colloidal system consisting of a solid and a liquid in a more solid form than a sol.<sup>30</sup> It has been found that gels can be formed with fatty acids with chain lengths from C<sub>12</sub> to C<sub>31</sub>, also with monoglycerides, fatty alcohols and dicarboxylic acids in various vegetable oils as described in a review by Perneti et al.,<sup>32</sup> some of which are described in the next section. As will be discussed in the results and discussion section, it has been possible to whip various gels to create a whipped oil stable for over 18 months. Therefore, it is important to discuss relevant previous work which involves the formation of oleo gels.

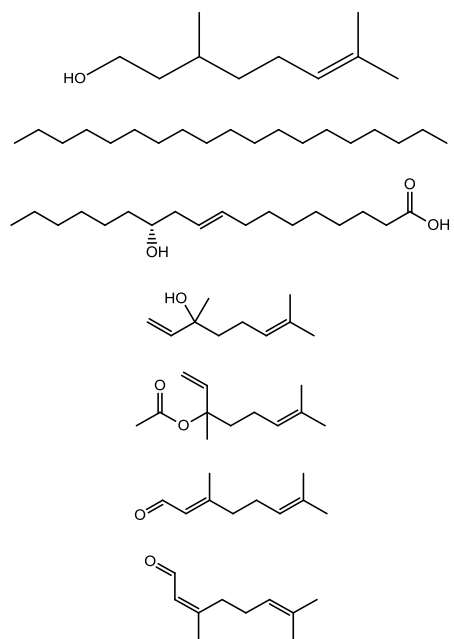
#### 1.4.2 Relevant previous work on organogels

There have been numerous studies conducted in the area of organogels. These include fatty acids, fatty alcohols and monoglycerides in various oils. Table 1.1 displays some of the oils investigated and their main fatty acid chain lengths which are referred to in the following review.

**Table 1.1.** Approximate main fatty acid chain length of various edible oils. For example in C<sub>18:2</sub> the digit before the colon is the chain length, the digit after the colon refers to the number of double bonds present. The references refer to where the oil composition was obtained.

| Oil                            | Approximate main fatty acid group(s)  |
|--------------------------------|---|
| Sunflower <sup>33</sup>        | 20 % C <sub>18:1</sub> and 68 % C <sub>18:2</sub>   |
| Diet <sup>33</sup>             | 22 % C <sub>18:1</sub> and 66 % C <sub>18:2</sub>   |
| Sal fat olein <sup>30</sup>    | 24 % C <sub>18</sub> and 56 % C <sub>18:1</sub>   |
| Cocoa butter <sup>34</sup>     | 85 % C <sub>16</sub> , C <sub>18</sub> and C <sub>18:1</sub>  |
| Palm super olein <sup>30</sup> | 49 % C <sub>18:1</sub> , 13.5 % C <sub>18:2</sub> and 32 % C <sub>16</sub>  |
| Olive oil <sup>30</sup>        | 79 % C <sub>18:1</sub>  |
| Soybean oil <sup>35</sup>      | 24 % C <sub>18:1</sub> , 11 % C <sub>16</sub> and 52 % C <sub>18:2</sub>  |
| Rapeseed oil <sup>36</sup>     | 63 % C <sub>18:1</sub> , 19 % C <sub>18:2</sub> and 9 % C <sub>18:3</sub>   |
| Lavender <sup>37</sup>         | 48 % linalyl acetate 28 % linalool  |
| Rose <sup>38</sup>             | 40 % beta-citronellol, 18 % nonadecane  |
| Lemongrass <sup>39</sup>       | 25-53 % geranial, 20-45 % neral   |
| Castor <sup>40</sup>           | 84-90 % ricinoleic  |
| Peanut <sup>41</sup>           | 51 % C <sub>18:1</sub> and 30 % C <sub>18:2</sub>   |
| Canola <sup>35</sup>           | 60 % C <sub>18:1</sub> and 22 % C <sub>18:2</sub>   |
| Sesame <sup>42</sup>           | 46 % C <sub>23</sub> -C <sub>33</sub>   |
| Virgin olive oil <sup>43</sup> | 55 % C <sub>18:1</sub>  |
| Palm <sup>44</sup>             | 45 % C <sub>16</sub> and 39 % C <sub>18:1</sub>   |
| Cod liver oil <sup>45</sup>    | 17 % C <sub>18:1</sub> , 11 % C <sub>16</sub> and 10 % C <sub>16:1</sub> , C <sub>18</sub> ,<br>C <sub>20:1</sub> |

**Figure 1.18.** Structure of various components in the oils stated in Table 1.1, from top to bottom, beta-citronellol, nonadecane, ricinelaic acid, linalool, linalyl acetate, geranial and neral.



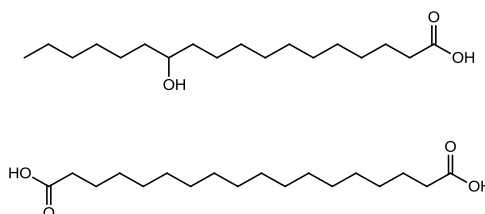
#### 1.4.2.1 Effect of fatty acids and fatty alcohols on gelation

Gandolfo et al.<sup>46</sup> have studied the formation of organogels from straight chain acids and alcohols  $C_{16}$  to  $C_{22}$ . The acids and alcohols were added to sunflower, soybean and rapeseed oil. The samples were heated to 60-80 °C, then cooled at room temperature with stirring to 40 °C, followed by storage at 5 °C for one day before experimentation. 2 wt.% of the acid or alcohol in sunflower oil was required to produce a gel. The ‘hardness’ of the mixtures formed was studied with the use of a texture profile analyser. Generally the alcohols formed a harder gel-like material than the acids. The soybean and rapeseed oil was found to produce similar results to that obtained with sunflower oil. Combinations of the acids and alcohols of the same chain length were investigated finding that with the  $C_{18}$  chain length a higher value of hardness was identified with a ratio of 8:2, acid:alcohol, compared to that obtained with only the alcohol or acid in the sunflower oil.

Work by Daniel and Rajasekharan<sup>47</sup> furthered the findings of Gandolfo et al. Saturated fatty acids with a chain length of  $C_{10}$  to  $C_{31}$  were studied with oils such as sunflower, lavender, castor, rapeseed, peanut, rose and lemongrass. The required amount of the fatty acid and oil were placed into a vessel which was heated to 60-65 °C and shaken

until the acid had dissolved. The solution was then left to cool to room temperature. Gelation was recognised as formation of a homogeneous substance with no gravitational flow. Fatty acids of chain length 10 to 31 were able to gel vegetable oils. It was found that the minimum amount of fatty acid required to create the gel decreased as the chain length increased (60 % for decanoic acid, 15 % for dodecanoic, 6 % for tetradecanoic acid, 4 % hexadecanoic acid and 2 % for octadecanoic acid). Concentration requirements for gelation remained relatively similar to that for octadecanoic acid as the chain length further increased to C<sub>31</sub>. The melting temperature of the gels increased from 30-70 °C as the chain lengths of the fatty acid increased. The effect of a hydroxyl group in the middle of the alkyl chain in C<sub>18</sub> (12-hydroxyoctadecanoic acid) was also studied (Figure 1.19) with the finding that only half of the substance was required to create a gel (1 %) compared to that with C<sub>18</sub> (2 %) in sunflower oil. The effect of changing the hydroxyl group with a methyl group (12-methyloctadecanoic acid) was then investigated in sunflower oil, finding that almost 10 % was required to create a gel. A similar result was obtained with the addition of a methyl group to the C<sub>22</sub> acid whereby 4 % was required to make a gel compared to 2 %. In contrast, the addition of a methyl group to C<sub>26</sub> and C<sub>30</sub> acid had little effect on the amount required to create a gel in sunflower oil. It was found that with a combination of C<sub>18</sub> and C<sub>20</sub> acids, on average, approximately 5 % more of the acid combination was required (~7 %) to create a gel than it did to create a gel with the acids alone (~2 %). The gelled oils produced were found to be stable for at least 3 months.

**Figure 1.19.** Structure of 12-hydroxyoctadecanoic acid (upper) and dihydroxyoctadecanoic acid (lower).



Higaki et al.<sup>30</sup> used ‘high melting fats’ which were either fully hydrogenated rapeseed oil rich in behenic acid (FHR-B), fully hydrogenated rapeseed oil rich in stearic acid (FHR-S), tristearoyl-glycerol (SSS), triarachidonoyl-glycerol (AAA) and tribehenoyl-glycerol (BBB). The ‘low melting fats’ used were sal fat olein (SFO), palm super olein (PSO), olive oil and cocoa butter. A high melting fat was added to a low melting fat at

70 °C, the mixture was then cooled to a crystallisation temperature which was between 20-38 °C. The sample was then heated at 2 °C/min. to a final temperature which was between 30-45 °C (the final temperature was between the melting temperatures of the low and high melting fats). The effect of the cooling rate (10 °C/min. and 1.5 °C/min.), the crystallisation temperature and the final temperature was investigated. The formation of a gel-like substance was identified by placing the vessel with the mixture present at an angle of 45 ° for an hour. The gel-like behaviour was identified when deformation did not occur and the liquid and solid phase did not separate. It was found that a cooling rate of 10 °C/min. was necessary for the formation of a gel-like substance as it was suggested that the fast cooling rate caused the production of  $\alpha$ -crystals. It was suggested that the heating to the final temperature used in the study then caused the  $\alpha$ -crystal to transform into a  $\beta$ -crystal. The fast cooling rate created a random distribution of the  $\alpha$ -crystal, therefore the nucleation sites for the transformation into  $\beta$ -crystals is also randomly distributed. The  $\beta$ -crystals (formed through melt-mediated transformation) then created a network which incorporated the liquid low melting fat. A gel-like substance could be produced at various crystallisation temperatures with cooling from 70 °C to the crystallisation temperature, then heating to a final temperature of 38 °C. This is shown in Table 1.2 below.

**Table 1.2.** Effect of crystallisation temperature ( $T_c$ ) (cooled from 70 °C at 10 °C/min.) on the gelation of FHR-B in SFO. The final temperature was 38 °C. – liquid, G gel-like, S somewhat gel-like.<sup>30</sup>

| Concentration of FHR-B (wt. %) | Concentration of SFO (wt.%) | $T_c$ (°C) |    |    |    |    |
|--------------------------------|-----------------------------|------------|----|----|----|----|
|                                |                             | 20         | 25 | 30 | 35 | 38 |
| 0                              | 100                         | -          | -  | -  | -  | -  |
| 0.5                            | 99.5                        | -          | -  | -  | -  | -  |
| 1.0                            | 99.0                        | -          | -  | -  | -  | -  |
| 1.5                            | 98.5                        | S          | -  | -  | -  | -  |
| 2.0                            | 98.0                        | G          | G  | -  | -  | -  |
| 3.0                            | 97.0                        | G          | G  | S  | -  | -  |
| 4.0                            | 96.0                        | G          | G  | G  | -  | -  |

For a crystallisation temperature of 20 °C, varying the final temperature from 30-45 °C affected the gelation behaviour as shown in Table 1.3.

**Table 1.3.** Effect of the final temperature ( $T_f$ ) on the gelation of FHR-B in SFO which was cooled from 70 °C to 20 °C at 10 °C/min. – liquid, G gel-like, S somewhat gel-like.<sup>30</sup>

|                                |                             | $T_f$ (°C) |    |    |    |    |    |
|--------------------------------|-----------------------------|------------|----|----|----|----|----|
| Concentration of FHR-B (wt. %) | Concentration of SFO (wt.%) | 30         | 35 | 38 | 41 | 43 | 45 |
| 0                              | 100                         | -          | -  | -  | -  | -  | -  |
| 0.5                            | 99.5                        | -          | -  | -  | -  | -  | -  |
| 1.0                            | 99.0                        | -          | -  | -  | -  | -  | -  |
| 1.5                            | 98.5                        | G          | G  | S  | -  | -  | -  |
| 2.0                            | 98.0                        | G          | G  | G  | -  | -  | -  |
| 3.0                            | 97.0                        | G          | G  | G  | G  | G  | -  |
| 4.0                            | 96.0                        | G          | G  | G  | G  | G  | G  |

It is clear from Tables 1.2 and 1.3 that a gel could not be formed at a FHR-B concentration less than 1.5 wt.%. The only systems that did produce a gel were FHR-B in SFO or cocoa butter. The lack of gel formation with PSO and olive oil was thought to be due to the absence of  $\alpha$ -crystal formation. The addition of all the high melting fats to SFO resulted in the creation of  $\alpha$ -crystals which melt-mediated into  $\beta$ -crystals, therefore it was suspected that the ‘randomness’ of the distribution of the fat crystals in the oils was essential to gel formation. The  $\beta$ -crystal was found to have needle-like morphology.

Schaink et al.<sup>31</sup> investigated the effect of various ratios of stearyl alcohol and stearic acid on hardness and rheology in sunflower oil and diet oil. The sample was heated to 70-80 °C and stirred for 10 minutes, then cooled to room temperature followed by storage at 4 °C. Sample analysis occurred within 4 hours of sample preparation. 3.5 % of the structurant was required to create a gel. It was found that with a ratio of 3:7 of acid:alcohol, the hardness of the mixture (5 % in total) was a factor of 2.5 harder than any other acid to alcohol combination or the pure component, which supported findings

by Gandolfo et al.<sup>46</sup> Further findings showed a decrease in elasticity with increasing temperature (from 5 °C to 30 °C). The appearance of the crystals in 3:7 was needle-like with the smallest average crystal size; therefore the small crystal size was thought to have been responsible for the strength of the gel. When only one structurant was present (stearic acid or stearyl alcohol) the structure of the crystals was plate-like. The pure components were thought to be  $\beta'$ -type crystals, whereas the mixtures of stearyl alcohol and stearic acid were thought to be  $\beta$ -type crystals. At temperatures above 35 °C all samples were liquid-like.

Wright and Marangoni<sup>48</sup> have studied ricinelaidic acid (REA) (see Figure 1.18)) in detail with canola oil, where it was found that a gel could be produced with a minimum of 1 % of the structurant. The mixture was produced with initial heating to 80 °C, with gelation studies at 15, 20 and 25 °C. A clear gel was formed with 0.5-1 % which occurred at below ~7 °C (with 0.5 %) and at below ~13 °C (with 1 %); with 1-3.5 % a non-transparent gel was formed which was observed below ~18 °C. The gel increased in stability with an increase in temperature as REA concentration was increased. The gel was present up to ~33 °C with 3.5 % and up to 35 °C with 4-5 %. The texture of 3.5 to 5 % REA in canola oil was described as fat-like. 5 % ricinelaidic acid was identified through polarised light microscopy as being long, thin fibres which were thought to intertwine into a cluster, immobilising the oil.

Rogers et al.<sup>49</sup> studied 12-hydroxystearic acid (HSA) in canola oil. The required amount of 12-hydroxystearic acid was added to the canola oil at 85 °C, then held at this temperature for 30 minutes, then stored at 5, 15, 20 or 30 °C for a day, week or month. It was found that 0.5 % of the structurant in the oil could produce a gel. With 2 % of the structurant in the oil at 30 °C a gel was stable for a week and remarkably when held at 5 °C the gel was found to be stable for up to 6 months. A gel could be formed with as little as 1 % HSA which was present at as high as 50 °C after 1 month. The melting temperature was found to increase as the structurant concentration increased. It was found that the amount of crystalline mass in the samples increased as the storage time increased.

#### 1.4.2.2 Effect of monoglycerides and diglycerides on gelation

In work by Ojijo et al.<sup>43</sup> Adochan 98 (monoglyceride consisting of 46 % C<sub>16</sub>, 54 % C<sub>18</sub>) was used in a mixture with virgin olive oil. The required amount of Adochan was added

to the virgin olive oil at 75 °C, then cooled to (taking roughly 4 hours) and stored at 25 °C. A cylindrical probe was used for hardness measurements. It was found that 7 % Adochan created a gel in the olive oil. The structure of the Adochan in the oil was found to be elongated/rod-like aggregates. The hardness of the gel increased as storage time increased. This may have been due to an increase in crystallinity with storage time. It was thought that the crystals observed after 2 months were smaller than that observed at the onset of storage as the larger crystals initially formed disintegrated into smaller crystals which reorganised into more compact aggregates (closer packing of acyl chains) creating the increased hardness.

Work by Lupi et al.<sup>50</sup> concentrated on Myverol (monoglyceride consisting of 60 % C<sub>14</sub>, 40 % C<sub>18:1</sub>) in olive oil and cocoa butter. The required amount of Myverol was added to the oil or cocoa butter at 70 °C, then maintained at 70 °C until experimentation was performed. The minimum amount of Myverol needed to create a gel in cocoa butter was 1 % and in olive oil was 1.5 % at 32 °C. It was thought that a  $\beta'$  crystal was responsible for the gel formation.

Saberi et al.<sup>44</sup> studied the gelation of a palm oil diglyceride (PO-DAG) (46 % C<sub>16</sub>, 38 % C<sub>18:1</sub>) in palm oil (PO). The investigated mixtures consisted of two components which were heated to 80 °C, then cooled to 18 °C, held at the temperature for 1 hour, then stored at 25 °C for 24 hours before analysis. A gel was formed with 10 % of the palm oil diglyceride in palm oil. The hardness of the palm oil increased as the palm oil diglyceride content increased (lowest concentration of palm oil was 0 %, the content increased by an increment of 10 % until 100 % palm oil was reached). The melting temperature of the palm oil diglyceride was found to increase as the content in the palm oil increased. The increased hardness as the PO-DAG content increased was thought to be due to the strength of the hydrogen bond formed among the free hydroxyl groups. This suggested that the use of a PO-DAG was ideal for structuring the oil. It was thought that the crystal present with 10 % palm oil diglyceride was  $\beta'$ , with 10 – 90 % the crystal was  $\beta$ .

Da Pieve et al.<sup>51</sup> used cod liver oil with 5, 7 and 9 % Myverol (60 % C<sub>14</sub>, 40 % C<sub>16</sub>). The Myverol in cod liver oil was heated to 80 °C, and then reached 20 °C under static conditions for 24 hours before analysis of the formed substance. Organogels were produced with all three concentrations of the Myverol. The melting temperature of the gel increased as the Myverol concentration increased. It was thought that as the monoglyceride content increased a more structured network was formed.

A brief summary of the findings from the relevant work in the area of the gelation of various 'structurant' in oil combinations are shown in Table 1.4.

**Table 1.4.** Summary of organogel formation studies.

| Structurant   | Oil   | Brief findings  | Reference |
|---|---|---|-----------|
| Saturated C <sub>16</sub> to C <sub>22</sub> alcohols and acids | Sunflower, soybean and rapeseed oil                                     | 2 wt.% required. Alcohols normally harder than the acids. C <sub>16</sub> acid produced hardest gel. Hardest gel with 5 % 3:7 acid:alcohol in soybean oil. Minimum hardness 7:3 acid:alcohol.   | 46        |
| Saturated C <sub>10</sub> to C <sub>31</sub> fatty acids        | Sunflower, castor, rapeseed, peanut, lavender, rose and lemongrass oil. | 2 % required. All fatty acids created a gel. Hydroxyl group (12-hydroxyoctadecanoic acid) reduced amount of acid required for gelation. Dicarboxylic acids created a gel in sunflower and lavender oil.                               | 47        |
| FHR-B, FHR-S, SSS, AAA and BBB                                  | Sal fat olein, cocoa butter, palm super olein and olive oil.            | Gel formed at 1.5 wt.% FHR-B in sal fat olein. Stability of gel increased as structurant concentration increased. Gel only formed with FHR-B in sal fat olein and cocoa butter. Cooling rate of 10 °C/min was essential for gelation. | 30        |
| Stearyl alcohol and stearic acid                                | Sunflower and diet oil  | 3-4 % required. Hardest gel formed with 3:7 acid:alcohol.   | 33        |
| Ricinelaidic acid (REA)   | Canola oil  | 2 % required. 5 % REA demonstrated long, thin fibres.   | 48        |
| 12-   | Canola oil  | 0.5 % required. 2 % at 5 °C was   | 49        |

|  |                            |  |    |
|--|----------------------------|--|----|
| hydroxystearic acid  |                            | stable for up to 6 months. Melting temperature increased as concentration increased.   |    |
| Adochan 98<br>(46 % C <sub>16</sub> ,<br>54% C <sub>18</sub> )           | Virgin olive oil           | 7% required. Elongated/rod-like aggregates in the olive oil. Hardness increased but melting temperature decreased as storage time increased. | 43 |
| Myverol (60 % C <sub>14</sub> , 40 % C <sub>16</sub> )                   | Olive oil and cocoa butter | 1 % required. β' crystal required for gelation.  | 50 |
| Palm oil diglyceride<br>(46 % C <sub>16</sub> , 38 % C <sub>18:1</sub> ) | Palm oil                   | 10 % required. Hardness and melting temperature increased as palm oil diglyceride % increased..  | 44 |
| Myverol (60 % C <sub>14</sub> , 40 % C <sub>16</sub> )                   | Cod liver oil              | 5 % required. Melting temperature of the gel increased as the Myverol concentration increased.   | 51 |

## 1.5 Aims and objectives

The aim of this research was to further knowledge in the area of non-aqueous foams with the use of numerous edible surfactants and oils with various aeration methods. It is known from previous literature that a foam can be produced with industrial oils and also with some vegetable oils such as olive oil and sunflower oil when there is polymers, surfactants or particles present. It is also known that a foam can be created through aeration with dissolved gas and also with a foaming column. However, there is still very little literature in the area of oil foams particularly with the use of edible surfactants and oils. It is not known what the effect of various edible surfactants and oils, along with other parameters such as aeration type, gas type and temperature, have on foam formation and stability. Therefore these factors have been investigated to understand their influence. These parameters are also extremely important for companies in the areas of food, oil and cosmetics; this thesis aims to investigate these factors as described in the presentation of thesis.

## 1.6 Presentation of thesis

The initial aim of this work was to find out which oil and surfactant combinations could create a foam and with which aeration method. The subsequent foam stability was then monitored. The effect of surfactant concentration and temperature was studied with numerous combinations. Chapter 2 describes the experimental methods conducted along with the surfactants and oils used.

Chapter 3 describes the results on the effect of phospholipids on the creation of a foam with various oils. The phospholipid concentration along with the amount of phosphatidylcholine and phosphatidylethanolamine in the mixtures on foamability and foam stability was also investigated.

Chapter 4 contains the data from investigating a mono-diglyceride surfactant on foamability and foam stability in high oleic sunflower oil. It includes the discussion of foams produced with a total of 4 different aeration methods. The effect of concentration, temperature and gas type was also studied along with comparison of the effect of saturation of the surfactant.

Chapter 5 introduces the gelled mixture of myristic acid in HOSO. The effect of myristic acid concentration on gelation, crystal structure, viscosity, melting temperature and solid content was investigated.

Chapter 6 comprises a detailed study of the foamability and foam stability of myristic acid in HOSO aerated with a hand held double beater electric whisk. The effect of concentration, temperature (on the foam stability and on the foam preparation) and oil type (both edible and non-edible) is discussed. The effect of cooling rate was also a parameter studied.

Numerous surfactant and oil combinations were analysed with the whipping technique in Chapter 7. The surfactants included monoglycerides and triglycerides as well as investigating the effect of fatty acid and fatty alcohol chain length on foamability and foam stability. The effect of stearic acid concentration in HOSO along with temperature on foam formation and stability was studied. The foam produced with Dimodan HR kosher in HOSO was very intriguing as it highlighted the importance of a further parameter necessary for foam formation (the temperature the mixture was cooled to). It was also found that the whipping technique was very applicable for a food company such as Nestlé which was identified by the concept samples produced.

Finally, a summary of the conclusions and suggestions for future work are described in Chapter 8.

## 1.7 References

1. Foams: Basic Principles, L. Schramm and F. Wassmuth, American Chemical Society, Washington, 1994.
2. C.J.W. Beward and P.D. Howell, *J. Fluid Mech.*, **458**, 379 (2002).
3. N. Vandewalle, H. Caps, G. Delon, A. Saint-Jalmes, E. Rio, L. Saulnier, M. Adler, A.L. Biance, O. Pitois, S. Cohen Addad, R. Hohler, D. Weaire, S. Hutzler and D. Langevin, *J. Phys. Conf. Ser.*, **327**, 1 (2011).
4. L. K. Shrestha, K. Aramaki, H. Kato, Y. Takase and H. Kunieda, *Langmuir*, **22**, 8337 (2006).
5. H. Kunieda, L. K. Shrestha, D. P. Acharya, H. Kato, Y. Takase and J. M. Gutierrez, *J. Disp. Sci. Technol.*, **28**, 133 (2007).
6. L. K. Shrestha, R. G. Shrestha, S. C. Sharma and K. Aramaki, *J. Colloid Interface Sci.*, **328**, 172 (2008).
7. R. G. Shrestha, L. K. Shrestha, C. Solans, C. Gonzalez and K. Aramaki, *Colloids Surf. A*, **353**, 157 (2010).
8. M. Mellema and J. Benjamins, *Colloids Surf. A*, **237**, 113 (2004).
9. M. Van den Temple, J. Lucassen and E. H. Lucassen-Reynders, *J. Phys. Chem.*, **69**, 1798 (1965).
10. *Applied Colloid and Surface Chemistry*, R. M. Pashley and M. E. Karaman, Wiley, Canberra, 2004.
11. W. C. Griffin, *J. Soc. Cosmetic Chem.*, **5**, 249 (1954).
12. L. K. Shrestha, M. Kaneko, T. Sato, D. P. Acharya, T. Iwanaga and H. Kunieda, *Langmuir*, **22**, 1449 (2006).
13. B. P. Binks and A. Rocher, *Phys. Chem. Chem. Phys.*, **12**, 9169 (2010).
14. B. P. Binks, A. Rocher and M. Kirkland, *Soft Matter*, **7**, 1800 (2011).
15. B. P. Binks, C. A. Davies, P. D. I. Fletcher and E. L. Sharp, *Colloids Surf. A*, **360**, 198 (2010).
16. S. E. Friberg, C. S. Wohn, B. Greene and R. Vangilder, *J. Colloid Interface Sci.*, **101**, 593 (1984).
17. S. Ross and G. Nishioka, *Colloid Polym. Sci.*, **255**, 560 (1977).
18. I. C. Callaghan and E. L. Neustadter, *Chem. Ind.*, 53 (1981).
19. A. Waseda and H. Iwano, *Geofluids*, **8**, 286 (2008).
20. R. H. Ottewill, D. L. Segal and R. C. Watkins, *Chem. Ind.*, 57 (1981).
21. V. Bergeron, J. E. Hanssen and F. N. Shoghl, *Colloids Surf. A*, **123**, 609 (1997).

22. Fatty Acid and Lipid Chemistry, F. Gunstone, Chapman & Hall, Bodmin, 1996.
23. R. Murakami and A. Bismarck, *Adv. Funct. Mater.*, **20**, 732 (2010).
24. T. A. L. Do, J. R. Mitchell, B. Wolf and J. Vieira, *React. Funct. Polym.*, **70**, 856 (2010).
25. Ethylcellulose,  
[http://www.dow.com/dowwolff/en/industrial\\_solutions/polymers/ethylcellulose/](http://www.dow.com/dowwolff/en/industrial_solutions/polymers/ethylcellulose/),  
Accessed 13th July, 2012.
26. S. Su-Jia, C. Dong, X. Shi-Chao, *J. Food Process Eng.*, **36**, 544 (2013).
27. C. Himawan, V. M. Starov and A. G. F. Stapley, *Adv. Colloid Interface Sci.*, **122**, 3 (2006).
28. Fat Crystal Networks, A. G. Marangoni, Marcel Dekker, New York, 2005.
29. Crystallization Processes in Fats and Lipid Systems, ed. N. Garti and K. Sato, Marcel Dekker Inc., New York, 2001.
30. K. Higaki, Y. Sasakura, T. Koyano, I. Hachiya and K. Sato, *J. Am. Oil Chem. Soc.*, **80**, 263 (2003).
31. K. Sato, *Eur. J. Lipid Sci. Technol.*, **12**, 467 (1999).
32. M. Perneti, K. F. van Malssen, E. Floter and A. Bot, *Curr. Opin. Colloid Interface Sci.*, **12**, 221 (2007).
33. H. M. Schaink, K. F. van Malssen, S. Morgado-Alves, D. Kalnin and E. van der Linden, *Food Res. Int.*, **40**, 1185 (2007).
34. P. Fryer and K. Pinschower, *MRS Bulletin*, **25**, 25 (2000).
35. M. Dubois, A. Tarres, T. Goldmann, G. Loeffelmann, A. Donaubauer and W. Seefelder, *J. Agric. Food Chem.*, **59**, 12291 (2011).
36. M. Tynek, R. Pawlowicz, J. Gromadzka, R. Tylingo, W. Wardencki and G. Karlovits, *Eur. J. Lipid Sci. Technol.*, **114**, 357 (2012).
37. R. S. Verma, L.U. Rahman, C. S. Chanotiya, R. K. Verma, A. Chauhan, A. Yadav, A. Singh and A. K. Yadav, *J. Serb. Chem. Soc.*, **75**, 343 (2010).
38. T. Shamspur, M. Mohamadi and A. Mostafavi, *Ind. Crop. Prod.*, **37**, 451 (2012).
39. V. D. Zheljzakov, C. L. Cantrell, T. Astatkie and J. B. Cannon, *Agron. J.*, **103**, 805 (2011).
40. Castor, J.M. Fernandez-Martinez and L. Velasco, Springer, New York, 2012.
41. H. Fayyaz ul and M. Ahmed, *Pak. J. Bot.*, **44**, 627 (2012).
42. Edible Oil Processing, W. De Greyt and M. Kellens, Sheffield Academic Press, Sheffield, 2000.

43. N.K.O. Ojijo, E. Kesselman, V. Shuster, S. Eichler, S. Eger, I. Neeman and E. Shimoni, *Food Res. Int.*, **37**, 385 (2004).
44. A. H. Saberi, T. Chin-Ping and L. Oi-Ming, *J. Am. Oil Chem. Soc.*, **88**, 1857 (2011).
45. F. O. Ayorinde, Q. L. Keith and L.W. Wan, *Rapid Commun. Mass Spectrom.*, **13**, 1762 (1999).
46. F. G. Gandolfo, A. Bot and E. Floter, *J. Am. Oil Chem. Soc.*, **81**, 1 (2004).
47. J. Daniel and R. Rajasekharan, *J. Am. Oil Chem. Soc.*, **80**, 417 (2003).
48. A. J. Wright and A. G. Marangoni, *J. Am. Oil Chem. Soc.*, **84**, 3 (2007).
49. M. A. Rogers, A. J. Wright and A. G. Marangoni, *Food Res. Int.*, **41**, 1026 (2008).
50. F. R. Lupi, D. Gabriele, D. Facciolo, N. Baldino, Seta, L. and B. de Cindio, *Food Res. Int.*, **46**, 177 (2012).
51. S. Da Pieve, S. Calligaris, A. Panozzo, G. Arrighetti and M. C. Nicoli, *Food Res. Int.*, **44**, 2978 (2011).

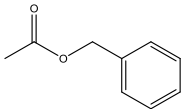
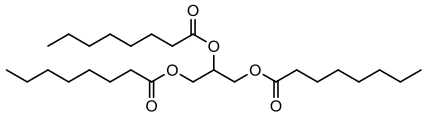
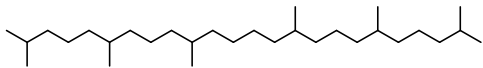
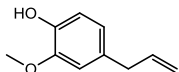
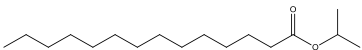
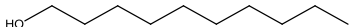
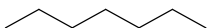
## 2 EXPERIMENTAL

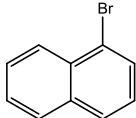
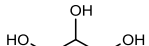
This chapter describes the numerous materials and experimental methods used throughout.

### 2.1 Materials

#### 2.1.1 Oils

**Table 2.1.** Name, source, purity and batch of the oils used.

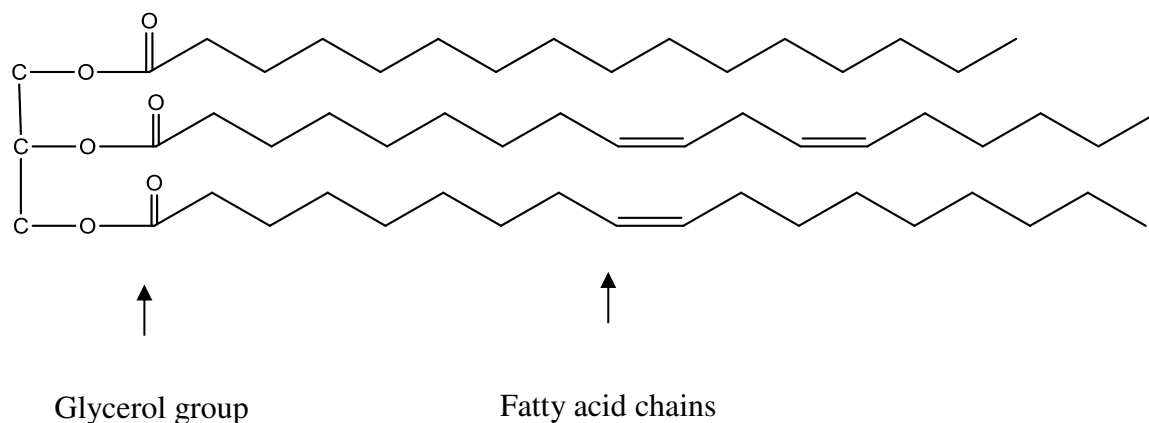
| Name   | Source                      | Purity  | Batch     |
|--|-----------------------------|---------|-----------|
| Benzyl acetate<br>        | Acros<br>Organics           | 99+ %   | A0229321  |
| Tricaprylin<br>          | Sigma<br>Aldrich            | ≥ 99 %  | BCBB4760  |
| Squalane<br>            | Acros<br>Organics           | 99 %    | A0286479  |
| Eugenol<br>             | Sigma<br>Aldrich            | 99 %    | MKBC6619V |
| Isopropyl myristate<br> | SAFC<br>supply<br>solutions | ≥98 %   | MKBC8765  |
| Decanol<br>             | Sigma<br>Aldrich            | ≥99 %   | 08810AH   |
| Hexadecane<br>          | Sigma<br>Aldrich            | ≥99 %   | STBB4053  |
| Cyclohexane<br>         | Sigma<br>Aldrich            | ≥99.9 % | MKBD0455  |
| Heptane<br>             | Sigma<br>Aldrich            | ≥99 %   | SZBA237M  |

|   |                      |                     |           |
|---|----------------------|---------------------|-----------|
| 1-dodecanol<br>        | Sigma<br>Aldrich     | 98 %                | 68953-105 |
| Toluene<br>            | Fisher<br>Scientific | 99.99 %             | 1070871   |
| Dodecane<br>           | Avocado              | 99+ %               | E3289A    |
| Ethylene glycol<br>    | Sigma<br>Aldrich     | ≥ 99 %              | BCBG1446V |
| α-Bromonaphthalene<br> | Sigma<br>Aldrich     | 97 %                | BCBC0497  |
| Diiodomethane<br>      | Sigma<br>Aldrich     | 99 %                | STBC6720V |
| Glycerol<br>         | Sigma<br>Aldrich     | 99 %                | BCBF4651V |
| Formamide<br>        | Sigma<br>Aldrich     | ≥ 99 %              | 69796TMV  |
| High oleic sunflower oil (HOSO)<br>Main chain length 83.5 % oleic <sup>1</sup>                          | EULIP                | Commercial<br>grade | 002/12    |
| Rapeseed oil from Brassica rapa<br>Main chain lengths 60 % oleic, 21.5 % linoleic <sup>2</sup>          | Acros<br>Organics    | Commercial<br>grade | BCBJ4393V |
| Coconut oil, pure, refined<br>Main chain lengths 48 % lauric, 18.5 % myristic <sup>2</sup>              | Acros<br>Organics    | Commercial<br>grade | A0338345  |
| Sesame oil<br>Main chain lengths 40 % oleic, 45 % linoleic <sup>2</sup>                                 | Acros<br>Organics    | Commercial<br>grade | A0338971  |
| Soybean oil<br>Main chain lengths 52 % linoleic, 24 % oleic <sup>2</sup>                                | Acros<br>Organics    | Commercial<br>grade | MKBN8800V |
| Cottonseed oil, pure  | Acros                | Commercial          | A0338268  |

|   |                   |                     |            |
|---|-------------------|---------------------|------------|
| Main chain lengths 53 % linoleic, 24 % palmitic, 17 % oleic <sup>3</sup>        | Organics          | grade               |            |
| Corn oil<br>Main chain lengths 56 % linoleic, 28 % oleic <sup>3</sup>           | Acros<br>Organics | Commercial<br>grade | A0341121   |
| Castor oil<br>Main chain length 72 % ricinoleic <sup>4</sup>                    | Acros<br>Organics | Commercial<br>grade | A0335275   |
| Olive oil, pure, refined<br>Main chain length 72.5 % oleic <sup>2</sup>         | Acros<br>Organics | Commercial<br>grade | A0335272   |
| Refined peanut oil<br>Main chain lengths 48 % oleic, 30 % linoleic <sup>2</sup> | EULIP             | Commercial<br>grade | 50784      |
| Peanut oil SN610642   | IFF               | Commercial          | 0004578643 |
| Hazelnut oil  | AAK               | Commercial          | 247889     |
| Deliair NH 50 (vegetable fat)   | AAK               | Commercial<br>grade | 47265000   |
| Fractionated palm kernel oil  | Cargill           | Commercial<br>grade | RMC009973  |
| Vegetable fat   | EULIP             | Commercial          | 248710     |
| Milk chocolate SMP cheaper  | Nestlé            | Commercial          | 245466     |

High oleic sunflower oil is an oil used throughout the work. It is a vegetable oil comprising of a mixture of triglycerides whose fatty acid chains constitute 83.5% oleic, 9.6% linoleic, 3.7% palmitic, 3.1% stearic and 0.1% linolenic.<sup>1</sup> A typical triglyceride structure with the main constituents of high oleic sunflower oil is shown in Figure 2.1.

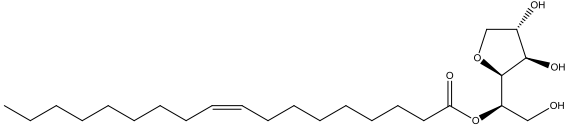
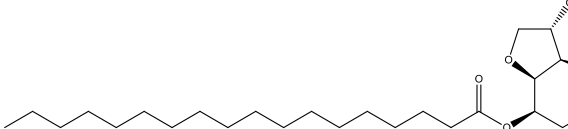
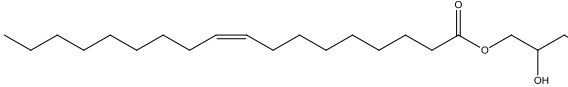
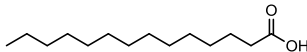
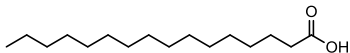
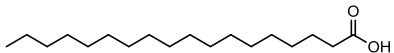
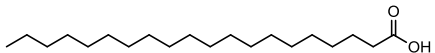
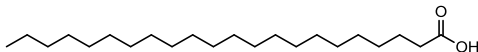
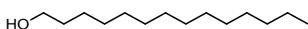
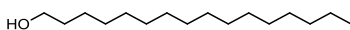
**Figure 2.1.** Structure of a triglyceride. The first chain (top to bottom) is palmitic (C<sub>16</sub>), the second chain is linoleic (C<sub>18</sub>) and the third is oleic (C<sub>18:1</sub>).



### 2.1.2 Surfactants

**Table 2.2** Name, source, purity and batch of the surfactants used.

| Name              | Source                              | Purity              | Batch  |
|-------------------|-------------------------------------|---------------------|--------|
| Epikuron 130 P IP | Cargill<br>texturizing<br>solutions | Commercial<br>grade | 193023 |
| Epikuron 145 V    | Cargill<br>texturizing<br>solutions | Commercial<br>grade | 199026 |
| Epikuron 170      | Cargill<br>texturizing<br>solutions | Commercial<br>grade | 199042 |
| Epikuron 200      | Cargill<br>texturizing<br>solutions | Commercial<br>grade | 199060 |
| Zonyl FSN 100     | Du Pont<br>de<br>Nemours<br>& co.   | Commercial<br>grade | CB20A  |

|  |                   |                  |                                |
|--|-------------------|------------------|--------------------------------|
| Crill 4 (Sorbitan Oleate)<br>                 | Croda             | Commercial grade | 331380<br>SD<br>01400/S<br>AMP |
| Crill 3 (Sorbitan Stearate)<br>               | Croda             | Commercial grade | 18022<br>SD<br>80054/S<br>AMP  |
| MONOMULS 90-O 18 PH (Glycerol Monooleate)<br> | Cognis            | Commercial grade | GR8155<br>4301                 |
| Grindsted Citrem LR 10 Extra Kosher  | Danisco           | Commercial grade | 4011539<br>885                 |
| Grindsted Citrem N12 veg   | Danisco           | Commercial grade | 4011480<br>119                 |
| Myristic acid<br>                           | Acros Organics    | 99 %             | A033770<br>2                   |
| Palmitic acid<br>                           | Acros Organics    | 98 %             | A029892<br>0                   |
| Stearic acid<br>                            | Fisher Scientific | 97+ %            | 1153859                        |
| Arachidic acid<br>                          | Sigma Aldrich     | ≥99 %            | 041M11<br>53V                  |
| Behenic acid<br>                            | Sigma Aldrich     | 99 %             | MKBH5<br>517V                  |
| 1-tetradecanol<br>                          | Acros Organics    | 99+ %            | A030922<br>0                   |
| 1-hexadecanol<br>                           | Sigma Aldrich     | 99 %             | BCBD82<br>20V                  |

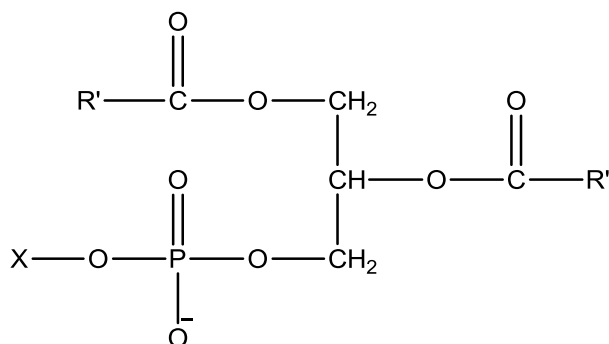
|  |                          |                     |                |
|--|--------------------------|---------------------|----------------|
| 1-octadecanol<br> | Sigma<br>Aldrich         | 99 %                | 1398531<br>V   |
| 1-eicosanol<br>   | Acros<br>Organics        | 98 %                | A030463<br>1   |
| 1-docosanol<br>   | Acros<br>Organics        | 98 %                | A030531<br>1   |
| Dimodan HR Kosher  | Danisco                  | Commercial          | 4011836<br>037 |
| Fully hydrogenated rapeseed oil rich in behenic acid   | Adeka<br>corporatio<br>n | Commercial<br>grade | N/A            |
| Cetostearyl alcohol (mixture of C <sub>16</sub> and C <sub>18</sub> chain lengths)                 | Cognis                   | > 96 %              | 242967         |

The Epikuron phospholipids are the focus of Chapter 3. Their composition, as stated by the manufacturer, is given in Table 2.3. The structure of the constituents of the Epikuron phospholipids is given in Figure 2.2.

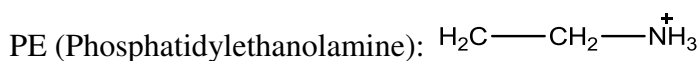
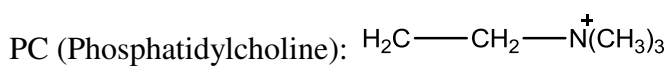
**Table 2.3.** Composition of the Epikuron surfactants studied. Phosphatidylcholine (PC), Phosphatidylethanolamine (PE), Phosphatidylinositol (PI) and Phosphatidic acid (PA).

| Epikuron | PC (%)    | PE (%)    | Lysophosphatidylcholine (%) | PI (%) | PA (%) |
|----------|-----------|-----------|-----------------------------|--------|--------|
| 130 P IP | 31.6      | 20.0      | 1.6                         | 13.6   | 4.4    |
| 145V     | 50.2-50.3 | 13.3-12.7 | 2.7-2.4                     | <1.0   | <1.0   |
| 170      | 78.0      | 6.3       | 1.0                         | <1.0   | -      |
| 200      | 93.4      | 0         | 1.3                         | -      | -      |

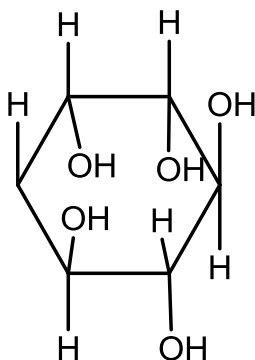
**Figure 2.2.** Molecular structure of the main phospholipids present in the Epikuron surfactants.<sup>5</sup>



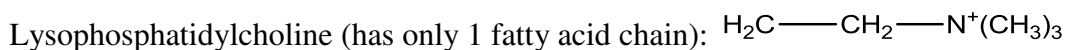
X is:



PI (Phosphatidylinositol):

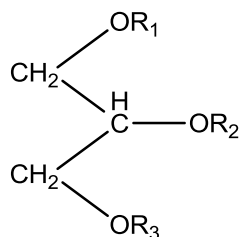


PA (Phosphatidic acid): H



Grindsted Citrem LR 10 Extra Kosher, which is studied in detail in Chapter 4, has the structure shown in Figure 2.3. The surfactant is a citric acid ester of a mono/diglyceride from sunflower oil where at least one of  $\text{R}_1$ ,  $\text{R}_2$  or  $\text{R}_3$  = citric acid, one = fatty acid moiety and the remainder = citric acid, fatty acid or hydrogen. The main fatty acid group is oleic acid ( $\text{C}_{18:1}$ ).

**Figure 2.3.** Structure of Grindsted Citrem LR 10 Extra Kosher.



Grindsted Citrem N12 veg is a mono/diglyceride made from fully hydrogenated palm-based oil with typical main chain lengths of 1 % myristic, 36-63 % palmitic, 35-58 % stearic and <1 % arachidic.

Dimodan HR Kosher is a monoglyceride with typically 93 % stearic chains.

### 2.1.3 Particles

Fumed silica particles are initially hydrophilic with SiOH groups present at the particle surface. The spherical fumed silica nanoparticles have a diameter of 20-30 nm<sup>6</sup>, however they aggregate during the manufacturing process to 200 nm sized clusters<sup>7</sup>. The hydrophilicity of the particles is determined by the percentage of SiOH present. The latter can be changed using dichlorodimethylsilane (DCDMS) with the modification by CH<sub>3</sub> groups. Fumed silica particles which are fully coated with DCDMS and partially coated with fluoro groups have also been used. The PTFE particles are larger (0.3-10 μm) than the nanoparticles, have a rough surface and are irregular in shape. Table 2.4 indicates the particles used and their source. The particles mentioned are used in Chapter 3.

**Table 2.4.** Name, source and batch of the particles used.

| Name  | Source          | Batch                     |
|---|-----------------|---------------------------|
| 100 % SiOH fumed silica   | Wacker-Chemie   | Wacker HDKN20             |
| 51 % SiOH fumed silica  | Wacker-Chemie   | SLM 4330002/68_10         |
| 14 % SiOH fumed silica  | Wacker-Chemie   | SLM<br>4433002/MM004_1c_f |
| Fully coated fluorosilica particles   | Wacker-Chemie   | SLM 433002-MM049/1        |
| Partially coated fluorosilica particles   | Wacker Chemie   | SLM 433002-MM049/2        |
| Polytetrafluoroethylene (PTFE) particles; Ultraflon MP-8T (2.5 $\mu\text{m}$ ) <sup>8</sup> | Laurel products | PA19520                   |
| Polytetrafluoroethylene (PTFE) particles; Zonyl MP1400 (10 $\mu\text{m}$ ) <sup>8</sup>     | DuPont          | N/A                       |

#### 2.1.4 Additional edible ingredients

Various edible ingredients have been used in the creation of concept samples which are given in Table 2.5.

**Table 2.5.** Name, source and batch of the additional edible ingredients used.

| Name                                    | Source                 | Batch     |
|---|------------------------|-----------|
| Natural cocoa powder 10-12 % fat        | Nestlé                 | 119978    |
| White sugar 0.01-0.015 mm particle size | Nestlé                 | 70784     |
| Caramelised milk powder caramilk 80654  | Dr. Suwelack           | 234217    |
| Peanut flour dark roast 28 % fat        | Golden peanut company  | 212795    |
| Finest Belgium white callets            | Callebaut Belgium 1911 | 123140601 |
| Finest Belgium milk chocolate callets   | Callebaut Belgium 1911 | 123370502 |
| Plain wafer                             | Nestlé                 | 24242     |

#### 2.1.5 Gases

Various gases have also been used and are stated in Table 2.6.

**Table 2.6.** Name, source and purity of the gases used.

| Name             | Source            | Purity   |
|------------------|-------------------|----------|
| Compressed air * | University supply | N/A      |
| CO <sub>2</sub>  | Energas           | < 99.9 % |
| N <sub>2</sub> O | Energas           | < 99 %   |

\*The main constituents of unpolluted air are 78 % nitrogen, 21 % oxygen and 1 % argon.<sup>9</sup>

## 2.2 Methods

### 2.2.1 Visual solubility determination of additive in oil

The initial visual solubility determination measurements (conducted with Epikuron and Grindsted Citrem in HOSO) were performed with this method. A specimen tube (internal diameter 53 mm, internal length 74 mm) containing the oil and the required amount of phospholipid/diglyceride (total mass 10 g) and 10 mm magnetic flea was placed into a water jacket (with an internal diameter of 85 mm and an internal length of 90 mm) containing water (connected to an R1 Grant water bath). The oil temperature was measured approximately 20 mm from the top of the air-oil surface into the solution with a thermometer (with increments of 0.1 °C) which was held in place by a clamp stand. The water jacket was placed on top of a Corning PC-420D magnetic stirrer operating at 500 rpm.

The temperature of the mixture was initially 20 °C and was increased 1 °C/min. When the solution changed from cloudy/ visual particles to a transparent solution the temperature was noted as the temperature at which the solute became soluble in the HOSO (one phase). The temperature was then increased 5 °C and subsequently decreased 1 °C/min. If the phospholipid became insoluble or there was any change in the mixture visually then this was noted along with the temperature this occurred at.

The above visual solubility method was then modified when investigating the myristic acid in HOSO system. The theoretical temperature of the dissolution of myristic acid in HOSO, assuming ideal mixing, was calculated with the equation shown below:<sup>10</sup>

$$\ln x_B = \frac{\Delta_{fus}H}{R} \left( \frac{1}{T_f} - \frac{1}{T} \right) \quad (2.1)$$

where  $x_B$  is the mole fraction of myristic acid, R is the gas constant, T is temperature,  $\Delta_{fus}H$  is the enthalpy of fusion (45 KJ mol<sup>-1</sup>)<sup>11</sup> and  $T_f$  is the temperature of fusion (326.6 K).<sup>11</sup>

The amount of myristic acid required to in theory precipitate/dissolve in HOSO at specific temperatures, T, was calculated. That calculated amount was then added to HOSO to make a sample with a total mass of 1 g. The sample (in a 37 mm x 10 mm vial) was placed into the well of a Grant thermostat as a clear homogeneous liquid (at 10 °C higher than the calculated precipitation temperature). A thermocouple (Omega engineering HH806WE) was used to monitor the temperature of a separate sample of 1g

of HOSO in a 37 mm x 10 mm vial in the same water bath. The mixture was then cooled, at a rate of 0.2 °C/ min., then held for 5 minutes at a temperature 5 °C below the temperature of gelation (the temperature the mixture became a gel), and then heated at 2 °C/min. The precipitation and dissolution temperatures were determined through visual observations. The precipitation temperature was defined as the temperature at which a crystal was observed in the HOSO. The dissolution temperature was defined as the temperature at which the mixture was visually less turbid and no longer a gel (flowed when inverted in the sample tube).

### 2.2.2 Differential scanning calorimetry

Through the use of a Perkin Elmer Differential Scanning Calorimeter 7 (DSC) various fats, fatty acids, alcohols and diglycerides, both neat and in HOSO, were studied. The samples were cooled from 90-80 °C (depends on the system) to as low as -20 °C and then heated back up to 90-80 °C with also the reverse investigated for some systems (heating followed by cooling). Heating and cooling rates of both 2 °C/min. and 20 °C/min. were investigated. The samples were placed into an unsealed aluminium sample pan with an unsealed aluminium sample pan as a reference. Indium was used to calibrate the instrument.

### 2.2.3 X-ray diffraction

An X-ray diffractometer was used to identify the crystal structure of myristic acid in a 10 wt.% myristic acid in HOSO gel. It was a PANalytical Empyrean instrument with Highscore Plus processing software. The radiation was CuK $\alpha$  radiation ( $\lambda = 1.54 \text{ \AA}$ ) and the  $2\theta$  angles investigated were 2 ° to 50 ° with a step size of 0.02 °. An additional X-ray diffractometer was used to identify the crystal structure of a 50  $\mu\text{m}$  aggregate of myristic acid (taken from a gel of 10 wt.% myristic acid in HOSO). This was a STOE X-ray IPDS2 diffractometer with MoK $\alpha$  radiation of 0.71073  $\text{\AA}$  with the  $2\theta$  angles investigated ranging from 2 ° to 50 °. The temperature of the investigated samples was  $20 \pm 2 \text{ }^\circ\text{C}$ . The 10 wt.% myristic acid in HOSO gel which was created for both measurements was heated to 80 °C, then cooled 1 °C/min. to 9.2 °C before measurements at  $20 \pm 2 \text{ }^\circ\text{C}$ .

#### 2.2.4 Optical microscopy

Various samples (including neat oils, neat surfactants, oil and surfactant mixtures, gels and foams) were placed onto a glass microscope slide with a cover slip and observed through an optical microscope (Leica DME). The microscopic analysis was carried out with and without cross polarising lenses. Images were captured with a Leica DFC 290 camera and analysed using a Leica V3 application suite calibrated with a PYSER-SGI limited graticule. The temperature of the slide was controlled with a Linkam PE120 heat stage attached to a Linkam T95-PE processor.

#### 2.2.5 Cryo-Scanning Electron Microscopy (SEM)

Myristic acid in HOSO mixtures (both gelled and aerated) were analysed with Cryo-SEM with Zeiss Smart SEM software. A sample of the foam was added to a perforated aluminium stub and placed into liquid nitrogen slush (-210 °C). The frozen sample was then transferred to a cryo system (Quorum Technologies PP3010T), where it was held at a pressure of  $10^{-6}$  mbar and at -140 °C in a nitrogen gas atmosphere. The sample was sputter coated with platinum. The sample then entered the SEM chamber of an EVO 60 microscope at a temperature of -140 °C and pressure of  $10^{-6}$  mbar at a beam voltage of 15 kV and probe current of between 20 and 35 pA. The images were collected at various locations on a sample.

#### 2.2.6 Surface tension

A Krüss K12 digital tensiometer with a Wilhemly plate was used at 25 °C. To ensure the equipment was working accurately, prior to use, the surface tension of ultrapure Milli Q water was measured ( $72.2 \text{ mN m}^{-1}$  at 25 °C). The meniscus was broken after each measurement (20 measurements with each oil), the plate was then washed firstly with ethanol and then rinsed with Milli Q water, finally the plate was heated until glowing in a blue flame. The glass vessel that contained the oils was initially rinsed with alcoholic KOH and then Milli-Q water, then placed in an oven at 100 °C for roughly 30 minutes whilst wrapped in foil to reduce any potential contamination. The glass vessel was not taken out of the foil until it was required and the investigated sample was placed into it. The Milli Q water is water that is first passed through an

Elgastat Prima reverse osmosis unit and then through a Milli-Q reagent water system (Millipore). The resistivity of the Milli-Q water was around 18 M $\Omega$  cm.

### 2.2.7 Contact angle determination

0.05 mL of a liquid (probe liquid) was added to the surface of a myristic acid solid pellet (thickness 2 mm, diameter 15 mm). The advancing and receding liquid-solid contact angle in air was measured through the liquid phase with the use of a Krüss DSA10 apparatus. Up to 20 measurements were taken with each oil (on average 4 measurements on each pellet). The pellet (shown in Figure 2.4) was produced by grinding the myristic acid into a fine powder with a pestle and mortar, then compressing the powder with the use of a Perkin Elmer hydraulic press with a weight of 12 tons.

**Figure 2.4.** Photograph of a myristic acid pellet used for contact angle measurements. Scale bar 1 cm.



### 2.2.8 Rheology

Rheological measurements of oil gels and oil foams were conducted with a Physica MCR301 Anton Parr rheometer with two different geometries. The first was a parallel plate geometry (oscillatory rheology- with 0.01 % strain and 1 Hz) where approximately 0.5 g of the sample (0.2 g if a foam) was added to the lower plate which had a Peltier system for temperature control (the effect of an increase and decrease in temperature over a range of 10 °C to as high as 90 °C was investigated). The distance between the plates (the sandblasted upper plate was 50 mm in diameter) with a liquid sample was 0.5 mm, with a foam the distance was 1 mm. The second geometry used was with concentric cylinders (flow rheology- at 1 Hz). Approximately 15 g of the mixture was added to the outer cylinder, the internal cylinder had a diameter of 28.9 mm and the

distance between the cylinders was 1 mm. The effect of an increase in shear rate (from  $0.01$ - $1000 \text{ s}^{-1}$ ) followed by a decrease ( $1000$  to  $0.01 \text{ s}^{-1}$ ) was investigated at a constant temperature.

With both geometries the non-aerated oil mixtures were added to the rheometer at  $80 \text{ }^\circ\text{C}$  (myristic acid in oil) or  $90 \text{ }^\circ\text{C}$  (Dimodan HR Kosher in oil). The temperature of the sample was then decreased at a rate of  $1 \text{ }^\circ\text{C}/\text{min.}$  to  $30$ ,  $20$  or  $10 \text{ }^\circ\text{C}$  where the effect of amplitude, frequency, time or shear rate was investigated. With aerated mixtures the sample was added to the rheometer at  $20 \text{ }^\circ\text{C}$ , the amplitude and frequency was then measured. The stability of the foam was also investigated by increasing the temperature of the sample at a rate of  $1 \text{ }^\circ\text{C}/\text{min.}$

#### 2.2.9 Pulsed nuclear magnetic resonance

The solid phase content of the oil-surfactant mixture was investigated with the use of pulsed NMR<sup>12-14</sup> (Maran 25 resonance instrument) with RINMR software. The measurements were conducted by heating to and then holding the sample at  $80 \text{ }^\circ\text{C}$  for 15 minutes, then holding the sample at  $60 \text{ }^\circ\text{C}$  for 30 minutes, then holding the sample at  $0 \text{ }^\circ\text{C}$  for 17 hours (the cooling rate for both decreases in temperature was  $1 \text{ }^\circ\text{C}/\text{min.}$ ). The solid content could then be measured at  $0$ ,  $10$ ,  $20$ ,  $25$ ,  $30$ ,  $32.5$ ,  $35$ ,  $37.5$ ,  $40$ ,  $45$  and  $50 \text{ }^\circ\text{C}$ . The sample (approximately  $2 \text{ g}$  in an NMR tube) was at the specified temperature for 30 minutes before a solid phase content measurement was conducted. The instrument was calibrated with  $0$ ,  $29.1$  and  $70.4 \%$  solid content samples at each temperature prior to solid content measurements of the investigated samples.

#### 2.2.10 Viscosity measurements

The kinematic viscosities of the liquid mixtures were examined with an Ostwald viscometer which was mounted in a thermostatted tank at  $25 \text{ }^\circ\text{C}$ . The viscometer was calibrated with squalane ( $99 \%$  purity) from data produced by Dubey and Sharma.<sup>15</sup> An average of three viscosity measurements were used which agreed within  $0.2 \text{ s}$ .

### 2.2.11 Grinding mill

21 g of myristic acid was added to a 80 mL milling cup and then ground with 30 stainless steel grinding balls (25 with a 10 mm diameter, 5 with a 20 mm diameter) for 1 hr at 100 rpm, then 15 minutes of no milling, followed by 1 hr at 150 rpm in a Retsch GmbH PM100 (Germany) grinding ball mill. This technique was used to grind the myristic acid to a significantly smaller size (to around 30  $\mu\text{m}$  from 2-5 mm).

### 2.2.12 Sonication

This method was necessary to disperse the solid particles in the selected oils. The required oil and particles were placed into a sample tube (cylindrical 75 mm x 25 mm, i.d. 24 mm). An ultrasonic probe attached to a Sonics and Materials vibracell processor was placed into the mixture for 2 minutes at 10 Watts. The mixture was then placed into a 100  $\pm$  1 mL Jaytec glass measuring cylinder with a ground glass joint and a stopper for the hand shaking/sparging gas technique.

### 2.2.13 Sample preparation of surfactant in oil mixtures for aeration via hand shaking or gas sparging

The required amount of surfactant and oil was placed into a Samco soda glass specimen tube (cylindrical 75 mm x 25 mm, i.d. 24 mm) along with a 10 mm magnetic flea. The sample was placed onto a Corning PC-420D hotplate operating at 380 rpm at 40 – 60  $^{\circ}\text{C}$  (temperature depended on the surfactant used). The temperature was measured with a thermometer with 0.1  $^{\circ}\text{C}$  increments. Once the surfactant had dissolved in the oil the mixture was then placed into a 100  $\pm$  1 mL Jaytec glass measuring cylinder with a ground glass joint and a stopper for the hand shaking/gas sparging at the investigated temperature.

### 2.2.14 Aeration techniques

The mixtures were aerated by various methods which include hand shaking, gas sparging, a soda siphon, a foaming column, whipping and a Hobart mixer. The volume of foam produced was not defined by overrun but by the foam volume (in the case of

hand shaking, gas sparging, using a soda siphon and a foaming column) and by the volume fraction of air present (with the whipping technique and Hobart mixer). Foam volume was recorded due to the low stability of these foams-transfer of the samples to a vessel with a fixed volume would cause substantial foam collapse. The volume fraction of the foams was recorded due to the value being easier to interpret than overrun, the definition of which differs within industry. The stability of the foam has been recorded by both the time until complete foam collapse and also by the foam half-life ( $t_{1/2}$ ) which is the time taken for the foam to decrease by half of its initial volume.

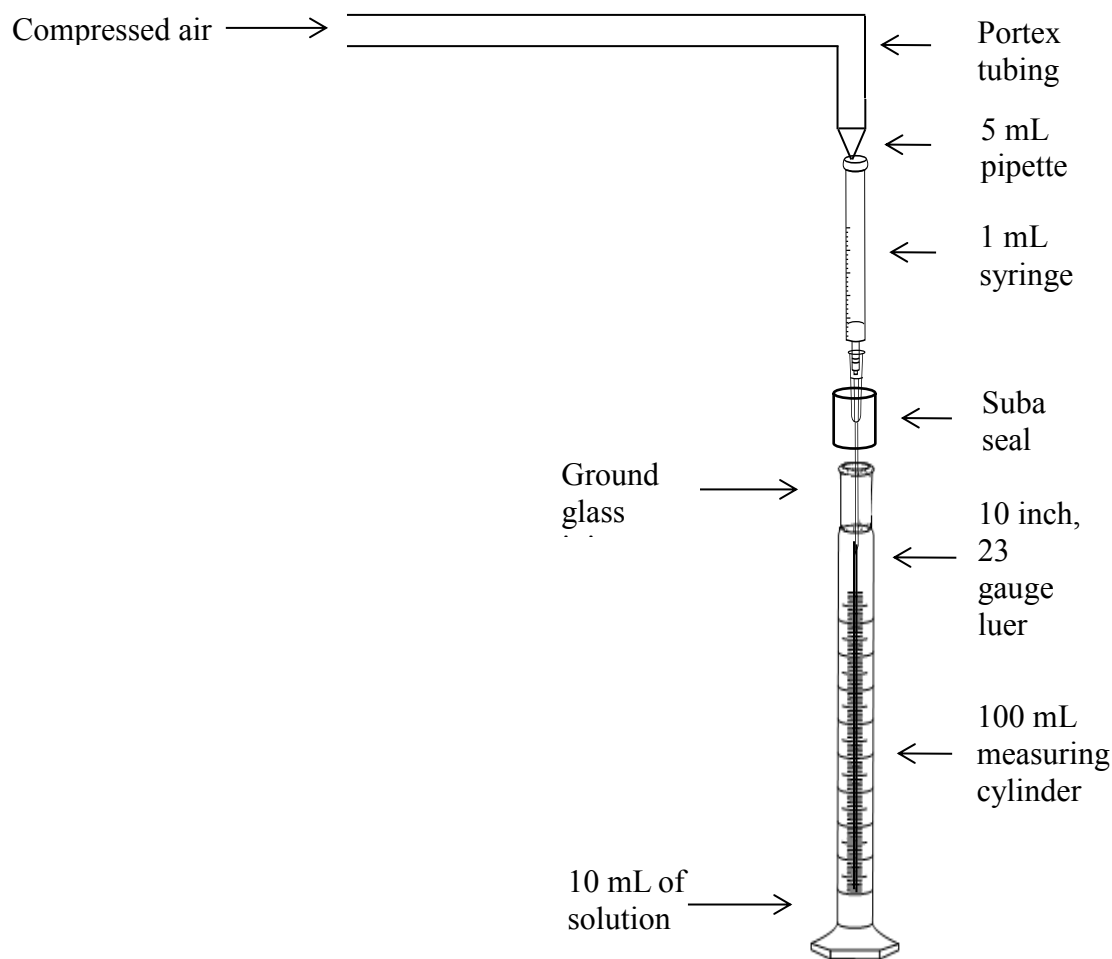
#### 2.2.14.1 Hand shaking

The mixture of particles/surfactants and oil in a  $100 \pm 1$  mL Jaytec glass measuring cylinder with a ground glass joint with a plastic stopper was shaken vigorously for one minute at  $20 \pm 2$  °C. The appearance of the solution was recorded before and after shaking and if foam was formed the height of the foam immediately after shaking was recorded.

#### 2.2.14.2 Gas sparging

A diagram of the aeration method is depicted in Figure 2.5 where roughly 190 cm of Portex tubing (9.0 mm ID, 13.5 mm OD) with a compressed air tap on one end and a 5 mL pipette tip on the other end was used. The 5 mL pipette tip then leads to a 1 mL syringe which has a 10 inch (in length), 23 gauge, luer stainless steel needle (i.d. 0.3 mm o.d. 0.6 mm). The needle is put through a suba seal that fits a  $100 \pm 1$  mL measuring Jaytec glass cylinder with a ground glass joint; this is because the solution is not sealed whilst it is aerated but becomes sealed if any foam is produced. The measuring cylinder containing the solution (10 mL oil with surfactant/particles) is placed into a water jacket, containing water if aerated at temperatures above room temperature ( $20 \pm 2$  °C). The needle is placed 5 mL below the air-oil interface of the solution and the compressed air tap is switched on the same amount (flow rate of 1 L/min.) each time for 1 minute/30 seconds. If a foam was created after the specific aeration time then the suba seal was pushed onto the measuring cylinder and the needle was removed leaving a sealed aerated solution to be monitored.

**Figure 2.5.** Diagram of the gas sparging method.



The experiments were conducted at room temperature ( $20\text{ }^{\circ}\text{C} \pm 2\text{ }^{\circ}\text{C}$ ).

#### 2.2.14.3 Soda siphon

This method was conducted to investigate an additional aeration method which was to dissolve and then release a gas from the mixture. 30 mL of the Grindsted Citrem LR 10 Extra Kosher in HOSO at the required temperature (stirred for 1 hour in a 250 mL flask in a water jacket at  $80\text{ }^{\circ}\text{C}$ ) was pipetted into a soda siphon (MOSA 0.25 L) residing in the well of the thermostat (also at the required temperature). The soda siphon (Figure 2.6) was then removed from the thermostat and one  $\text{CO}_2/\text{N}_2\text{O}$  cartridge was then inserted and dispensed gas through an insertion hole which had a diameter of 0.1 mm into the sample in the soda siphon. The siphon was then vigorously shaken by hand for

1 minute. Excess gas was gently released from the siphon whilst it was held upright through the dispensing nozzle to create minimum disturbance to the aerated sample. Once the gas was released through the dispensing nozzle, the lid of the siphon was carefully unscrewed and the aerated sample was transferred to a graduated 250 mL glass measuring cylinder (with a glass ground joint) using a spatula, then immediately sealed with a plastic stopper. The measuring cylinder was in a water jacket connected to a R1 Grant thermostat at the required temperature. The foamability and foam stability of the system was measured and recorded.

**Figure 2.6.** Photograph of the soda siphon.

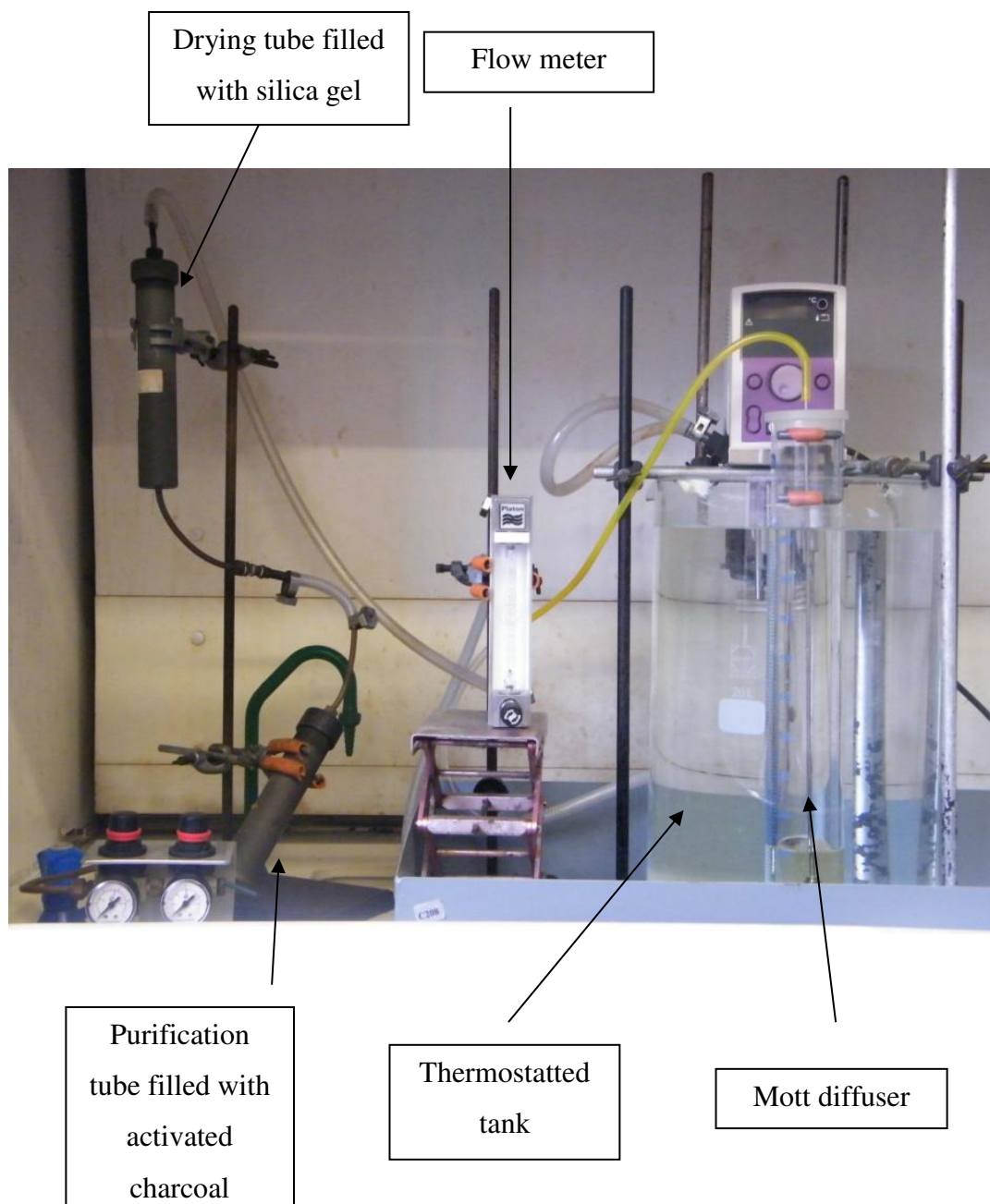


#### 2.2.14.4 Foaming column

As can be seen from Figure 2.7 gas was passed through a purification column filled with activated charcoal (VWR Ltd.), a drying tube filled with silica gel (Fisher Scientific) and then a flow meter either at a flow rate of  $94 \text{ cm}^3 \text{ min}^{-1}$  (Platon) or at a flow rate of  $2 \text{ L min}^{-1}$  (Whatman). The gas then entered a Mott diffuser (Stanhope Seta) with a mean pore diameter of  $22 \text{ }\mu\text{m}$  and permeability of  $5100 \text{ mL air min}^{-1}$  at a pressure drop of  $2.45 \text{ kPa}$ . The Mott diffuser was placed at the bottom of  $200 \text{ cm}^3$  of the sample liquid (liquid depth  $7 \text{ cm}$ , distance from top of the diffuser to liquid surface  $4.5 \text{ cm}$ ) which was in a  $1 \text{ L}$  graduated measuring cylinder held within a thermostatted tank. The sample liquid was equilibrated for 30 minutes at the experimental temperature

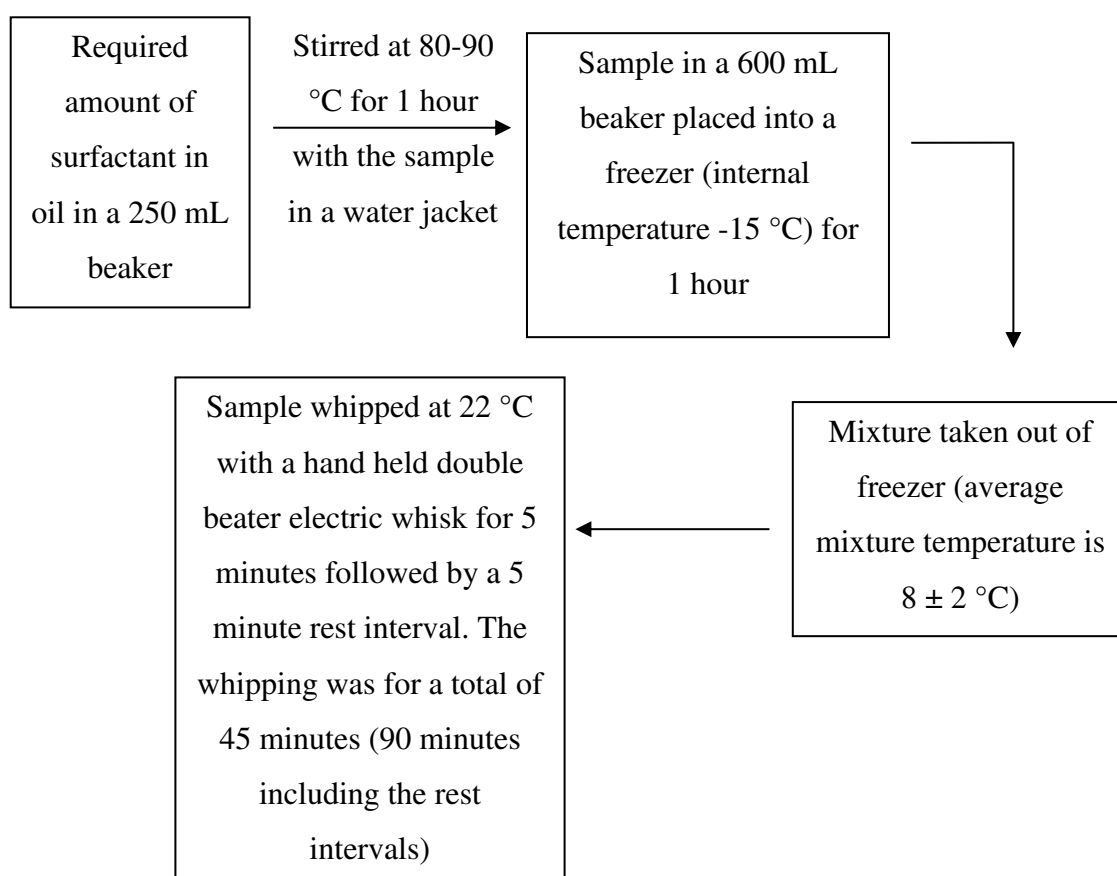
before aeration by the Mott diffuser for 5 minutes. Once 5 minutes of aeration ceased the foam was then in a sealed system, the amount of liquid and foam present was continuously recorded as a function of time.

**Figure 2.7.** Photograph of the thermostatted foaming column.



### 2.2.14.5 Whipping technique

The whipping technique was conducted to investigate the effect of a different aeration method on the ability to create a foam and any subsequent foam stability. The technique involves, as seen in the flow scheme below, mixing the surfactant and oil mixture at a high temperature to create a clear, homogeneous mixture. The mixture was then cooled to  $8 \pm 2$  °C at approximately 1 °C/min. followed by whipping with a hand held double beater electric whisk for 45 minutes.



The sample (total weight 200 g) was measured with an ADAM balance. The sample, once heated in a water jacket connected to a Grant GR150 thermostat and a Grant R1 water circulator, was transferred from a 250 mL beaker to a 600 mL beaker, and then placed into a Bio cold laboratory freezer. The sample was then whisked at 22 °C with an Argos value range hand held double beater electric whisk (blade size 6 cm) on speed setting 1. The foam mass was measured in a 67 cm<sup>3</sup> beaker at regular intervals (after each 5 minutes of whipping).

After each 5 minute interval of whipping, a sample (~ 1 mL) was placed onto a microscope slide with 1 mL of oil along with a cover slip and analysed with a

microscope (Leica DME). The microscopic analysis was with and without crossed polarising lenses. A Linkam PE120 heat stage with a Linkam T95-PE processor was also used. Images were captured with a Leica DFC 290 camera and then analysed using the Leica V3 application suite. If after 45 minutes of whipping a whipped oil was produced, the stability of the whipped product was then investigated by keeping a sample (30 g) at room temperature ( $20 \pm 2$  °C) and also heating a sample (10 g). The stability of the whipped product to an increase in temperature was investigated by placing 10 g of the foam into a 71 mm high by 26 mm wide glass bottle which was in the well of a Grant thermostat with a thermometer inside (submerged into approximately 20 mm of the sample) and heated 1 °C/min. Microscopy of the whipped product was undertaken at 25 °C, then with every 5 °C increase in the sample temperature until foam collapse occurred.

#### 2.2.14.6 Hobart mixer

The required amount of Dimodan HR Kosher was added to the required oil (total mass 400 g) and then heated to  $85 \pm 2$  °C. The mixture was then cooled via a freezer (internal temperature  $-18 \pm 1$  °C) to the required temperature. The mixture (in a 2 L capacity bowl) was then whipped (at  $20 \pm 1$  °C) with a Hobart mixer (see Figure 2.8) on speed setting 2 (130 rpm) for up to 1 hour. The mass of the foam was measured at regular intervals with a 26 cm<sup>3</sup> vessel.

**Figure 2.8.** Photograph of the Hobart mixer used.



#### 2.2.15 Concept samples

Concept samples have been created which involve the aeration of various edible ingredients to make a variety of products. The various methods for the creation of the products are to be described in detail.

##### 2.2.15.1 Indulgent chocolate filling

Two chocolate shell fillings were made, the first with HOSO, Dimodan HR Kosher and chocolate, the second with hazelnut oil, Dimodan HR Kosher and chocolate. The whipped fillings were then added to chocolate shells followed by the addition of a final layer of chocolate to encase the filling. There was in total approximately  $3.6 \pm 0.1$  g of the whipped oil in the chocolate shell. The chocolate (shell and back) was approximately 6 g.

To make the filling with HOSO, 440 g of 10 wt.% Dimodan HR Kosher in HOSO was heated to 85 °C, then cooled approximately 1 °C/min. to 10 °C. 880 g of chocolate (at 25 °C) was then added. The mixture was then heated, whilst stirring by hand, to 35 °C to create a homogeneous liquid, then cooled to 19.6 °C at approximately 1 °C/min. The mixture was then whipped with a Hobart mixer on speed setting 2 at 20 ± 1 °C for 20 minutes.

To make the filling with hazelnut oil, 200 g of 10 wt.% Dimodan HR Kosher in hazelnut oil was heated to 85 °C, then cooled approximately 1 °C/min. to 10 °C. 400 g of chocolate (at 25 °C) was then added. The mixture was then heated, whilst stirring by hand, to 35 °C to create a homogeneous liquid, then cooled to 20.3 °C at approximately 1 °C/min. The mixture was then whipped with a Hobart mixer on speed setting 2 at 20 ± 1 °C for 20 minutes.

#### 2.2.15.2 Extruded filling

The ability to create an aerated filling which could be placed into an extruded chocolate cereal tube (provided by Nestlé) was investigated. The filling was placed into the chocolate cereal tube with the use of a piping bag. The aerated fillings were created with both HOSO and peanut oil. The average weight of the cereal tubes was 1 ± 0.1 g. The average amount of the HOSO based filling added to the cereal tubes was 0.8 ± 0.05 g, with the peanut oil based filling 0.7 ± 0.05 g was added.

To create the aerated extruded filling with HOSO 10 wt.% Dimodan HR Kosher in HOSO (200 g) was heated to 90 °C, then 50 g cocoa powder, 200 g white sugar and 100 g caramelised milk powder was added. Once the additional materials were added to the mixture it was mixed by hand at 60 °C to create homogeneity. The mixture was then cooled to 20.8 °C at approximately 1 °C/min., then whipped with a Hobart mixer on speed setting 2 at 20 ± 1 °C for 60 minutes.

To create the aerated filling with peanut oil 10 wt.% Dimodan HR Kosher in peanut oil (source:IFF) (200 g) was heated to 90 °C, then 25 g cocoa powder, 200 g white sugar, 25 g peanut flour dark roast and 25 g caramelised milk powder was then added to the mixture. Once the additional materials were added to the mixture it was stirred by hand at 60 °C to create homogeneity. The mixture was then cooled to 19.8 °C at

approximately 1 °C/min., and then whipped with a Hobart mixer with speed setting 2 at  $20 \pm 1$  °C for 60 minutes.

#### 2.2.15.3 Biscuit filling

An aerated biscuit filling was also created with 10 wt.% Dimodan HR Kosher in HOSO (200 g) which was heated to 90 °C, then 200 g white sugar and 150 g white chocolate callets was added. The mixture was stirred by hand at 45 °C, then cooled to 18.7 °C at approximately 1 °C/min. The mixture was then whipped with a Hobart mixer with speed setting 2 at  $20 \pm 1$  °C for 20 minutes.

The whipped product ( $2.5 \pm 0.2$  g) was then placed between two oreo biscuits to demonstrate the application of the whipping technique to biscuit fillings.

#### 2.2.15.4 Whipped spread

To create a whipped spread 10 wt.% Dimodan HR Kosher in hazelnut oil (200 g) was heated to 90 °C, then 400 g milk chocolate callets and 200 g white sugar was added. The homogeneous fluid like paste (at 50 °C) was cooled to 21.0 °C at approx. 1 °C/min. The sample was then whipped for 30 minutes with a Hobart mixer with speed setting 2 at  $20 \pm 1$  °C.

#### 2.2.15.5 Wafer filling

The ability to create an aerated wafer filling was also investigated by using the mixture used to create the whipped spread as a wafer filling. The mixture was placed between wafers (4 wafer layers and 3 whipped filling layers) with a ratio of 60 % filling, 40 % wafer. The wafer and filling was then cut into 10 cm x 2 cm pieces.

## 2.3 References

- 1 V. Dossat, D. Combes and A. Marty, *Enzyme and Microbial Technology*, **30**, 90 (2002).
- 2 V. Dubois, S. Breton, M. Linder, J. Fanni and M. Parmentier, *Eur. J. Lipid Sci. Technol.*, **109**, 710 (2007).
- 3 M. Dubois, A. Tarres, T. Goldmann, G. Loeffelmann, A. Donaubaauer and W. Seefelder, *J. Agric. Food Chem.*, **59**, 12291 (2011).
- 4 E.J.L. de Medeiros, R. de Cassia Ramos do Egypto Queiroga, A.G. de Souza, A.M.T. de M. Cordeiro, A.N. de Medeiros, D.L. de Souza and M.S. Madruga, *J. Therm. Anal. Calorim.* **112**, 1515 (2013).
- 5 *Fatty acid and lipid chemistry*, F. Gunstone, Chapman & Hall, Bodmin, 1996
- 6 A. Stocco, E. Rio, B. P. Binks and D. Langevin, *Soft Matter*, **7**, 1260 (2010).
- 7 J. Nordstrom, A. Matic, J. Sun, M. Forsyth and D. R. MacFarlane, *Soft Matter*, **6**, 2293 (2010).
- 8 B. P. Binks, A. Rocher and M. Kirkland, *Soft Matter*, **7**, 1800 (2011).
- 9 *Air composition & chemistry*, P. Brimblecombe, second edition, Cambridge University Press, Cambridge, 1996.
- 10 *Atkins' Physical Chemistry*, P.W. Atkins, ninth edition, Oxford University Press, Oxford, 2010.
- 11 J.A. Wilson and J.S. Chickos, *J. Chem. Eng. Data*, **58**, 322 (2013).
- 12 K.P.A.M. van Putte and J. van den Enden, *J. Phys. E Sci. Instrum.*, **6**, 910 (1973).
- 13 K. van Putte and J. van den Enden, *J. Am. Oil Chem. Soc.*, **51**, 316 (1974)
- 14 M.A.J.S. van Boekel, *J. Am. Oil Chem. Soc.*, **58**, 768 (1981).
- 15 G.P. Dubey and M. Sharma, *J. Chem. Thermodyn.*, **41**, 115 (2009).

### 3 PHOSPHOLIPIDS IN OIL

#### 3.1 Introduction

It is clear from previous work<sup>1-18</sup> that non-aqueous foams can be produced in a variety of systems. The effect of the surface tension of various oils on their foamability and subsequent foam stability upon addition of surfactants with different functional groups and fumed silica particles was investigated. The foamability and foam stability of edible oils is of great importance to the food industry so the ability of a foam to be produced and its subsequent stability with the use of a series of edible phospholipids in high oleic sunflower oil (HOSO) was studied in detail with the use of two aeration methods. The effect of the phosphatidylcholine (PC) and phosphatidylethanolamine (PE) content present in the phospholipids on the foam formation and stability was also investigated.

#### 3.2 Initial foamability investigations

A study into the ability of various oils with surfactants and particles to generate a foam was conducted by both hand shaking and sparging compressed air into a cylinder which contained the surfactant/particle in oil mixture.

##### 3.2.1 Surfactants

Table 3.1 contains data on whether a foam could be produced with ten oils with a surface tension ranging from 36.8 mN m<sup>-1</sup> (benzyl acetate) to 20.2 mN m<sup>-1</sup> (heptane) with various surfactants. The table indicates which surfactant in oil combination could produce a foam: √ represents foam production, x represents no foam production. It was clear that the oils which produced a foam had a surface tension above approx. 33 mN m<sup>-1</sup>. This was found to be the case when 5 wt.% of each surfactant was added to the oils and then hand shaken for one minute and also aerated with the sparging gas technique for 30 sec. 5 wt.% was chosen as it was assumed that if a foam cannot be produced with 5 wt.% then a foam is unlikely to be produced at any other concentration of the surfactant with the oil with these aeration methods. Foam was only produced with the four edible Epikuron phospholipids in benzyl acetate, eugenol and HOSO.

**Table 3.1.** Various oil and surfactant combinations both hand shaken for 1 minute and sparged with compressed air for 30 seconds at  $22 \pm 2$  °C. X represents no foam produced,  $\checkmark$  represents foam produced.

| Oil                 | Surface tension/<br>$\text{mN m}^{-1}$ | Crill 3 & 4 | MONO-MULS 90-18 PH | Epikuron 130 P IP | Epikuron 145 V | Epikuron 170 | Epikuron 200 |
|---------------------|--|-------------|--------------------|-------------------|----------------|--------------|--------------|
| Benzyl acetate      | 36.8                                   | X           | X                  | X                 | $\checkmark$   | $\checkmark$ | $\checkmark$ |
| Eugenol             | 36.5                                   | X           | X                  | $\checkmark$      | X              | X            | X            |
| HOSO                | 33.4                                   | X           | X                  | $\checkmark$      | $\checkmark$   | $\checkmark$ | $\checkmark$ |
| Tricaprylin         | 29.6                                   | X           | X                  | X                 | X              | X            | X            |
| Squalane            | 28.6                                   | X           | X                  | X                 | X              | X            | X            |
| Decanol             | 28.6                                   | X           | X                  | X                 | X              | X            | X            |
| Isopropyl myristate | 28.6                                   | X           | X                  | X                 | X              | X            | $\checkmark$ |
| Hexadecane          | 27.6                                   | X           | X                  | X                 | X              | X            | X            |
| Cyclohexane         | 24.9                                   | X           | X                  | X                 | X              | X            | X            |
| Heptane             | 20.2                                   | X           | X                  | X                 | X              | X            | X            |

### 3.2.2 Particles

The ability of particles with a modified surface to generate a foam in the oils with a surface tension above  $33 \text{ mN m}^{-1}$  was investigated through hand shaking as shown in Table 3.2. The particles used included fumed silica particles. The hydrophilic particles had a surface with 100 % SiOH, the partially hydrophobic particles had a surface with 51 % SiOH and the very hydrophobic particles had a surface with 14 % SiOH. 2 wt.% of the particles were added to benzyl acetate, eugenol and HOSO and then, once dispersed in the oils, were hand shaken for 1 minute. It was found that a foam could not be produced with any of the chosen particles. This is anticipated because it is known

that a foam can be produced when fluorinated particles are added to sunflower oil, eugenol and benzyl acetate.<sup>5,6,10</sup>

**Table 3.2.** Various oils and particles hand shaken for 1 minute at  $22 \pm 2$  °C both with and without sonication. X represents that a foam was not produced.

|                | Fumed silica 14% SiOH | Fumed silica 51% SiOH | Fumed silica 100% SiOH | Zonyl MP1400 PTFE | Ultraflon MP-8T PTFE | Fluoro fumed silica 51% SiOH | Fluoro fumed silica 19% SiOH |
|----------------|-----------------------|-----------------------|------------------------|-------------------|----------------------|------------------------------|------------------------------|
| Benzyl acetate | X                     | X                     | X                      | X                 | X                    | X                            | X                            |
| Eugenol        | X                     | X                     | X                      | X                 | X                    | X                            | X                            |
| HOSO           | X                     | X                     | X                      | X                 | X                    | X                            | X                            |

### 3.3 Characterisation of phospholipids in high oleic sunflower oil

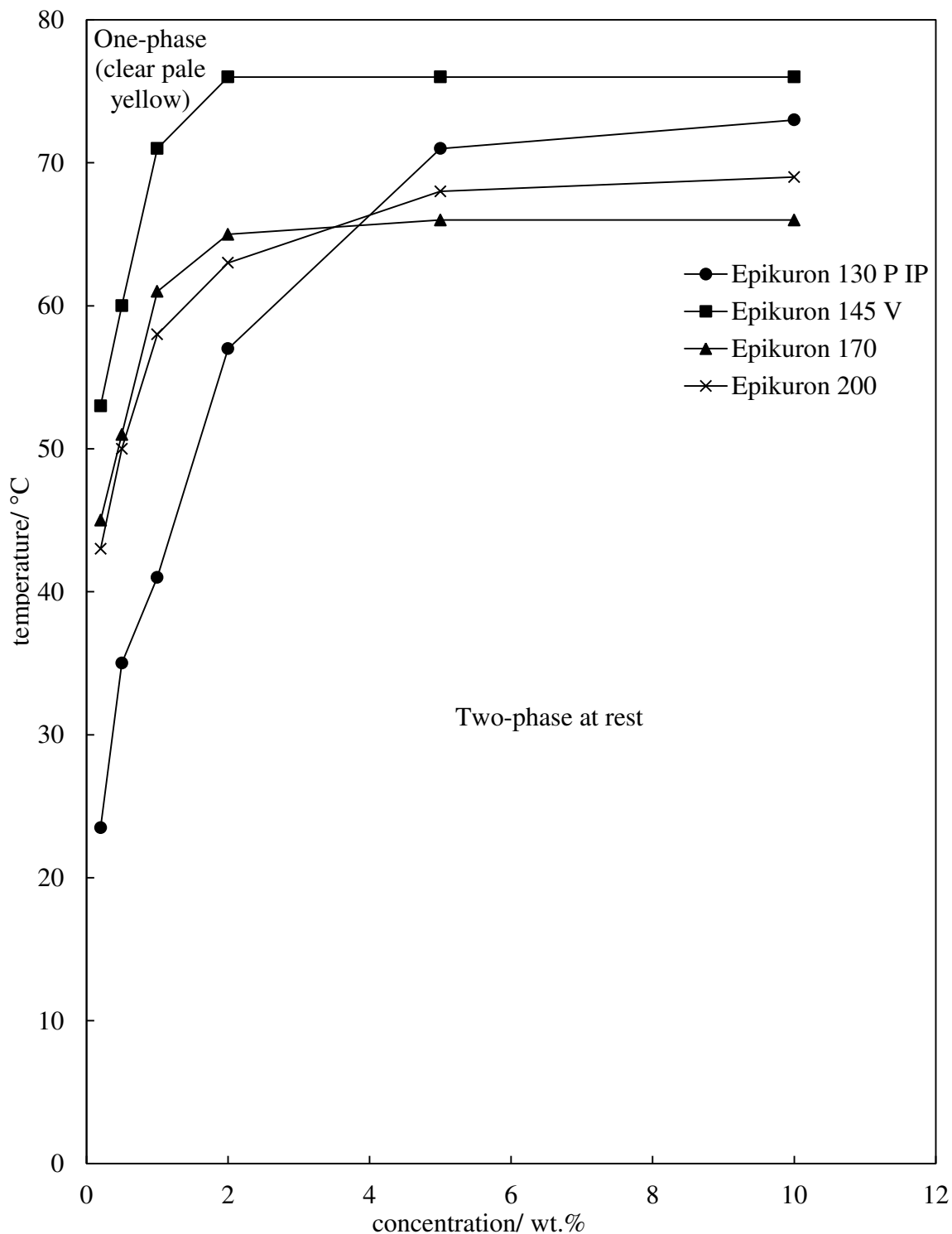
As shown in Table 3.1 it was clear that all four of the edible phospholipids in HOSO created a foam, therefore the aeration of this combination was further studied.

#### 3.3.1 Visual solubility determination

The Epikuron phospholipid foaming agents were then studied in further detail which began by measuring the temperature at which the phospholipid in HOSO became visibly soluble when it was heated from room temperature at a rate of 1 °C/min. This was conducted because it is known that the solubility of a surfactant in the oil has a significant effect on foamability.<sup>7,17-18</sup> The visible solubility measurements of all four studied Epikuron phospholipids in HOSO are shown in Figure 3.1. The figure demonstrates that when heating the mixture from room temperature, above the solubility line the mixture was one-phase (a clear homogeneous liquid) and below the line was a turbid two-phase mixture. It was found that when the mixture was then cooled from 5 °C above the measured solubility temperature at 1 °C/min. it remained a clear homogeneous mixture even when 25 °C was reached. It was only when the mixture had been left at 25 °C for around 10 minutes that the mixture became turbid. This was found to occur with every mixture except for 10 wt.% Epikuron 130 P IP in

HOSO and 10 wt.% Epikuron 145 V in HOSO where a turbid mixture was observed at 41.2 °C and 30.7 °C, respectively. It was clear with all four phospholipids that as temperature increased the solubility in HOSO increased.

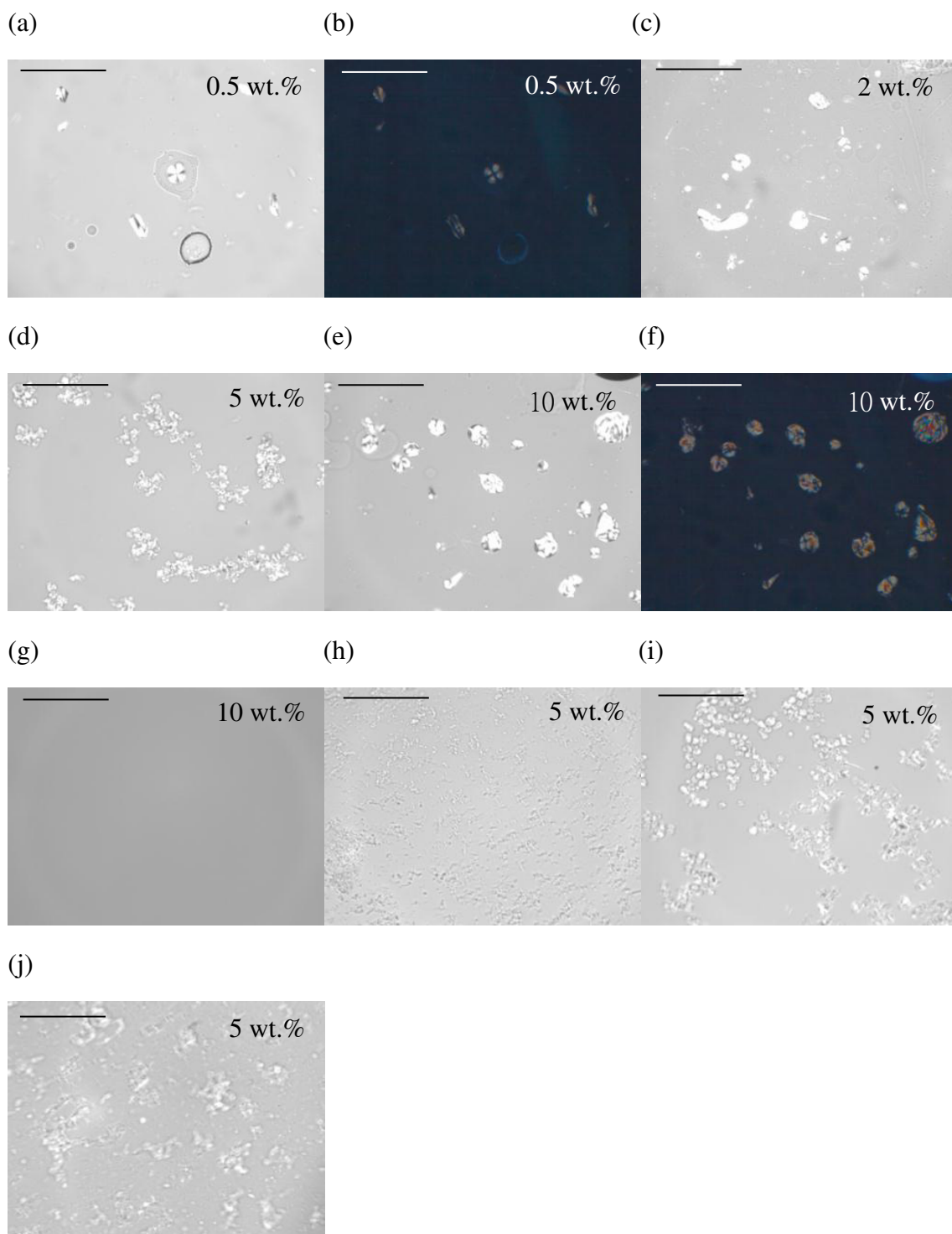
**Figure 3.1.** Visual solubility of four Epikuron phospholipids in HOSO heated at a rate of 1 °C/ min. from room temperature ( $22 \pm 2$  °C). Above the line a clear homogeneous one-phase mixture was observed, below the line was a turbid two-phase mixture.



### 3.3.2 Microscopy

Microscopy was conducted on the two-phase mixtures at 25 °C after heating into the one-phase region. It was found that at 25 °C birefringent crystals of the phospholipid were present in oil as shown in Figure 3.2. However the crystals could not be observed by eye. At 25 °C (after heating to 80 °C) the Epikuron surfactant is present in the oil both as a molecular solution and as a crystal dispersion. The crystals were present with as little as 0.5 wt.% of phospholipid, the concentration of these crystals increased as the Epikuron concentration increased as also shown in Figure 3.2. It is also clear that at 80 °C there was not any surfactant aggregates present.

**Figure 3.2.** Microscopy images at 25 °C after cooling from 80 °C of (a) to (g) Epikuron 145 V in HOSO, (h) Epikuron 130 P IP in HOSO, (i) Epikuron 170 in HOSO and (j) Epikuron 200 in HOSO (concentrations given). (b) and (f) are viewed through crossed polarising lenses. (g) is at 80 °C. Scale bar 200 μm.



## 3.4 Aeration

### 3.4.1 Gas sparging

The foamability and foam stability of all four phospholipids as a function of concentration in HOSO was then investigated at 25 °C (after heating to 80 °C) with the sparging gas technique. Figure 3.3 shows the foamability and foam stability of Epikuron 145 V as a function of concentration in HOSO. The foam collapsed once the bubbles had become large polyhedral ones with a thin foam lamella from initially small relatively spherical bubbles with a thick foam lamella shown in Figure 3.4. Figure 3.3 demonstrates that, over time, the foam collapsed in either gradual stages of approximately 10-40 mL at a time, or, in some cases there was a catastrophic foam collapse at the same time. It was found that the foam generation with Epikuron 145 V in HOSO reached a maximum at 2 wt.%. A further increase in the phospholipid concentration from 2 to 10 wt.% caused no change in the foamability. However, the maximum capacity of the vessel containing the foam was reached at 2 wt.%. It is worth noting that the time taken for the samples to reach this maximum was the same (within 22 seconds), therefore demonstrating that the foamability (time for this maximum amount to be generated) was the same.

The time for the volume of foam produced immediately after aeration to collapse was found to increase as the surfactant concentration increased; foam produced with 10 wt.% surfactant collapsed after 85 minutes compared with 32 minutes at 0.5 wt.%. Figure 3.5 (a) shows the initial foam volume and Figure 3.5 (b) shows the foam half-life (time taken for the foam to decrease by half of its initial volume) of all four Epikuron phospholipids studied as a function of concentration in HOSO after aeration with the sparging gas technique. It can be seen that the highest foamability at 2 wt.% was also observed with Epikuron 130 P IP, 170 and 200. Again, it is not possible to conclude whether this was due to the capacity of the vessel used for the aeration being reached or due to the Epikuron surfactant not encouraging further gas incorporation into the mixture when the content is above 2 wt.%. As the phospholipid concentration increased the foam stability also generally increased. For Epikuron 200, it was found that the foam stability increased up to 2 wt.%, remained constant to 5 wt.% and decreased slightly at 10 wt.%. The stability of the foams appears to be Epikuron 145 V > Epikuron 170 > Epikuron 130 P IP > Epikuron 200. It is clear that this aeration method is effective

at generating a foam but the foam produced is relatively unstable, therefore an additional method using a foaming column was used to aerate the mixture.

**Figure 3.3.** Foam collapse profile of Epikuron 145 V as a function of concentration in HOSO. The foam was generated with sparged compressed air for 30 seconds at  $22 \pm 2$  °C.

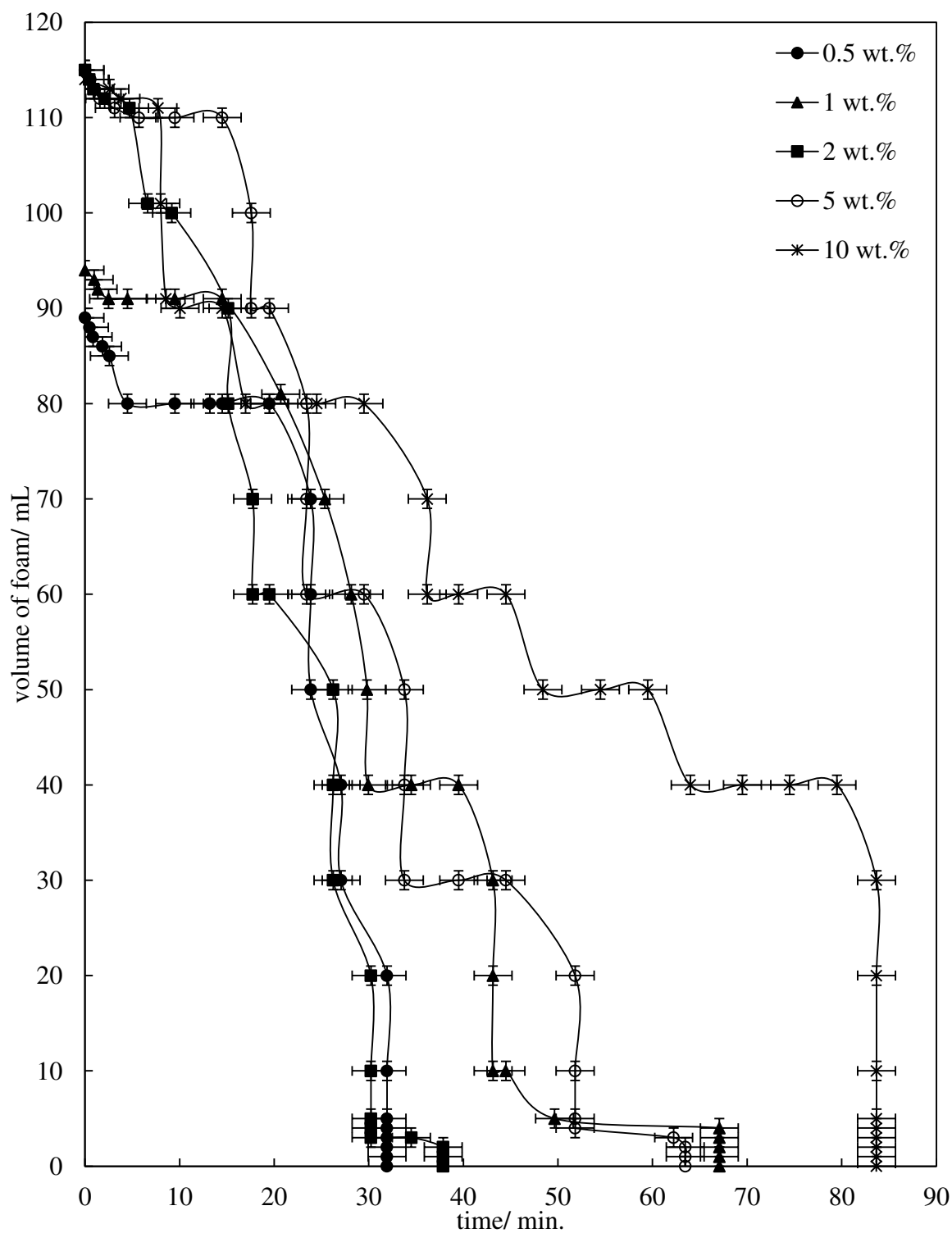


**Figure 3.4.** Appearance of the foam produced with 5 wt.% Epikuron 145 V in HOSO (a) immediately after aeration, (b) 10 minutes after aeration and (c) 30 minutes after aeration with sparged compressed air for 30 seconds at  $22 \pm 2$  °C. Scale bar 1 cm.

(a)

(b)

(c)

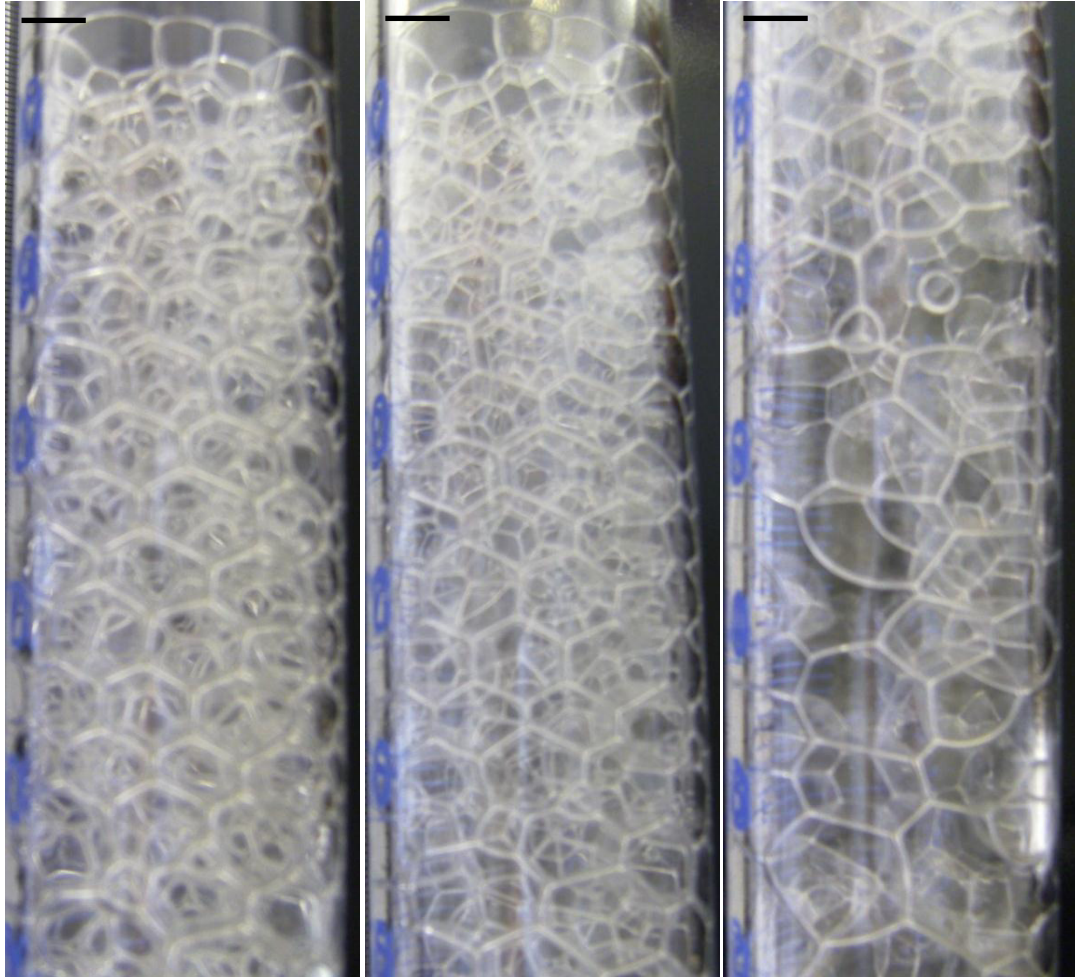
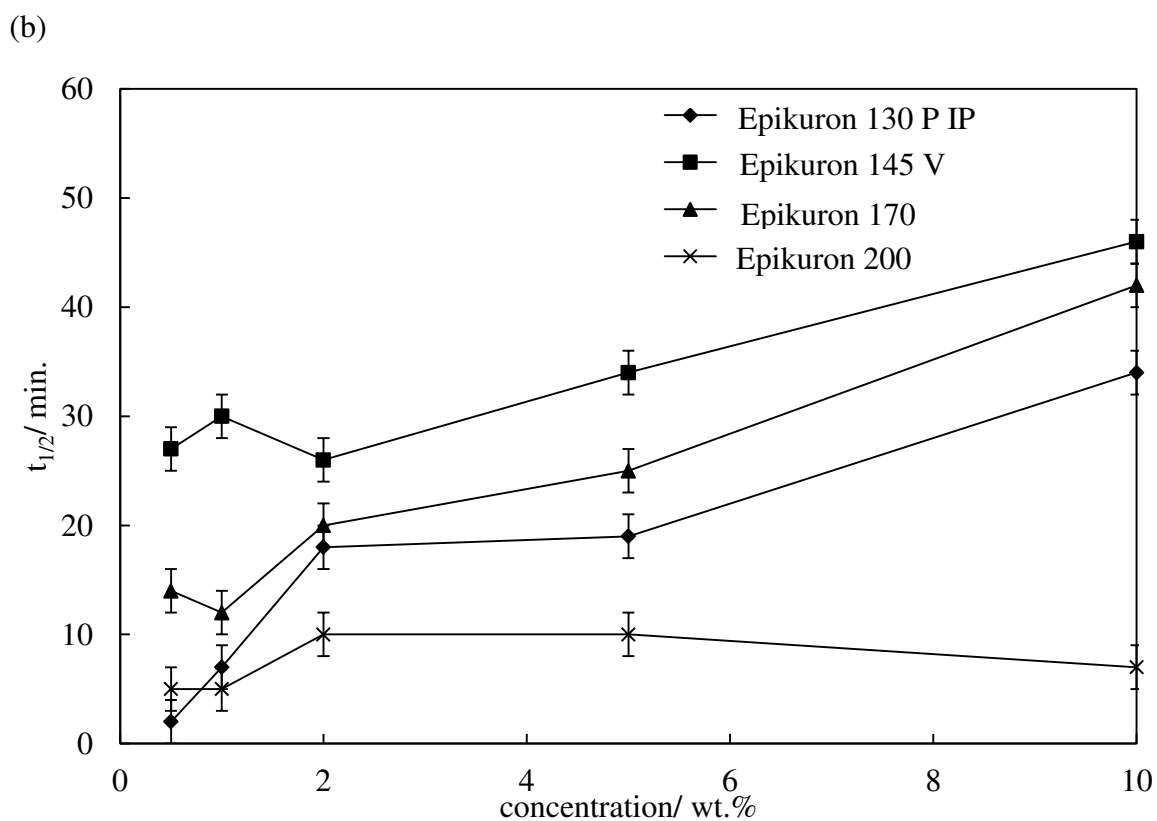
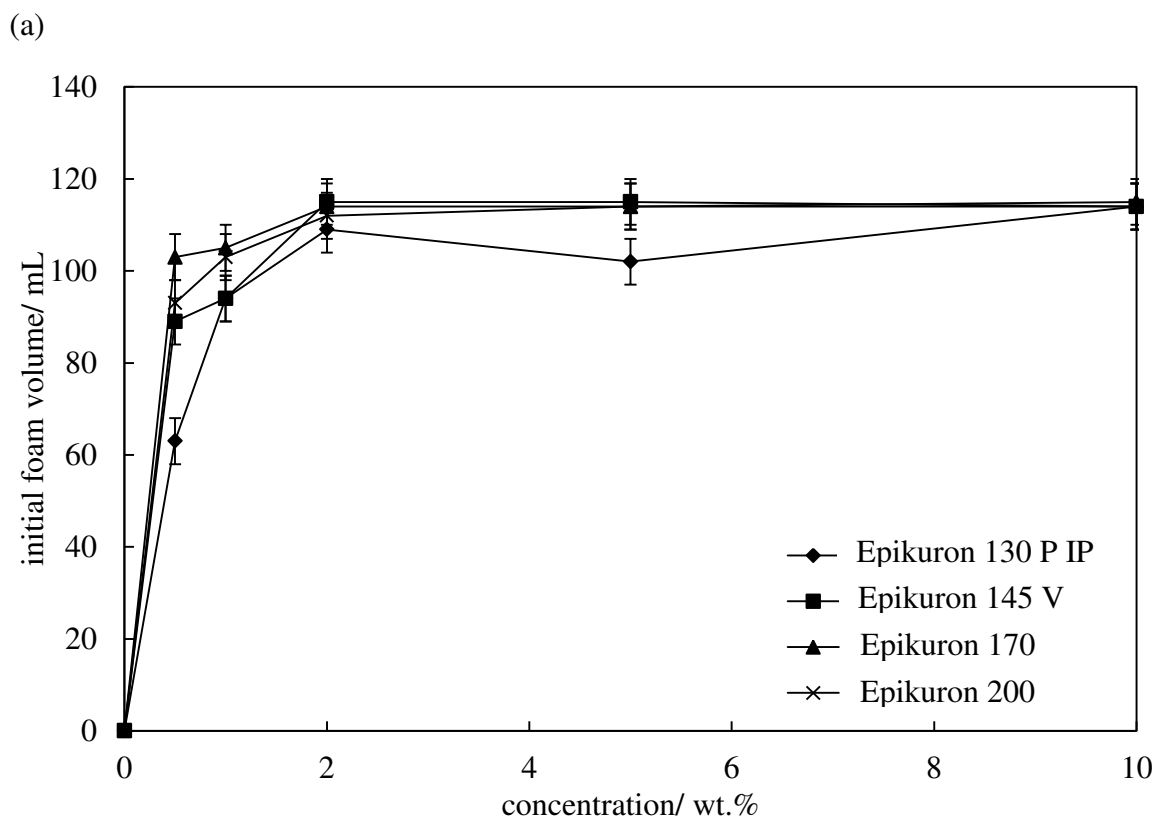


**Figure 3.5.** Effect of phospholipid concentration in HOSO on (a) initial foam volume and (b) foam half-life ( $t_{1/2}$ ). Foam was produced through sparging compressed air for 30 seconds into the sample at  $22 \pm 2$  °C.



### 3.4.2 Foaming column

The phospholipid in HOSO mixtures were aerated using the foaming column not only because of the low foam stability with the sparging gas technique but also because the gas flow was not controlled (was found to be on average  $1 \text{ L min.}^{-1}$ ). The aeration with the foaming column included the use of a flow meter, so the compressed air flow could be monitored and controlled to remain at  $94 \text{ mL min.}^{-1}$  for the entire 5 minutes of aeration. The aerated mixture was placed into a 1 L capacity measuring cylinder, therefore a flow rate of  $94 \text{ mL min.}^{-1}$  for 5 minutes was chosen as all the gas inputted into the system, if encapsulated into the foam, could be monitored. All four phospholipids in HOSO were aerated with the foaming column technique with compressed air for 5 minutes at  $25 \text{ }^{\circ}\text{C}$  after cooling from  $80 \text{ }^{\circ}\text{C}$  at approx.  $1 \text{ }^{\circ}\text{C/min}$ . As can be seen from the following figures the amount of foam generated with the foaming column was considerably higher than that produced with the sparging gas technique. The increase in the amount of foam generated compared to that found with the sparging gas technique is thought to be due to the increase in the volume of the phospholipid and oil mixture- 10 mL with the sparging gas, 100 mL with the foaming column. If 470 mL of foam was produced then all of the gas that entered the mixture had been incorporated in the foam which indicates that the system had a high foamability.

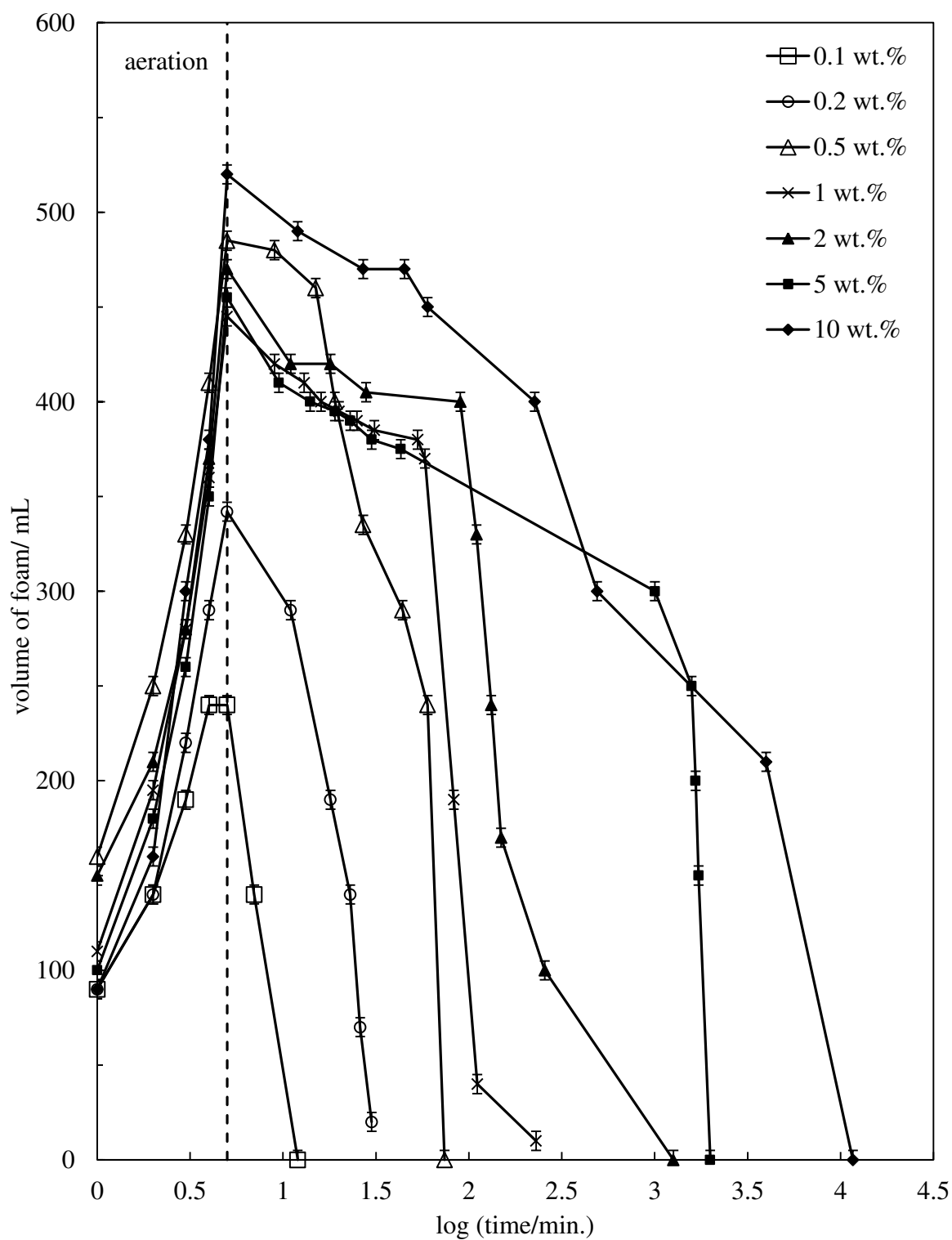
#### 3.4.2.1 Epikuron 145 V in HOSO

Figure 3.6 demonstrates the effect of the Epikuron 145 V concentration in HOSO on the ability to create a foam and the collapse profile of that foam. It is interesting to see that a large amount of foam, 480 mL, was produced even with as little as 0.5 wt.% of the phospholipid present. Figure 3.7 shows the initial foam volume and the foam half-life of Epikuron 145 V as a function of concentration in HOSO. It is clear that the initial foam volume increased as the surfactant concentration increased from 0.1 to 0.5 wt.%, as the concentration further increased to 10 wt.% the initial foam volume was between 450 mL and 530 mL. The Figure also shows that the half-life of the foam increased as the Epikuron concentration increased from 2 minutes with 0.1 wt.% to almost 65 hours with 10 wt.%.

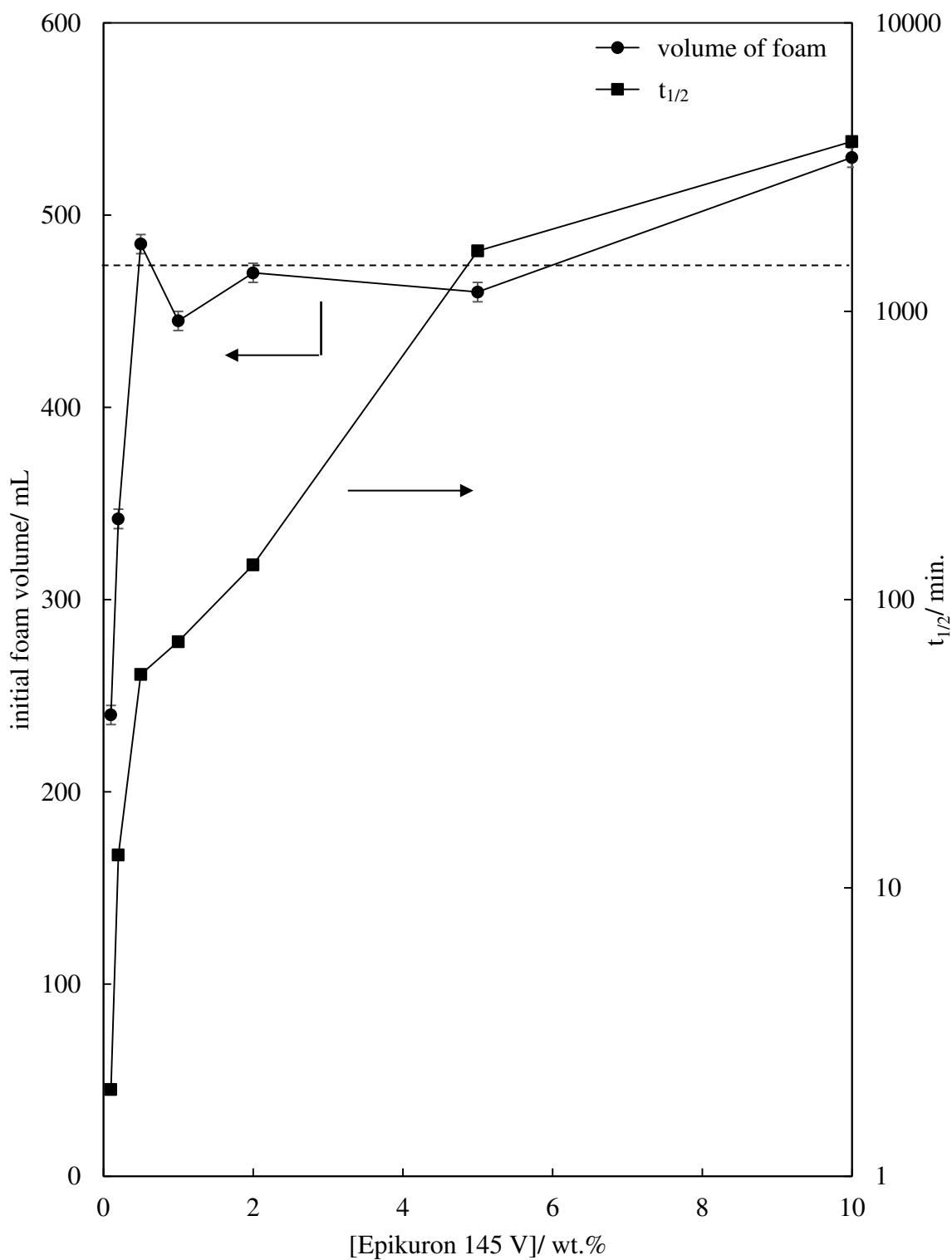
The visual change of the foam was similar for all four phospholipids as it collapsed and is clearly shown in Figure 3.8. The foam bubbles immediately after aeration were

spherical with a diameter of less than 1 mm. Over time they gradually increased to a diameter of 2-3 mm with some polyhedral bubbles. The bubbles then increased to 10 mm in diameter with more polyhedral bubbles. These larger bubbles then merged and finally collapsed. The increase in bubble size initially occurred at the upper surface of the foam but gradually over time then occurred with the bubbles lower in the foam (closer to the drained liquid). Through visual observations of the foam collapse it was seen that the liquid drained gradually. At 10 wt.% Epikuron 145 V the time for the liquid to drain to the original volume (100 mL) was 8 hours, at 0.5 wt.% the drainage time was 45 minutes. As the phospholipid concentration increased, the time for the liquid to drain from the foam also increased, therefore causing the rate of coalescence and disproportionation to decrease, consequently the time until complete foam collapse increased.

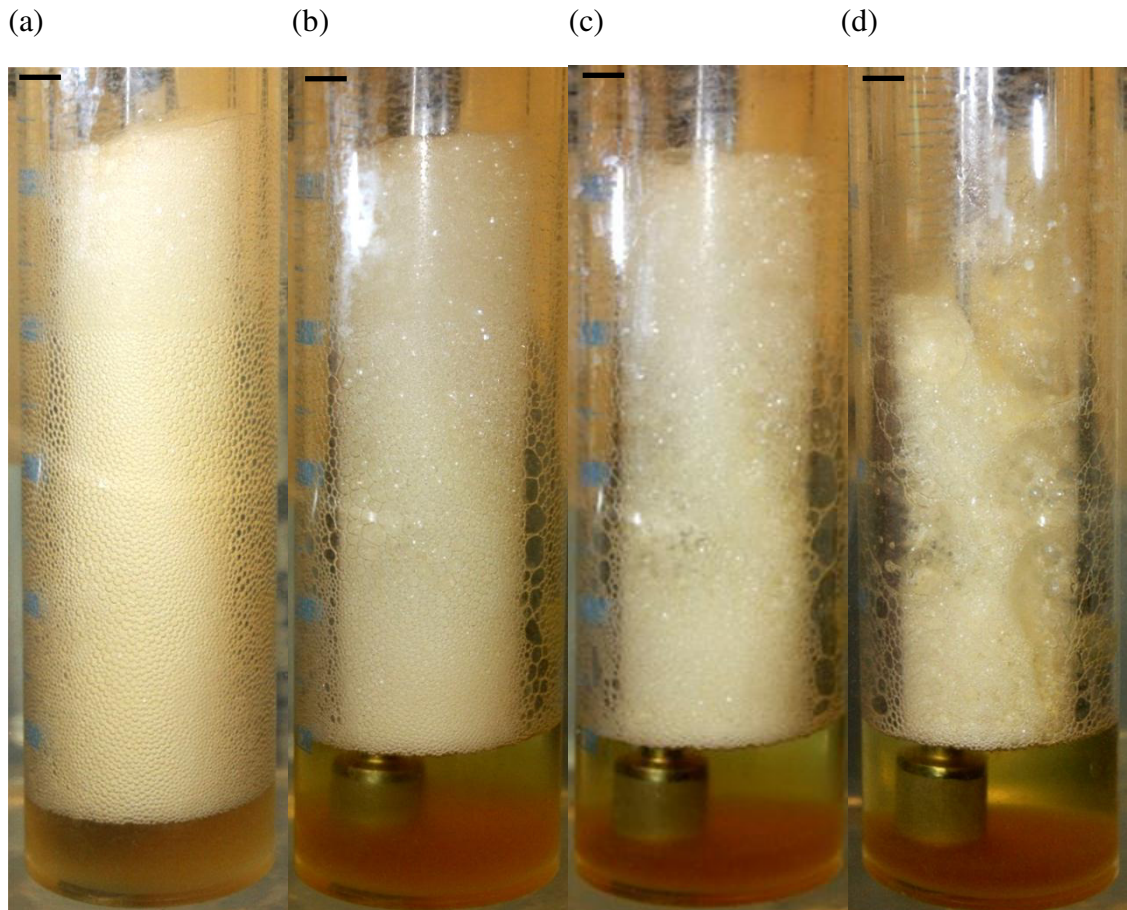
**Figure 3.6.** Foam collapse profile of Epikuron 145 V as a function of concentration in HOSO after aerating for 5 minutes with compressed air in the foaming column at 25 °C. Dashed vertical line indicates end of aeration.



**Figure 3.7.** Initial foam volume and foam half-life of foams produced with Epikuron 145 V as a function of concentration in HOSO. Foam produced with the foaming column with compressed air at 25 °C. Dashed horizontal line indicates that all the air that entered the system was incorporated into the mixture.



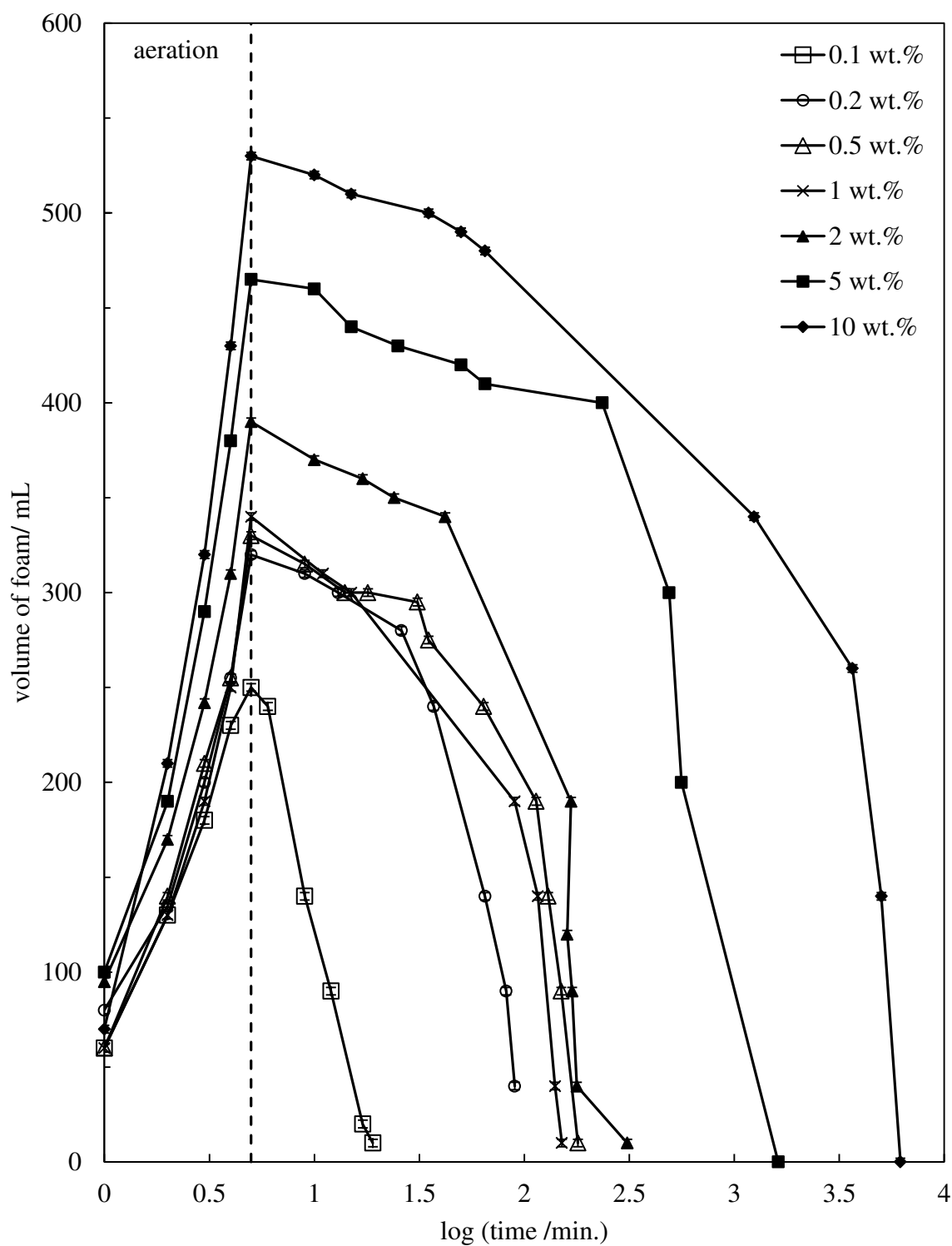
**Figure 3.8.** Appearance of foam from 5 wt.% Epikuron 145 V in HOSO after aeration with compressed air via the foaming column technique for 5 minutes at 25 °C (a) immediately after aeration, (b) after 1 hour, (c) after 2 hours and (d) after 6 hours. Scale bar 1 cm.



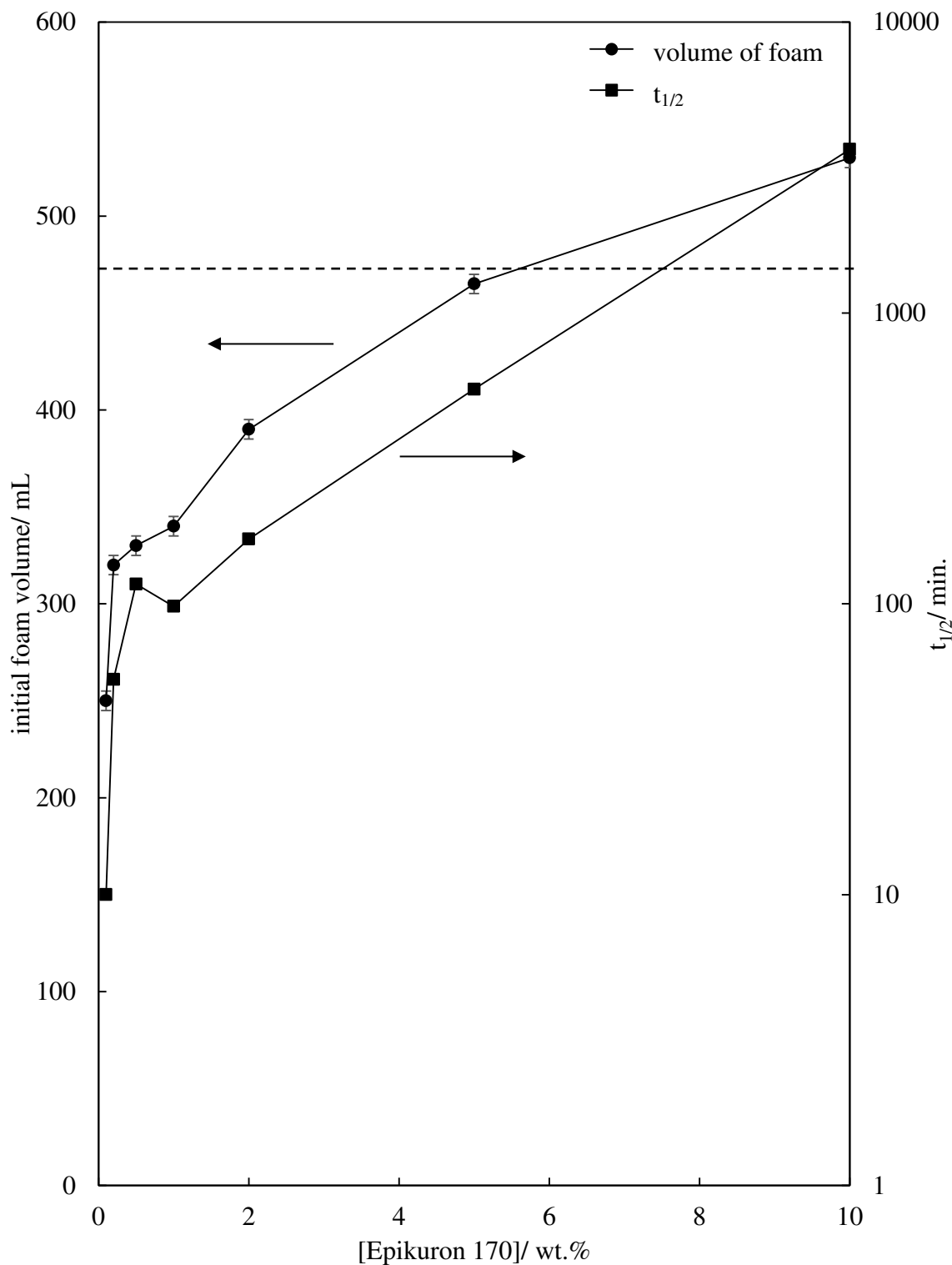
#### 3.4.2.2 Epikuron 170 in HOSO

Figure 3.9 shows that the foam volume generated with 0.1-10 wt.% Epikuron 170 in HOSO increased rapidly over the 5 minutes of aeration. The foam was then found to collapse gradually over time. The figure also shows that as the Epikuron 170 concentration was increased there was clearly an increase in the foamability and the foam stability. The high foamability of the system is clear in Figure 3.10 as even with as little as 0.1 wt.% 250 mL of foam was produced.

**Figure 3.9.** Foam collapse profile of Epikuron 170 as a function of concentration in HOSO aerated with compressed air with the foaming column for 5 minutes at 25 °C. Dashed vertical line indicates end of aeration.



**Figure 3.10.** Initial volume of foam and foam half-life of Epikuron 170 as a function of concentration in HOSO at 25 °C aerated with the foaming column with compressed air for 5 minutes. Dashed horizontal line indicates that all the air that entered the system was incorporated into the mixture.



### 3.4.2.3 Epikuron 130 P IP in HOSO

It is clear from Figure 3.11 that the foam volume reached a maximum at between 0.5 and 1 wt.% Epikuron 130 P IP in HOSO. The foamability then decreased at 2 wt.% and then gradually increased as the concentration increased up to 10 wt.%. As the phospholipid concentration increased, the foam stability also increased as shown in Figure 3.11. It was interesting to find that foams produced particularly below 3 wt.% had little foam collapse up to 60 minutes (time increased as concentration increased) from the initial foam generation. The foam then collapsed relatively quickly over 20 minutes. This may have been because as the liquid drained from the foam lamella, coalescence and disproportionation then occurred which caused the foam collapse. The liquid uptake and subsequent drainage of foams produced with Epikuron 130 P IP as a function of concentration in HOSO is shown in Figure 3.12. It can be seen that when a foam was generated at 0.1 and 0.2 wt.% there was no liquid uptake which was clearly necessary for any substantial foam stability as the foams produced collapsed after 16 and 31 minutes, respectively. Between 0.3 and 3 wt.% of the phospholipid the foam collapsed as the liquid drained, which again showed the importance of the liquid in the foam lamella for the foam stability. It is also shown in the figure that at 5 and 10 wt.% the liquid drained hours prior to the foam collapse suggesting that the liquid, at these phospholipid concentrations, was not essential for the foam stability. This may be due to the presence of a larger amount of phospholipid crystals in the foam lamella which created some resistance to coalescence and disproportionation. The liquid drainage from the foam at 5 and 10 wt.% was slower compared to the drainage times at lower phospholipid content. This suggests that as the concentration increased the viscosity of the continuous phase also increased. The half-life of the foams produced as a function of concentration in HOSO and the initial foam volumes are shown in Figure 3.13. The half-life of the foams were found to generally increase from 0.1 to 10 wt.%, with a plateau between 0.3 and 3 wt.%.

**Figure 3.11.** Foam collapse profile of Epikuron 130 P IP as a function of concentration in HOSO aerated with the foaming column with compressed air for 5 minutes at 25 °C. Dashed vertical line indicates end of aeration.

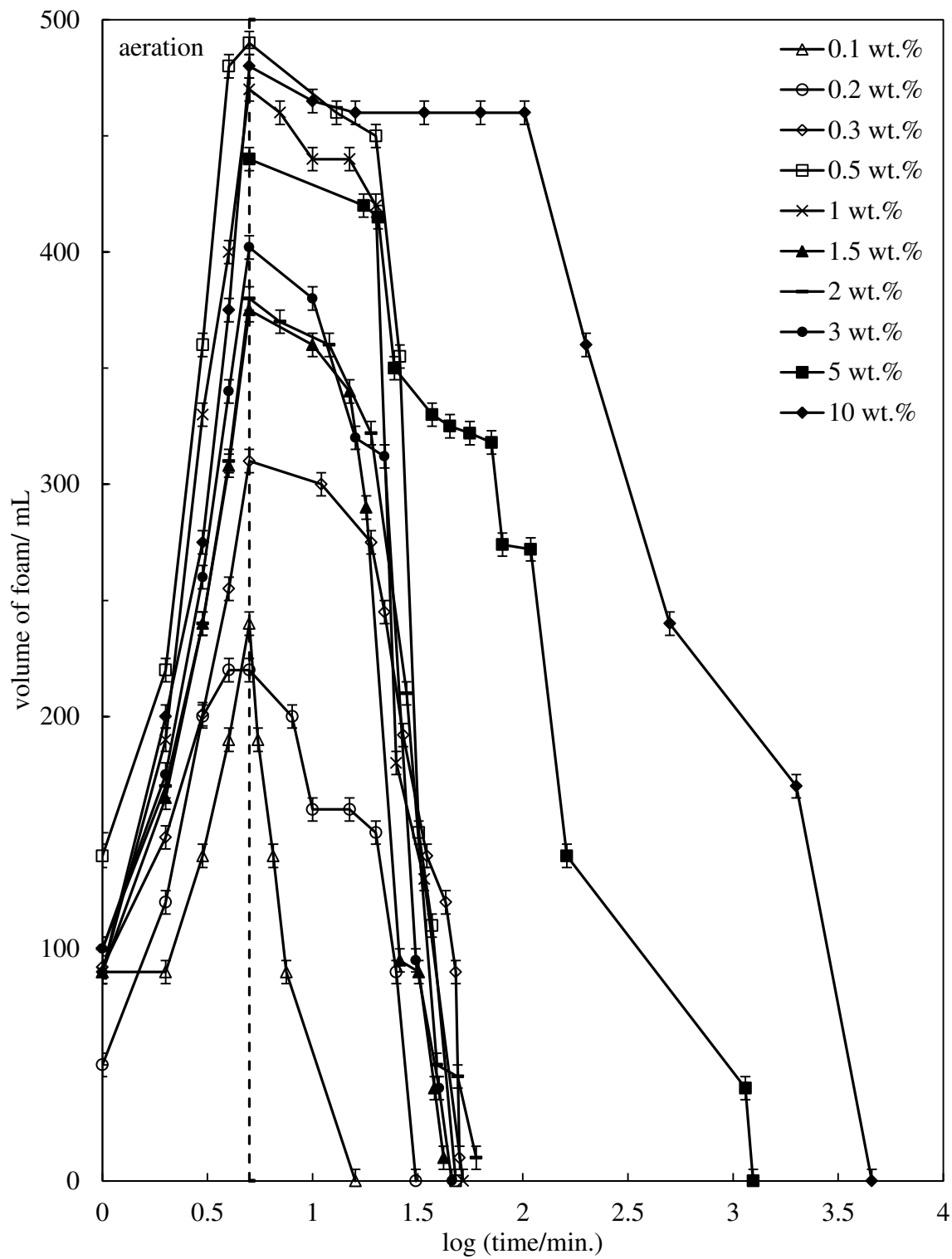


**Figure 3.12.** Liquid uptake and subsequent drainage from a foam produced with Epikuron 130 P IP as a function of concentration in HOSO aerated with the foaming column with compressed air for 5 minutes at 25 °C. Dashed vertical line indicates end of aeration.

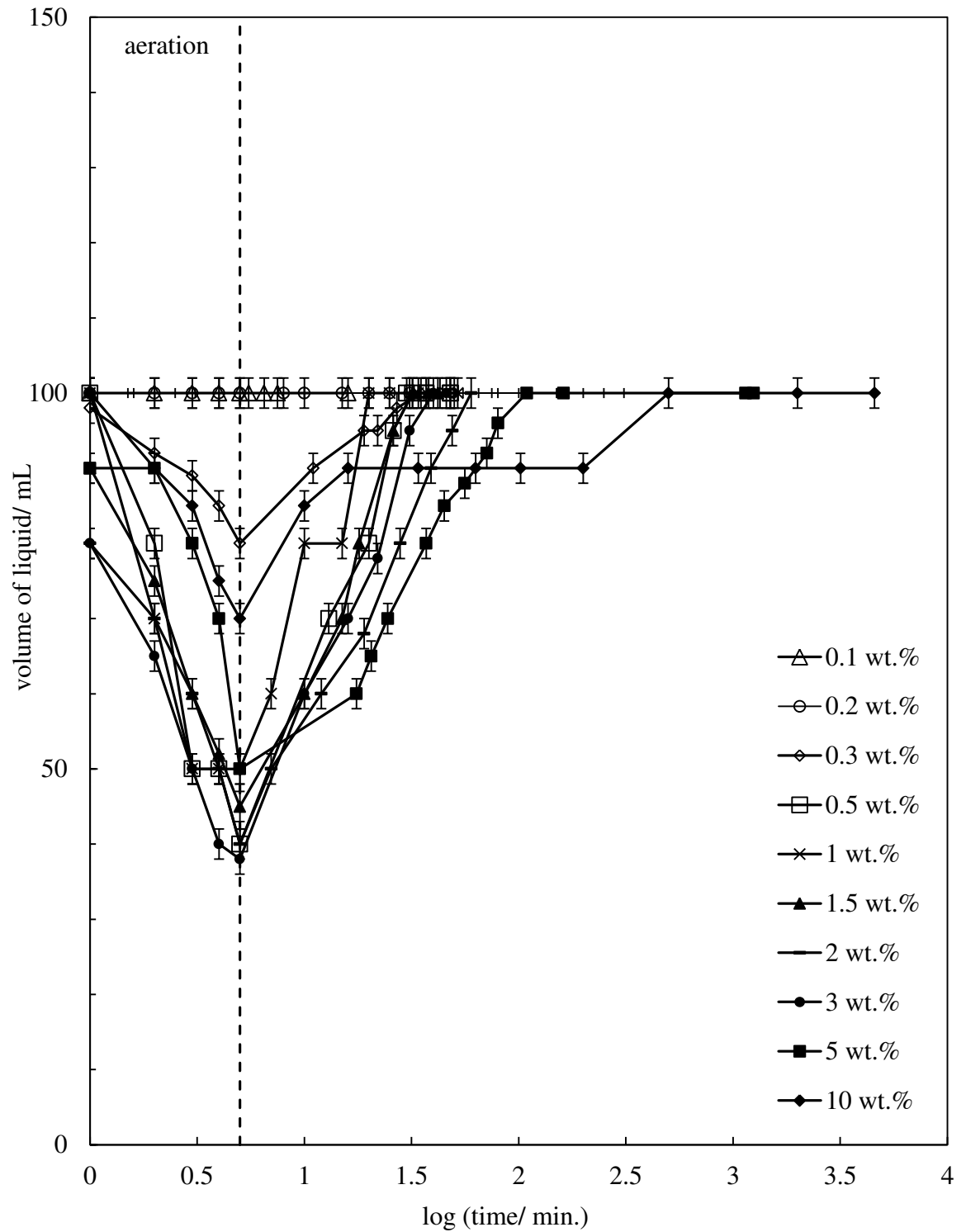
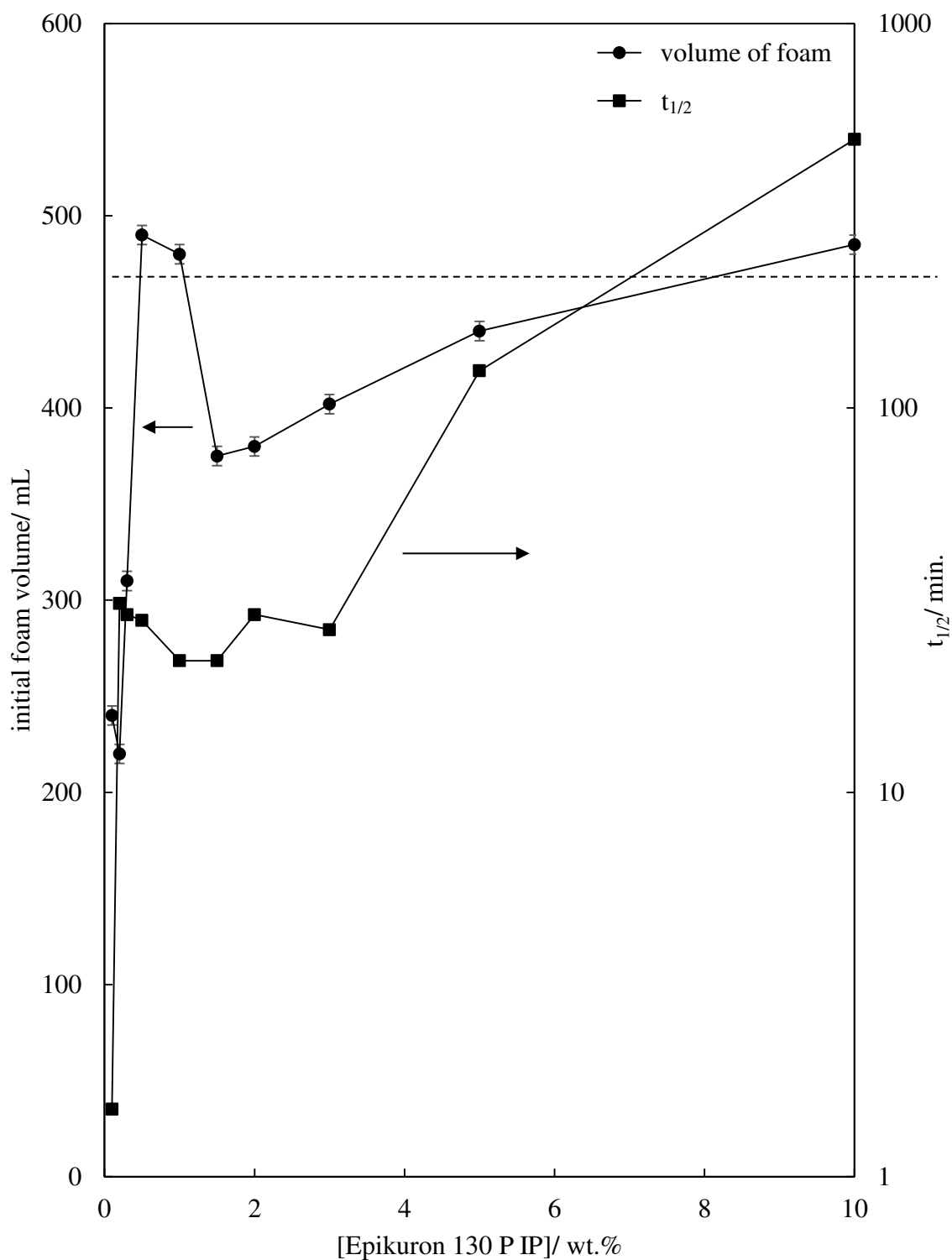


**Figure 3.13.** Initial volume of foam and foam half-life of Epikuron 130 P IP as a function of concentration in HOSO aerated with the foaming column with compressed air for 5 minutes at 25 °C. Dashed horizontal line indicates that all the air that entered the system was incorporated into the mixture.



#### 3.4.2.4 Epikuron 200 in HOSO

The foam generation and subsequent stability of the foams produced with Epikuron 200 in HOSO is presented in Figure 3.14. It is observed that the foams produced with as little as 0.1 wt.% surfactant (440 mL of foam) had a remarkable stability fully collapsing after 98 minutes. This was significant because with 0.1 wt.% Epikuron 130 P IP the time for complete collapse was 16 minutes, with 145 V it was 7 minutes and with 170 it was 14 minutes. However, even though the foam stability did increase as concentration increased (Figure 3.15), the significantly higher stability of the foams produced with Epikuron 200 was only seen at this lower concentration. It is known that Epikuron 200 has the highest PC content (93.4 %) and the lowest PE content (0 %). Therefore this amount may initially aid the foam stability with the lower concentrations of the Epikuron 200 in HOSO, but then limit the stability of the foams formed with the higher concentrations.

**Figure 3.14.** Foam collapse profile of Epikuron 200 as a function of concentration in HOSO aerated with the foaming column with compressed air for 5 minutes at 25 °C. Dashed vertical line indicates end of aeration.

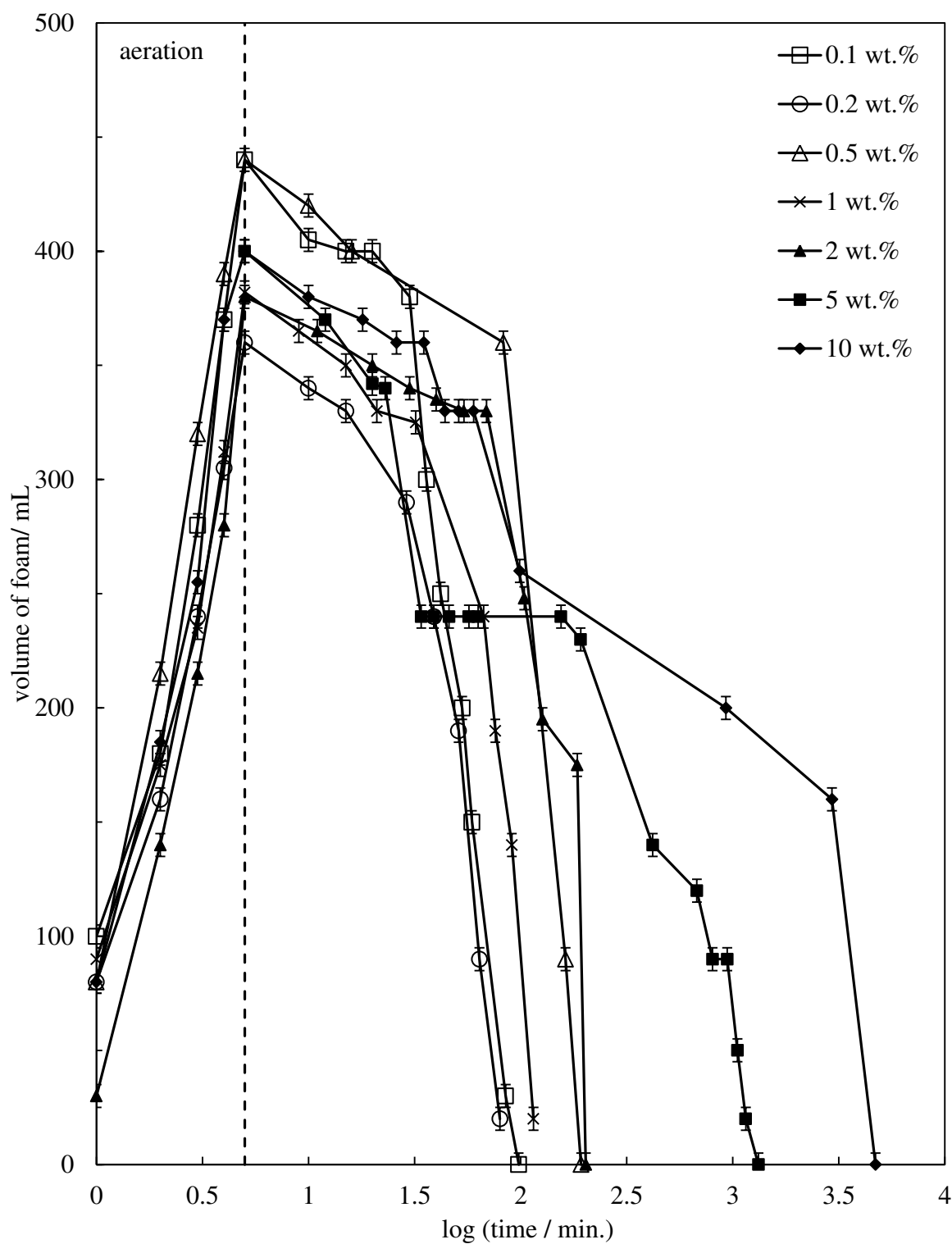
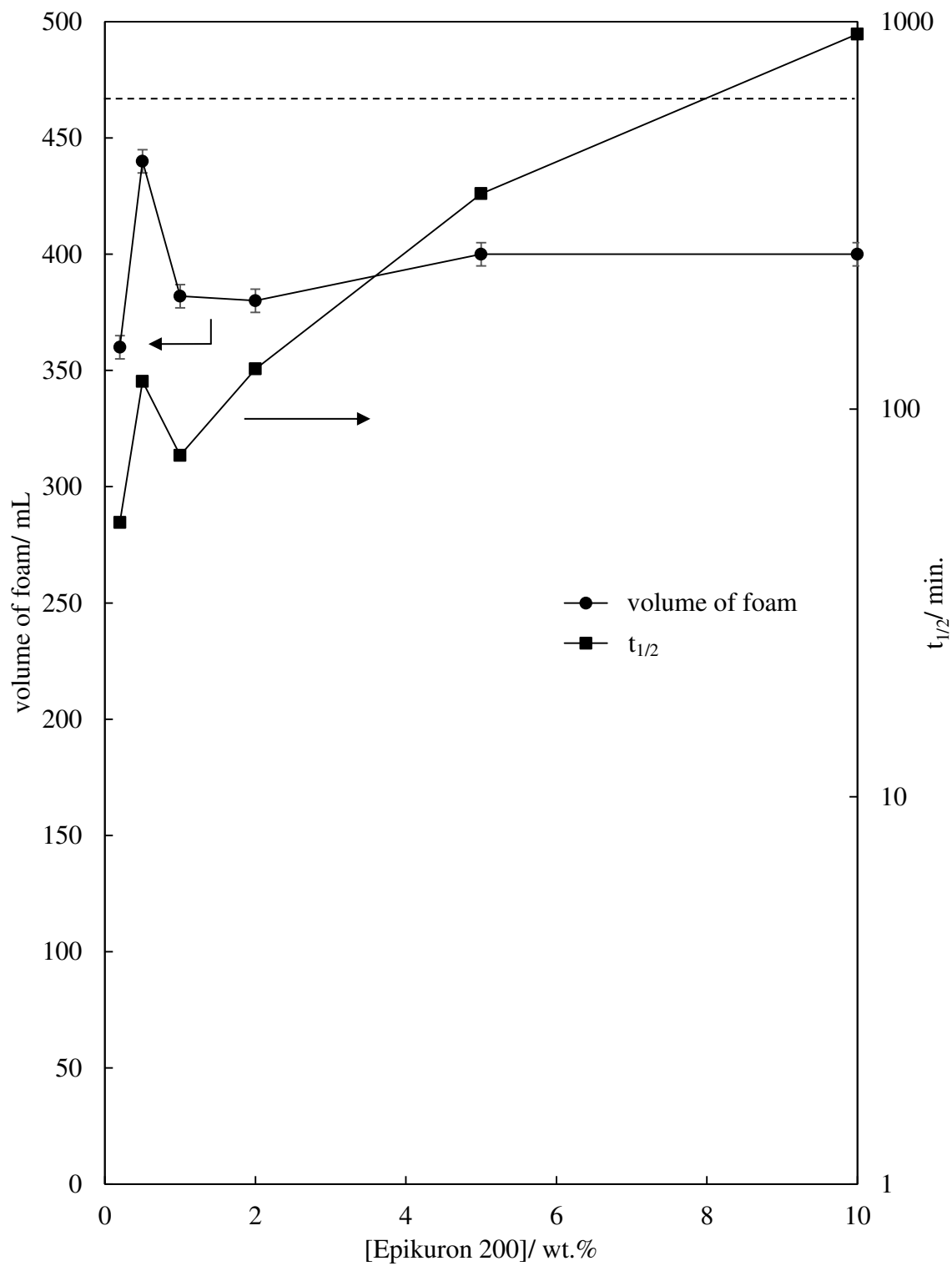


**Figure 3.15.** Initial volume of foam and foam half-life of Epikuron 200 as a function of concentration in HOSO at 25 °C aerated with the foaming column with compressed air for 5 minutes. Dashed horizontal line indicates that all the air that entered the system was incorporated into the mixture.

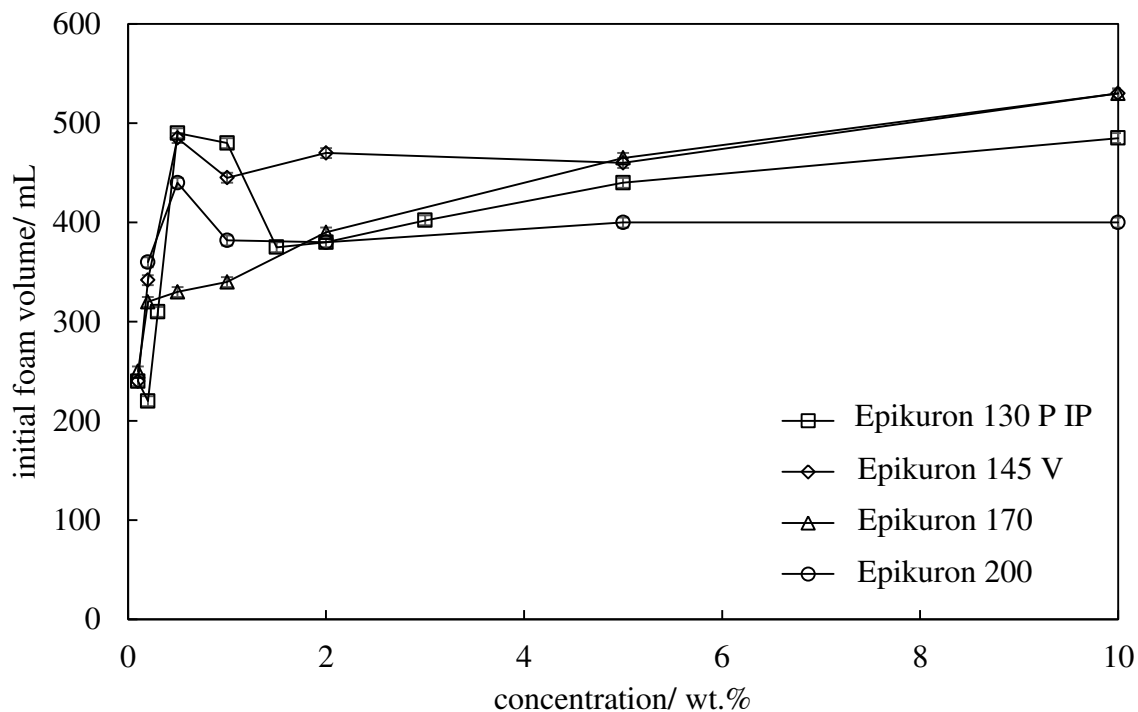


#### 3.4.2.5 Comparison of Epikuron phospholipids

It was found that the foamability was not significantly affected by the PC and PE content in general as seen in Figure 3.16 (a). This highlights that the amount of foam produced was independent of the PC and PE content shown in Figure 3.17 at 5 wt.% of phospholipid. This was not be the case with phospholipids in cocoa butter as found by Su-Jia et al.<sup>19</sup> where it was clear that the foamability increased as the PC content increased and the PE content decreased. Figure 3.17 however does illustrate the clear effect of the PC and PE content on the foam stability observed at 5 wt.%, which was also seen with 2 wt.% and 10 wt.% in Figure 3.16 (b). The foam produced with Epikuron 145 V, where the PE content was approximately 13 % and the PC content was approximately 50.25 %, was found to have the highest stability. It was interesting to find that with the sparged gas technique the Epikuron 200 had the least stable foams, with Epikuron 130 P IP having the second least stable foams, whereas with the foaming column this was reversed with the least stable foams being produced with Epikuron 130 P IP. It was proposed that this may be due to the initially uniform, spherical bubbles which were produced with the foaming column causing the rate of disproportionation to reduce. Therefore, the foams produced with the Epikuron 130 P IP may coalesce faster, after the liquid drained from the foam lamella, than foams produced with the other three Epikurons resulting in the lower foam stability. This theory is supported by Figure 3.11 and Figure 3.12 which demonstrate that complete/ almost complete liquid drainage was followed by foam collapse with concentrations of 0.3 to 3 wt.% Epikuron 130 P IP in HOSO.

**Figure 3.16.** Foams of the 4 Epikuron surfactants in HOSO aerated with the foaming column with compressed air for 5 minutes at 25 °C. (a) Initial foam volume, (b) foam half-life.

(a)



(b)

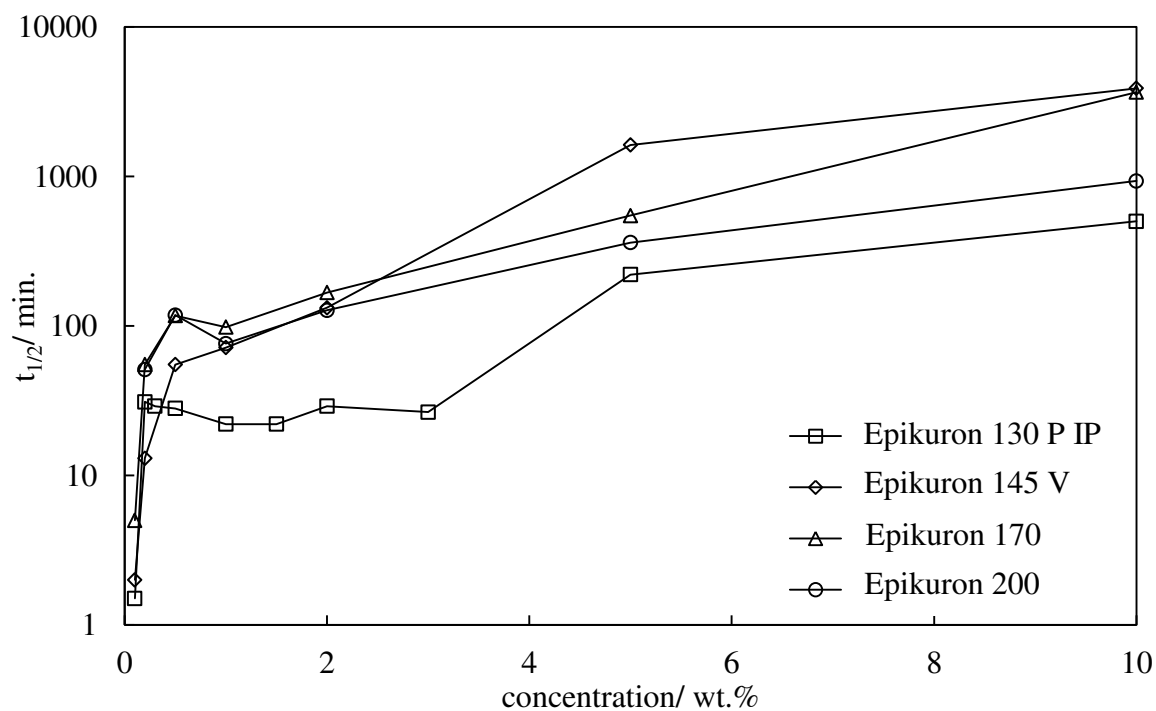
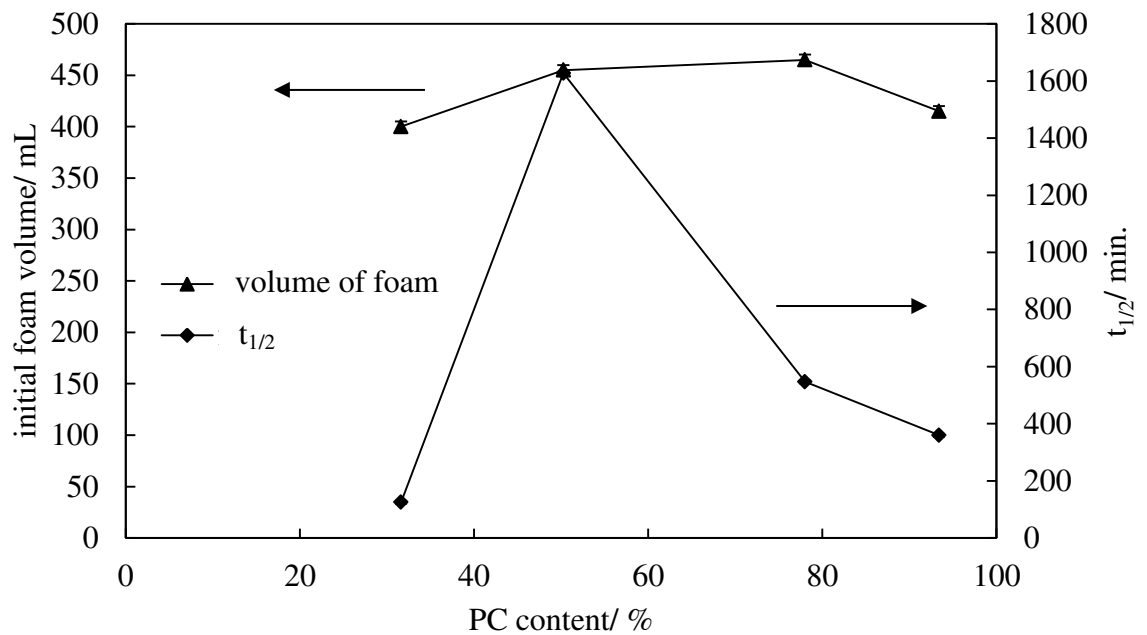
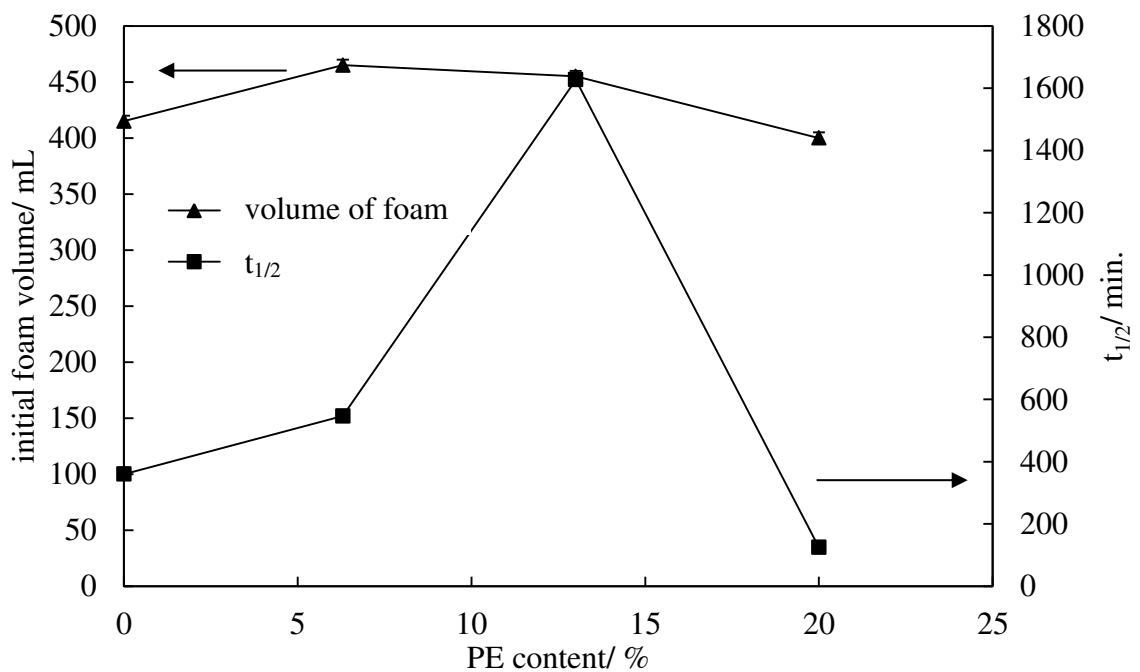


**Figure 3.17.** Effect of (a) phosphatidylcholine content (PC) and (b) phosphatidylethanolamine content (PE) in the Epikuron phospholipid foaming agents on the initial foam volume and foam half-life. 5 wt.% of phospholipid in HOSO was aerated with the foaming column with compressed air for 5 minutes at 25 °C.

(a)



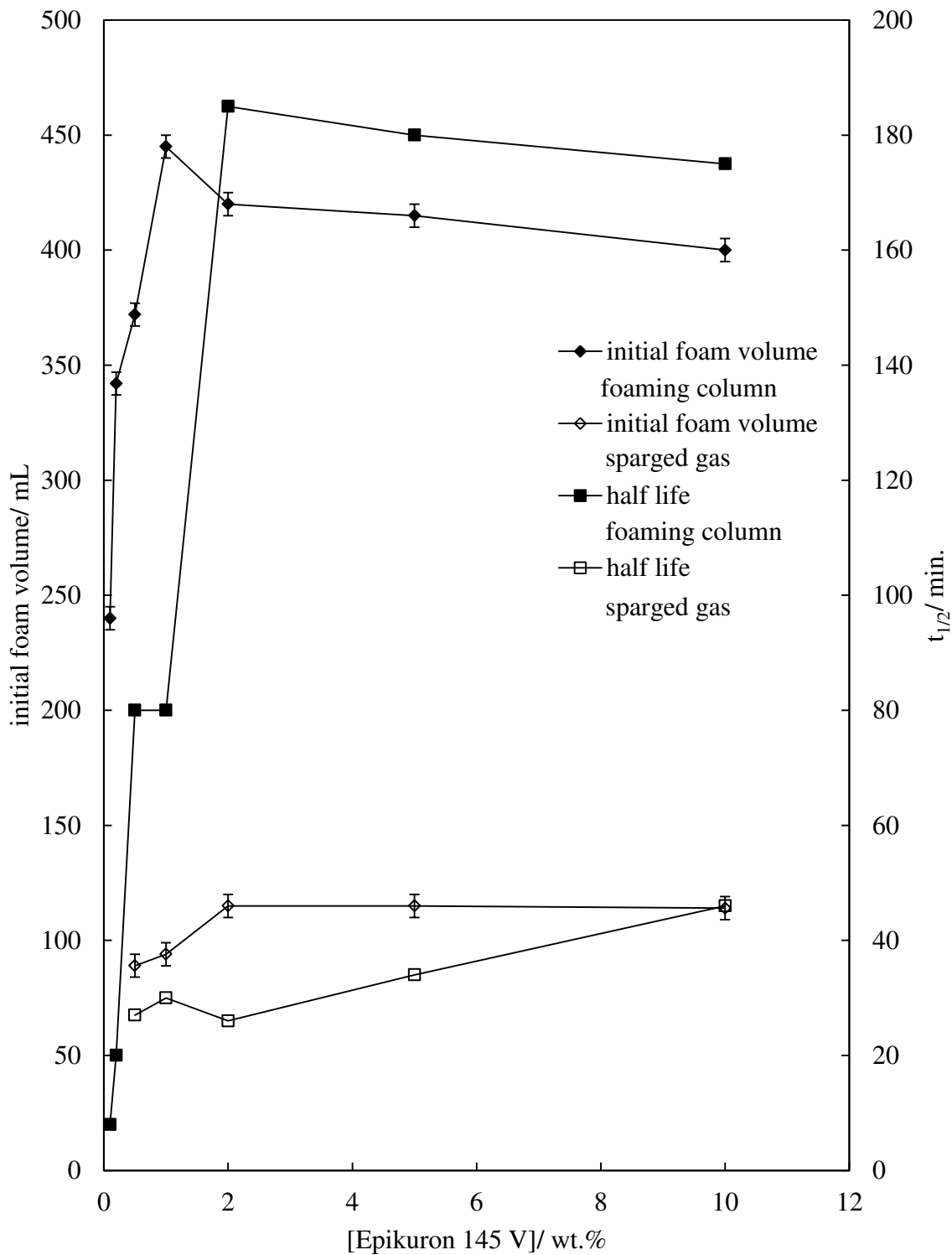
(b)



### 3.4.3 Effect of aeration method

The stability of the foam was significantly greater with the foaming column; the foam half-life was almost 65 hours, whereas with the sparged gas the half-life was approximately 45 minutes at 10 wt.% Epikuron 145 V in HOSO. This was thought to be due to the generated bubbles initially having a smaller, uniform initial bubble size with the foaming column and therefore coalescence once the foam was created was limited. The initial smaller uniform spherical bubbles (< 1 mm) compared to that observed with the sparging technique (initially 3-5 mm spherical bubbles) was thought to be due to the size of the needle/ pores the compressed air flowed through. The foaming column pore size was on average 22  $\mu\text{m}$ , with the sparging technique, the needle internal diameter was 318  $\mu\text{m}$ . As can be seen from Figure 3.18, the volume of foam generated with the foaming column was significantly higher than that produced with the sparged gas. This is because 470 mL of compressed air entered the mixture with the foaming column, whereas with the sparged gas technique on average 250 mL entered the mixture, yet the foam produced was almost a quarter of that produced with the foaming column.

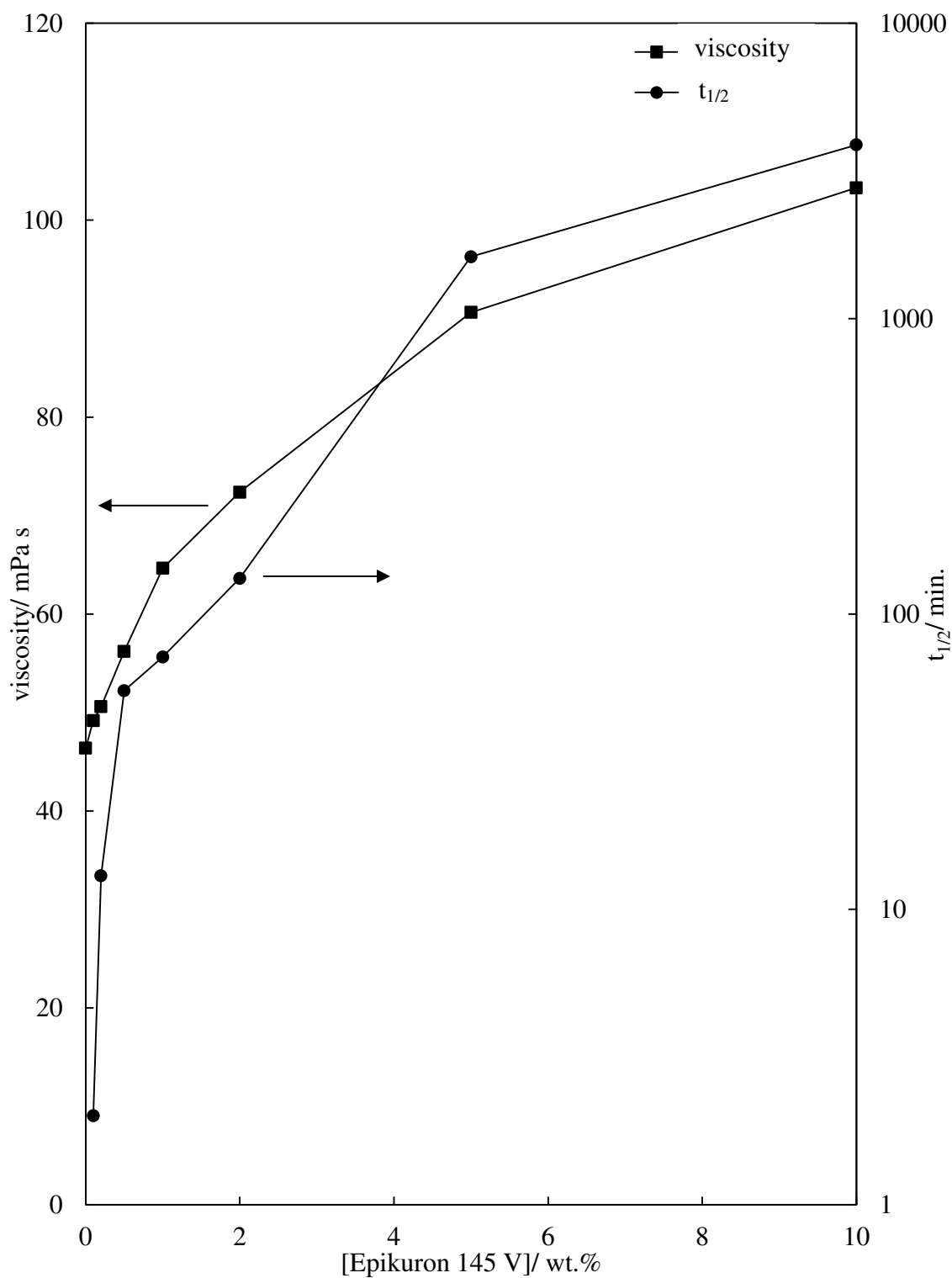
**Figure 3.18.** Effect of aeration method on the initial foam volume and foam half-life with Epikuron 145 V as a function of concentration in HOSO. Foaming column at 25 °C, and with sparged gas at 20 ± 2 °C, aerated with compressed air.



#### 3.4.4 Viscosity of phospholipid-oil dispersions

The stability of a foam can be increased by the addition of surfactant particularly if the surfactant causes an increase in viscosity. This is due to the surfactant causing a decrease in the rate of liquid drainage; the presence can also cause a resistance to coalescence and also slow down the rate of disproportionation. Therefore the viscosity of Epikuron 145 V as a function of concentration in HOSO (shown in Figure 3.19) was measured to identify the effect of the viscosity of the continuous phase on the half-life of the foam. With 10 wt.% Epikuron 145 V present in HOSO the mixture was measured to be extremely viscous (over double the viscosity of the neat HOSO). With as little as 1 wt.% Epikuron 145 V present in the HOSO the viscosity was found to increase by 20 mPa s (HOSO was measured to be 46 mPa s). It is clear that as the concentration of the Epikuron 145 V increased, the viscosity of the mixture dramatically increased, which was therefore thought to cause the increased foam stability due to a decrease in the rate of liquid drainage from the foam. A correlation between the foam stability and the viscosity of the continuous phase was also found by Binks et al.,<sup>7</sup> when studying foams produced with a mixture of polymers and detergent particles in lubricating oils. In the study it was found that as the viscosity of the continuous phase increased, the time for foam collapse also increased (as the liquid drained the foam collapsed).

**Figure 3.19.** Viscosity of Epikuron 145 V-HOSO mixtures as a function of concentration and foam half-life produced with the foaming column with compressed air for 5 minutes at 25 °C. Viscosity values were an average of three measurements with an Ostwald viscometer which agreed within 0.2 seconds at 25 °C.



### 3.5 Conclusions

It has been found that a foam can be produced with edible phospholipid foaming agents with oils with a surface tension above  $33.4 \text{ mN m}^{-1}$ . Through microscopy it can be concluded that the mixture of Epikuron phospholipids in HOSO prior to aeration was two-phase. It was also found that birefringent crystals were present at phospholipid concentrations as low as 0.5 wt.% in HOSO with all four Epikurons. The foaming agent concentration was important for the amount of foam generated and its stability. It was clear that the foam stability increased significantly as the phospholipid concentration increased. The amount of foam produced with the foaming column technique was significantly higher and had a higher stability than when the same sample was aerated with the sparged gas technique. This was thought to be due to how the air entered the mixture, which in turn effected the initial bubble size and dispersity. It was also found that the phosphatidylcholine and phosphatidylethanolamine content within the phospholipid did not have a significant effect on the volume of foam generated, but did effect the stability of the generated foam with both the sparging gas technique and the foaming column. Viscosity measurements demonstrated that there was a considerable increase in oil viscosity as the phospholipid concentration increased which was thought to contribute to foam stability as liquid drained from the foam films at a slower rate. The presence of the molecular phospholipid was thought to be important in the generation of the foam. The presence of birefringent crystals (which adsorbed and desorbed from the air-oil surface) were thought to be essential for the foam stability (foam stable for up to several days).

### 3.6 References

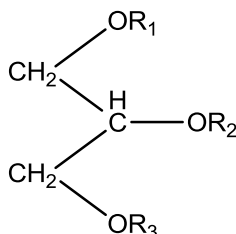
1. L. K. Shrestha, K. Aramaki, H. Kato, Y. Takase and H. Kunieda, *Langmuir*, **22**, 8337 (2006).
2. H. Kunieda, L.K. Shrestha and D.P. Acharya, *J. Disper. Sci. Technol.*, **28**, 133 (2007).
3. L. K. Shrestha, R. G. Shrestha, S. C. Sharma and K. Aramaki, *J. Colloid Interface Sci.*, **328**, 172 (2008).
4. R. G. Shrestha, L. K. Shrestha, C. Solans, C. Gonzalez and K. Aramaki, *Colloids Surf. A*, **353**, 157 (2010).
5. B. P. Binks and A. Rocher, *Phys. Chem. Chem. Phys.*, **12**, 9169 (2010).
6. B. P. Binks, A. Rocher and M. Kirkland, *Soft Matter*, **7**, 1800 (2011).
7. B. P. Binks, C. A. Davies, P. D. I. Fletcher and E. L. Sharp, *Colloid Surf. A*, **360**, 198 (2010).
8. S. E. Friberg, C. S. Wohn, B. Greene and R. Vangilder, *J. Colloid Interface Sci.*, **101**, 593 (1984).
9. S. E. Friberg, I. Blute, H. Kunieda and P. Stenius, *Langmuir*, **2**, 659 (1986).
10. B.P. Binks and A.T. Tyowua, *Soft Matter*, **9**, 834 (2013).
11. B.P. Binks, T. Sekine and A.T. Tyowua, *Soft Matter*, **10**, 578 (2014).
12. I.C. Callaghan and E.L. Neustadter, *Chem. Ind. (London)*, **17**, 53 (1981).
13. R.H. Ottewill, D.L. Segal and R.C. Watkins, *Chem. Ind. (London)*, **17**, 57 (1981).
14. V. Bergeron, J.E. Hanssen and F.N. Shoghl, *Colloids Surf. A.*, **123-124**, 609 (1997)
15. M. Mellema and J. Benjamins, *Colloids Surf. A.*, **237**, 113 (2004).
16. R. Murakami and A. Bismarck, *Adv. Funct. Mater.*, **20**, 732 (2010).
17. S. Ross and G. Nishioka, *J. Phys. Chem.*, **79**, 1561 (1975).
18. S. Ross and G. Nishioka, *Colloid Polym. Sci.*, **255**, 560 (1977).
19. S. Su-Jia, C. Dong and X. Shi-Chao, *J. Food Process Eng.*, **36**, 544 (2013).

## 4 SATURATED AND UNSATURATED MONO/DIGLYCERIDES IN HIGH OLEIC SUNFLOWER OIL

### 4.1 Introduction

The use of an edible mono/diglyceride to aerate an edible oil is of great interest to the food industry. Therefore, the foamability and foam stability of Grindsted Citrem LR 10 Extra Kosher (G. C. LR 10) and Grindsted Citrem N12 veg (G. C. N12 veg) in high oleic sunflower oil (HOSO) was studied, by investigating the effect of surfactant concentration, aeration temperature and aeration method. The effect of gas type on foamability and foam stability was also studied with G. C. LR 10. G.C. LR 10 is a citric acid ester of a mono/diglyceride from sunflower oil where at least one of  $R_1$ ,  $R_2$  or  $R_3$  = citric acid, one = fatty acid moiety and the remainder = citric acid, fatty acid or hydrogen (see Figure 4.1 below). The main fatty acid group is oleic acid ( $C_{18:1}$ ).

**Figure 4.1.** Structure of G. C. LR 10.



G. C. N12 veg is a mono/diglyceride made from fully hydrogenated palm-based oil with typical main chain lengths of 1 % myristic, 36-63 % palmitic, 35-58 % stearic and <1 % arachidic.

### 4.2 Unsaturated mono/diglyceride in high oleic sunflower oil

The foamability of the unsaturated mono/diglyceride has been studied extensively including the effect of concentration, temperature, gas type and aeration method. To do this, the mixture prior to aeration had to be studied which included measuring the temperature the mixture was either one phase or two phases and also the appearance with polarised light microscopy at various temperatures.

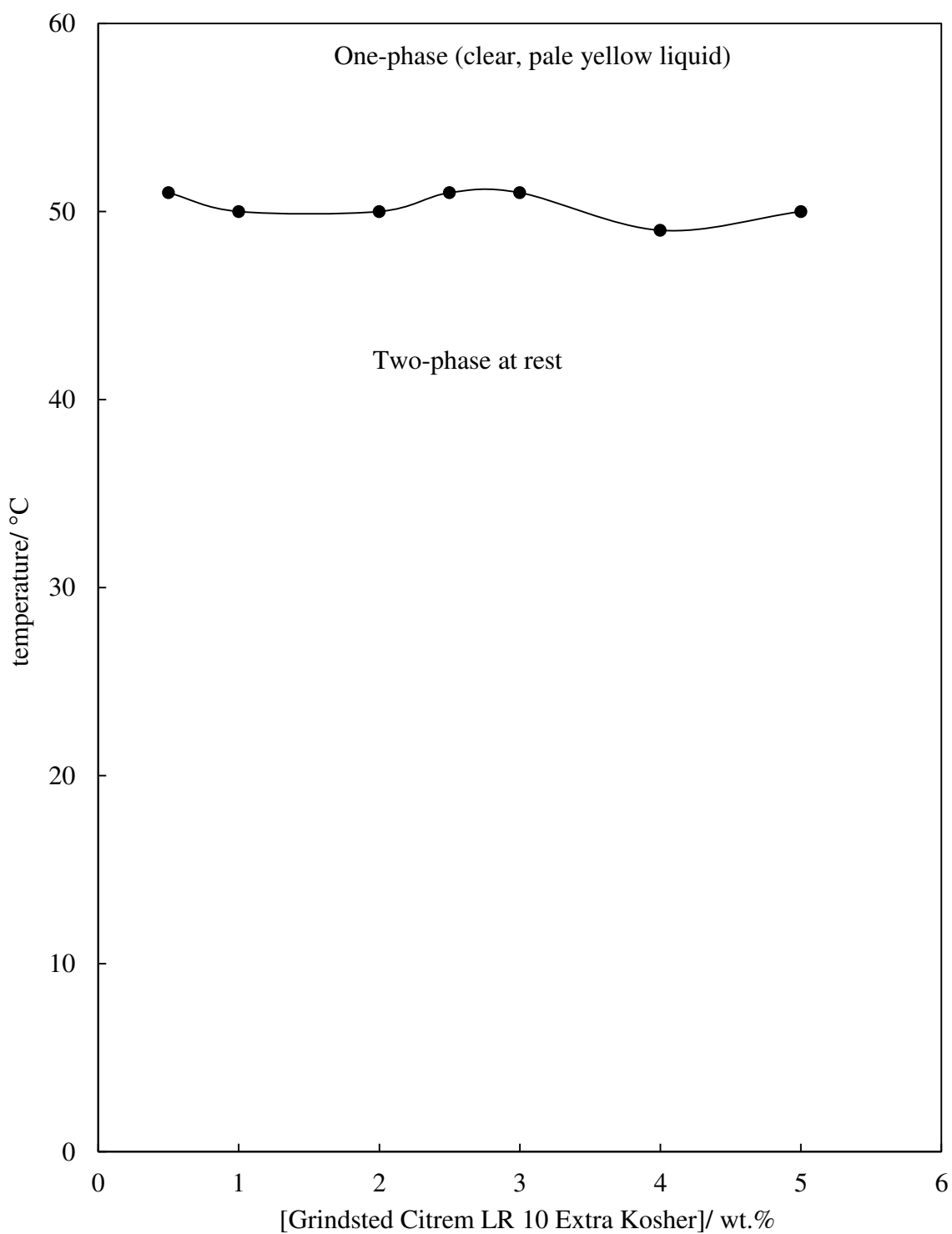
#### 4.2.1 Characterisation of surfactant in oil before aeration

The importance of the mixture prior to aeration was shown in the previous chapter where the presence of a molecular solution as well as the presence of birefringent crystals was able to aid the production of a foam with a stability of up to 4 days with the foaming column technique. Ross and Nishioka<sup>1,2</sup> and Binks et al.<sup>3</sup> have also shown that the solubility boundary is very important in the foamability of a mixture. In the studies it was found that a foam could be produced at the solubility temperature; when the conversion to two phases from one phase was imminent. Therefore, the solubility boundary of G. C. LR 10 in HOSO was determined along with microscopy at various concentrations at 25, 45 and 60 °C.

##### 4.2.1.1 Visual solubility determination

The mixture of surfactant and oil was heated from 20 °C at a rate of 1 °C/ min. until it became a clear homogeneous liquid (one-phase). It was then heated a further 5 °C, held for 5 minutes and then cooled at 1 °C/ min. until 40 °C where, at all the concentrations studied, the mixture was two-phase (a molecular solution and aggregate dispersion). The temperature at which the mixture became a clear homogeneous liquid was the dissolution temperature; the temperature at which the mixture was no longer clear was the precipitation temperature. As can be seen from Figure 4.2 these two temperatures were the same.

**Figure 4.2.** Visual solubility of G. C. LR 10 in HOSO heated at a rate of 1 °C/min. from 20 °C, then held for 5 minutes at 5 °C above the solubility line, then cooled 1 °C/min. to 40 °C.



#### 4.2.1.2 Microscopy

Figures 4.3 and 4.4 are microscopy images of 1-5 wt.% G. C. LR 10 in HOSO at various temperatures. It was found at 25 °C that prior heating to 60 °C did not have a significant effect on the aggregate appearance between 1 and 3 wt.% (Figure 4.3). However, at 4 and 5 wt.% at 25 °C with prior heating to 60 °C more surfactant aggregates were present which were smaller in size (aggregate diameter as high as 25 µm without prior heating). It is also clear from Figure 4.3 (d) that the surfactant aggregates were not birefringent crystals. Figure 4.4 shows that the aggregate diameter at between 1 and 5 wt.% at 45 °C was < 10 µm, therefore smaller than at 25 °C. Also, that at 60 °C at up to 5 wt.% the mixture was a clear homogeneous liquid with no aggregates present.

**Figure 4.3.** Optical microscopy of G. C. LR 10 in HOSO (a), (b), (c) and (d) at 25 °C, (e) and (f) at 25 °C after cooling from 60 °C. (d) is viewed through crossed polarising lenses. G. C. LR 10 concentrations are given in upper right of images. Scale bar 100  $\mu$ m.

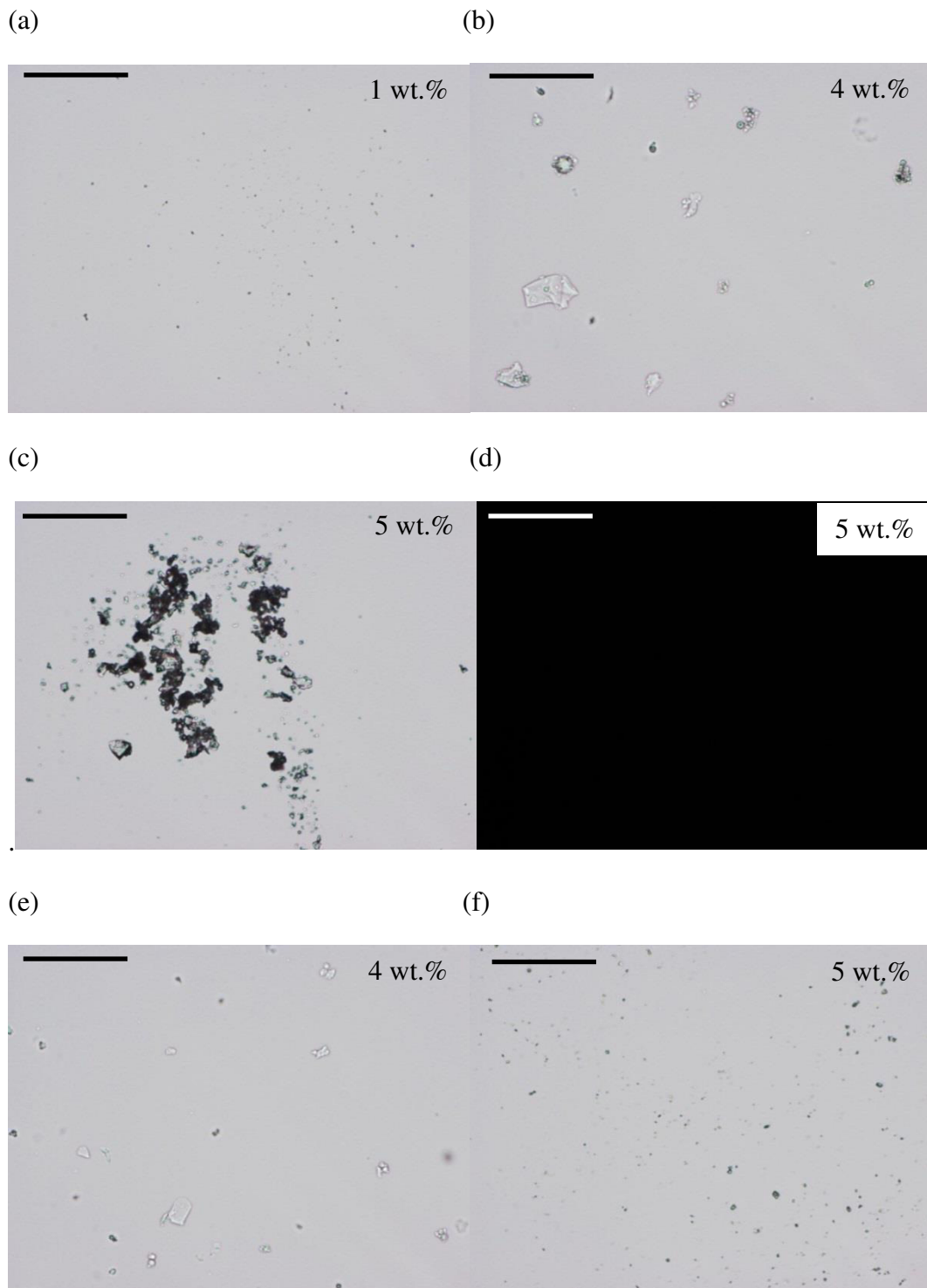
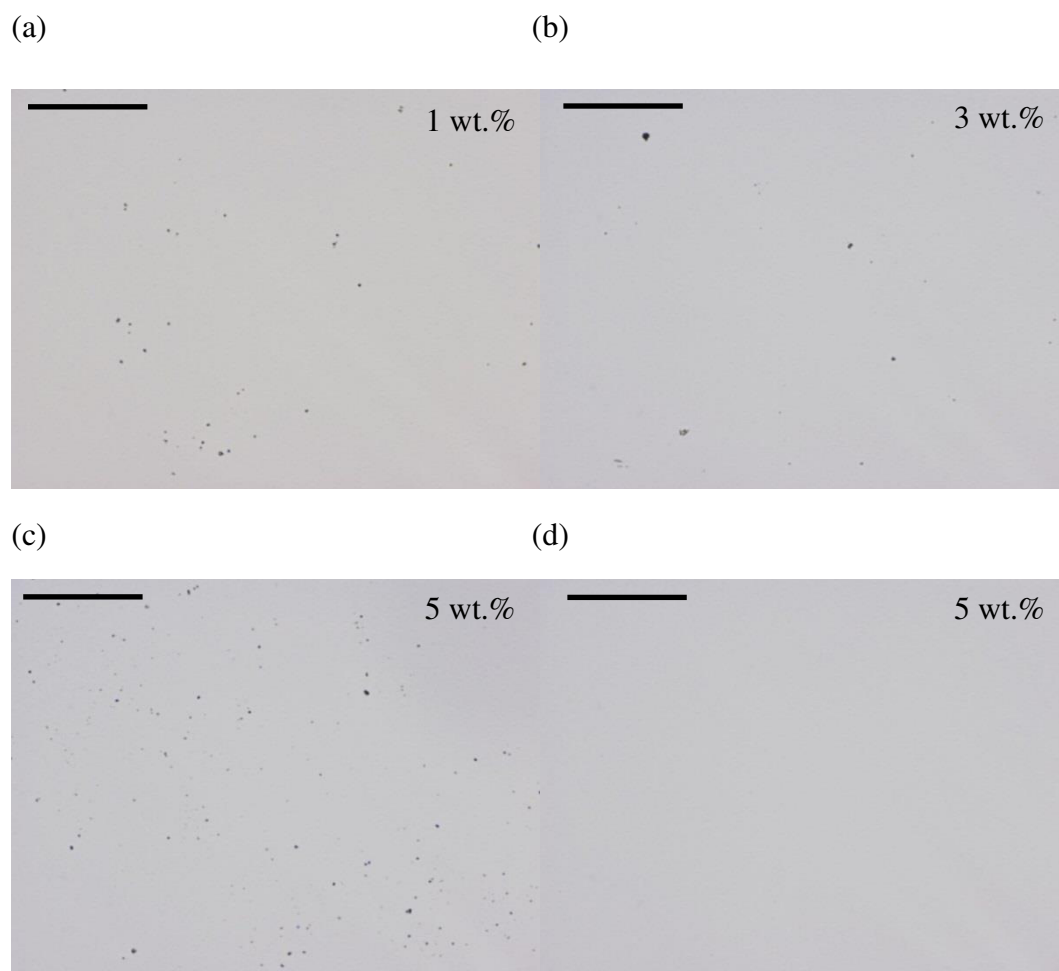


**Figure 4.4.** Optical microscopy of G. C. LR 10 in HOSO (a), (b) and (c) at 45 °C, (d) at 60 °C. G. C. LR 10 concentrations are given in upper right of images. Scale bar 100  $\mu$ m.



## 4.2.2 Aeration

Various concentrations of G. C. LR 10 in HOSO were aerated at numerous temperatures with different gases with both the foaming column and a soda siphon. The effect of these parameters on the initial foam volume, liquid drainage, foam half-life and total foam collapse was investigated along with any significant visual change. Optical microscopy of the foams was found to not be possible as the foam collapsed when transferring to a microscope slide.

### 4.2.2.1 Foaming column

Investigations into the foamability and any subsequent foam stability of G. C. LR 10 in HOSO were conducted with the foaming column. It was clear from the aeration of the Epikuron phospholipids in HOSO that the foaming column was an effective aeration method.

#### 4.2.2.1.1 Effect of concentration at 45 °C

From the visual solubility measurement it was decided that 1-5 wt.% G. C. LR 10 would be aerated with the foaming column for 5 minutes with compressed air at 45 °C. The mixture was aerated at 45 °C after heating to 60 °C as the mixture was two-phase and relatively close to the solubility boundary.

Figure 4.5 shows how, over time, the < 1 mm diameter spherical foam bubbles observed immediately after aeration gradually increased in size to 2-3 mm in diameter 30 minutes after the aeration. It was seen that the bubbles at the top of the foam column could increase to approximately 4 mm in diameter. The bubbles did deform over time to become polyhedral in shape with a diameter of up to 20 mm (mainly at the top of the foam column) with the majority of the bubbles remaining spherical at < 4 mm diameter. The increase in bubble size originates from coalescence and disproportionation.

Figure 4.6 shows the foam collapse profile of 1-5 wt.% G. C. LR 10 in HOSO aerated with compressed air at 45 °C via the foaming column. As the surfactant concentration increased the foamability remained between 400 mL and 460 mL, however the foam stability increased from approximately 50 minutes at 1 wt.% to over three days at 5

wt.%. The gradual foam collapse was typical of the mixture when it was aerated with this method. It can also be noticed that the foam volume did not reach zero at 4 and 5 wt.% by 3.5 days.

The liquid drainage from the foams produced is shown in Figure 4.7 at 5 wt.%. It was found that the majority of the liquid drained within approximately 30 minutes after aeration. This liquid drainage resulted in gradual foam collapse. The volumes of drained liquid and foam present were then constant until 5 hours after aeration at which 160 mL of foam collapsed and 10 mL of liquid was released causing the drained liquid to be at the original volume prior to aeration (200 mL). The remaining volume of foam (140 mL) then gradually collapsed over 3.5 days. It was found that after 3.5 days 40 mL of foam remained. In general, at the higher concentrations (2-5 wt.%), the foam collapse was relatively independent of the liquid drainage. This suggests that once the liquid drained the presence of the mono/diglyceride provided some stability to coalescence.

The half-life of the foam (time for half of the initial foam volume to collapse) is plotted in Figure 4.8. It is clear that the foam half-life was independent of concentration and relatively low up to 2 wt.%, it then dramatically increased up to 3 wt.%, then remained approximately the same with 4 and 5 wt.%.

Shrestha et al.<sup>4,7</sup> also found that non-aqueous foams could have a relatively high stability (up to a month). As the surfactant concentration increased the foamability increased by a small amount, but the foam stability increased significantly. It was stated that the increased stability of the foam was due to the presence of lamellar liquid crystal particles and also solid surfactant particulates. As the concentration increased the diameter of the solid surfactant particles decreased which possibly allowed better packing at the gas-liquid interface causing the foam to be more resilient to film rupture.

**Figure 4.5.** Appearance of 3 wt.% G. C. LR 10 in HOSO aerated with compressed air for 5 minutes at 45 °C (after prior heating to 60 °C) via the foaming column (a) immediately after aeration, (b) 30 minutes after aeration. Scale bar is 1 cm.

(a)

(b)

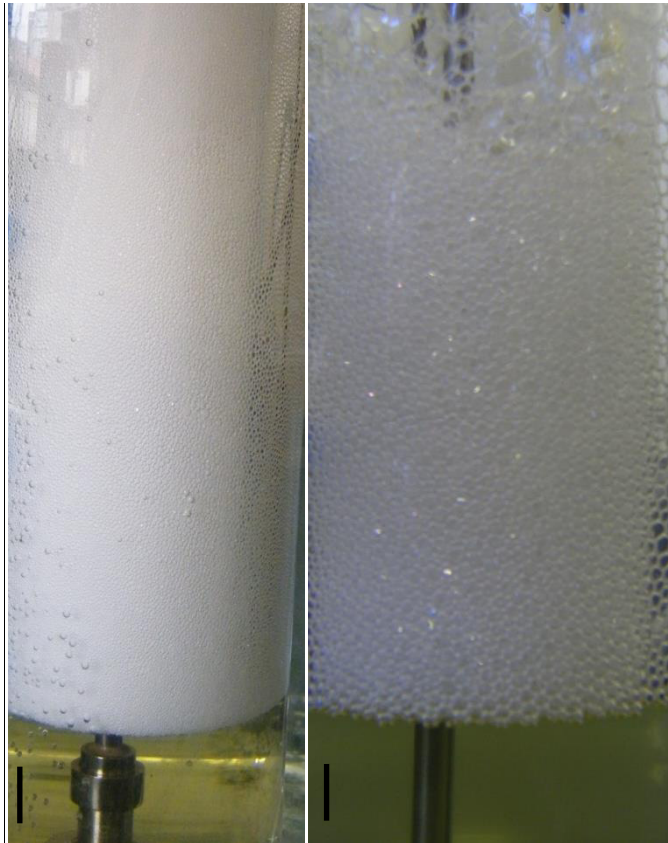


**Figure 4.6.** Foam collapse profile of G. C. LR 10 as a function of concentration in HOSO aerated with compressed air for 5 minutes with the foaming column at 45 °C (after prior heating to 60 °C).

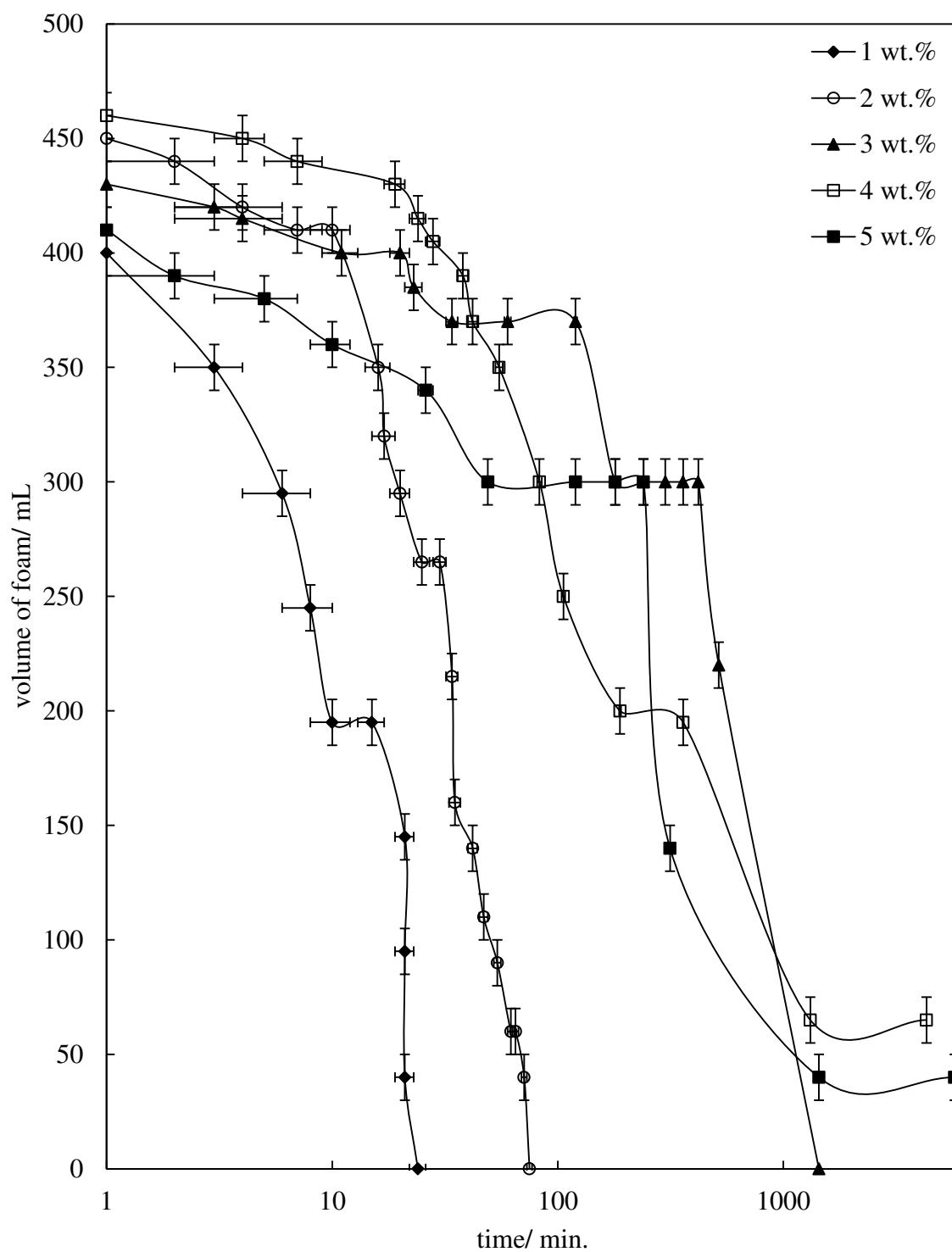


**Figure 4.7.** Foam collapse and liquid drainage of a foam produced with 5 wt.% G. C. LR 10 in HOSO at 45 °C (after prior heating to 60 °C). The aeration was for 5 minutes with compressed air via the foaming column.

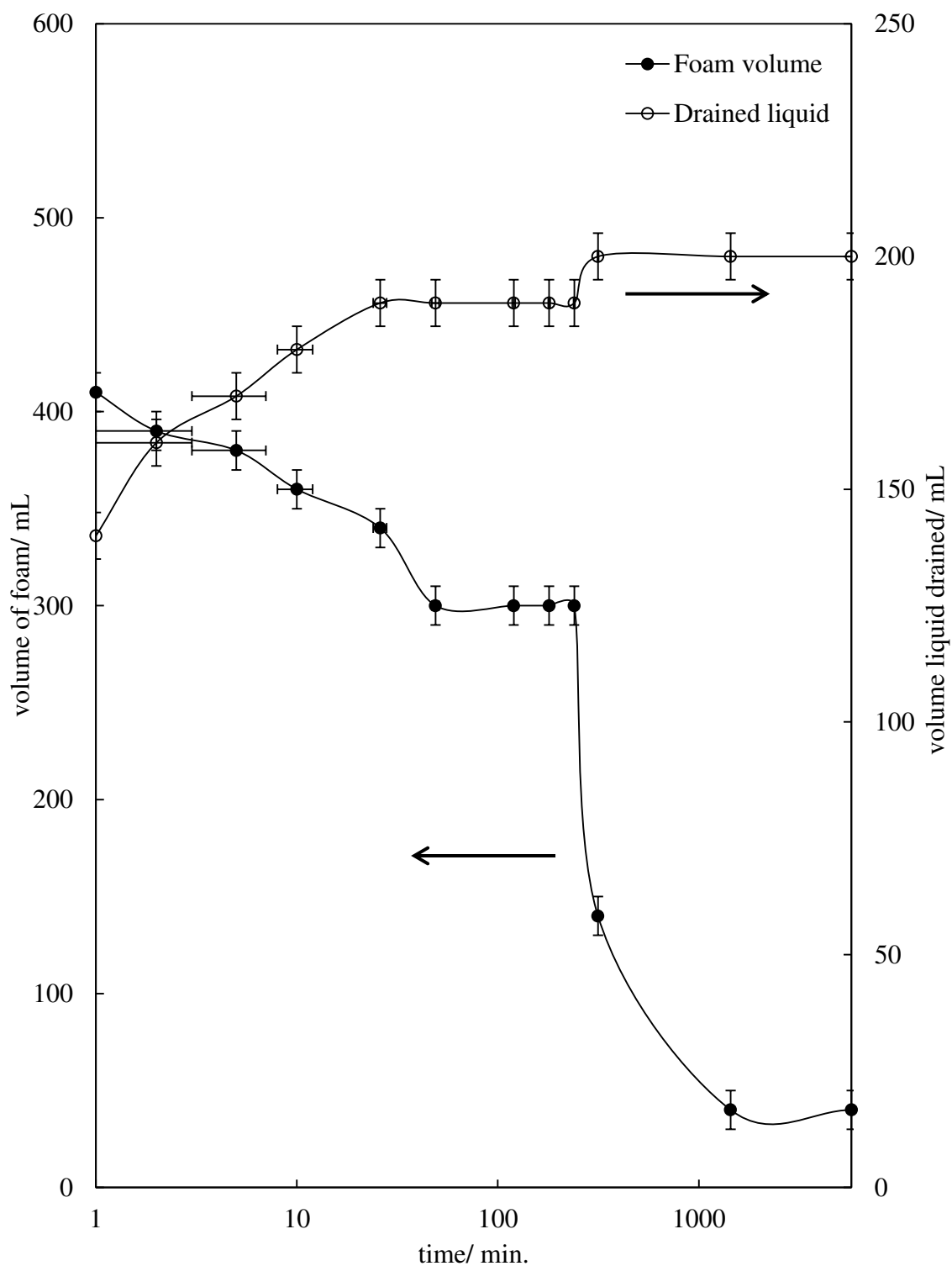
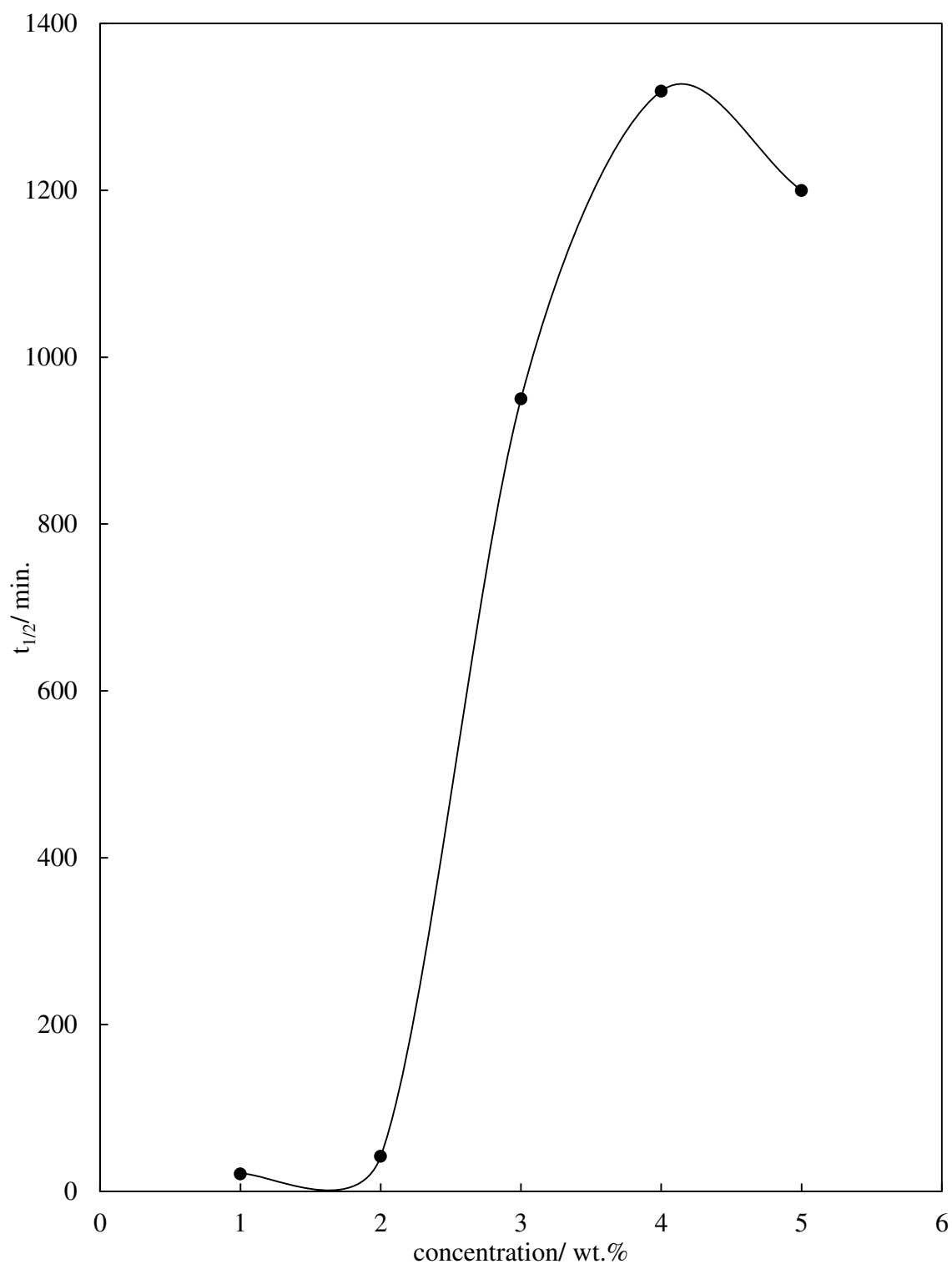


**Figure 4.8.** Half-life of the foam produced with G. C. LR 10 as a function of concentration in HOSO aerated with compressed air for 5 minutes with the foaming column at 45 °C (after prior heating to 60 °C).



#### 4.2.2.1.2 Effect of temperature

The effect of aeration temperature was investigated. It is known from visual solubility measurements that there was a phase boundary around 50 °C. Therefore, aeration was also conducted at 25 °C and 60 °C where the mixture was two-phase and one-phase respectively.

##### 4.2.2.1.2.1 Aeration at 25 °C and 45 °C

As shown in Figure 4.9 it was found that as the surfactant concentration increased the foamability, in general, was found to increase with aeration at 25 °C both with and without prior heating to 60 °C. At 3-5 wt.% surfactant, between 400 mL and 470 mL of foam was produced.

As can be seen from Figure 4.10 it was found that the foam stability was significantly higher at 25 and 45 °C than at 60 °C. The stability of the foam produced at 25 and 45 °C was found to increase from approximately 15 minutes at 1 wt.% to over a day with 4 wt.%, the stability was then found to remain constant with a further concentration increase to 5 wt.%. It was also found that the prior heating to 60 °C before aeration at 25 and 45 °C did not have a significant effect on the foam stability. The foam half-life is quoted rather than the time until complete foam collapse due to some of the foams being forcibly collapsed after several days. This shows that the foam stability was considerably higher than that observed with the phospholipids.

**Figure 4.9.** Initial foam volume of the foam produced from G. C. LR 10 as a function of concentration in HOSO aerated at various temperatures with compressed air for 5 minutes via the foaming column. Dashed horizontal line indicates that all the air that entered the system was incorporated into the mixture.

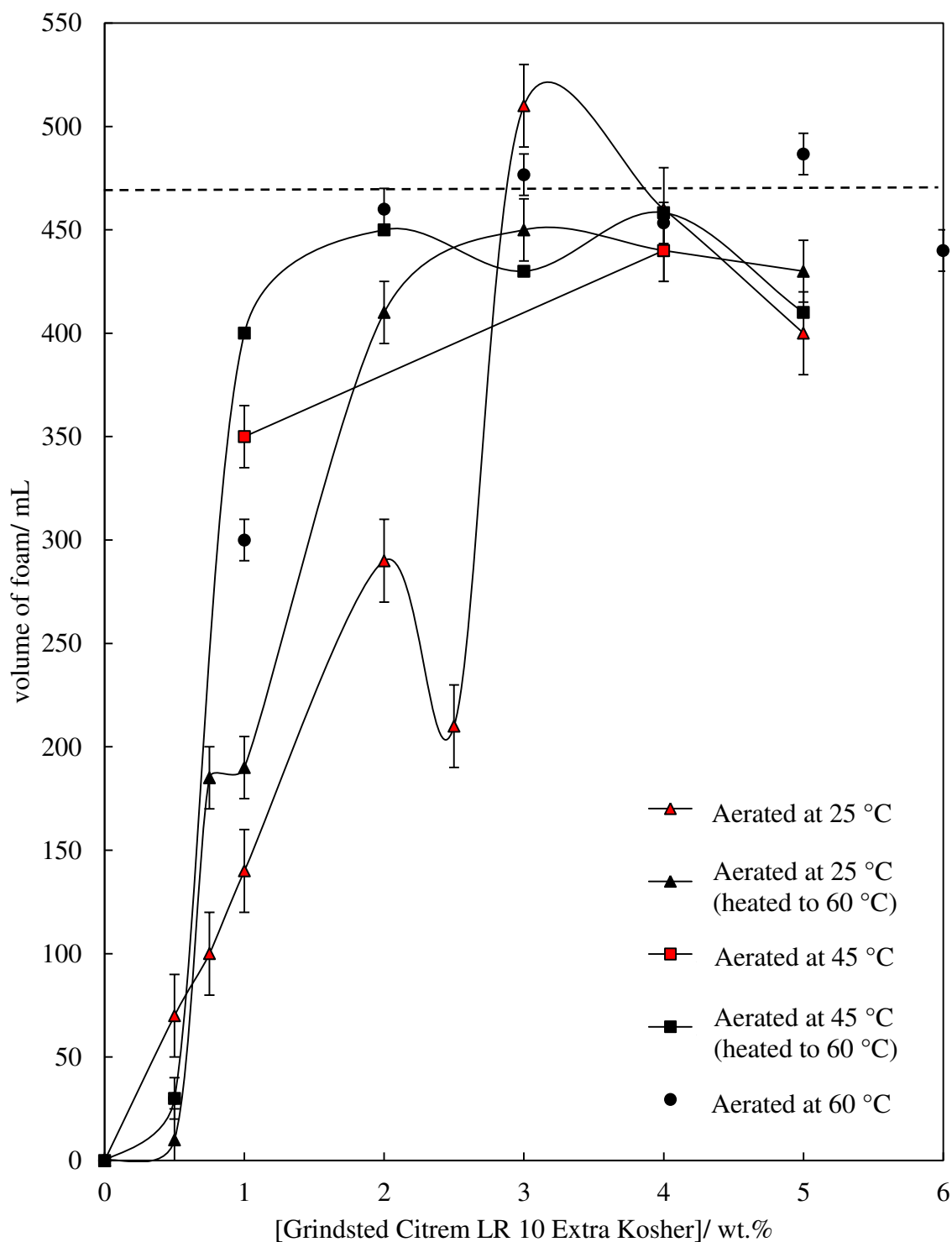
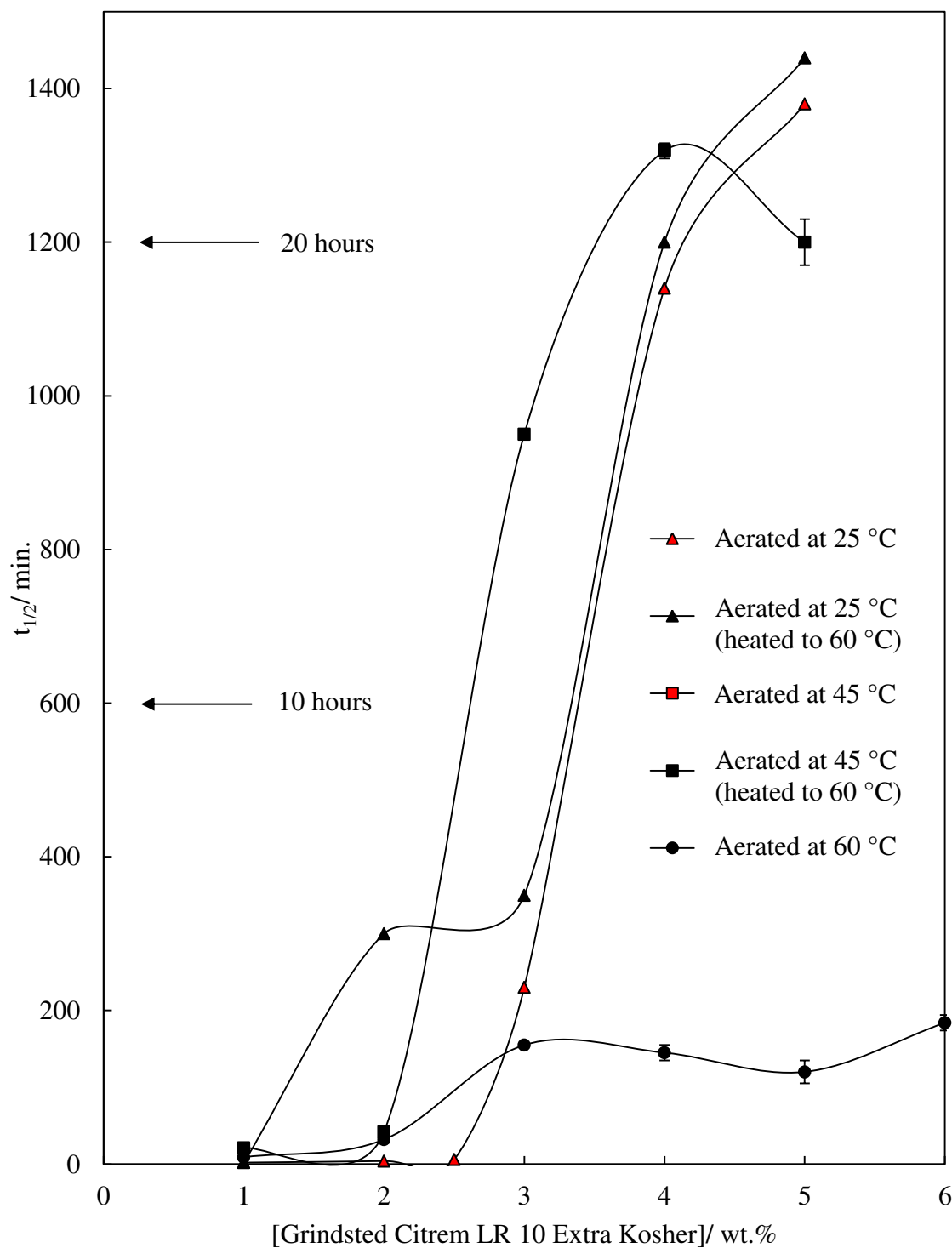


**Figure 4.10.** Half-life of the foam produced with G. C. LR 10 as a function of concentration in HOSO aerated for 5 minutes with compressed air via the foaming column at various temperatures.



#### 4.2.2.1.2.2 Aeration at 60 °C

Figure 4.9 shows that the foamability at 60 °C increased as surfactant concentration increased. A large amount of foam was produced which increased dramatically from zero to 460 mL with 0 to 2 wt.% surfactant present. A further increase in surfactant concentration from 2 to 5 wt.% kept the foamability between 450 and 490 mL. It can be concluded that temperature does not significantly affect the foamability of the system.

Figure 4.10 shows that as the surfactant concentration increased from 0 to 3 wt.% the half-life increased to 2.5 hours, the half-life then remained constant with a further increase to 6 wt.%. A half-life of 2.5 hours was significantly lower than the half-life of the foams produced at 25 and 45 °C as the half-life at these temperatures with 5 wt.% was approximately a day. This suggests that a solid surfactant particle dispersion was necessary for high stability of the foams. As shown in Figure 4.2, G. C. LR 10 in HOSO became soluble at  $50 \pm 1$  °C. Therefore, at 60 °C only surfactant molecules will be present at the gas-liquid interface which may explain the decrease in foam stability compared to the stability observed at 25 and 45 °C.

#### 4.2.2.1.2.3 Summary

In summary, as the concentration of G. C. LR 10 in HOSO increased at all the aeration temperatures the volume of foam produced generally increased. Prior heating to 60 °C before aeration at 25 °C and at 45 °C did not significantly affect the volume of foam produced. At concentrations of 3, 4 and 5 wt.% almost all of the air inputted into the system was incorporated into the mixture indicating a high foamability. The temperature of aeration significantly affected the foam stability. Aeration at 60 °C (when the mixture was a molecular solution) produced a foam that was found to have a half-life of several hours whereas at 25 and 45 °C the half-life was over a day (prior heating to 60 °C did not have an effect). It was clear that the presence of surfactant particles/aggregates was necessary for foam stability.

#### 4.2.2.1.3 Effect of gas type

The effect of the gas type was studied by aerating at 45 °C and 60 °C. CO<sub>2</sub> and N<sub>2</sub>O were used and the foam appearance, foamability and foam stability investigated. Figure 4.11 shows the appearance of 200 mL of 5 wt.% G.C. LR 10 in HOSO aerated at 45 °C immediately after aeration and 30 minutes after with air, CO<sub>2</sub> and N<sub>2</sub>O. The appearance of the foam produced with all three gases was similar (spherical bubbles of diameter < 1 mm). All foams change very little within 30 minutes.

Figure 4.12 shows the appearance of the foam produced with air, CO<sub>2</sub> and N<sub>2</sub>O with the foaming column at 60 °C immediately after aeration and 30 minutes after aeration. The foams were similar and comprised spherical bubbles of diameter < 1 mm. The foam appearance changed very little with CO<sub>2</sub> and air, although with N<sub>2</sub>O it was found that numerous cavities of foam almost 10 mm in diameter had collapsed.

##### 4.2.2.1.3.1 CO<sub>2</sub>

Figure 4.13 shows that aerating the mixture with CO<sub>2</sub> generated a large amount of foam. As the surfactant concentration was increased from 0 to 2 wt.% the amount of foam produced increased from 0 to 500 mL. The amount of foam produced then remained constant between 2-5 wt.%; this was found to be the case at both 45 °C and 60 °C. The stability of the foam at both temperatures was found to increase gradually from several minutes to almost 10 hours as the surfactant concentration increased from 1 to 5 wt.% (Figure 4.14). It was found that at 5 wt.% the foam stability at 45 °C was only approximately one hour longer than that observed at 60 °C. The time for total foam collapse was thus not significantly affected by the aeration temperature.

The half-life of the foam produced (Figure 4.15) also clearly showed the gradual increase in foam stability at both temperatures. The stability of the foam was similar to that observed at 60 °C with air.

**Figure 4.11.** Appearance of 5 wt.% G. C. LR 10 in HOSO immediately after aeration for 5 minutes at 45 °C with (a) compressed air, (b) CO<sub>2</sub> and (c) N<sub>2</sub>O immediately after aeration (upper) and 30 minutes after aeration (lower) via the foaming column. Scale bar 1 cm.

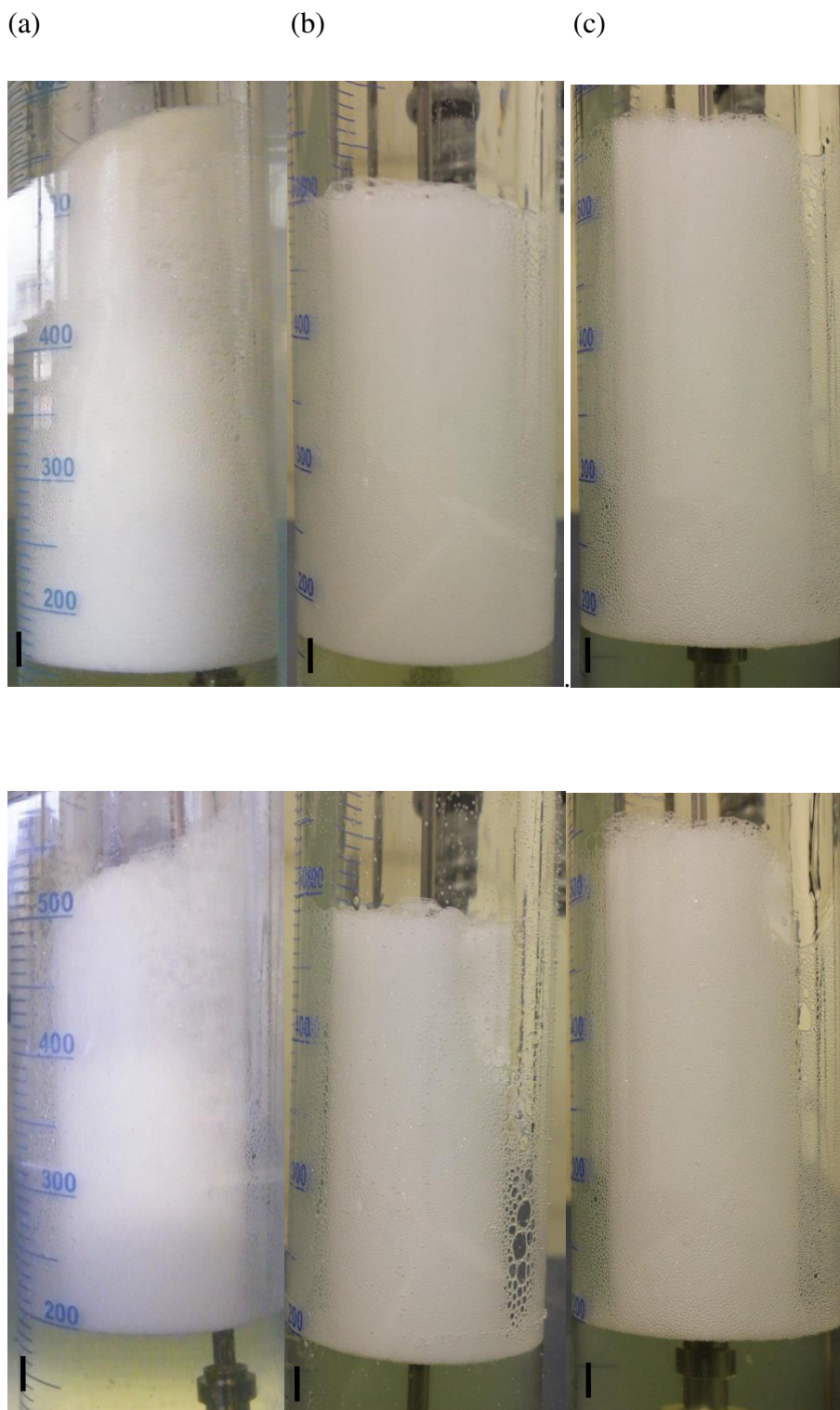


**Figure 4.12.** Appearance of 5 wt.% G. C. LR 10 in HOSO immediately after aeration for 5 minutes at 60 °C with (a) compressed air, (b) CO<sub>2</sub> and (c) N<sub>2</sub>O immediately after aeration (upper) and 30 minutes after aeration (lower) via the foaming column. Scale bar 1 cm.



**Figure 4.13.** Initial volume of foam produced with G. C. LR 10 as a function of concentration in HOSO aerated with compressed air, CO<sub>2</sub> and N<sub>2</sub>O for 5 minutes at 45 °C and 60 °C with the foaming column. Dashed horizontal line indicates that all the air that entered the system was incorporated into the mixture.

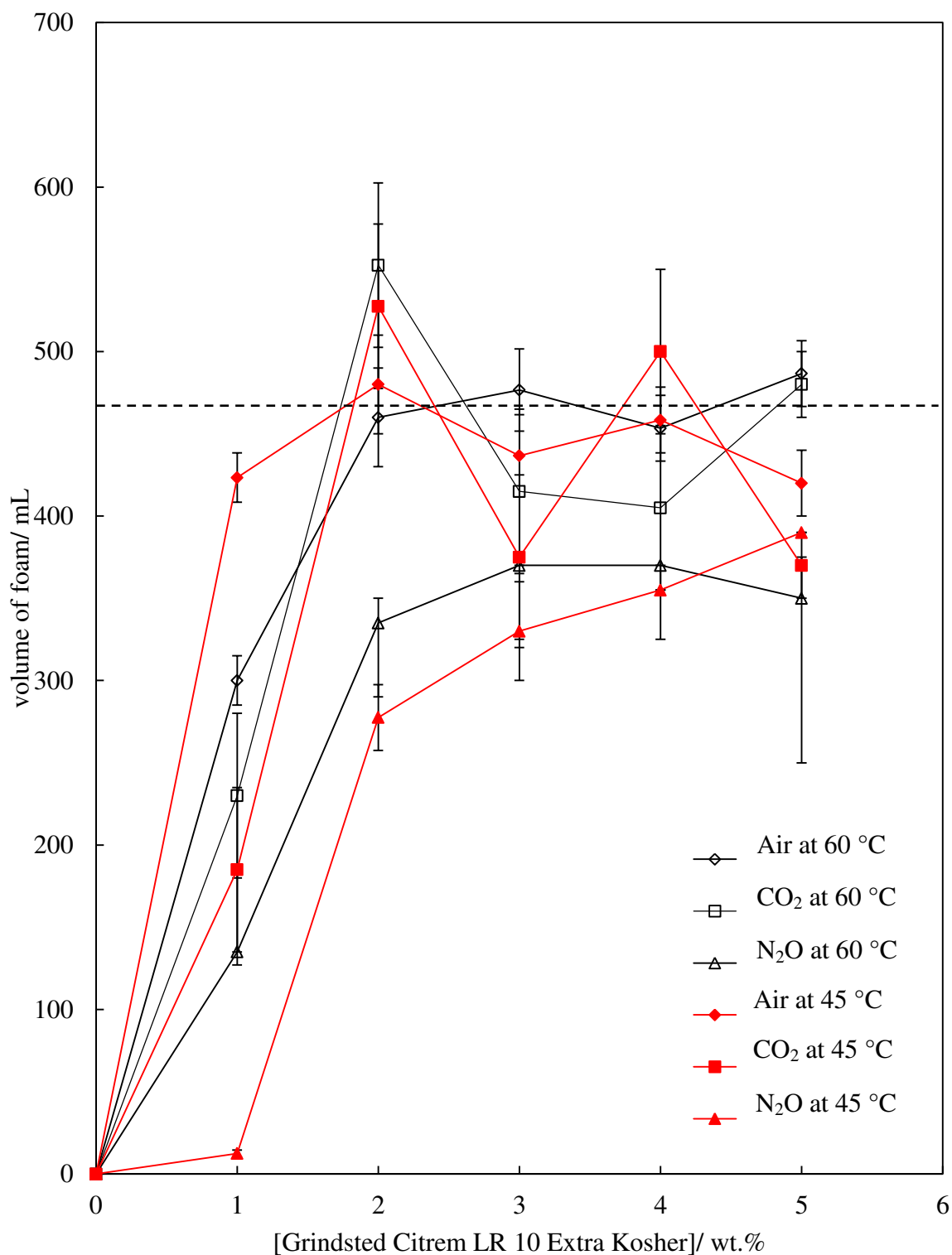
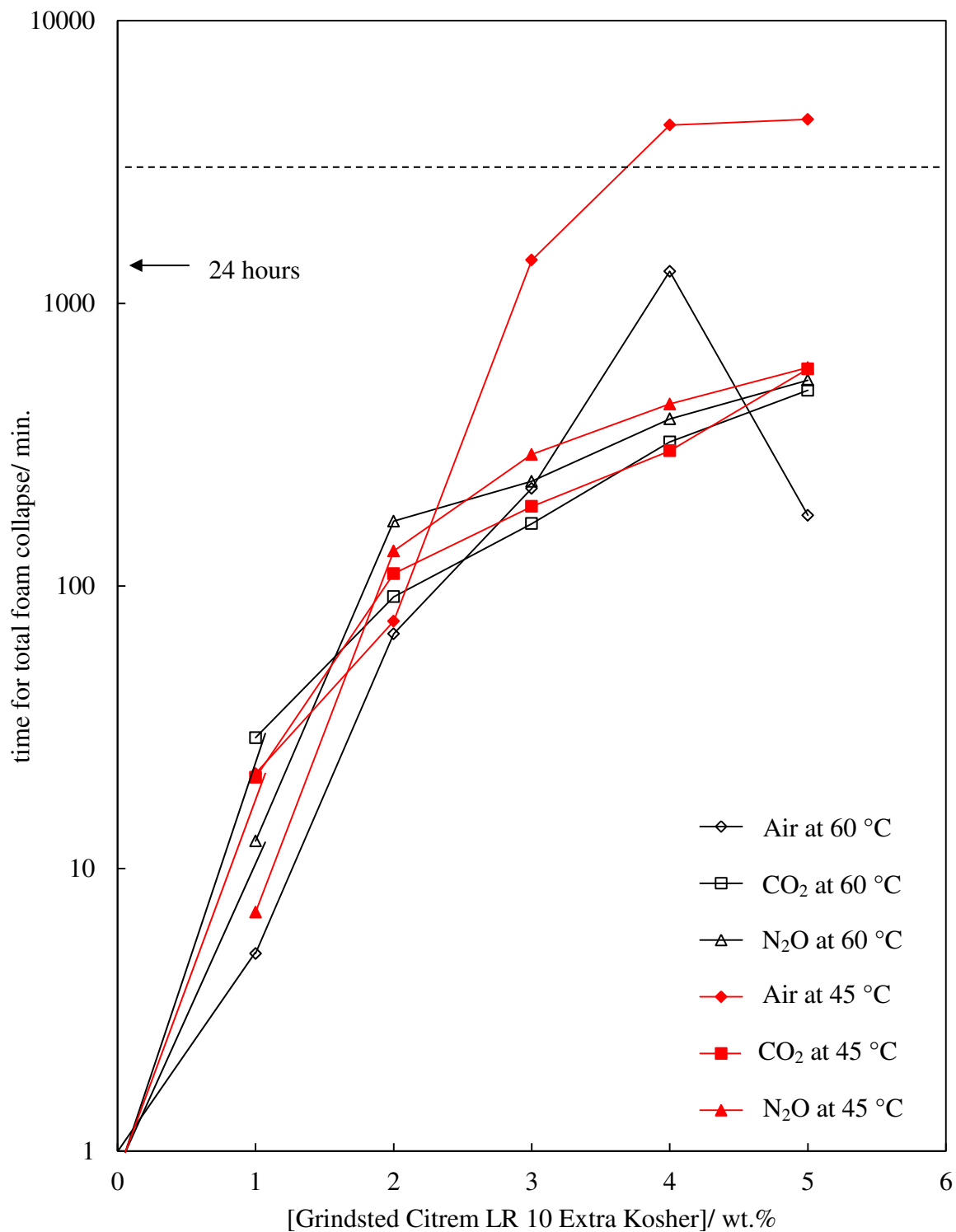


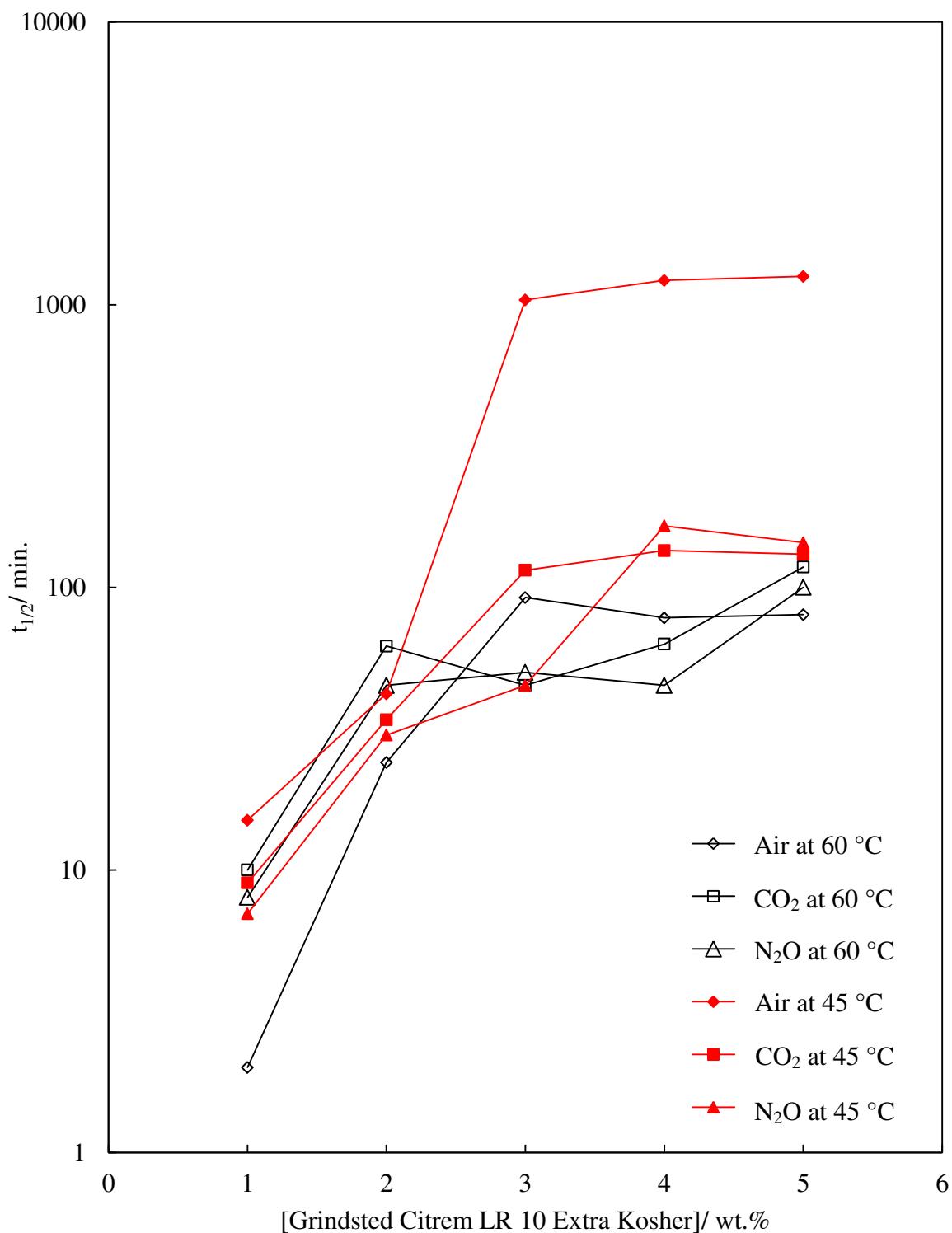
**Figure 4.14.** Time for total collapse of foams produced with G. C. LR 10 as a function of concentration in HOSO aerated with compressed air, CO<sub>2</sub> and N<sub>2</sub>O for 5 minutes at 45 °C and 60 °C with the foaming column. Above the dashed line the foam was forcibly collapsed through stirring.



#### 4.2.2.1.3.2 N<sub>2</sub>O

The foamability of G. C. LR 10 in HOSO aerated with N<sub>2</sub>O (Figure 4.13) was found to gradually increase with surfactant concentration; however, the increase in foamability was not as dramatic as that seen with compressed air and CO<sub>2</sub>. However, with a further increase of surfactant (2-5 wt.%) the foamability of the system did increase and then plateau (like with CO<sub>2</sub> and compressed air) although the overall foamability (360 ± 30 mL) was slightly lower than that observed with CO<sub>2</sub> and compressed air (375-550 mL). The foamability was not found to be affected by the aeration temperature. Figure 4.14 shows that the stability of foams produced with N<sub>2</sub>O increased as the surfactant concentration increased. The stability was not significantly affected by the aeration temperature which was shown clearly by the foam half-life (Figure 4.15). The half-life of a foam produced at 45 °C was found to collapse on average only 1 hour later than foams produced at 60 °C (at 4 and 5 wt.%).

**Figure 4.15.** Half-life of the foam produced with G. C. LR 10 as a function of concentration in HOSO aerated with compressed air, CO<sub>2</sub> and N<sub>2</sub>O for 5 minutes at 45 °C and 60 °C via the foaming column.



#### 4.2.2.1.3.3 Summary

The foamability of G. C. LR 10 in HOSO was not affected by temperature with any of the three gases studied. It was found that the foamability with N<sub>2</sub>O was slightly lower than that seen with compressed air and CO<sub>2</sub>. The stability of the foams produced with compressed air was affected by the aeration temperature with the foams produced at 45 °C being considerably more stable than the foams produced at 60 °C. The stability of foams produced with CO<sub>2</sub> and N<sub>2</sub>O were not significantly affected by the aeration temperature. This may be due to the CO<sub>2</sub> and N<sub>2</sub>O being more soluble in the continuous phase than air.<sup>8</sup> The gas solubility of N<sub>2</sub>, CO<sub>2</sub> and N<sub>2</sub>O in olive oil has been investigated by Snedden et al.<sup>8</sup> The gas solubility at 37 °C increased in the order of N<sub>2</sub> < CO<sub>2</sub> < N<sub>2</sub>O. Kubie<sup>9</sup> studied the solubility of N<sub>2</sub> and CO<sub>2</sub> in mineral oil and found also that CO<sub>2</sub> was more soluble than N<sub>2</sub>. Therefore, it is assumed that the high stability observed at 45 °C with compressed air may not be possible with CO<sub>2</sub> and N<sub>2</sub>O as disproportionation may have occurred at a faster rate inducing foam collapse through coalescence causing any effect of temperature to be limited.

#### 4.2.2.2 Soda siphon

G. C. LR 10 in HOSO was also aerated with a soda siphon with the effect of concentration, temperature and gas type investigated. The results could then be used to compare the foamabilities and foam stabilities produced with the foaming column. The concentrations studied were 1 to 5 wt.% at 25, 45 and 60 °C with CO<sub>2</sub>. The aerations were also conducted at 45 and 60 °C with N<sub>2</sub>O. The soda siphon technique was similar to the aeration technique used in the work conducted by Shrestha et al.<sup>4-7</sup> The gas was initially dissolved into the mixture (30 mL) which was then hand shaken for one minute. The gas was then released with any generated foam being poured into a vessel to be measured. Figure 4.16 for 3 wt.% surfactant shows the appearance of the foam immediately after pouring it into a measuring cylinder and then 30 minutes later. It shows that the spherical foam bubbles with thick foam lamellae were initially 2-3 mm in diameter (larger than the bubbles in the foams immediately after aeration with the foaming column). The foam gradually collapsed after liquid drainage had occurred (liquid drainage caused the foam lamella to become thinner) through coalescence and disproportionation. The bubbles increased in size to up to 5 mm in diameter, became polydisperse and polyhedral in shape. The foam was found to collapse in 5-10 mL sections; however larger foam sections (20-40 mL) were found to collapse after liquid drainage had occurred.

##### 4.2.2.2.1 Effect of concentration with CO<sub>2</sub> as gas

It is clear from Figure 4.17 that concentration had a significant effect on the amount of foam produced. At 1 and 2 wt.% there was approximately 90 mL of foam produced. The amount then increased to approximately 140 mL at 3 wt.%. The foam volume reached a maximum of 180 mL at 4 wt.% before decreasing to 140 mL at 5 wt.%. As can also be seen, as the surfactant concentration increased the foam stability increased. The foam produced collapsed sporadically with up to 50 mL collapsing at a time due to liquid drainage, shown in Figure 4.18. The liquid drained rapidly immediately after the foam was poured into the measuring cylinder causing rapid foam collapse until 20 minutes had elapsed. The liquid drainage then occurred gradually. When it did occur it caused a large amount of foam to then coalesce and collapse.

As shown in Figure 4.19, the half-life of the foam increased as the surfactant concentration increased. The stability increased from 6 minutes at 1 wt.% to 32 minutes at 5 wt.%.

**Figure 4.16.** Images of a foam produced with 3 wt.% G. C. LR 10 in HOSO aerated with a CO<sub>2</sub> cartridge in a soda siphon at 45 °C. Image (a) is immediately after the foam was poured in a measuring cylinder from the soda siphon and (b) 30 minutes after. Scale bar 1 cm.

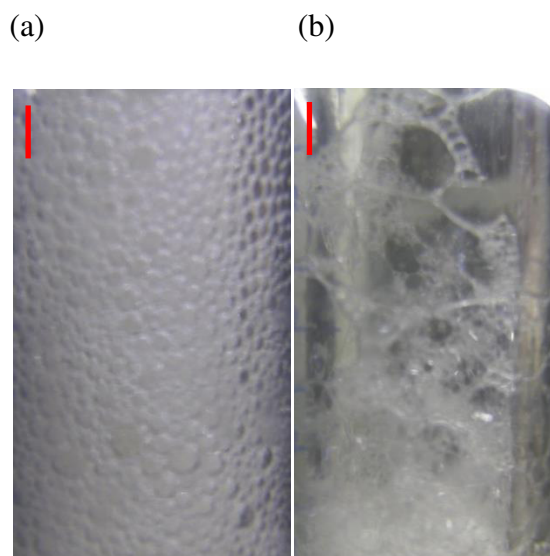


**Figure 4.17.** Foam collapse profile of G. C. LR 10 as a function of concentration in HOSO at 45 °C aerated in a soda siphon with a CO<sub>2</sub> cartridge.

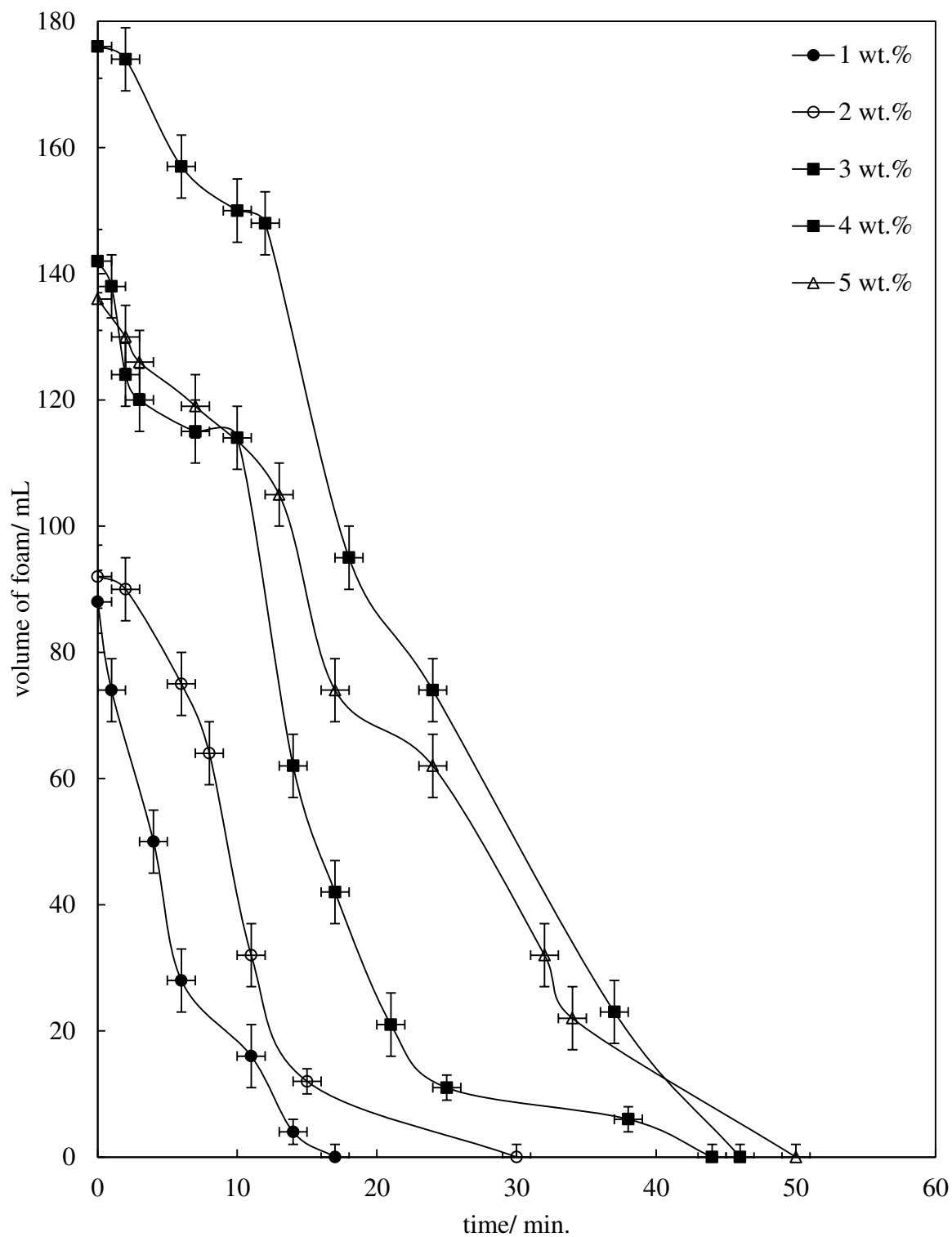


**Figure 4.18.** Foam collapse and liquid drainage of a foam produced with 5 wt.% G. C. LR 10 in HOSO aerated at 45 °C in a soda siphon with a CO<sub>2</sub> cartridge.

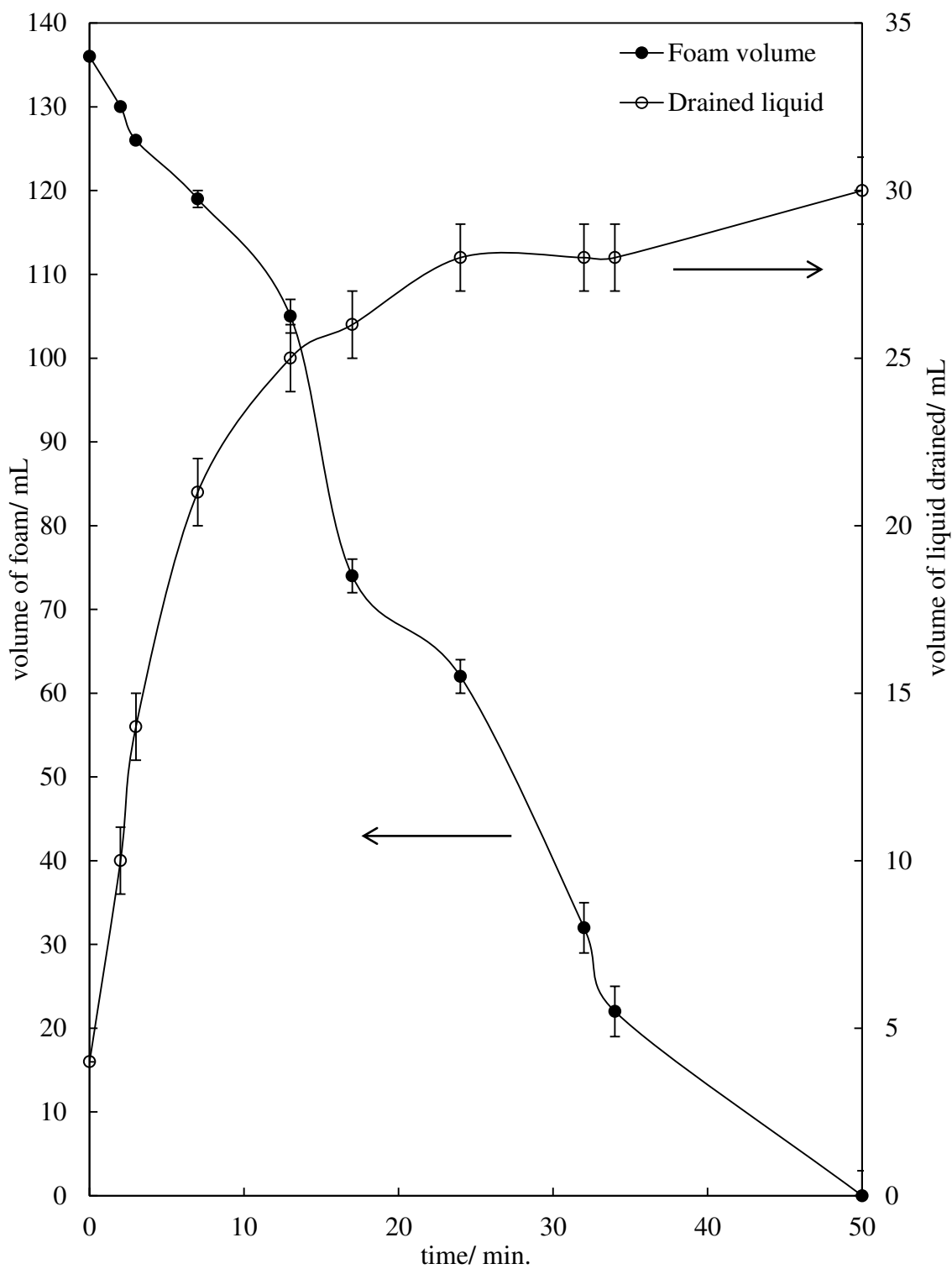
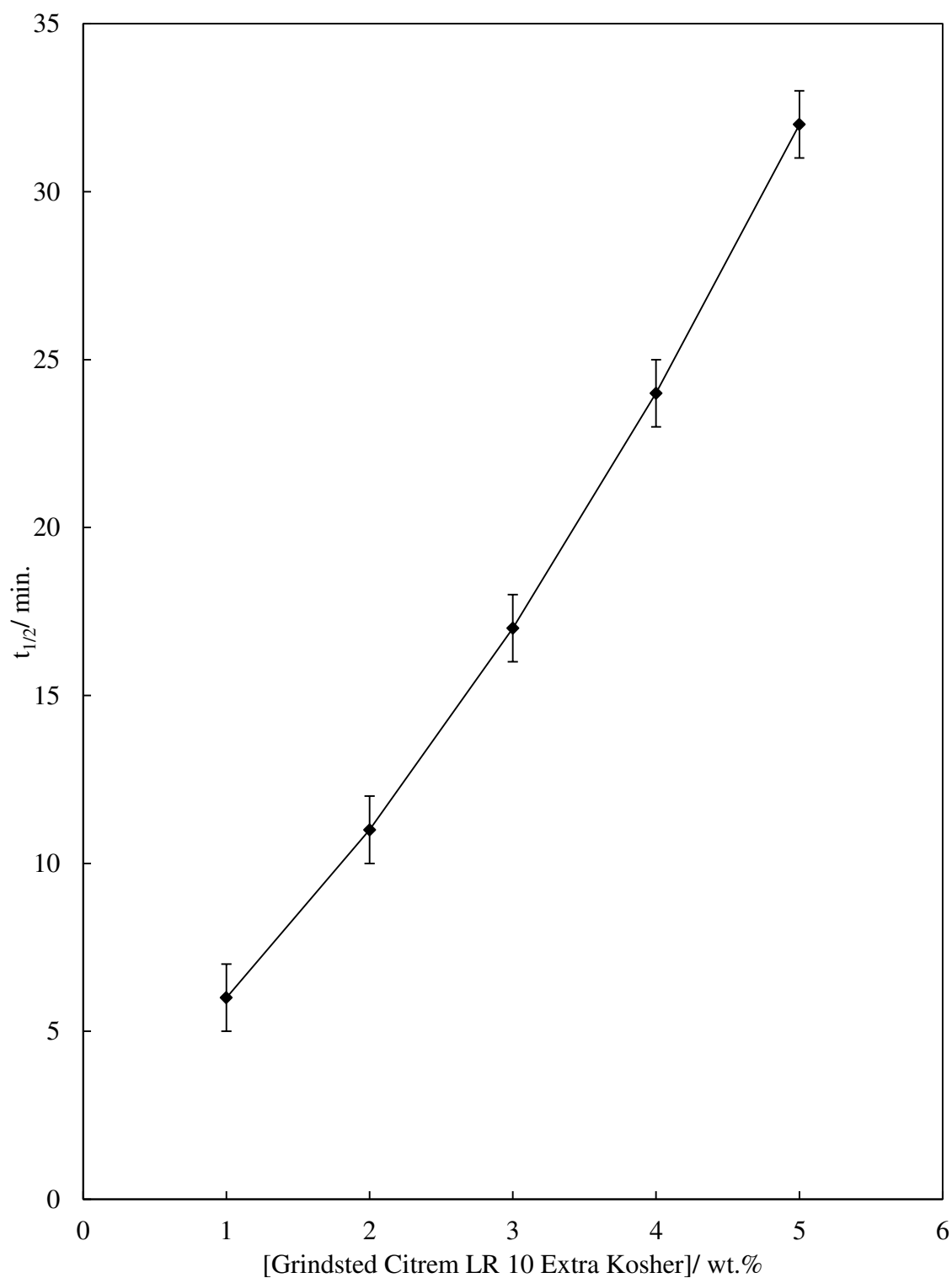


**Figure 4.19.** Half-life of the foam produced with G. C. LR 10 as a function of concentration in HOSO aerated at 45 °C in a soda siphon with a CO<sub>2</sub> cartridge.



#### 4.2.2.2.2 Effect of temperature

The effect of the aeration temperature on the foamability and foam stability of G. C. LR 10 in HOSO with the soda siphon with CO<sub>2</sub> was studied. The aerations were conducted at 25 °C, and 60 °C as well as at 45 °C to investigate the effect of aerating the mixture in the one-phase and two-phase regions. The results could then be compared to that obtained with the foaming column.

##### 4.2.2.2.2.1 Aeration at 25 °C

The amount of foam produced with G. C. LR 10 in HOSO was found to increase as the surfactant concentration increased; however as can be seen in Figure 4.20 the foamability did not increase linearly. The amount of foam produced with 5 and 6 wt.% was between 140-200 mL at 25 °C both with and without prior heating to 60 °C indicating that the prior heating to 60 °C did not affect the foamability.

The foam stability increased a large amount as the surfactant concentration increased from 1-2 wt.% from 1 minute to 2 hours for complete foam collapse (Figure 4.21). The foam stability at 25 °C increased with a further concentration increase to 6 wt.% where the foam fully collapsed after 24 hours. The foams produced at 25 °C after prior heating to 60 °C had a significantly higher stability than foams produced at 25 °C without heating. The foam produced at 1 wt.% was stable for 90 minutes, as the concentration increased to 6 wt.% the stability increased dramatically to over 6 days where 29 % of the foam remained.

Figure 4.22 demonstrates that, in general, as the surfactant concentration increased the half-life increased. There was clearly a decrease in the foam half-life at 4 and 5 wt.%. This was because a large amount of foam (30 mL) spontaneously collapsed causing the half-life to be lower than expected. Figure 4.17 shows that relatively large sections of the foam produced with the soda siphon can collapse at the same time. Figure 4.22 also shows that the aeration at 25 °C with prior heating to 60 °C has a significantly higher foam half-life than at 25 °C without heating. This increase in foam stability was thought to be due to the aggregates being more in number and smaller due to the heating and then cooling prior to aeration (the effect of heating and cooling on the aggregates is shown earlier by microscopy). This difference may cause the aggregates to arrange at the bubble surface more favourably. The effect was not observed with the foaming

column. This is thought to be because the aeration method with the soda siphon involves more disruption to the foam, therefore the enhanced stability of the foam by the amount of aggregates and their size became more pronounced.

**Figure 4.20.** Initial volume of foam produced with G. C. LR 10 as a function of concentration in HOSO at various temperatures aerated with a soda siphon with CO<sub>2</sub>.

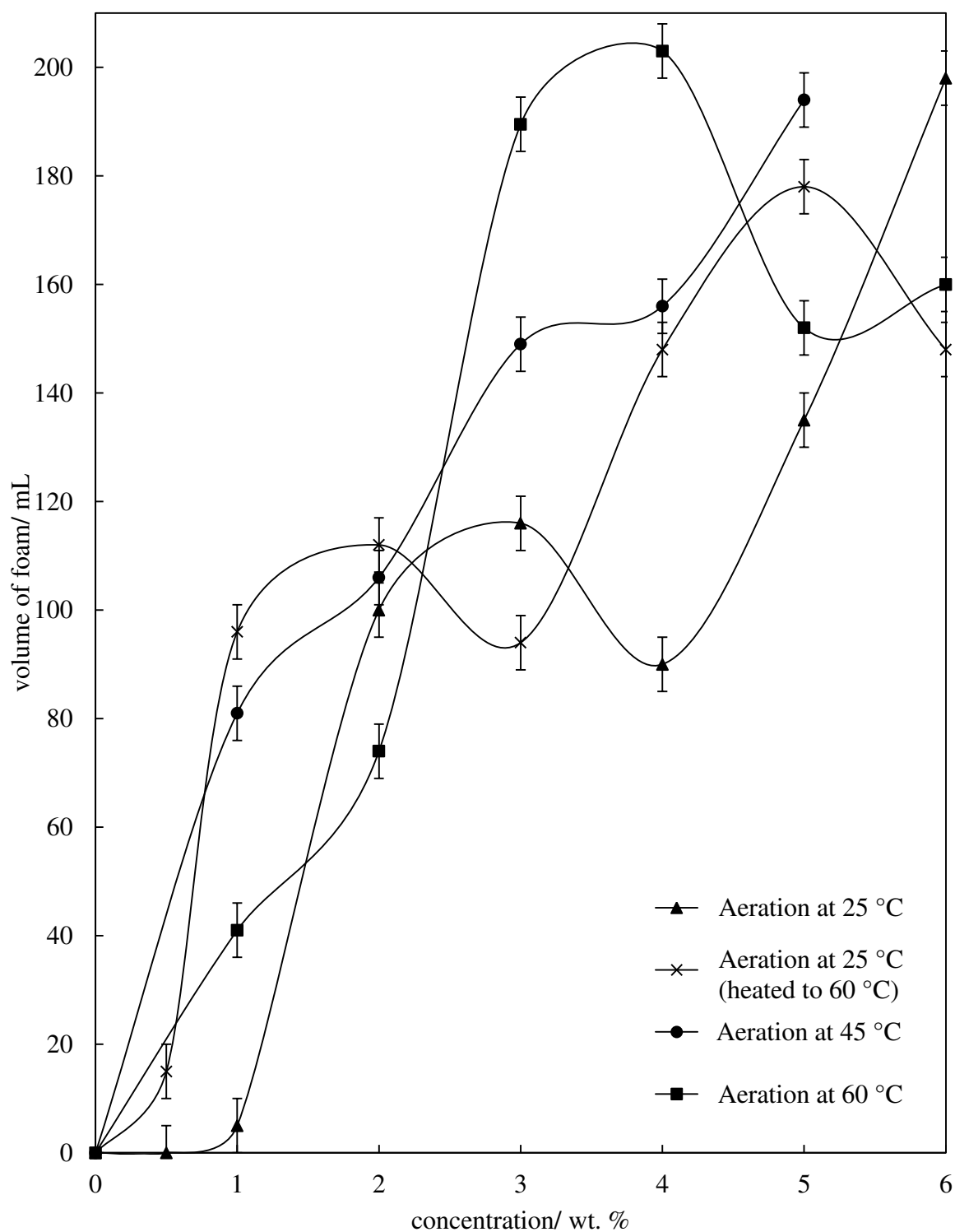


**Figure 4.21.** Time for total foam collapse of the foam produced from G. C. LR 10 as a function of concentration in HOSO at various temperatures aerated with a soda siphon with CO<sub>2</sub>. Above the dashed line is the percentage of residual foam remaining at the designated time prior to forcible collapse.

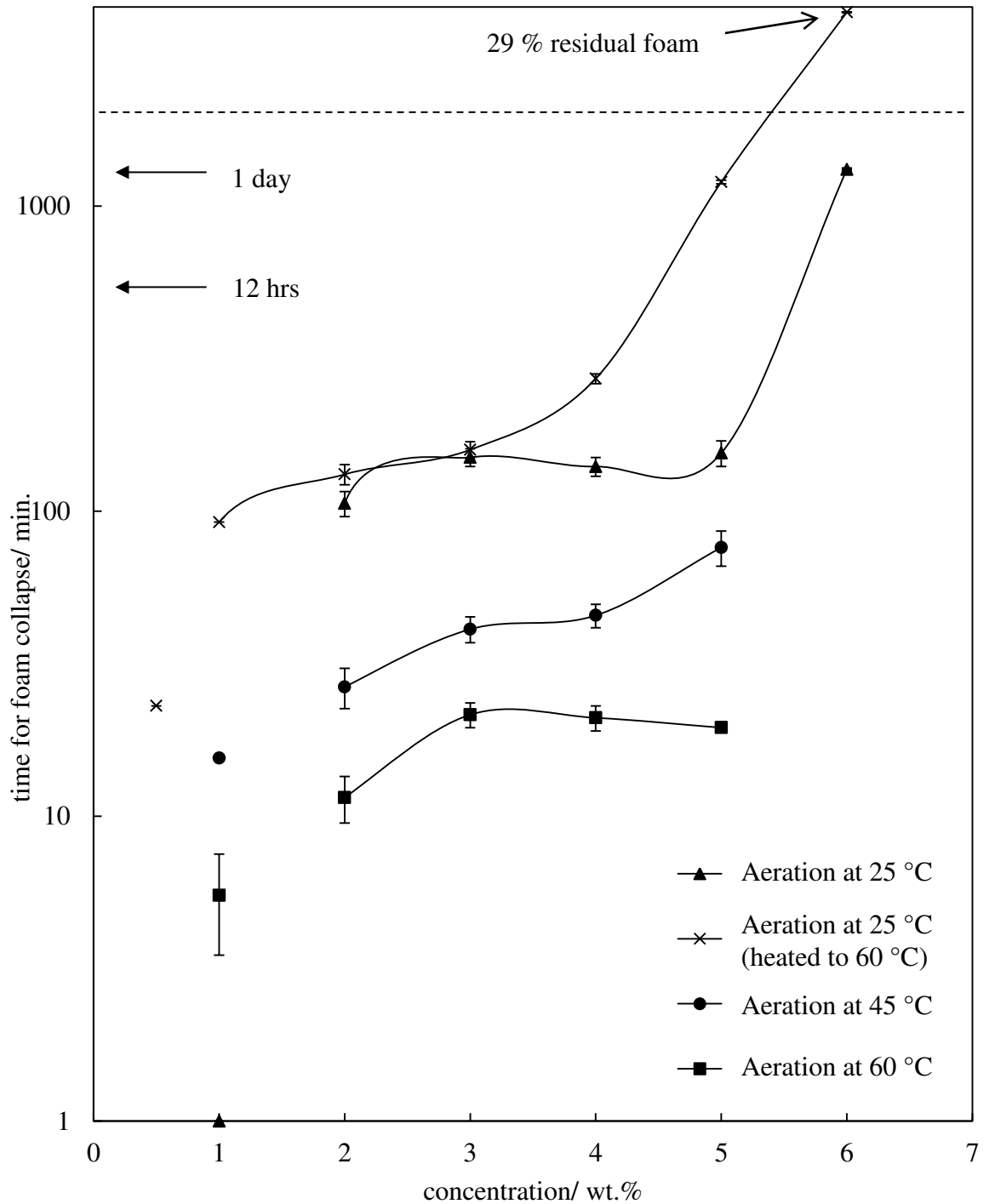
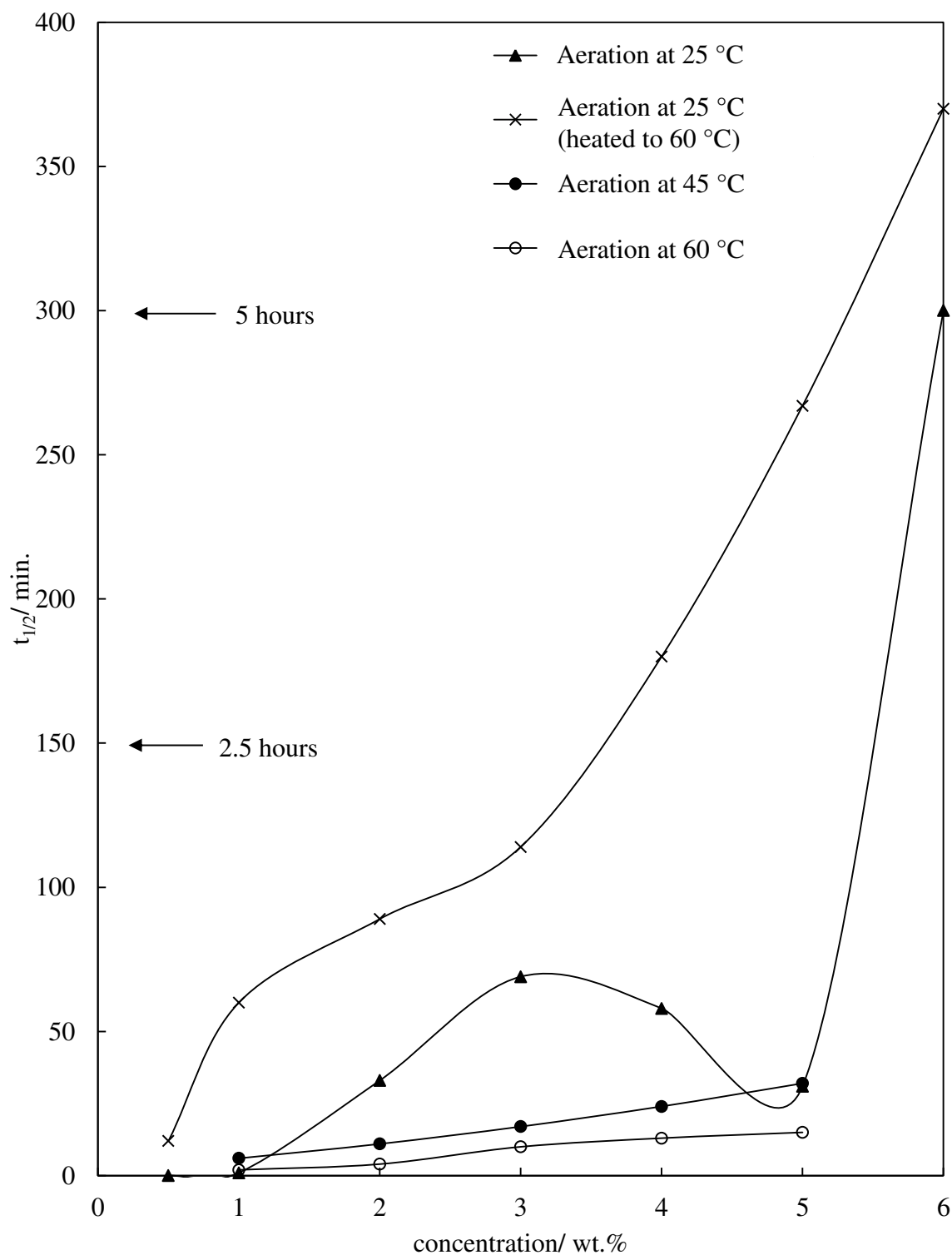


**Figure 4.22.** Half-life of the foam produced with G. C. LR 10 as a function of concentration in HOSO aerated with a soda siphon with CO<sub>2</sub> at various temperatures.



#### 4.2.2.2.2.2 Aeration at 60 °C

Figure 4.20 shows that foamability generally increased with an increase in surfactant concentration, however, the foamability did fluctuate a large amount. The fluctuations were thought to be due to the method used, as pouring the mixture from the soda siphon into the measuring cylinder could cause some of the foam to collapse. The stability of the foam produced at 60 °C was found to be surprisingly low (with 5 wt.% the foam fully collapsed within 20 minutes) as shown in Figure 4.21. The half-life of the foam produced at 60 °C is demonstrated in Figure 4.22. The figure shows that the half-life gradually increased to 10 minutes as the surfactant concentration increased to 3 wt.%; the half-life plateaus at 15 minutes between 4 and 6 wt.%.

#### 4.2.2.2.2.3 Summary

In summary the aeration temperature did not have an effect on the foamability of the mixture. However, there was a clear effect on the foam stability; as temperature increased there was a decrease in the foam stability. Therefore, the most stable foams were produced at 25 °C, the least stable foams were produced at 60 °C. This may be because as the temperature increased the viscosity decreased causing the rate of liquid drainage to increase and the foam to collapse due to disproportionation and coalescence.

#### 4.2.2.2.3 Effect of gas type

The effect of aerating G.C. LR 10 as a function of concentration in HOSO with N<sub>2</sub>O at 45 °C and 60 °C was studied. It is clear from Figure 4.23 and Figure 4.24 that the foam produced consisted of spherical bubbles which were 2-3 mm in diameter. After 10 minutes it was found, particularly at 60 °C, that the bubbles had become significantly larger in diameter with polydisperse bubbles ranging from 2 mm to as high as 20 mm.

Figure 4.25 shows that the foamability of the G. C. LR 10 in HOSO increased as the surfactant concentration increased at both 45 °C and 60 °C with N<sub>2</sub>O gas. The foamability was not affected by the aeration temperature. The stability of the foam was found to increase as the surfactant concentration increased at 45 °C as shown in Figure 4.26. The stability of the foam produced at 60 °C increased at 0 to 3 wt.%, then remained constant with a further increase. It was clear that the foam was more stable at 45 °C than at 60 °C which was also shown in Figure 4.27 with the foam half-life.

##### 4.2.2.2.3.1 Summary

As can be seen from Figure 4.25 the gas type did have an effect on the foamability of the mixture. The volume of foam produced with the CO<sub>2</sub> was found to be greater than that produced with the N<sub>2</sub>O by at least 50 mL at 3-5 wt.%. This may be because N<sub>2</sub>O is more soluble in the oil, therefore upon release of the dissolved gas from the soda siphon CO<sub>2</sub> more readily leaves the oil than N<sub>2</sub>O generating more foam. Snedden et al.<sup>8</sup> have found that N<sub>2</sub>O is more soluble in olive oil than CO<sub>2</sub>, this may also be the case in HOSO. Figure 4.26 and Figure 4.27 show clearly that the temperature of aeration did have an effect on the foam stability, however gas type did not.

**Figure 4.23.** 5 wt.% G. C. LR 10 in HOSO aerated with the soda siphon with CO<sub>2</sub> at 45 °C (a) immediately after pouring the aerated mixture into a measuring cylinder, (b) after 10 minutes, and at 60 °C (c) immediately after pouring the aerated mixture into the measuring cylinder, (d) after 10 minutes. Scale bar 1 cm.

(a)

(b)

(c)

(d)

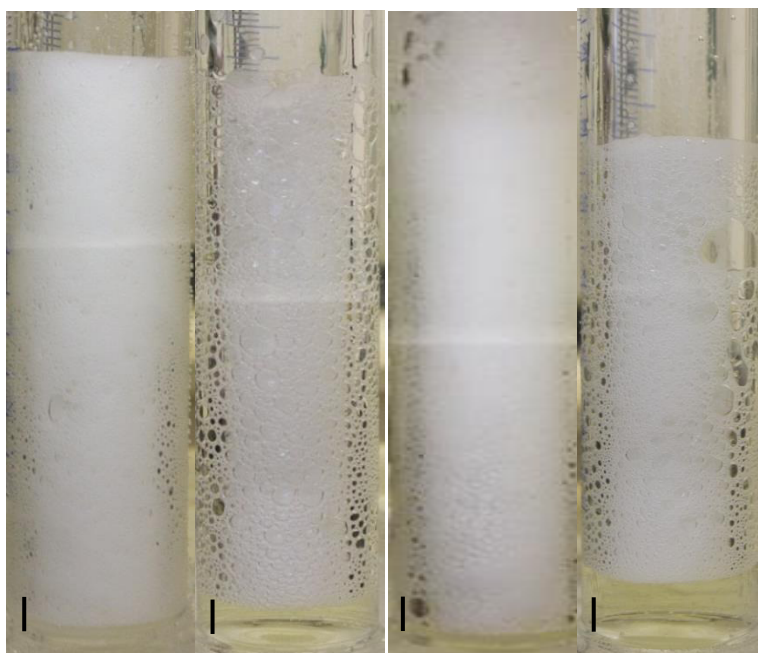


**Figure 4.24.** 5 wt.% G. C. LR 10 in HOSO aerated with a soda siphon with  $N_2O$  at 45 °C (a) immediately after the aerated mixture was poured into the measuring cylinder, (b) after 10 minutes, and at 60 °C (c) immediately after the aerated mixture was poured into the measuring cylinder, (d) after 10 minutes. Scale bar 1 cm.

(a)            (b)            (c)            (d)

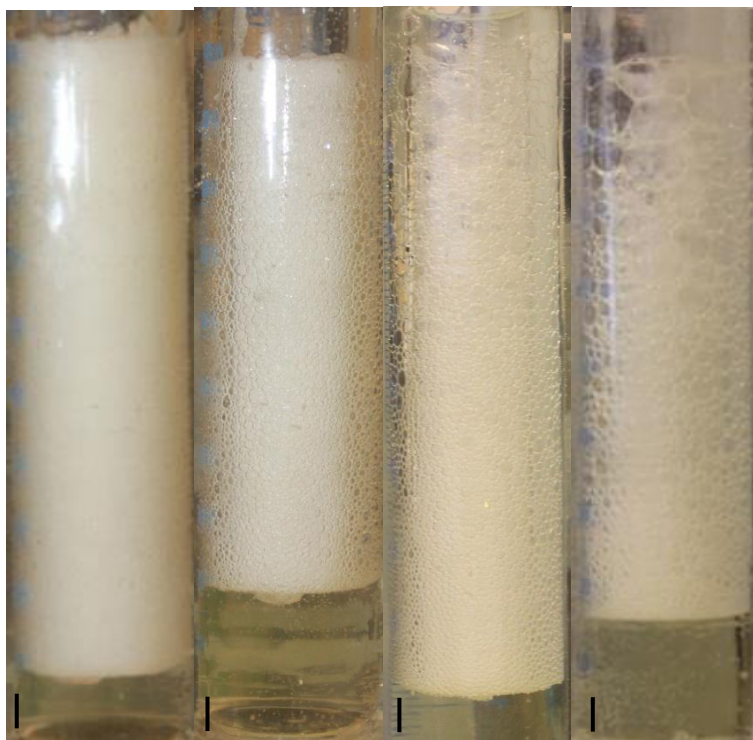


**Figure 4.25.** Initial foam volume of the foam produced with G. C. LR 10 as a function of concentration in HOSO aerated with the soda siphon with CO<sub>2</sub> and N<sub>2</sub>O at 45 and 60 °C.

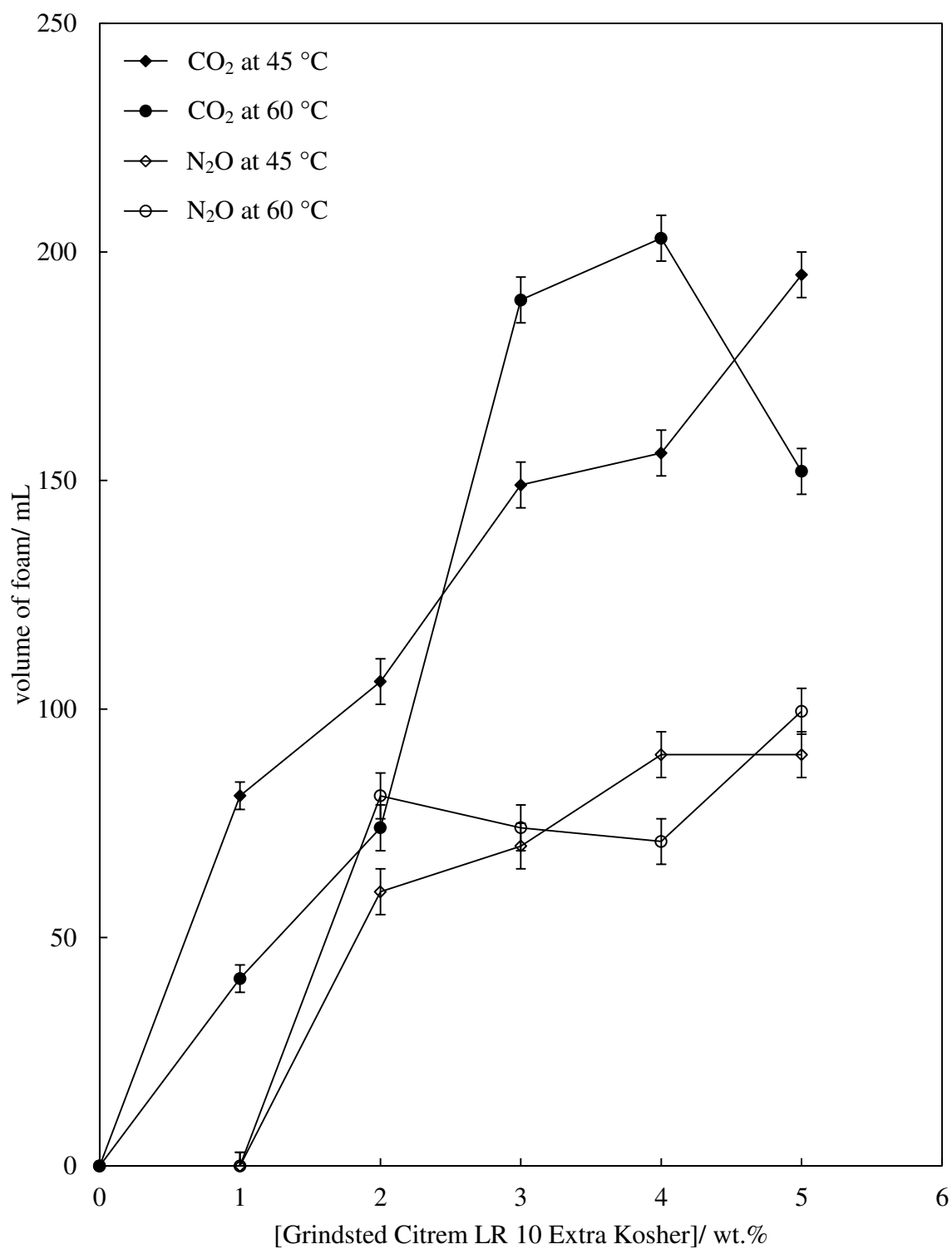


**Figure 4.26.** Time for total foam collapse of the foam produced with G. C. LR 10 as a function of concentration in HOSO aerated with a soda siphon with CO<sub>2</sub> and N<sub>2</sub>O at 45 and 60 °C.

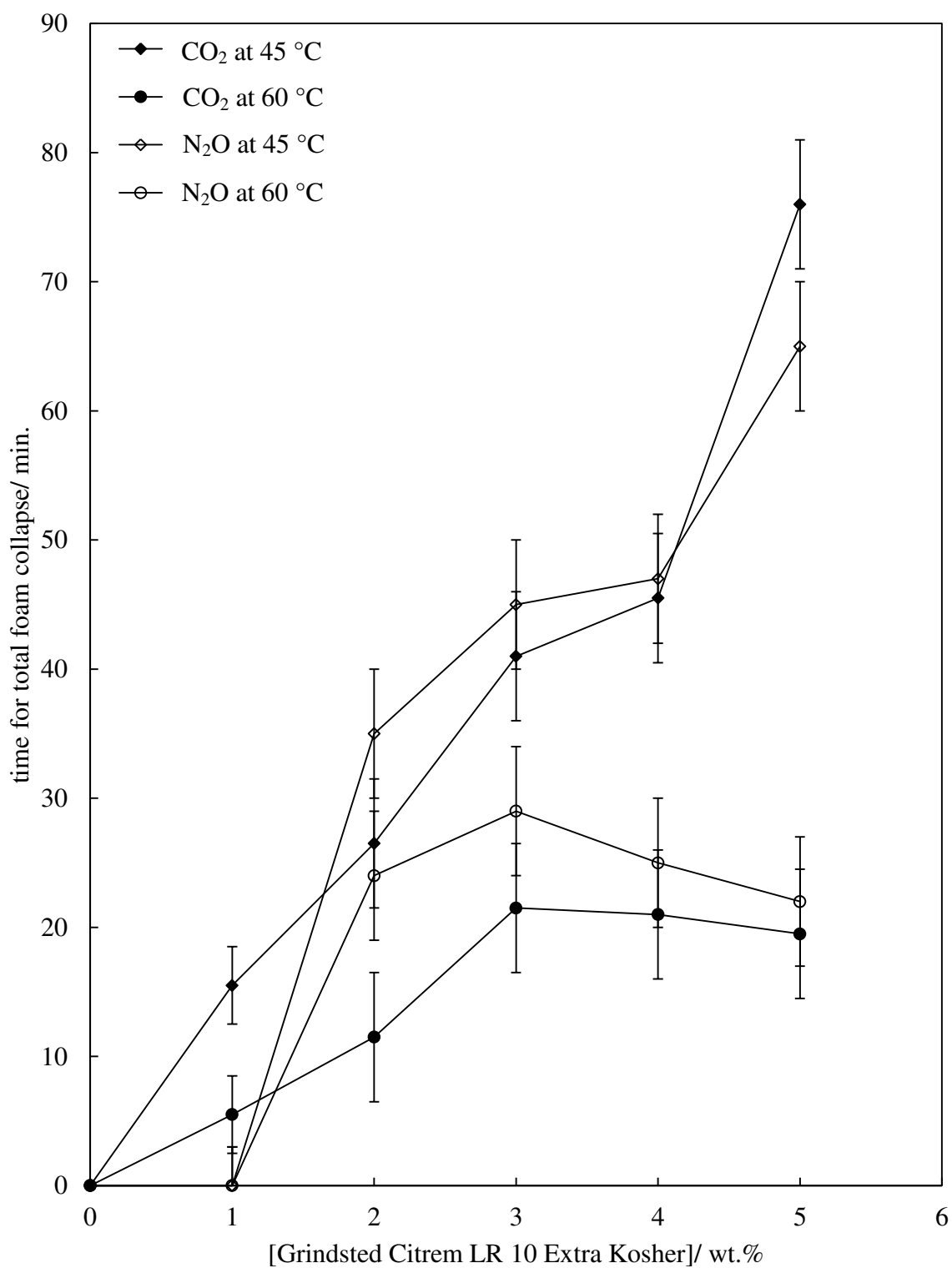
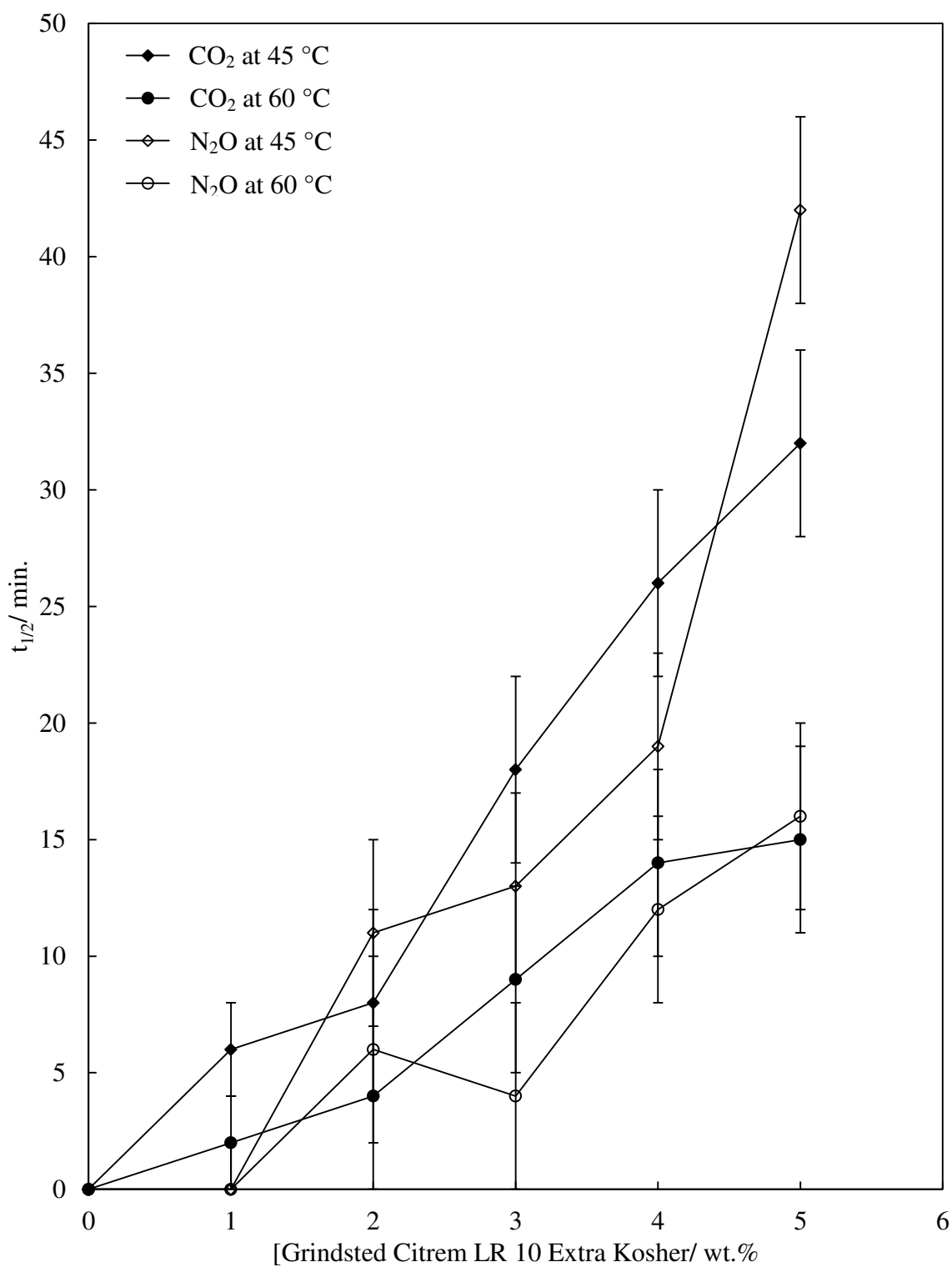


**Figure 4.27.** Half-life of the foam produced with G. C. LR 10 as a function of concentration in HOSO aerated with a soda siphon with CO<sub>2</sub> and N<sub>2</sub>O at 45 and 60 °C.



### 4.3 Saturated mono/diglyceride in high oleic sunflower oil

A saturated surfactant (Grindsted Citrem N12 veg) in HOSO was then investigated to understand what the difference in structure may have on foamability and foam stability. Grindsted Citrem N12 veg (G. C. N12 veg) in HOSO was initially analysed with differential scanning calorimetry (DSC) to determine the solubility boundary of the mixture. With this knowledge the system was then aerated at selected temperatures with gas sparging, the foaming column and the whipping technique.

#### 4.3.1 Characterisation

The G. C. N12 veg both with and without HOSO was characterised by DSC to determine the melting temperature and phase behaviour.

##### 4.3.1.1 Differential scanning calorimetry

The DSC curve for neat HOSO is given in Figure 4.28 and for neat G. C. N12 veg in Figure 4.29. Neat HOSO does not have a peak across the temperature range of 10 °C to 80 °C indicating that it is liquid. Figure 4.29 for neat G. C. N12 veg was where the sample was cooled from 80 °C at 5 °C/min. to 10 °C, held at 10 °C for 5 minutes, then heated to 80 °C at 2 °C/min. It can be seen that there were two temperatures of crystallisation and one temperature (with a shoulder) where the mixture melted. As shown in Figure 4.30 as the concentration of the G. C. N12 veg in HOSO increased, the melting and crystallisation peaks occurred at increasing temperature. The peaks are labelled as crystallisation peak 1 (Tc 1) and 2 (Tc 2) and melting peak 1 (Tm). The two crystallisation peaks indicate the presence of different crystal polymorphs.

**Figure 4.28.** DSC of neat HOSO with a protocol of cooling from 80 °C to 10 °C (5 °C/ min.), held at 10 °C for 5 minutes, then heating to 80 °C (2 °C/ min.).

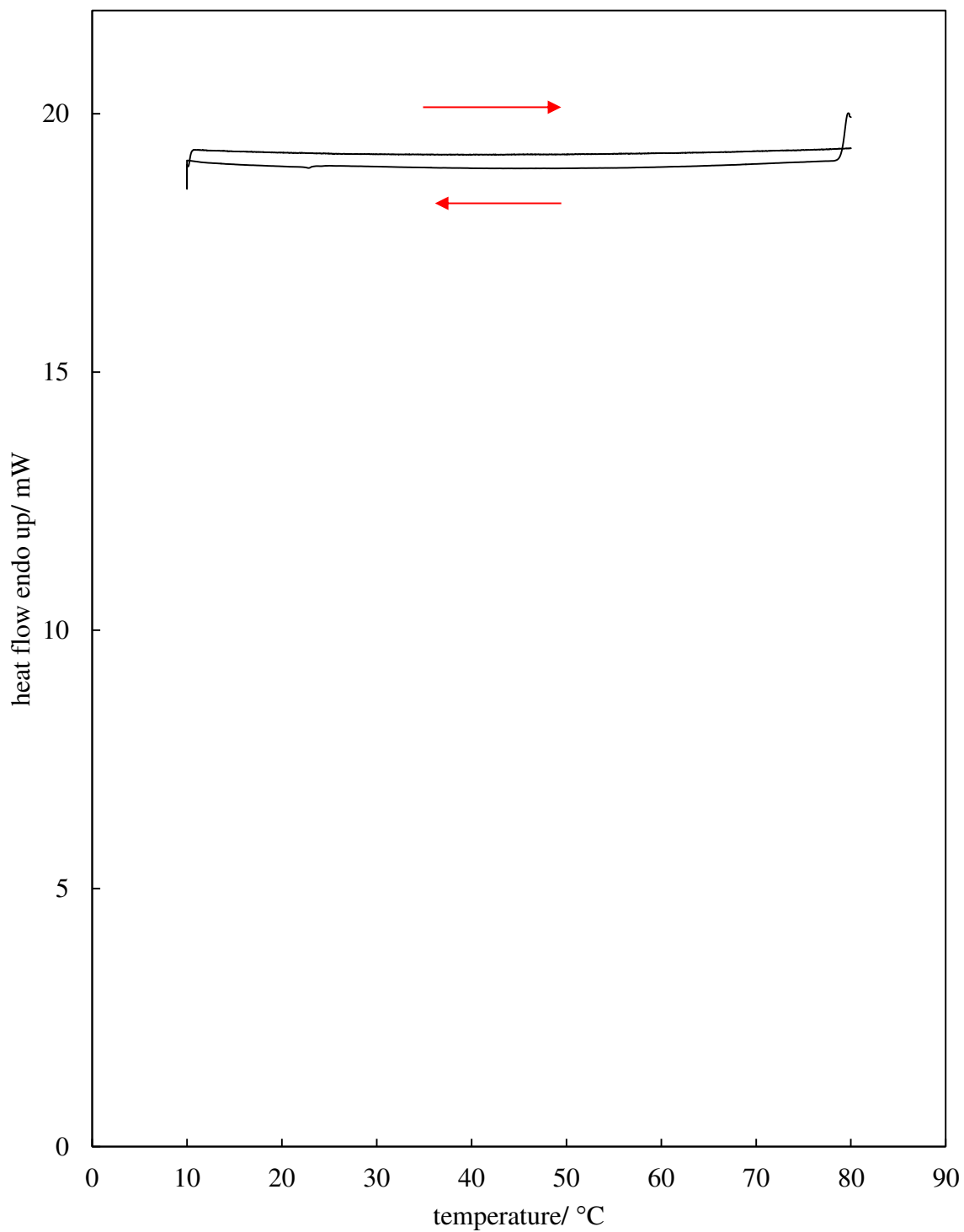


**Figure 4.29.** DSC of neat G. C. N12 veg cooled from 80 °C to 10 °C (5 °C/ min.), held at 10 °C for 5 minutes, then heated to 80 °C (2 °C/ min.).

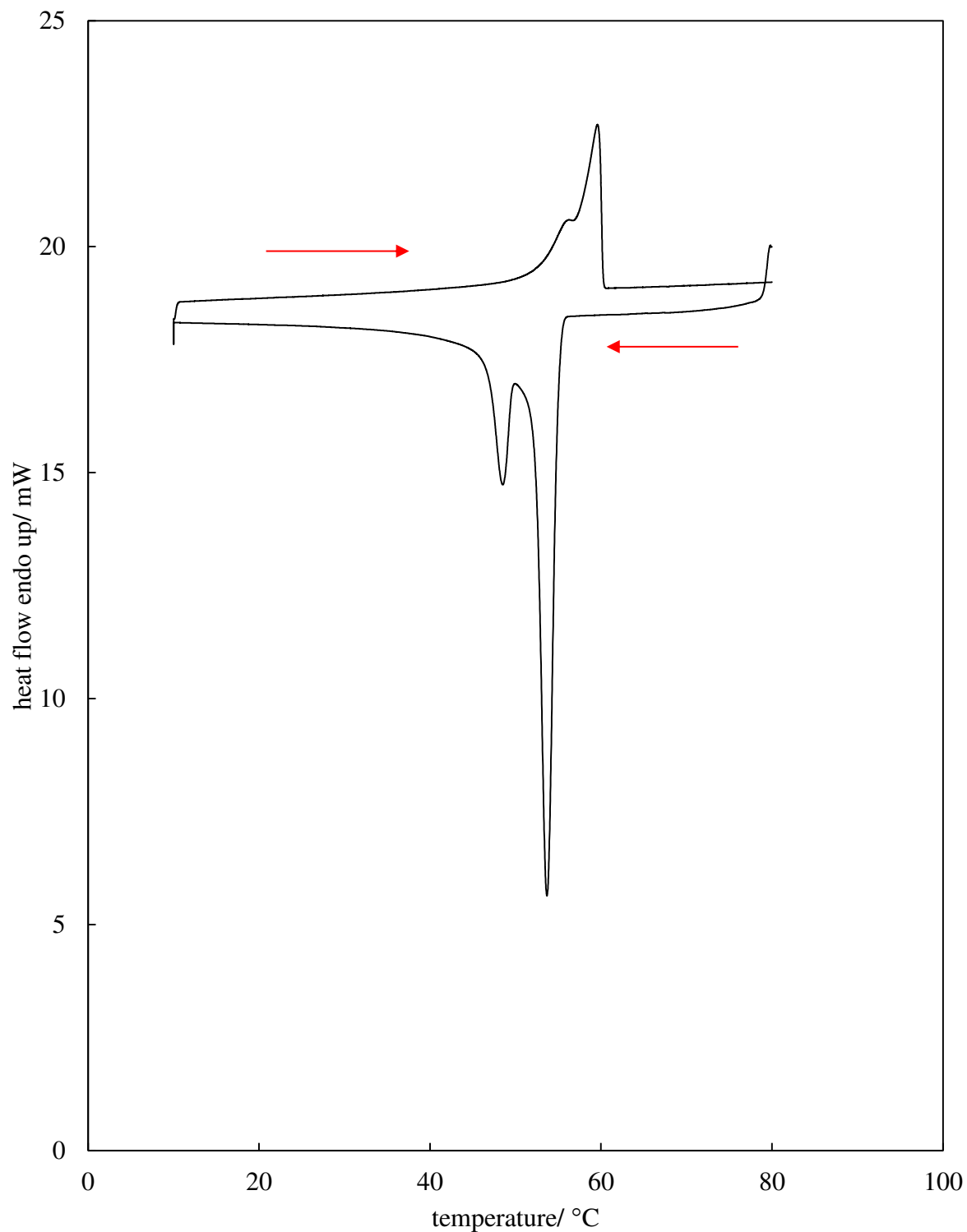
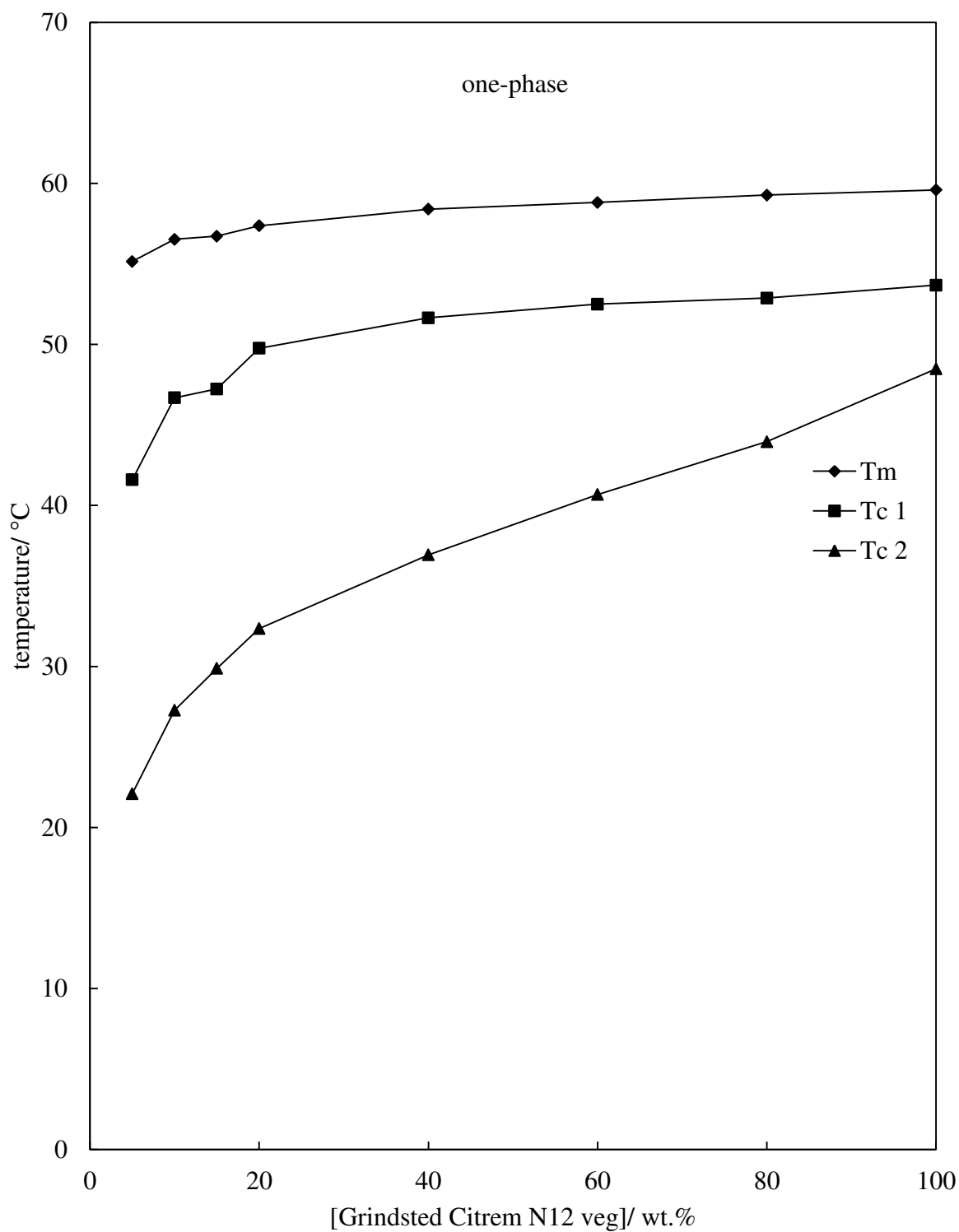


**Figure 4.30.** The melting temperature ( $T_m$ ), temperature of crystallisation peak 1 ( $T_c$  1) and temperature of crystallisation peak 2 ( $T_c$  2) of mixtures of G. C. N12 veg in HOSO. A protocol of cooling from 80 °C to 10 °C (5 °C/ min.), held at 10 °C for 5 minutes, then heating to 80 °C (2 °C/ min.) was followed.



### 4.3.2 Aeration

The mixtures were aerated using sparging with compressed air, the foaming column with compressed air and the whipping technique with air.

#### 4.3.2.1 Sparged gas

As shown in Table 4.1 the G. C. N12 veg in HOSO was aerated at various temperatures. The temperatures were chosen based on the DSC curves, i.e. when the mixture was one-phase or two-phase and also after heating to 80 °C when the mixture had crystallised to different extents between Tc1 and Tc2. It was interesting to see that a foam could only be produced at 60 °C and 80 °C (when the mixture was one-phase as seen in Figure 4.31). A foam could not be produced at 25, 35 and 45 °C or by heating the mixtures to 80 °C then cooling and aerating at either 35 °C or 45 °C.

##### 4.3.2.1.2 Aeration at 60 °C and 80 °C

As shown in Table 4.1 a foam could be produced at 5 and 10 wt.% G. C. N12 veg in HOSO aerated at 60 °C and 2.5, 5 and 10 wt.% aerated at 80 °C with sparged compressed air. As Figure 4.31 demonstrates the bubbles produced immediately after aeration at both 60 and 80 °C were polyhedral in shape with thin foam films of diameter 5 mm. The foam begins to collapse immediately after foam formation as shown in Figure 4.32 due to liquid drainage and then coalescence and disproportionation. The initial foam volume produced with 5 and 10 wt.% at 60 °C was 95 mL and 85 mL respectively, with the foam completely collapsing 8 and 20 minutes after aeration, respectively. As the G. C. N12 veg concentration in HOSO was increased from 2.5 to 10 wt.% the foamability and subsequent foam stability both increased. The foamability of the system was found to increase from 70 mL to 100 mL as shown in Figure 4.32. The foam fully collapsed after 4 minutes at 2.5 wt.% and after 22 minutes at 10 wt.%.

**Table 4.1.** Sparging of 2.5, 5 and 10 wt.% G. C. N12 veg in HOSO at various temperatures with compressed air for 30 seconds. X represents no foam, √ represents foam.

| Temperature/ °C          | Grindsted Citrem N12 veg concentration/ wt.% |   |    |
|--------------------------|--|---|----|
|                          | 2.5  | 5 | 10 |
| 25                       | X  | X | X  |
| 35                       | X  | X | X  |
| 45                       | X  | X | X  |
| 60                       | X  | √ | √  |
| 80                       | √  | √ | √  |
| 35 (after heating to 80) | X  | X | X  |
| 45 (after heating to 80) | X  | X | X  |

**Figure 4.31.** Photographs immediately after aeration of (a) 5 and (b) 10 wt.% G. C. N12 veg in HOSO aerated at 80 °C and (c) 10 wt.% G. C. N12 veg in HOSO aerated at 60 °C with sparged compressed air for 30 seconds. Scale bar 1 cm.

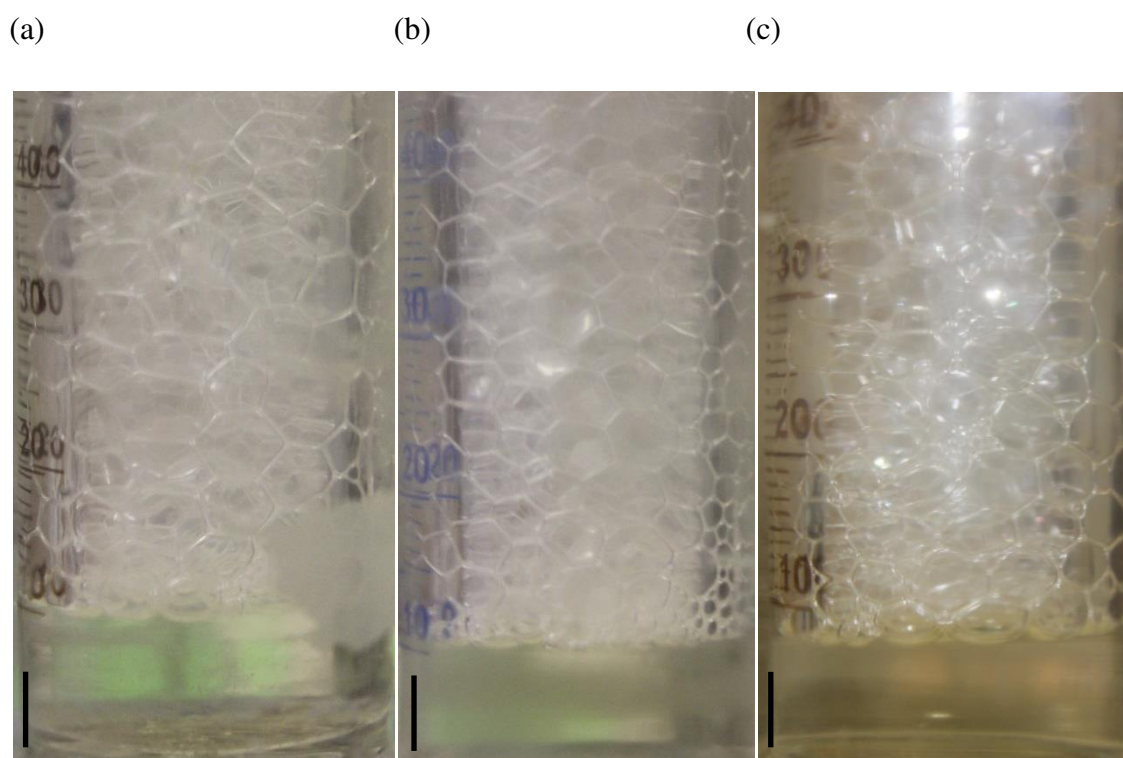
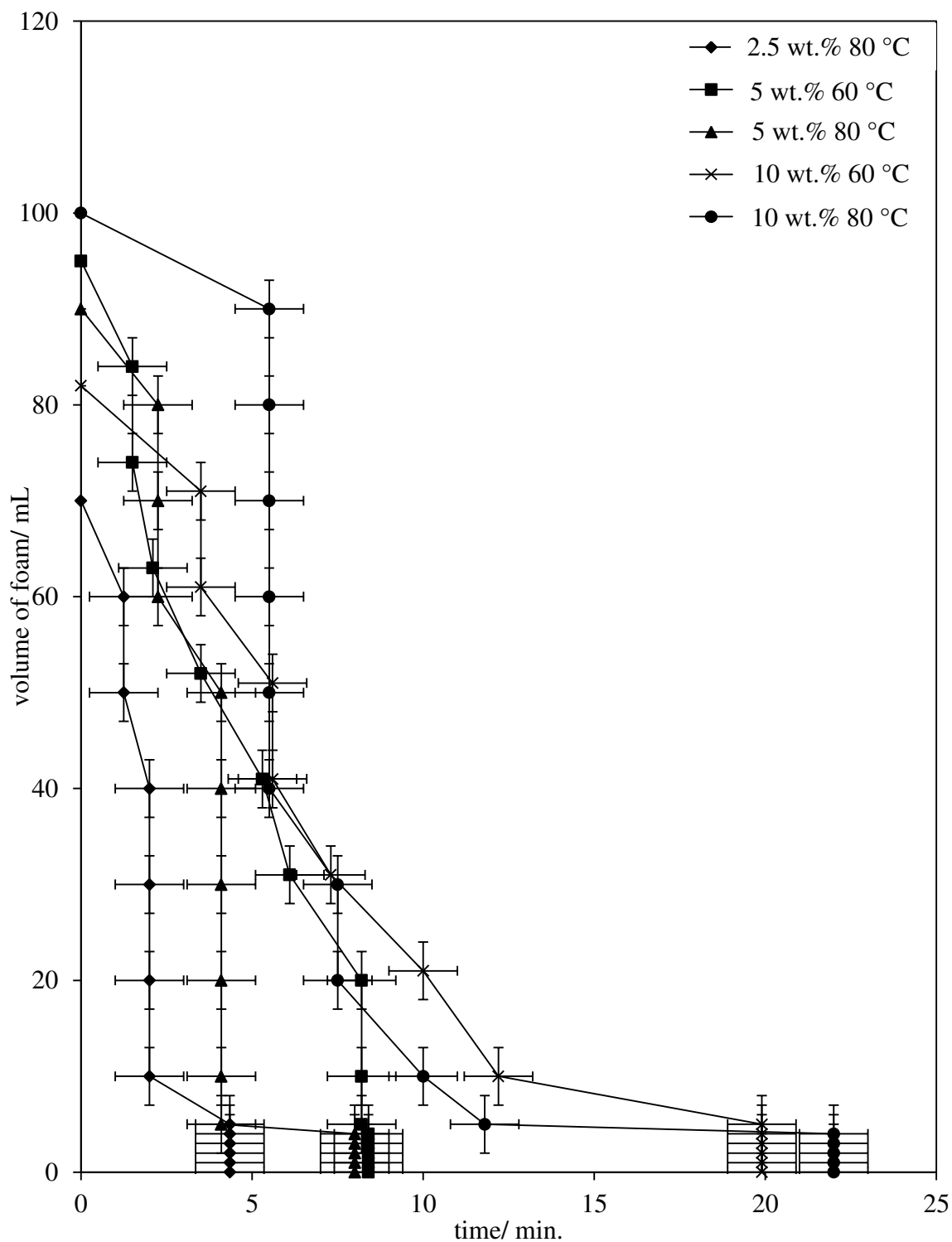


**Figure 4.32.** Foam collapse profile of the foam produced with various concentrations of G. C. N12 veg in HOSO at various temperatures aerated with sparged compressed air for 30 seconds.



#### 4.3.2.2 Foaming column

G. C. N12 veg in HOSO was aerated at 25, 35 and 60 °C with the foaming column with compressed air for 5 minutes. The foaming column was chosen because a consistent air flow can be maintained with this technique.

##### 4.3.2.2.1 Aeration at 25 and 35 °C

As seen in Table 4.2 aerations were conducted with 1 and 5 wt.% G. C. N12 veg in HOSO at 25 °C with and without prior heating to 60 °C and also at 35 °C. It was found that a foam could not be produced with the foaming column at 25 °C and 35 °C. The results obtained with the foaming column support those obtained with the needle aeration method. The mixture was a viscous liquid at 25 and 35 °C, and it may be difficult to disperse gas into it.

##### 4.3.2.2.2 Aeration at 60 °C

A foam was produced with 1-5 wt.% G. C. N12 veg in HOSO as shown in Table 4.2. Figure 4.33 shows the visual difference in the foam immediately after aeration as G. C. N12 veg concentration increased at 1 to 5 wt.%. It is clear that the bubbles in the foam with 1 and 2 wt.% were both spherical and polyhedral in shape with a diameter ranging from 3 to 20 mm and started to collapse immediately after the aeration had ceased. The foam produced with 3, 4 and 5 wt.% immediately after aeration consisted of spherical bubbles which were < 1 mm in diameter.

The foamability of the mixture increased as the surfactant concentration increased as shown in Figure 4.34. The foam stability (shown in Figure 4.35) was found to increase as the surfactant concentration increased. The time for total foam collapse increased from 20 minutes at 2 wt.% to 16 hours at 5 wt.%. The foam half-life (Figure 4.36) was found to be very similar to the time taken for the foam to completely collapse, whereby the foam half-life increased gradually from 0-2 wt.% surfactant to 10 minutes, then increased significantly to just over 4 hours at 5 wt.% surfactant.

The higher stability of the foams produced with the foaming column compared to that seen with the sparged gas aeration was likely to be due to the initial size of the bubbles

being uniform and much smaller ( $< 1$  mm in diameter, shown in Figure 4.33) than the polydisperse, polyhedral bubbles with the sparged gas aeration (5 mm in diameter, shown in Figure 4.31). The initial larger, polyhedral, polydisperse bubbles with the sparged gas aeration was likely to be due to factors such as the needle having to be removed from the foam causing foam disruption and also the large needle size (inner diameter of 318  $\mu\text{m}$ ). The gas entered the mixture aerated with the foaming column via a Mott diffuser which had an average pore size of 22  $\mu\text{m}$ .

**Table 4.2.** G. C. N12 veg as a function of concentration in HOSO aerated with the foaming column for 5 minutes with compressed air at various temperatures. X represents no foam,  $\surd$  represents foam and N/A means aeration has not been conducted.

| Temperature/ $^{\circ}\text{C}$ | Grindsted Citrem N12 veg concentration/ wt.% |         |         |         |         |
|---------------------------------|--|---------|---------|---------|---------|
|                                 | 1  | 2       | 3       | 4       | 5       |
| 25                              | X  | N/A     | N/A     | N/A     | X       |
| 25 after heated to<br>60        | X  | N/A     | N/A     | N/A     | X       |
| 35                              | X  | N/A     | N/A     | N/A     | X       |
| 60                              | $\surd$                                      | $\surd$ | $\surd$ | $\surd$ | $\surd$ |

**Figure 4.33.** Photographs of (a) 1 wt.%, (b) 2 wt.%, (c) 3 wt.%, (d) 4 wt.% and (e) 5 wt.% G. C. N12 veg in HOSO immediately after aeration with the foaming column for 5 minutes with compressed air at 60 °C. Scale bar 1 cm.

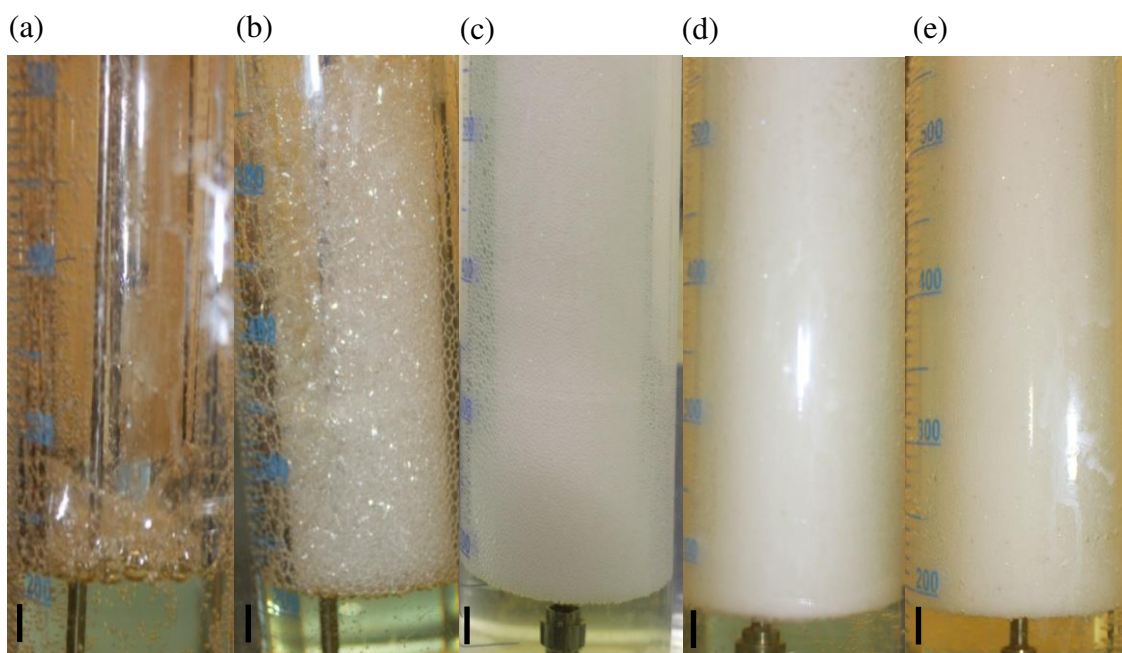


**Figure 4.34.** Initial foam volume of a foam produced with G. C. N12 veg as a function of concentration in HOSO aerated with the foaming column with compressed air for 5 minutes at 60 °C.

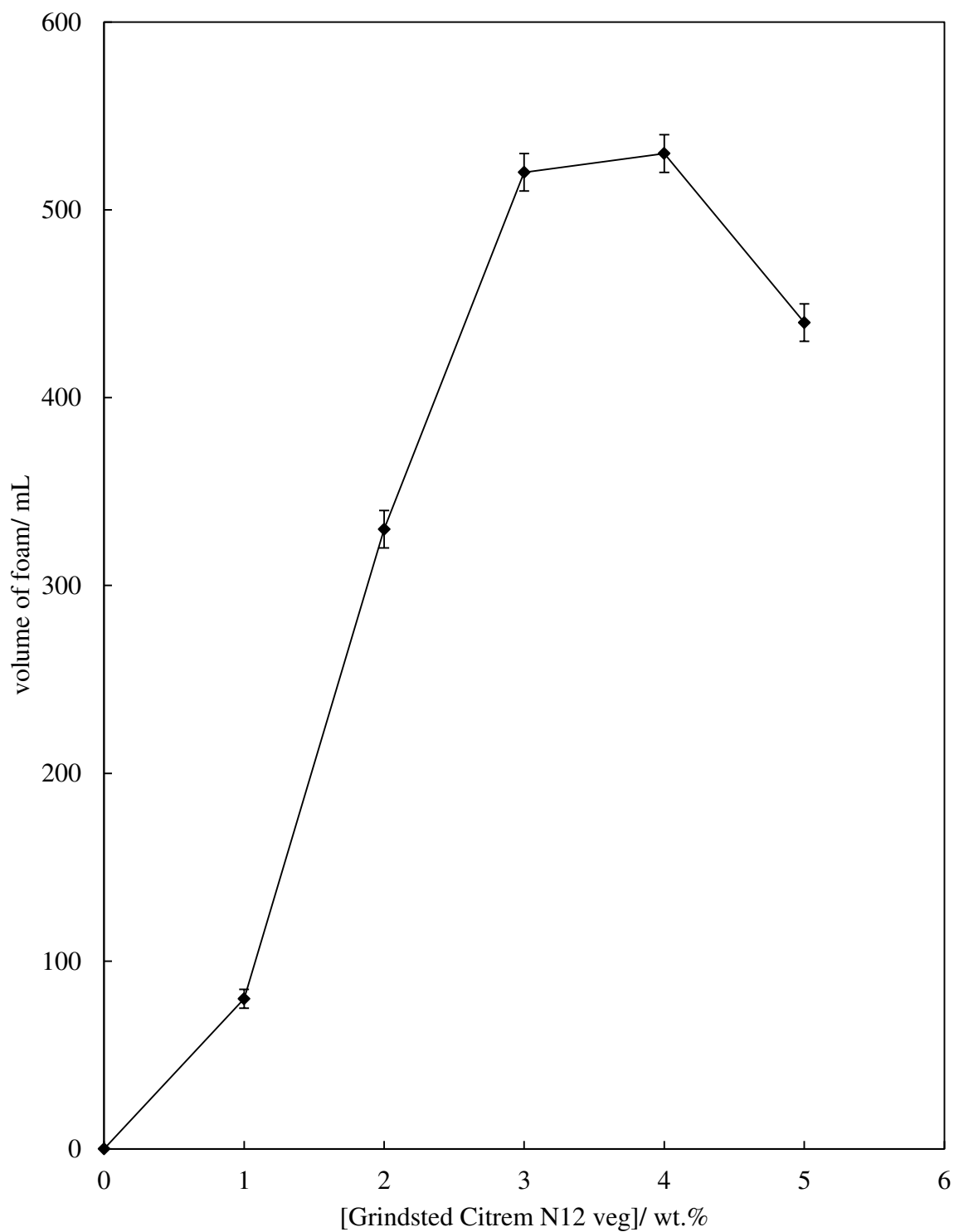


**Figure 4.35.** Time for total foam collapse of a foam produced with G. C. N12 veg as a function of concentration in HOSO aerated with the foaming column with compressed air for 5 minutes at 60 °C.

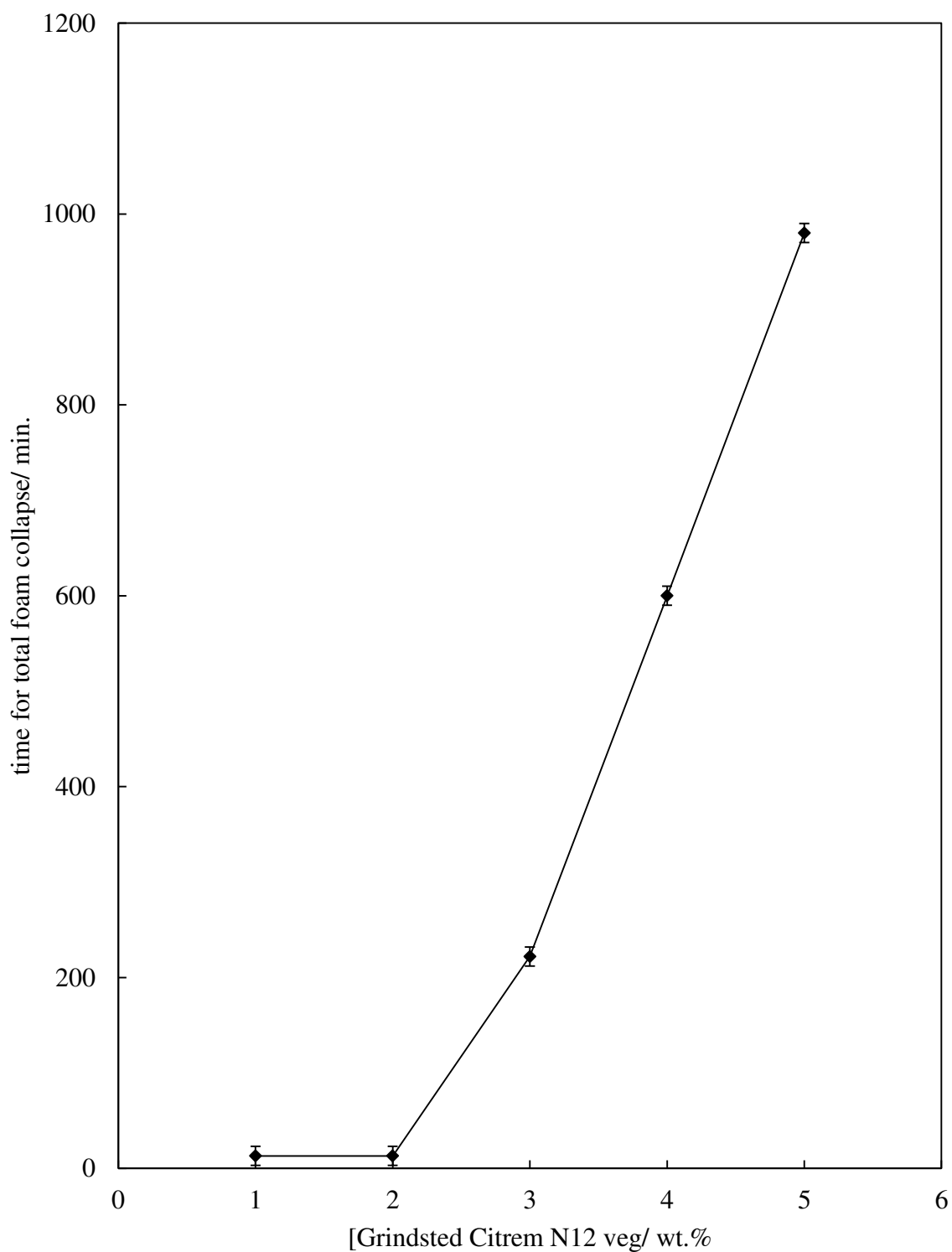
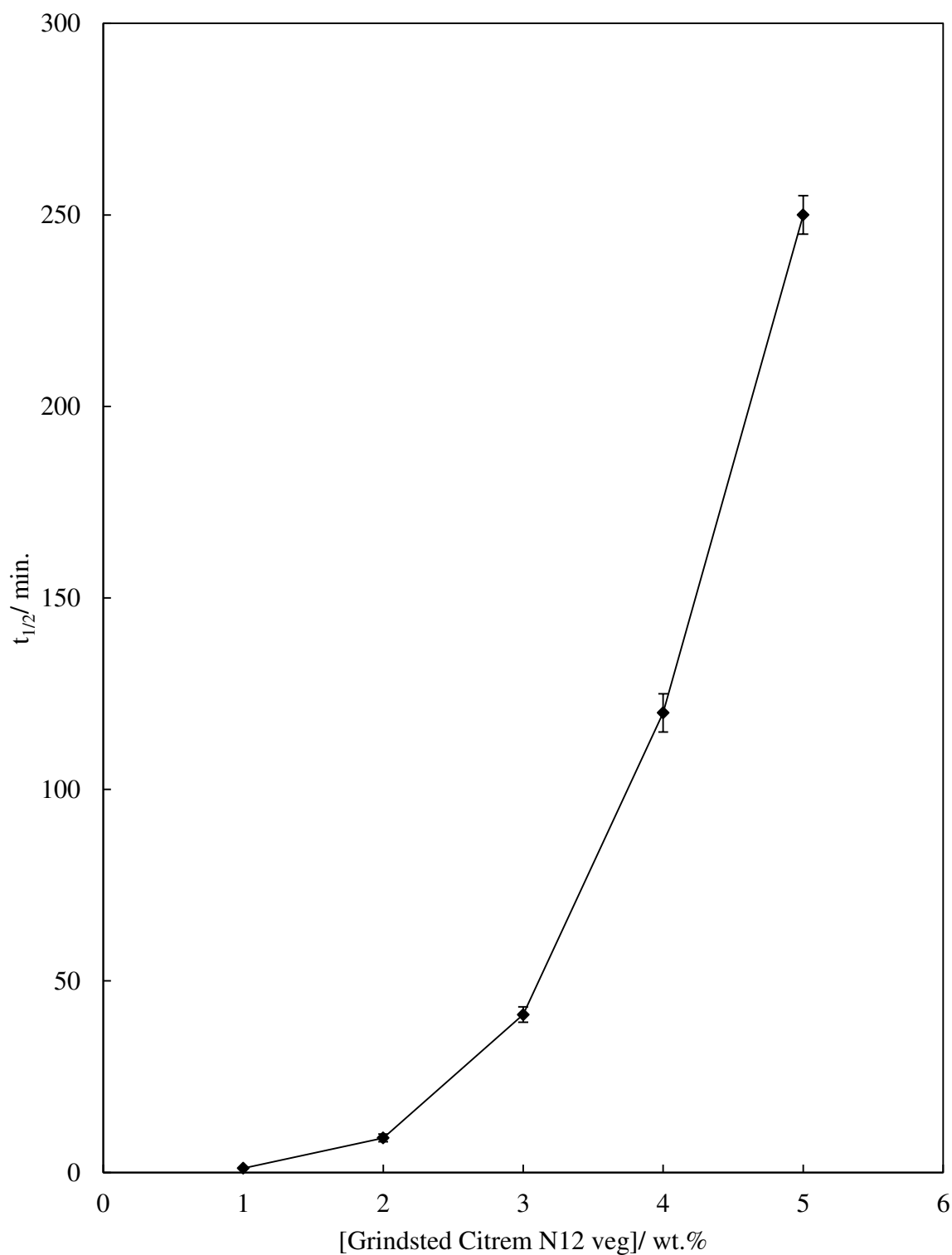


**Figure 4.36.** Half-life of foam produced with G. C. N12 veg as a function of concentration in HOSO aerated with the foaming column with compressed air for 5 minutes at 60 °C.



#### 4.3.2.2.3 Summary

In summary, highly stable foams were produced with G. C. LR 10 with compressed air with the foaming column at 25 °C and 45 °C (in two-phase), however with G. C. N12 veg foams could not be produced at these temperatures. Foaming was possible at 60 °C (one-phase) with both surfactants. This may be due to the high viscosity of G. C. N12 veg in HOSO at 25 °C and 45 °C causing it to be difficult for gas to disperse and therefore create a foam. The foamability with both surfactants at 60 °C was found to be similar; however the foam stability with the G. C. N12 veg was higher.

#### 4.3.2.3 Whipping technique

It was noticed that when the mixture was at 25 °C it was gel-like. This was not surprising as is known that gels can be produced with vegetable oils with various fatty acids, fatty alcohols, monoglycerides and hydrogenated oils such as rapeseed oil.<sup>10-16</sup> Therefore, the gelled mixture was whipped with a hand held double beater electric whisk for 45 minutes to investigate if the mixture could be aerated with this method. The gel was produced by heating 10 wt.% G. C. N12 veg in HOSO to 80 °C for one hour and then cooling it with the use of a freezer for one hour. It was found that a whipped oil could not be produced when the mixture was cooled to 15 °C and then whipped for 45 minutes at 22 °C as shown in Figure 4.37 and Figure 4.38 where in Figure 4.38 (b) bubbles were not present in the mixture. However, when the mixture was cooled to 20 °C prior to whipping for 45 minutes at 22 °C it was found that 400 mL of foam could be produced as shown in Figure 4.39 which had a volume fraction of air of 0.62. This is thought to be due to the mixture being more viscous at 15 °C than at 20 °C which restricted the foam formation. From microscopy (Figure 4.40) it was found that the mixture prior to aeration after cooling to 20 °C consisted of aggregates that were up to 30 µm in diameter. Therefore, the appearance of the mixture prior to aeration was similar to that seen in Figure 4.38 where the mixture was cooled to 15 °C prior to whipping. However, as can be seen in Figure 4.40 (b) a large volume of spherical bubbles with a diameter of < 25 µm were incorporated into the mixture. It was found that the foam was very stable as it did not decrease in volume nor was there any liquid drainage 3 weeks after foam formation as shown in Figure 4.41.

**Figure 4.37.** Photos of 10 wt.% G. C. N12 veg in HOSO (a) prior to whipping and (b) after the mixture was whipped for 45 minutes at 22 °C with a double beater hand held electric whisk after cooling to 15 °C from 80 °C. Scale bar 1 cm.

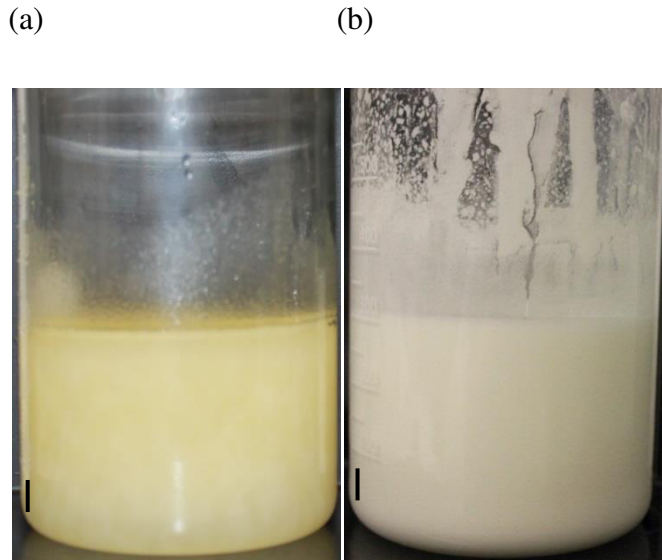


**Figure 4.38.** Microscopy of 10 wt.% G. C. N12 veg in HOSO heated to 80 °C, then cooled to 15 °C (a) prior to whipping and (b) after whipping for 45 minutes at 22 °C with a double beater hand held electric whisk. Scale bar 100  $\mu\text{m}$ . The gel was diluted 1:1 with HOSO.

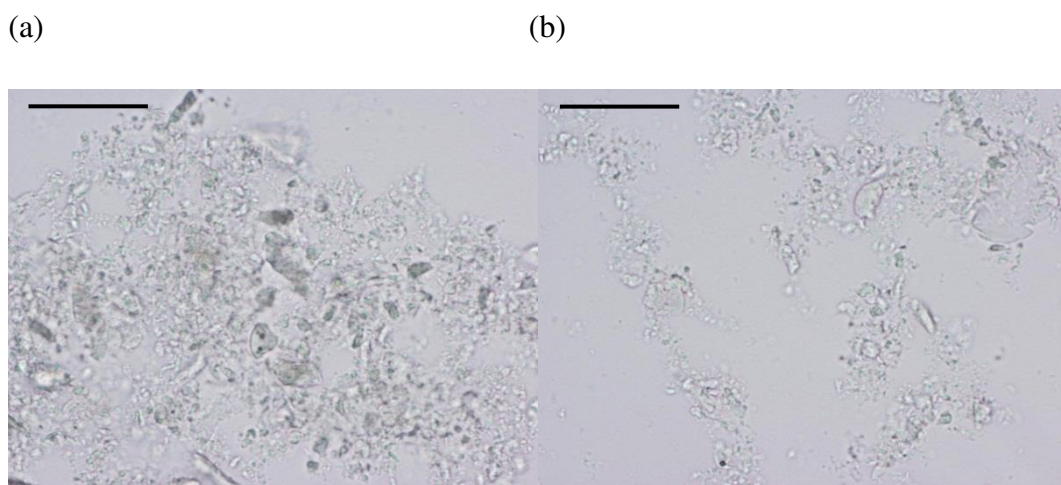


**Figure 4.39.** Photograph of 10 wt.% G. C. N12 veg in HOSO (a) prior to whipping and (b) after whipping for 30 minutes with a hand held double beater electric whisk at 22 °C after cooling the mixture to 20 °C from 80 °C. Scale bar 1 cm.

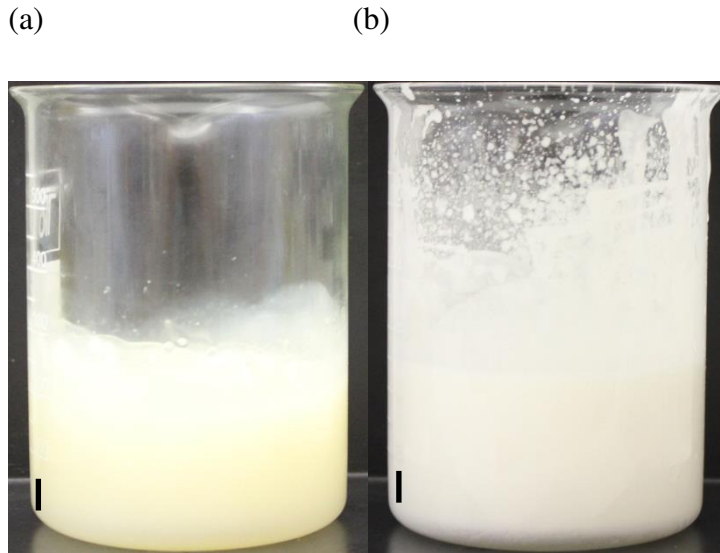


**Figure 4.40.** Microscopy of 10 wt.% G. C. N12 veg in HOSO (a) prior to whipping and (b) after whipping for 30 minutes with a hand held double beater electric whisk at 22 °C after cooling the mixture to 20 °C from 80 °C. Scale bar 100  $\mu$ m. The gel was diluted 1:1 with HOSO.

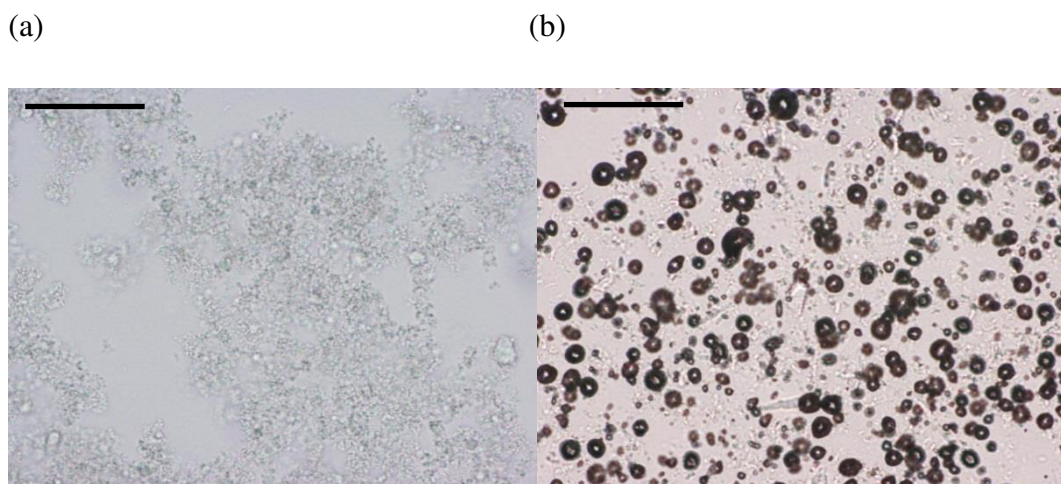


**Figure 4.41.** 10 wt.% G. C. N12 veg in HOSO (a) immediately after whipping with a hand held double beater electric whisk for 45 minutes at 22 °C after cooling the mixture to 20 °C from 80 °C (b) 3 weeks after whipping. Scale bar 1 cm.



#### 4.3.2.3.1 Effect of temperature increase

The stability of the whipped oil to an increase in temperature at a rate of 1 °C/min. from 22 °C was remarkable as it was found that liquid drainage did not occur until the mixture was heated to 45 °C. Total foam collapse did not occur until the mixture was heated to 58.4 °C. The change in the foam appearance as the temperature was increased is shown in Figure 4.42. It is clear that the foam collapsed when the surfactant aggregates melted (Figure 4.30) indicating the importance of the gelled structure for both foam formation and foam stability. As temperature increased, liquid drained from the foam causing the foam to collapse. Figure 4.43 shows through microscopy the change in the foam bubbles as temperature was increased; the bubbles increased in diameter as temperature increased. It was also interesting to see that there were still some aggregates present at 60 °C. It is clear from Figure 4.43 (f) that the aggregates were plate-like. Figure 4.44 represents the foam collapse and the liquid drainage from the foam as temperature was increased. It clearly shows the high temperature stability of the foam. The temperature the mixture was cooled to prior to aeration is very important for foam production with the whipping technique. This may be due to a specific solid content or viscosity being required for the air to be incorporated into the mixture.

**Figure 4.42.** Photograph of 10 wt.% G. C. N12 veg in HOSO whipped with a hand held double beater electric whisk for 45 minutes at 22 °C after heating to 80 °C and then cooling to 20 °C. The foam produced was then heated from (a) 22 °C at 1 °C/min. until foam collapse. (b) 30 °C, (c) 40 °C, (d) 50 °C, (e) 55 °C and (f) 60 °C. Scale bar 1 cm.

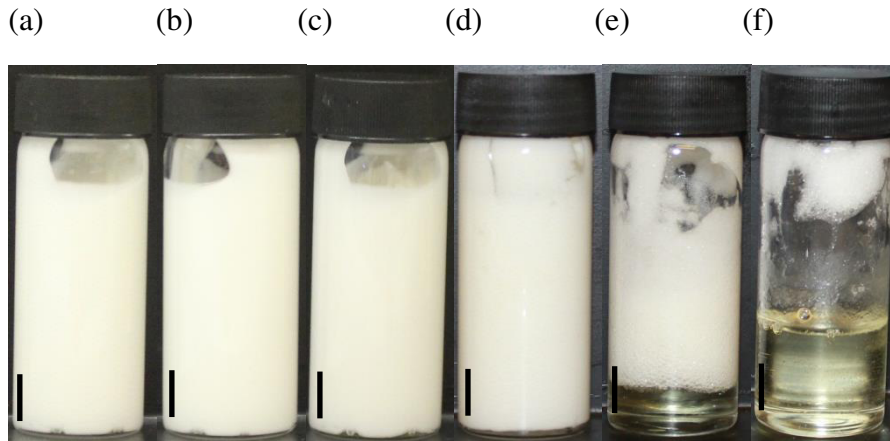


**Figure 4.43.** Microscopy of 10 wt.% G. C. N12 veg in HOSO whipped with a hand held double beater electric whisk at 22 °C after heating to 80 °C and then cooling to 20 °C. The foam produced was then heated from (a) 22 °C at 1 °C/min. until foam collapse. (b) 30 °C, (c) 40 °C, (d) 50 °C, (e) 55 °C and (f) 60 °C. Scale bar 100 μm. The foam was diluted 1:1 with HOSO.

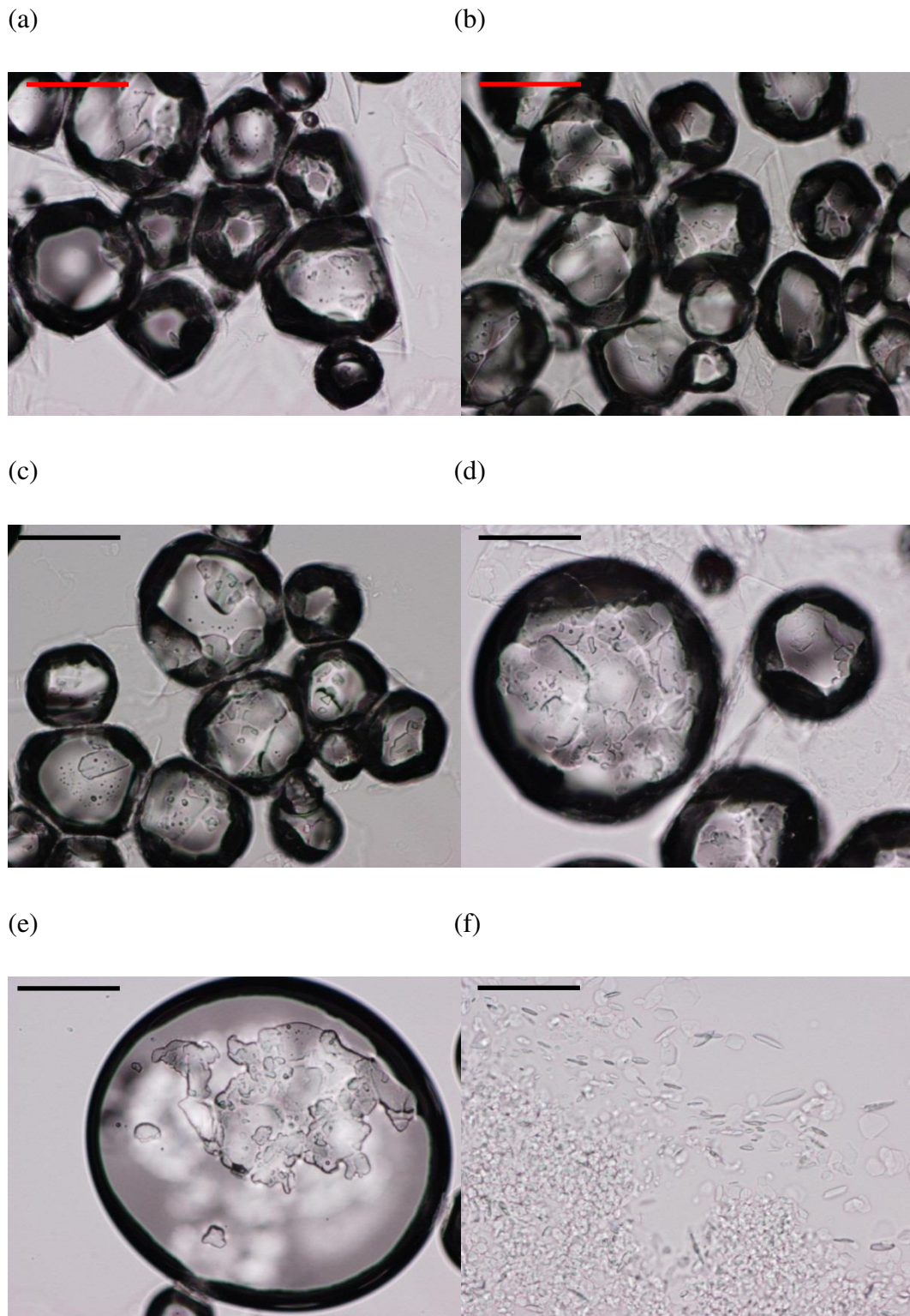
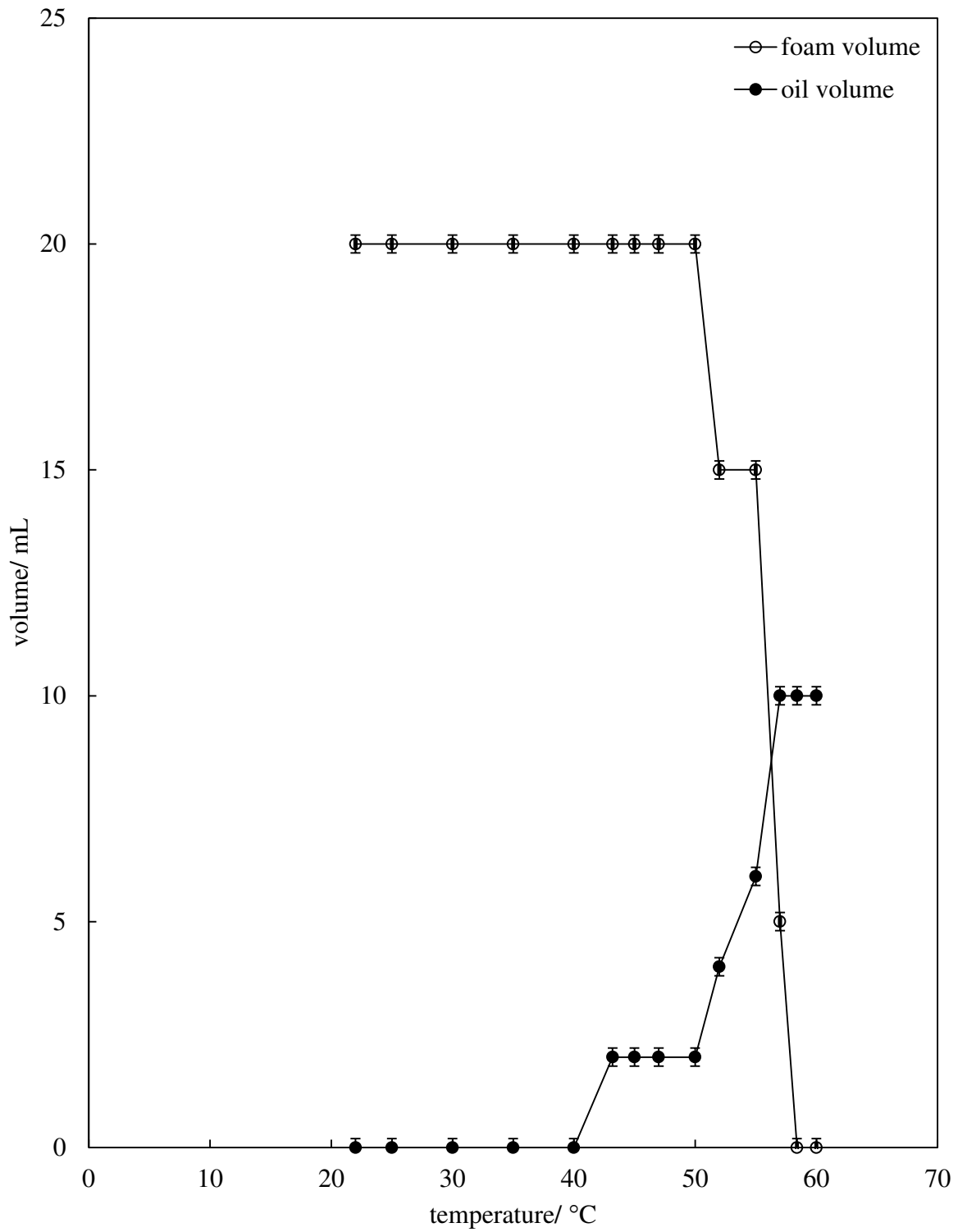


**Figure 4.44.** Liquid drainage and foam collapse of 10 wt.% G. C. N12 veg in HOSO whipped for 45 minutes with a hand held double beater electric whisk at 22 °C after cooling to 20 °C from 80 °C. The foam was heated at 1 °C/min. from 22 °C.



## 4.4 Conclusions

### 4.4.1 Unsaturated mono/diglyceride

A foam could be produced with G. C. LR 10 in HOSO with both the foaming column and soda siphon. A summary of the effect of the parameters investigated on foamability and foam stability are shown in Table 4.3. It is clear that the surfactant in oil in two-phase is crucial for the foam stability. Gas type was also an important parameter as the foam stability at 45 °C with air with the foaming column was significantly higher than that seen with CO<sub>2</sub> and N<sub>2</sub>O. Gas type was also extremely important with the soda siphon for foam generation as more foam was produced with CO<sub>2</sub> than with N<sub>2</sub>O.

**Table 4.3.** Summary of the effect of surfactant concentration, temperature and gas type with both the soda siphon and foaming column on foamability and foam stability.

|                | Aeration method                      |  |   |                                      |   |                                |
|----------------|--------------------------------------|--|---|--------------------------------------|---|--------------------------------|
|                | Foaming column                       |  |   | Soda siphon                          |   |                                |
| Parameter      | Surfactant concentration             | temperature  | Gas type  | Surfactant concentration             | temperature                                   | Gas type                       |
| Foamability    | Increased as concentration increased | No effect  | No effect   | Increased as concentration increased | No effect                                     | More foam with CO <sub>2</sub> |
| Foam stability | Increased as concentration increased | As temperature increased stability decreased (with air). No effect with CO <sub>2</sub> and N <sub>2</sub> O | Stability similar except at 45 °C with air where foams were highly stable | Increased as concentration increased | As temperature increased stability decreased. | No effect                      |

#### 4.4.2 Saturated mono/diglyceride

A foam could only be produced at 60 and 80 °C with sparging air and at 60 °C with the foaming column. The foam produced by sparging was found to be significant; however the foam stability was relatively low. The foam produced with the foaming column was also significant and had a reasonably high stability. The foam produced with the foaming column with compressed air at 60 °C with 5 wt.% G. C. N12 veg in HOSO had a higher stability than that observed with the G.C. LR 10 in HOSO by 15 hours. It was interesting that a foam could only be produced with these methods when the surfactant-oil mixture was one phase. A foam could be produced with G. C. LR 10 in HOSO when the mixture was one-phase and two-phase, however the foam stability was higher at 45 °C and 25 °C (two phase). It was found that the temperature the mixture was cooled to prior to aeration with the whipping protocol was important for foam formation. A foam was not produced when aerating the mixture with the whipping protocol at 22 °C after cooling to 15 °C from 80 °C, however when the mixture was cooled to 20 °C from 80 °C a foam was produced. The foam produced was highly stable when it was heated at 1 °C/min. and did not fully collapse until 58.4 °C (collapsed as the surfactant melted). It was found that the foam was very stable as it did not decrease in volume and there was not any liquid drainage 3 weeks after foam formation. It was clear that a larger volume of foam was more likely to be produced with a viscous mixture aerated with the whipping technique than with the foaming column or soda siphon and the reverse is the case when the mixture is fluid-like. The stability of the foam produced with the whipping technique was considerably higher than that observed with the foaming column and soda siphon, therefore the whipping technique is the focus of Chapter 6.

#### 4.5 References

1. S. Ross and G. Nishioka, *J. Phys. Chem-US.*, **79**, 1561 (1975).
2. S. Ross and G. Nishioka, *Colloid Polym. Sci.*, **255**, 560 (1977).
3. B.P. Binks, C.A. Davies, P.D.I. Fletcher and E.L. Sharp, *Colloids Surf. A*, **360**, 198 (2010).
4. R.G. Shrestha, L.K. Shrestha, C. Solans, C. Gonzalez and K. Aramaki, *Colloids Surf. A*, **353**, 157 (2010).
5. L.K. Shrestha, R.G. Shrestha, S.C. Sharma and K. Aramaki, *J. Colloid Interface Sci.*, **328**, 172 (2008).
6. H. Kunieda, L.K. Shrestha and D.P. Acharya, *J. Disp. Sci. Technol.*, **28**, 133 (2007).
7. L.K. Shrestha, K. Aramaki, H. Kato, Y. Takase and H. Kunieda., *Langmuir*, **22**, 8337 (2006).
8. W. Snedden, K. Ledez and H. J. Manson, *J. Appl. Physiol.*, **80**, 1371 (1996).
9. L. Kubie, *J. Biol. Chem.*, (1927).
10. F. G. Gandolfo, A. Bot and E. Floter, *J. Am. Oil Chem. Soc.*, **81**, 1 (2004).
11. J. Daniel and R. Rajasekharan, *J. Am. Oil Chem. Soc.*, **80**, 417 (2003).
12. H. M. Schaink, K. F. van Malssen, S. Morgado-Alves, D. Kalnin and E. van der Linden, *Food Res. Int.*, **40**, 1185 (2007).
13. M. Perneti, K. F. van Malssen, E. Floter and A. Bot, *Curr. Opin. Colloid Interface Sci.*, **12**, 221 (2007).
14. K. Higaki, Y. Sasakura, T. Koyano, I. Hachiya and K. Sato, *J. Am. Oil Chem. Soc.*, **80**, 263 (2003).
15. K.W. Smith, K. Bhaggan, G. Talbot, K.F. van Malssen, *J. Am. Oil Chem. Soc.*, **88**, 1085 (2011).
16. N.K.O. Ojijo, E. Kesselman, V. Shuster, S. Eichler, S. Eger, I. Neeman and E. Shimoni, *Food Res. Int.*, **37**, 385 (2004).

## 5 CHARACTERISATION OF GELS OF MYRISTIC ACID IN HIGH OLEIC SUNFLOWER OIL

### 5.1 Introduction

The ability to gel a vegetable oil with the use of a fatty acid or fatty alcohol is known.<sup>1-6</sup> It is known from previous literature that a gel of myristic acid in various oils including sunflower, castor, rapeseed and peanut oil along with other straight chained acids (up to C<sub>31</sub>) can be created. Daniel and Rajasekharan found that myristic acid could gel sunflower oil with as little as 2 wt.% of the fatty acid present.<sup>1</sup> Gandolfo et al. have also studied the gelation capability of saturated straight chained acids and alcohols ranging from C<sub>16</sub> to C<sub>22</sub> with sunflower, soybean and rapeseed oil.<sup>2</sup> It was also found that only 2 wt.% of the fatty acids and alcohols was required for a gel to be created in sunflower oil.<sup>2</sup> It was found with both studies that the gels were created by cooling the mixtures from between 60 to 80 °C to room temperature or 5 °C. From these findings it was proposed that myristic acid may have the ability to gel high oleic sunflower oil and that the sample preparation procedure would be to heat the required amount of myristic acid in HOSO to 80 °C for one hour, then cool to 8 ± 2 °C before analysis at room temperature (20 ± 2 °C). In this chapter the myristic acid in HOSO gel was characterised by methods including visual solubility determination, differential scanning calorimetry (DSC), X-ray diffraction (XRD), microscopy, surface energy determination, rheology and pulsed nuclear magnetic resonance (pNMR) spectroscopy. The effect of myristic acid concentration, temperature and cooling rate on gel formation was also investigated. This was to further understand the system which, in turn, aided the interpretation of the results obtained when the myristic acid in HOSO system was aerated with the whipping protocol which will be discussed in Chapter 6.

### 5.2 Solubility determination in HOSO

The visual solubility determination was conducted by cooling a sample at 0.1 °C/min. from 80 °C to observe the temperature at which a crystal was formed (precipitation temperature) and then heating the mixture at 0.1 °C/min. until the mixture returned to a clear homogeneous liquid (dissolution temperature). The theoretical solubility temperature, assuming ideal behaviour, was calculated using:<sup>7</sup>

$$\ln x_B = \frac{\Delta_{fus}H}{R} \left( \frac{1}{T_f} - \frac{1}{T} \right) \quad (5.1)$$

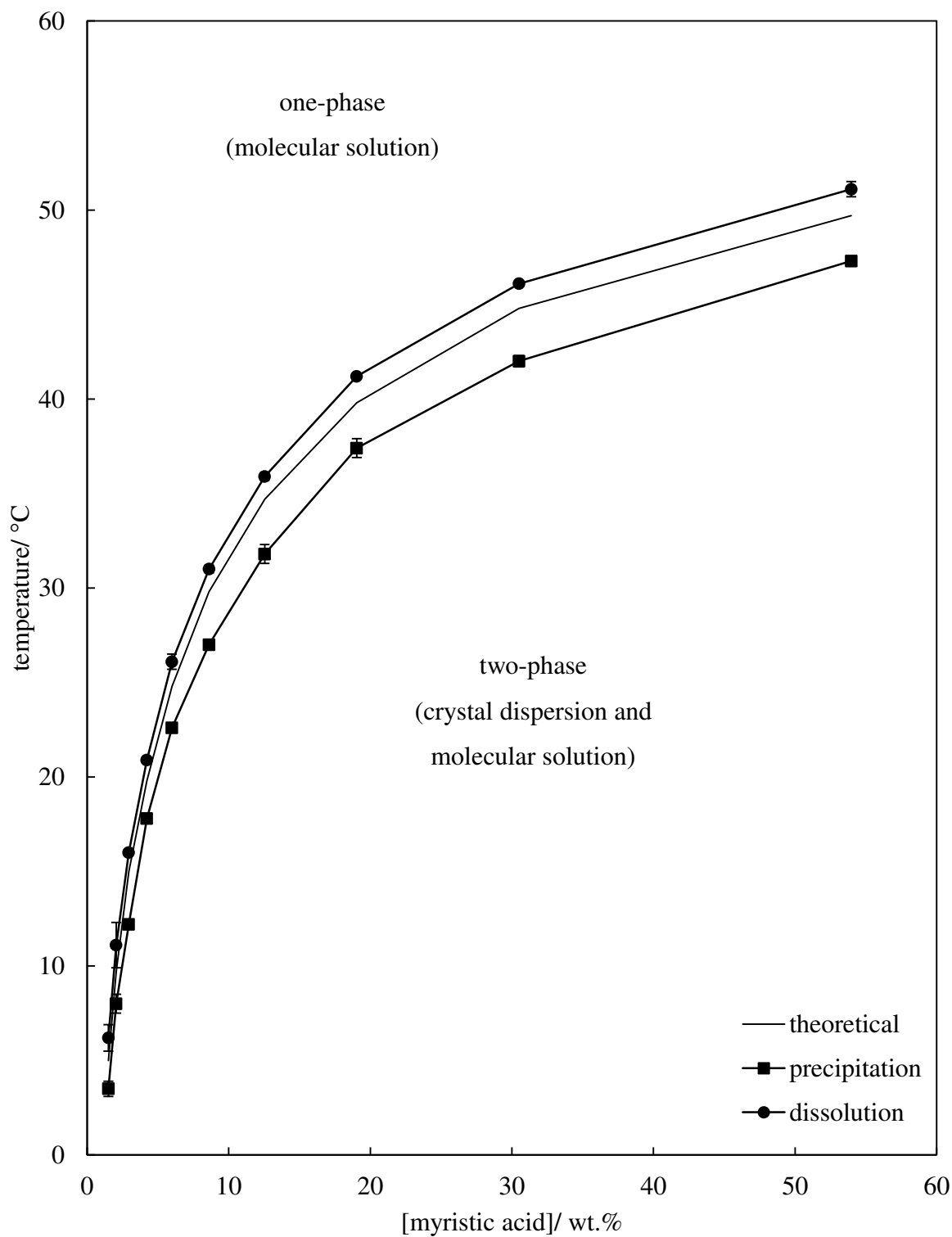
where  $x_B$  is the mole fraction of myristic acid, R is the gas constant, T is temperature,  $\Delta_{fus}H$  is the enthalpy of fusion ( $45 \text{ KJ mol}^{-1}$ )<sup>8</sup> and  $T_f$  is the temperature of fusion ( $326.6 \text{ K}$ ).<sup>8</sup>

Figure 5.1 shows the appearance of the myristic acid in HOSO mixture when it was (a) a one-phase mixture which was a clear, pale yellow homogeneous liquid and (b) a two-phase mixture which was a turbid, pale yellow gel/soft solid. It was found that a gel could be produced at  $22 \text{ }^\circ\text{C}$  with as little as 4 wt.%. Figure 5.2 clearly shows that the solubility curve is closer to the dissolution points than the precipitation points. It is thought that with an extremely slow heating rate the measured dissolution temperatures would overlay the theoretical solubility curve.

**Figure 5.1.** Photographs of 10 wt.% myristic acid in HOSO at  $22 \text{ }^\circ\text{C}$  demonstrating the appearance of (a) the clear, homogeneous liquid and (b) the turbid, two-phase mixture. Scale bar 1 cm.



**Figure 5.2.** Visual solubility measurements of myristic acid as a function of concentration in HOSO cooled from 80 to 5 °C below the precipitation temperature at 0.1 °C/min., held at that temperature for 5 min., then heated to 5 °C above the dissolution temperature at 0.1 °C/min. The theoretical curve was calculated with the ideal solubility equation.



### 5.3 Differential scanning calorimetry

Differential scanning calorimetry (DSC) was conducted to verify the results found with the visual observations. The protocol followed consisted of cooling the mixture from 80 to -20 °C at 2 °C/min., holding the mixture at -20 °C for 5 minutes and then heating the mixture to 80 °C at 2 °C/min. The previous chapter shows that there was not any component in the HOSO which solidified/melted over the temperature range of 80 to -20 °C. It is clear from Figure 5.2 hysteresis occurs between the precipitation and dissolution temperature. This was also seen in Figure 5.3 with the DSC measurement of 10 wt.% myristic acid in HOSO. The temperature at which the heat flow was the lowest on the crystallisation peak was recorded as the precipitation temperature and the temperature at which the heat flow was the highest on the melting peak was recorded as the dissolution temperature. Figure 5.4 shows that the solubility curve, like with the visual solubility measurements, is closer to the dissolution points than the precipitation points.

**Figure 5.3.** DSC of 10 wt.% myristic acid in HOSO cooled from 80 to -20 °C, held at -20 °C for 5 minutes and then heated to 80 °C. The heating and cooling rates were 2 °C/min.

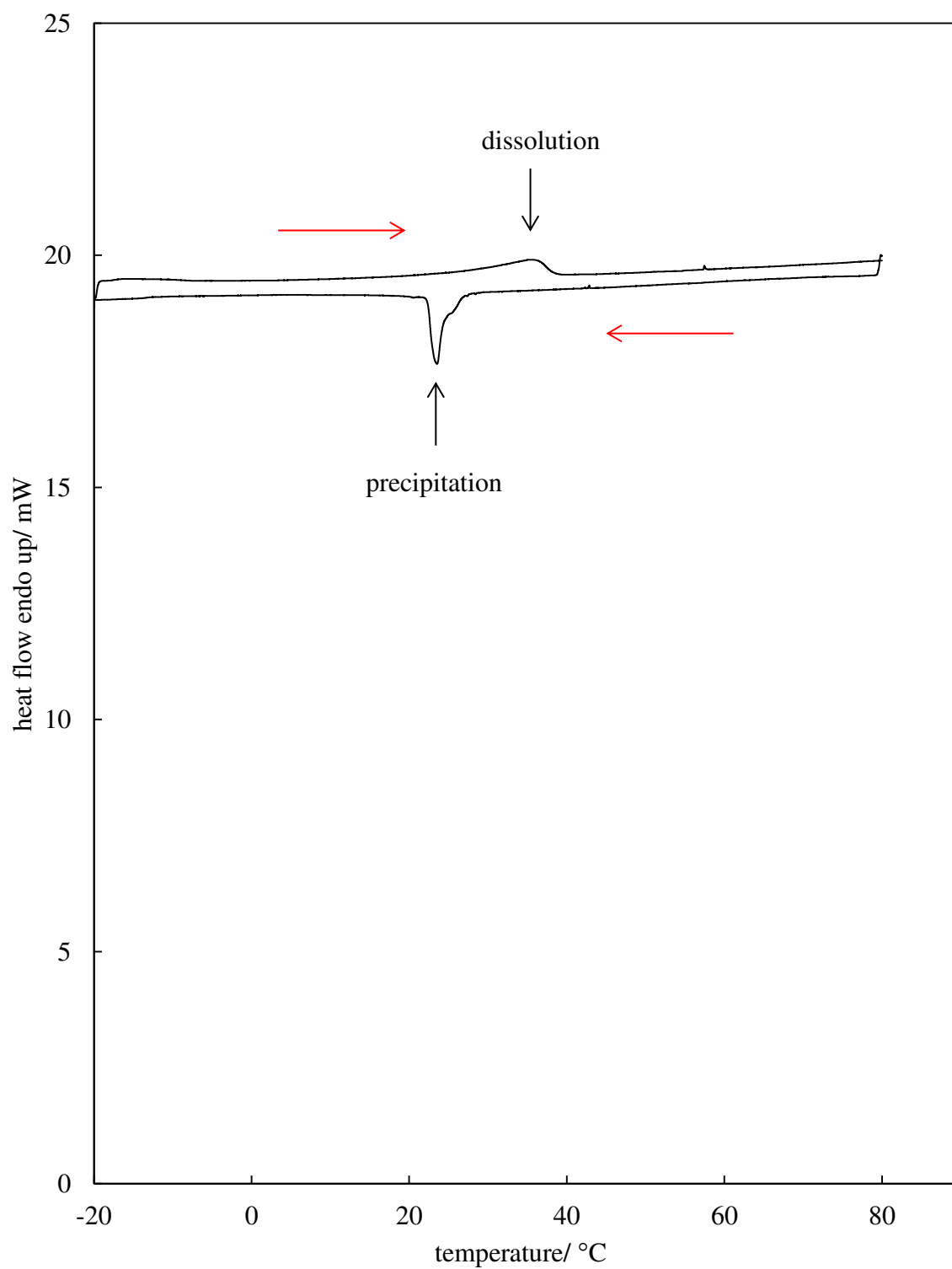
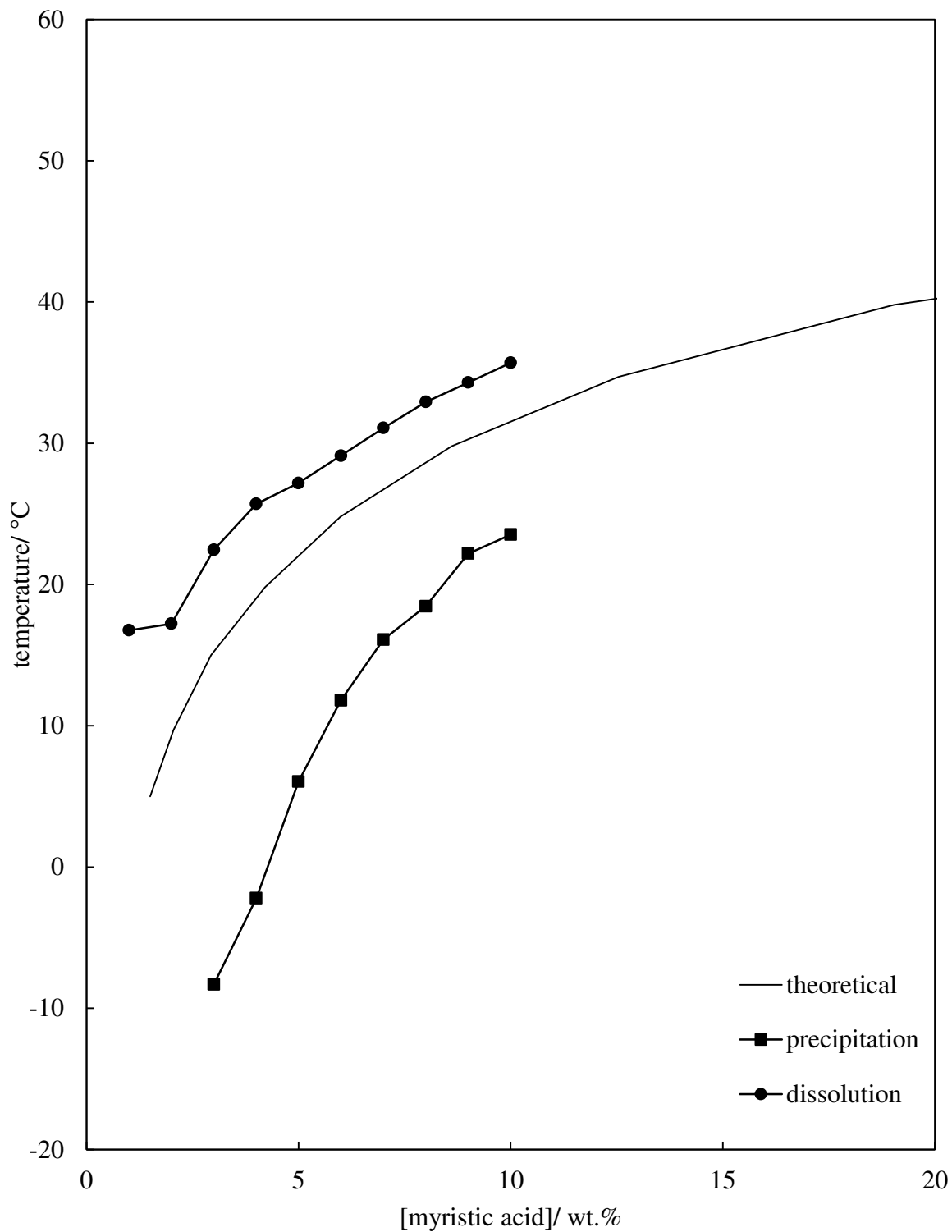


**Figure 5.4.** Precipitation and dissolution temperatures from DSC of myristic acid as a function of concentration in HOSO cooled from 80 to -20 °C, held at -20 °C for 5 minutes and then heated to 80 °C. The theoretical curve was calculated with equation 5.1.



### 5.3.1 Effect of cooling rate

The effect of cooling rate on the precipitation and dissolution peaks identified by DSC was investigated. The heating and cooling rates were 2 °C/min. and 20 °C/min. with concentrations ranging from 1 to 10 wt.% myristic acid in HOSO. The effect of cooling and heating rate was investigated due to literature stating that the cooling rate of a mixture can affect the gelled structure produced. Higaki et al.<sup>9</sup> investigated the effect of cooling rate on the gel produced with 'high-melting and low-melting fats'. The high-melting fats had melting temperatures over 60 °C such as fully hydrogenated rapeseed oil rich in behenic acid and fully hydrogenated rapeseed oil rich in stearic acid. The low-melting fats that these high-melting fats were added to included cocoa butter and olive oil which had a melting temperature of 34 °C and 5 °C, respectively. It was found that the faster cooling rate of 10 °C/min. rather than 1.5 °C/min. was necessary for the formation of a gel. This was because the high cooling rate induced the creation of smaller crystals that were randomly distributed in the liquid oil causing a crystal network which could incorporate an oil to develop, whereas the slower cooling rate caused the creation of large crystals which were not distributed throughout the oil. As can be seen from Figure 5.5 the cooling rate had a significant effect on the precipitation temperature of 2-10 wt.% myristic acid in HOSO. It was clear that as the cooling rate increased, from 0.1 °C/min. (from visual measurements), to 2 °C/min. and then 20 °C/min. (from DSC) the temperature of precipitation decreased. From Figure 5.6 it is clear that the heating rate had a significant effect on the dissolution temperature. It was found that as the heating rate increased from 0.1 °C/min. (from visual measurements) to up to 20 °C/min. (from DSC) the dissolution temperature increased. This is thought to be due to the slower cooling and heating rate causing there to be more time for the solution to equilibrate, therefore the values are closer to the theoretical value. From these results, it was decided that further measurements with the gel would be conducted when the gel was formed through cooling the myristic acid in HOSO mixture from 80 °C to  $8 \pm 2$  °C with the use of a freezer for one hour (cooling rate of approximately 1 °C/min.). In various measurements where the effect of heating the mixture was investigated, such as with pNMR measurements, the heating rate used was 1 °C/min.

**Figure 5.5.** Precipitation temperature of myristic acid as a function of concentration in HOSO as the cooling rate was increased from 0.1 °C/min. to 20 °C/min. The temperature determined with a rate of 0.1 °C/min. was through visual measurements, with 2 °C/min. and 20 °C/min. was with DSC. The theoretical dissolution temperature was determined from the ideal solubility equation.

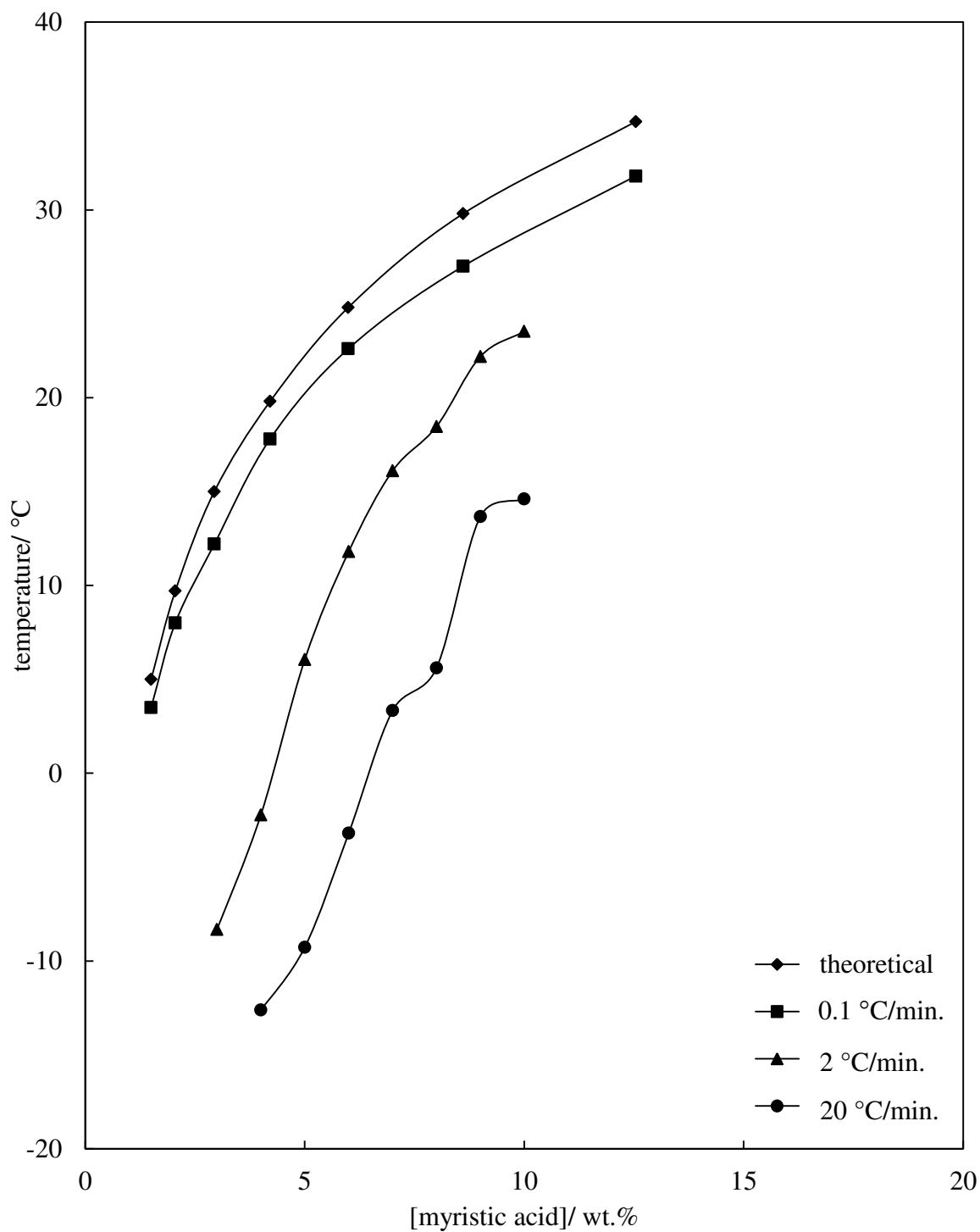
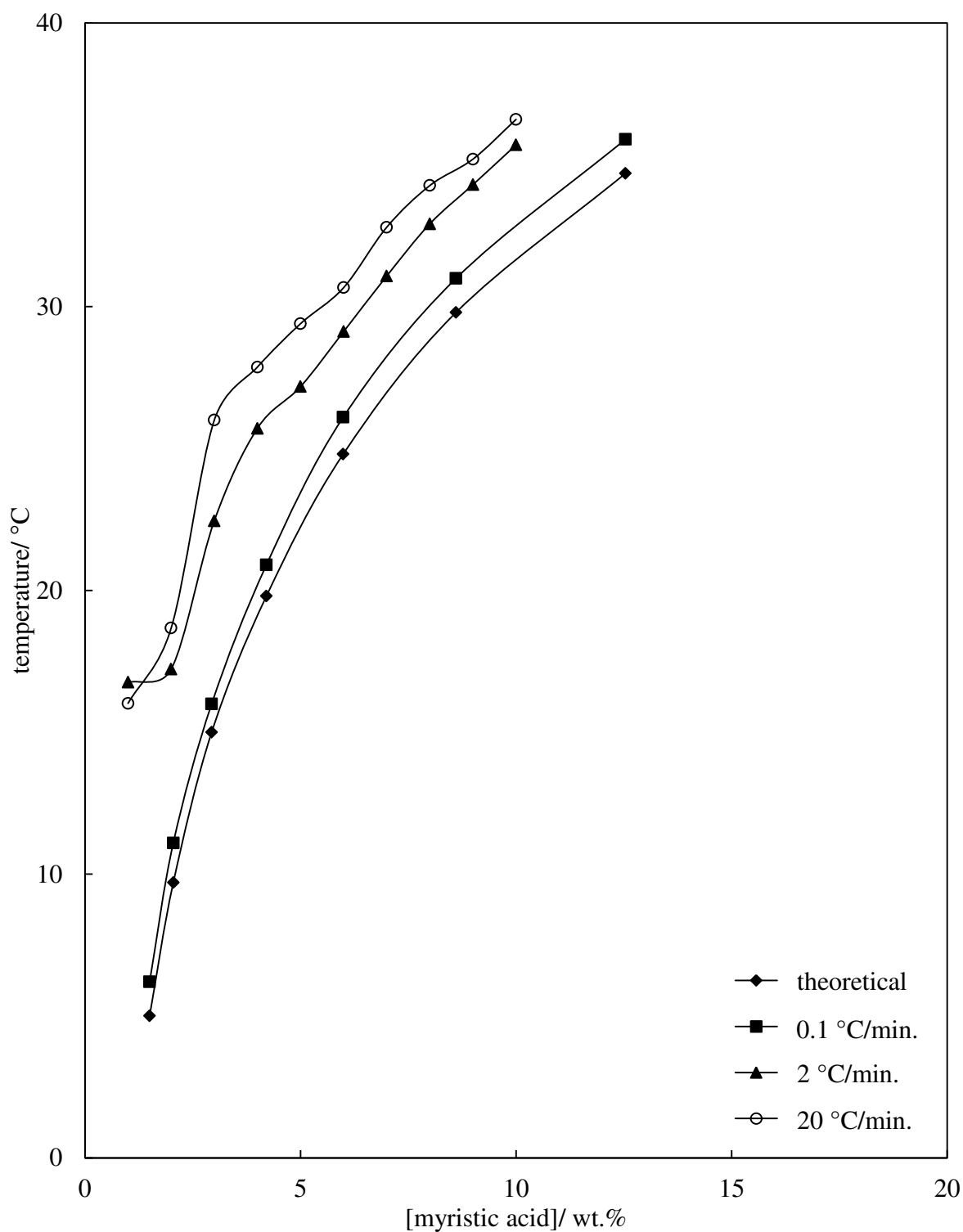


**Figure 5.6.** Dissolution temperature of myristic acid as a function of concentration in HOSO as the heating rate was increased from 0.1 °C/min. to 20 °C/min. The temperature determined with 0.1 °C/min. was through visual measurements, 2 °C/min. and 20 °C/min. was with DSC. The theoretical precipitation temperature was determined from the ideal solubility equation.



## 5.4 XRD

X-ray diffraction (XRD) was conducted to determine the crystal structure of myristic acid in HOSO at 25 °C. To do this two X-ray diffractometers were used which involved the same sample preparation method (10 wt.% myristic acid in HOSO gel was heated to 80 °C, then cooled 1 °C/min. to 9.2 °C) before measurements at  $20 \pm 2$  °C. Figure 5.7 shows the X-ray diffraction pattern of 10 wt.% myristic acid in HOSO with the use of a PANalytical empyrean X-ray diffractometer with  $\text{CuK}\alpha$  radiation ( $\lambda = 1.54$  Å). From the figure it can be determined that the peaks observed are the same as that found with neat myristic acid by Bond<sup>10</sup> (see Appendix Figure A1.1). It is clear that there were three prominent peaks identified which were at  $2\theta$  of 2.84, 5.64 and 8.43 ° which from Bragg's law (see equation 5.2) give d-spacings (distances between crystal planes) of 32.08, 15.70 and 10.55 Å, respectively. Bond found that the  $2\theta$  values of the prominent peaks have d-spacing values of 31.47, 15.73 and 10.49 Å. This confirms that the structure of the myristic acid in the HOSO was the same as that found by Bond, i.e. monoclinic.

A crystal from a gel of 10 wt.% myristic acid in HOSO was studied with a second X-ray diffractometer (Stoë IPDS2 with a molybdenum wavelength of 0.71 Å) to verify the findings with the PANalytical empyrean X-ray diffractometer. It was found that peaks were observed at similar d-spacings to before as shown in Figure 5.8. The d-spacings of 10.71, 4.12 and 3.65 Å, which are also shown in a simulated pattern in Figure 5.9, correspond to the d-spacings identified by Bond which are 10.45, 4.103 and 3.64 Å (see Appendix Figure A1.2). This therefore concludes that the myristic acid crystals present were monoclinic. The d-spacings from the  $2\theta$  values were calculated by the following equation:

$$\sin\theta = \frac{\lambda}{2d} \quad (5.2)$$

where  $\lambda$  is wavelength of the incident wave and  $d$  is the d-spacing.<sup>7</sup>

**Figure 5.7.** X-ray diffraction pattern of a 10 wt.% myristic acid in HOSO gel with a PANalytical empyrean X-ray diffractometer with CuK $\alpha$  radiation ( $\lambda = 1.54 \text{ \AA}$ ) with the prominent d-spacings labelled in  $\text{\AA}$ .

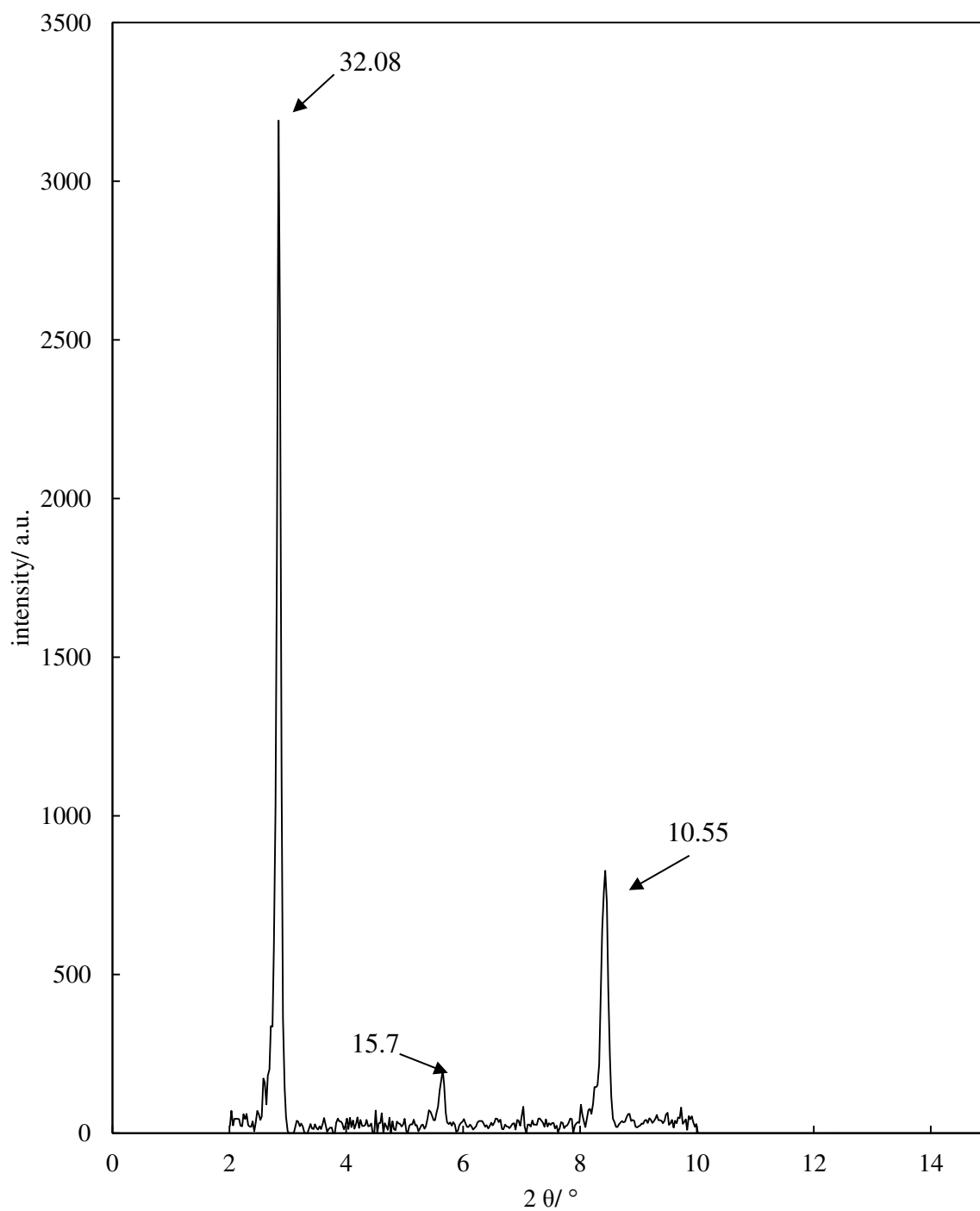


**Figure 5.8.** Powder diffraction pattern for a 50  $\mu\text{m}$  aggregate of myristic acid taken from a 10 wt.% myristic acid in HOSO gel. The pattern is from a Stöe IPDS2 diffractometer with a molybdenum wavelength of 0.71  $\text{\AA}$  with the prominent d-spacings labelled.

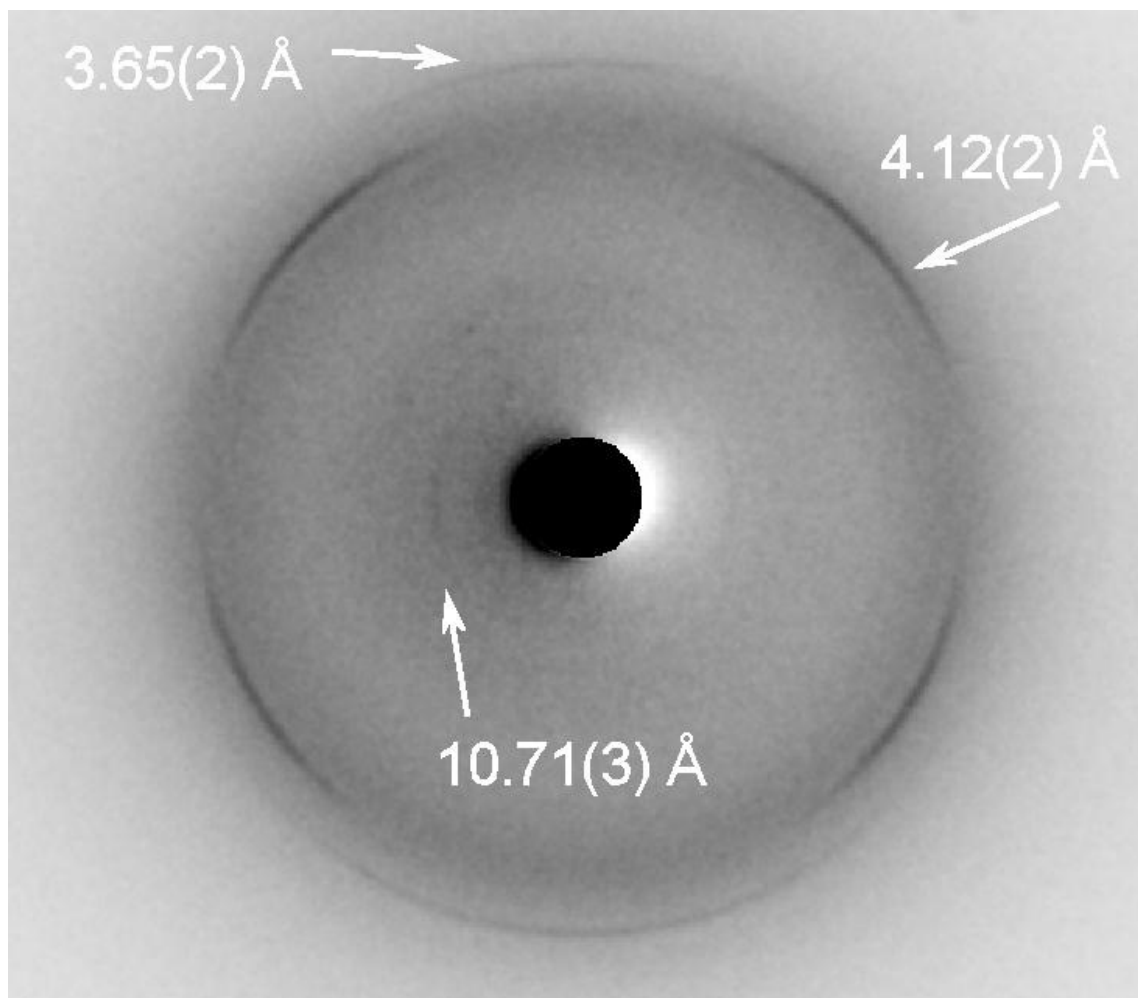
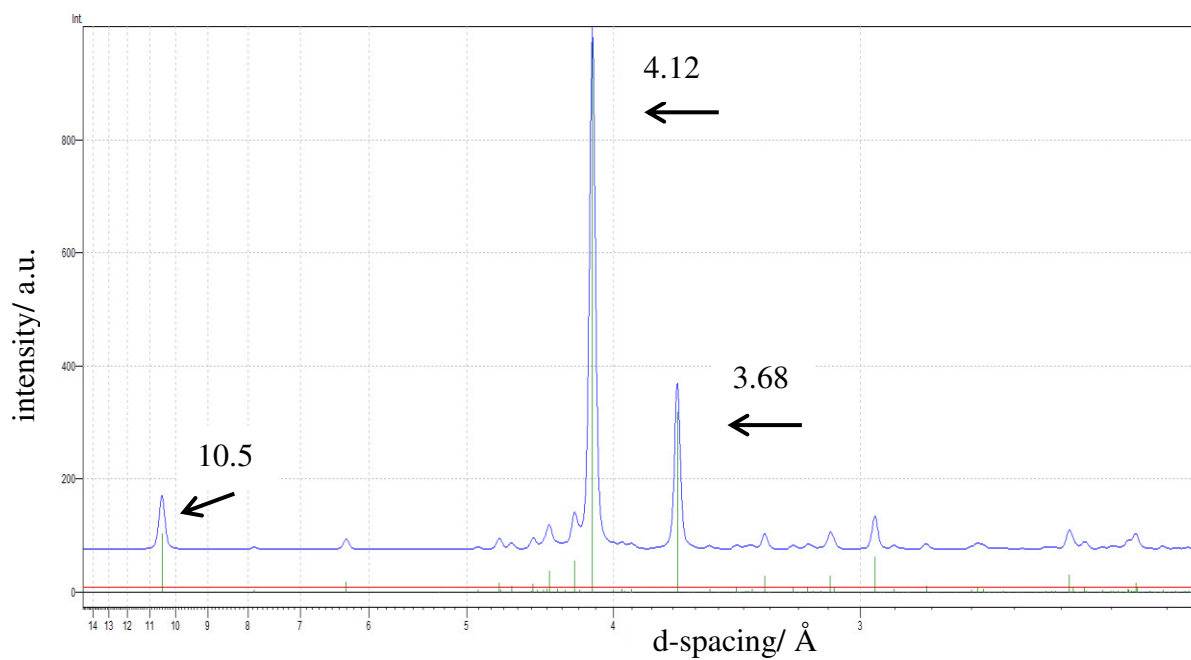


**Figure 5.9.** Simulated 1-D pattern for a 50  $\mu\text{m}$  aggregate of myristic acid taken from a 10 wt.% myristic acid in HOSO gel. Prominent d-spacings are labelled.



## 5.5 Microscopy

Both optical microscopy and cryogenic scanning electron microscopy (cryo SEM) were used to investigate the shape and size of myristic acid crystals in HOSO gels.

### 5.5.1 Optical microscopy

The gel was created by heating the mixture to 80 °C for 1 hour and then cooling to  $8 \pm 2$  °C, with microscopy conducted at 22 °C. As can be seen from Figure 5.10, when neat HOSO was heated and then cooled there was not any solid component present. With 1 and 2 wt.% myristic acid present there were small aggregates ( $< 10 \mu\text{m}$  in diameter) in the oil. As the myristic acid concentration increased from 3 to 4 wt.% these small aggregates were observed but there was also needles present which were up to 100  $\mu\text{m}$  in length. As the myristic acid concentration increased to up to 12 wt.% plate-like crystals with a width of  $< 50 \mu\text{m}$  were formed. As the myristic acid concentration increased from 7 wt.% to 12 wt.%, the size of the plates was found to decrease. It was also interesting to see that the crystals present in the oil through crossed polarising lenses indicating that they were birefringent crystals. As can be seen from Figure 5.2 at 22 °C a clear homogeneous mixture is observed at concentrations below 4 wt.%, therefore crystals were not expected to be observed through optical microscopy below this concentration. However crystals were observed with as little as 2 wt.%. This is thought to be because the microscope slide and cover slip induced heterogeneous crystallisation.

**Figure 5.10.** Optical microscopy of myristic acid (concentration given) in HOSO mixtures at 22 °C after prior heating to 80 °C and then cooling to  $8 \pm 2$  °C. (b), (m) and (p) are viewed through crossed polarising lenses. The samples with myristic acid present were diluted 1:1 with HOSO. Scale bar 200  $\mu\text{m}$ .

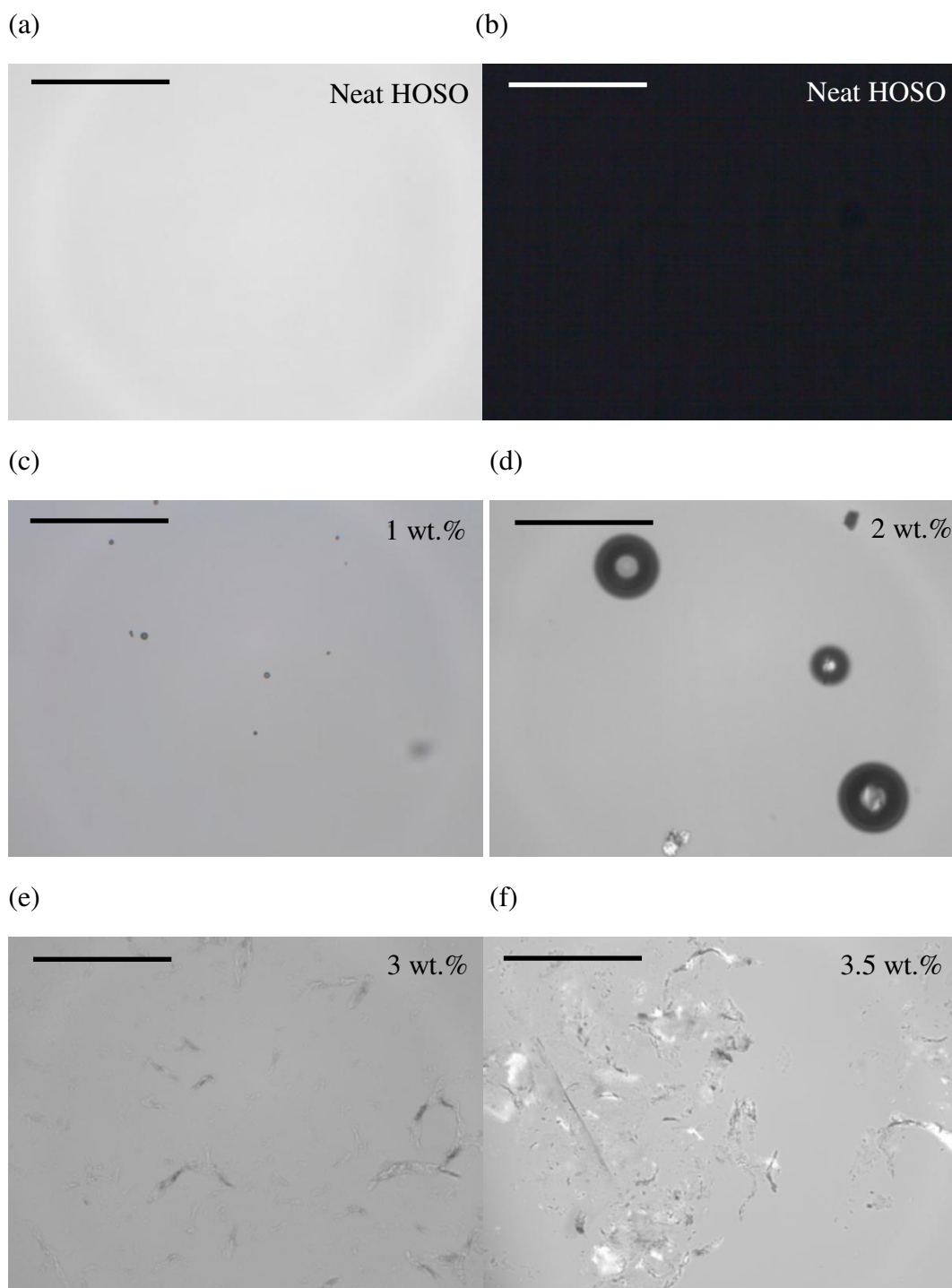


**Figure 5.10** (continued)

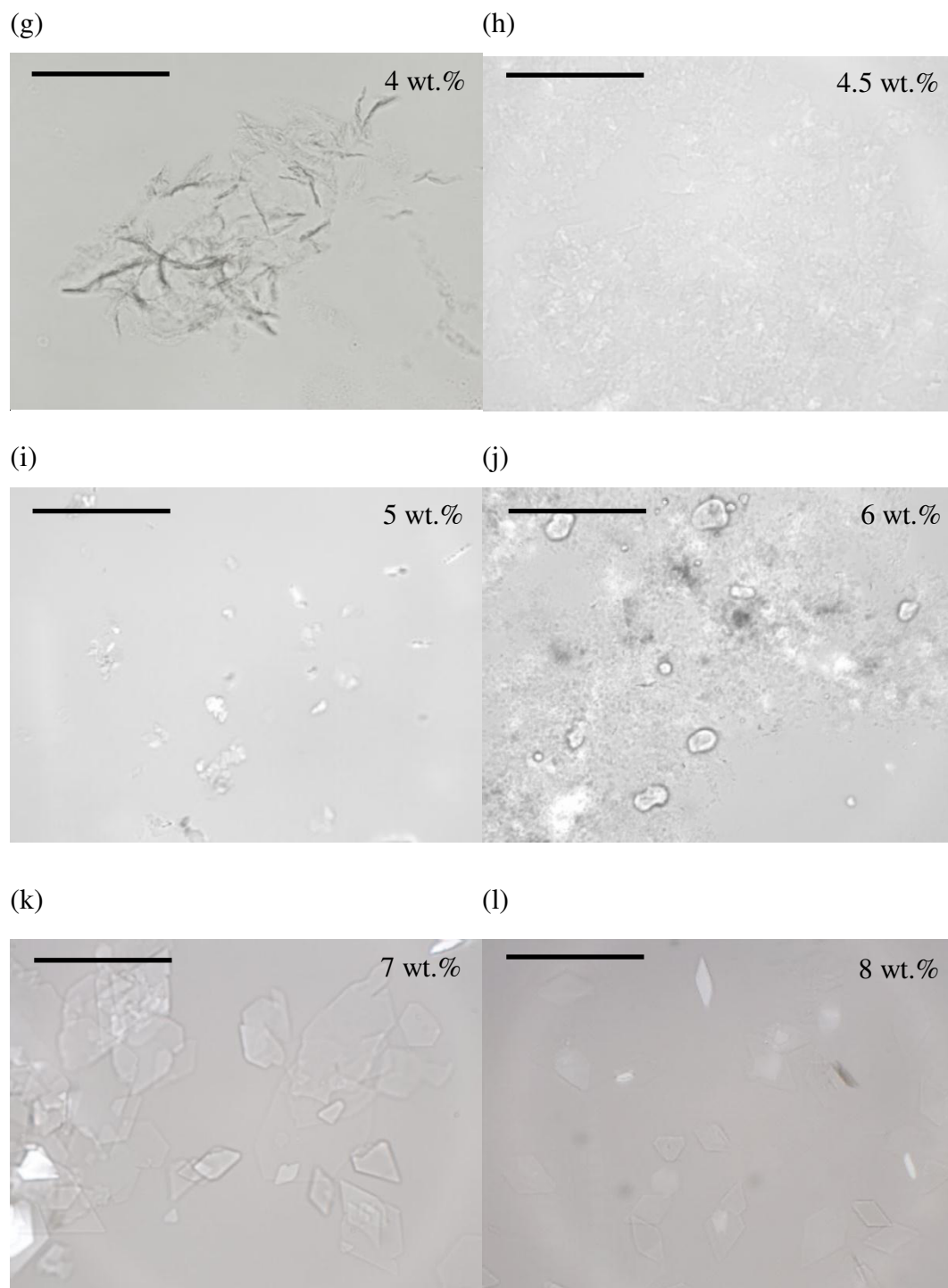
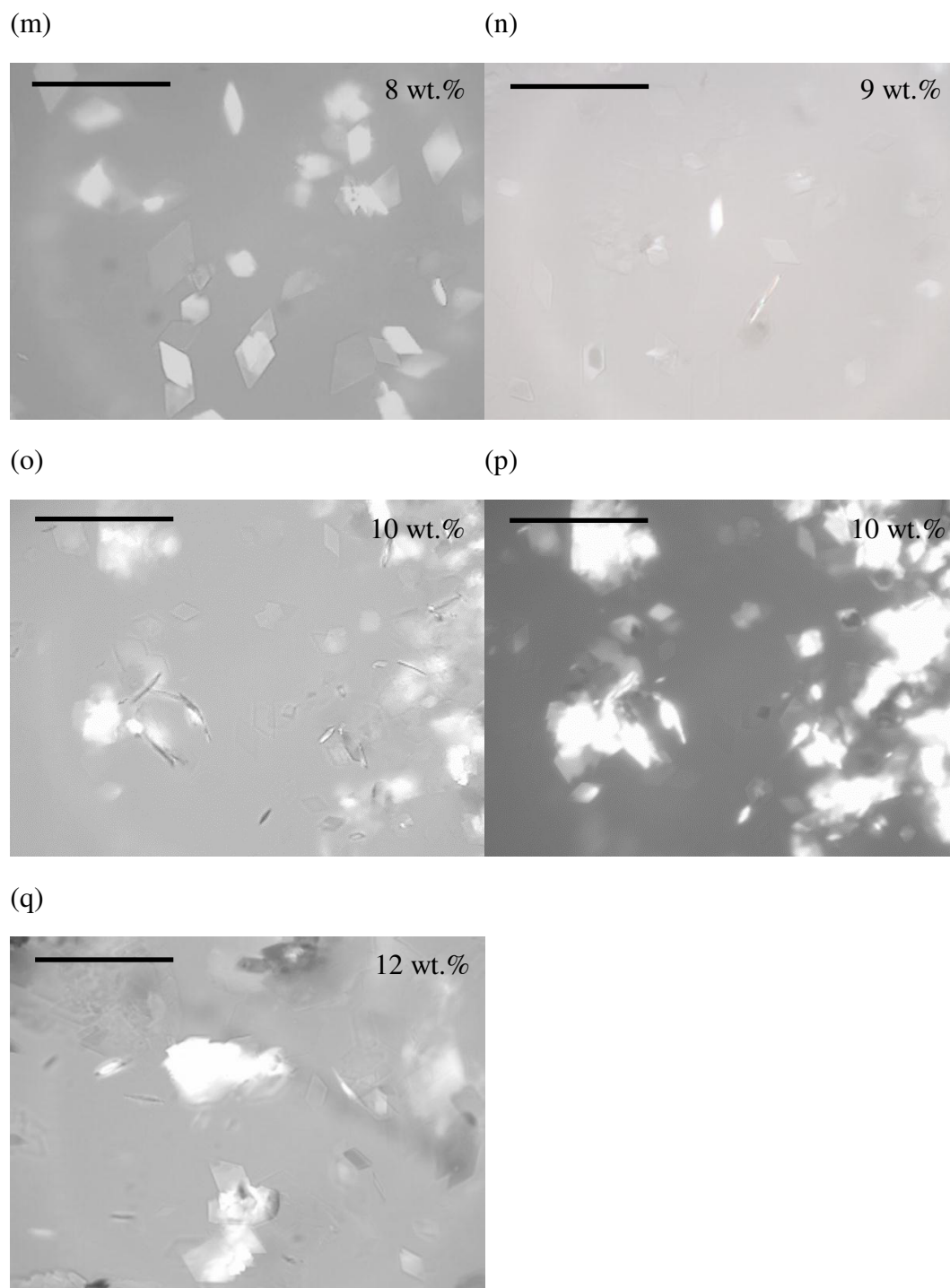


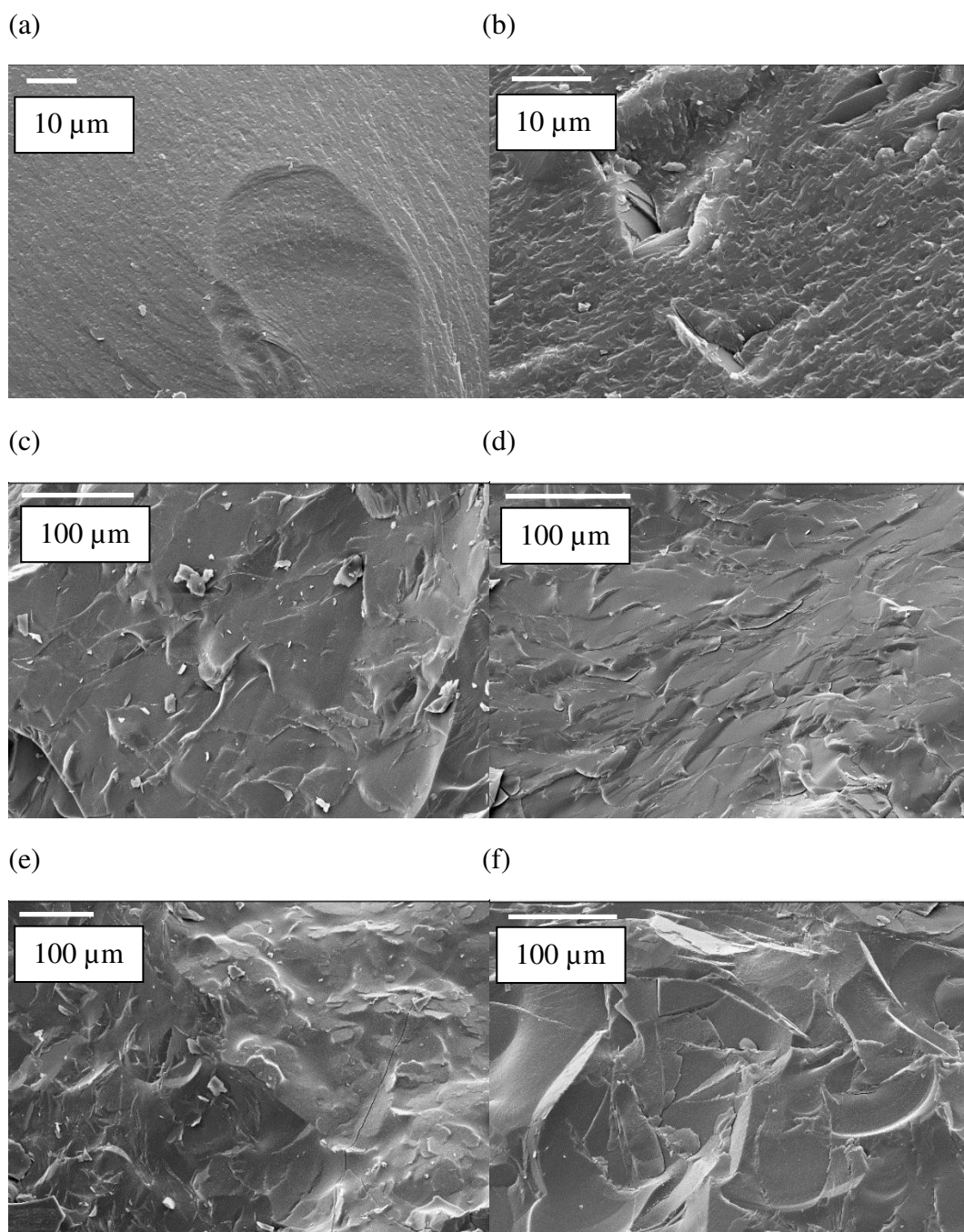
**Figure 5.10** (continued)



### 5.5.2 Cryogenic scanning electron microscopy

Cryogenic scanning electron microscopy (Cryo-SEM) was conducted at -140 °C (samples were fractured after cooling to -140 °C prior to microscopy) with neat HOSO and with 4, 6, 8, 10 and 12 wt.% myristic acid in HOSO. As can be seen from Figure 5.11, it was clear that myristic acid crystallised into plates and that they became more visible as the myristic acid concentration increased, unfortunately the crystal size could not be determined.

**Figure 5.11.** Cryo-SEM images at  $-140\text{ }^{\circ}\text{C}$  of (a) 0 wt.%, (b) 4 wt.%, (c) 6 wt.%, (d) 8 wt.%, (e) 10 wt.% and (f) 12 wt.% myristic acid in HOSO after prior heating to  $80\text{ }^{\circ}\text{C}$ , then cooling to  $8 \pm 2\text{ }^{\circ}\text{C}$ .



## 5.6 Surface energy determination

It is known that the contact angle of a liquid on a solid particle surface is important for the creation and stability of foam. If the contact angle is  $0^\circ$  then the liquid fully wets the solid surface, if the contact angle is  $180^\circ$  then the solid surface is not wetted, an angle in between these values indicates that the solid surface is partially wetted and therefore the particle is present at the air-oil interface.<sup>11</sup> Surface energy measurements were conducted by contact angle measurements with a compressed pellet of myristic acid with various oils. The values in Table 5.1 were from 30 measurements with each liquid on 8 compressed pellets. It is clear that there is a significant hysteresis between the advancing and receding contact angle indicating that the myristic acid pellet surface was particularly rough.<sup>12</sup> The obvious roughness of the surface may have caused the contact angles to be lower than if the contact angles were measured on a smooth surface.<sup>13</sup> However, the surface of myristic acid is hydrophobic. An advancing contact angle of  $89^\circ$  into the water phase is similar to that on PTFE ( $108^\circ$ ).<sup>14</sup> The results also show that high oleic sunflower oil partially wets the myristic acid inferring that the myristic acid may sit at the air-oil interface.

**Table 5.1.** Advancing and receding contact angle measurements of different liquids on pellets of myristic acid in air at  $22 \pm 2^\circ\text{C}$ .

| Liquid                      | Surface tension/<br>$\text{mN m}^{-1}$ | Advancing contact<br>angle/ $\pm 1^\circ$ | Receding contact<br>angle/ $\pm 1^\circ$ |
|-----------------------------|--|---|--|
| Hexadecane                  | 27.05 <sup>15*</sup>                   | 23  | 14                                       |
| High oleic sunflower<br>oil | 33.4*                                  | 39  | 18                                       |
| 1-bromonaphthalene          | 44.6 <sup>16+</sup>                    | 28  | 14                                       |
| Ethylene glycol             | 47.99 <sup>15*</sup>                   | 47  | 38                                       |
| Diiodomethane               | 50.8 <sup>16+</sup>                    | 48  | 24                                       |
| Formamide                   | 57.03 <sup>15*</sup>                   | 32  | 18                                       |
| Glycerol                    | 63.4 <sup>16+</sup>                    | 89  | 56                                       |
| Milli Q water               | 72.0 <sup>15*</sup>                    | 89  | 71                                       |

\* at  $25^\circ\text{C}$ , + at  $20^\circ\text{C}$ .

## 5.7 Rheology

Rheology is a study of the flow behaviour of a mixture. The effect of frequency and temperature on the rheology of myristic acid in HOSO was investigated. Initial tests were conducted to identify the viscoelastic region of 8 and 12 wt.% myristic acid in HOSO at 10 °C. The mixtures were cooled 1 °C/min. from 80 °C to 10 °C prior to the gradual increase in strain from 0.001 to 1 % over 22 minutes. Figure 5.12 shows that the linear viscoelastic region was clearly in the area of 0.01 % as in this area  $G'$  was independent of the increase in strain ( $G'$  is the solid nature of a mixture<sup>17</sup>). Therefore the strain was set at 0.01 %.

### 5.7.1 Effect of oscillation frequency

The effect of oscillation frequency on mixtures of 4, 8 and 12 wt.% myristic acid in HOSO was then investigated as shown in Figure 5.13. The figure shows that the mixtures at all concentrations investigated demonstrated a gelled network<sup>17</sup> as  $G'$  was independent of frequency. The values of  $G'$  were found to be similar to those observed with 5-9 % Myverol monoglyceride in cod liver oil<sup>18</sup> and a volume fraction of 0.063 and 0.075 Adochan 98 (monoglyceride) in olive oil<sup>19</sup> where  $G'$  was found to be in the area of  $10^5$ - $10^6$  Pa. It was decided that a frequency of 1 Hz would be used to study the effect of temperature and shear rate on the gel characteristics.

**Figure 5.12.** Amplitude sweep at 10 °C of 8 and 12 wt.% myristic acid in HOSO (after cooling from 80 °C at 1 °C/min.). The strain gradually increased from 0.001 to 1 % over 22 minutes and was conducted with a frequency of 1 Hz using parallel plates.

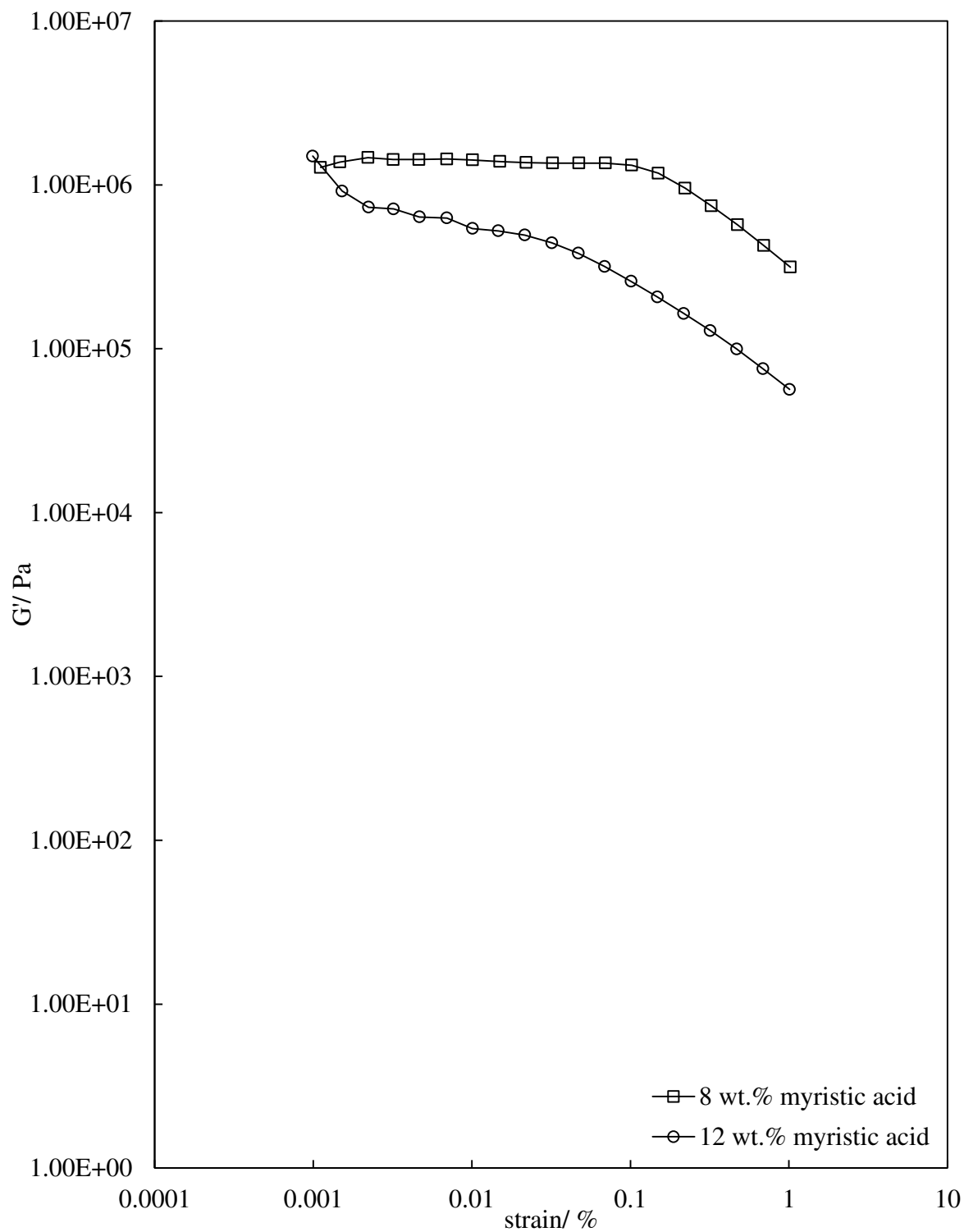
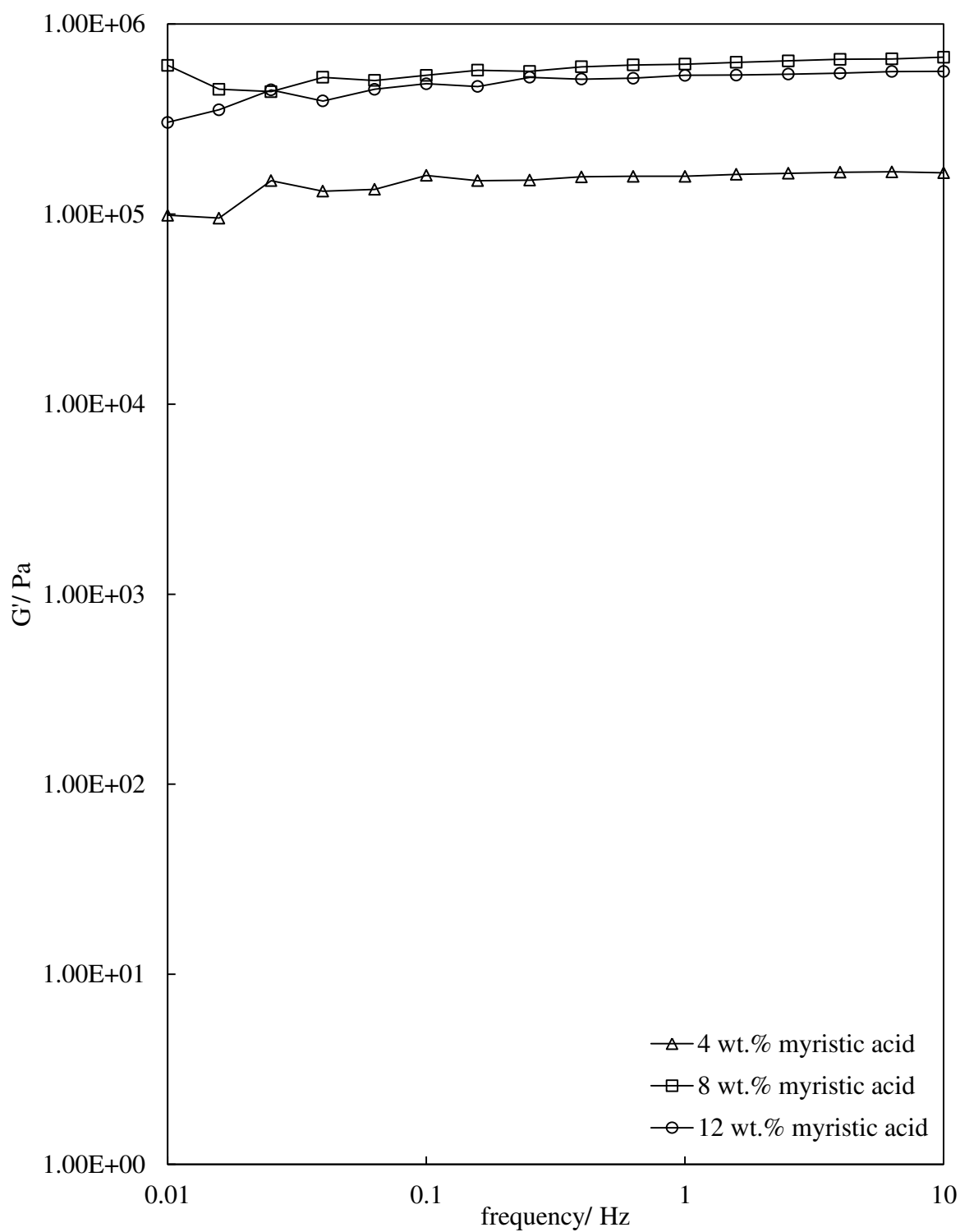


**Figure 5.13.** Frequency sweep at 10 °C of 4, 8 and 12 wt.% myristic acid in HOSO (after cooling from 80 °C with a cooling rate of 1 °C/min.). The measurements were conducted with 0.01 % strain using parallel plates.

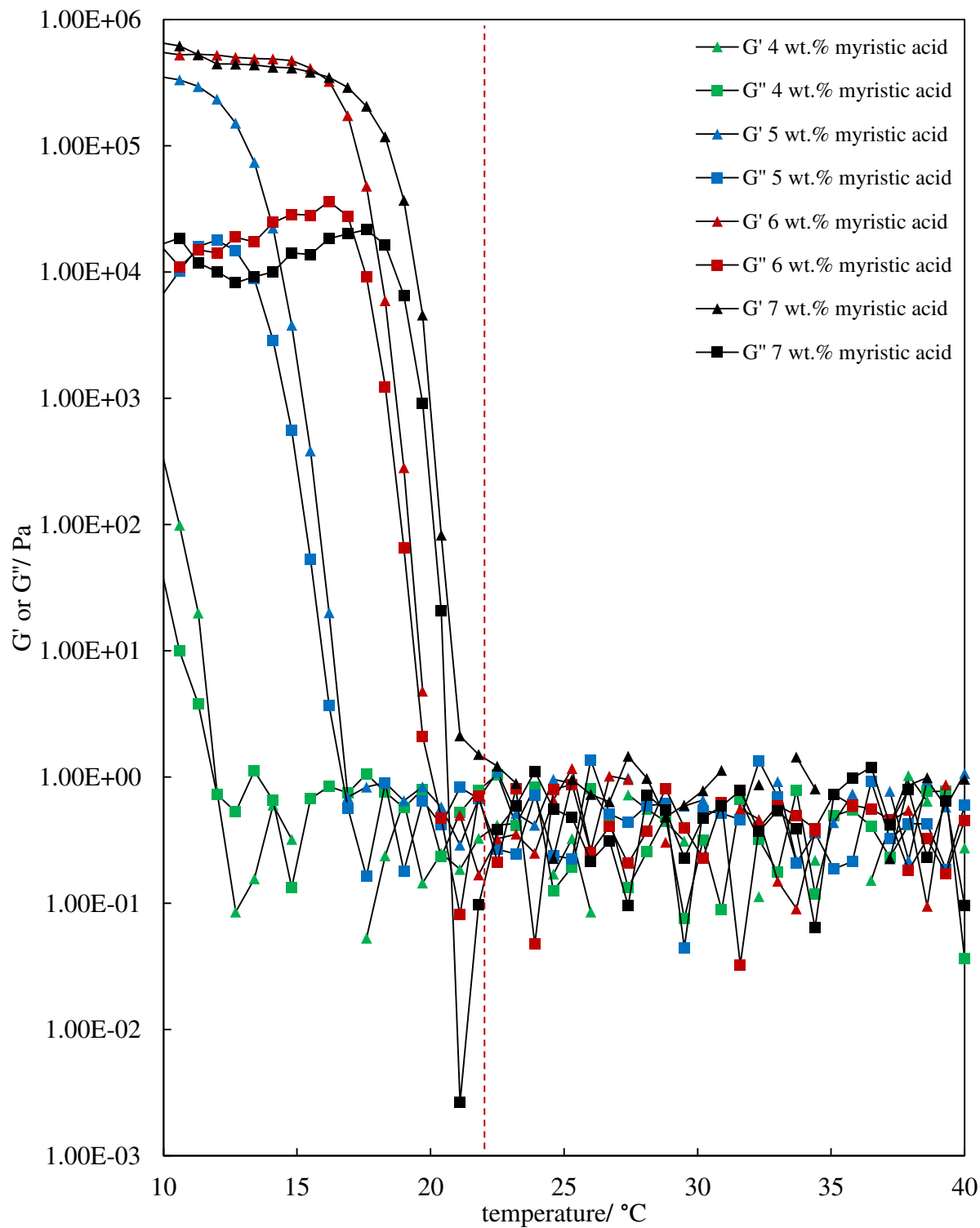


### 5.7.2 Effect of temperature

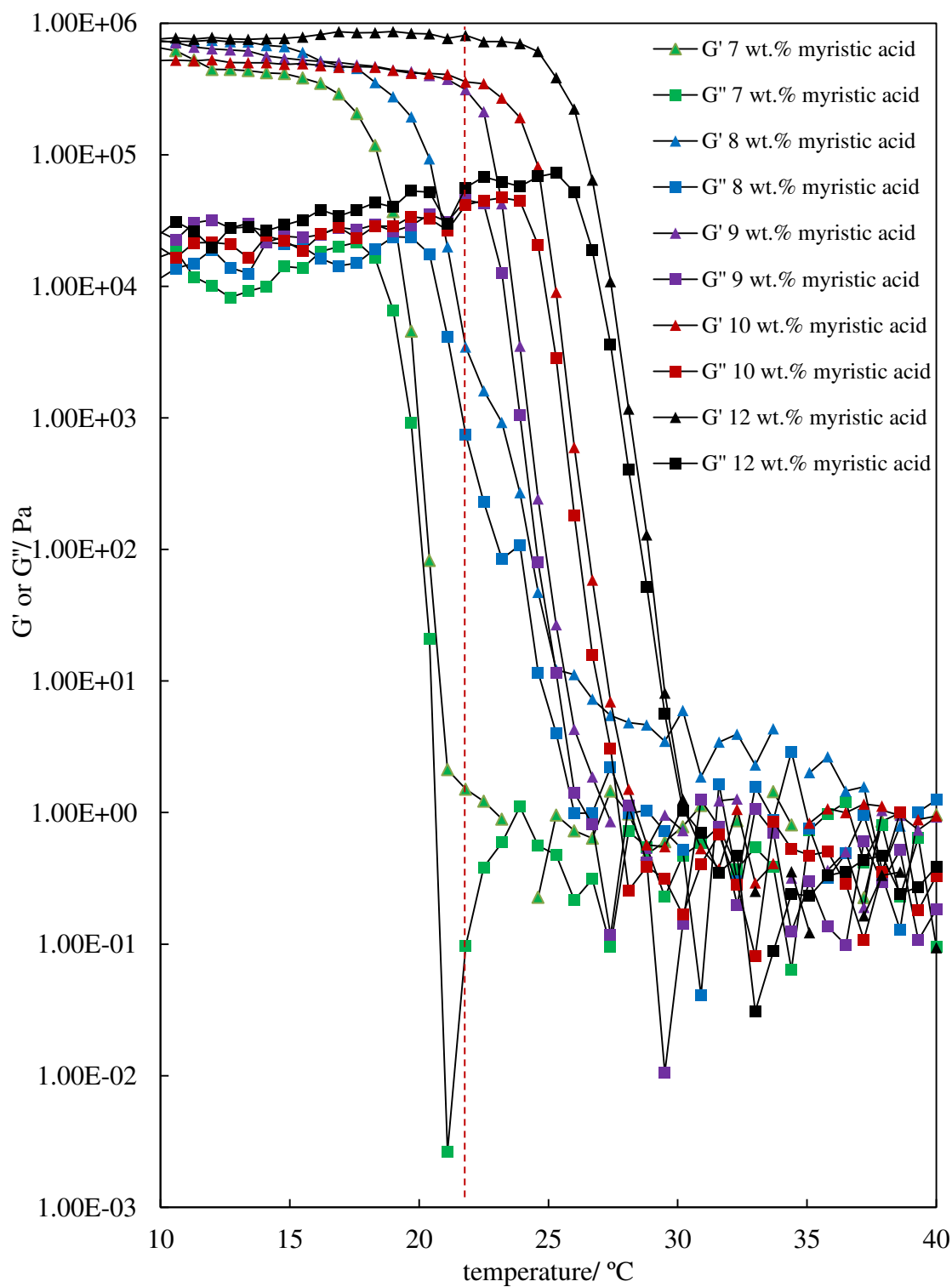
Figure 5.14 shows that as the temperature of mixtures of myristic acid in HOSO decreased from 80 °C to 10 °C both the  $G'$  and  $G''$  ( $G''$  is the liquid nature of a mixture<sup>17</sup>) increased dramatically at a specific temperature. A  $G'$  value which is higher than the  $G''$  indicates that the mixture is not a liquid. As the myristic acid concentration increased from 4 to 5 wt.% values of  $G'$  and  $G''$  increased significantly at 10 °C.  $G'$  and  $G''$  only slightly increased as the myristic acid concentration was further increased to up to 10 wt.% as shown in both Figure 5.14 and Figure 5.15. As the myristic acid concentration increased the temperature at which  $G'$  reached a maximum occurred at a higher temperature. The temperature of gelation is taken as the mid-point between the minimum and maximum  $G'$  value. This gelation temperature increased as the myristic acid concentration increased.

Figure 5.16 shows that the precipitation temperature (identified through visual observations) is higher than the gelation temperature. This indicates that for a gel to be formed there needs to be a certain volume fraction of crystals present.

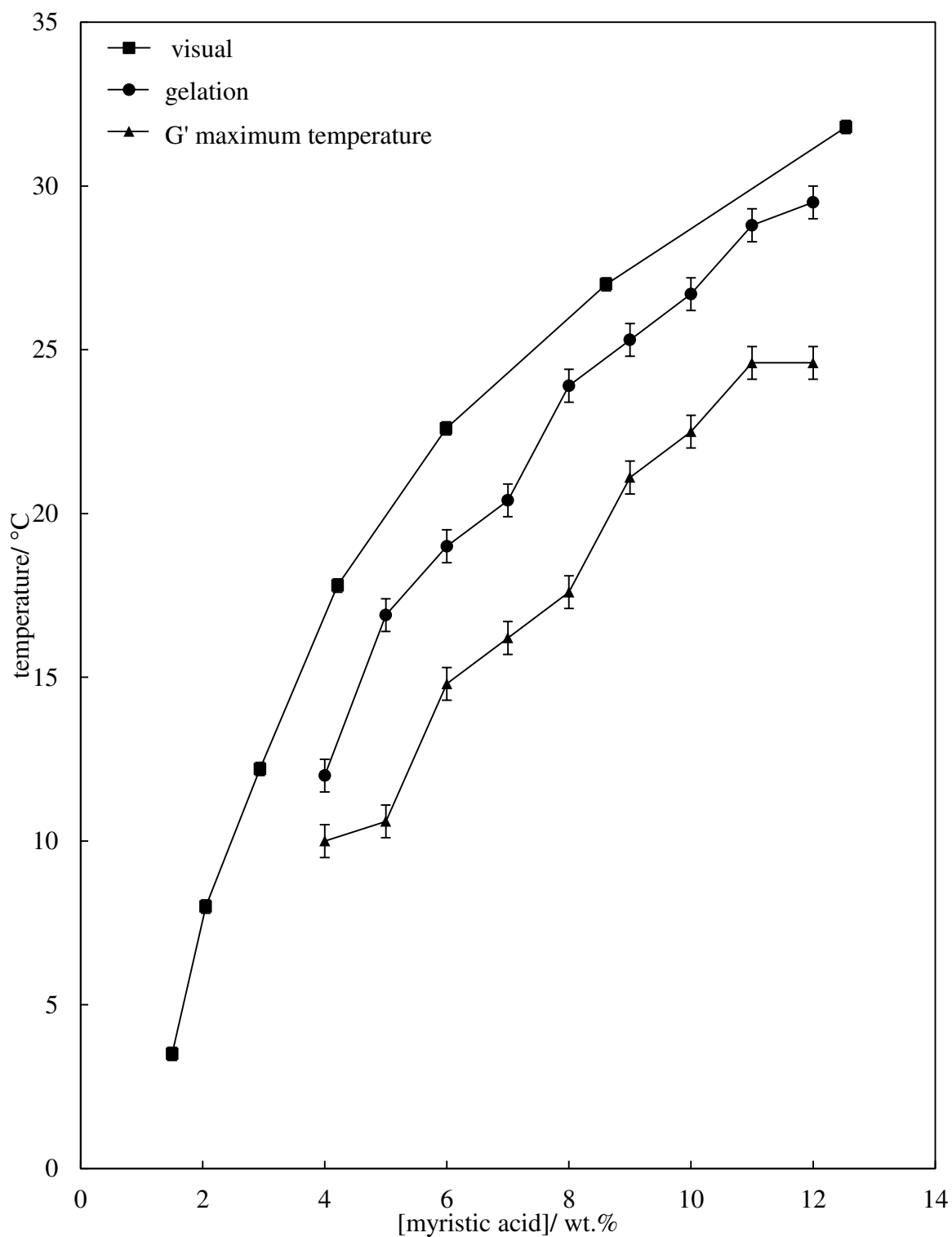
**Figure 5.14.** Storage modulus ( $G'$ ) and loss modulus ( $G''$ ) of 4-7 wt.% myristic acid in HOSO as temperature was decreased from 80 °C to 10 °C at a rate of 1 °C/min. Measurements were conducted with parallel plates at 0.01 % and 1 Hz. The red dashed line indicates 22 °C.



**Figure 5.15.** Storage modulus ( $G'$ ) and loss modulus ( $G''$ ) of 7-12 wt.% myristic acid in HOSO as temperature was decreased from 80 °C to 10 °C at a rate of 1 °C/min. Measurements were conducted with parallel plates at 0.01 % and 1 Hz. The red dashed line indicates 22 °C.



**Figure 5.16.** Gelation temperature and the temperature at which G' is maximum (determined by rheology measurements) and the visual precipitation temperature of myristic acid as a function of concentration in HOSO. The rheology measurements were conducted with a cooling rate of 1 °C/min. and the cooling rate with the visual measurements was 0.1 °C/min.

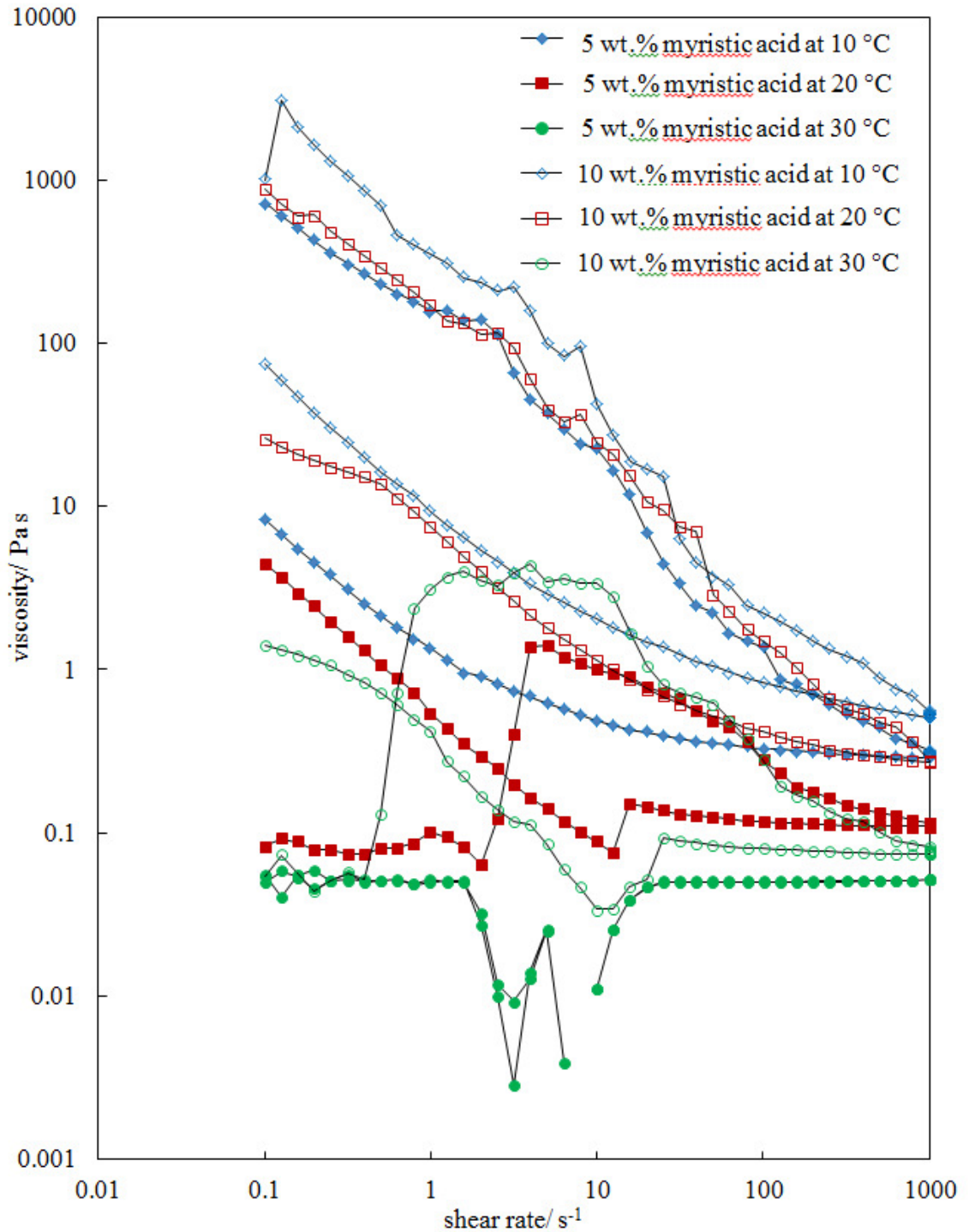


### 5.7.3 Viscosity

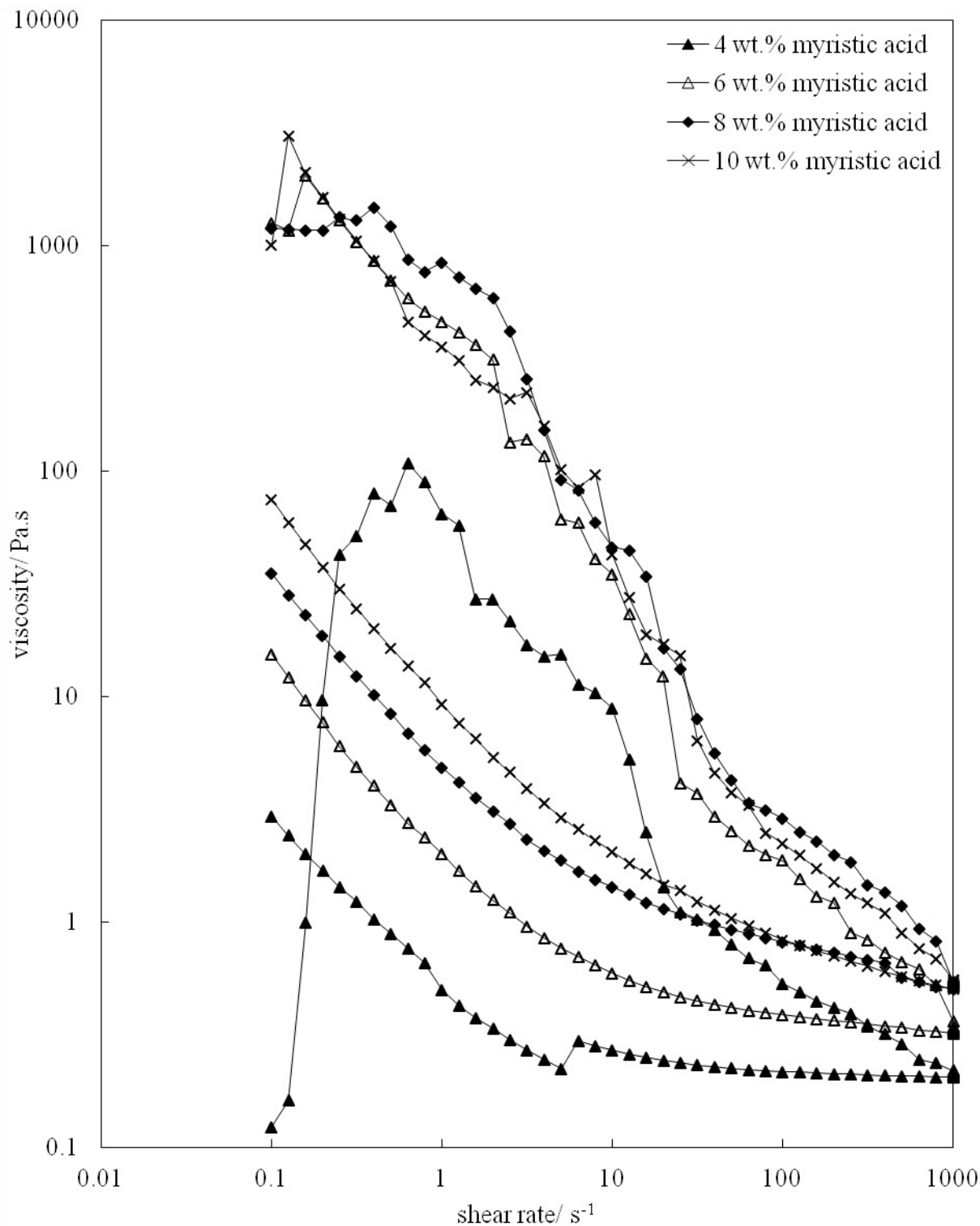
The viscosity measurements were conducted at 10, 20 and 30 °C after cooling from 80 °C at a rate of 1 °C/min. At the final temperature (10-30 °C) the shear rate was then increased from 0.01 to 1000 s<sup>-1</sup> over 30 minutes, held at 1000 s<sup>-1</sup> for 5 minutes, then reduced back to 0.01 s<sup>-1</sup> over 30 minutes. The sample was held at 1000 s<sup>-1</sup> for 5 minutes to simulate the shear that the sample experiences during the whipping technique. Figure 5.17 demonstrates that as the shear rate was increased from 0.01 to 1000 s<sup>-1</sup> the network of crystals of myristic acid in HOSO was disrupted. Upon decreasing the shear rate to 0.01 s<sup>-1</sup> the gel network partially reformed (the viscosity increased). However, the viscosity did not return to the value prior to the increase in shear rate suggesting the shear induced a possible reorientation of the fatty acid in the oil. The figure also shows that the viscosity increased as the fixed temperature decreased. Also, as the concentration of myristic acid in HOSO decreased from 10 to 5 wt.% the viscosity of the mixture decreased.

Figure 5.18 shows viscosity measurements of 4, 6, 8 and 10 wt.% myristic acid in HOSO at 10 °C. Again, as the myristic acid concentration increased, the viscosity increased. Also, 8 and 10 wt.% myristic acid in HOSO at 10 °C have a similar viscosity within the shear range of 50 to 1000 s<sup>-1</sup>.

**Figure 5.17.** Viscosity of 5 and 10 wt.% myristic acid in HOSO at 10, 20 and 30 °C with a strain of 0.01 % and a frequency of 1 Hz using concentric cylinders. The shear rate increased from 0.01 to 1000 s<sup>-1</sup>, then decreased from 1000 to 0.01 s<sup>-1</sup>.



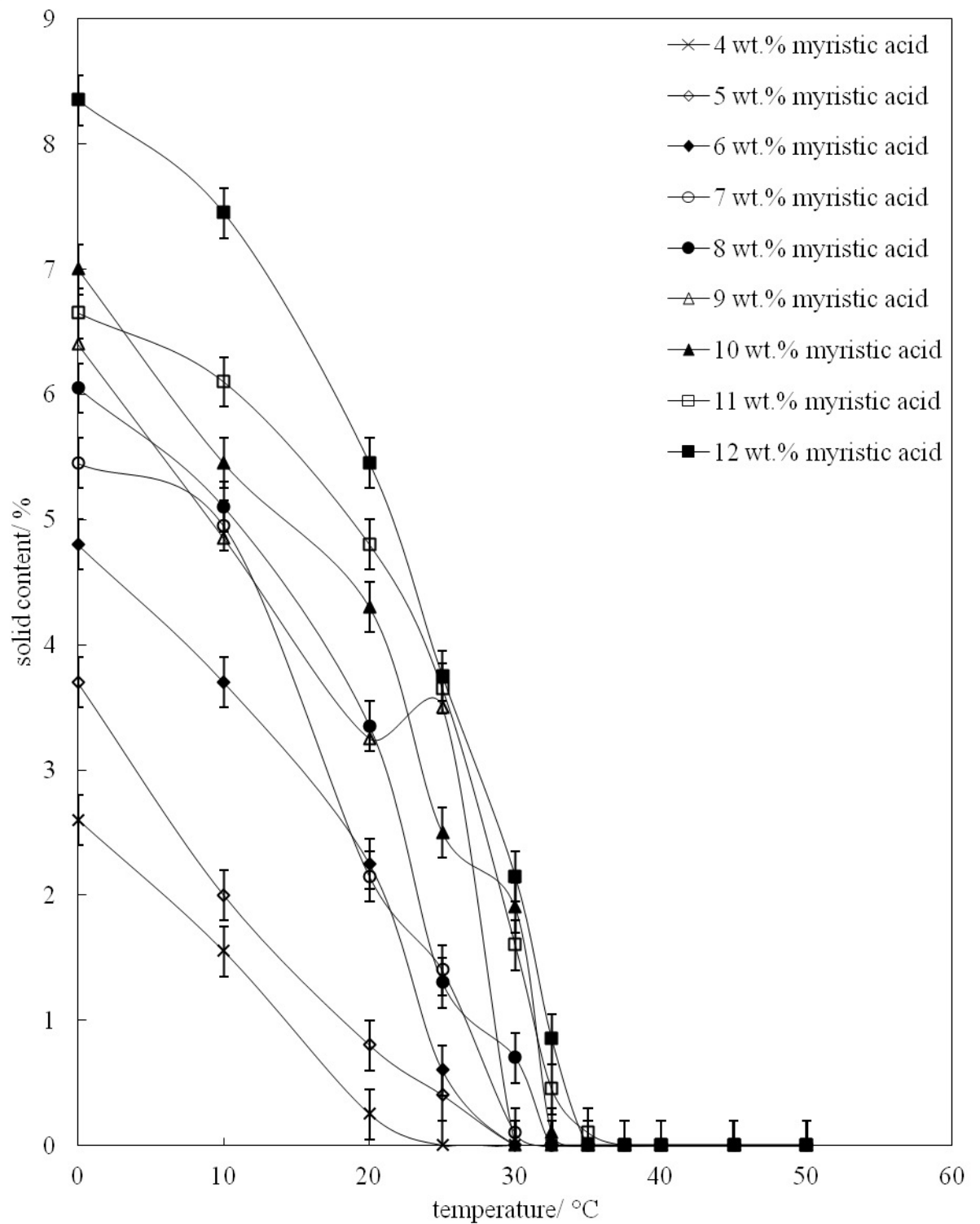
**Figure 5.18.** Viscosity of 4, 6, 8 and 10 wt.% myristic acid in HOSO at 10 °C with a strain of 0.01 % and a frequency of 1 Hz. The shear rate increased from 0.01 to 1000 s<sup>-1</sup>, then decreased from 1000 to 0.01 s<sup>-1</sup> using concentric cylinders.



## 5.8 Pulsed nuclear magnetic resonance

Pulsed nuclear magnetic resonance (pNMR) was conducted to investigate if there was a significant difference in the solid content of the myristic acid in HOSO mixture as both temperature and the myristic acid concentration was increased. pNMR can measure the solid content in the mixture from the free induction decay of the protons in the sample after a radio frequency pulse at 90 °. The solid and liquid content can be determined due to signals from solids decaying faster than signals from liquids.<sup>20-22</sup> Figure 5.19 shows that there was a decrease in the solid phase content as the concentration of the myristic acid decreased and also as temperature increased. It can therefore be concluded that a gel could be created with as little as 2.5 % of solid.

**Figure 5.19.** Solid phase content analysis with the use of pulsed NMR of myristic acid as a function of concentration in HOSO following the standard Nestlé preparation procedure.



## 5.9 Conclusions

It was found that as the cooling rate of the mixture of myristic acid in HOSO was increased, the crystallisation temperature decreased, and as the heating rate increased the dissolution temperature increased. Myristic acid crystals, as identified by XRD, were found to have a monoclinic structure. Myristic acid in HOSO at low concentrations (1-4 wt.%) existed as both small aggregates < 10  $\mu\text{m}$  in diameter and needles up to 100  $\mu\text{m}$  in length. At higher concentrations (5-12 wt.%) the birefringent crystals were plate-like which decreased in size as concentration increased. Contact angle measurements of various probe liquids on a myristic acid pellet confirmed that myristic acid is hydrophobic and that HOSO partially wets a myristic acid substrate. It was confirmed by rheology measurements that myristic acid gels HOSO, and that the gelation temperature increased as the myristic acid concentration increased. The solid content of myristic acid in HOSO mixture decreased as myristic acid concentration decreased and as temperature increased.

## 5.10 References

1. J. Daniel and R. Rajasekharan, *J. Am. Oil Chem. Soc.*, **80**, 417 (2003).
2. F. G. Gandolfo, A. Bot and E. Floter, *J. Am. Oil Chem. Soc.*, **81**, 1 (2004).
3. H. M. Schaink, K. F. van Malssen, S. Morgado-Alves, D. Kalnin and E. van der Linden, *Food Res. Int.*, **40**, 1185 (2007).
4. M. Perneti, K. F. van Malssen, E. Floter and A. Bot, *Curr. Opin. Colloid Interface Sci.*, **12**, 221 (2007).
5. K.W. Smith, K. Bhaggan, G. Talbot and K.F. van Malssen, *J. Am. Oil Chem. Soc.*, **88**, 1085 (2011).
6. A. Sein, J.A. Verheij and W.G.M. Agterof, *J. Colloid Interface Sci.*, **249**, 412 (2002).
7. *Atkins' Physical Chemistry*, P.W. Atkins, Ninth edition, Oxford University Press, Oxford, 2010.
8. J.A. Wilson and J.S. Chickos, *J. Chem. Eng. Data*, **58**, 322 (2013).
9. K. Higaki, Y. Sasakura, T. Koyano, I. Hachiya and K. Sato, *J. Am. Oil Chem. Soc.*, **80**, 263 (2003).
10. A.D. Bond, *New. J. Chem.*, **28**, 104 (2004).
11. B.P. Binks, A. Rocher and M. Kirkland, *Soft Matter*, **7**, 1800 (2011).
12. *Wetting and spreading dynamics*, V.M. Starov, M.G. Velarde and C.J. Radke, CRC Press, Boca Raton, 2007.
13. R.N. Wenzel, *Ind. Eng. Chem.*, **28**, 988 (1936).
14. H.W. Fox and W.A. Zisman, *J. Colloid Sci.*, **5**, 514 (1950).
15. *Handbook of Chemistry and Physics*, D. R. Lide, CRC Press, Boca Raton, 1997.
16. B.P. Binks and A.T. Tyowua, *Soft Matter*, **9**, 834 (2013).
17. *Rheology for chemists-an introduction*, J.W. Goodwin and R.W. Hughes, Royal Society of Chemistry, Cambridge 2000.

18. S. Da Pieve, S. Calligaris, A. Panozzo, G. Arrighetti and M.C. Nicoli, *Food Res. Int.*, **44**, 2978 (2011).
19. E. Tarabukina, F. Jago, J-M. Haudin, P. Navard and E. Peuvrel-Disdier, *J. Food Sci.*, **74**, 405 (2009).
20. K.P.A.M. van Putte and J. van den Enden, *J. Phys. E Sci. Instrum.*, **6**, 910 (1973).
21. K. van Putte and J. van den Enden, *J. Am. Oil Chem. Soc.*, **51**, 316 (1974).
22. M.A.J.S. van Boekel, *J. Am. Oil Chem. Soc.*, **58**, 768 (1981).

## 6. AERATION OF MIXTURES OF MYRISTIC ACID IN OIL

### 6.1 Introduction

It was found that a gel could be produced with myristic acid in HOSO. This was not surprising as a gel has been known to be produced with fatty acids and fatty alcohols in various vegetable oils.<sup>1-6</sup> With this knowledge the ability to create a foam with the gelled mixture was investigated. The effect of myristic acid concentration, temperature, aeration time and oil type amongst other parameters on foam generation and foam stability have been investigated. The mixture was aerated with a hand held double beater electric whisk for 45 minutes (the whipping protocol) at a selected temperature. The technique includes heating the myristic acid and oil mixture to as high as 80 °C, then cooling to as low as  $8 \pm 2$  °C at a specific cooling rate (ranging from 0.5-2 °C/min.) with the use of a freezer prior to aeration.

### 6.2 Effect of myristic acid concentration

The investigation of the effect of myristic acid concentration in HOSO was conducted by heating the mixture to 80 °C, then cooling to  $8 \pm 2$  °C at 1 °C/min. followed by aeration at 22 °C with a hand held double beater electric whisk for 45 minutes. As can be seen from Table 6.1 and Figure 6.1 a significant amount of foam can be produced. The volume of the aerated phase was zero for 0-3 wt.% myristic acid. The amount of foam produced then increased dramatically with an increase in myristic acid concentration from 3.5 wt.% to 5 wt.% where the foamability reached 400 mL. The foamability then remained constant up to 10 wt.% and then decreased slightly at 12 wt.% myristic acid (350 mL). It was established that the volume fraction of air present in the mixture followed a similar trend. It is interesting that a foam was produced at concentrations above 4 wt.% because at 22 °C aggregates were observed in the mixture (identified through visual observations) at and above this concentration (see Chapter 5 Figure 5.2). Below this concentration a clear homogeneous mixture was observed and remarkably a foam was not produced demonstrating that the presence of aggregates was necessary for foam formation. At each concentration, once the maximum amount of foam was produced the foam volume then remained constant as the mixture was

whipped for a total of 45 minutes. The maximum amount of air incorporated into the mixture was almost 60 % at 8 wt.% myristic acid in HOSO.

A sample of the foam produced after 45 minutes of whipping was heated at 1 °C/min. until the foam completely collapsed. As can be seen from Table 6.1 the temperature of foam collapse increased with concentration increase. The effect of temperature on foam stability will be discussed in detail later in the chapter. Since a foam could not be formed at lower concentrations, this indicates that a gel was necessary for foam formation. At 12 wt.%, the incorporation of air into the mixture may have been limited by the increase in solid-like behaviour of the mixture. The change in the mixture from fluid to solid-like as the myristic acid concentration increased was clear from visual observations as shown in Figure 6.2. The solid-like behaviour with the myristic acid in HOSO can be seen in Figure 6.2 (n) where there is an indentation in the mixture due to a thermometer. Figure 6.3 shows that as the myristic acid concentration increased the appearance of the crystals changed from < 10 µm in diameter aggregates and needle-like with 3-4 wt.% to plate-like with 4.5-12 wt.%. The size of the myristic acid plates decreases with concentration. Birefringent crystals are clear under the crossed polarising lenses.

**Table 6.1.** Volume of the aerated phase, whipping time for maximum foam production, volume fraction of air incorporated into the mixture and temperature of complete foam collapse for myristic acid as a function of concentration in HOSO aerated with a hand held double beater electric whisk for 45 minutes at 22 °C.

| [myristic acid]/<br>wt. % | Volume of<br>aerated phase/<br>± 10 mL | Whipping time<br>for maximum<br>foam/ min. | Volume<br>fraction of<br>air<br>± 0.02 | Temperature of<br>complete foam<br>collapse/ ± 0.1 °C |
|---------------------------|--|--|--|---|
| 1                         | No foam                                | 45   | 0                                      | N/A   |
| 2                         | No foam                                | 45   | 0                                      | N/A   |
| 3                         | No foam                                | 45   | 0                                      | N/A   |
| 3.5                       | 25                                     | 15   | 0.2                                    | 30.2  |
| 4                         | 170                                    | 10   | 0.2                                    | 37.0  |
| 4.5                       | 300                                    | 15   | 0.21                                   | 37.5  |
| 5                         | 400                                    | 15   | 0.25                                   | 37.8  |
| 6                         | 400                                    | 15   | 0.28                                   | 38.0  |
| 7                         | 400                                    | 15   | 0.41                                   | 39.0  |
| 8                         | 400                                    | 15   | 0.58                                   | 40.0  |
| 9                         | 400                                    | 15   | 0.55                                   | 40.0  |
| 10                        | 400                                    | 10   | 0.56                                   | 40.9  |
| 12                        | 350                                    | 15   | 0.55                                   | 41.4  |

**Figure 6.1.** Volume of aerated phase and volume fraction of air incorporated into myristic acid-HOSO mixtures as a function of concentration after whipping for 45 minutes with a hand held double beater electric whisk at 22 °C.

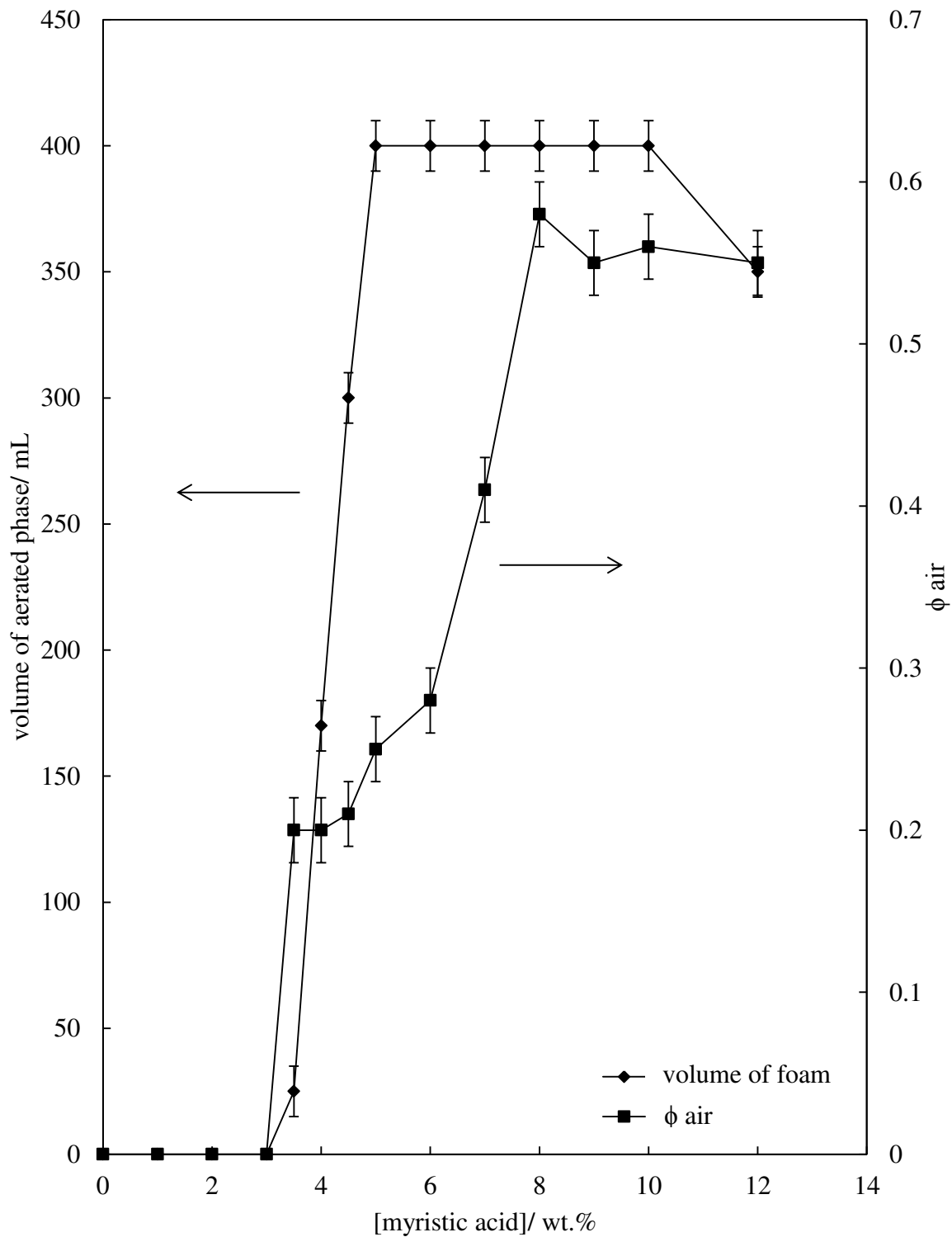


**Figure 6.2.** Photographs of (a) 1 wt.%, (b) 2 wt.%, (c) 3 wt.%, (d) 3.5 wt.%, (e) 4 wt.%, (f) 4.5 wt.%, (g) 5 wt.%, (h) 6 wt.%, (i) 7 wt.%, (j) 8 wt.%, (k) 9 wt.%, (l) 10 wt.%, (m) 12 wt.% and (n) 7 wt.% (from above) myristic acid in HOSO after cooling from 80 °C to  $8 \pm 2$  °C prior to aeration at 22 °C. Scale bar 1 cm.

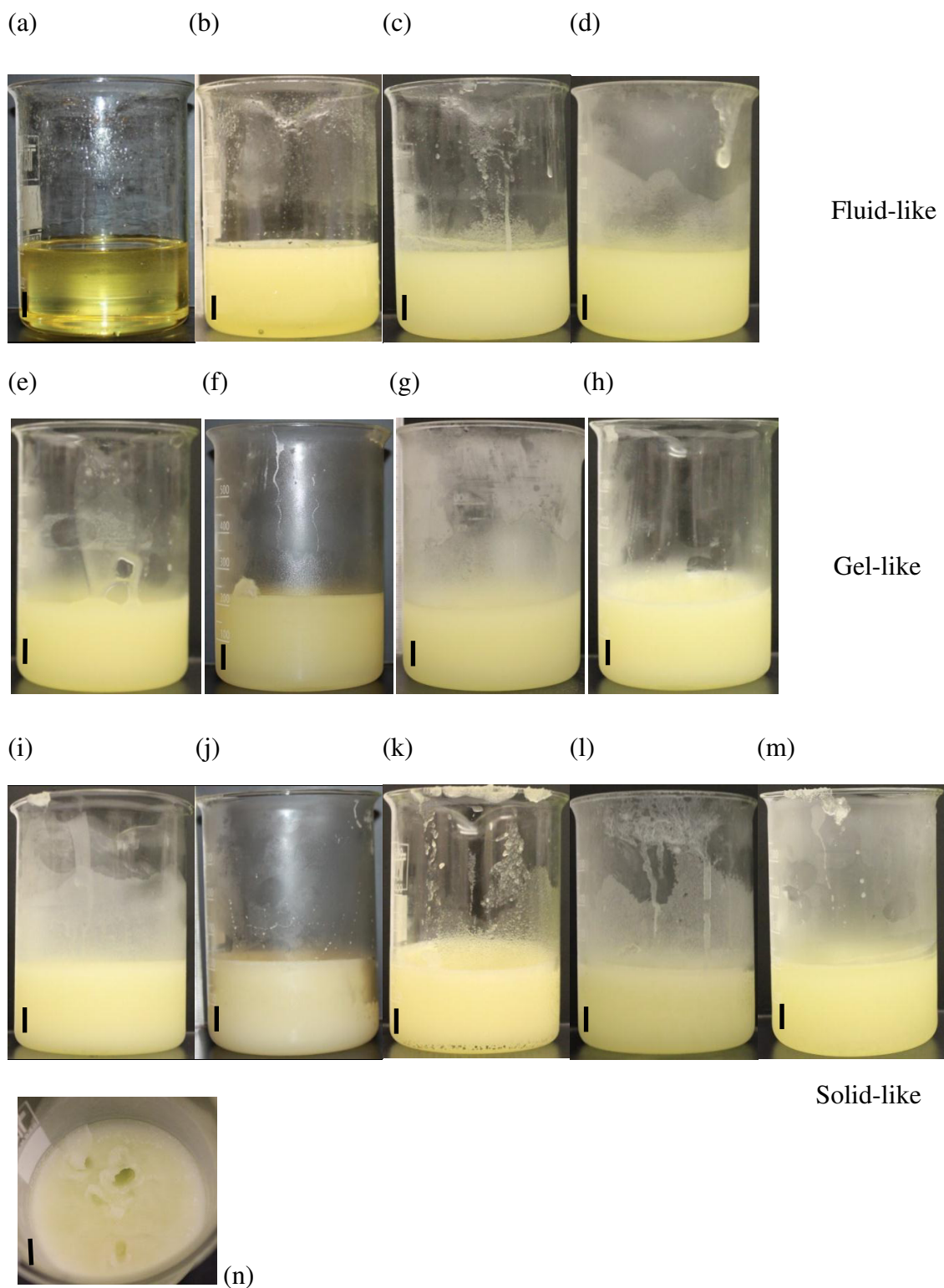


**Figure 6.3.** Optical microscopy as a function of myristic acid concentration in HOSO at 22 °C after prior heating to 80 °C and then cooling to  $8 \pm 2$  °C. (b) is neat HOSO viewed with crossed polarising lenses, (g) is 8 wt.% viewed with crossed polarising lenses, and (i) is 10 wt.% viewed with crossed polarising lenses. Scale bar 200  $\mu\text{m}$ .

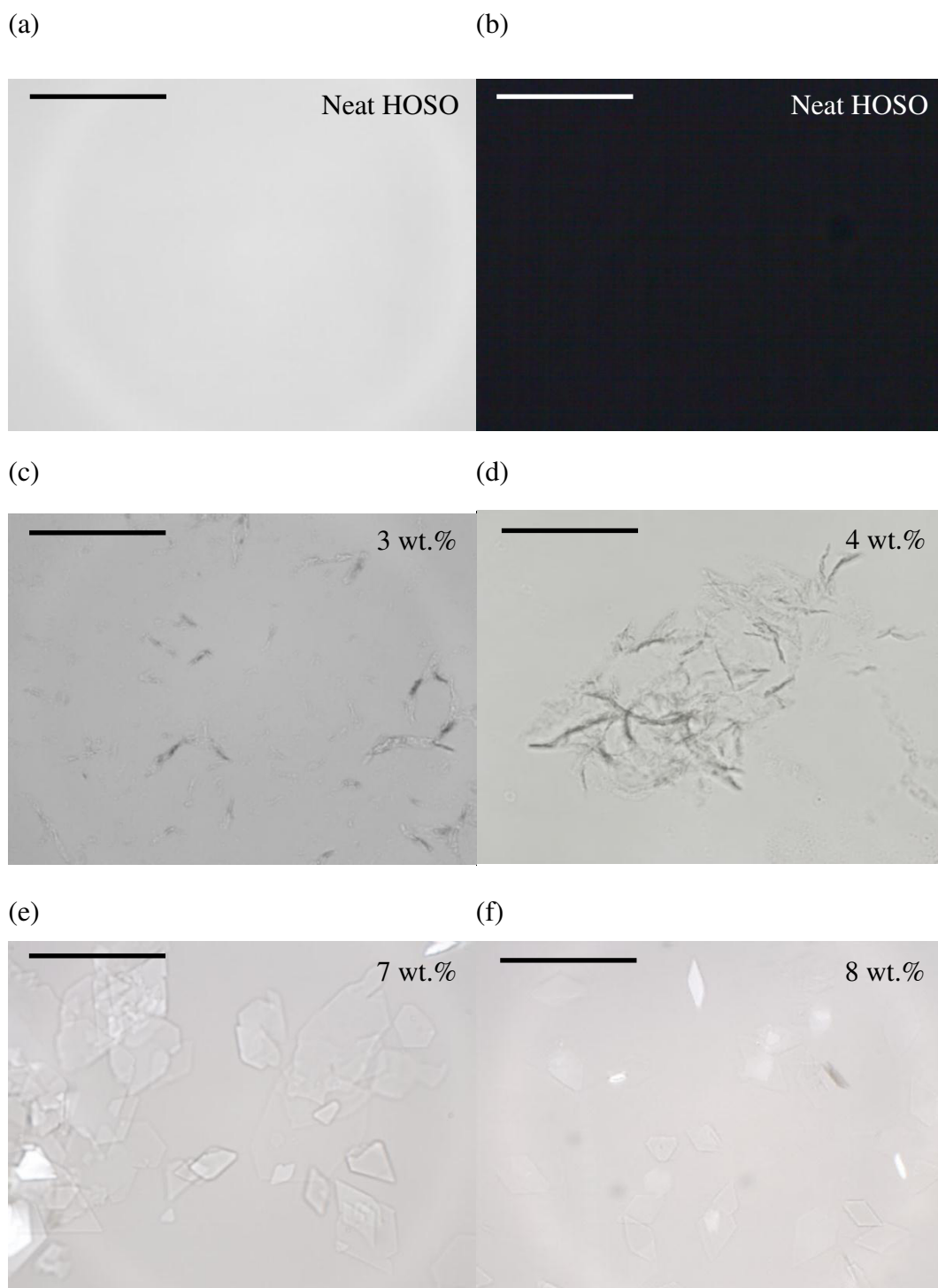


**Figure 6.3** (continued)

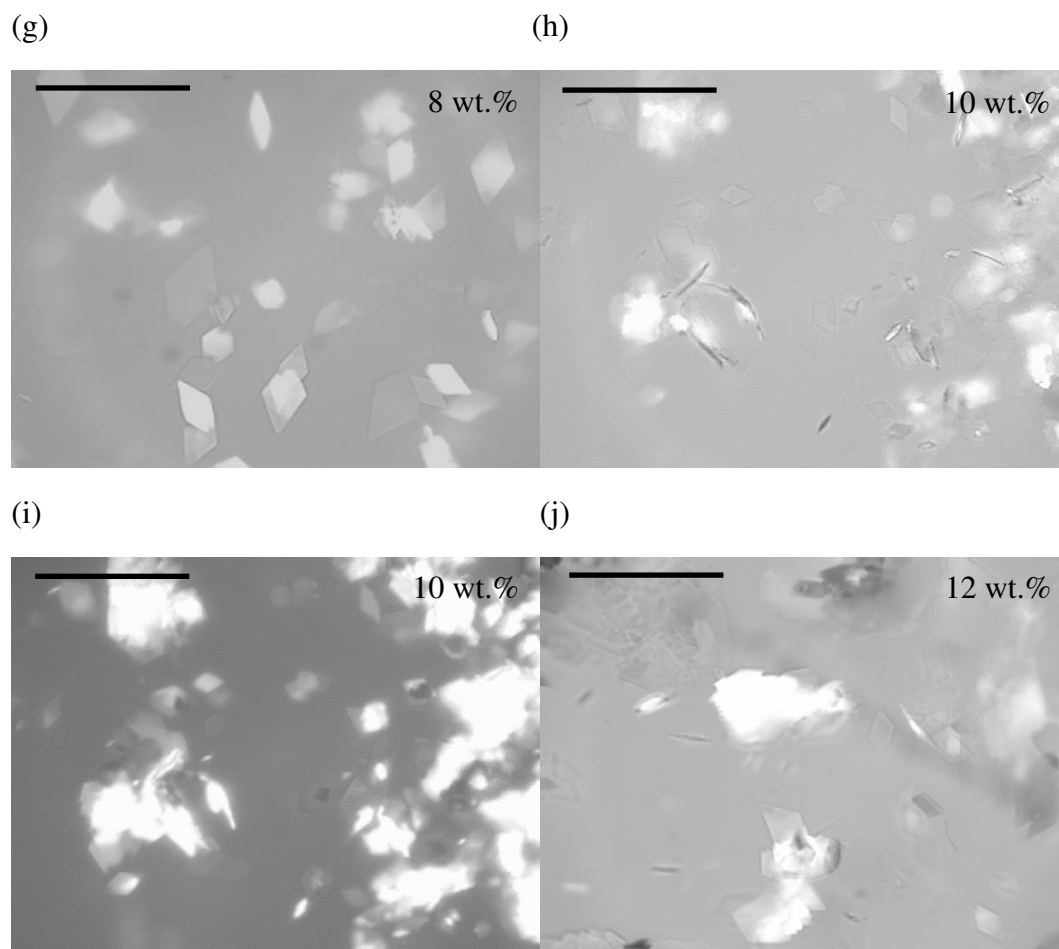
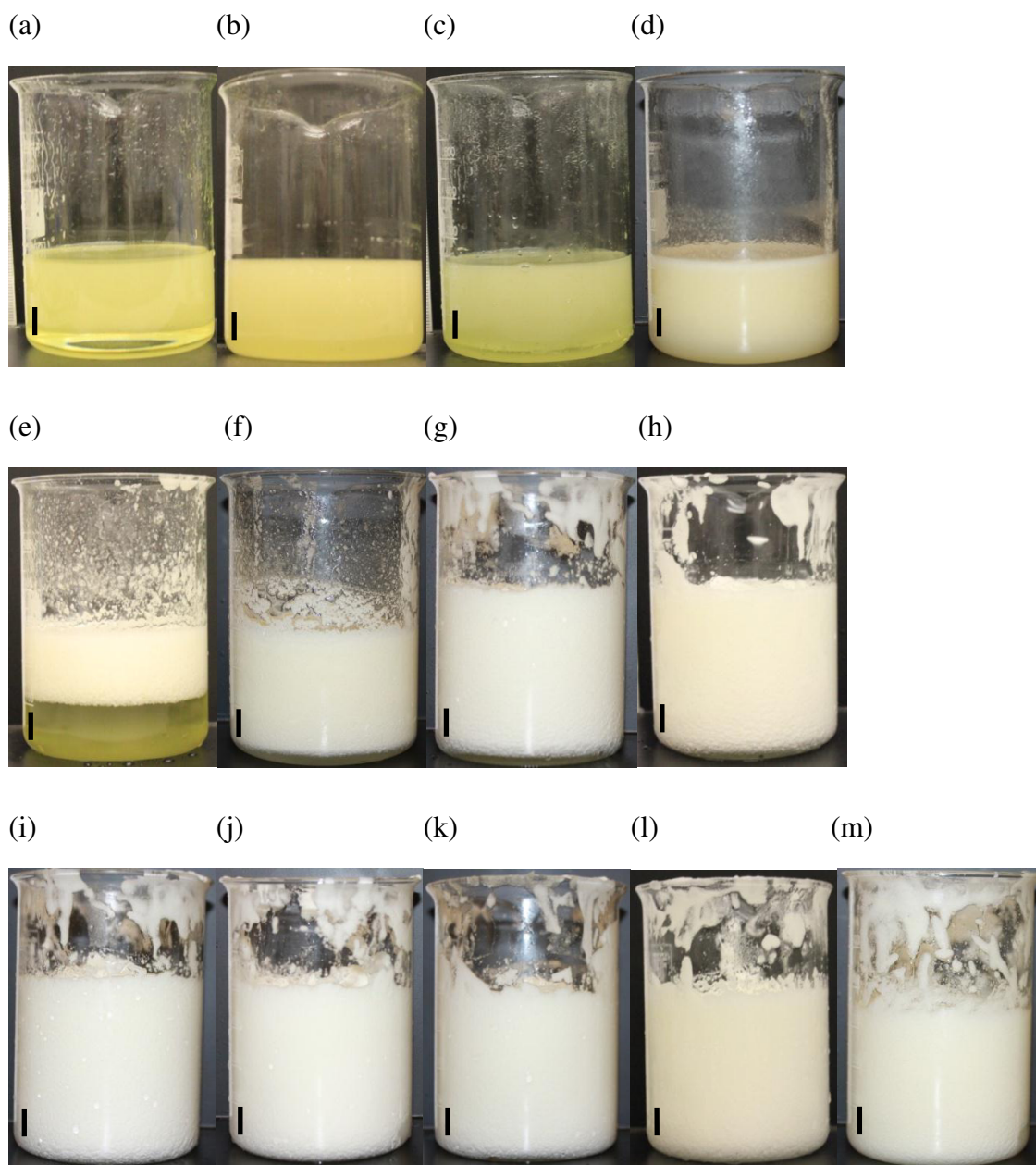


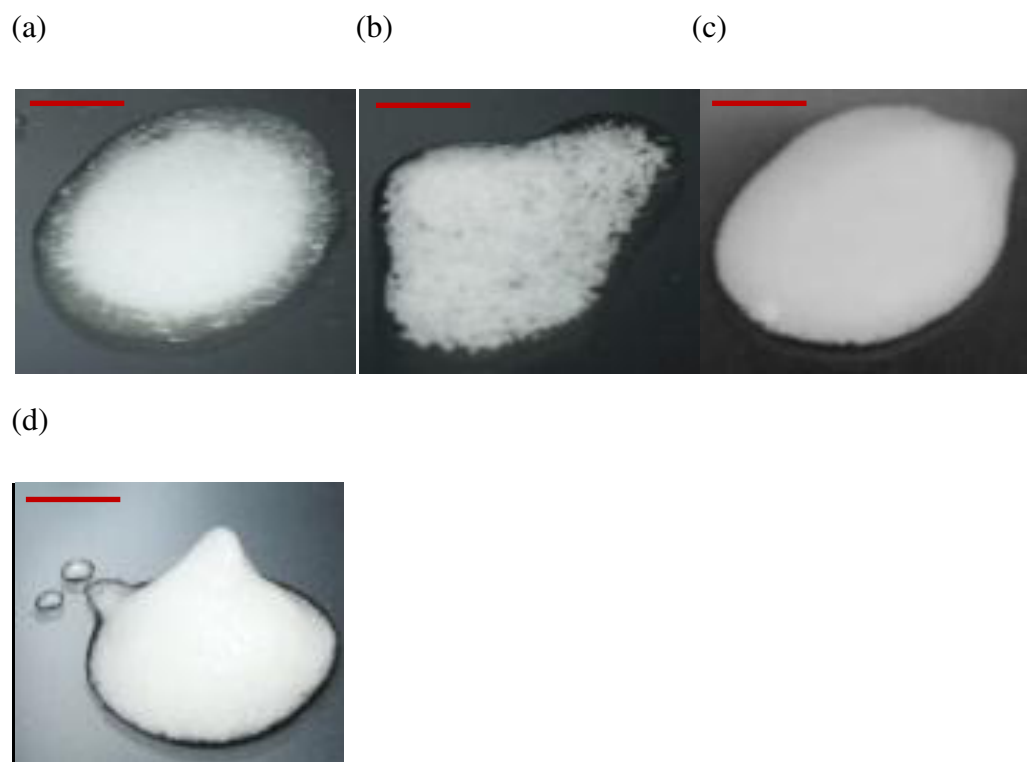
Figure 6.4 shows photographs of the vessels after 30 minutes of whipping. After whipping 1-3 wt.% myristic acid for 30 minutes, where the mixture was fluid-like prior to aeration, there was little or no foam production. As the mixture prior to aeration became gel-like and then increased in viscosity to become solid-like there was an increase in the amount of foam. Figure 6.5 shows the visual change in the foam produced from fluid-like to relatively structured and resistant to deformation as the myristic acid concentration in the HOSO increased.

Figure 6.6 presents the optical microscopy images of the foams. The number of bubbles present increased as the myristic acid concentration increased which was expected because, as already shown in Table 6.1, the volume fraction of air in the mixture increased as the myristic acid concentration increased. The bubbles at a concentration of 3.5 wt.% did not have a textured surface and were spherical. At higher concentration the bubbles became less spherical and the bubble surface became more textured. The change in the bubbles was thought to be due to an increase in the presence of myristic acid crystals at the bubble surface. The size of the bubbles were found to decrease from 300  $\mu\text{m}$  to between 20-100  $\mu\text{m}$  as the myristic acid concentration increased from 4 to 10 wt.%. The bubble size was then found to slightly increase at 12 wt.% (50-100  $\mu\text{m}$ ). It may be that as the myristic acid concentration increased there was an optimum crystal size, solid content or viscosity or a combination of all three parameters for foam production and subsequent foam stability. It was clear from microscopy, pNMR measurements and viscosity measurements of the myristic acid in HOSO mixture prior to aeration that the crystal size, solid content and viscosity all changed as the myristic acid concentration increased.

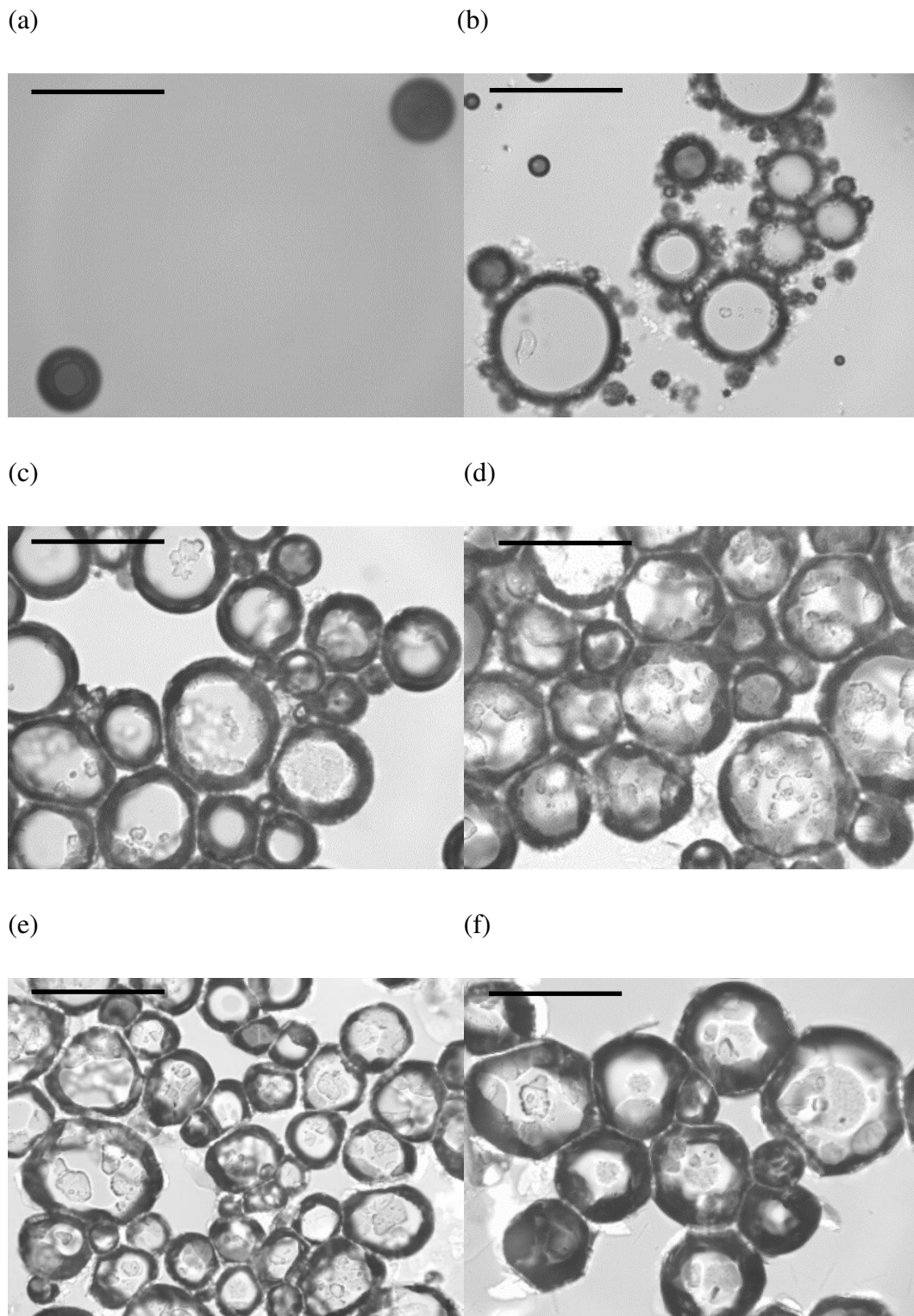
**Figure 6.4.** Photographs of (a) 1 wt.% , (b) 2 wt.% , (c) 3 wt.% , (d) 3.5 wt.% , (e) 4 wt.% , (f) 4.5 wt.% , (g) 5 wt.% , (h) 6 wt.% , (i) 7 wt.% , (j) 8 wt.% , (k) 9 wt.% , (l) 10 wt.% , (m) 12 wt.% myristic acid in HOSO whipped for 30 minutes with a hand held double beater electric whisk at 22 °C. Scale bar 1 cm.



**Figure 6.5.** Photographs of (a) 3 wt.%, (b) 4 wt.% (c) 5 wt.% and (d) 8 wt.% myristic acid in HOSO foams after whipping for 30 minutes with a hand held double beater electric whisk at 22 °C. Scale bar 1 cm.



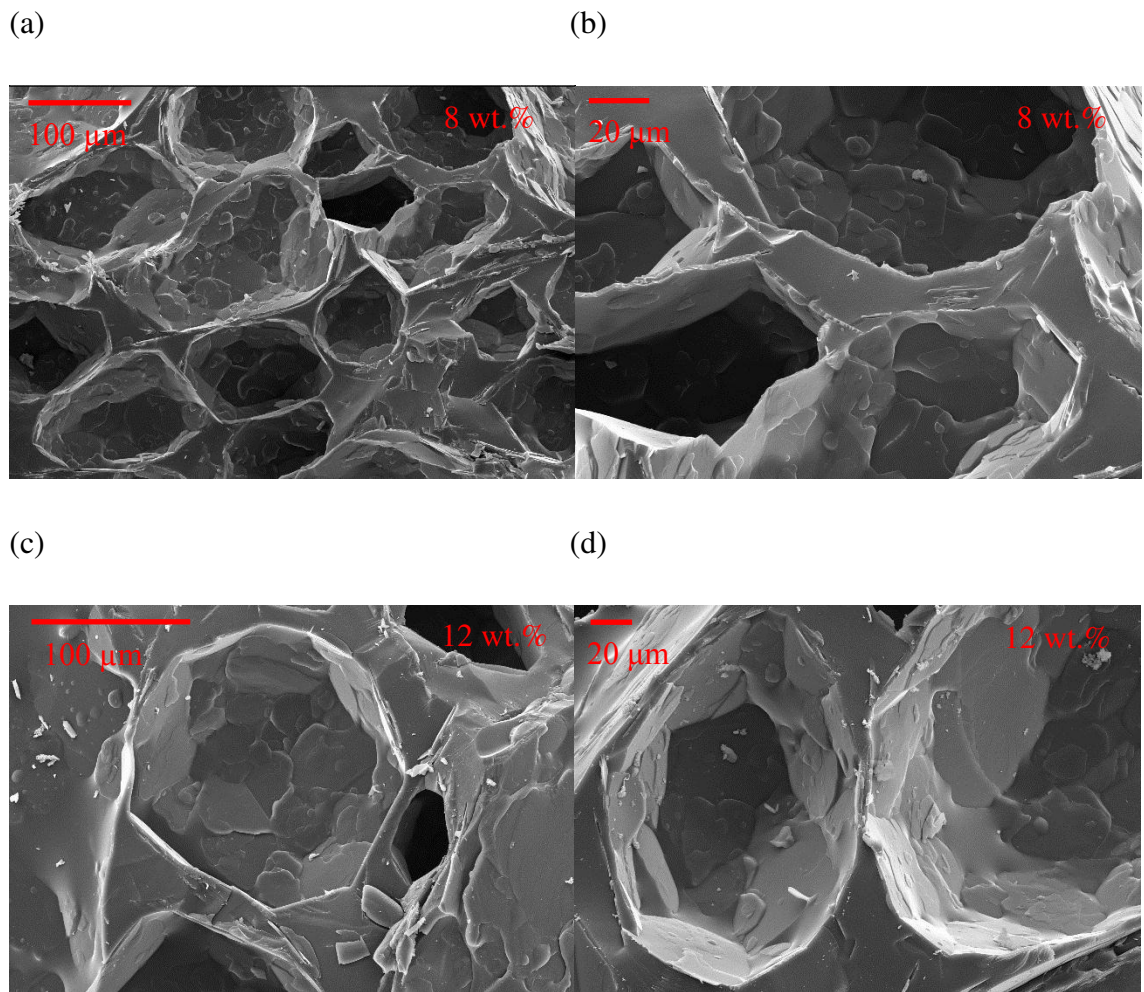
**Figure 6.6.** Optical microscopy images of (a) 1 wt.%, (b) 3.5 wt.%, (c) 5 wt.%, (d) 7 wt.%, (e) 8 wt.% and (f) 12 wt.% myristic acid in HOSO foams whipped for 30 minutes with a hand held double beater electric whisk at 22 °C. Scale bar 200  $\mu$ m.



### 6.2.1 Cryogenic scanning electron microscopy

The samples shown in the cryo-SEM images in Figure 6.7 were produced by heating myristic acid in HOSO to 80 °C, then cooling to  $8 \pm 2$  °C at a rate of approximately 1 °C/min. and then whipping for 45 minutes at 22 °C. The foam was then cooled quickly to -210 °C and then held at -140 °C where the foam was then fractured followed by images being taken. Figure 6.7 agrees with Figure 6.6 as the bubble size is clearly between 20-100  $\mu\text{m}$  at 8 wt.% and 50-100  $\mu\text{m}$  at 12 wt.%. The figure also indicates the presence of the plate-like crystals of myristic acid around the air bubbles in the foams. The considerable foam stability that is observed (over 18 months) is due to their presence.

**Figure 6.7.** Cryo-SEM images of 8 wt.% and 12 wt.% myristic acid in HOSO foams whipped for 45 minutes with a hand held double beater electric whisk at 22 °C.



### 6.3 Effect of storage time

It was found, as shown in Figure 6.8 with a 30 g sample of the foam (produced after heating the myristic acid in HOSO mixture to 80 °C, then cooling to  $8 \pm 2$  °C at approximately 1 °C/min. followed by whipping at 22 °C for 45 minutes), that 3 weeks after whipping oil had drained from the foam. The volume of liquid drainage decreased as myristic acid concentration increased (10 mL with 4-7 wt.% and 3 mL with 12 wt.%). The oil drainage occurred within 24 hours of foam formation. After 24 hours (the sealed sample was held at  $22 \pm 2$  °C) the only change in foam appearance was a slight decrease in the foam volume (approximately 5 mL), this may be due to compaction of the foam bubbles in the vessel (see Figure 6.8). The foam did not change further in appearance for 18 months. This was remarkable as previous literature shows that a non-aqueous foam could only be stable for up to a month.<sup>7-11</sup> After 18 months, the foam started to collapse with up to 3 mm spherical cavities at a time which caused gradual liquid drainage (approximately 2 mL/month). The liquid also became slightly turbid in appearance as it now contains myristic acid. This foam collapse occurred gradually over 6 months to 1 year.

**Figure 6.8.** Photographs of myristic acid in HOSO (upper) immediately after whipping with a hand held double beater electric whisk for 45 minutes at 22 °C and (lower) 3 weeks after foam formation at 22 ± 2 °C. Scale bar 1 cm.

4 wt.%    5 wt.%    6 wt.%    7 wt.%    8 wt.%    9 wt.%    10 wt.%    12 wt.%



## 6.4 Effect of storage and aeration temperature

The effect of an increase in temperature at 1 °C/min. on a 10 g sample of the foam produced after whipping for 45 minutes at 22 °C was investigated. The effect on foamability and foam stability of aerating 8 wt.% myristic acid in HOSO with a hand held double beater electric whisk for 45 minutes at different aeration temperatures was also studied. 8 wt.% myristic acid was chosen because at this concentration there was a maximum amount of air incorporated into the system when aerated at 22 °C. Therefore, if a foam is to be produced at the different temperatures it is likely to be at this concentration. It is known that the formation of a gel prior to aeration is important for foam production and foam stability. It is also known from rheology and pNMR of myristic acid in HOSO that the viscosity and the solid content of the mixture decreased as temperature increased. Therefore, the effect of an increase in temperature on a foam already formed at 22 °C and on foam formation at higher whipping temperatures are interesting to investigate.

### 6.4.1 Effect of storage temperature on foam stability

As seen in Table 6.1, the temperature at which the foam collapsed increased significantly from 30.2 to 37 °C between 3.5 and 4 wt.% myristic acid and then increased gradually to 41.4 °C at 12 wt.%. As shown in Figure 6.9 with 8 wt.%, the foam collapsed gradually as temperature was increased from 22 °C to 30 °C, a large volume of foam then collapsed between 30 °C and 40 °C. Initially liquid drainage occurred (likely to be due to a decrease in viscosity), then as temperature further increased there was bubble coalescence and disproportionation along with further liquid drainage. Figure 6.10 shows the corresponding optical microscopy images. As the foam was heated from room temperature to 30 °C there was very little change in the structure of the whipped oil (other than some bubbles decreasing in size and some increasing in size suggesting possible disproportionation and coalescence had occurred). However at 35 °C the bubbles in the foam had increased in size to up to 500 µm, clearly indicating a large amount of foam collapse. At 40 °C the foam had completely collapsed with no bubbles visible. Figure 6.11 presents the volume of foam and the volume of oil released from a 10 g sample as a function of temperature. The foam collapse is due to the melting of myristic acid crystals which were stabilising the foam. It is thought that the

foam melting temperatures are higher than the dissolution temperatures due to the foam not conducting heat as effectively as a liquid.

**Figure 6.9.** Appearance of 8 wt.% myristic acid in HOSO whipped for 45 minutes with a hand held double beater electric whisk at 22 °C, then heated 1 °C/min. to (a) 22 °C, (b) 25 °C, (c) 30 °C, (d) 35 °C and (e) 40 °C. Scale bar 1 cm.

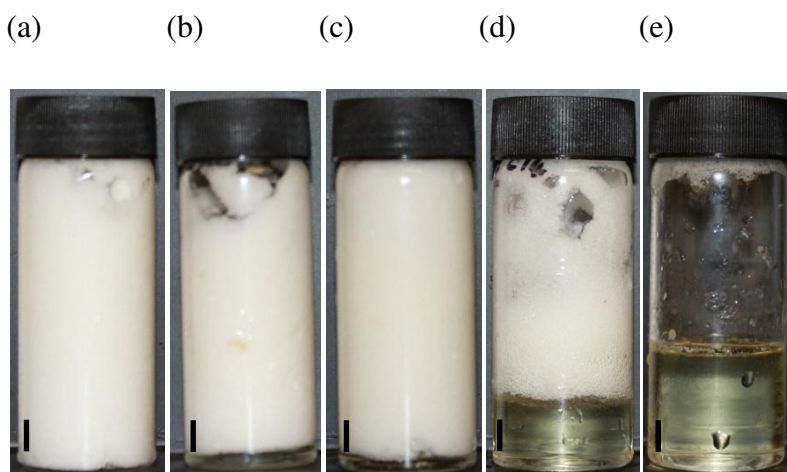


**Figure 6.10.** Optical microscopy of 8 wt.% myristic acid in HOSO whipped for 45 minutes with a hand held double beater electric whisk at 22 °C, then heated 1 °C/min. to (a) 22 °C, (b) 25 °C, (c) 30 °C, (d) 35 °C, (e) 40 °C and (f) 80 °C. Scale bar 200  $\mu$ m.

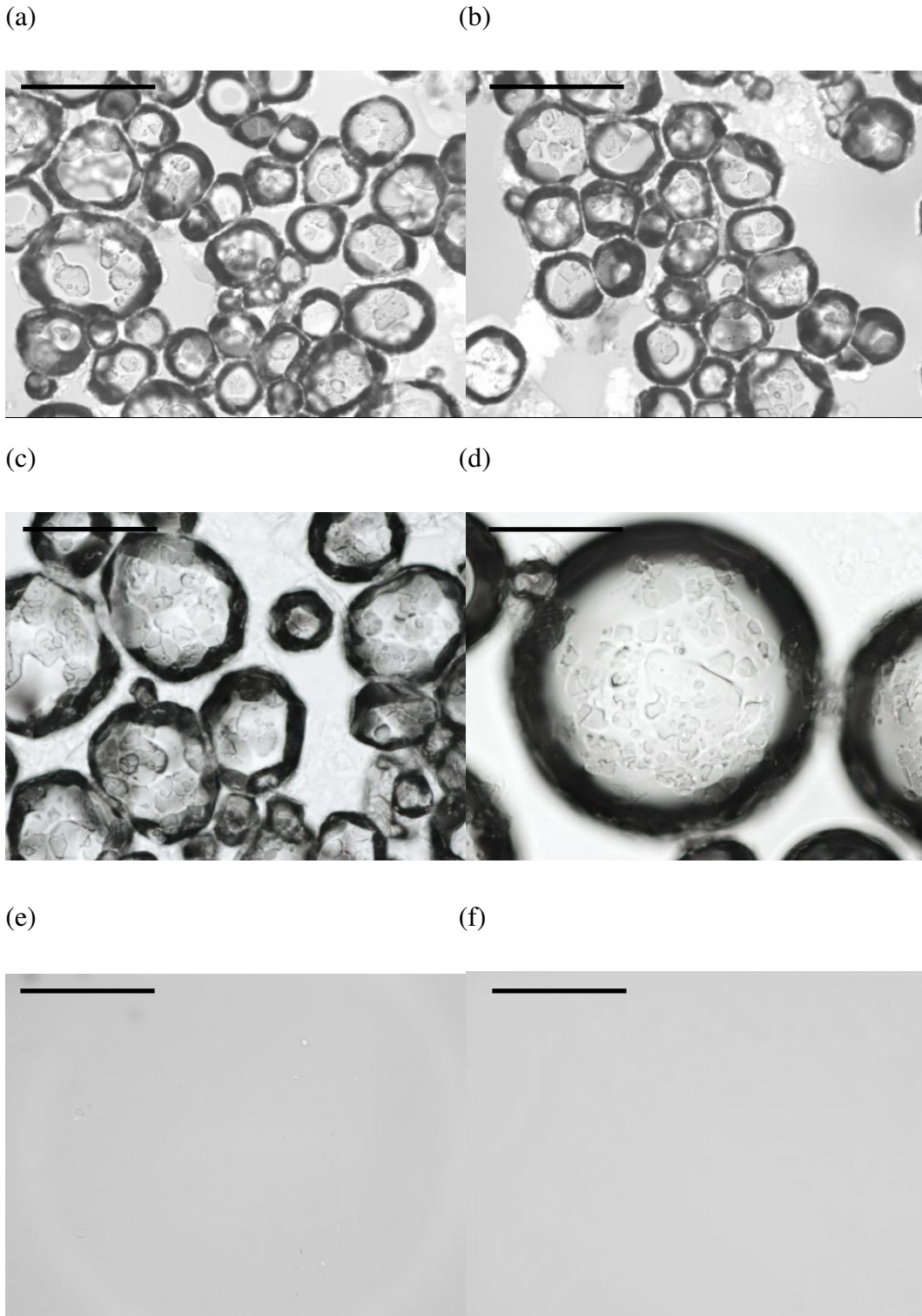
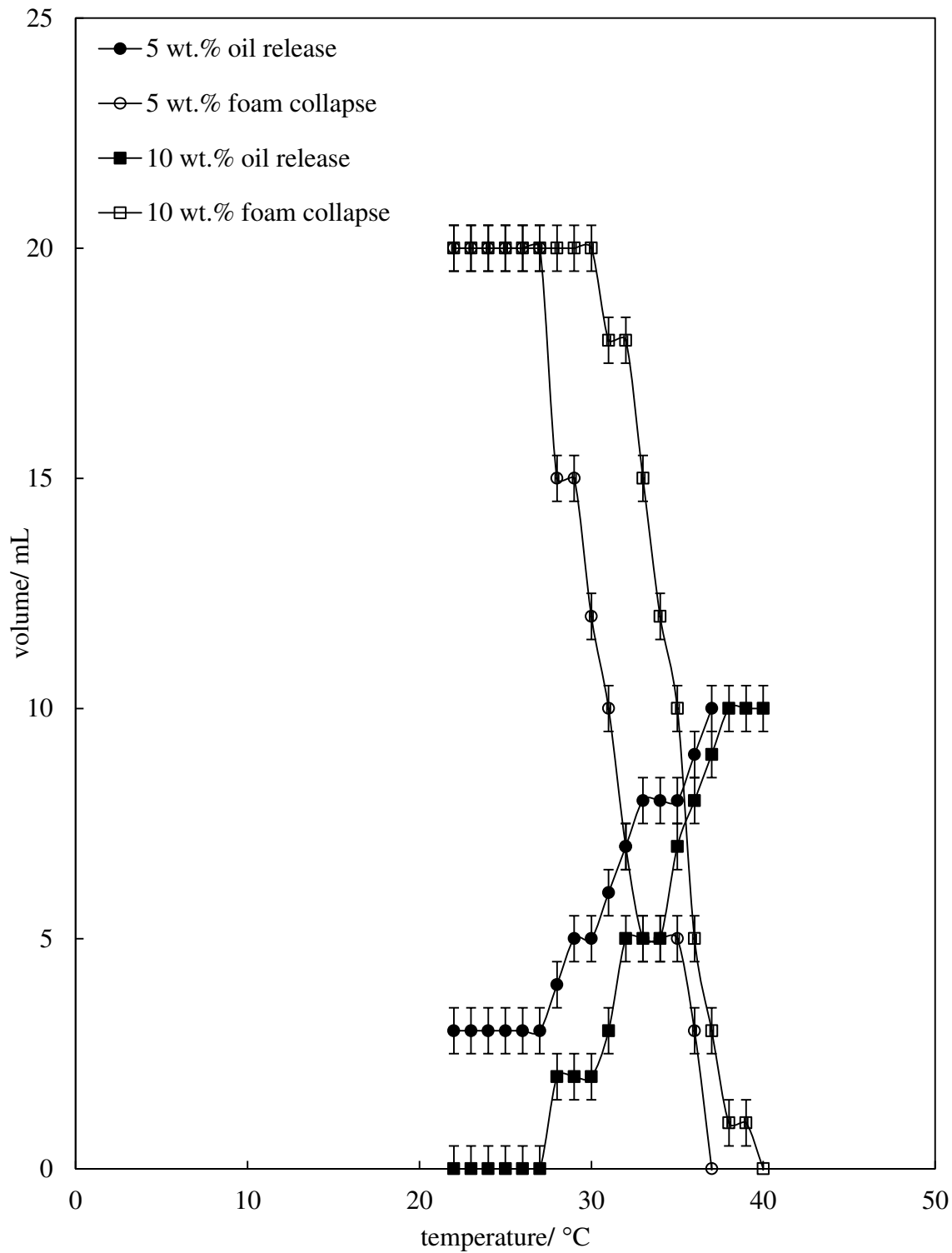


**Figure 6.11.** Volume of oil release and foam remaining from a 10 g sample of foam produced with 5 and 10 wt.% myristic acid in HOSO whipped for 45 minutes with a hand held double beater electric whisk at 22 °C then heated 1 °C/min. until total foam collapse.



#### 6.4.2 Effect of aeration temperature on foamability

The effect of aeration temperature was also investigated which consisted of heating the mixture to 80 °C, then cooling the mixture to  $8 \pm 2$  °C at approximately 1 °C/min., followed by heating the mixture to 22, 30, 35 or 40 °C. The mixture was then whipped with a hand held double beater electric whisk. As can be seen from Figure 6.12 the mixtures prior to aeration at 22 and 30 °C were relatively similar visually as they were both turbid, although the mixture was less viscous at 30 °C. At 35 and 40 °C mixtures were a clear, homogeneous liquid. From Figure 6.13 the appearance of the crystals was different at the various temperatures. They are plate-like at 22 °C, but at 30 °C needle-like and also < 20 µm sized spherical aggregates. At 35 and 40 °C needle-like crystals also exist. The presence of crystals identified through optical microscopy at 35 and 40 °C are thought to be due to heterogeneous crystallisation on the microscope slide and cover slip. Figure 6.14 shows visually the difference in the mixtures after whipping for 45 minutes. It is clear that as the aeration temperature increased from 22 to 30 °C, the amount of foam produced decreased from 400 mL to 250 mL. As the aeration temperature further increased to 35 °C and 40 °C a foam was not produced. Optical microscopy of the foams is shown in Figure 6.15. A significant amount of air was clearly incorporated into the mixture at 22 °C, whereas at 30 °C there was less air incorporated into the mixture. At both 22 °C and 30 °C the bubbles had a textured surface and were non-spherical, suggesting the presence of myristic acid crystals at bubble surfaces. Bubbles were not observed at 35 and 40 °C as a foam was not produced. Figure 6.16 shows clearly the decrease in foamability as aeration temperature increased. Also, the volume fraction of air incorporated decreased from 0.58 (at 22 °C) to 0.15 (at 30 °C) to 0 (at 35 and 40 °C). The lack of foam production at 35 and 40 °C is due to the absence of myristic acid crystals. From pNMR measurements it was seen that with 8 wt.% myristic acid in HOSO at 35 and 40 °C the solid content was 0 %. The investigation into the effect of temperature on foam stability and foam formation clearly showed that the myristic acid presence was necessary for both foamability and foam stability.

**Figure 6.12.** Photographs of 8 wt.% myristic acid in HOSO at (a) 22 °C, (b) 30 °C, (c) 35 °C and (d) 40 °C after cooling approximately 1 °C/min. from 80 °C to  $8 \pm 2$  °C and subsequent heating. Scale bar 1 cm.

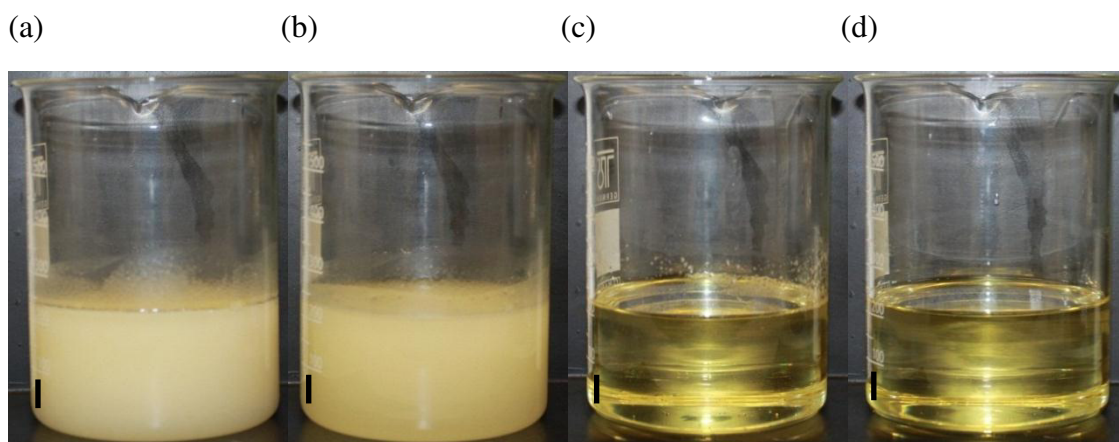


**Figure 6.13.** Optical microscopy of 8 wt.% myristic acid in HOSO at (a) 22 °C, (b) 30 °C, (c) 35 °C and (d) 40 °C after cooling approximately 1 °C/min. from 80 °C to  $8 \pm 2$  °C and subsequent heating. Scale bar 200  $\mu$ m.

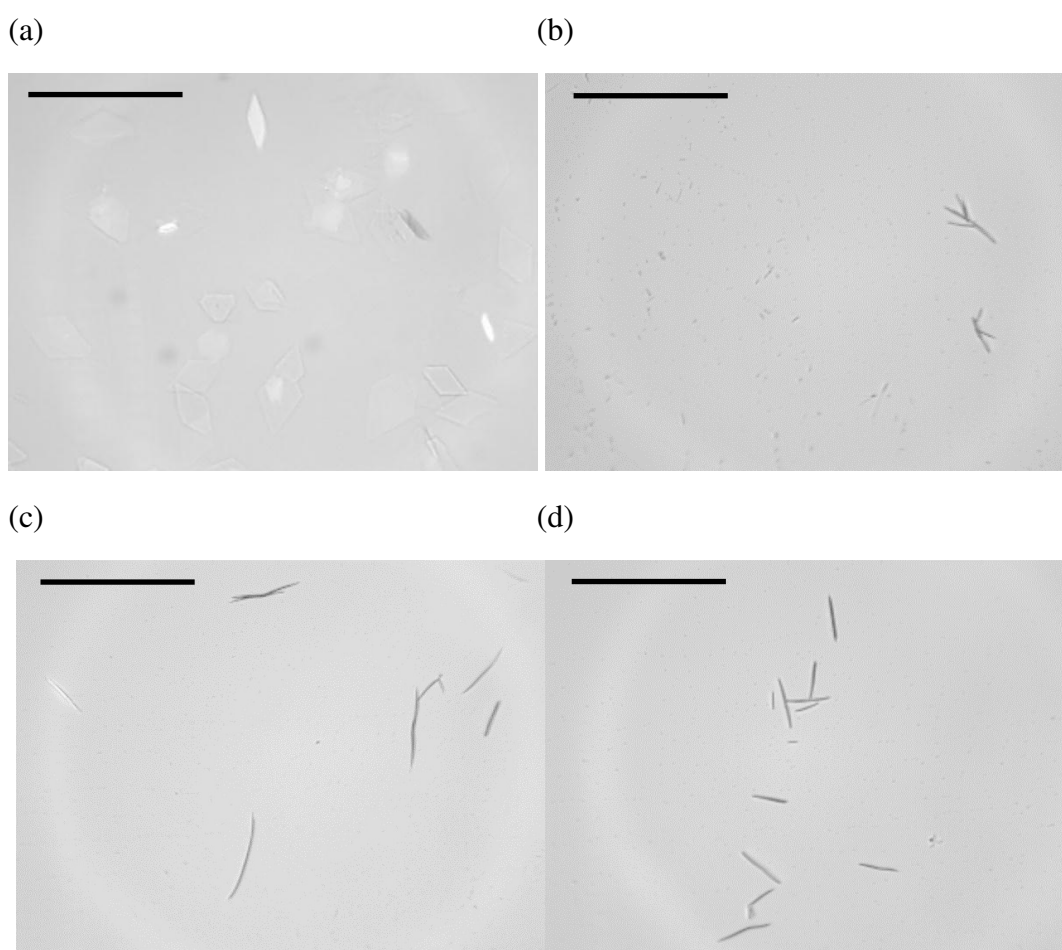


**Figure 6.14.** Photographs of 8 wt.% myristic acid in HOSO after whipping for 45 minutes with a hand held double beater electric whisk at (a) 22 °C, (b) 30 °C, (c) 35 °C and (d) 40 °C. Scale bar 1 cm.

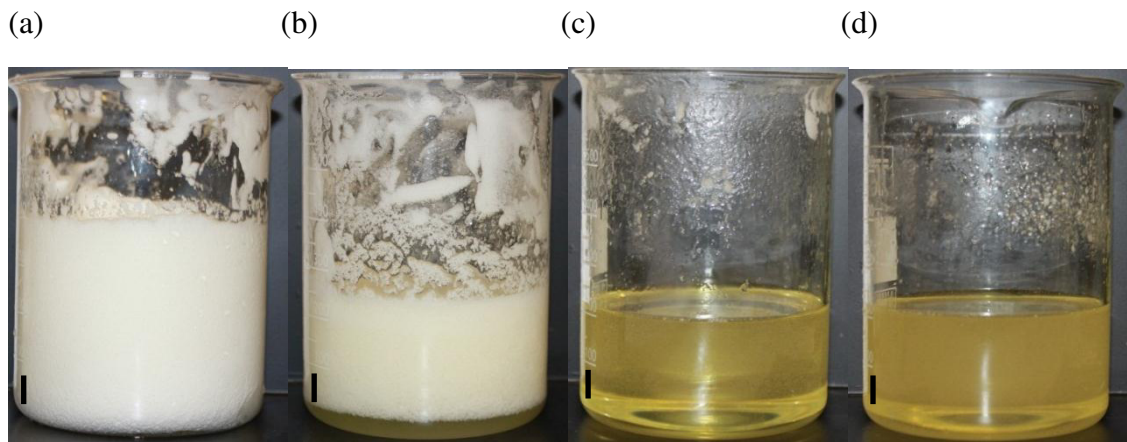


**Figure 6.15.** Optical microscopy of 8 wt.% myristic acid in HOSO after whipping for 45 minutes with a hand held double beater electric whisk at (a) 22 °C, (b) 30 °C, (c) 35 °C and (d) 40 °C. Scale bar 200  $\mu\text{m}$ .

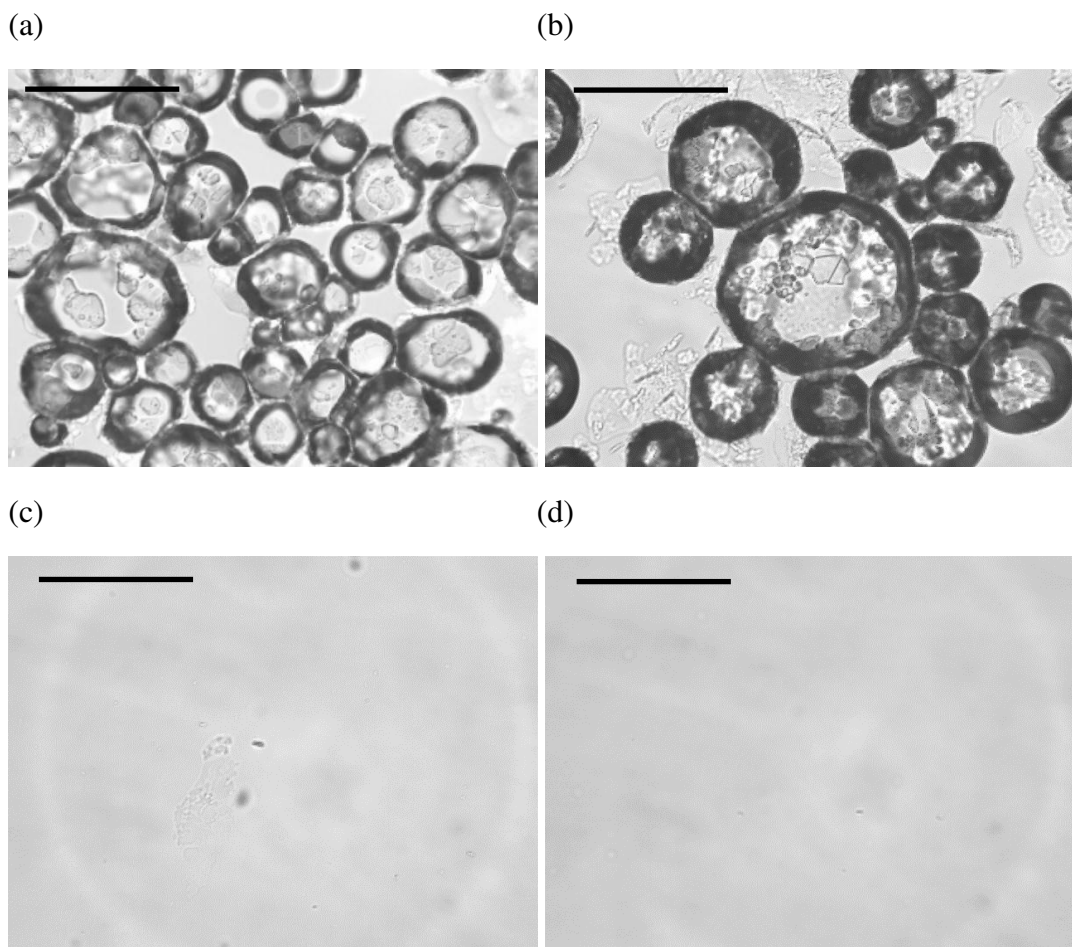
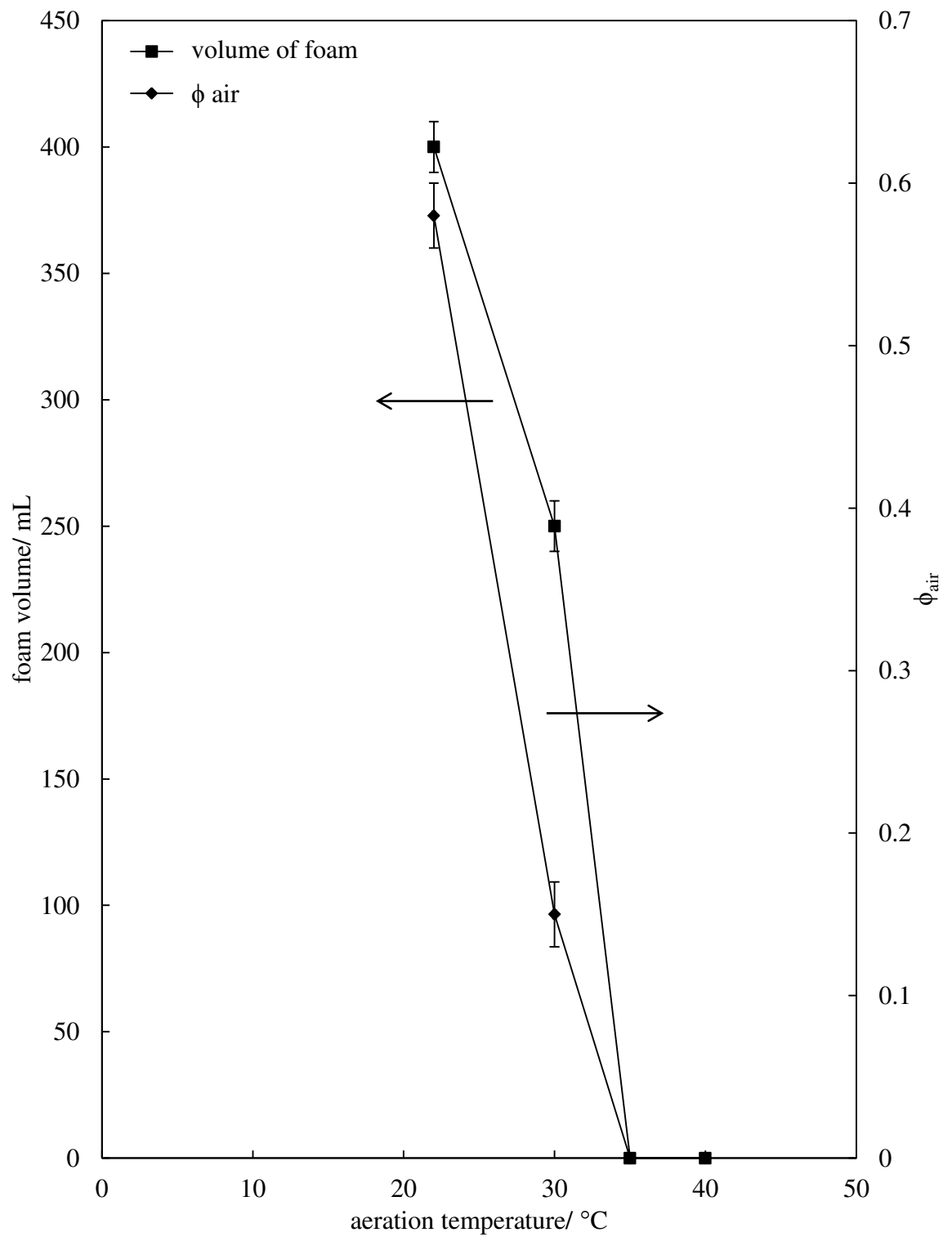


**Figure 6.16.** Volume of foam and volume fraction of air incorporated into 8 wt.% myristic acid in HOSO aerated with a hand held double beater electric whisk for 45 minutes at various temperatures.



## 6.5 Effect of cooling rate

The effect of varying the cooling rate and time before whipping 8 wt.% myristic acid in HOSO has been investigated. Again, the concentration of 8 wt.% was chosen with the assumption that if a foam can be produced under these conditions then it will be at this concentration. The effect of cooling rate and time was studied due to literature<sup>12</sup> stating that the cooling rate of a mixture can affect the ability to gel a vegetable oil, the presence of which was important for foam production. Therefore, the two additional cooling rates stated as a 'fast cool' and a 'slow cool' from 80 °C to 8.3 °C and 20.5 °C, respectively prior to whipping at 22 °C. The effect of these on the foamability and foam stability of 8 wt.% myristic acid was compared to that obtained with the 'standard cool' which was where the mixture was cooled approximately 1 °C/min. from 80 °C to 8 ±2 °C prior to whipping at 22 °C. The fast cool was with a cooling rate of 2 °C/min. to 8.3 °C, the slow cool was with a cooling rate of 0.5 °C/min to 20.5 °C. It took 2 hours for the mixture to cool to 20.5 °C from 80 °C. The effect of time with the slow cool was also studied in that the sample was aerated 24 hours and 48 hours after reaching 20.5 °C.

As can be seen in Table 6.2, the volume of foam produced and the amount of air incorporated into the mixture is affected by the cooling rate and the time the sample is left at 20.5 °C prior to aeration. The table shows that aerating the mixture after the fast cool and the slow cool creates a large amount of foam (400 mL versus 350 mL) and a relatively large amount of air is incorporated into the mixture. The volume of foam produced and the amount of air incorporated into the mixture with the slow cool aerated immediately is considerably higher than that seen with the slow cool after 24 and 48 hours. The volume fraction of air incorporated into the mixture with the longer time period prior to whipping is approximately half that obtained after whipping the mixture once 20.5 °C was reached. The table suggests that the standard cool gave the optimum foaming. Interestingly the temperature of foam collapse was not noticeably affected by the cooling rate and the time before whipping.

Figure 6.17 shows that the appearance of the mixture prior to aeration after the different cooling protocols was different. After the standard cool and the fast cool the mixtures were more turbid with a higher viscosity compared to after the slow cool. This is likely to be due to the mixture being cooled to a lower temperature prior to aeration yielding a higher concentration of myristic acid crystals. The lower temperature the mixtures were

cooled to prior to aeration may explain the slightly higher foamability and larger amount of air incorporated into the mixture after the standard and fast cool prior to whipping than that seen with the slow cool prior to whipping.

**Table 6.2.** Volume of the aerated phase, time for maximum foam production, volume fraction of air incorporated into the mixture and melting temperature of a whipped oil produced with 8 wt.% myristic acid in HOSO after cooling the mixture from 80 °C with various cooling rates. The mixture was aerated with a hand held double beater electric whisk for 45 minutes at 22 °C. The mixture after the fast and standard cool was cooled to  $8 \pm 2$  °C. The mixtures after the slow cool were cooled to 20.5 °C.

| Cooling rate                           | Volume of aerated phase/ $\pm 10$ mL | Whipping time for maximum foam production/ min. | Volume fraction of air $\pm 0.02$ | Temperature of foam collapse/ $\pm 0.1$ °C |
|--|--------------------------------------|---|-----------------------------------|--|
| Fast cool (2 °C/min.)                  | 400                                  | 20  | 0.46                              | 40.6                                       |
| Slow cool immediately (0.5 °C/min.)    | 350                                  | 20  | 0.41                              | 41.5                                       |
| Slow cool after 24 hours (0.5 °C/min.) | 250                                  | 10  | 0.19                              | 39.6                                       |
| Slow cool after 48 hours (0.5 °C/min.) | 250                                  | 25  | 0.23                              | 39.8                                       |
| Standard cool (1 °C/min.)              | 400                                  | 15  | 0.58                              | 40.0                                       |

**Figure 6.17.** Photographs of 8 wt.% myristic acid in HOSO after (a) a fast cool, (b) a slow cool immediately, (c) a slow cool after 24 hours, (d) a slow cool after 48 hours and (e) a standard cool from 80 °C prior to aeration at 22 °C. Scale bar 1 cm.

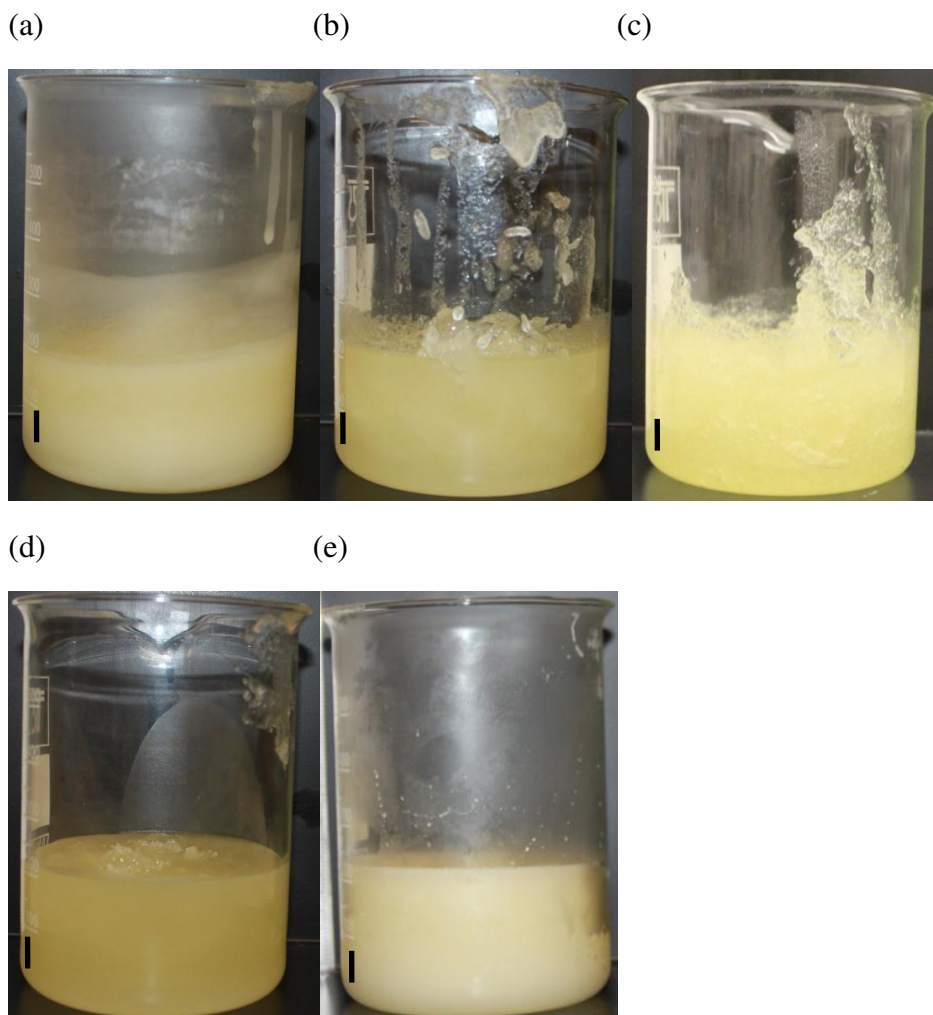
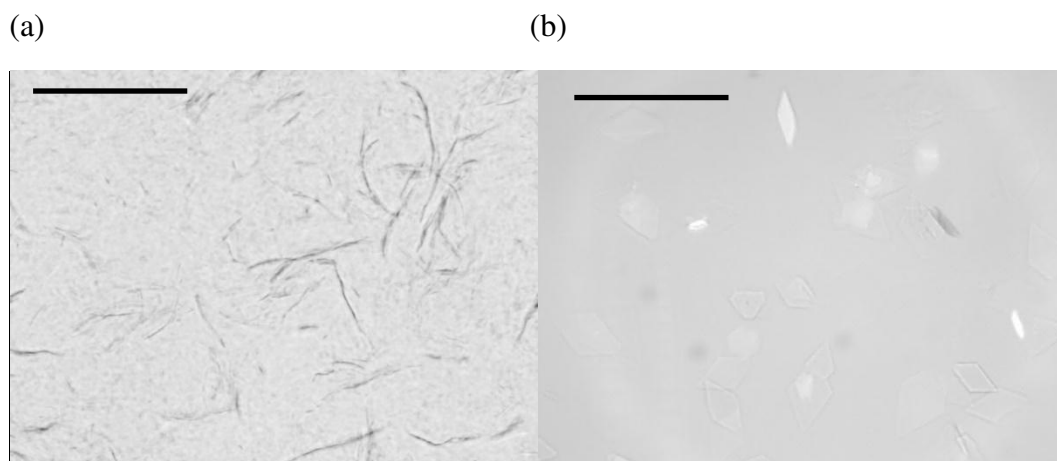


Figure 6.18 shows optical microscopy of the mixtures prior to aeration at 22 °C after the standard cool and the slow cool. It is clear that the cooling rates have an effect on the structure of myristic acid. After the standard cool the myristic acid was < 50 µm plates, whereas after the slow cool the myristic acid was approximately 200 µm aggregates and 100 µm long needles. The myristic acid 24 hours and 48 hours after the slow cool was found to be large aggregates (over 500 µm), after the fast cool the myristic acid was 200 µm aggregates.

Figure 6.19 shows the high foamability with the standard cool, the fast cool and the slow cool immediately. The figure also shows the lower foamability with the slow cool after 24 and 48 hours. It may be that the foamability of the mixture was lower 24 and 48 hours after the slow cool due to a larger aggregate size prior to aeration. The larger aggregate size may cause the aggregate to not orientate itself as effectively at the bubble surface as the smaller myristic acid aggregates produced after the other cooling rates causing the foamability to be lower.

The appearance of the foam bubbles using optical microscopy is relatively similar with all of the cooling rates and time scales prior to whipping (Figure 6.20). The similarity was that crystals were present at the bubble air-oil surface (identified by the non-spherical bubbles which had a textured surface). It was also clear that the amount of bubbles (air incorporated) was higher with the standard cool and fast cool than with the slow cool after all three time periods.

**Figure 6.18.** Optical microscopy of 8 wt.% myristic acid in HOSO after (a) a slow cool immediately and (b) a standard cool from 80 °C prior to aeration at 22 °C. Scale bar 200 µm.



**Figure 6.19.** Photographs of 8 wt.% myristic acid in HOSO after 30 minutes of whipping with a hand held double beater electric whisk at 22 °C after cooling from 80 °C with (a) a fast cool, (b) a slow cool immediately, (c) a slow cool after 24 hours, (d) a slow cool after 48 hours and (e) after the standard cool. Scale bar 1 cm.

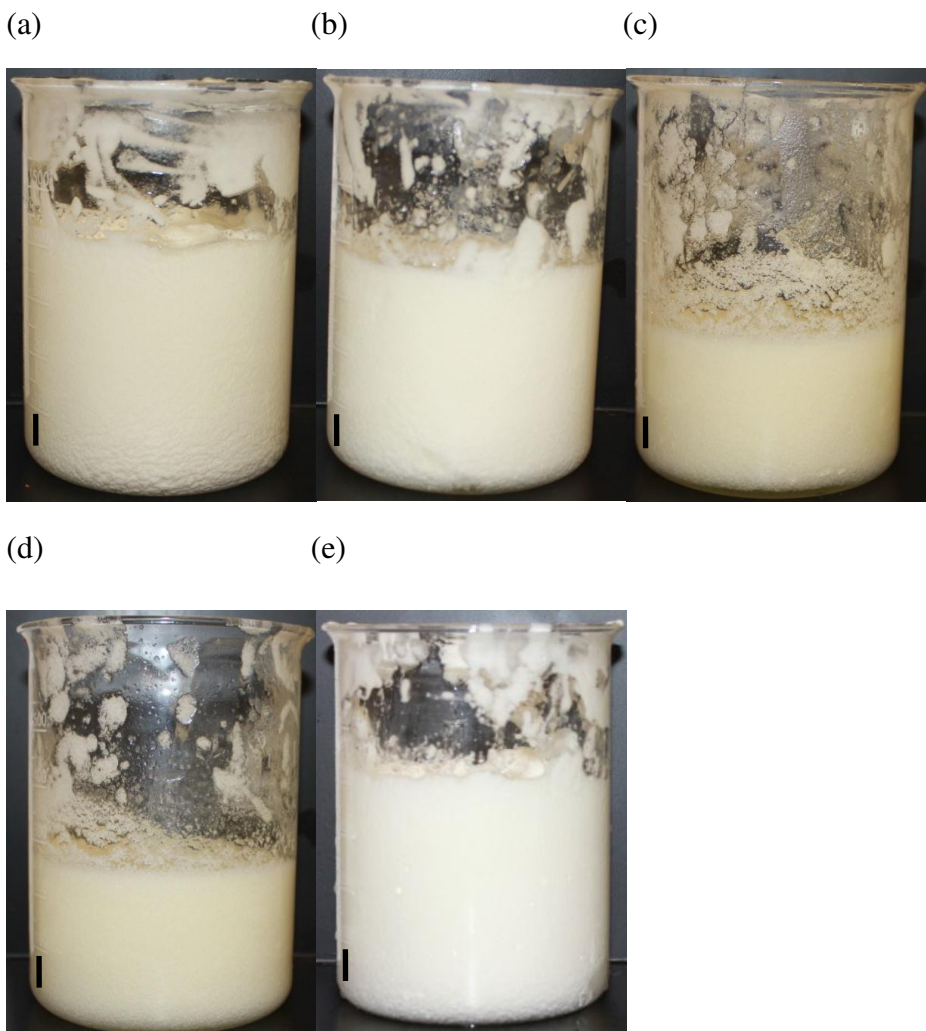
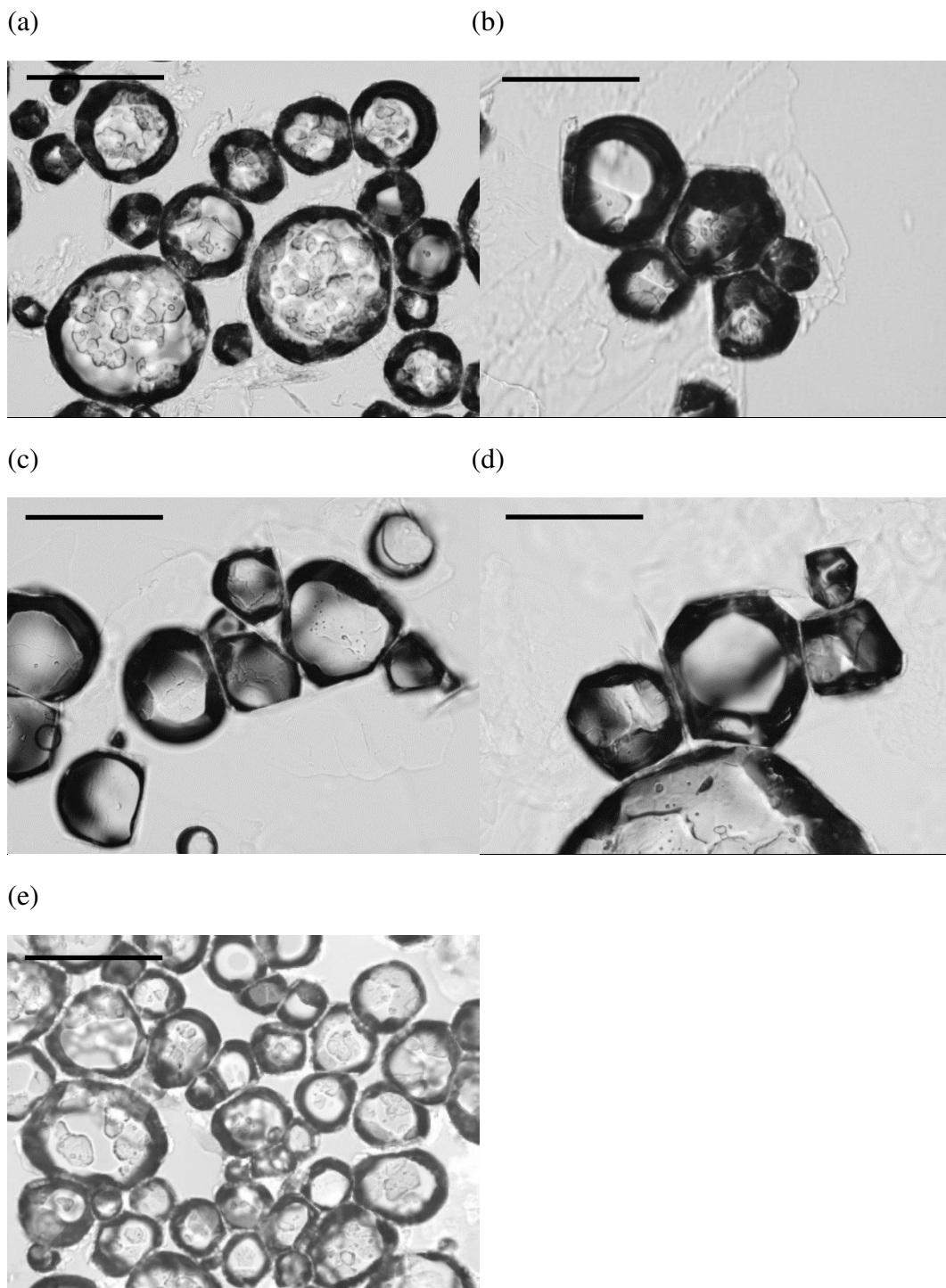


**Figure 6.20.** Optical microscopy images of 8 wt.% myristic acid in HOSO after 30 minutes of whipping with a hand held double beater electric whisk at 22 °C after cooling from 80 °C with (a) a fast cool, (b) a slow cool immediately, (c) a slow cool after 24 hours, (d) a slow cool after 48 hours and (e) after the standard cool. Scale bar 200  $\mu\text{m}$ .



## 6.6 Effect of oil type

The effects of the oil type on foam formation was investigated. This was to discover which other oils could be gelled by the myristic acid and then subsequently aerated with the hand held double beater electric whisk. 5 wt.% myristic acid was added to the various oils as it was clear that a foam could be produced at this concentration, therefore it was thought that this concentration would be sufficient to investigate the effect of oil type.

### 6.6.1 Vegetable oils

10 vegetable oils with differing main fatty acid chain lengths were studied in detail with 5 wt.% myristic acid as shown in Table 6.3. A gel was produced with all of the oils except castor oil. The crystals prior to aeration were either needle-like, plate-like or < 25  $\mu\text{m}$  aggregates.

A foam was produced at 22 °C with all 10 of the vegetable oils investigated, however the volume of the aerated phase after whipping the mixture for 45 minutes varied significantly (Table 6.4). It is also clear that the mixture in rapeseed, sesame, castor, olive and peanut oil only needed to be whipped for 5 minutes before maximum foam production. Once the maximum amount of foam was produced it was found that the foam volume then remained constant until 45 minutes of whipping had elapsed. The foam volume varied from 240 mL (volume fraction of air incorporated 0.13) with sesame oil to 450 mL (volume fraction 0.6) with castor oil. The volume of foam produced with castor oil is surprising as the mixture was not a gel prior to aeration, although the foam fully collapsed within an hour, suggesting that a gelled structure prior to aeration may be necessary for any considerable foam stability. A 10 g sample of each foam was heated from 22 °C at 1 °C/min. to measure the temperature for complete foam collapse which varied from 29.4 °C with castor oil to 43.7 °C with olive oil. When the neat oils were aerated using the same protocol it was found that a foam was only generated with coconut oil indicating that the presence of myristic acid was necessary for a foam to be generated with the other vegetable oils.

**Table 6.3.** Main fatty acid chain length(s) in the oil to which 5 wt.% myristic acid was added, existence of gel prior to aeration, crystal shape prior to aeration and appearance of the foam 24 hours after aeration with a hand held double beater electric whisk for 45 minutes at 22 °C. The foam was stored for 24 hours at 22 ± 2 °C.

| Oil            | Main fatty acid chain length(s)                        | Prior to aeration | Crystal shape prior to aeration  | Appearance of the foam 24 hrs after aeration         |
|----------------|--|-------------------|----------------------------------|--|
| HOSO           | 83.5 % oleic <sup>13</sup>                             | Gel               | < 25 µm aggregates               | 10 mL liquid drainage, 30 mL foam for over 18 months |
| Rapeseed oil   | 60 % oleic, 21.5 % linoleic acid <sup>14</sup>         | Gel               | Needle-like and 50 µm aggregates | 20 mL liquid, 15 mL foam                             |
| Coconut oil    | 48 % lauric, 18.5 % myristic acid <sup>14</sup>        | Gel               | Needle-like                      | 45 mL foam   |
| Sesame oil     | 40 % oleic, 45 % linoleic acid <sup>14</sup>           | Gel               | Needle-like                      | 20 mL liquid, 5 mL foam                              |
| Soybean oil    | 52 % linoleic, 24 % oleic acid <sup>14</sup>           | Gel               | Plate-like                       | 15 mL liquid, 20 mL foam                             |
| Cottonseed oil | 53 % linoleic, 24 % palmitic, 17 % oleic <sup>15</sup> | Gel               | Plate-like and needles           | Foam collapsed within 24 hrs                         |
| Corn oil       | 56 % linoleic, 28 % oleic <sup>15</sup>                | Gel               | Plate-like                       | 10 mL liquid, 20 mL foam                             |
| Castor oil     | 72 % ricinoleic acid <sup>16</sup>                     | No gel            | < 25 µm aggregates               | Foam collapsed within 1 hour.                        |
| Olive oil      | 72.5 % oleic acid <sup>14</sup>                        | Gel               | < 25 µm aggregates               | 15 mL liquid, 10 mL foam                             |
| Peanut oil     | 48 % oleic, 30 % linoleic <sup>14</sup>                | Gel               | Needle-like                      | Foam collapsed within 24 hrs                         |

**Table 6.4.** Volume of the aerated phase, whipping time for maximum foam production, volume fraction of air incorporated into the mixture and the temperature of complete foam collapse of 5 wt.% myristic acid in vegetable oils whipped with a hand held double beater electric whisk at 22 °C.

| Oil            | Volume of aerated phase/<br>± 10 mL | Whipping time for maximum foam/ min. | Volume fraction of air ± 0.02 | Temperature of complete foam collapse/ ± 0.1 °C |
|----------------|-------------------------------------|--------------------------------------|-------------------------------|---|
| HOSO           | 400                                 | 15                                   | 0.25                          | 37.0  |
| Rapeseed oil   | 350                                 | 5                                    | 0.46                          | 41.8  |
| Coconut oil    | 300                                 | 15                                   | 0.36                          | 32.3  |
| Sesame oil     | 240                                 | 5                                    | 0.13                          | 42.4  |
| Soybean oil    | 300                                 | 15                                   | 0.35                          | 39.4  |
| Cottonseed oil | 250                                 | 10                                   | 0.15                          | 41.3  |
| Corn oil       | 300                                 | 10                                   | 0.36                          | 43.4  |
| Castor oil     | 450                                 | 5                                    | 0.60                          | 29.4  |
| Olive oil      | 270                                 | 5                                    | 0.20                          | 43.7  |
| Peanut oil     | 250                                 | 5                                    | 0.16                          | 42.4  |

As seen from Figure 6.21, 5 wt.% myristic acid had the ability to gel all of the vegetable oils once they had been heated to 80 °C, followed by cooling to  $8 \pm 2$  °C at approximately 1 °C/min. except for myristic acid in castor oil which was a clear pale yellow viscous liquid. From optical microscopy (Figure 6.22) it can be seen that the myristic acid formed various structures in the different oils. The myristic acid in HOSO, castor and olive oil appeared to be small aggregates which were < 25 µm in diameter, whereas in rapeseed oil the myristic acid appeared to be both a needle-like structure (up to 100 µm long) and aggregates which were < 50 µm in diameter. This needle-like structure (needles up to 100 µm long) was also observed with the myristic acid in coconut, sesame and peanut oil. The myristic acid, when in soybean, cottonseed and corn oil, was a plate-like structure which had a diameter ranging from 25 µm with cottonseed oil to 200 µm with corn oil.

**Figure 6.21.** Photographs of 5 wt.% myristic acid in (a) HOSO, (b) rapeseed oil, (c) coconut oil, (d) sesame oil, (e) soybean oil, (f) cottonseed oil, (g) corn oil, (h) castor oil, (i) olive oil and (j) peanut oil prior to whipping at 22 °C. Scale bar 1 cm.

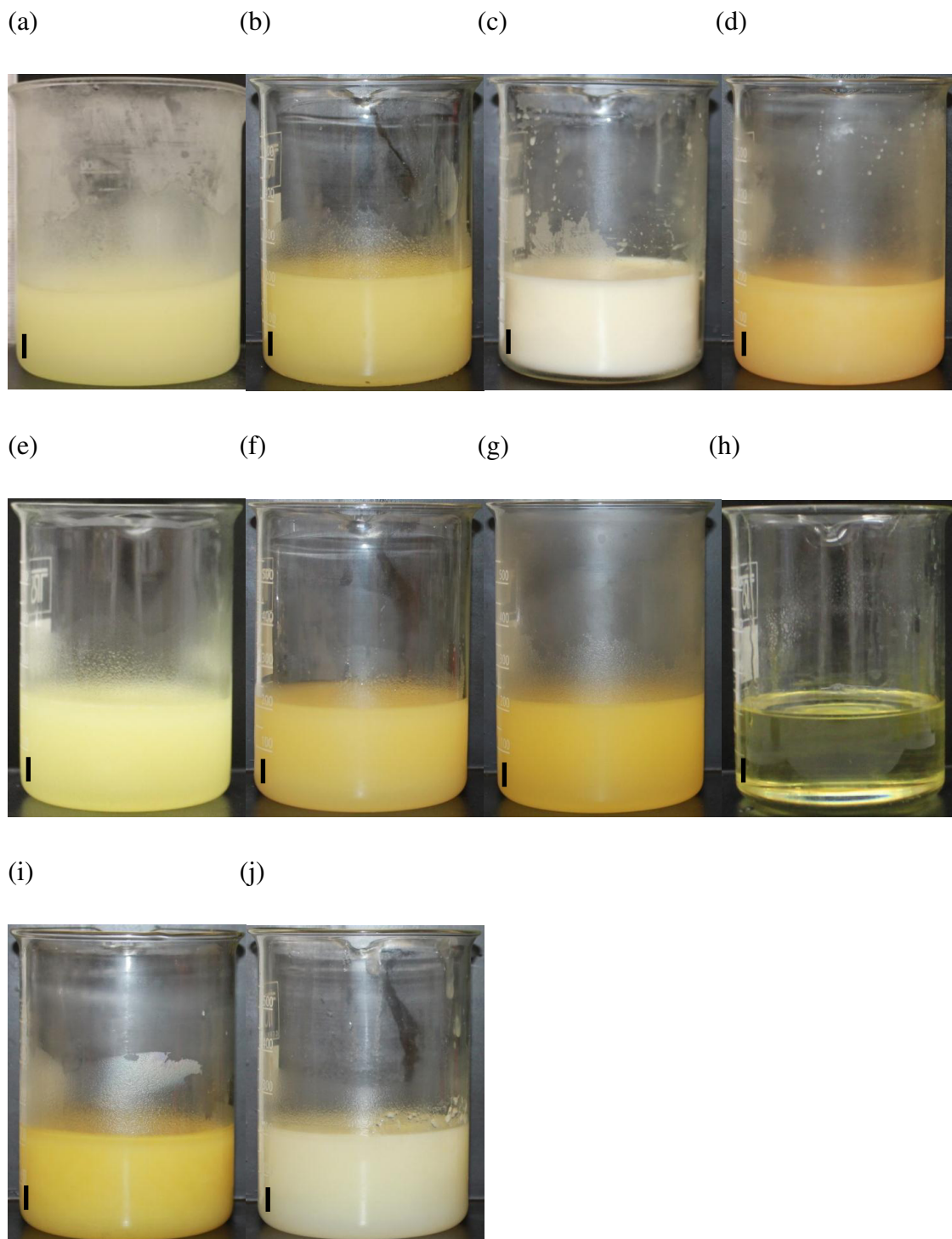
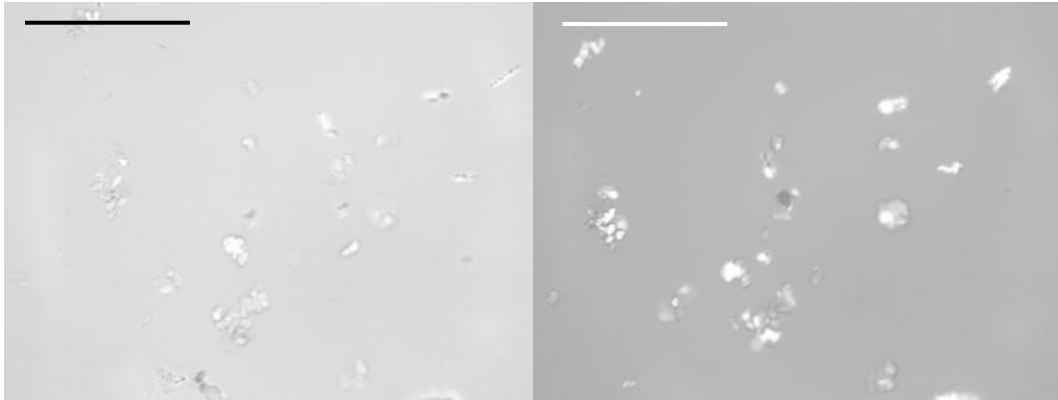
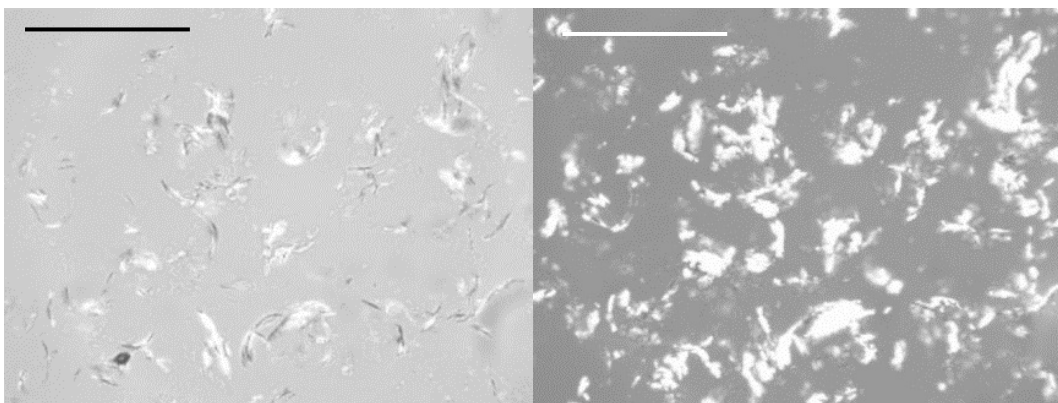


**Figure 6.22.** Optical microscopy of 5 wt.% myristic acid in (a) HOSO, (b) rapeseed oil, (c) coconut oil, (d) sesame oil, (e) corn oil and (f) castor oil prior to whipping at 22 °C. Images on the right are corresponding micrographs viewed through crossed polarising lenses. Scale bar is 200  $\mu\text{m}$ .

(a)



(b)



(c)

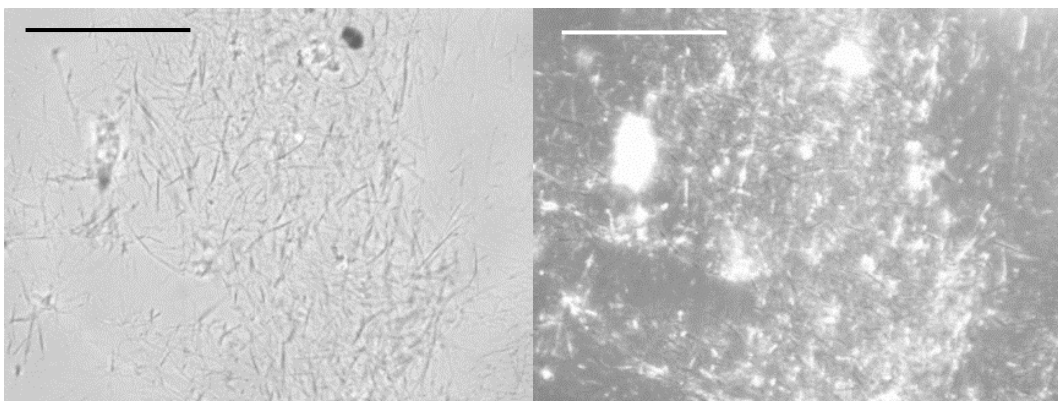
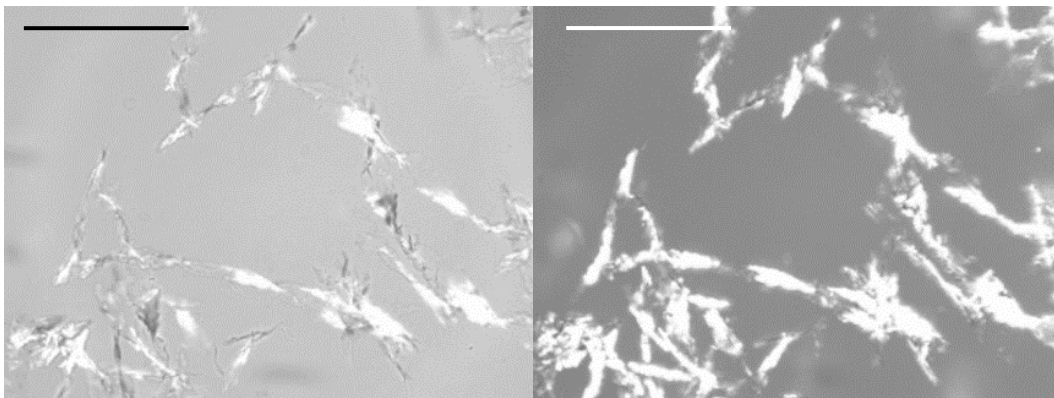
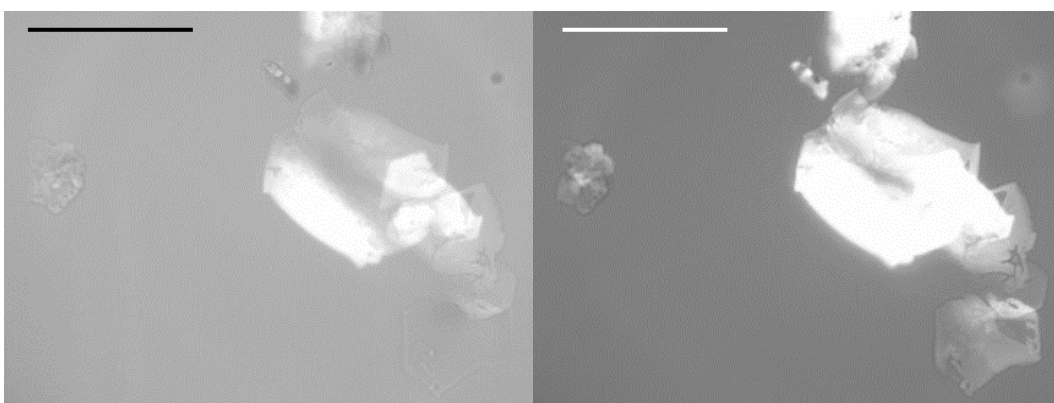


**Figure 6.22** (continued)

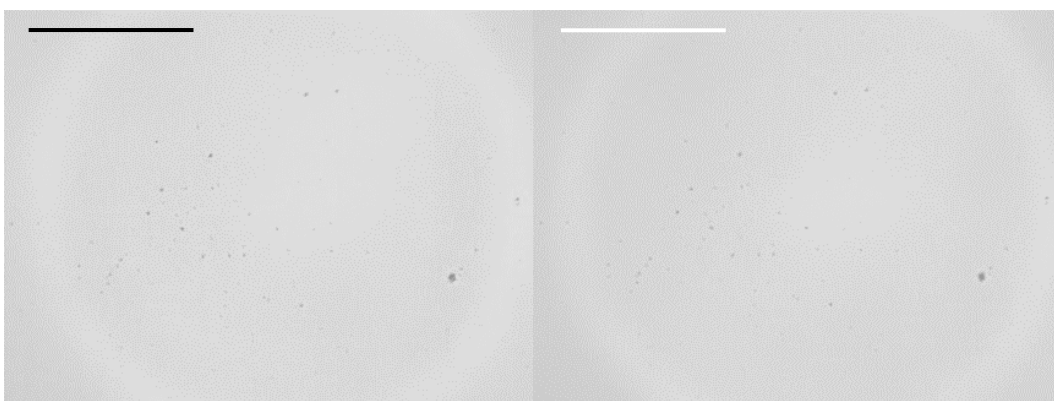
(d)



(e)



(f)



Remarkably a foam was formed with all of the oils (as shown in Table 6.4 and seen in Figure 6.23) suggesting that the ability to create a foam is independent of the type of crystals in the oil and also a gel prior to aeration is, in fact, not necessary for foam

formation. Figure 6.23 shows visually that myristic acid in sesame, cottonseed, olive and peanut oil once whipped does not produce as much foam as that seen with the other six oils studied. The optical microscopy shown in Figure 6.24 is very interesting as it shows that the bubbles in the foams produced with the different oils are very different. The bubbles in the foams produced with sesame, cottonseed, olive and peanut oil where the foam volume is relatively low (< 300 mL) were all similar in appearance (< 50  $\mu\text{m}$ ). The mainly spherical bubbles in the myristic acid in coconut oil system where the foam was stable for over 4 months without any liquid drainage were also, on average, < 50  $\mu\text{m}$ . The foam bubbles in castor oil were over 400  $\mu\text{m}$  in diameter which shows the instability of the system (the foam fully collapsed 1 hour after the whipping had ceased). The foams formed with the remaining oils were found to consist of non-spherical bubbles with an average diameter of 100  $\mu\text{m}$ , the bubble surface was also textured. It is interesting that the bubble appearance does not appear to have an effect on the foam stability.

Figure 6.25 shows the foams produced with 5 wt.% myristic acid in various vegetable oils 24 hours after formation. The foams produced remained as shown in the figure for at least 2 weeks before further liquid drainage and gradual foam collapse occurred. The foam produced with HOSO (where there was 10 mL of liquid drainage) did not change in appearance until after 18 months. The foam produced with coconut oil did not change in appearance for at least 4 months. The foam produced with peanut and cottonseed oil collapsed 24 hours after formation (as seen in Table 6.3 and Figure 6.25 where only a small amount of bubbles remained at the air-oil surface on the side of the glass). It is therefore unclear what determined the stability of the foams. The appearance of the foam changed up to 24 hours after aeration, after 24 hours the foam did not significantly change at room temperature ( $22 \pm 2$  °C) until 2 weeks had elapsed, the foam then gradually collapsed (except for foams produced with HOSO and coconut oil). It is clear that the difference in the mixture prior to whipping (gel or not a gel) did not have an effect on the foam formation (450 mL of foam produced with castor oil where the mixture was not a gel prior to aeration). However, the foam stability was found to clearly be effected as the foam produced with castor oil fully collapsed 1 hour after the aeration and collapsed at 29.4 °C when a sample of foam was heated at 1 °C/min. as shown in Table 6.4. It was found that a foam produced with olive oil had the highest stability to a temperature increase (fully collapsed at 43.7 °C), however when the sample was left at room temperature for 24 hours over half of the foam volume

collapsed (only 10 mL remained). The foam produced with corn oil fully collapsed at 43.4 °C, but was found to also be relatively stable when left at room temperature as after 24 hours 20 mL of foam remained. The foam produced with castor oil was found to fully collapse at 29.4 °C when the temperature of the sample increased, when the sample was left at room temperature the foam was found to fully collapse after 1 hour. It is interesting to see that the foam produced with the coconut oil was found to fully collapse at 32.3 °C, however when the sample was left at room temperature the mixture was found to be highly stable with no liquid drainage. It is therefore clear that the myristic acid presence was necessary for the foam stability but how favourably the myristic acid attached at the air-oil surface, and therefore the stability of the foams over time, was dependent on the oil type.

**Figure 6.23.** Photographs of 5 wt.% myristic acid in (a) HOSO, (b) rapeseed oil, (c) coconut oil, (d) sesame oil, (e) soybean oil, (f) cottonseed oil, (g) corn oil, (h) castor oil, (i) olive oil and (j) peanut oil after whipping for 30 minutes with a hand held double beater electric whisk at 22 °C. Scale bar 1 cm.

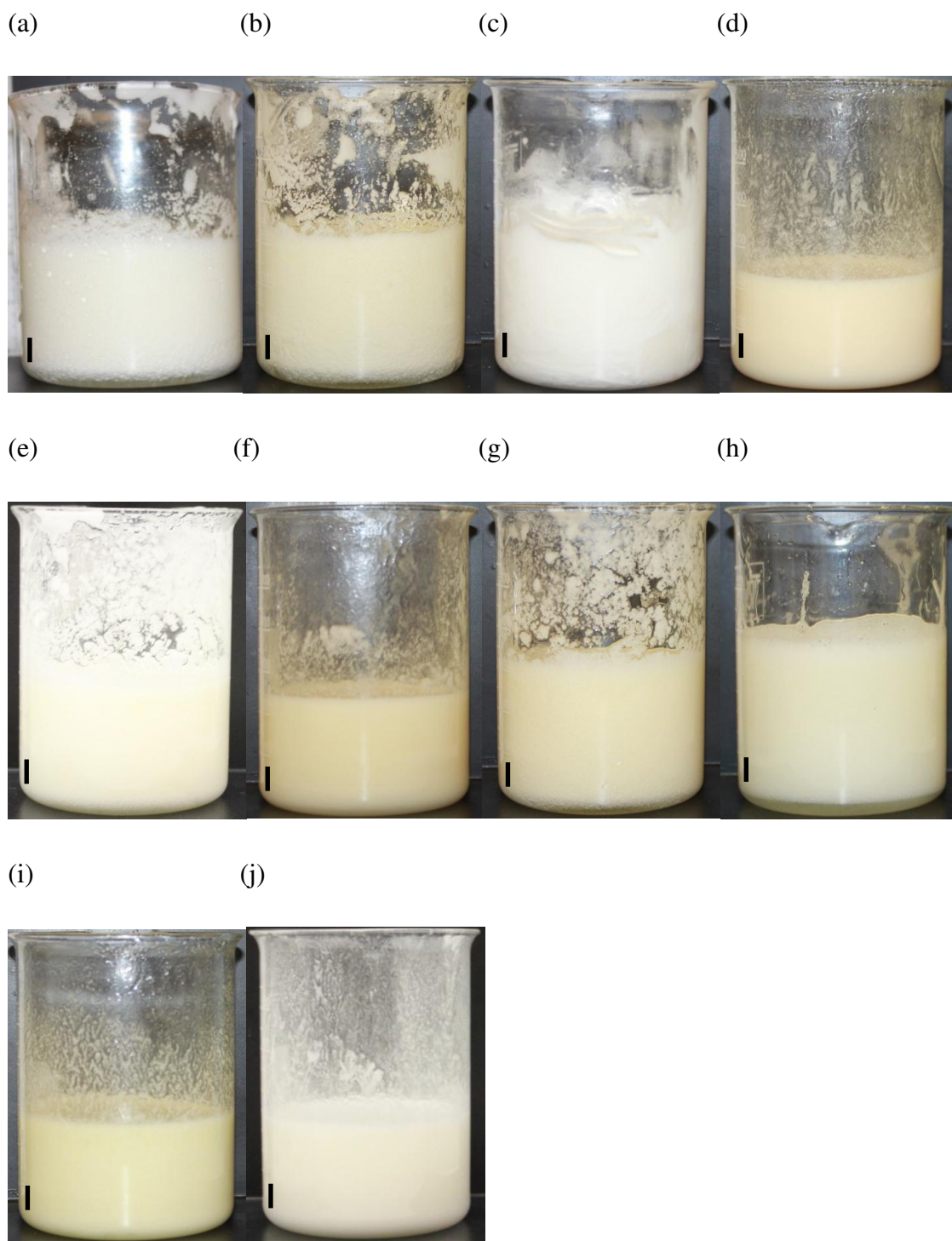
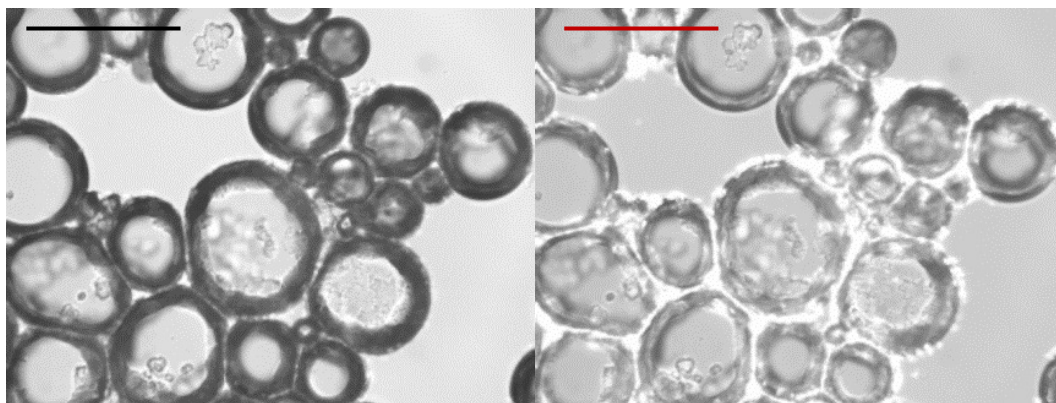
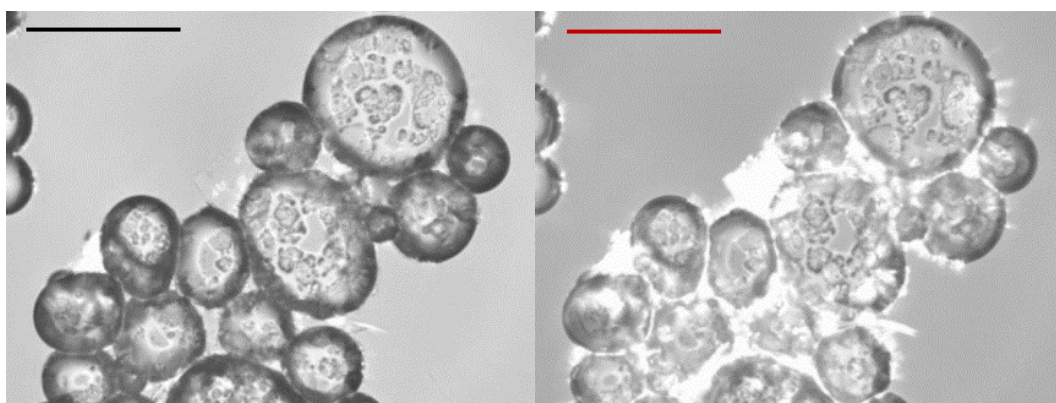


**Figure 6.24.** Optical microscopy of 5 wt.% myristic acid in (a) HOSO, (b) rapeseed oil, (c) coconut oil, (d) sesame oil, (e) corn oil and (f) castor oil after 30 minutes of whipping with a hand held double beater electric whisk at 22 °C. Images on right are corresponding micrographs viewed through crossed polarising lenses. Scale bar 200  $\mu\text{m}$ .

(a)



(b)



(c)

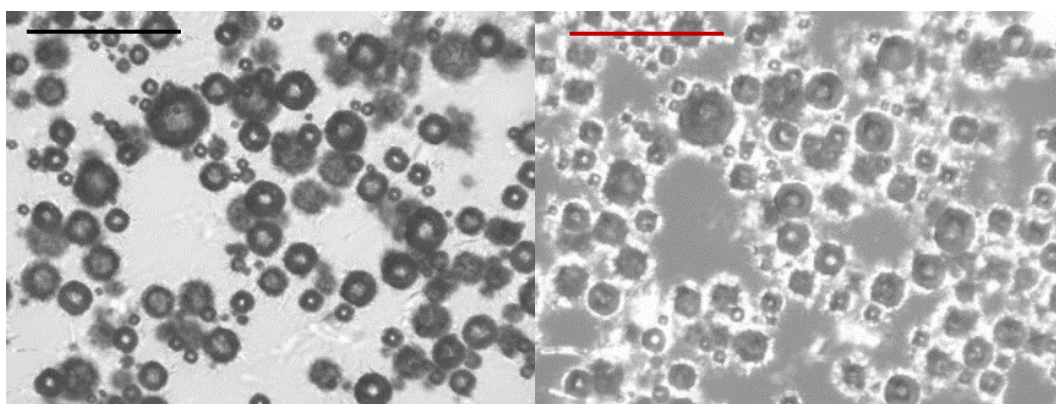
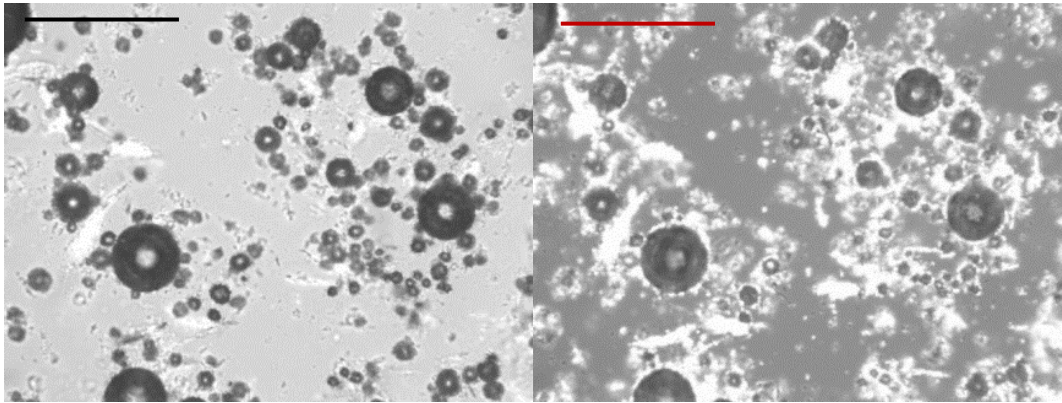
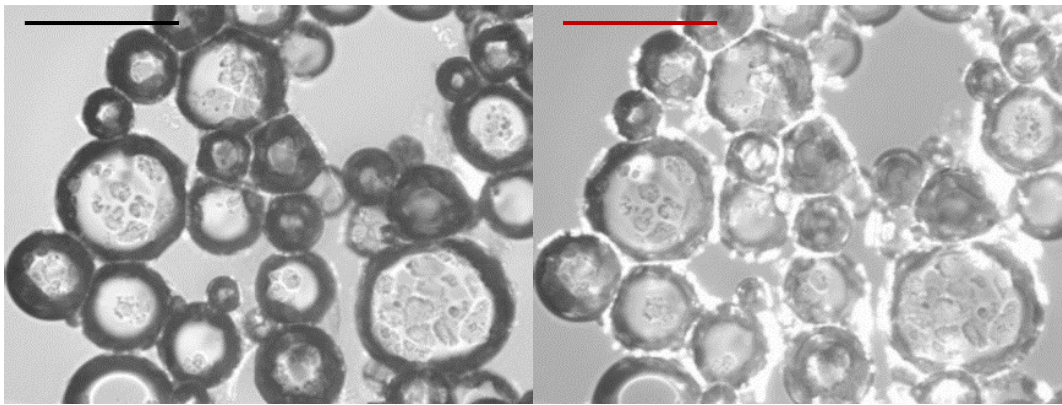


**Figure 6.24** continued

(d)



(e)



(f)

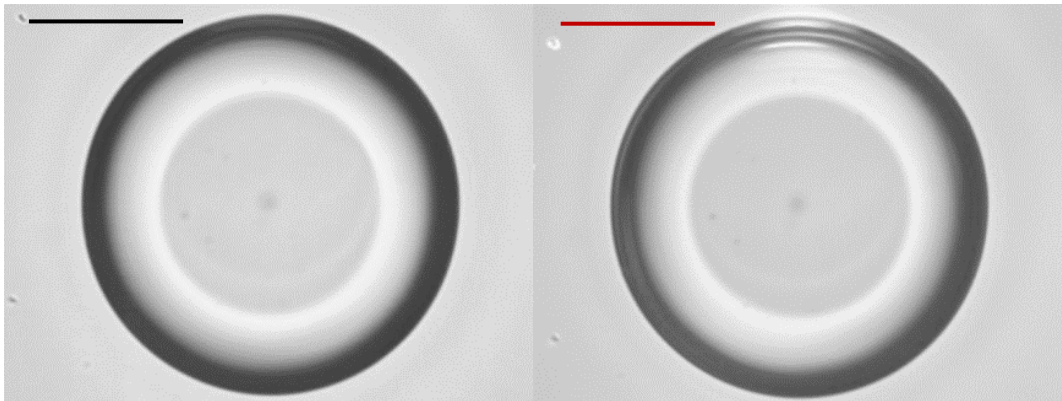
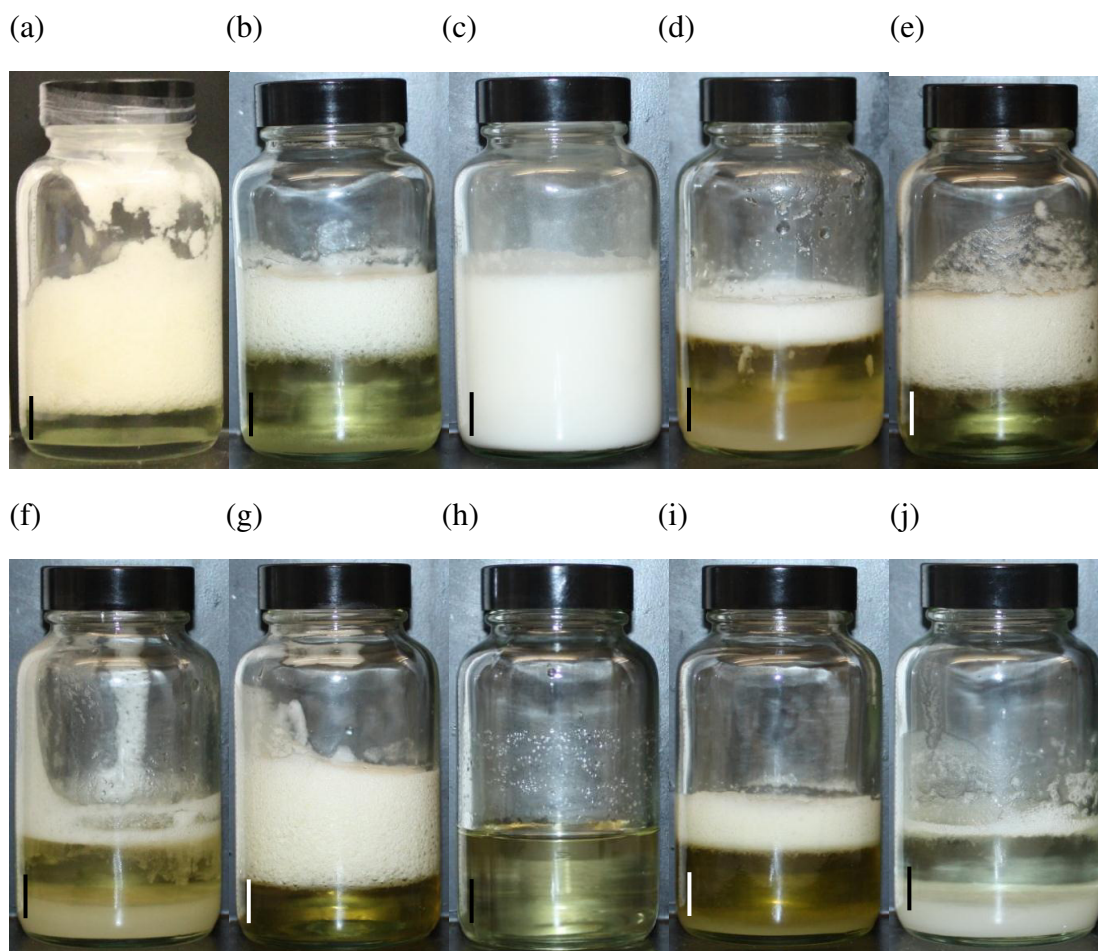


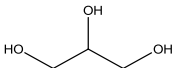
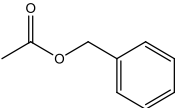
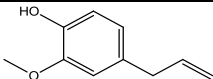
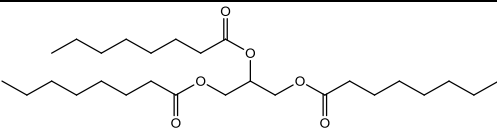
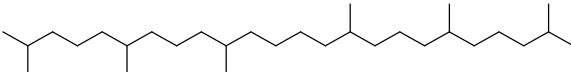
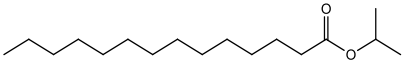
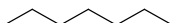
**Figure 6.25.** Photographs of 5 wt.% myristic acid in (a) HOSO, (b) rapeseed oil, (c) coconut oil, (d) sesame oil, (e) soybean oil, (f) cottonseed oil, (g) corn oil, (h) castor oil, (i) olive oil and (j) peanut oil at  $22 \pm 2$  °C 24 hours after whipping for 45 minutes with a hand held double beater electric whisk at 22 °C. Scale bar 1 cm.



### 6.6.2 Non-edible oils

The ability of myristic acid in various non-edible oils to create a foam with the whipping protocol was investigated. The investigated liquids had varying surface tensions and structures as can be seen from Table 6.5. The table also shows that a foam could be produced with 5 wt.% myristic acid in eugenol, HOSO, ethylene glycol and squalane. The surface tension did not appear to have an effect on the foamability of the oil.

**Table 6.5.** Liquid type, structure, air-liquid surface tension and whether a foam could be produced after whipping 5 wt.% myristic acid in the liquid with a hand held double beater electric whisk for 45 minutes at 22 °C.

| Non-aqueous liquid  | Structure  | Foam production<br>Y (Yes)/N (NO) | Air-oil surface tension/ mN m <sup>-1</sup> at 25 °C |
|---------------------|--|-----------------------------------|--|
| Glycerol            |     | N                                 | 63.4 <sup>17</sup>                                   |
| Ethylene glycol     |     | Y                                 | 47.7 <sup>17</sup>                                   |
| Benzyl acetate      |     | N                                 | 36.8   |
| Eugenol             |     | Y                                 | 36.5   |
| HOSO                | Triglyceride with ~84 % oleic acid   | Y                                 | 33.4   |
| Tricaprylin         |  | N                                 | 29.6   |
| Squalane            |  | Y                                 | 28.6   |
| Isopropyl myristate |   | N                                 | 28.6   |
| Toluene             |   | N                                 | 28.4 <sup>17</sup>                                   |
| Cyclohexane         |   | N                                 | 24.9   |
| Heptane             |   | N                                 | 20.2   |
| 1-dodecanol         |   | N                                 | solid  |

6.6.2.1 5 wt.% myristic acid in ethylene glycol, eugenol, high oleic sunflower oil and squalane

Table 6.6 summarises the volume of the aerated phase, the amount of air incorporated into the mixture along with the foam stability for eugenol, squalane, ethylene glycol and HOSO with 5 wt.% myristic acid at  $22 \pm 2$  °C. 50 mL of foam was formed in eugenol and squalane, however the foam was only stable for 6 and 2 minutes, respectively. Due to this instability a temperature of complete foam collapse was not recorded for either of these foams. A value for the volume fraction of air incorporated into the mixture is not stated for squalane as the foam produced was very unstable; the foam collapsed when it was transferred to a vessel to be weighed. A large amount of air was incorporated into the foam formed in ethylene glycol (0.63), almost three times more than that found with HOSO (0.25), however the foam was found to not be particularly stable (only stable for 48 hours). It is interesting that the temperature the foam fully collapsed was found to be high (54.2 °C) showing that the crystals were necessary for foam stability. Foams with eugenol, squalane and ethylene glycol were found to not be particularly stable compared to that with HOSO.

**Table 6.6.** Volume of aerated phase, amount of air incorporated into the mixture and subsequent foam stability after whipping 5 wt.% myristic acid in various liquids with a hand held double beater electric whisk for 45 minutes at 22 °C.

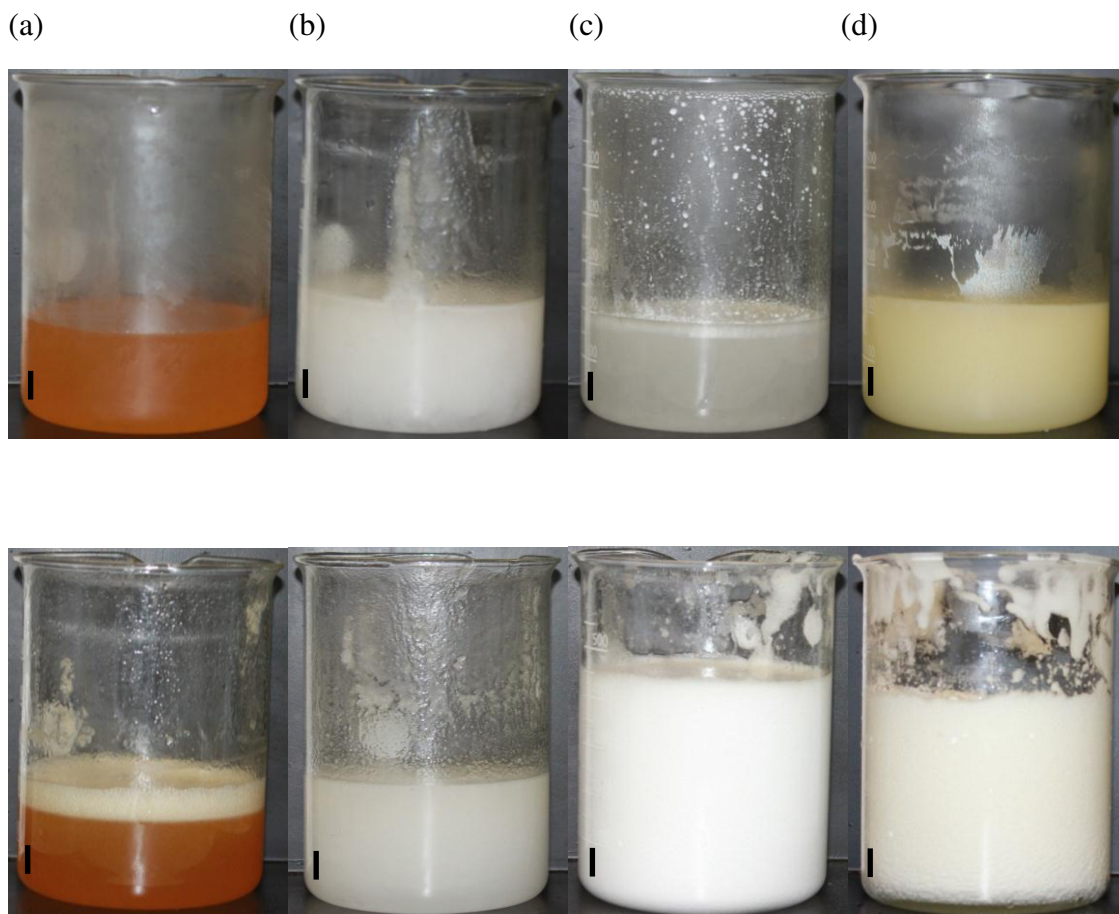
| Oil             | Volume of aerated phase/ mL | Volume fraction of air | Foam stability | Temperature of complete foam collapse/ $\pm 0.1$ °C |
|-----------------|-----------------------------|------------------------|----------------|---|
| Ethylene glycol | 450                         | 0.63                   | 48 hours       | 54.2  |
| Eugenol         | 50                          | 0.15                   | 6 minutes      | -   |
| HOSO            | 400                         | 0.25                   | 18 months      | 37.0  |
| Squalane        | 50                          | -                      | 2 minutes      | -   |

Figure 6.26 gives the appearance of these systems prior to whipping. As seen, myristic acid in eugenol, squalane and HOSO was a soft, turbid gel. Myristic acid appeared solidified at the air-ethylene glycol surface however. The figure also demonstrates the visual appearance of the foams produced in these liquids. It is clear from the figure that a large amount of foam (450 mL) was generated when the myristic acid was in ethylene glycol, whereas with eugenol and squalane only 50 mL of foam was produced.

As seen in Figure 6.27, prior to whipping the myristic acid was irregular shaped aggregates approximately 200-250  $\mu\text{m}$  in size in eugenol which was also the case in squalane and ethylene glycol. The myristic acid in HOSO was approximately 40  $\mu\text{m}$  aggregates. In all four oils the myristic acid is visible with crossed polarising lenses. It may be that the smaller myristic acid aggregates were able to arrange better at the air-oil surface than the larger aggregates causing the high stability at  $22 \pm 2$  °C of the foam produced with HOSO.

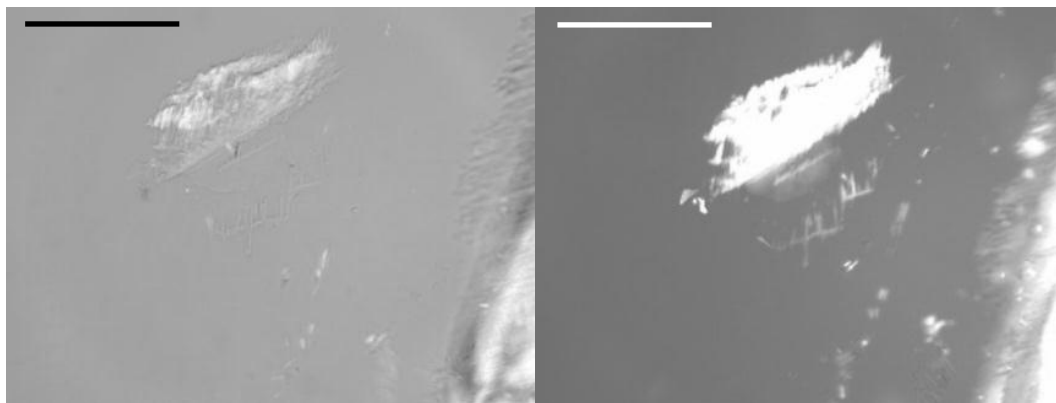
Figure 6.28 shows optical microscopy images of the foams produced. The foam produced with myristic acid in squalane was not observed under the microscope due to its instability. Figure 6.28 (c) demonstrates that the foam produced with ethylene glycol had bubbles ranging from 50 to 250  $\mu\text{m}$  and that the surface of the bubbles appeared to be textured, indicating the presence of crystals. It is clear from the figure with the foams viewed through crossed polarising lenses that the myristic acid was present at the air-oil surface of the bubbles in a foam produced with eugenol, ethylene glycol and HOSO.

**Figure 6.26.** Photographs of 5 wt.% myristic acid in (a) eugenol, (b) squalane, (c) ethylene glycol and (d) HOSO (upper) prior to whipping and (lower) after whipping for 45 minutes with a hand held double beater electric whisk at 22 °C. Scale bar 1 cm.



**Figure 6.27.** Optical microscopy of 5 wt.% myristic acid in (a) eugenol and (b) HOSO prior to whipping with a hand held double beater electric whisk at 22 °C. Images on the right are corresponding micrographs viewed through crossed polarising lenses. Scale bar 200  $\mu\text{m}$ .

(a)



(b)

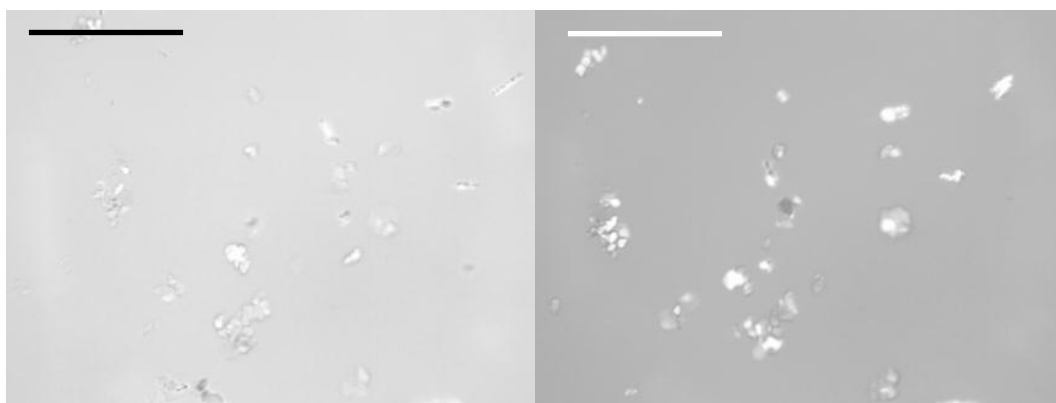
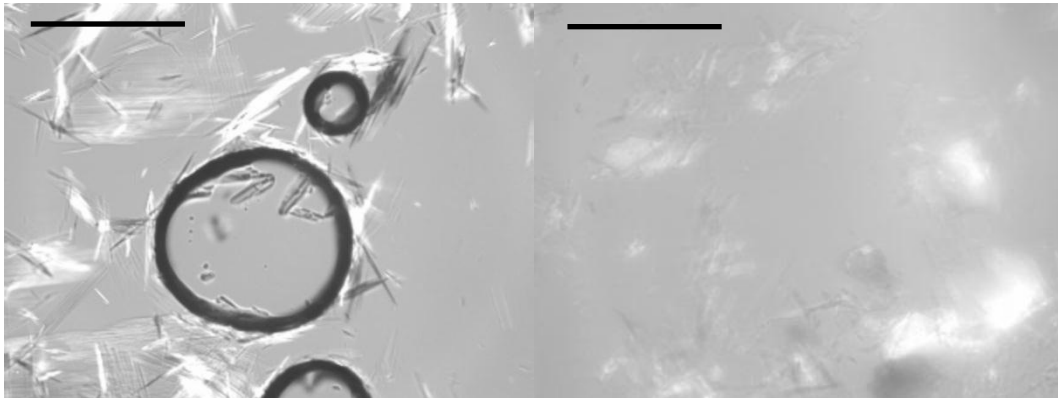
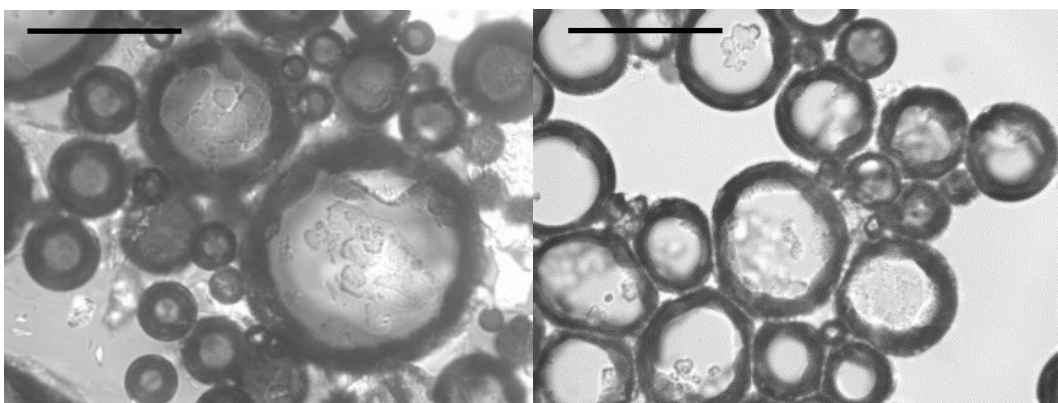


**Figure 6.28.** Optical microscopy of 5 wt.% myristic acid in (a) eugenol, (b) squalane, (c) ethylene glycol and (d) HOSO after whipping for 45 minutes with a hand held double beater electric whisk at 22 °C. Scale bar 200  $\mu\text{m}$ .

(a)



(b)



6.6.2.2 5 wt.% myristic acid in benzyl acetate, cyclohexane, 1-dodecanol, glycerol, heptane, isopropyl myristate, toluene and tricaprylin

5 wt.% myristic acid was added to benzyl acetate, cyclohexane, 1-dodecanol, glycerol, heptane, isopropyl myristate, toluene and tricaprylin. The mixtures were cooled from 80 °C to  $8 \pm 2$  °C at approximately 1 °C/min. except with cyclohexane, heptane and toluene where the mixture was at 40 °C and then cooled to  $8 \pm 2$  °C at approximately 1 °C/min. The mixtures were whipped with a hand held double beater electric whisk for 45 minutes at 22 °C, it was then found that a foam could not be produced.

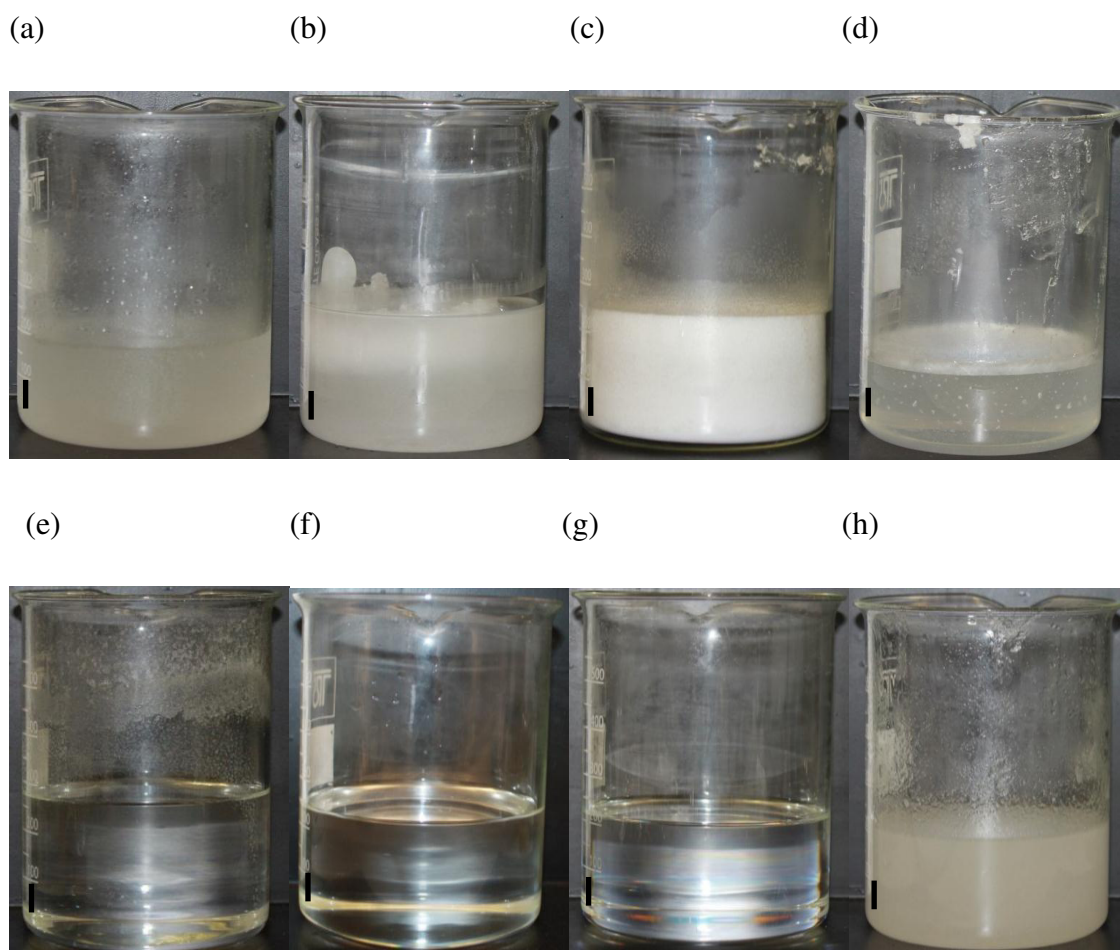
Figure 6.29 shows the appearance of the systems prior to whipping. As shown in the figure myristic acid was completely soluble in heptane, isopropyl myristate and toluene forming a clear, homogeneous liquid. Myristic acid in benzyl acetate was a turbid, fluid liquid, in tricaprylin and glycerol the mixture was a turbid, viscous liquid and in 1-dodecanol the mixture was a white solid. It is worth noting that although the myristic acid in cyclohexane prior to whipping was a turbid fluid, after 5 minutes of whipping the mixture was a clear homogeneous liquid.

Figure 6.30 shows optical microscopy images of the systems prior to whipping at 22 °C. It is clear that myristic acid is soluble in heptane, isopropyl myristate and toluene. In benzyl acetate and tricaprylin the myristic acid had a plate-like structure. It is therefore puzzling why a foam was not produced with these oils after whipping for 45 minutes.

It is clear from Figure 6.31 that there was not a foam produced with 5 wt.% myristic acid in benzyl acetate, cyclohexane, 1-dodecanol, glycerol, heptane, isopropyl myristate, toluene and tricaprylin after 45 minutes of whipping at 22 °C. After whipping cyclohexane the myristic acid dissolved in the oil, whereas after whipping glycerol and isopropyl myristate the mixture became a turbid, white liquid. Figure 6.32 also confirms that a foam was not produced after whipping 5 wt.% myristic acid in the oils for 45 minutes. Figure 6.32 (b) shows that some bubbles were incorporated into the 5 wt.% myristic acid in glycerol mixture, but a foam was not produced. It is interesting that a foam could not be produced with myristic acid in benzyl acetate, cyclohexane, 1-dodecanol, glycerol, heptane, isopropyl myristate, toluene and tricaprylin (all other images were featureless) because when myristic acid was added to various vegetable oils a foam could be generated regardless of whether the mixture prior to aeration was a turbid gel or a clear viscous liquid. It was also found with myristic acid in the vegetable

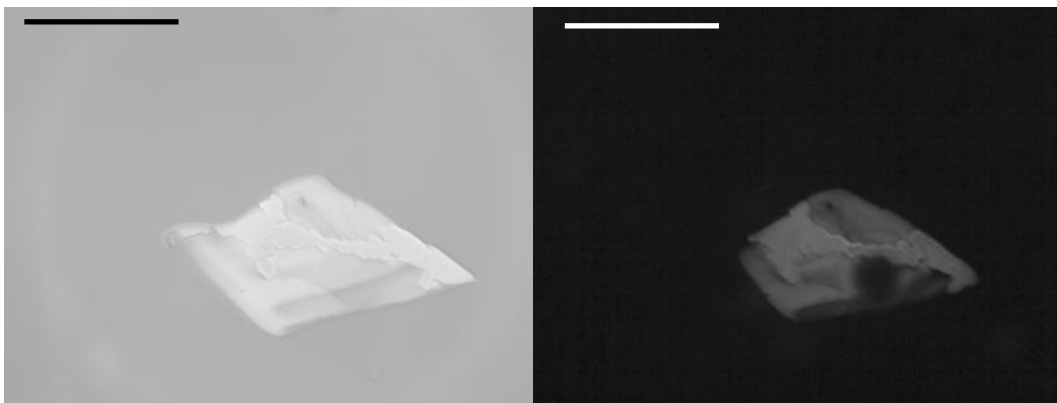
oils that the ability to generate a foam was independent of the structure of the myristic acid.

**Figure 6.29.** Photographs of 5 wt.% myristic acid in (a) benzyl acetate, (b) cyclohexane, (c) 1-dodecanol, (d) glycerol, (e) heptane, (f) isopropyl myristate, (g) toluene and (h) tricaprylin prior to whipping at 22 °C. Scale bar 1 cm.

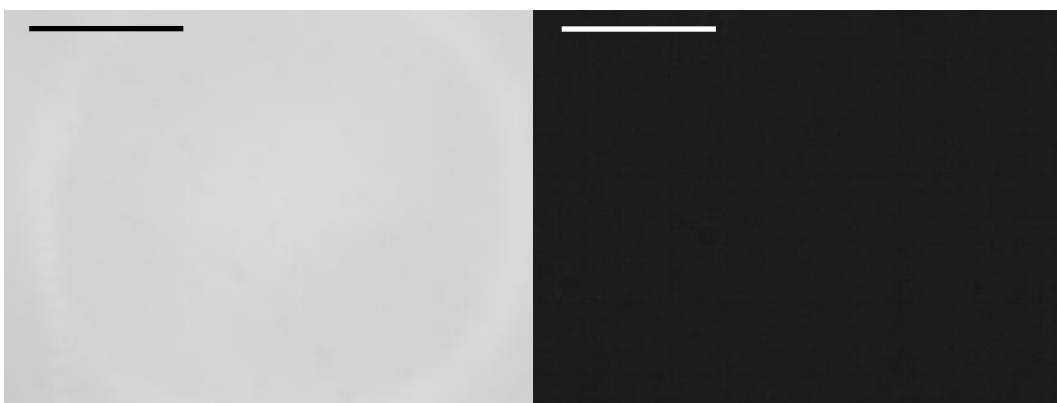


**Figure 6.30.** Optical microscopy of 5 wt. % myristic acid in (a) benzyl acetate, (b) heptane and (c) tricapyrylin prior to whipping. Images on the right are corresponding micrographs viewed through crossed polarising lenses. Scale bar 200  $\mu\text{m}$ .

(a)



(b)



(c)

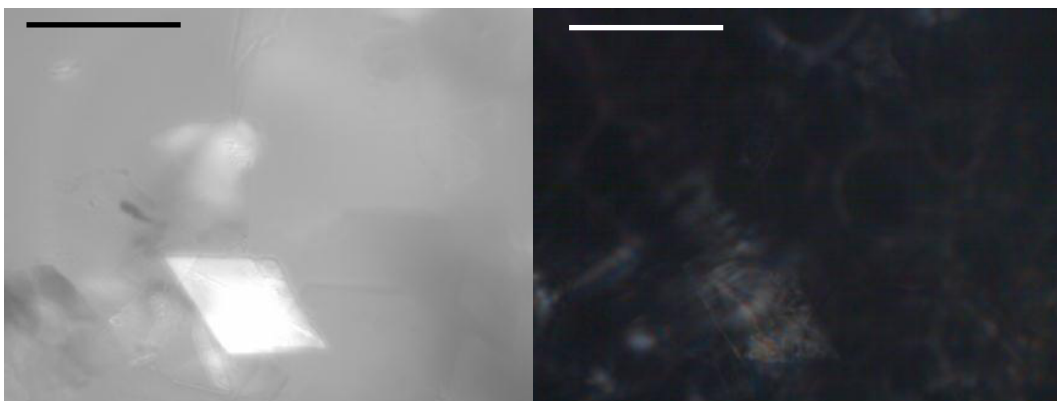


**Figure 6.31.** Photographs of 5 wt.% myristic acid in (a) benzyl acetate, (b) cyclohexane, (c) 1-dodecanol, (d) glycerol, (e) heptane, (f) isopropyl myristate, (g) toluene and (h) tricaprylin after whipping for 45 minutes with a hand held double beater electric whisk at 22 °C. Scale bar 1 cm.

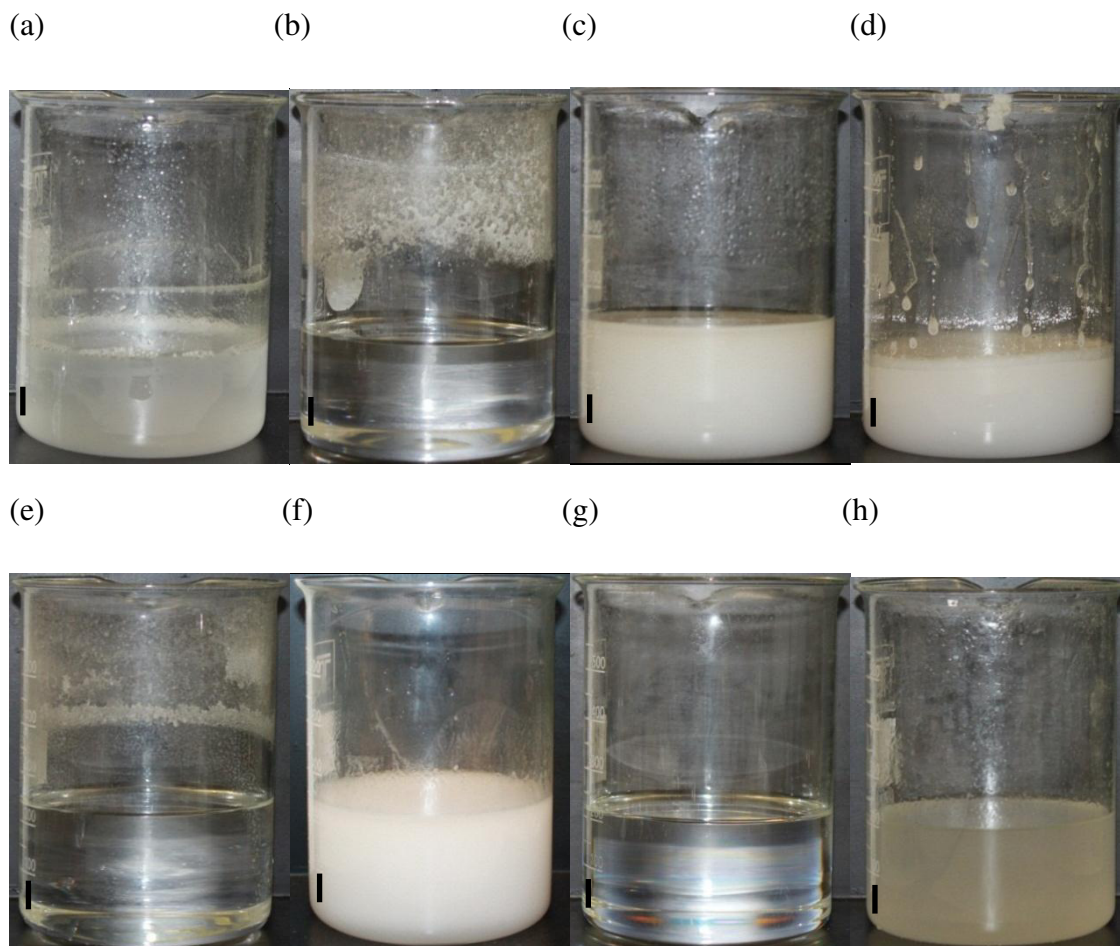
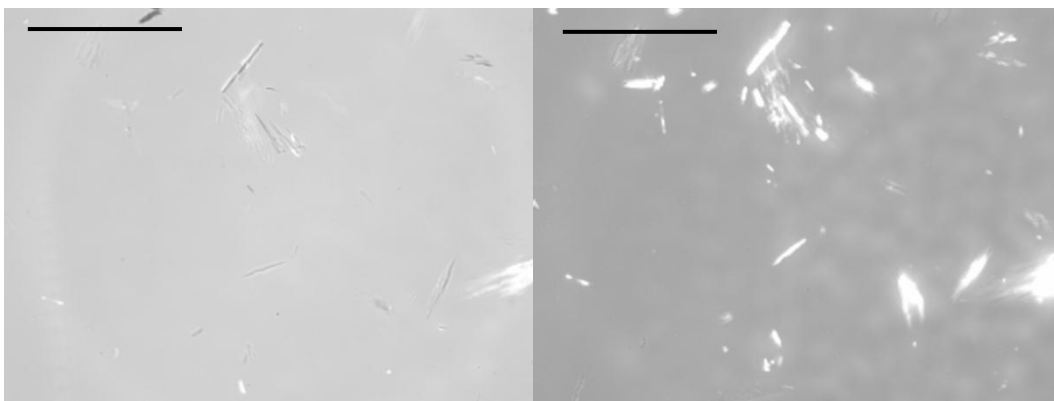
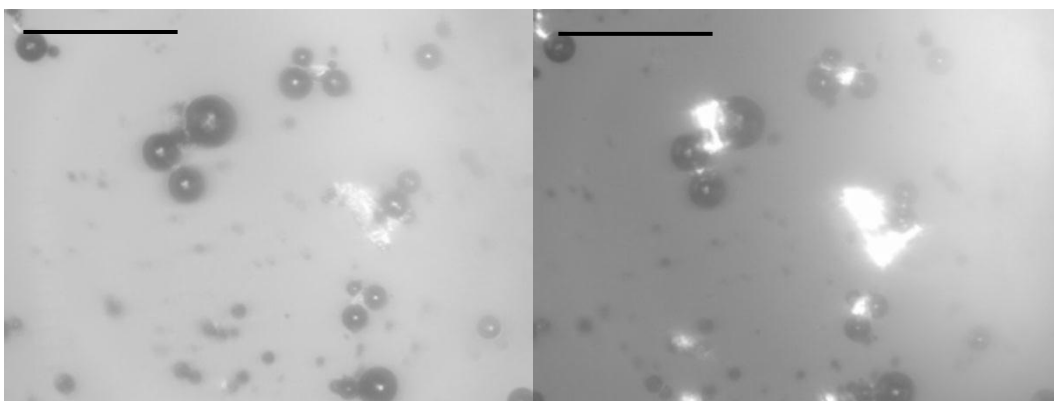


**Figure 6.32.** Optical microscopy of 5 wt. % myristic acid in (a) benzyl acetate, (b) glycerol and (c) tricapylin after whipping for 45 minutes with a hand held double beater electric whisk at 22 °C. Images on the right are corresponding micrographs viewed through crossed polarising lenses. Scale bar 200  $\mu\text{m}$ .

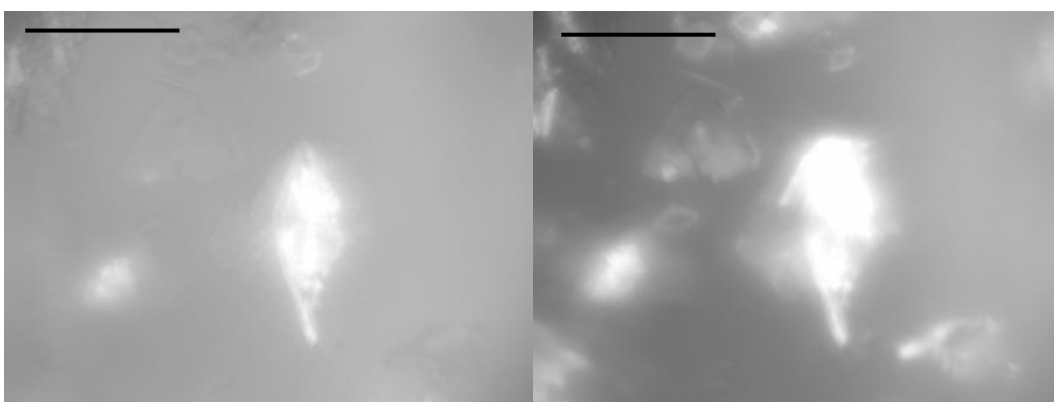
(a)



(b)



(c)



## 6.7 Effect of ground myristic acid in HOSO

The effect of simply grinding myristic acid and then adding it to HOSO on foam formation was investigated. The myristic acid powder prior to grinding consisted of aggregates around 2-5 mm, significantly larger than the size of ground myristic acid, 30  $\mu\text{m}$  in diameter (Figure 6.33). 6 wt.% of the ground myristic acid was added to HOSO. It was found that the ground myristic acid sedimented in the oil, as shown in Figure 6.34. The size of the crystals once added to HOSO prior to whipping did not change as shown in Figure 6.35. After the mixture was whipped for 45 minutes with a hand held double beater electric whisk (no prior heating) it was found that a foam could not be formed as shown in Figure 6.34 and Figure 6.35 (b). It is therefore clear that the plate-like crystals are not surface active and also that the absence of the dissolved myristic acid molecules is detrimental to foam formation.

**Figure 6.33.** Optical microscopy of neat myristic acid powder. Image on the right is a corresponding micrograph viewed through crossed polarising lenses. Myristic acid was ground with the use of a grinding ball mill with 30 stainless steel balls (10-20 mm diameter) for 1 hour at 100 rpm and then 1 hour at 150 rpm. Scale bar 200  $\mu\text{m}$ .

(a)

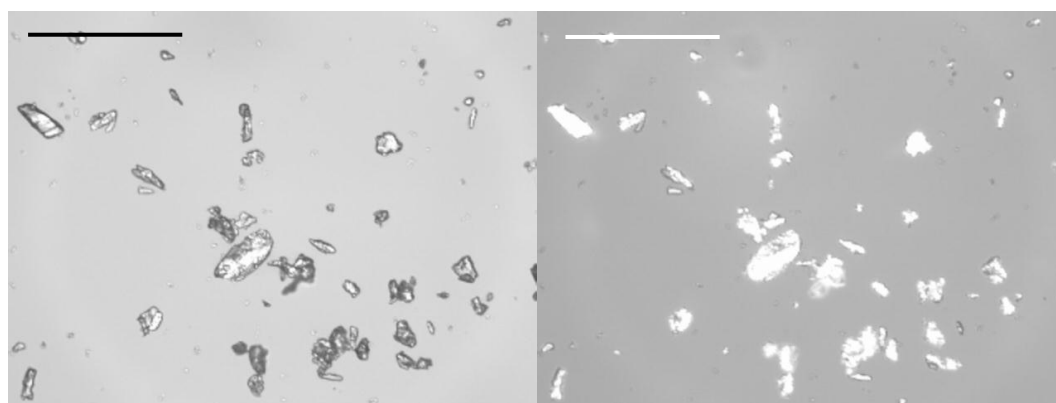


**Figure 6.34.** Photographs of 6 wt.% ground myristic acid in HOSO (a) prior to whipping and (b) after whipping for 45 minutes with a hand held double beater electric whisk at 22 °C. Scale bar 1 cm.

(a)

(b)

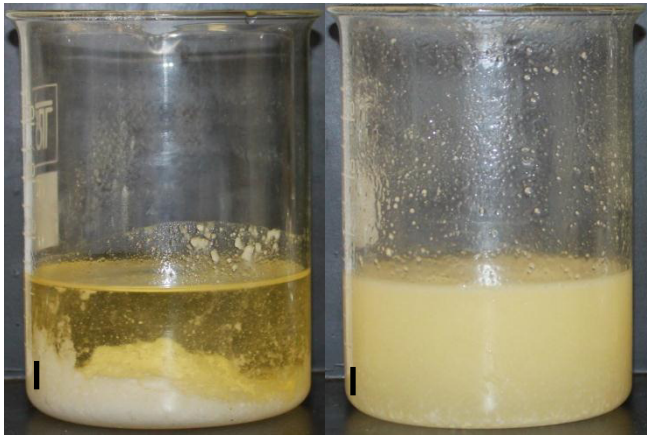
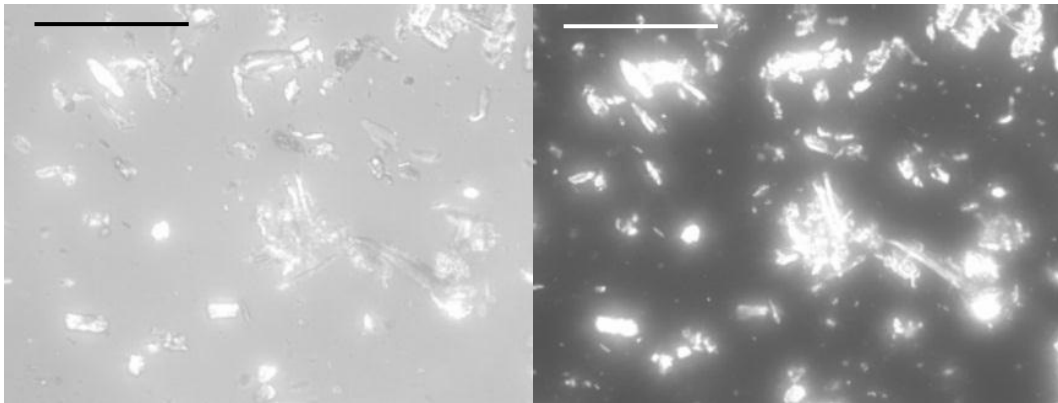
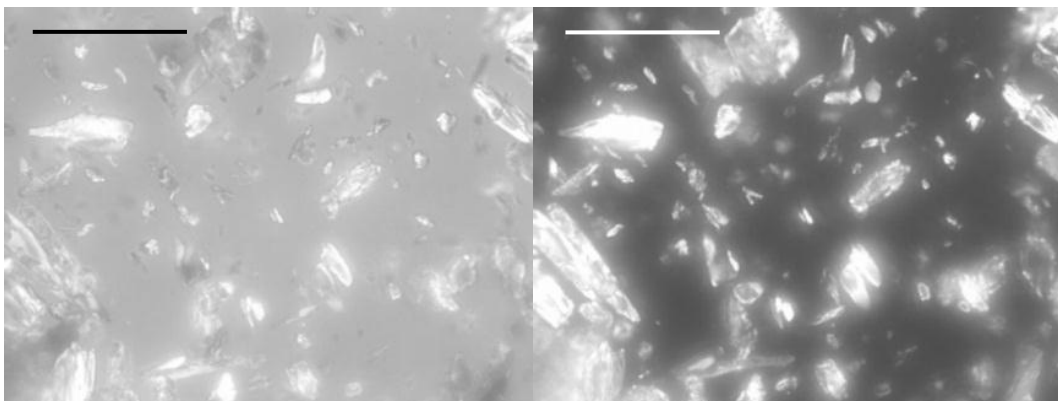


**Figure 6.35.** Optical microscopy of 6 wt.% ground myristic acid in HOSO (a) prior to whipping and (b) after whipping for 45 minutes with a hand held double beater electric whisk at 22 °C. Images on the right are corresponding micrographs viewed through crossed polarising lenses. Scale bar 200  $\mu\text{m}$ .

(a)



(b)



## 6.8 Conclusions

It was found that a foam could be produced with over 3.5 wt.% myristic acid in HOSO; the foam was found to be stable for over 18 months. As a sample of the foam was heated the foam was found to collapse, the temperature of the foam collapse was found to increase as the myristic acid concentration increased. A volume fraction of up to 0.58 of air could be incorporated into the mixture. It was found that the volume of foam produced with 12 wt.% was less than that observed with 10 wt.%. It was also found that a gel of myristic acid in HOSO was necessary for the formation of a foam and that as aeration temperature increased foamability dramatically decreased. Cryo-SEM and optical microscopy with and without crossed polarising lenses of the foams indicated that the plate-like myristic acid was present at the oil-air surface. Cooling rate had an effect on foamability, as cooling rate decreased foamability decreased. It is clear that a favourable viscosity/solid content is necessary for foam formation.

A foam could be produced with all 10 of the chosen vegetable oils, however foamability and foam stability varied considerably. It ranged from a large volume of foam with castor oil (450 mL), which had a relatively low stability, to 300 mL with coconut oil which was stable for 4 months without any visible change in appearance over time. However, a foam which was highly stable was also observed with coconut oil without the addition of myristic acid. Relatively stable foams were produced with rapeseed, soybean and corn oil (stable for over 2 weeks). It was found that the myristic acid structure in the oils was not important for foamability or foam stability. It was clear that a gelled structure was important for foam stability, however the presence of a gel didn't guarantee the production of highly stable foams. The foams produced did collapse indicating that the myristic acid does not irreversibly attach at the air-oil interface.

It was found that when myristic acid was added to non-edible oils a foam could only be produced with eugenol, squalane and ethylene glycol and that unfortunately the foam produced was not particularly stable. It can be concluded that surface tension does not have a significant effect on the foamability and subsequent stability of any foam produced.

It was also found that a foam could not be produced when ground myristic acid was added to HOSO and then whipped. It is therefore clear that the plate-like crystals are not surface active and also that the absence of the dissolved myristic acid molecules is detrimental to foam formation.

## 6.9 References

1. J. Daniel and R. Rajasekharan, *J. Am. Oil Chem. Soc.*, **80**, 417 (2003).
2. F. G. Gandolfo, A. Bot and E. Floter, *J. Am. Oil Chem. Soc.*, **81**, 1 (2004).
3. H. M. Schaink, K. F. van Malssen, S. Morgado-Alves, D. Kalnin and E. van der Linden, *Food Res. Int.*, **40**, 1185 (2007).
4. M. Perneti, K. F. van Malssen, E. Floter and A. Bot, *Curr. Opin. Colloid Interface Sci.*, **12**, 221 (2007).
5. K.W. Smith, K. Bhaggan, G. Talbot and K.F. van Malssen, *J. Am. Oil Chem. Soc.*, **88**, 1085 (2011).
6. A. Sein, J.A. Verheij and W.G.M. Agterof, *J. Colloid Interface Sci.*, **249**, 412 (2002).
7. B.P. Binks, C.A. Davies, P.D.I. Fletcher and E.L. Sharp, *Colloids Surf. A*, **360**, 198 (2010).
8. R.G. Shrestha, L.K. Shrestha, C. Solans, C. Gonzalez and K. Aramaki, *Colloids Surf. A*, **353**, 157 (2010).
9. L.K. Shrestha, R.G. Shrestha, S.C. Sharma and K. Aramaki, *J. Colloid Interface Sci.*, **328**, 172 (2008).
10. H. Kunieda, L.K. Shrestha and D.P. Acharya, *J. Disp. Sci. Technol.*, **28**, 133 (2007).
11. L.K. Shrestha, K. Aramaki, H. Kato, Y. Takase and H. Kunieda., *Langmuir*, **22**, 8337 (2006).
12. K. Higaki, Y. Sasakura, T. Koyano, I. Hachiya and K. Sato, *J. Am. Oil Chem. Soc.*, **80**, 263 (2003).
13. V. Dossat, D. Combes and A. Marty, *Enzyme and Microbial Technol.*, **30**, 90 (2002).
14. V. Dubois, S. Breton, M. Linder, J. Fanni and M. Parmentier, *Eur. J. Lipid Sci. Technol.*, **109**, 710 (2007).

15. M. Dubois, A. Tarres, T. Goldmann, G. Loeffelmann, A. Donaubaer and W. Seefelder, *J. Agric. Food Chem.*, **59**, 12291 (2011).
16. E.J.L. de Medeiros, R. de Cassia Ramos do Egypto Queiroga, A.G. de Souza, A.M.T. de M. Cordeiro, A.N. de Medeiros, D.L. de Souza and M.S. Madruga, *J. Therm. Anal. Calorim.*, **112**, 1515 (2013).
17. B.P. Binks, A. Rocher and M. Kirkland, *Soft Matter*, **7**, 1800 (2011).

## 7 INVESTIGATION OF STRUCTURING AGENTS IN OIL

### 7.1 Introduction

The ability of a surfactant in various oils to create a foam through the whipping technique has been investigated. As has been previously stated, a gel can be created with myristic acid in various oils, both non-edible and vegetable. The gel was then whipped with a hand held double beater electric whisk for 45 minutes at various temperatures and myristic acid concentrations finding that a foam can be produced. Therefore, additional surfactants (various fatty acid and alcohol chain lengths, monoglycerides, diglycerides) and oils were then studied for the ability to create a foam by whipping with a hand held double beater electric whisk.

### 7.2 Fully hydrogenated rapeseed oil rich in behenic acid in HOSO

It is known that fully hydrogenated rapeseed oil rich in behenic acid (FHR-B) can gel various oils such as sunflower oil, olive oil, palm olein and cocoa butter.<sup>1-3</sup> Therefore, it was investigated whether FHR-B can gel HOSO and then be aerated with a hand held double beater electric whisk. As can be seen from Figure 7.1, neat FHR-B cooled from 80 °C to 10 °C was found to solidify at 53.9 °C. As the surfactant was then heated to 80 °C, it was found that it melted at 59.1 °C. Therefore, 10 wt.% FHR-B in HOSO was cooled from 80 °C to 9.8 °C at approximately 1 °C/min. and then whipped at 22 °C as it is known that at 22 °C the FHR-B is a solid in the HOSO. The FHR-B in HOSO prior to whipping can be seen in Figure 7.2 where the mixture was a turbid, pale yellow gel. It can be seen from Figure 7.3 that particles of < 25 µm in diameter in the oil were not visible through crossed polarising lenses. Once the mixture had been whipped for 30 minutes 400 mL of foam was produced (see Figure 7.2) which had an air volume fraction of 0.43. Optical microscopy of the foam (Figure 7.3) shows that the bubbles were spherical with a diameter of < 25 µm. In the oil continuous phase it appeared that the < 25 µm aggregates had broken up to become almost plate-like which were < 10 µm in diameter. The amount of foam produced was remarkable, along with the foam stability (foam stable for over 18 months at room temperature and was found to fully collapse at 59.2 °C when a sample was heated 1 °C/min). This suggests that the FHR-B

presence is clearly necessary for the foam stability as when the FHR-B melted the foam collapsed; it may be that the gelled HOSO created a resistance to foam collapse.

**Figure 7.1.** DSC of FHR-B cooled from 80 °C to 10 °C at 2 °C/min., held at 10 °C for 5 minutes and then heated to 80 °C at 2 °C/min. Arrows indicate direction of heating and cooling.

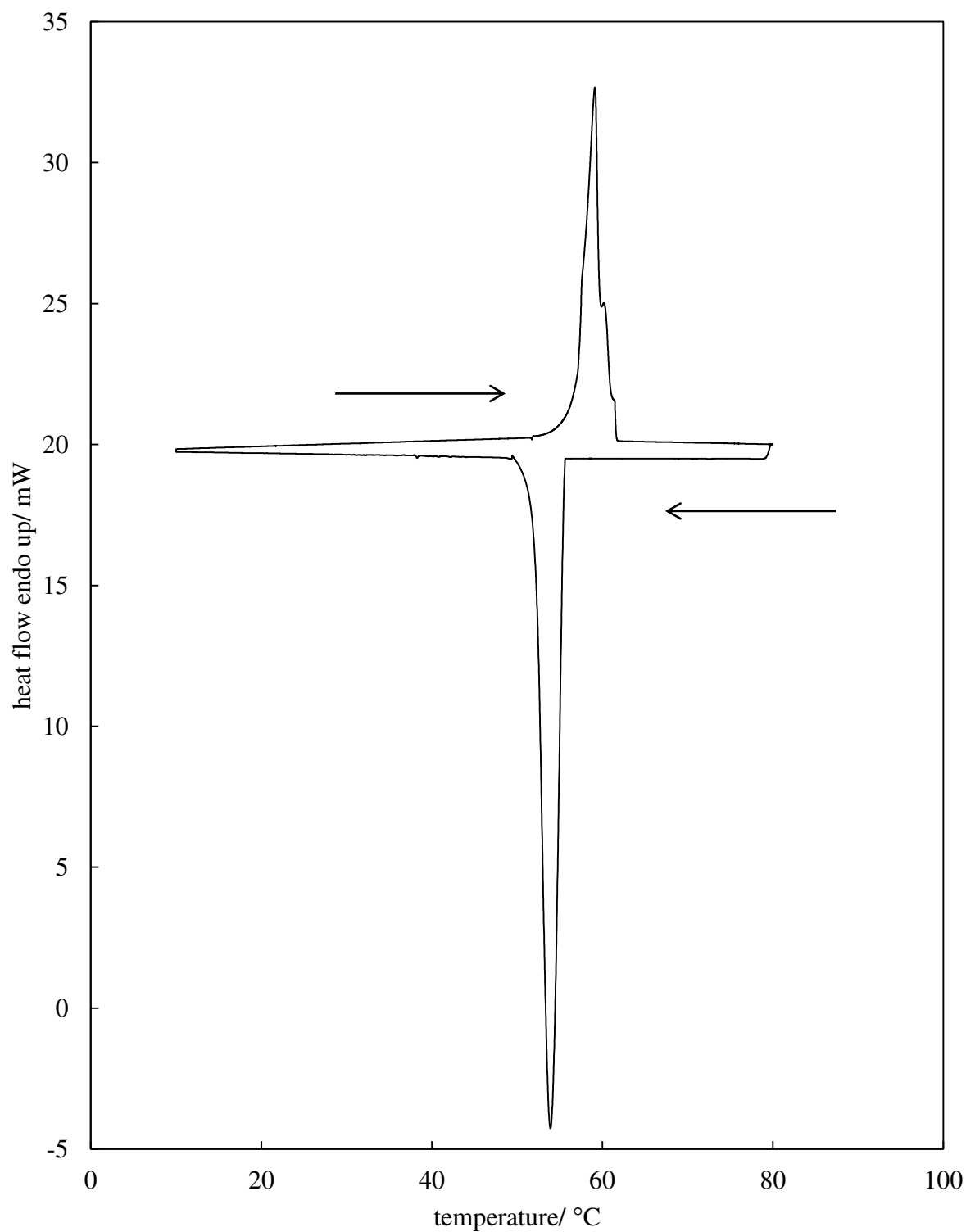


**Figure 7.2.** 10 wt.% FHR-B in HOSO (a) prior to whipping and (b) after whipping for 30 minutes with a hand held double beater electric whisk for 30 minutes at 22 °C. Scale bar 1 cm.

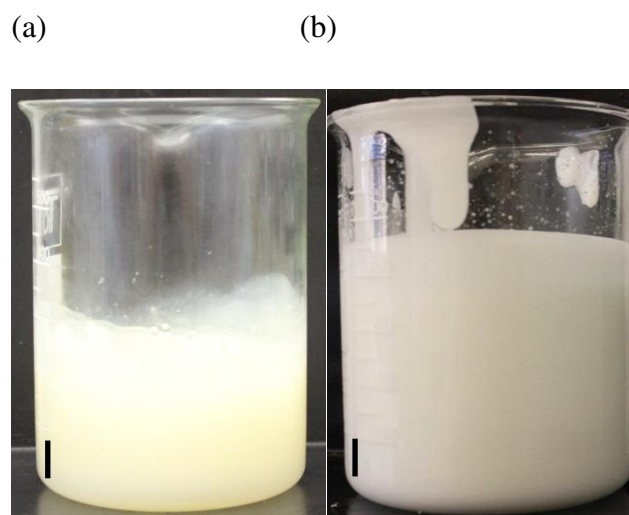
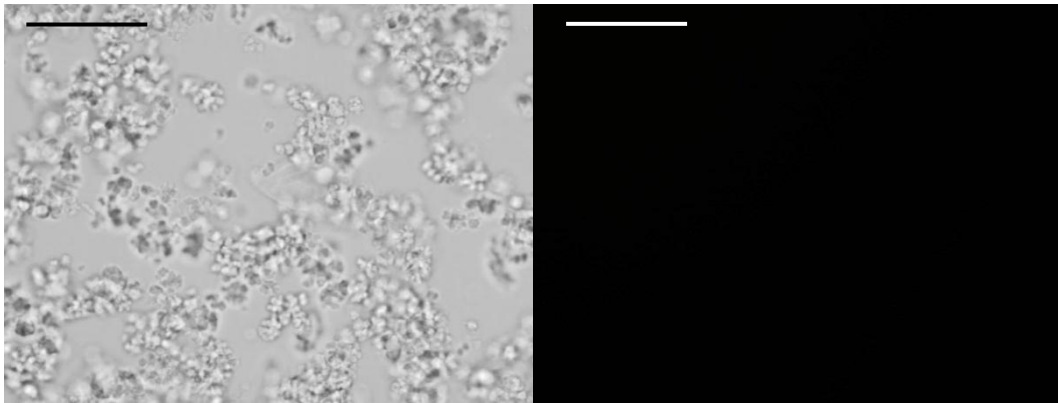
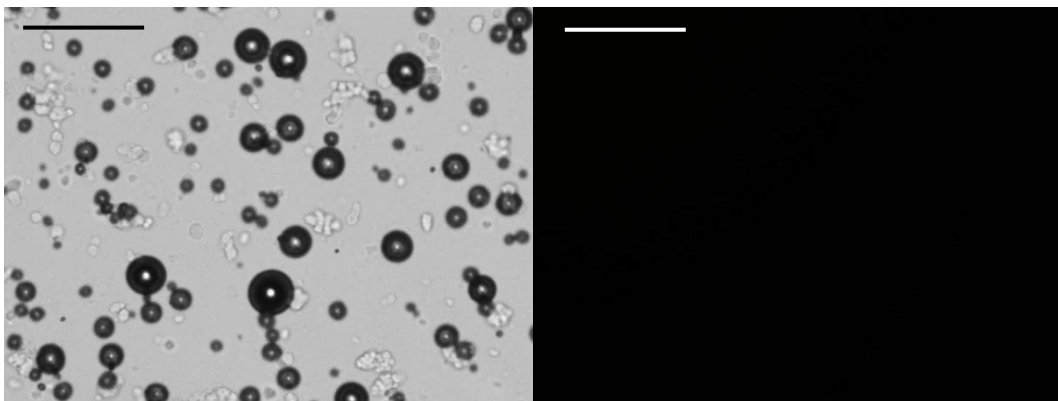


**Figure 7.3.** Optical microscopy of 10 wt.% FHR-B in HOSO (a) prior to whipping and (b) after whipping for 30 minutes with a hand held double beater electric whisk at 22 °C. Images on the right are corresponding micrographs viewed through crossed polarising lenses. Scale bar 100  $\mu\text{m}$ .

(a)



(b)



### 7.3 Cetostearyl alcohol

Cetostearyl alcohol is a mixture of C<sub>16</sub> and C<sub>18</sub> straight chained alcohols (typical ratio is unknown). It has been stated<sup>4-7</sup> that straight chained alcohols can gel various oils. Therefore, it was investigated if a gel could be produced by adding 10 wt.% cetostearyl alcohol to both HOSO and dodecane and if also a foam could be produced by whipping the mixture with a hand held double beater electric whisk.

#### 7.3.1 HOSO

10 wt.% cetostearyl alcohol in HOSO was heated to 80 °C, then cooled to 8.6 °C at approximately 1 °C/min., then whipped at 22 °C. It is clear from Figure 7.4 that the mixture at 22 °C prior to aeration was a white gel. The structure of the cetostearyl alcohol in HOSO was found to be both needle-like (200 μm in length) and aggregates up to 100 μm in diameter as shown in Figure 7.5. After whipping the mixture for 30 minutes it was clear from Figure 7.4 that a foam was produced (200 mL). As seen in Figure 7.5, the irregular shaped bubbles in the foam produced were < 50 μm in diameter with the cetostearyl alcohol clearly at the air-oil bubble surface. Crystals were not birefringent. It was also found that the foam produced had a volume fraction of 0.11 of air present. The foam collapsed at 39.4 °C when a sample was heated 1 °C/min. from 22 °C. The foam was held at 22 ± 2 °C, finding that the foam collapsed over 4 months after formation. Once 4 months had elapsed it was found that the foam gradually collapsed over 1 month. Cetostearyl alcohol presence was necessary for the foam formation and stability, however as the foam was only stable for over 4 months at 22 ± 2 °C, it is clear that the crystals did not irreversibly attach at the air-oil surface.

**Figure 7.4.** 10 wt.% cetostearyl alcohol in HOSO (a) prior to whipping and (b) after whipping for 30 minutes with a hand held double beater electric whisk at 22 °C. Scale bar 1 cm.

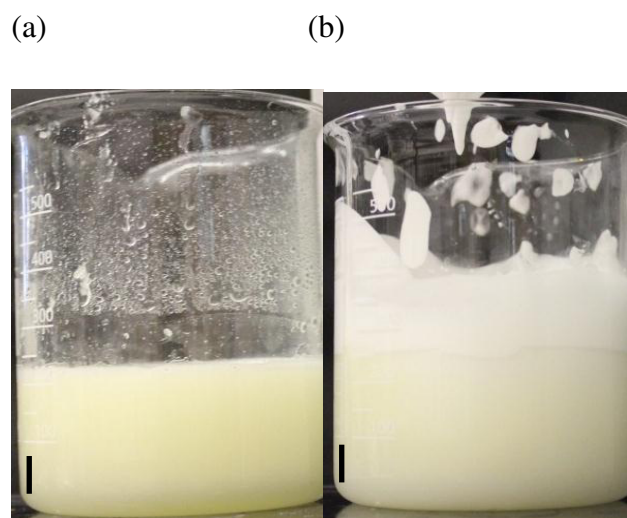
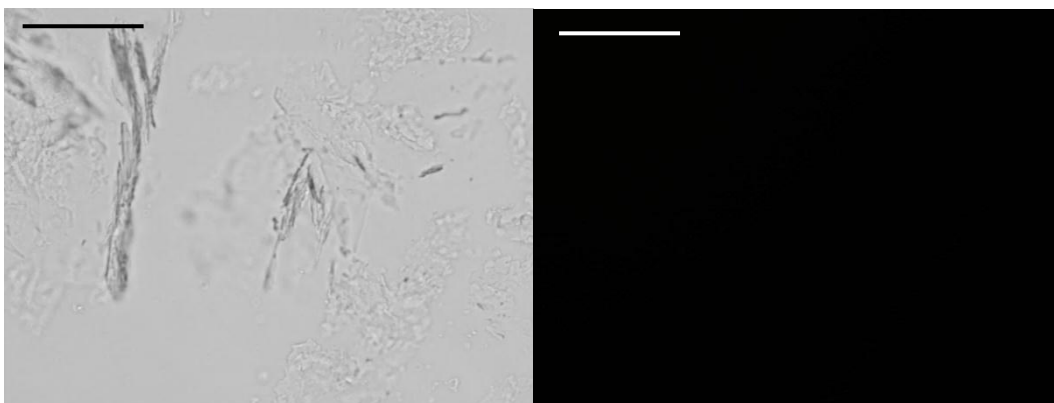
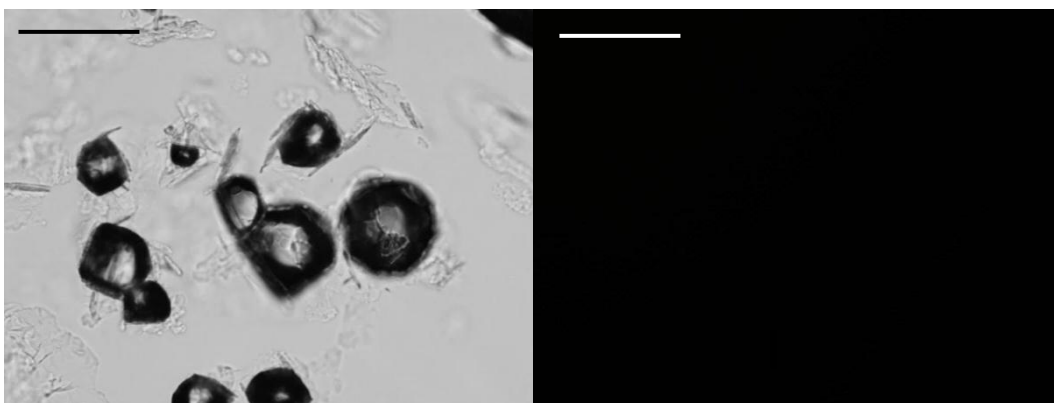


**Figure 7.5.** Optical microscopy of 10 wt.% cetostearyl alcohol in HOSO (a) prior to whipping and (b) after whipping for 30 minutes with a hand held double beater electric whisk at 22 °C. Images on the right are corresponding micrographs viewed through crossed polarising lenses. Scale bar 100  $\mu\text{m}$ .

(a)



(b)



### 7.3.2 Dodecane

Figure 7.6 shows that 10 wt.% cetostearyl alcohol in dodecane at 22 °C after cooling from 80 °C to 7.4 °C at approximately 1 °C/min. was a white soft solid. Figure 7.7 shows that the structure of the alcohol in dodecane was very different to that seen in HOSO. In dodecane the alcohol had a plate-like structure with a diameter of < 10 µm and also needles which were found to be < 10 µm in length. After whipping the mixture for 30 minutes it was found that 400 mL of foam was produced as shown in Figure 7.6. The volume fraction of air incorporated into the foam was 0.31. Figure 7.7 shows that the spherical foam bubbles were almost 100 µm in diameter and that the solid alcohol may be at the air-oil surface. The foam was not particularly stable as it fully collapsed 5 days after formation at 22 ± 2 °C. As temperature of the foam was heated 1 °C/min. it was found that the foam collapsed at 36.6 °C.

**Figure 7.6.** Photographs of 10 wt.% cetostearyl alcohol in dodecane (a) prior to whipping (b) after whipping for 30 minutes with a hand held double beater electric whisk at 22 °C. Scale bar 1 cm.

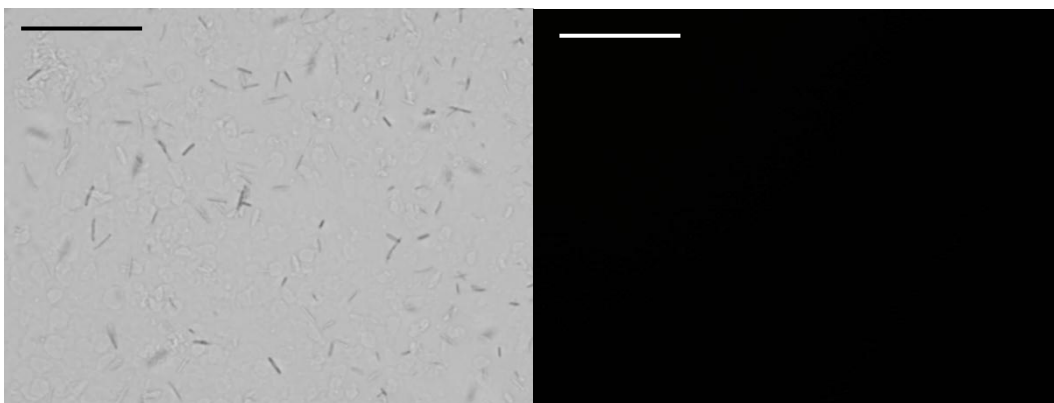
(a)

(b)

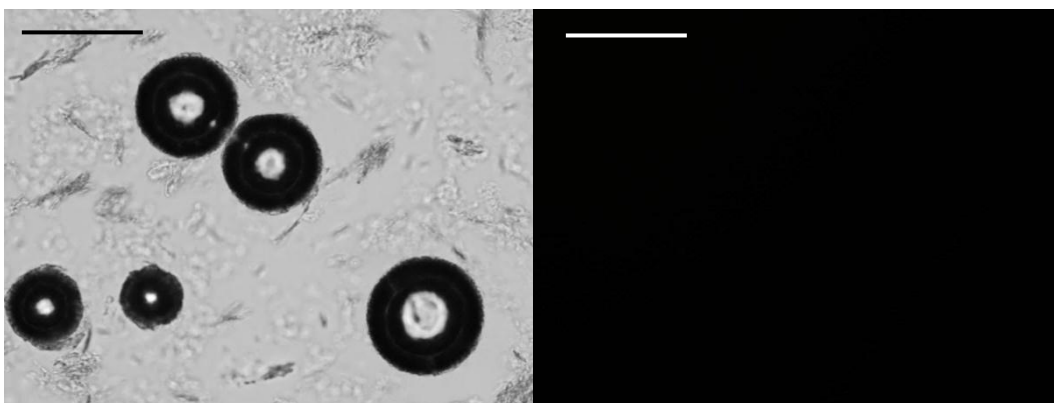


**Figure 7.7.** Optical microscopy of 10 wt.% cetostearyl alcohol in dodecane (a) prior to whipping (b) after whipping for 30 minutes with a hand held double beater electric whisk at 22 °C. Images on the right are corresponding micrographs viewed through crossed polarising lenses. Scale bar 100  $\mu\text{m}$ .

(a)



(b)



## 7.4 Dimodan HR kosher in HOSO

An investigation into the use of Dimodan HR kosher as a structuring agent in HOSO was studied. Dimodan HR kosher is a monoglyceride with a main chain length (93 %) of stearic acid. The ability to create a gel was initially investigated which included visual observations along with the use of DSC, pNMR and rheology. The gel was also whipped with two aeration methods, a Hobart mixer and a hand held double beater electric whisk, to investigate if air can be incorporated into the gel. The effect of temperature on foam production was also studied with the Hobart mixer.

### 7.4.1 Gel characterisation

The gelled mixture was studied with DSC, optical microscopy, pNMR and rheology. The effect of temperature and Dimodan HR kosher concentration on the behaviour of the mixture was probed with rheology.

#### 7.4.1.1 DSC

10 wt.% Dimodan HR Kosher in HOSO was analysed with DSC by cooling the mixture from 90 °C to 0 °C, then holding the sample at this temperature for 5 minutes before heating the mixture to 90 °C with a heating and cooling rate of 2 °C/min. as shown in Figure 7.8. From the figure it is clear that at 58.9 °C the mixture was a liquid and that at 39.7 °C the mixture was a solid. It is also clear from the figure that there are 2 crystal forms of the monoglyceride in HOSO identified by the 2 peaks upon melting and solidifying. This is interesting because it was observed visually that the temperature the mixture was cooled to (between 25 and 0 °C) from 90 °C had an effect on the appearance of the mixture (more solid-like the lower the mixture was cooled to). This may be due to the amount of time the mixture was below the precipitation temperature, meaning that the surfactant had more time to create a matrix, and therefore entrap the oil prior to any analysis.

#### 7.4.1.2 Optical microscopy

It could be seen visually (as shown in Figure 7.9) that at 22 °C a gel was produced when 5 wt.% and 10 wt.% Dimodan HR kosher was cooled from 90 °C to 5 and 20 °C respectively, prior to heating to 22 °C. From the optical microscopy images shown in Figure 7.10 it is clear that both 5 and 10 wt.% Dimodan HR kosher in HOSO had a plate-like structure (< 50 µm in diameter) in the HOSO which behaved as birefringent crystals in the oil as shown by the bright appearance through crossed polarising lenses.

**Figure 7.8.** DSC of 10 wt.% Dimodan HR kosher in HOSO cooled from 90 °C to 0 °C, held at 0 °C for 5 minutes and then heated to 90 °C. The heating and cooling rates were 2 °C/min. Arrows indicate the direction of heating and cooling.

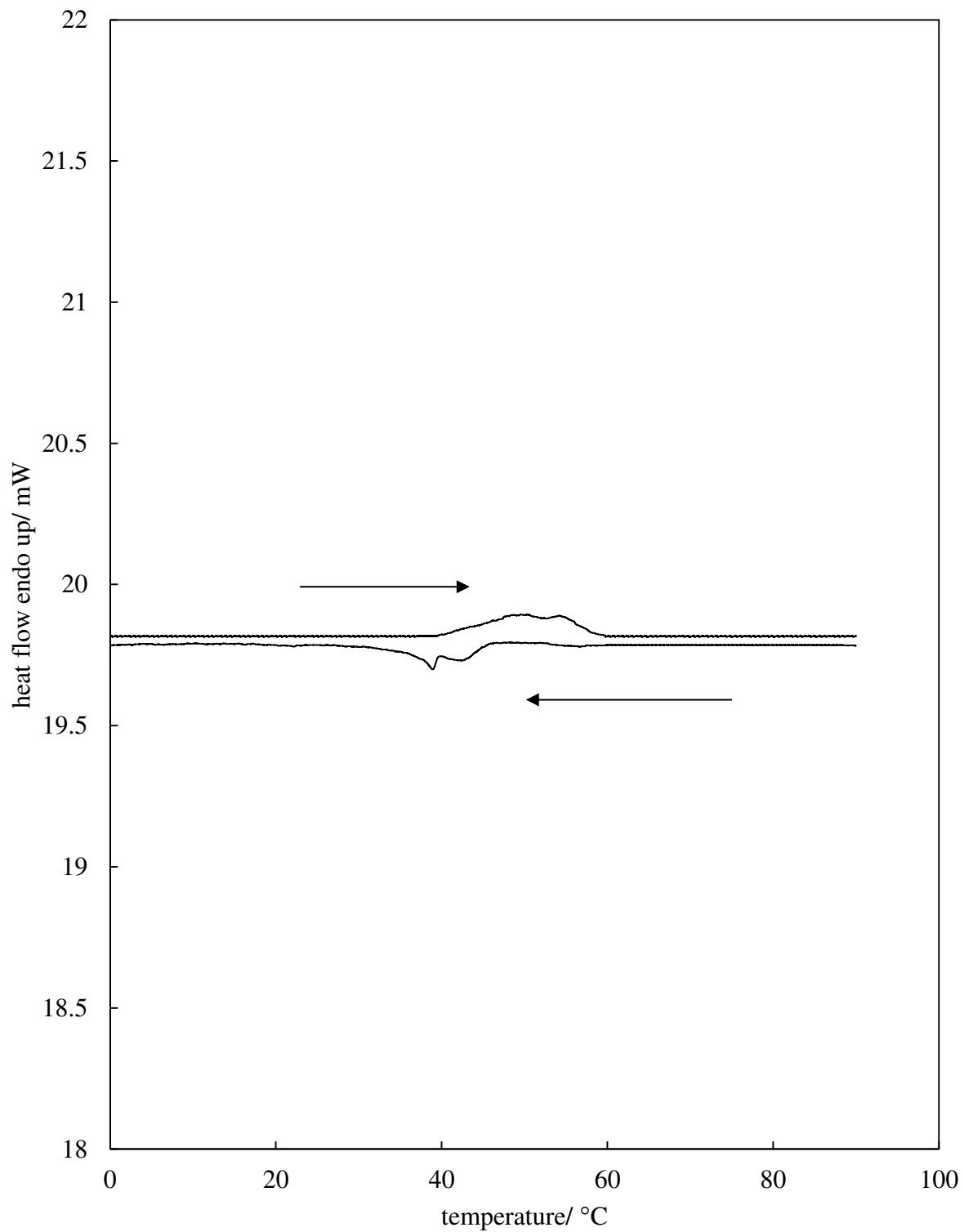


**Figure 7.9.** Photographs of (a) 5 wt.% Dimodan HR kosher in HOSO, (b) 10 wt.% Dimodan HR kosher in HOSO at 22 °C after cooling approximately 1 °C/min. from 90 °C to 5 and 20 °C respectively. Scale bar 1 cm.

(a)

(b)

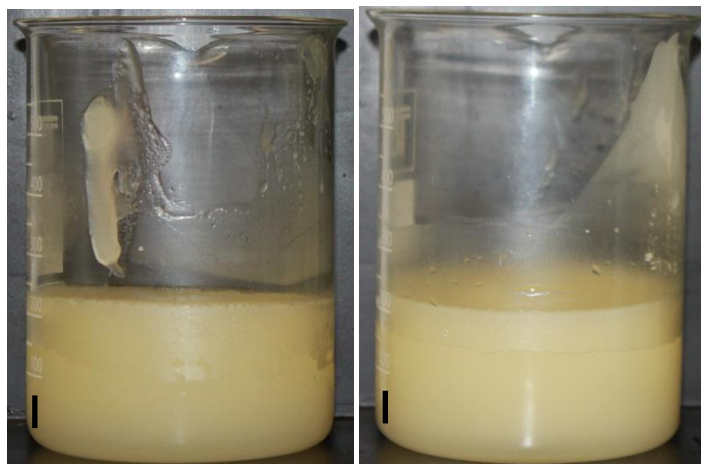
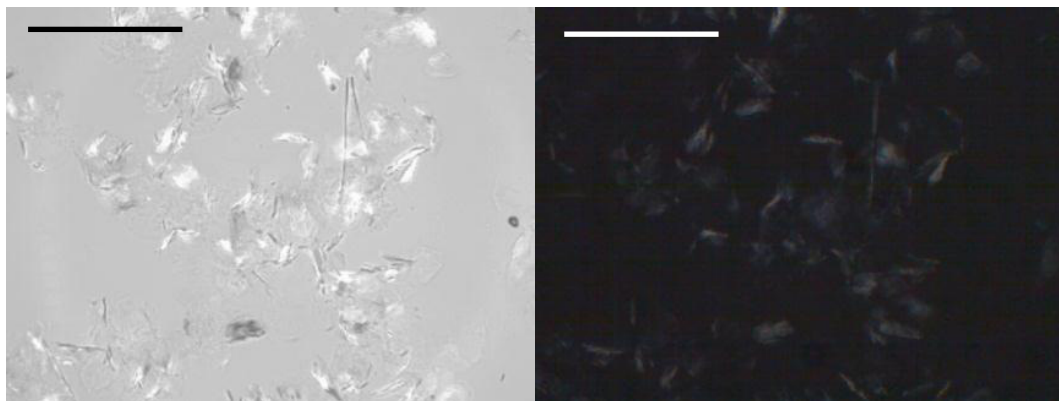
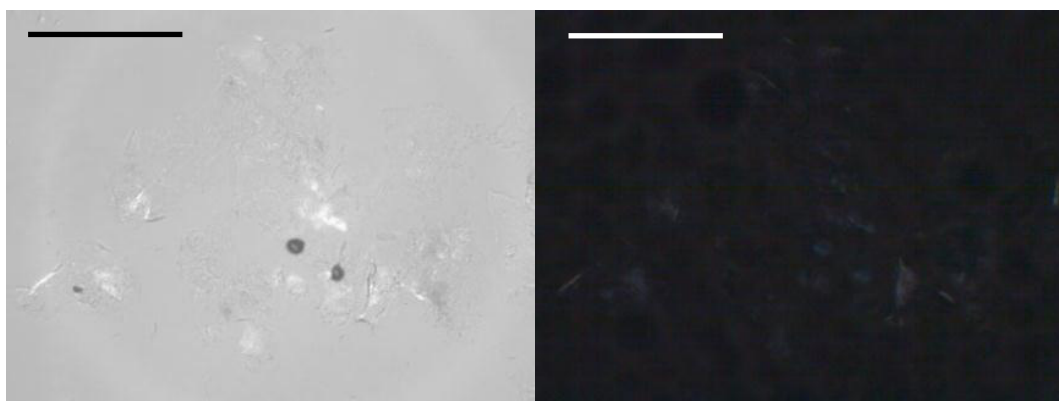


**Figure 7.10.** Optical microscopy of (a) 5 wt.% Dimodan HR kosher in HOSO (cooled from 90 °C to 5 °C) and (b) 10 wt.% Dimodan HR kosher in HOSO (cooled from 90 °C to 20 °C) at 22 °C. Images on the right are corresponding micrographs viewed through crossed polarising lenses. Scale bar 200  $\mu$ m.

(a)



(b)



### 7.4.1.3 Rheology

Dimodan HR kosher in HOSO was studied with the use of rheology to examine the flow behaviour of the mixture. The effect of frequency, shear rate, temperature and time on the behaviour of the mixture was investigated.

#### 7.4.1.3.1 Effect of frequency

Initial tests were conducted to identify the viscoelastic region of Dimodan HR kosher in HOSO. Figure 7.11 shows that the viscoelastic region of Dimodan HR kosher in HOSO was clearly in the area of 0.01 % as  $G'$  was independent of strain. Therefore, the strain for further measurements such as the effect of frequency and temperature was 0.01 %.

The effect of frequency on mixtures of 5 wt.% Dimodan HR kosher in HOSO at 10 °C and 10 wt.% Dimodan HR kosher in HOSO at 10, 20 and 30 °C was then investigated. As can be seen from Figure 7.12, the mixtures at all concentrations investigated demonstrated a gelled network<sup>8</sup> as  $G'$  was independent of the change in frequency. The values of the  $G'$  recorded are found to be similar to that observed with samples of 5-9 % Myverol monoglyceride in cod liver oil<sup>9</sup> and  $\Phi = 0.063$  and 0.075 Adochan 98 (monoglyceride) in olive oil<sup>10</sup> where  $G'$  was found to be in the region of  $10^5$ - $10^6$  Pa. Figure 7.12 shows that the  $G'$  values observed with 10 wt.% Dimodan HR kosher at 30 °C is similar to that of 10 wt.% Dimodan HR kosher at 20 °C and 5 wt.% Dimodan HR kosher at 10 °C. It was decided that a frequency of 1 Hz would be used for the study of the effect of temperature on the gel and an increase in shear rate.

**Figure 7.11.** Amplitude sweep at 10 °C of 5 and 10 wt.% Dimodan HR kosher in HOSO (after cooling 1 °C/min. from 90 °C). The measurements were conducted at 1 Hz with parallel plates after cooling the mixtures at a rate of 1 °C/min.

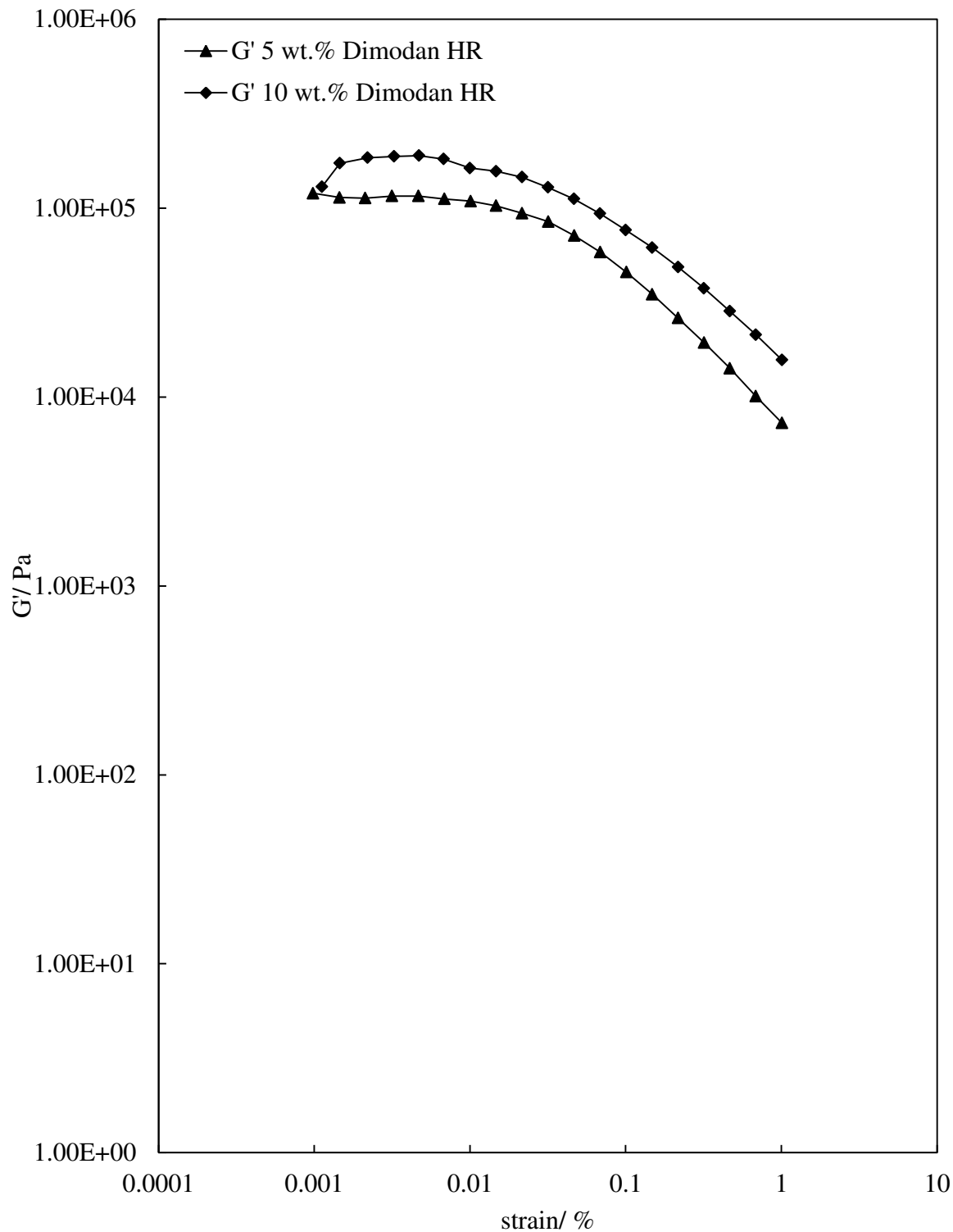
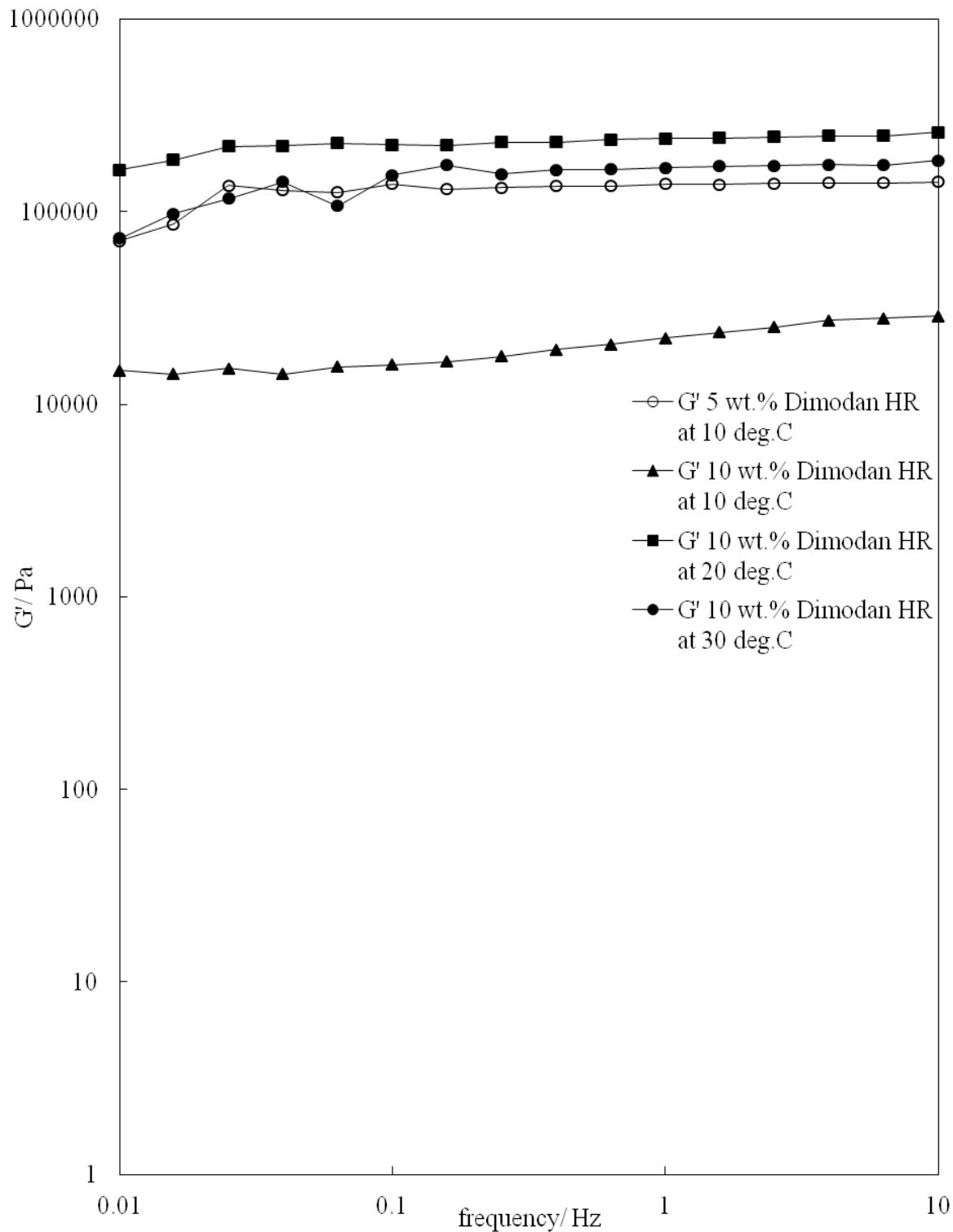


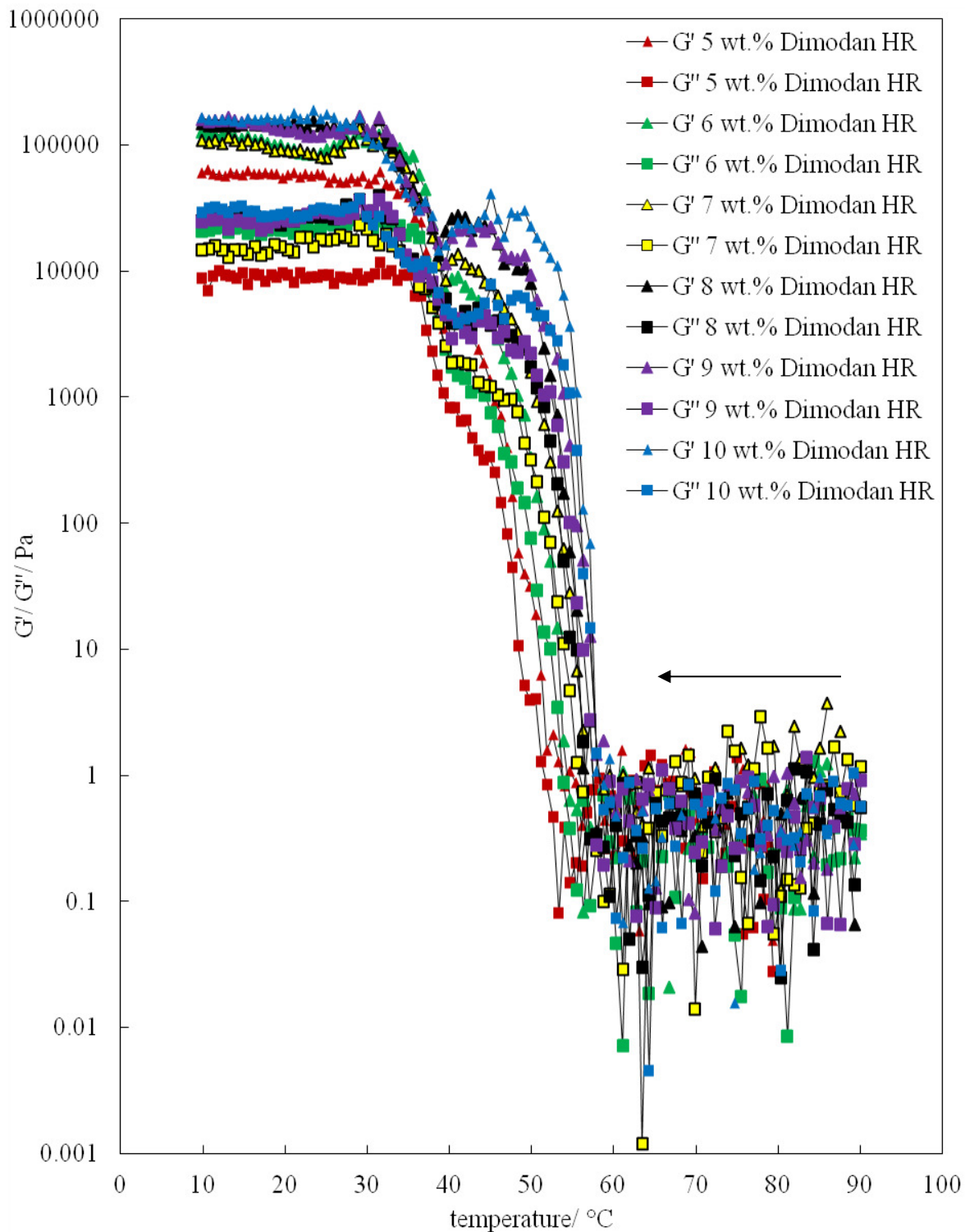
**Figure 7.12.** Frequency sweep at 10 °C of 5 wt.% Dimodan HR kosher in HOSO and at 10, 20 and 30 °C of 10 wt.% Dimodan HR kosher in HOSO. The measurements were conducted at 0.01 % with parallel plates after cooling from 90 °C at a rate of 1 °C/min.



#### 7.4.1.3.2 Effect of temperature decrease from 90 °C to 10 °C

The effect of the Dimodan HR kosher concentration in HOSO on the values of  $G'$  and  $G''$  as the temperature of the mixture decreased from 90 to 10 °C at a rate of 1 °C/min. was measured. Figure 7.13 shows that as the concentration of the surfactant increased from 5 to 10 wt.% in HOSO values of  $G'$  and  $G''$  increased a relatively small amount. It is clear that the mixture began to gel at an earlier temperature as the Dimodan HR kosher concentration increased (gelation temperature taken as the mid-point between the maximum  $G'$  and the minimum  $G'$ ). It is also clear that  $G'$  gradually increased as temperature decreased, at approximately 40 °C the  $G'$  plateaued and then increased again suggesting the formation of a second crystal form<sup>11</sup> (this second crystal form was also identified with DSC).

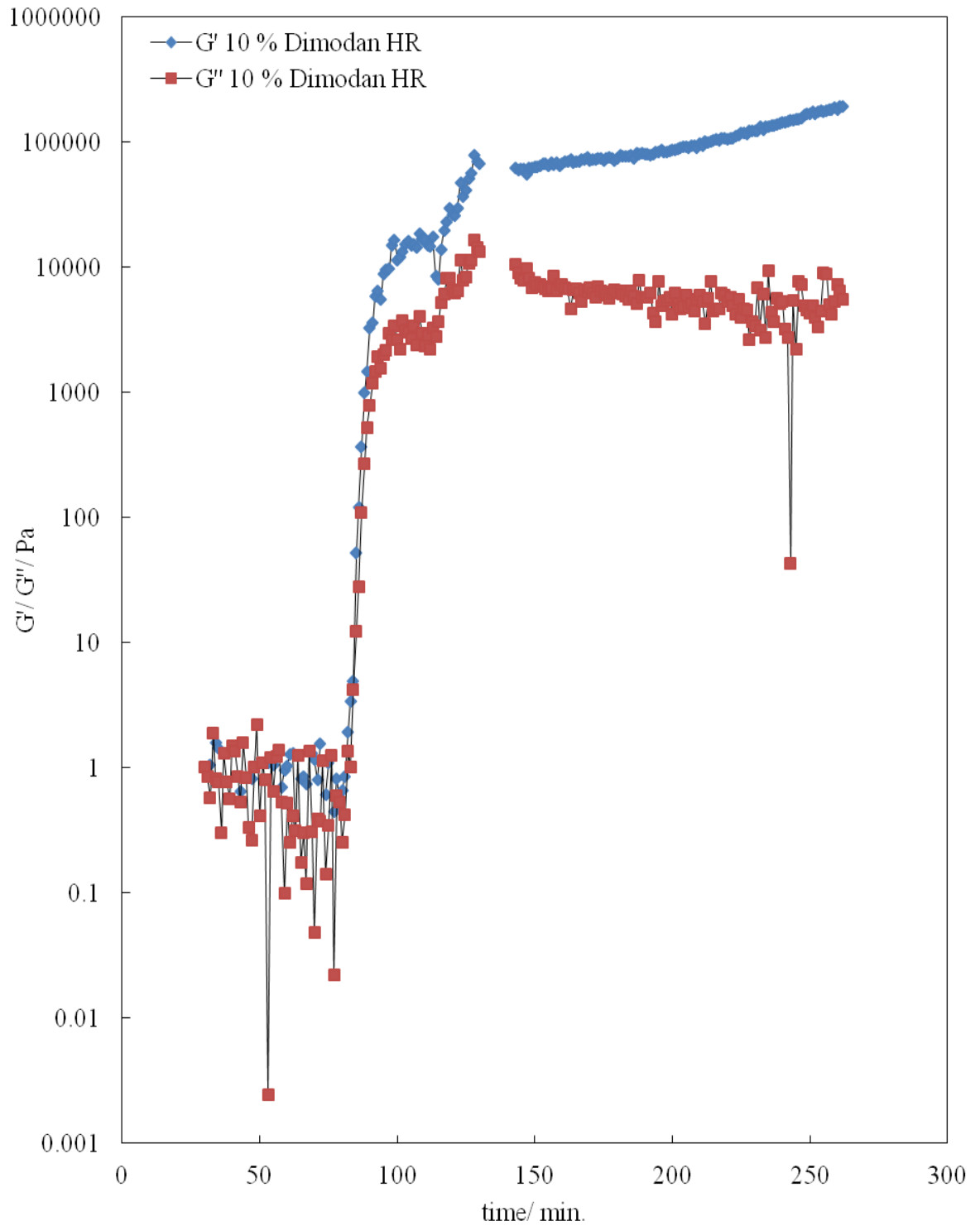
**Figure 7.13.** Storage modulus ( $G'$ ) and loss modulus ( $G''$ ) of 5 to 10 wt.% Dimodan HR kosher in HOSO as temperature decreased from 90 °C to 10 °C (as shown by the arrow) at a cooling rate of 1 °C/min. Measurements were conducted with parallel plates at 0.01% and 1 Hz.



#### 7.4.1.3.3 Effect of time

Figure 7.14 demonstrates that over a period of 3 hours the solid component ( $G'$ ) of Dimodan HR kosher in HOSO gradually increased, although  $G''$  remained constant. Therefore it may be possible that storage time had an effect on the foamability of the gel, however this parameter was not investigated.

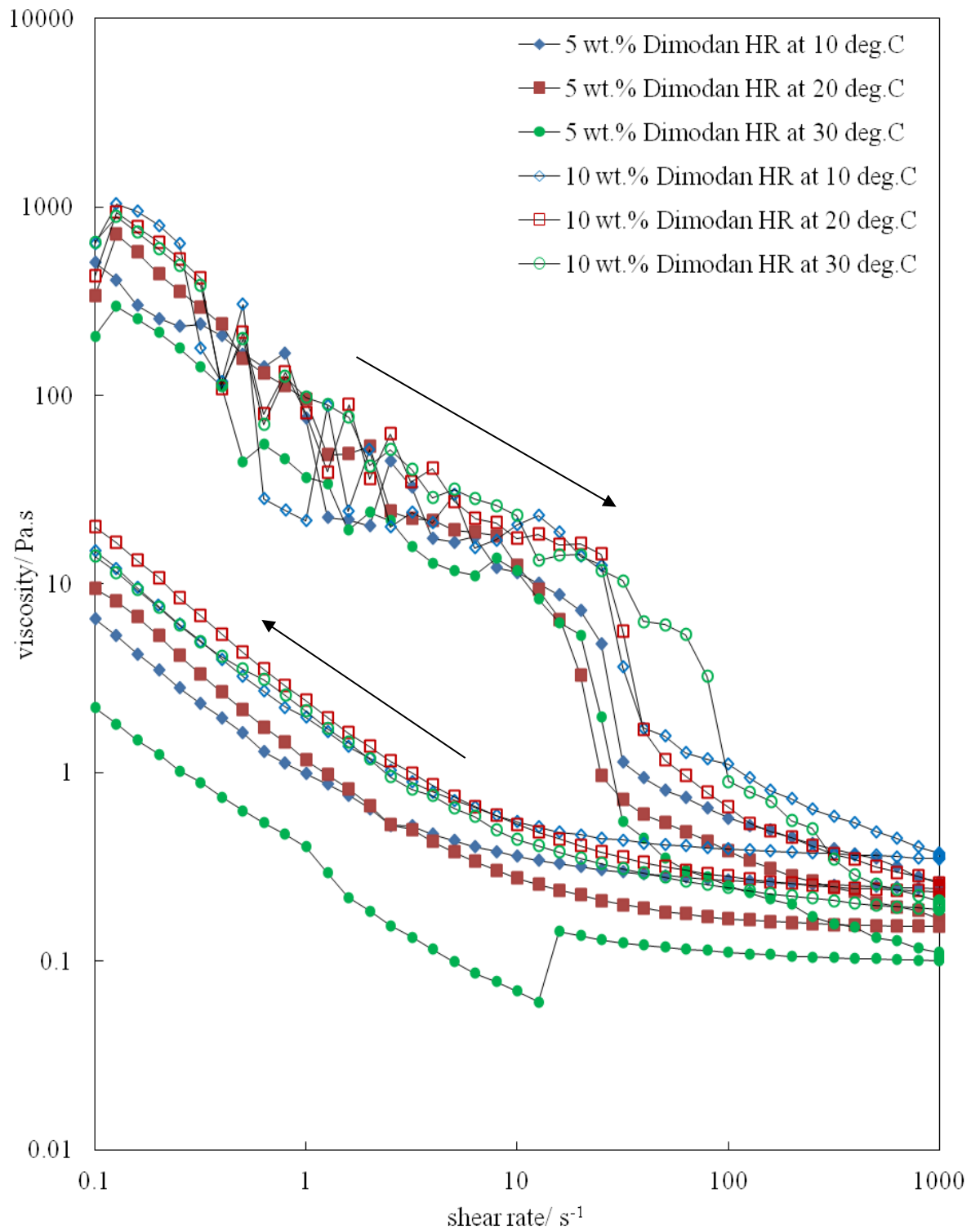
**Figure 7.14.** Gelation and effect of time on  $G'$  and  $G''$  components of 10 wt.% Dimodan HR kosher in HOSO as the sample was cooled from 90 °C to 30 °C at a rate of 1 °C/min. and then held at 30 °C for 3 hours. Measurements were conducted with parallel plates at 0.01% and 1 Hz.



#### 7.4.1.3.4 Viscosity measurement

Figure 7.15 demonstrates the increase and then decrease in shear rate on both 5 and 10 wt.% Dimodan HR kosher in HOSO after cooling from 90 °C/min. to various temperatures. It is clear that as the shear rate increased from 0.01 to 1000 s<sup>-1</sup> over 30 minutes the network of a gel produced with Dimodan HR kosher in HOSO appeared to break-up which was identified as a decrease in the viscosity. The network of the system then reformed as the shear rate decreased to 0.01 over 30 minutes. However, the viscosity was lower than that prior to the increase in shear rate suggesting that the high shear may have induced a reorientation of the monoglyceride in HOSO into another structure/packing arrangement.

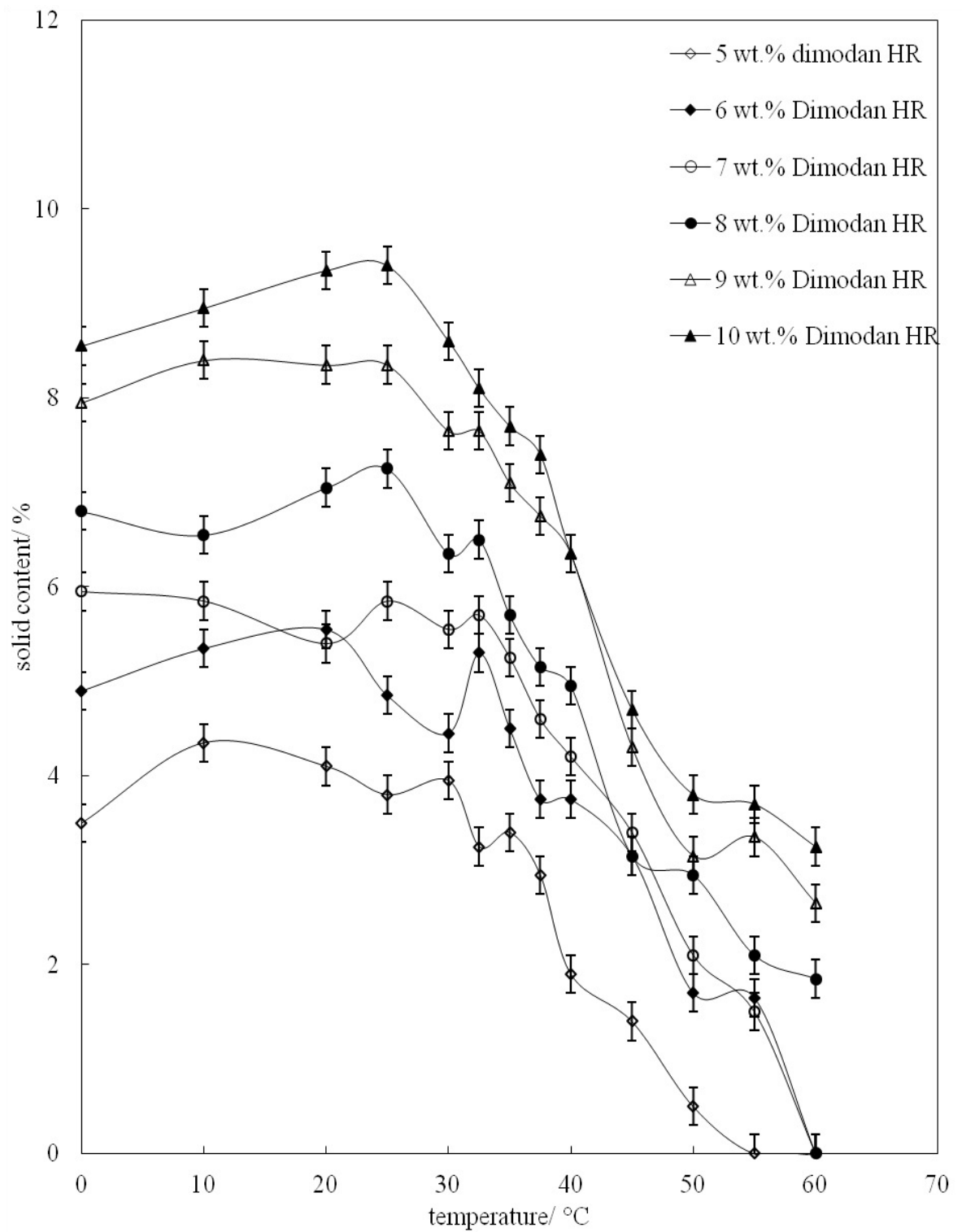
**Figure 7.15.** Viscosity measurements of 5 and 10 wt.% Dimodan HR kosher in HOSO at 10, 20 and 30 °C as shear rate was increased from 0.1 to 1000 s<sup>-1</sup> over 30 minutes, then decreased to 0.1 s<sup>-1</sup> over 30 minutes (as shown by arrows). Measurements were conducted after cooling 1 °C/min. from 90 °C with concentric cylinders at 1 Hz.



#### 7.4.1.4 Pulsed nuclear magnetic resonance

It is known that pulsed nmr can be used to investigate the proportion of a solid present in a mixture such as a gel as stated in Chapter 5.<sup>12-14</sup> Figure 7.16 and Figure 7.17 shows that, as expected, there was an increase in solid content as the concentration of Dimodan HR kosher was increased, also that as the temperature of the samples increased from 0 °C to 60 °C the solid content decreased.

**Figure 7.16.** Solid phase content analysis with the use of pulsed NMR of Dimodan HR kosher as a function of concentration in HOSO following the standard Nestlé preparation procedure.



## 7.4.2 Aeration

Dimodan HR kosher in HOSO was aerated with both the use of a Hobart mixer and a hand held double beater electric whisk. The aeration with the Hobart mixer consisted of whipping 5 and 10 wt.% Dimodan HR kosher in HOSO at 22 °C after cooling approximately 1 °C/min. from 90 °C to various temperatures. The aeration with the hand held double beater electric whisk consisted of cooling 5 and 10 wt.% Dimodan HR kosher in HOSO at approximately 1 °C/min. from 90 °C to a specific temperature and then whipping the mixture at 22 °C.

### 7.4.2.1 Hobart mixer

The effect of the temperature 5 and 10 wt.% Dimodan HR kosher in HOSO was cooled to prior to whipping was crucial in determining whether a whipped oil could be produced as shown in Table 7.1 and Table 7.2. It was clear from the measurements that there was an optimum temperature that the mixture had to be cooled to (from 90 °C at approximately 1 °C/min.) for a maximum volume fraction of air to be incorporated into the mixture. With 5 wt.% Dimodan HR kosher the temperature was 5 °C, with 10 wt.% Dimodan HR kosher the temperature was 20 °C. This optimum temperature was not surprising as Dimodan HR kosher is an impure surfactant, therefore there may be many different components solidifying at different temperatures. It was shown in both DSC and rheology measurements that there are clearly two crystal forms present in the surfactant and HOSO mixture. The effect of the temperature the mixture was cooled to on foamability was also found when G. C. N12 veg in HOSO was whipped as shown in Chapter 4. This finding supports the theory that a whipped oil can only be produced when the gelled mixture has specific characteristics (an optimum viscosity, solid content and/or crystal size for maximum air incorporation). It is thought that the shear rate of a Hobart mixer is between 100 to 500 s<sup>-1</sup>.<sup>15</sup> Therefore the behaviour of 5 and 10 wt.% Dimodan HR kosher in HOSO when the shear rate of the mixture was increased and decreased in the region of 100 to 500 s<sup>-1</sup> is of particular importance. It is not clear if there is a typical viscosity value required for the incorporation of air into all gels. The viscosity measured in the area of 100 to 500 s<sup>-1</sup> (Figure 7.15) with 5 wt.% Dimodan HR kosher at 10 °C and 10 wt.% Dimodan HR kosher at 20 °C is similar, yet the volume fractions of air after 1 hour of whipping is 0.25 and 0.59, respectively. Therefore it may be possible to predict the ability to create a foam from viscosity measurements, but not

the volume fraction of air incorporated. Foam formation cannot be related to the solid content of the mixture as at 5 wt.% at 0, 5 and 10 °C the solid content was clearly lower than at 10 wt.% at 15 °C and 20 °C. It was found that the foams produced were stable for over 18 months with only approximately 10 mL of liquid drainage occurring from a 30 g sample of foam (the liquid drainage occurred within 24 hours of foam formation).

**Table 7.1.** The temperature 5 wt.% Dimodan HR kosher in HOSO was cooled to from 90 °C at 1 °C/min. prior to whipping at  $20 \pm 1$  °C and the volume fraction of air present after 1 hour of whipping with a Hobart mixer.

| Temperature/ °C | Foam production | Volume fraction of air<br>$\pm 0.02$ |
|-----------------|-----------------|--------------------------------------|
| -5              | No              | -                                    |
| 0               | Yes             | 0.06                                 |
| 5               | Yes             | 0.62                                 |
| 10              | Yes             | 0.25                                 |
| 15              | No              | -                                    |
| 20              | No              | -                                    |
| 25              | No              | -                                    |
| 30              | No              | -                                    |

**Table 7.2.** The temperature 10 wt.% Dimodan HR kosher in HOSO was cooled to from 90 °C at 1 °C/min. prior to whipping at  $20 \pm 1$  °C and the volume fraction of air present after 1 hour of whipping with a Hobart mixer.

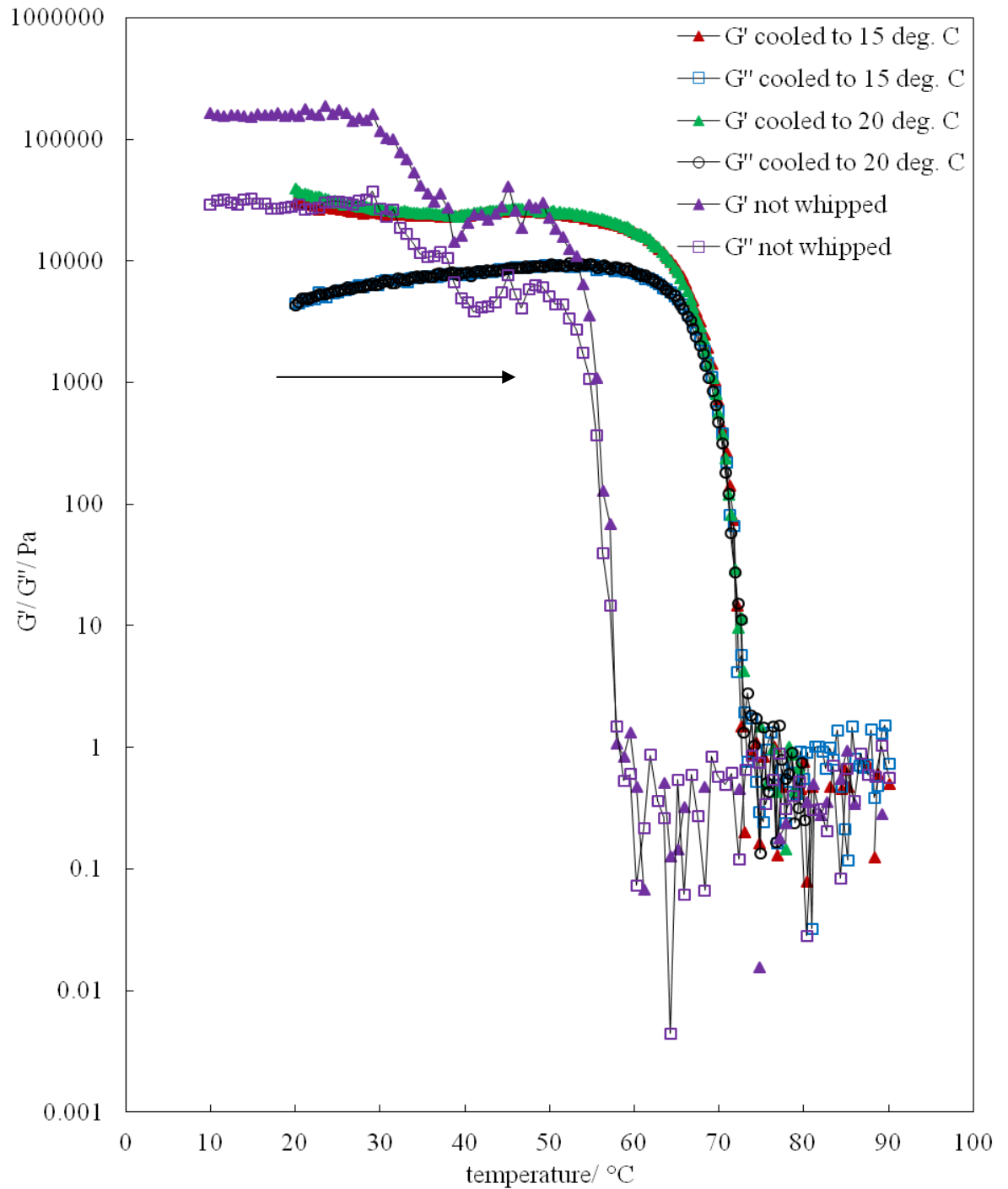
| Temperature/ °C | Foam production | Volume fraction of air<br>$\pm 0.02$ |
|-----------------|-----------------|--------------------------------------|
| 10              | No              | -                                    |
| 15              | Yes             | 0.55                                 |
| 20              | Yes             | 0.59                                 |
| 25              | No              | -                                    |
| 30              | No              | -                                    |

#### 7.4.2.1.2 Rheology of foam

A foam produced with 10 wt.% Dimodan HR kosher in HOSO was investigated with rheology. The foam was created by heating 10 wt.% Dimodan HR kosher in HOSO to 90 °C, then cooling to 15 and 20 °C at approximately 1 °C/min., then whipped at 22 °C for 1 hour. As can be seen from Figure 7.17  $G'$  and  $G''$  of the non-whipped gel of 10 wt.% Dimodan HR kosher which was cooled to 20 °C was found to be significantly larger than that of the foams. This was thought to be due to the presence of air in the foam.

The foam was heated at 1 °C/min, finding that the foam fully collapsed at 71.1 °C. The temperature the mixture was cooled to prior to whipping did not affect the temperature at which  $G'$  and  $G''$  of the foam significantly decreased (the temperature of foam collapse). Interestingly this temperature for both foams was considerably higher than the temperature the gel (not whipped) melted to become a liquid (decrease in  $G'$  and  $G''$ ). This may be due to the foam not conducting heat as efficiently as the gel.

**Figure 7.17.** Rheology measurements of a foam produced from whipping 10 wt.% Dimodan HR kosher in HOSO at 22 °C for 1 hour with a Hobart mixer with prior cooling from 90 °C to 15 and 20 °C at approximately 1 °C/min. Also, of the gel prior to whipping which was cooled to 20 °C from 90 °C at approximately 1 °C/min. Rheology measurements were with oscillating parallel plates (0.01 % strain at 1 Hz) as temperature increased to 90 °C (as shown by the arrow) at a rate of 1 °C/min.



#### 7.4.2.2 Whipping technique

5 and 10 wt.% Dimodan HR kosher in HOSO was aerated with a hand held double beater electric whisk for 45 minutes, the results were then compared to that found with the Hobart mixer. As can be seen in Table 7.3 the volume fraction of air incorporated into the foam produced at 5 and 10 wt.% was 0.43 and 0.47, respectively. The foam at 5 wt.% was produced after the mixture was cooled to 5 °C at approximately 1 °C/min. from 90 °C, at 10 wt.% the mixture was cooled to 20 °C, prior to whipping. It is clear that the volume fraction of air present in the foam produced with the Hobart mixer was significantly higher than with the hand held double beater electric whisk. This may be because the Hobart mixer agitated the mixture more, therefore more air was incorporated into the mixture.

As shown in Figure 7.18 at 5 and 10 wt.% prior to whipping there was a pale yellow soft gel. As can be seen in Figure 7.19 at both 5 and 10 wt.% the surfactant was found to be < 100 µm in diameter aggregates. It is interesting that again it appears that there is not a specific structure of the surfactant prior to whipping that is necessary to create a foam. As seen in Figure 7.20 a considerable amount of foam (450 mL) is produced after whipping 5 and 10 wt.% for 30 minutes. Figure 7.21 demonstrates that the bubbles in the foam were very small (< 50 µm in diameter). It also appears that the Dimodan HR kosher had a plate-like structure in the HOSO (it may be that the whipping caused the Dimodan HR kosher to break up to become plates). It is unclear if the Dimodan HR kosher was present at the air-oil surface of the bubbles. As can also be seen in Figure 7.21, where the foam was viewed through crossed polarising lenses, the Dimodan HR kosher was visible suggesting it was a birefringent crystal. The foams produced were heated 1 °C/min. until complete foam collapse was observed. The foam produced at 5 wt.% was found to fully collapse at 66.6 °C, the foam at 10 wt.% fully collapsed at 69.4 °C. These temperatures agree with that seen with Rheology measurements of the foam where G' and G'' values were found to begin to decrease at 62 ± 1 °C with the lowest G' at 71.1 °C, as stated earlier. It was found that a small amount of liquid drainage from the foam had occurred (approximately 10 mL from a 30 g foam sample) within 24 hours of foam formation. Over 18 months after foam formation there was little change in the appearance of the foams. The high stability of the foam may be due to the structured oil surrounding air bubbles in the foam and/or due to the Dimodan HR kosher being present at the air-oil surface.

The effect of the temperature 10 and 5 wt.% Dimodan HR kosher in HOSO was cooled to prior to whipping was not investigated with this method, however it was clear from whipping the mixture with a Hobart mixer that this was a crucial factor for the formation of foam.

**Table 7.3.** Volume fraction of air incorporated into a foam produced with 5 and 10 wt.% Dimodan HR kosher in HOSO with a Hobart mixer and with a hand held double beater electric whisk (electric whisk) at  $20 \pm 1$  °C and 22 °C, respectively. Prior to whipping 5 and 10 wt.% Dimodan HR kosher in HOSO was cooled from 90 °C at approximately 1 °C/min. to 5 °C and 20 °C, respectively.

| Dimodan HR concentration/<br>wt.% | Volume fraction of air with<br>Hobart mixer<br><br>$\pm 0.02$ | Volume fraction of air<br>with electric whisk<br><br>$\pm 0.02$ |
|-----------------------------------|---|---|
| 5                                 | 0.62  | 0.43  |
| 10                                | 0.59  | 0.47  |

**Figure 7.18.** Photographs of (a) 5 wt.% Dimodan HR kosher in HOSO cooled to 5 °C from 90 °C and (b) 10 wt.% Dimodan HR kosher in HOSO cooled to 20 °C from 90 °C. Scale bar 1 cm.

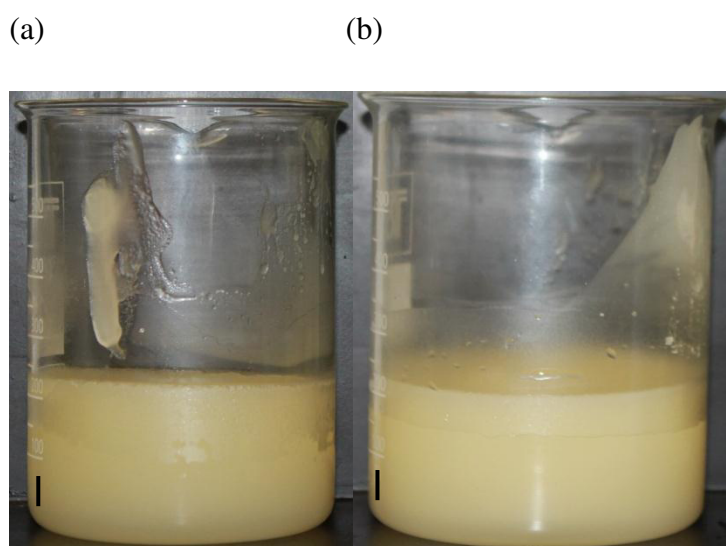
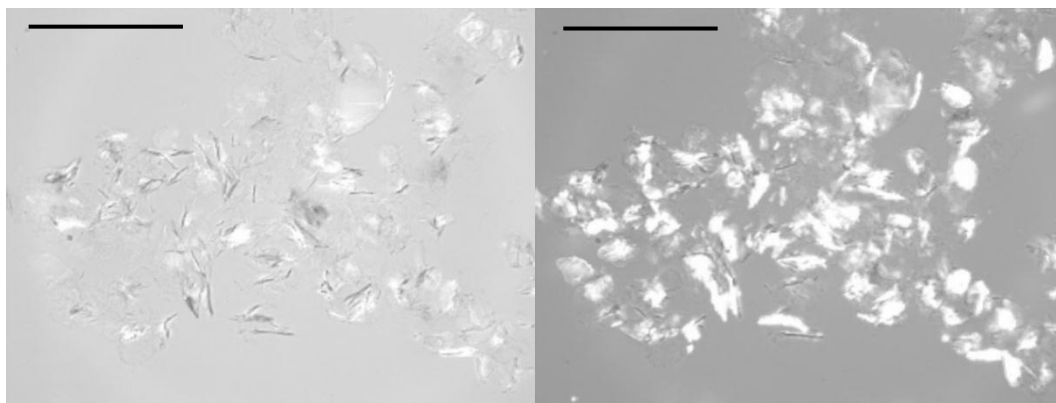


**Figure 7.19.** Optical microscopy at 22 °C of (a) 5 wt.% Dimodan HR kosher in HOSO cooled from 90 °C to 5 °C and (b) 10 wt.% Dimodan HR kosher in HOSO cooled from 90 °C to 20 °C. Images on the right are corresponding micrographs viewed through crossed polarising lenses. Scale bar 200 μm.

(a)



(b)

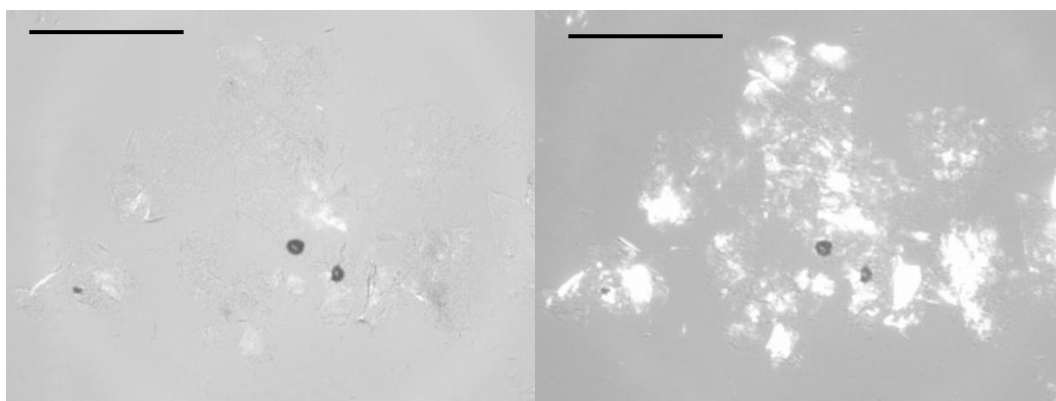


**Figure 7.20.** Photographs of (a) 5 wt.% Dimodan HR kosher in HOSO cooled from 90 °C to 5 °C and (b) 10 wt.% Dimodan HR kosher in HOSO cooled from 90 °C to 20 °C followed by whipping for 30 minutes at 22 °C with a hand held double beater electric whisk. Scale bar 1 cm.

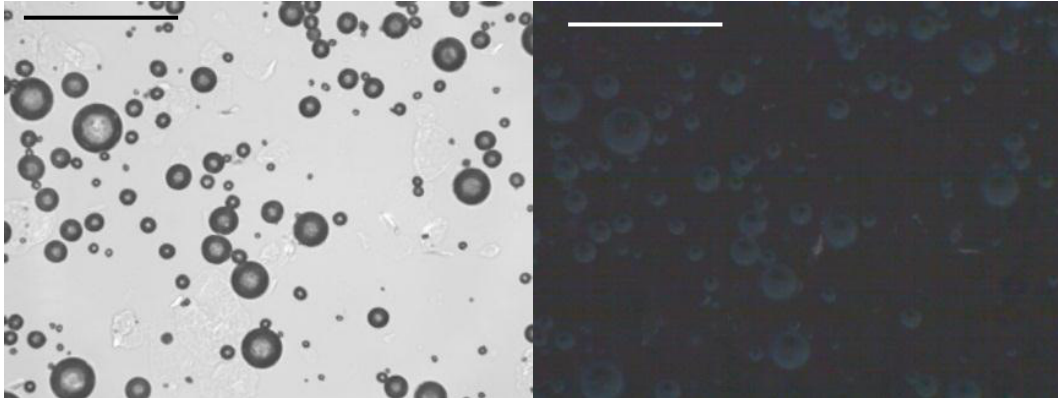
(a)

(b)

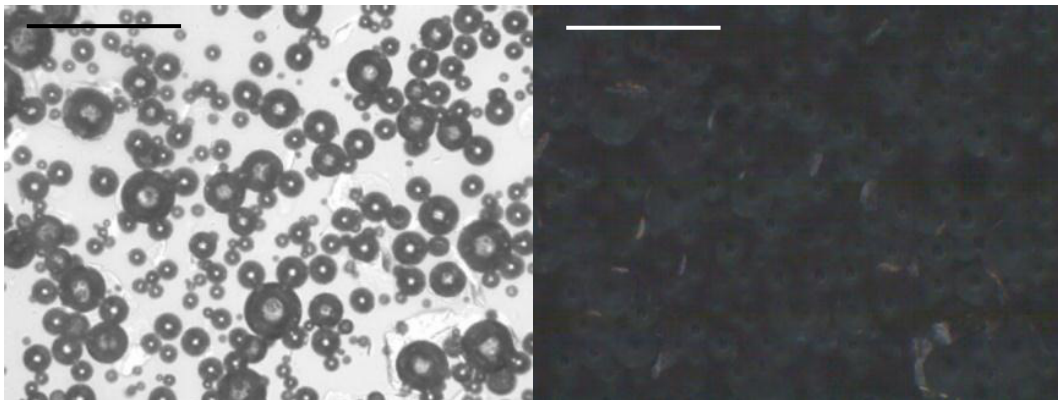


**Figure 7.21.** Optical microscopy of (a) 5 wt.% Dimodan HR kosher in HOSO cooled from 90 °C to 5 °C and (b) 10 wt.% Dimodan HR kosher in HOSO cooled from 90 °C to 20 °C followed by whipping for 30 minutes with a hand held double beater electric whisk at 22 °C. Images on the right are corresponding micrographs viewed through crossed polarising lenses. Scale bar 200  $\mu$ m.

(a)



(b)



## 7.5 Stearic acid in HOSO

The ability of stearic acid (an 18 carbon, straight chained, saturated carboxylic acid) to gel oils has previously been studied.<sup>6</sup> Therefore the formation of a gel followed by the ability to create a foam with 1-10 wt.% stearic acid in HOSO with a hand held double beater electric whisk was investigated.

The foam was produced by cooling the required amount of stearic acid in HOSO to  $8 \pm 2$  °C from 80 °C at approximately 1 °C/min., the mixture was then whipped for 45 minutes at 22 °C with a hand held double beater electric whisk. It can be seen from Table 7.4 that a foam was not produced at 1 and 2 wt.%. A foam (200 mL) could be produced at 3 wt.%, as the surfactant concentration further increased to 5 wt.% the amount of foam produced increased to 400 mL. The volume of foam produced then remained constant (400 mL) until 9 and 10 wt.% where the foam volume then decreased to 350 and 300 mL, respectively. The temperature of complete foam collapse, which increased as stearic acid concentration increased, will be discussed later.

It is clear from Figure 7.22 that the volume of foam produced reached a maximum (400 mL) at 5-8 wt.%. This maximum was also observed with the volume fraction of air incorporated into the mixture which was 0.36 to 0.38 at 5 to 7 wt.%. This maximum may be due to a specific mixture hardness/viscosity or possible optimum crystal size being required for a foam to be produced and for a maximum amount of air to be incorporated into the mixture. The maximum was not surprising as it was also observed with myristic acid in HOSO. The requirement of a specific mixture hardness/viscosity/crystal size was also necessary for foam formation with G.C. N12 veg in HOSO and Dimodan HR kosher in HOSO.

Figure 7.23 shows the appearance of 1-10 wt.%, once cooled from 80 °C to  $8 \pm 2$  °C at approximately 1 °C/min. At all stearic acid concentrations the mixture was turbid and pale yellow, 1 wt.% was fluid-like, 2-4 wt.% was gel-like, 5-10 wt.% was solid-like.

Figure 7.24 shows optical microscopy at 22 °C of 0-10 wt.% after cooling the mixture from 80 °C to  $8 \pm 2$  °C at approximately 1 °C/min. It was found at 1 wt.% that needles and aggregates were present, as the stearic acid concentration increased the aggregates became more plate-like as seen at 5 wt.%, although there were still needles present as seen at 6 wt.%. With a further concentration increase the structure then became all

plate-like as seen at 8 wt.%. It can also be seen from the figure through crossed polarising lenses that the stearic acid is a birefringent crystal.

At 1 and 2 wt.%, after whipping for 30 minutes, the appearance was relatively similar, as a foam was not produced as shown in Figure 7.25. After whipping 3 to 10 wt.% for 30 minutes a pale yellow to white foam was produced. The decrease in foam formation at 9 and 10 wt.% is also clear from Figure 7.25. Figure 7.26 shows that at 1 wt.% after whipping for 30 minutes there was some air present in the mixture. However the amount was clearly not substantial as a foam was not visible macroscopically and the volume fraction of air present in the mixture was 0. It is clear at 3-10 wt.% after whipping for 30 minutes that the stearic acid was present at the air-oil surface as the bubbles were irregular in shape and had a textured surface. The crystal presence at the air-oil bubble surface was visible when the foam produced at 6 wt.% was viewed through crossed polarising lenses. The size of the bubbles appeared to change very little with stearic acid concentration as they remained 20-150  $\mu\text{m}$  in diameter.

**Table 7.4.** Volume of the aerated phase, whipping time for maximum foam production, volume fraction of air incorporated into the mixture and temperature of complete foam collapse of stearic acid as a function of concentration in HOSO aerated with a hand held double beater electric whisk for 45 minutes at 22 °C.

| [stearic acid]/<br>wt.% | Volume of<br>aerated phase/<br>$\pm 10$ mL | Whipping time<br>for maximum<br>foam/ min. | Volume<br>fraction of air<br>$\pm 0.02$ | Temperature of<br>complete foam<br>collapse/ $\pm 0.1$ °C |
|-------------------------|--|--|---|---|
| 1                       | 0  | N/A  | 0                                       | N/A   |
| 2                       | 0  | N/A  | 0                                       | N/A   |
| 3                       | 200  | 25   | 0.08                                    | 46.0  |
| 4                       | 350  | 20   | 0.27                                    | 47.8  |
| 5                       | 400  | 15   | 0.36                                    | 54.4  |
| 6                       | 400  | 15   | 0.38                                    | 53.5  |
| 7                       | 400  | 15   | 0.37                                    | 55.8  |
| 8                       | 400  | 10   | 0.34                                    | 55.7  |
| 9                       | 350  | 25   | 0.19                                    | 55.8  |
| 10                      | 300  | 30   | 0.06                                    | 57.8  |

**Figure 7.22.** Volume of foam produced and volume fraction of air incorporated into stearic acid as a function of concentration in HOSO aerated with a hand held double beater electric whisk for 45 minutes at 22 °C.

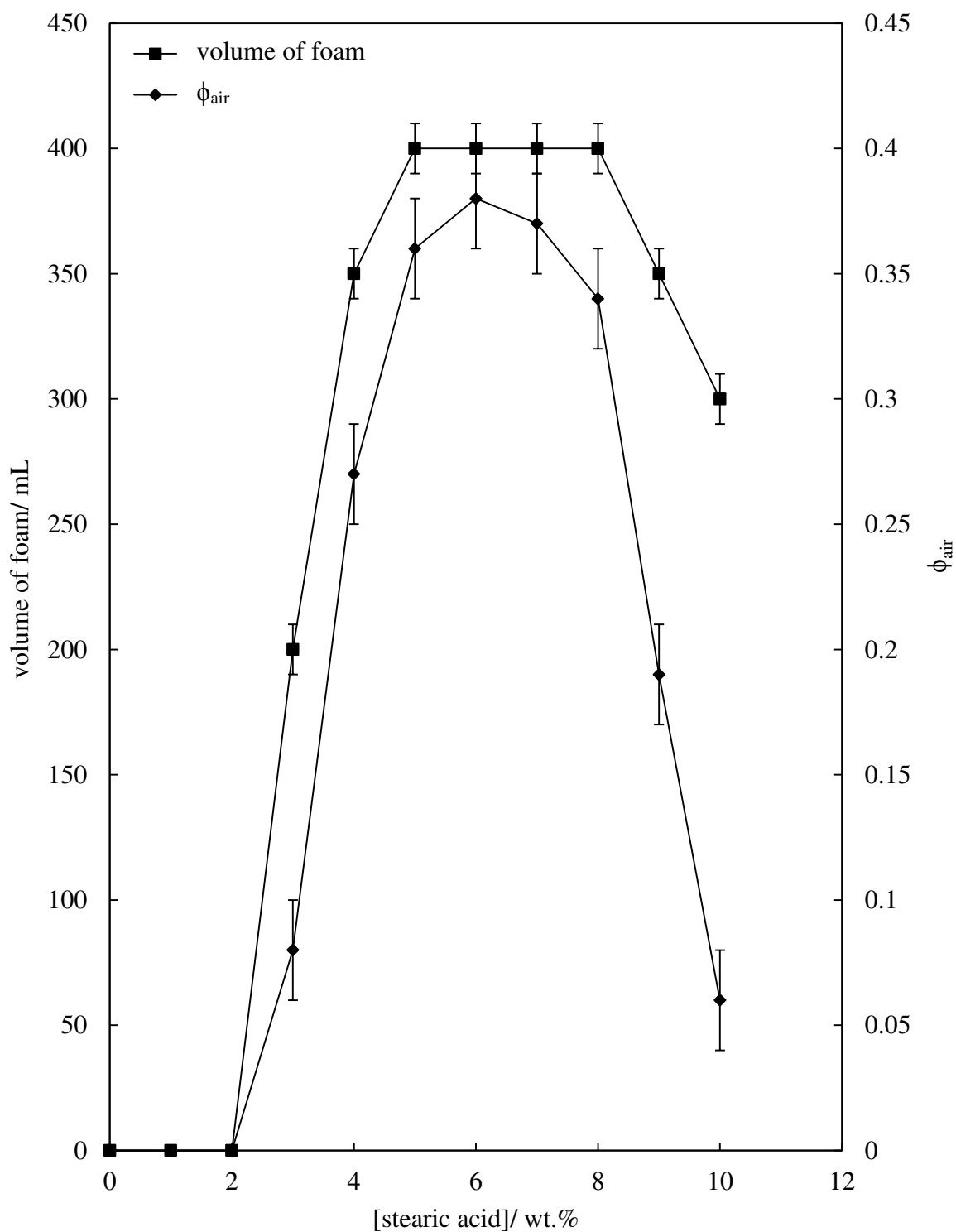


**Figure 7.23.** Photographs of (a) 1 wt.%, (b) 2 wt.%, (c) 3 wt.%, (d) 4 wt.%, (e) 5 wt.%, (f) 6 wt.%, (g) 7 wt.%, (h) 8 wt.%, (i) 9 wt.% and (j) 10 wt.% stearic acid in HOSO at 22 °C after cooling from 80 °C to  $8 \pm 2$  °C at approximately 1 °C/min. Scale bar 1 cm.

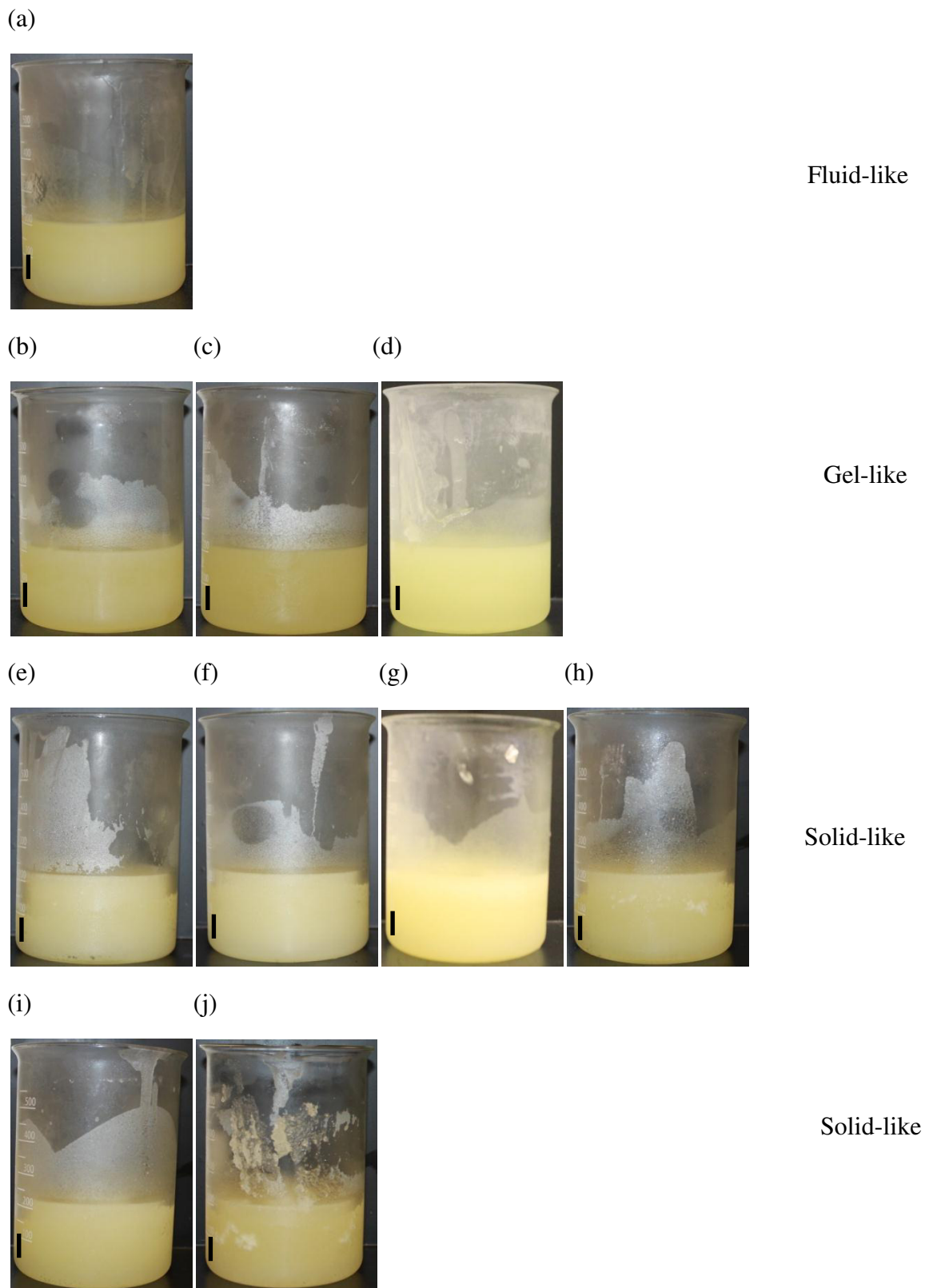


**Figure 7.24.** Optical microscopy of 1-8 wt.% stearic acid in HOSO at 22 °C after cooling from 80 °C to  $8 \pm 2$  °C at approximately 1 °C/min. (d) is the corresponding image of 6 wt.% stearic acid in HOSO viewed through crossed polarising lenses. Scale bar 200  $\mu$ m.

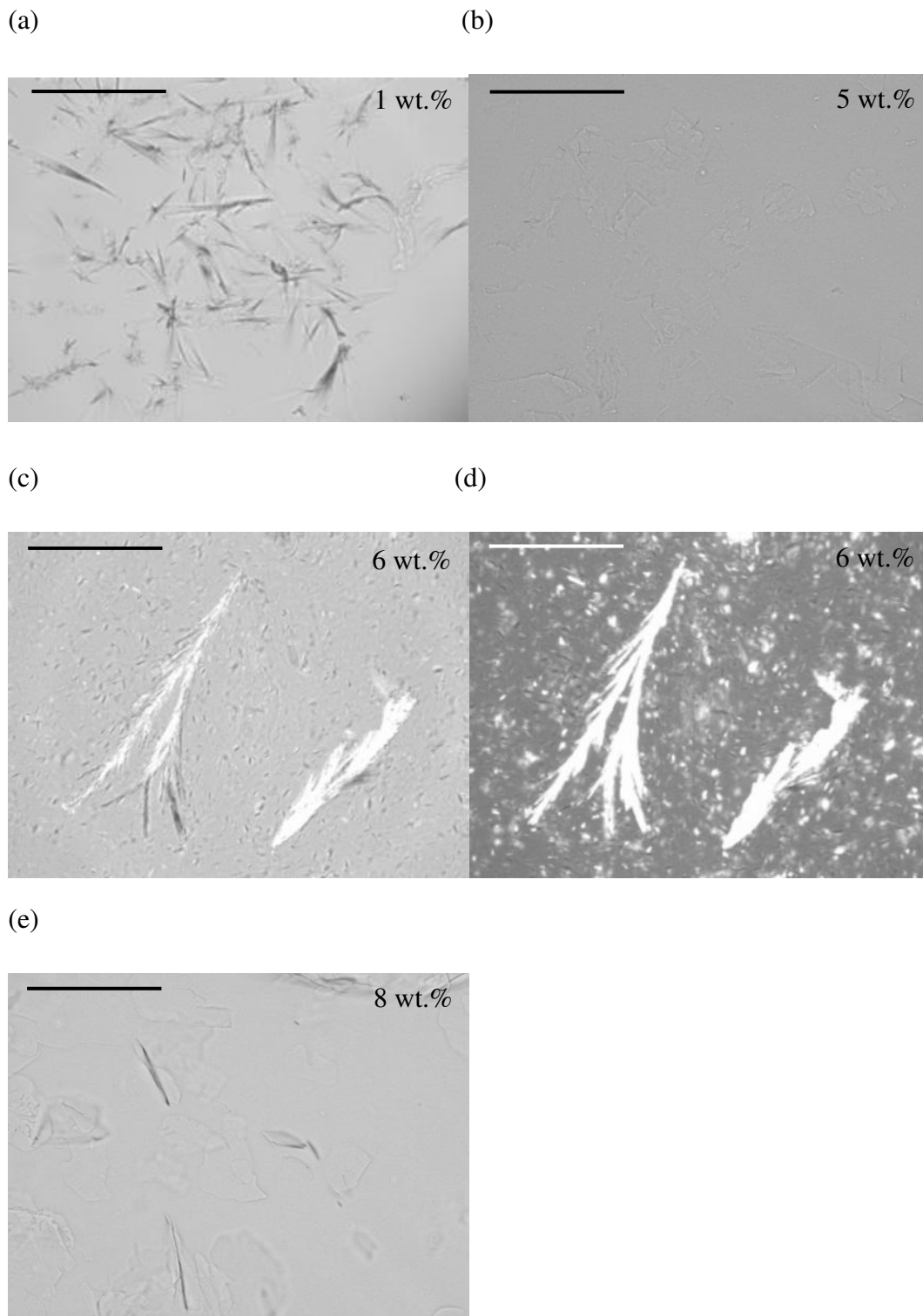


**Figure 7.25.** Photographs of (a) 1 wt.% , (b) 2 wt.% , (c) 3 wt.% , (d) 4 wt.% , (e) 5 wt.% , (f) 6 wt.% , (g) 7 wt.% , (h) 8 wt.% , (i) 9 wt.% and ( j) 10 wt.% stearic acid in HOSO aerated for 30 minutes with a hand held double beater electric whisk at 22 °C. Scale bar 1 cm.

(a)



(b)



(c)



(d)



(e)



(f)



(g)



(h)



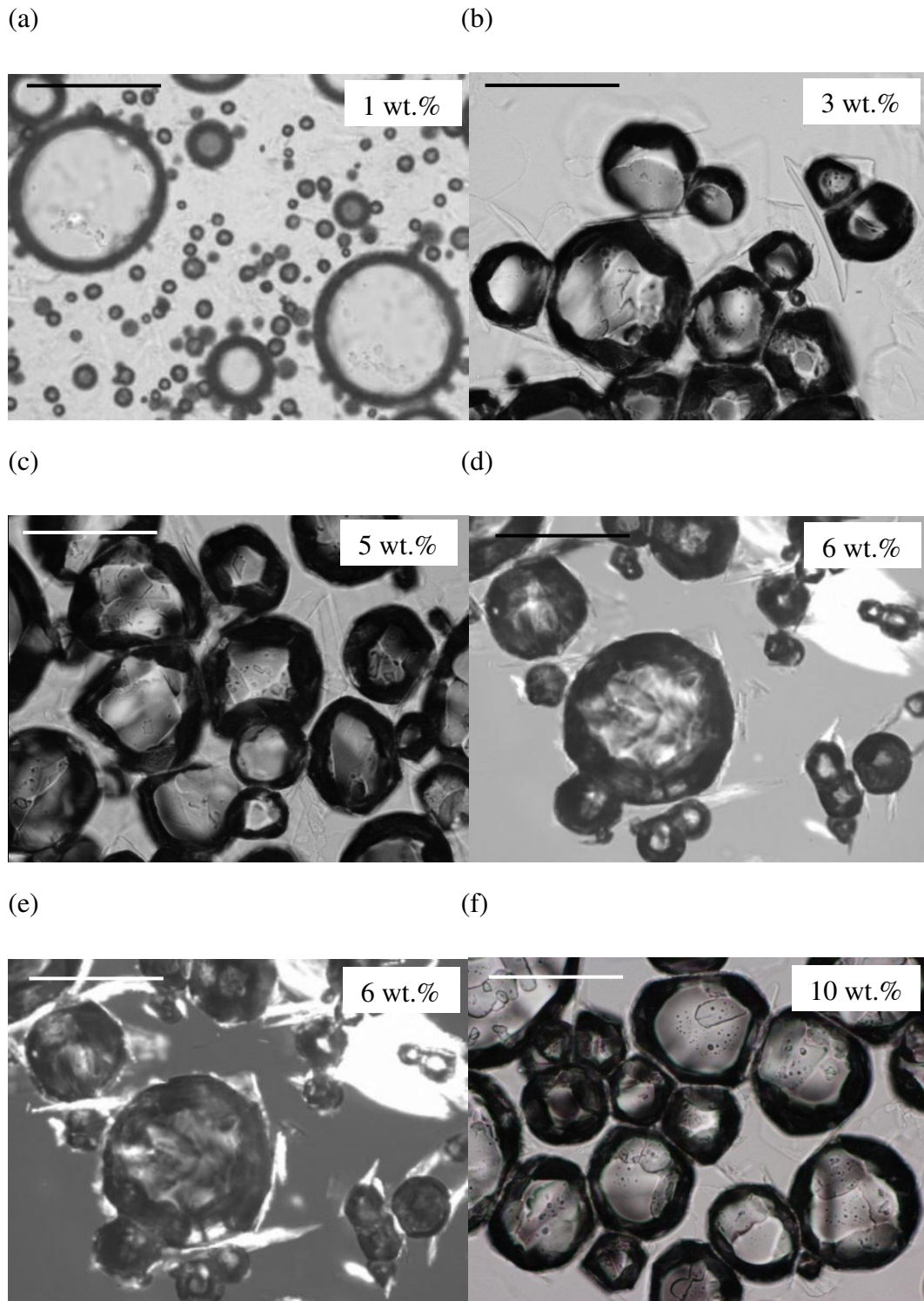
(i)



(j)



**Figure 7.26.** Optical microscopy images of 1-10 wt.% stearic acid in HOSO after whipping for 30 minutes with a hand held double beater electric whisk at 22 °C. (e) is the corresponding image of 6 wt.% stearic acid in HOSO viewed through crossed polarising lenses. Scale bar 200  $\mu\text{m}$ .



### 7.5.1 Effect of temperature increase

It was found, as shown in Table 7.4, that the temperature the foam fully collapsed increased as stearic acid concentration increased. Figure 7.27 shows that there was gradual liquid drainage and foam collapse as temperature increased. As the temperature of the foam increased from 22 °C to 35 °C there was little change in the foam macroscopically, the bubble appearance through optical microscopy, remained < 150 μm in diameter (Figure 7.28). As the temperature further increased the bubble diameter increased gradually to approximately 200 μm and then as high as 400 μm at 40 °C and 45 °C, respectively. At 50 °C and 55 °C the bubble diameter then increased to 800 μm. It is clear that at 60 °C all of the foam had collapsed, but some of the surfactant remained which was < 10 μm sized plates. Figure 7.29 also shows the gradual foam collapse and oil release which occurred from a 10 g sample of foam at 5 and 10 wt.% as temperature increased 1 °C/min. The foam collapsed before the stearic acid melted (melting temperature 68.8 °C) suggesting that the foam collapsed due to a decrease in viscosity (as temperature increased liquid drainage, disproportionation and coalescence occurred). However, the stearic acid is clearly necessary for foam stability, as at room temperature (22 ± 2 °C) the foam produced was stable for over 18 months without any foam collapse or liquid drainage.

**Figure 7.27.** Photographs of 10 wt.% stearic acid in HOSO after whipping for 45 minutes with a hand held double beater electric whisk at 22 °C heated 1 °C/min. at (a) 22 °C, (b) 30 °C, (c) 35 °C, (d) 40 °C, (e) 45 °C, (f) 50 °C, (g) 55 °C and (h) 60 °C. Scale bar 1 cm.

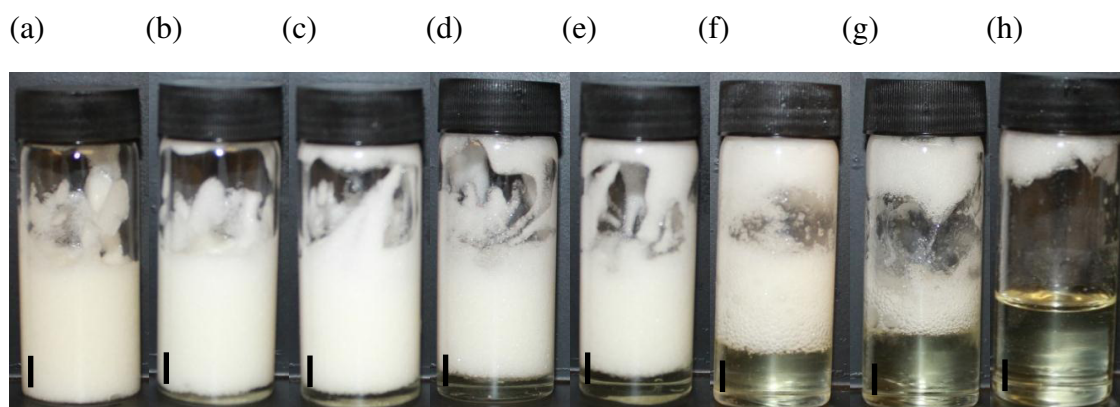


**Figure 7.28.** Optical microscopy of 10 wt.% stearic acid in HOSO after whipping for 45 minutes with a hand held double beater electric whisk at 22 °C heated 1 °C/min. at (a) 22 °C, (b) 25 °C, (c) 30 °C, (d) 35 °C, (e) 40 °C, (f) 45 °C, (g) 50 °C, (h) 55 °C and (i) 60 °C. Scale bar 200  $\mu$ m.

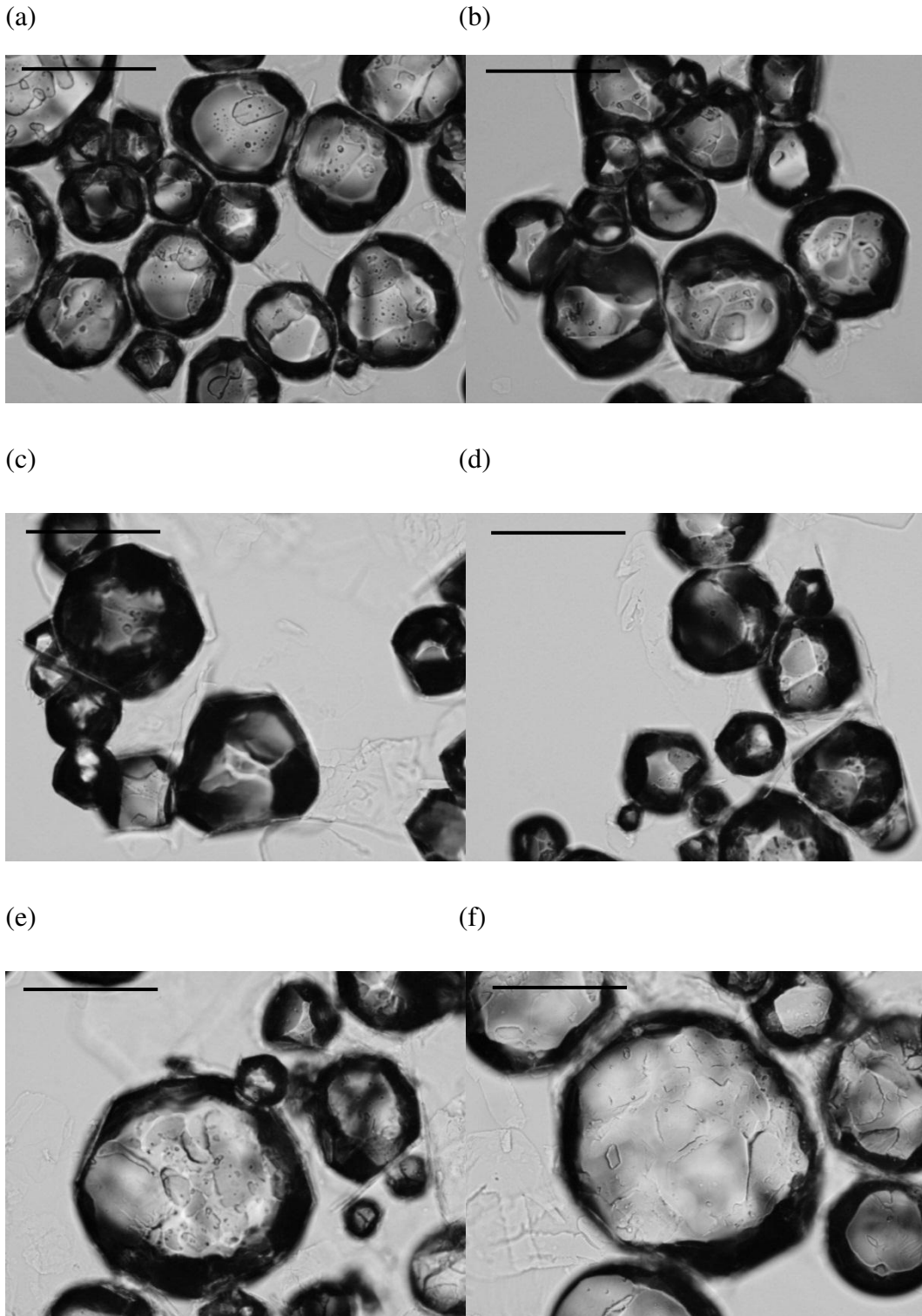
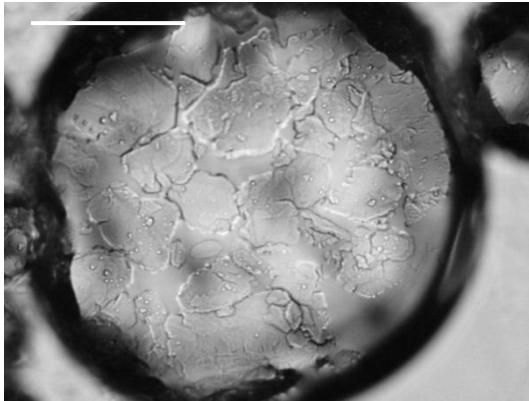
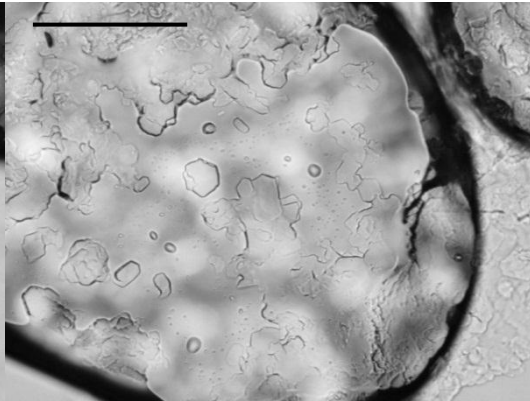


**Figure 7.28** (continued)

(g)



(h)



(i)

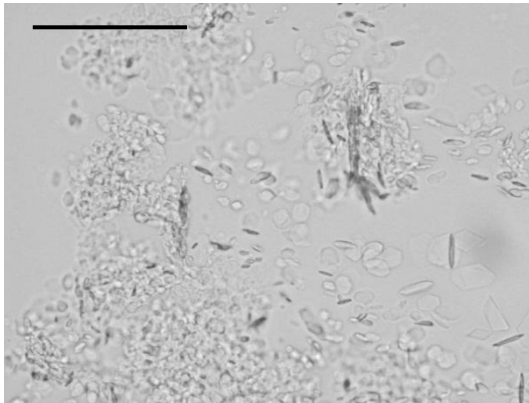
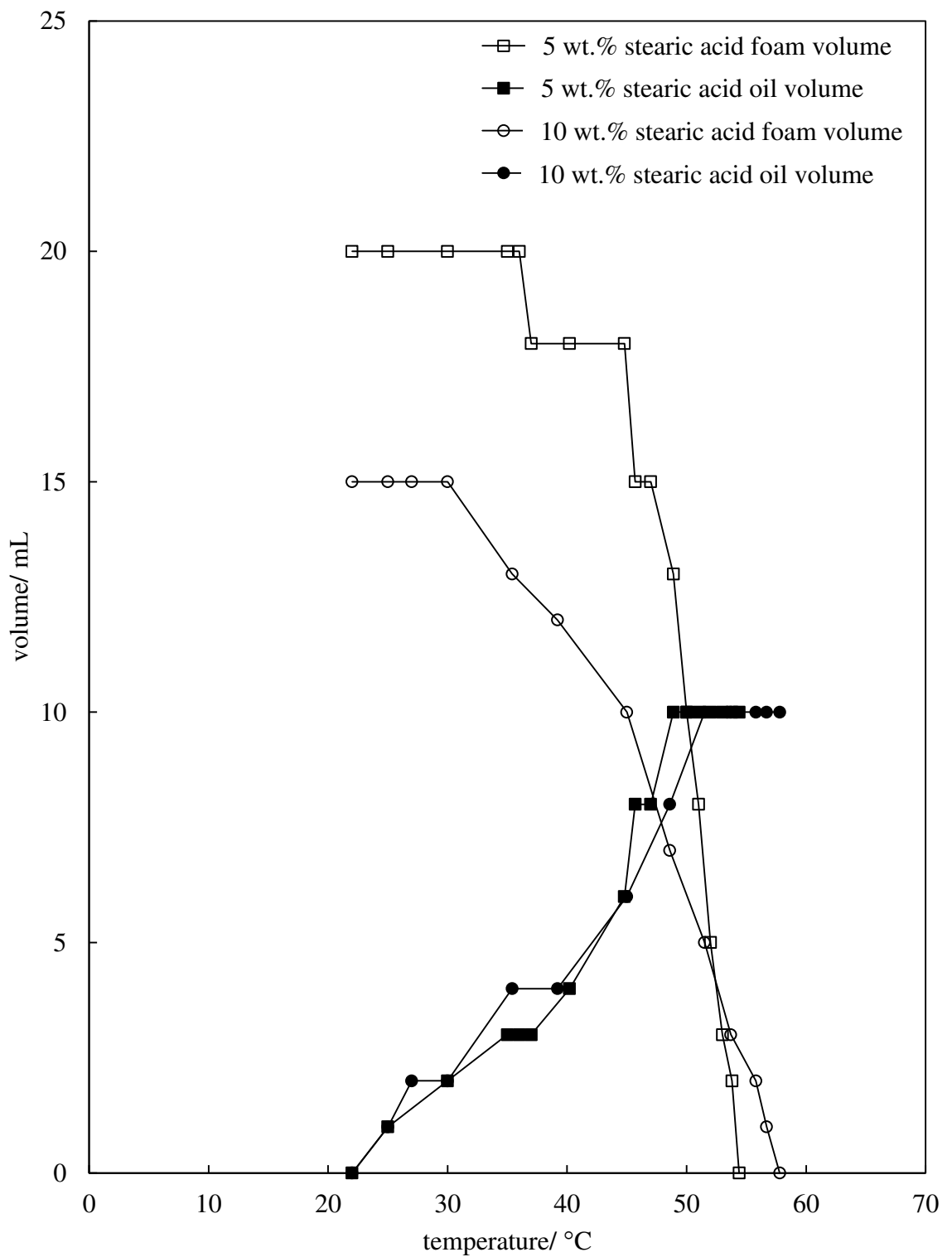


**Figure 7.29.** Oil release and foam collapse of a foam produced with a hand held double beater electric whisk for 45 minutes at 22 °C with 5 and 10 wt.% stearic acid in HOSO heated 1 °C/min.



### 7.5.2 Effect of whipping temperature

The effect of whipping temperature was investigated with 7 wt.% stearic acid in HOSO. As can be seen in Table 7.5 the temperatures the mixture was whipped at (after cooling from 80 °C to  $8 \pm 2$  °C at approximately 1 °C/min.) were 22, 30, 40 and 50 °C. It is clear that as the whipping temperature was increased to 30 °C from 22 °C the volume of foam produced decreased (50 mL less) and the amount of air incorporated into the mixture decreased to 0.29 from 0.37. The effect of whipping at 40 °C was found to be significant as the volume of foam produced was only 250 mL and the fraction of air incorporated into the mixture was 0.04. A foam could not be produced when whipping the mixture at 50 °C. The decrease in foam volume and volume fraction of air in the mixture as whipping temperature increased is clearly shown in Figure 7.30. The appearance of the mixture prior to aeration at 22, 30, 40 and 50 °C was different (see Figure 7.31). At 22 and 30 °C the mixture was a turbid, pale yellow gel, at 40 °C the mixture was a turbid, pale yellow liquid and at 50 °C the mixture was a clear yellow liquid. Through optical microscopy it appears that at all temperatures investigated, prior to aeration, the stearic acid was < 400 µm in diameter aggregates (Figure 7.32). Figure 7.33 shows the foam volume produced after whipping for 30 minutes at 22 °C, 30 °C and 40 °C decreased as temperature increased. At 50 °C the mixture remained a clear yellow liquid as foam was not produced. There was a change in the appearance of the foam through optical microscopy as the whipping temperature increased (Figure 7.34). At 22 and 30 °C the appearance of the foam was similar (non-spherical bubbles with a diameter of < 150 µm). At 40 °C, there were clearly less bubbles in the foam than at 22 and 30 °C, however the bubbles in the foam were similar in appearance as they were non-spherical with a diameter of < 150 µm. At 50 °C only < 100 µm stearic acid aggregates and up to 200 µm long needles were present in the oil (no bubbles). This change in aggregate size suggests that the whipping caused the < 400 µm aggregates to break up.

It was found that the increase in whipping temperature (from 22 °C to 40 °C) did not have a significant effect on the temperature of foam collapse when a sample of the foam was increased 1 °C/min. However, it did have an effect on the stability of the foam when the foam was held at the aeration temperature after whipping. It was found that the foam produced at 22 °C remained stable for 18 months without any liquid drainage or foam collapse, the foam produced at 30 °C was stable for 2 weeks. The foam

produced at 40 °C was only stable for 4 hours. This, again, shows the necessity of the stearic acid for foam formation, along with the stability of the foam.

**Table 7.5.** Volume of the aerated phase, whipping time for maximum foam production, volume fraction of air incorporated into the mixture and temperature of complete foam collapse of 7 wt.% stearic acid in HOSO after whipping for 45 minutes with a hand held double beater electric whisk at 22 °C, 30 °C, 40 °C and 50 °C.

| Aeration temperature/<br>°C | Volume of aerated phase/<br>± 10 mL | Whipping time for maximum foam/<br>min. | Volume fraction of air ± 0.02 | Temperature of complete foam collapse/<br>± 0.1 °C |
|-----------------------------|-------------------------------------|---|-------------------------------|--|
| 22                          | 400                                 | 15                                      | 0.37                          | 55.8   |
| 30                          | 350                                 | 25                                      | 0.29                          | 56.0   |
| 40                          | 250                                 | 10                                      | 0.04                          | 55.2   |
| 50                          | 0                                   | N/A                                     | 0                             | N/A  |

**Figure 7.30.** Volume of aerated phase and volume fraction of air incorporated into 7 wt.% stearic acid in HOSO aerated with a hand held double beater electric whisk for 45 minutes at 22 °C, 30 °C, 40 °C and 50 °C.

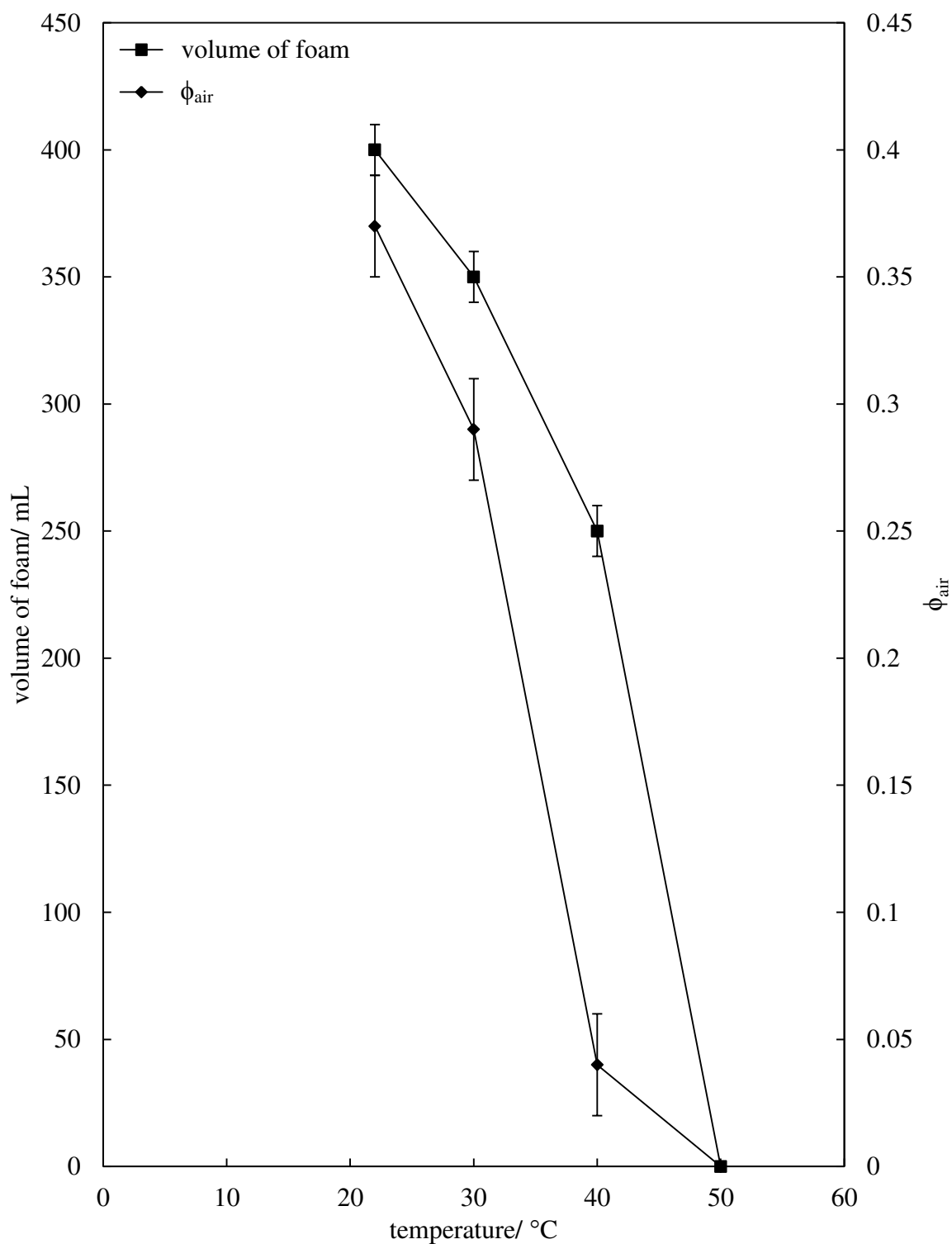


**Figure 7.31.** Photographs of 7 wt.% stearic acid in HOSO after cooling from 80 °C to  $8 \pm 2$  °C at approximately 1 °C/min. at (a) 22 °C, (b) 30 °C, (c) 40 °C and (d) 50 °C. Scale bar 1 cm.

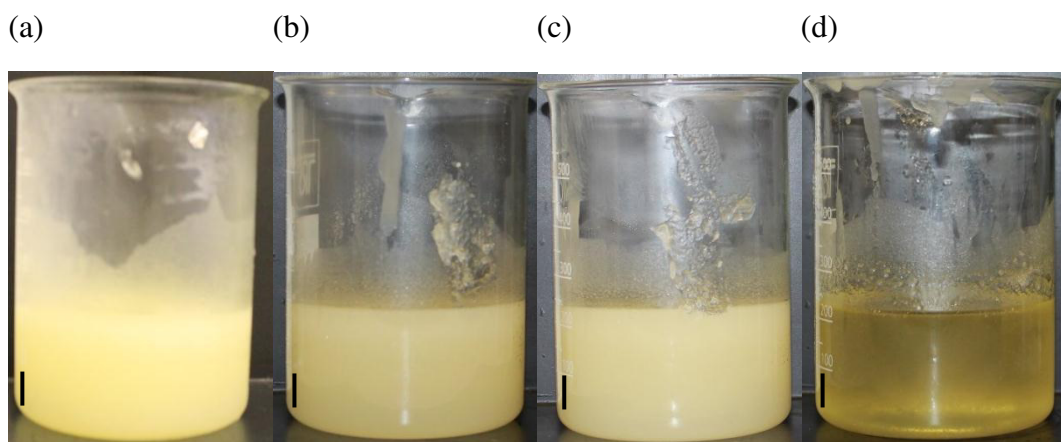


**Figure 7.32.** Optical microscopy of 7 wt.% stearic acid in HOSO after cooling from 80 °C to  $8 \pm 2$  °C at approximately 1 °C/min. at (a) 22 °C, (b) 30 °C, (c) 40 °C and (d) 50 °C. Scale bar 200  $\mu$ m.

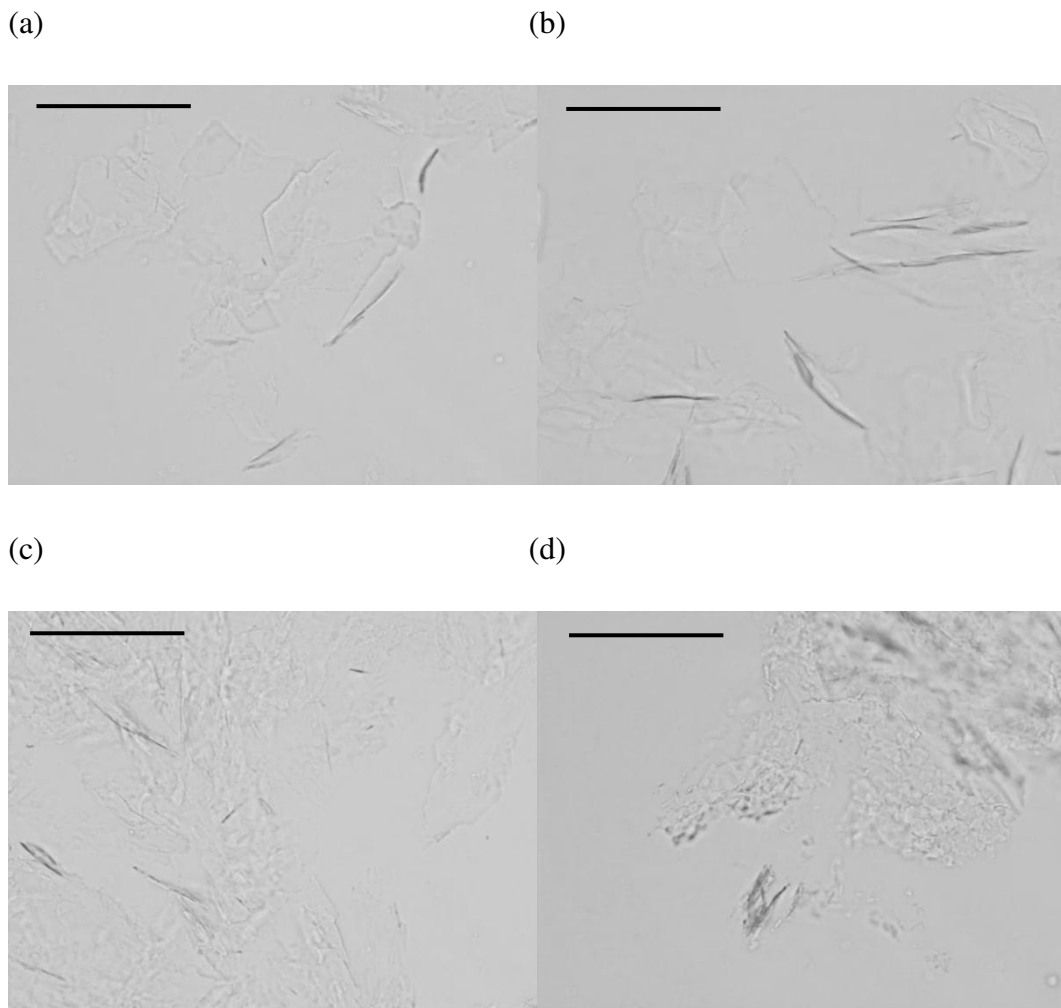


**Figure 7.33.** Photographs of 7 wt.% stearic acid in HOSO after cooling from 80 °C to  $8 \pm 2$  °C at approximately 1 °C/min. followed by whipping for 30 minutes with a hand held double beater electric whisk at (a) 22 °C, (b) 30 °C, (c) 40 °C and (d) 50 °C. Scale bar 1 cm.

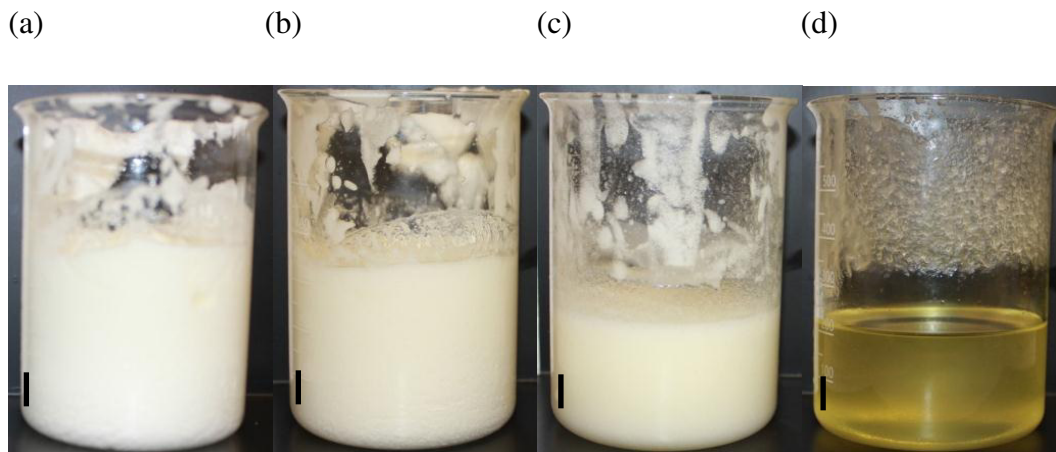
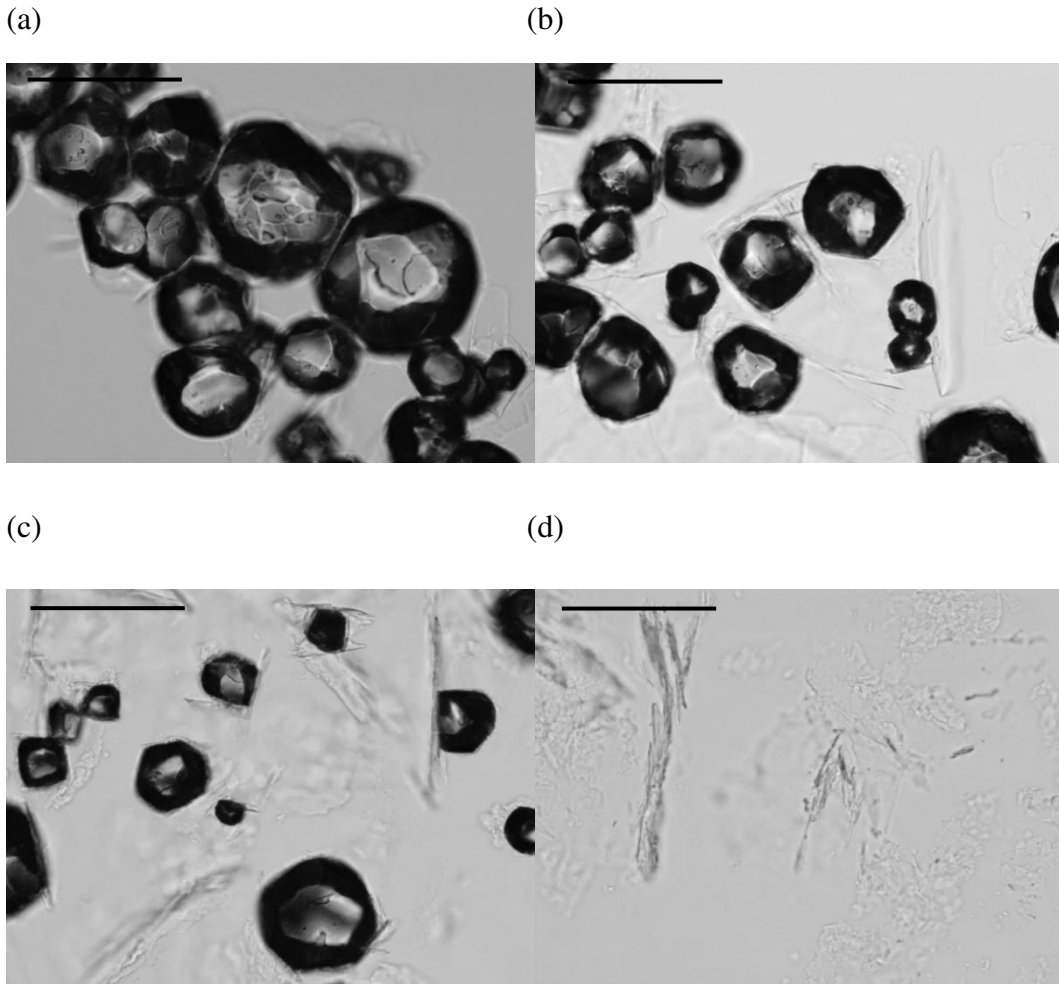


**Figure 7.34.** Optical microscopy of 7 wt.% stearic acid in HOSO after cooling from 80 °C to  $8 \pm 2$  °C at approximately 1 °C/min. followed by whipping for 30 minutes with a hand held double beater electric whisk at (a) 22 °C, (b) 30 °C, (c) 40 °C and (d) 50 °C. Scale bar 200  $\mu$ m.



## 7.6 Fatty acids and fatty alcohols in HOSO

After finding that both a gel and a foam could be created with myristic acid and stearic acid in HOSO the effect of fatty acid chain length on both characteristics was then investigated. It is known that a gel can be created with alcohols in vegetable oils<sup>5,6</sup> and also with cetostearyl alcohol in dodecane and HOSO. Also, that a foam could be produced when cetostearyl alcohol was added to both dodecane and HOSO, therefore the effect of fatty alcohol chain length on gel formation and foam creation was also investigated. The effect of chain length was studied by initially determining the melting temperature of neat fatty acids and alcohols with chain lengths of 14, 16, 18, 20 and 22 carbons by DSC.

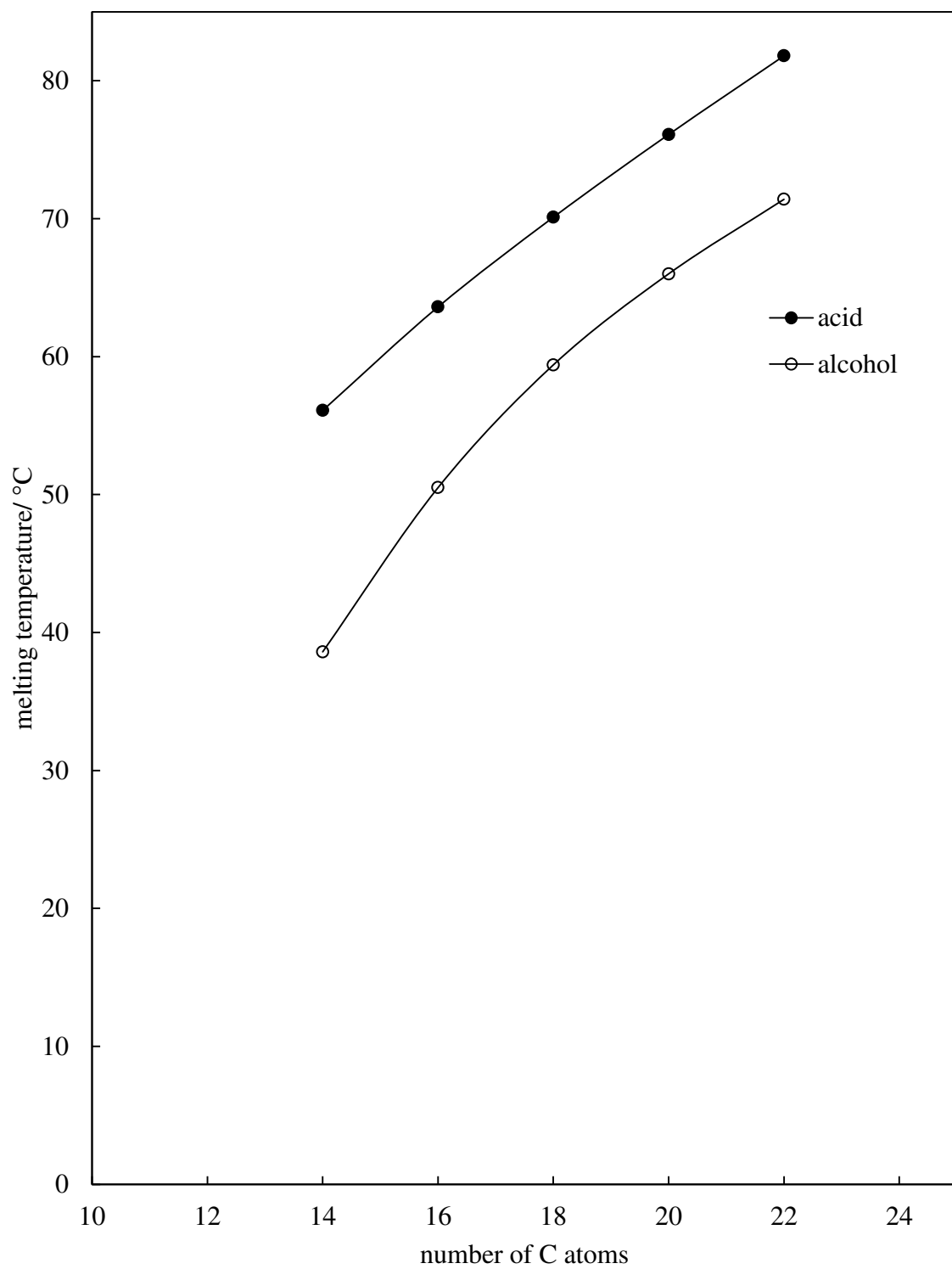
### 7.6.1 Differential scanning calorimetry

Table 7.6 gives the melting temperature, determined by DSC, of neat acids and alcohols with straight, saturated chain lengths ranging from C<sub>14</sub> to C<sub>22</sub>. Figure 7.35 shows how the melting temperature of the alcohols and acids increased as the chain length increased. It was therefore clear that with all acids and alcohols (except behenic acid) in HOSO the same protocol could be followed for gel formation and whipping as that used with stearic acid, myristic acid and cetostearyl alcohol in HOSO. This was where the mixture was heated to 80 °C, then cooled to 8 ± 2 °C at approximately 1 °C/min., then held at 22 °C to observe if there was a gel presence. The mixture was then whipped with a hand held double beater electric whisk for 45 minutes to investigate possible foam production. The protocol with behenic acid was the same except the mixture was initially heated to 85 °C, not 80 °C.

**Table 7.6.** Melting temperatures of acids and alcohols determined through DSC by heating from 10 °C to 90 °C at 2 °C/min.

| Name           | Hydrocarbon chain length | Melting temperature/ °C | Literature melting temperature/ °C <sup>16</sup> |
|----------------|--------------------------|-------------------------|--|
| Myristic acid  | C <sub>14</sub>          | 56.1                    | 53.9   |
| Palmitic acid  | C <sub>16</sub>          | 63.6                    | 61.8   |
| Stearic acid   | C <sub>18</sub>          | 70.1                    | 68.8   |
| Arachidic acid | C <sub>20</sub>          | 76.1                    | 75.4   |
| Behenic acid   | C <sub>22</sub>          | 81.8                    | 81.0   |
| 1-tetradecanol | C <sub>14</sub>          | 38.6                    | 39.5   |
| 1-hexadecanol  | C <sub>16</sub>          | 50.5                    | 49.3   |
| 1-octadecanol  | C <sub>18</sub>          | 59.4                    | 59.5   |
| 1-eicosanol    | C <sub>20</sub>          | 66.0                    | 66.1   |
| 1-docosanol    | C <sub>22</sub>          | 71.4                    | 72.5   |

**Figure 7.35.** Melting temperature of neat, straight chained, saturated hydrocarbon acids and alcohols.



## 7.6.2 Effect of fatty acid chain length in HOSO

As stated earlier it is known that a gel can be created with various fatty acids in oils.<sup>4,7</sup> Also, that a foam can be created with myristic acid and stearic acid in HOSO. Therefore it was not surprising that a gel and a subsequent foam, the details of which are shown in Table 7.7, could be created with palmitic, arachidic and behenic acid in HOSO. The gel formed prior to whipping with all 5 acids is shown in Figure 7.36. The appearance, through optical microscopy, of the fatty acids in HOSO prior to whipping was different as shown in Figure 7.37. Myristic acid was both plate-like and also 10  $\mu\text{m}$  sized aggregates, palmitic and stearic acid was a needle-like structure, stearic acid also had numerous  $< 10 \mu\text{m}$  aggregates present and arachidic and behenic acid had a plate-like structure which was  $< 200 \mu\text{m}$  in diameter. This therefore suggests that foamability was independent of the surfactant structure in the oil. A large amount of foam could be created with palmitic acid in HOSO (450 mL) as shown in Figure 7.38. It appeared that the volume of foam produced (and volume fraction of air present in the mixture) decreased as chain length increased from  $\text{C}_{16}$  to  $\text{C}_{22}$  (250 mL with behenic acid). This change in foamability may be due to the hardness of the mixture, therefore the foamability of behenic acid in HOSO may be higher when the mixture is cooled to a higher temperature prior to whipping as found with 10 wt.% Dimodan HR kosher in HOSO. Figure 7.39 shows the microscopic appearance of the foams after 30 minutes of whipping. The bubble appearance with all 5 fatty acids was relatively similar as they were non-spherical with textured surfaces ranging from 30-200  $\mu\text{m}$  in diameter. Although the bubble appearance was similar the stability of the foams at room temperature was found to differ as shown in Figure 7.40 with the foam appearance 24 hours after aeration. The amount of liquid that drained from a 30 g sample of foam with myristic acid was 10 mL, with palmitic acid was 5 mL, with stearic acid there was not any liquid drainage, with arachidic acid was 12 mL and finally with behenic acid was 15 mL. It appears that there was an optimum chain length for foamability, which was palmitic acid, and for foam stability (at room temperature), which was observed with stearic acid (as there was not any liquid drainage or foam collapse over 18 months). All of the foams produced had a relatively good foam stability as after the initial liquid drainage and foam collapse within 24 hours after formation the foam was stable for over 9 months (foams produced with myristic and stearic acid were stable for over 18 months) when kept at room temperature ( $22 \pm 2 \text{ }^\circ\text{C}$ ).

**Table 7.7.** Volume of the aerated phase, volume fraction of air incorporated into the mixture, time for maximum foam production and temperature of complete foam collapse of 6 wt.% fatty acids in HOSO after whipping for 45 minutes with a hand held double beater electric whisk at 22 °C.

| Fatty acid     | Volume of the aerated phase/<br>± 10 mL | Whipping time for maximum foam/ min. | Volume fraction of air<br>± 0.02 | Temperature of complete foam collapse/ ± 0.1 °C |
|----------------|---|--------------------------------------|----------------------------------|---|
| Myristic acid  | 400                                     | 15                                   | 0.28                             | 38.0  |
| Palmitic acid  | 450                                     | 25                                   | 0.48                             | 47.6  |
| Stearic acid   | 400                                     | 15                                   | 0.45                             | 53.5  |
| Arachidic acid | 300                                     | 15                                   | 0.23                             | 60.1  |
| Behenic acid   | 250                                     | 15                                   | 0.12                             | 61.8  |

**Figure 7.36.** Photographs of 6 wt.% (a) myristic acid, (b) palmitic acid, (c) stearic acid, (d) arachidic acid and (e) behenic acid in HOSO at 22 °C after cooling from 80 °C to  $8 \pm 2$  °C at approximately 1 °C/min. Scale bar 1 cm.

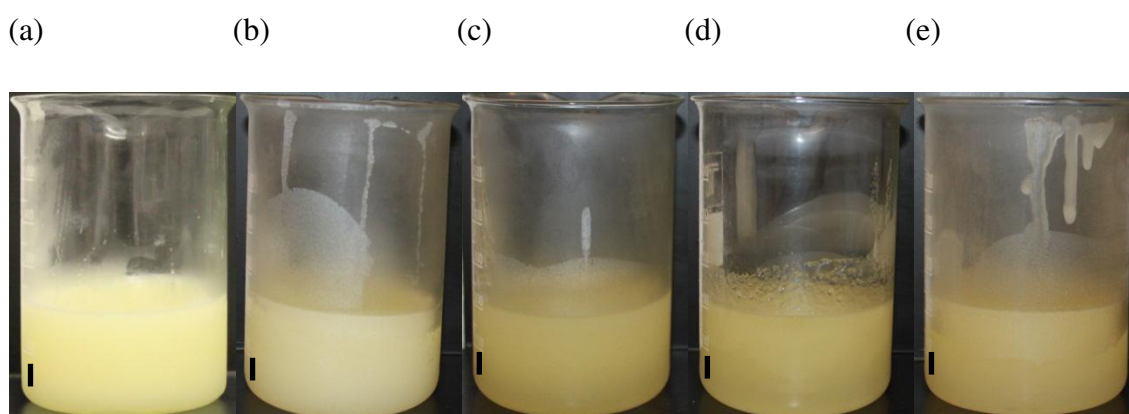
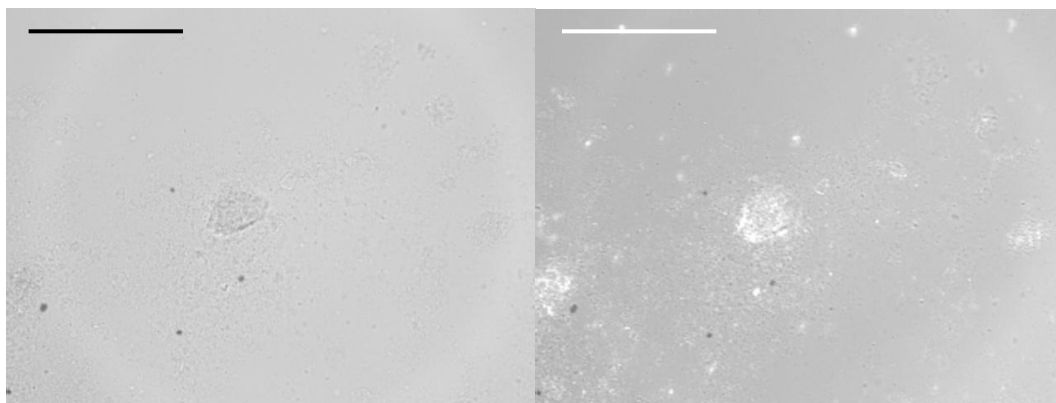
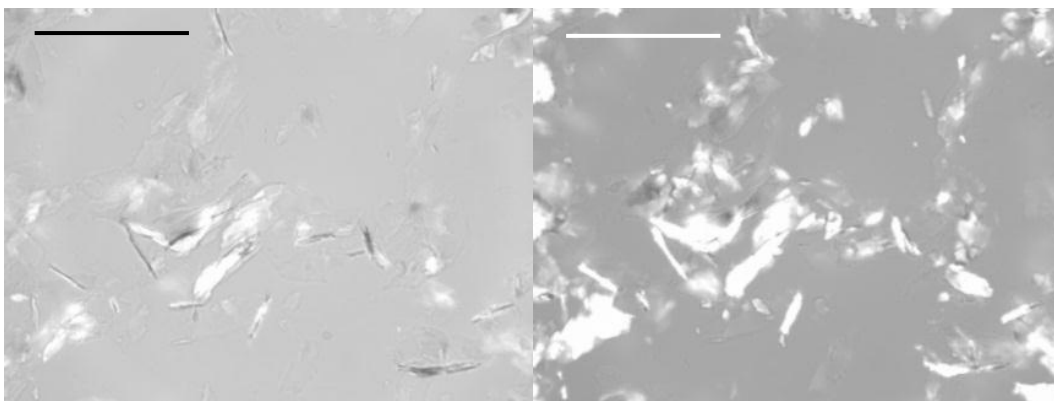


**Figure 7.37.** Optical microscopy of 6 wt.% (a) myristic acid, (b) palmitic acid, (c) stearic acid, (d) arachidic acid and (e) behenic acid in HOSO at 22 °C after cooling from 80 °C to  $8 \pm 2$  °C at approximately 1 °C/min. Images on the right are corresponding micrographs viewed through crossed polarising lenses. Scale bar 200  $\mu\text{m}$ .

(a)



(b)



(c)

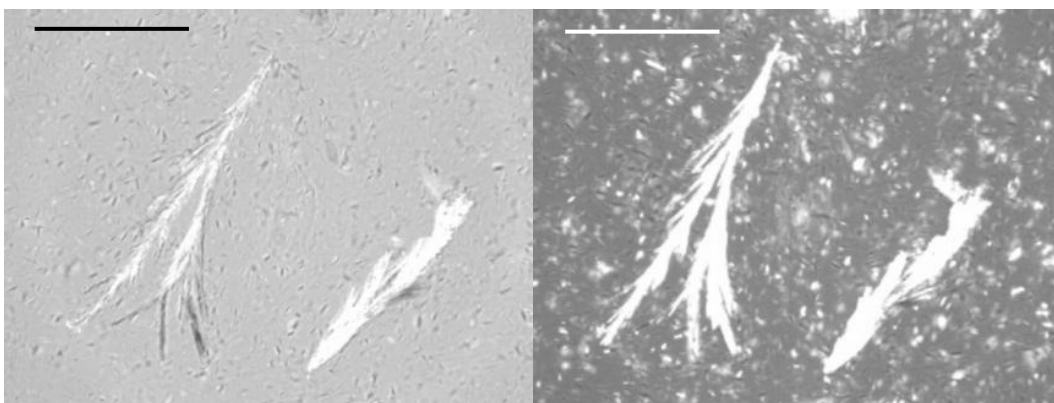
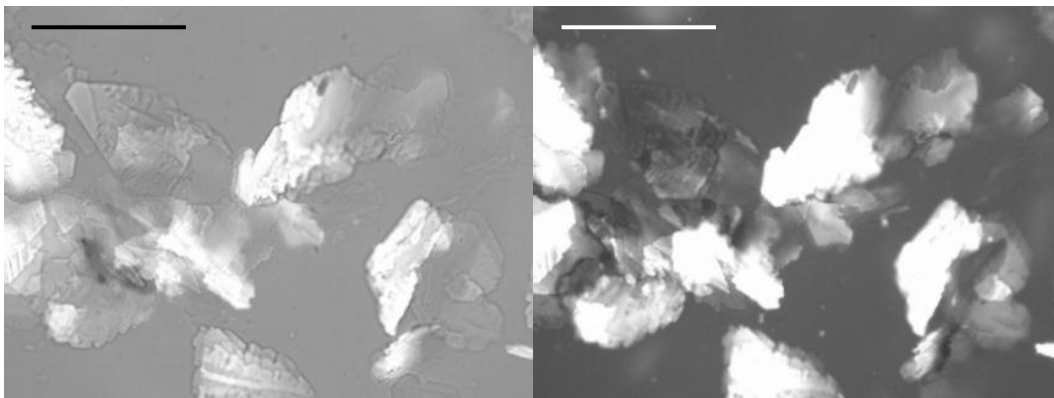


**Figure 7.37** (continued)

(d)



(e)

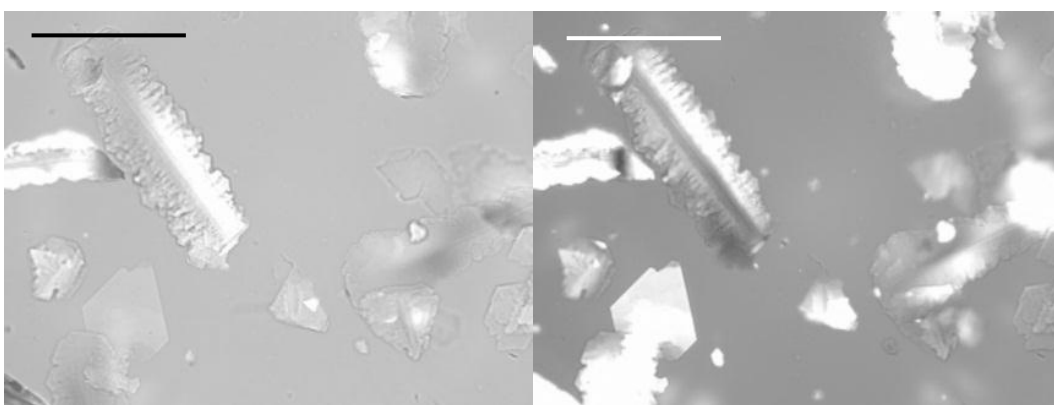


**Figure 7.38.** Photographs of 6 wt.% (a) myristic acid, (b) palmitic acid, (c) stearic acid, (d) arachidic acid and (e) behenic acid in HOSO at 22 °C after whipping for 30 minutes with a hand held double beater electric whisk. Scale bar 1 cm.

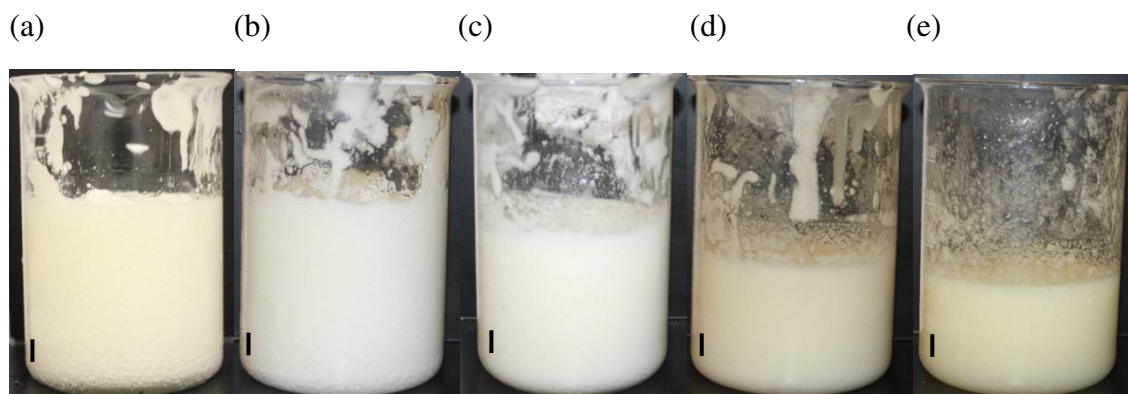
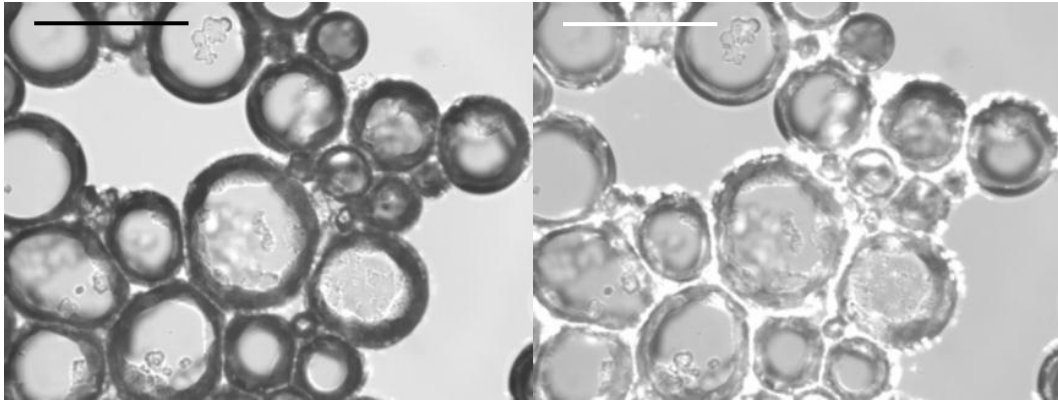
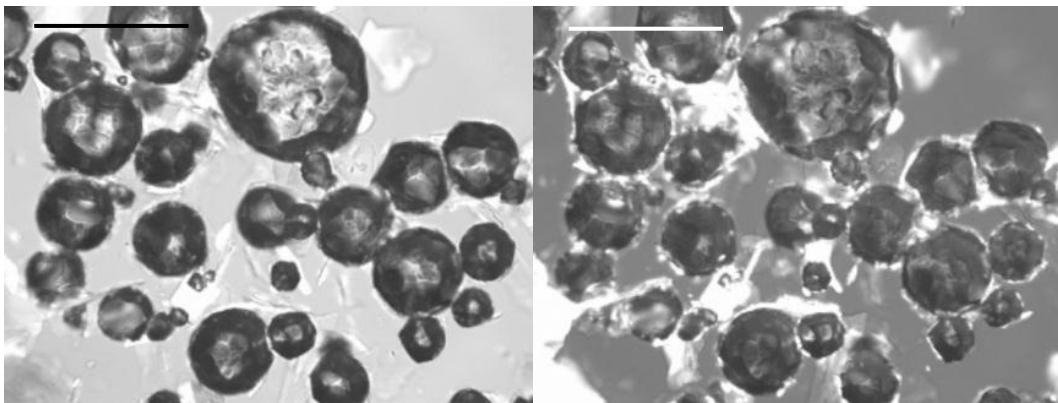


**Figure 7.39.** Optical microscopy of 6 wt.% (a) myristic acid, (b) palmitic acid, (c) stearic acid, (d) arachidic acid and (e) behenic acid in HOSO after whipping for 30 minutes with a hand held double beater electric whisk at 22 °C. Images on the right are corresponding micrographs viewed through crossed polarising lenses. Scale bar 200  $\mu\text{m}$ .

(a)



(b)



(c)

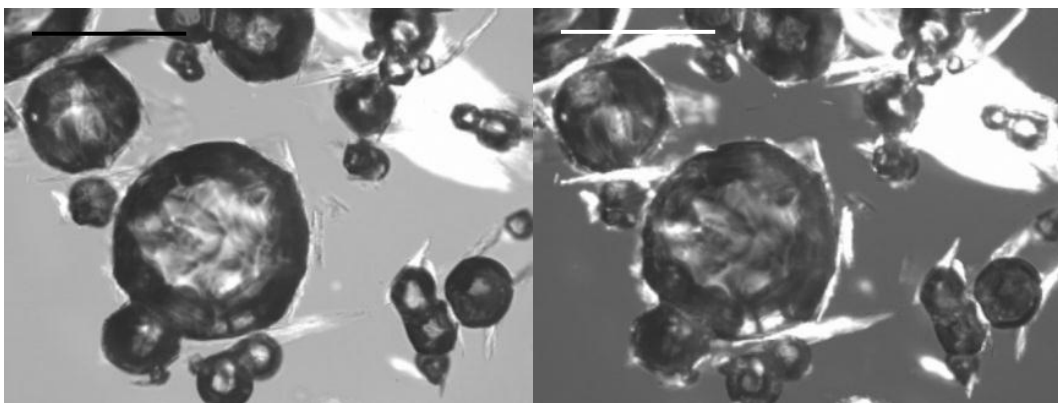
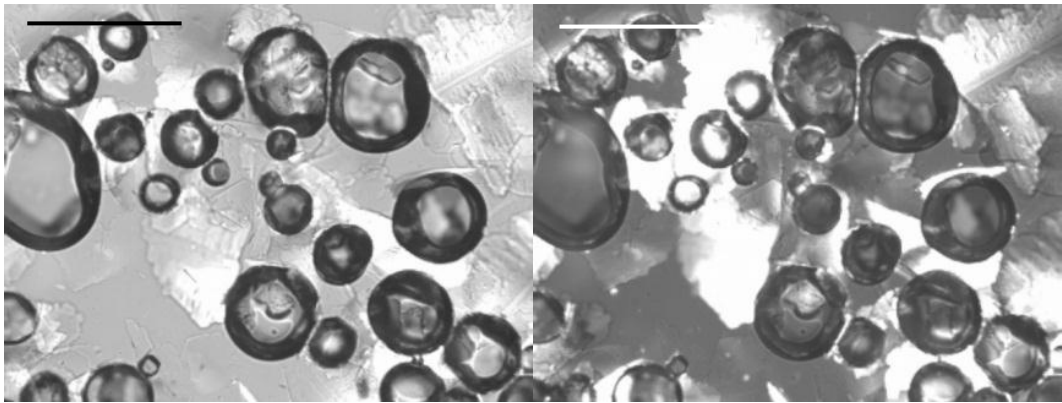


**Figure 7.39** (continued)

(d)



(e)

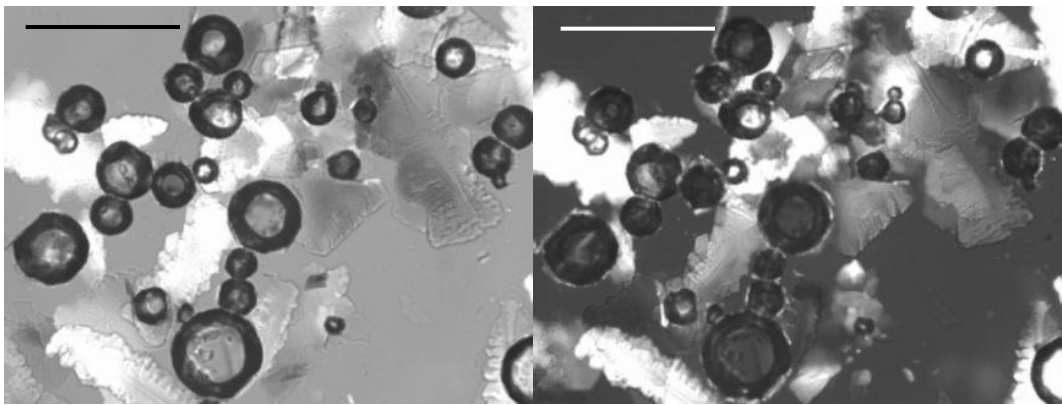
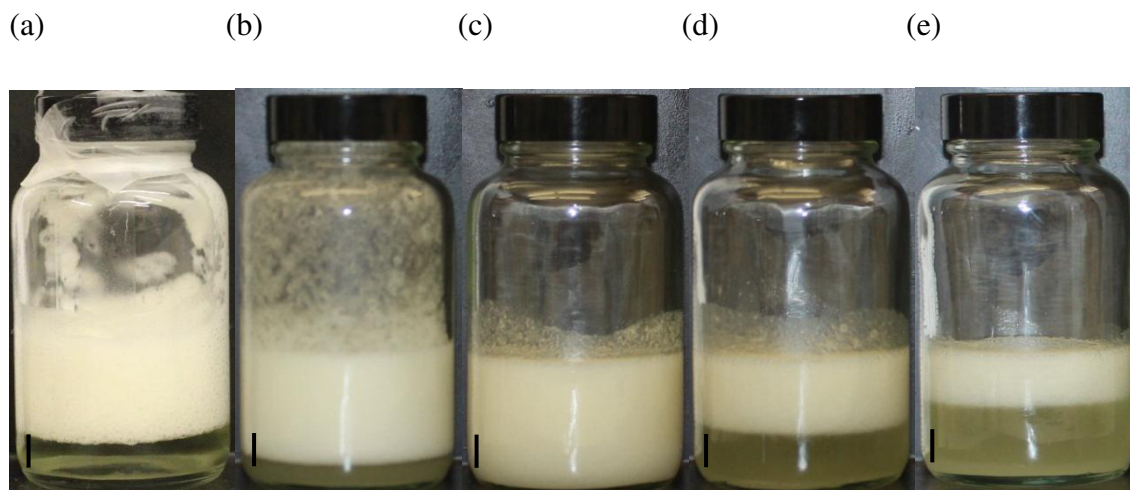


**Figure 7.40.** Photographs of 6 wt.% (a) myristic acid, (b) palmitic acid, (c) stearic acid, (d) arachidic acid and (e) behenic acid in HOSO at  $22 \pm 2$  °C 24 hours after aeration with a hand held double beater electric whisk for 45 minutes. Scale bar 1 cm.



### 7.6.3 Effect of fatty alcohol chain length in HOSO

As seen from Table 7.8 a foam could be produced with 6 wt. % 1-hexadecanol, 1-octadecanol, 1-docosanol and 1-eicosanol in HOSO after whipping the mixtures with a hand held double beater electric whisk for 45 minutes at 22 °C. Interestingly the foam volume and volume fraction of air in the mixture produced with the fatty alcohols was found to be on average lower than that produced with fatty acids of the same chain lengths in HOSO. A foam was not produced with 1-tetradecanol, it may be necessary to investigate a higher concentration of the surfactant in HOSO to discover if conclusively a foam cannot be produced through the whipping protocol with this alcohol in HOSO. It is also interesting from the table that a maximum amount of foam (300 mL) was produced with 1-octadecanol compared to that obtained with the other 3 alcohols (250 mL). This maximum volume of foam, and volume fraction of air incorporated into the mixture with a specific chain length was also observed with the fatty acids in HOSO (maximum with palmitic acid). It may be, again, that with this specific chain length at 22 °C the mixture had the required viscosity/ hardness/ crystal size that is necessary for a large amount of foam to be produced. Figure 7.41 shows that prior to whipping 1-tetradecanol the mixture was a turbid, pale yellow gel, therefore the appearance of the mixture was not significantly different to that observed with 1-hexadecanol, 1-octadecanol, 1-docosanol and 1-eicosanol. This was also found through optical

microscopy (Figure 7.42) as the fatty alcohols all had a plate-like structure in the HOSO prior to aeration. Figure 7.43 shows that the foam produced with the fatty alcohols was similar in appearance (pale yellow) and that foam was not produced with 1-tetradecanol. 50 mL more foam was produced with 1-octadecanol than with 1-hexadecanol, 1-eicosanol and 1-docosanol. Again, the foamability with the longer chain lengths may be improved by cooling the mixture to a higher temperature to gain an optimum viscosity/solid content/crystal presence for foam formation. Figure 7.44 shows that the bubbles in the foams produced with the fatty alcohols in HOSO were relatively similar in appearance (non-spherical with a textured surface ranging from 30-150  $\mu\text{m}$  in diameter). A sample of the foam produced with each fatty alcohol was heated 1  $^{\circ}\text{C}/\text{min.}$ , it was clear that the alcohol was necessary for the foam stability as the foam collapsed as temperature increased. The appearance of the foams at room temperature 24 hours after aeration was found to differ as shown by Figure 7.45. The liquid drainage which occurred was found to be similar (10 mL) apart from 12 mL with 1-docosanol. However, the foam volume was different, with 1-hexadecanol and 1-octadecanol there was 30 mL, with 1-eicosanol there was 40 mL and with 1-docosanol there was 20 mL.

It appears that there was not a particularly significant amount of foam produced with the fatty alcohols; however it appears that there was more foam produced with 1-octadecanol. The foam produced with 1-eicosanol clearly had a higher stability than that seen with the other alcohols investigated, however all of the foams produced remained as found after 24 hours for over 9 months.

**Table 7.8.** Volume of the aerated phase, whipping time for maximum foam production, volume fraction of air incorporated into the mixture and temperature of complete foam collapse of 6 wt.% fatty alcohols in HOSO after whipping for 45 minutes with a hand held double beater electric whisk at 22 °C.

| Fatty alcohol  | Volume of aerated phase/<br>± 10 mL | Whipping time for maximum foam/ min. | Volume fraction of air<br>± 0.02 | Temperature of complete foam collapse/ ± 0.1 °C |
|----------------|-------------------------------------|--------------------------------------|----------------------------------|---|
| 1-tetradecanol | -                                   | -                                    | -                                | -   |
| 1-hexadecanol  | 250                                 | 15                                   | 0.21                             | 45.0  |
| 1-octadecanol  | 300                                 | 20                                   | 0.33                             | 48.0  |
| 1-eicosanol    | 250                                 | 15                                   | 0.22                             | 59.7  |
| 1-docosanol    | 250                                 | 15                                   | 0.13                             | 62.2  |

**Figure 7.41.** Photographs of 6 wt.% (a) 1-tetradecanol, (b) 1-hexadecanol, (c) 1-octadecanol, (d) 1-eicosanol and (e) 1-docosanol in HOSO at 22 °C after cooling from 80 °C to 8 ± 2 °C at approximately 1 °C/min. Scale bar 1 cm.

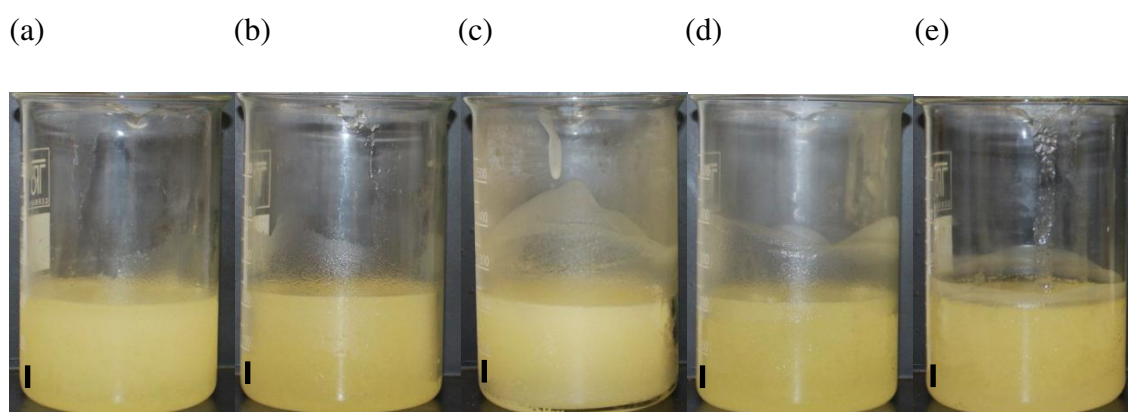
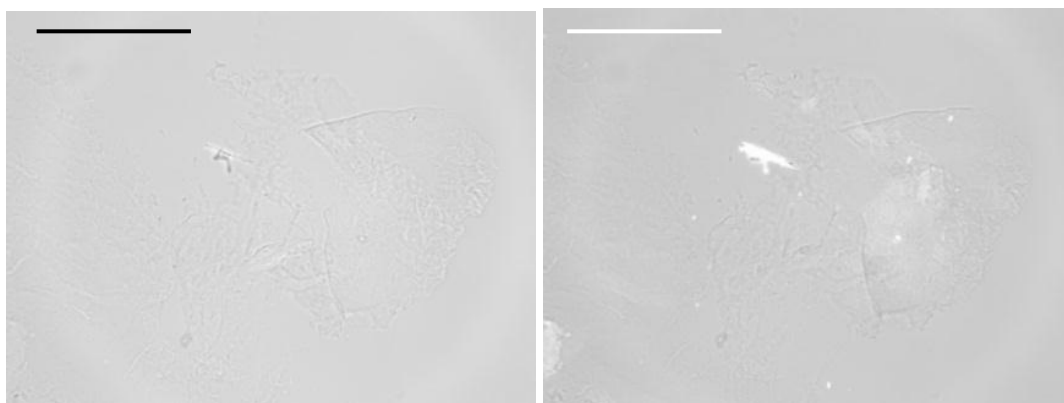
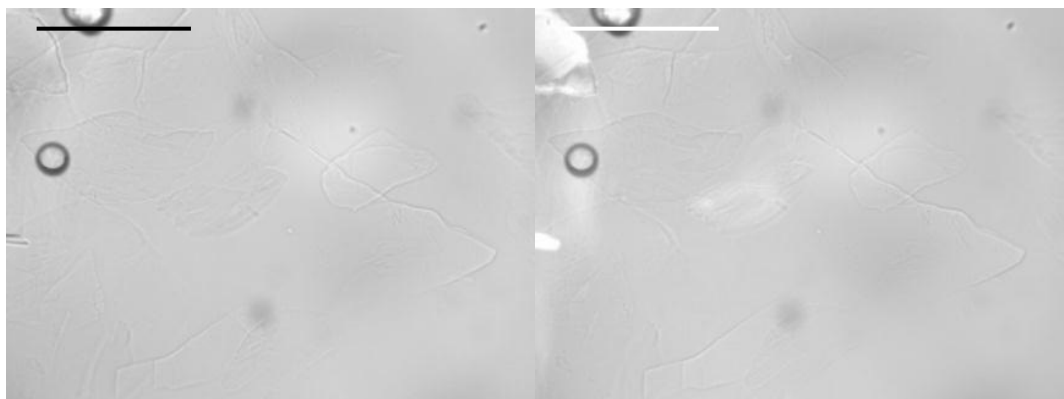


**Figure 7.42.** Optical microscopy of 6 wt.% (a) 1-tetradecanol, (b) 1-hexadecanol, (c) 1-octadecanol, (d) 1-eicosanol and (e) 1-docosanol (l) in HOSO at 22 °C after cooling from 80 °C to  $8 \pm 2$  °C at approximately 1 °C/min. Images on the right are corresponding micrographs viewed through crossed polarising lenses. Scale bar 200  $\mu$ m.

(a)



(b)



(c)

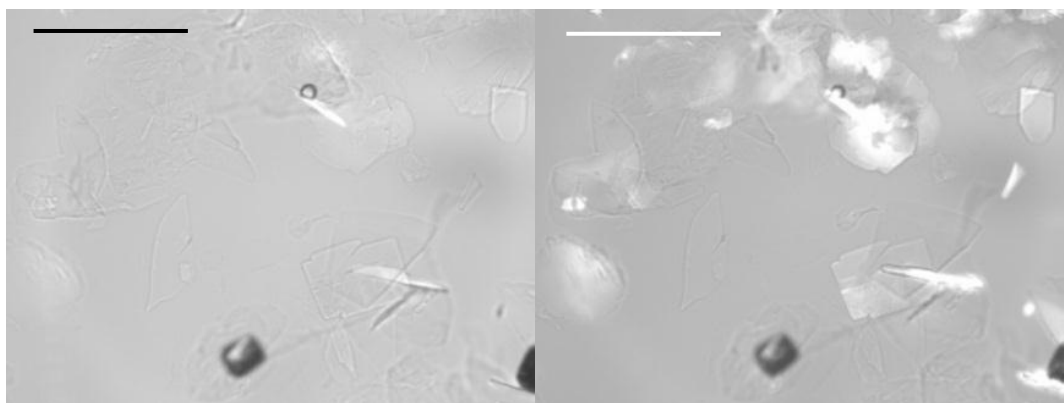
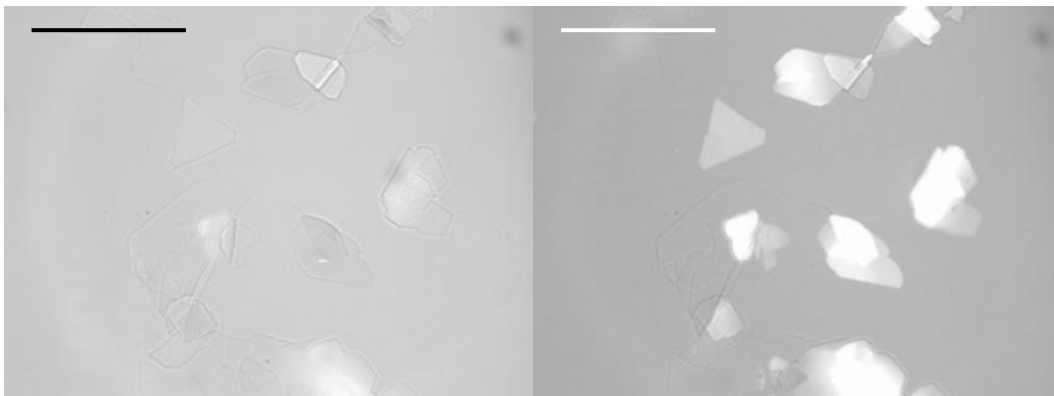


**Figure 7.42** (continued)

(d)



(e)

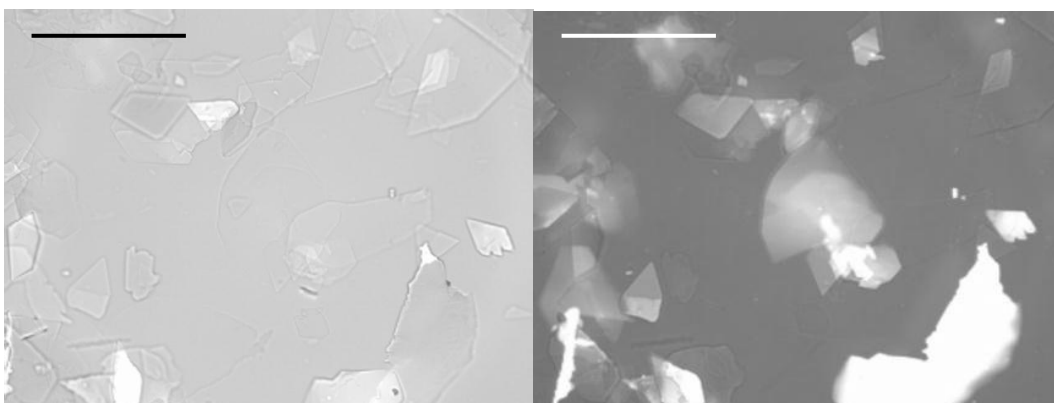


**Figure 7.43.** Photographs of 6 wt.% (a) 1-tetradecanol, (b) 1-hexadecanol, (c) 1-octadecanol, (d) 1-eicosanol and (e) 1-docosanol in HOSO after whipping for 30 minutes with a hand held double beater electric whisk at 22 °C. Scale bar 1 cm.

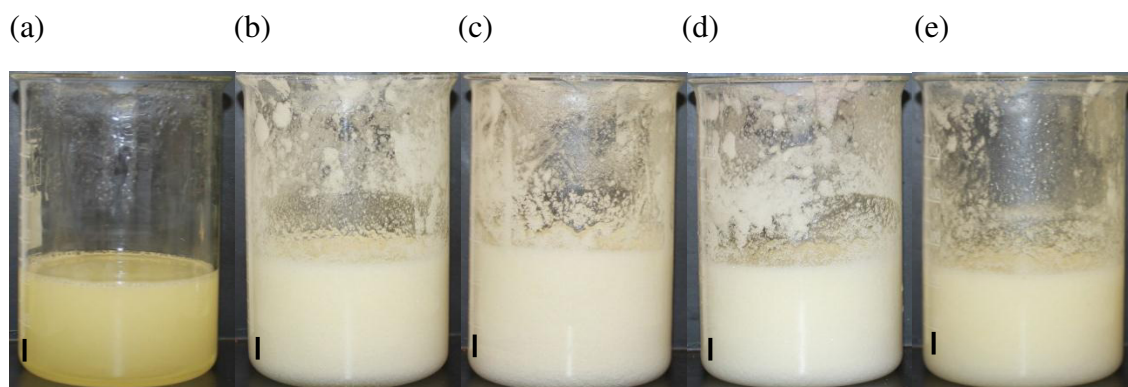
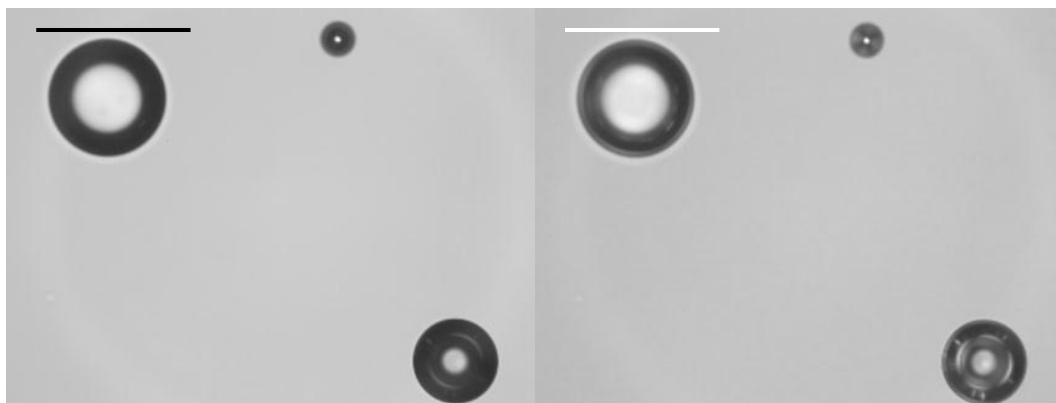
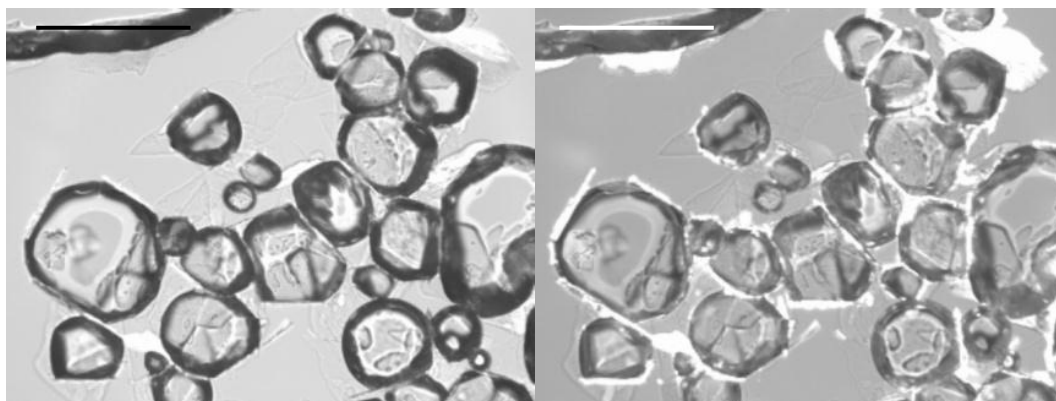


**Figure 7.44.** Optical microscopy of 6 wt.% (a) 1-tetradecanol, (b) 1-hexadecanol, (c) 1-octadecanol, (d) 1-eicosanol and (e) 1-docosanol in HOSO after whipping for 30 minutes with a hand held double beater electric whisk at 22 °C. Images on the right are corresponding micrographs viewed through crossed polarising lenses. Scale bar 200  $\mu\text{m}$ .

(a)



(b)



(c)

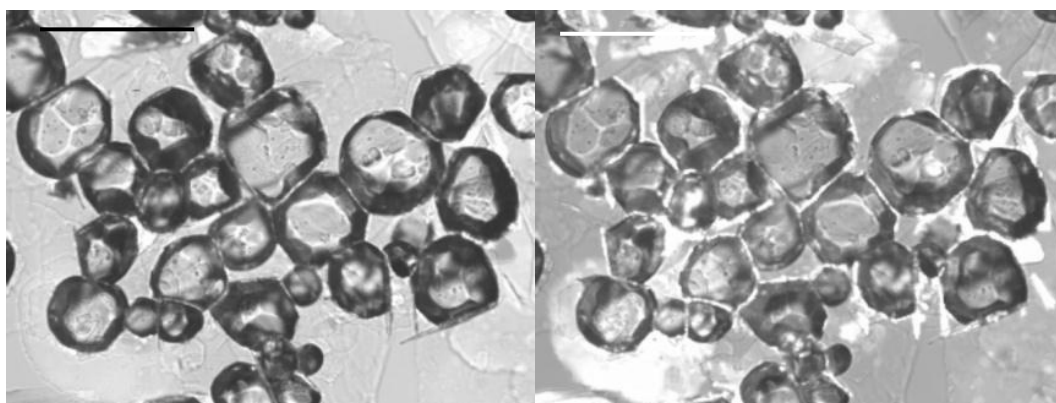
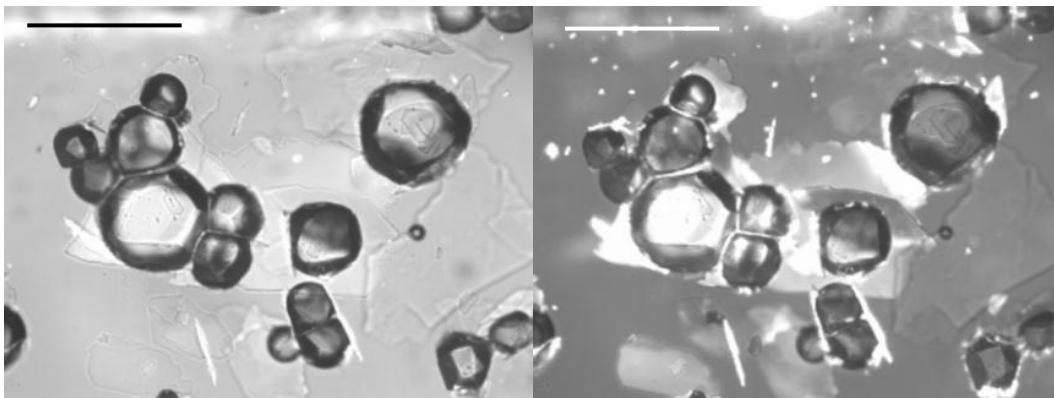


**Figure 7.44** (continued)

(d)



(e)

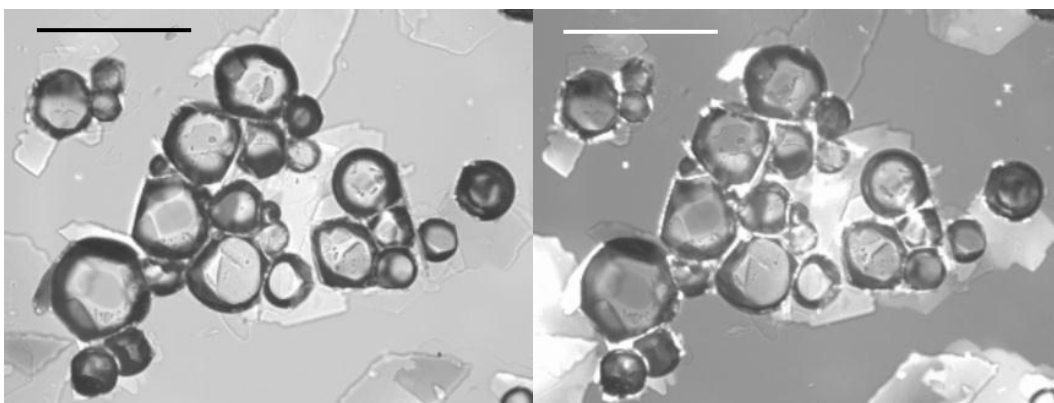


**Figure 7.45.** Photographs of 6 wt.% (a) 1-hexadecanol, (b) 1-octadecanol, (c) 1-icosanol, (d) 1-docosanol in HOSO at  $22 \pm 2$  °C 24 hours after aeration with a hand held double beater electric whisk at 22 °C. Scale bar 1 cm.

(a)

(b)

(c)

(d)



## 7.7 Concept samples

It is clear that the whipping aeration method can be applicable to many products including confectionary products. This is because it has the ability to aerate relatively viscous materials such as a fat filling. Dimodan HR was used in all of the concept samples as it is known to aid the aeration of HOSO, therefore it was used to investigate if it had the same effect with other edible ingredients such as sugar and chocolate. To prove this, the method was used with edible ingredients to create indulgent chocolate fillings, extruded fillings, biscuit fillings, whipped spreads and wafer fillings. The concept samples were produced by heating a mixture, then cooling it at approximately 1 °C/min., followed by whipping it at  $22 \pm 2$  °C with a Hobart mixer.

### 7.7.1 Indulgent chocolate filling

To make the indulgent chocolate filling a chocolate shell had to be made with liquid, tempered chocolate which was added to a mould and then placed into a fridge for an hour (internal temperature 7 °C). Two chocolate shell fillings were then made, the first with high oleic sunflower oil, Dimodan HR kosher and chocolate, the second with hazelnut oil, Dimodan HR kosher and chocolate. The different oils have been chosen to investigate if the aeration of the mixture is independent of the oil type.

#### 7.7.1.1 High oleic sunflower oil based filling

10 wt.% Dimodan HR kosher in HOSO was heated to 85 °C, then cooled to 10 °C at approximately 1 °C/min. Milk chocolate at 25 °C was then added to the mixture. The mixture was then heated to 35 °C to create a homogeneous viscous liquid, then cooled to 19.6 °C, again at approximately 1 °C/min. The mixture was then whipped with a Hobart mixer on speed setting 2 at  $20 \pm 1$  °C for 20 minutes. As can be seen from Table 7.9, after 20 minutes of whipping the volume fraction of air present in the mixture was 0.21. This was not a particularly significant amount of air incorporated into the mixture; however it was still very interesting to find that a foam could be produced with the edible ingredients.

**Table 7.9.** Volume fraction of air present in the HOSO based chocolate filling as whipping time increased with a Hobart mixer at  $20 \pm 1$  °C.

| Whipping time/ min. | Volume fraction of air<br>$\pm 0.02$ |
|---------------------|--------------------------------------|
| 5                   | 0.20                                 |
| 10                  | 0.20                                 |
| 15                  | 0.20                                 |
| 20                  | 0.21                                 |

#### 7.7.1.2 Hazelnut oil based filling

The procedure for creating an indulgent chocolate filling was then repeated with hazelnut oil replacing HOSO to determine if the ability to incorporate air into an edible mixture was possible with other oils. As can be seen from Table 7.10, which indicates that a foam was produced with hazelnut oil, the volume fraction of air in the mixture was 0.21 after 20 minutes of whipping. This value was the same as that observed with the HOSO based filling. Again, not much air was incorporated into the mixture; however a foam was produced which indicates that this technique could be used for this application.

**Table 7.10.** Volume fraction of air present in the hazelnut oil based chocolate filling as whipping time increased with a Hobart mixer at  $20 \pm 1$  °C.

| Whipping time/ min. | Volume fraction of air<br>$\pm 0.02$ |
|---------------------|--------------------------------------|
| 5                   | 0.12                                 |
| 10                  | 0.17                                 |
| 15                  | 0.23                                 |
| 20                  | 0.21                                 |

The whipped foam produced with both oils was then added to the chocolate shells followed by the addition of a final layer of chocolate to encase the filling. The resulting chocolate is shown in Figure 7.46. There was in total approximately  $3.6 \pm 0.1$  g of the whipped oil in the chocolate shell. The chocolate (shell and back) was approximately 6 g.

**Figure 7.46.** Photographs of 10 wt.% Dimodan HR kosher in HOSO whipped with chocolate encased in a chocolate shell at  $20 \pm 1$  °C. Scale bar 1 cm.



### 7.7.2 Extruded filling

The ability to create an aerated filling which could be placed into an extruded chocolate cereal tube (provided by Nestlé) was investigated. The filling, which was created with both HOSO and peanut oil, was placed into the chocolate cereal tube with the use of a piping bag. Different ingredients were chosen to that used for the chocolate filling to investigate if they could also be aerated along with two different oils, again, to investigate if the aeration of the mixture was independent of the oil type.

#### 7.7.2.1 High oleic sunflower oil based extruded filling

10 wt.% Dimodan HR kosher in HOSO was heated to 90 °C, then cocoa powder, white sugar and caramelised milk powder was added. Once the additional materials were added to the mixture it was mixed by hand at 60 °C to create homogeneity. The mixture was then cooled to 20.8 °C at approximately 1 °C/min., then whipped with a Hobart mixer on speed setting 2 at 20 ± 1 °C for 60 minutes. The volume fraction of air incorporated into the mixture after 60 minutes of whipping is shown in Table 7.11. It is clear that with this mixture a larger amount of air was incorporated (0.28 after 60 minutes of whipping) compared to that found with the indulgent chocolate filling. It may be that the addition of the sugar and caramelised milk powder created a more favourable viscosity for air to be incorporated into the mixture.

**Table 7.11.** Volume fraction of air incorporated into the whipped HOSO extruded filling as whipping time increased with a Hobart mixer at 20 ± 1 °C.

| Whipping time/ min. | Volume fraction of air<br>± 0.02 |
|---------------------|----------------------------------|
| 5                   | 0.18                             |
| 10                  | 0.22                             |
| 15                  | 0.25                             |
| 20                  | 0.29                             |
| 30                  | 0.28                             |
| 60                  | 0.28                             |

### 7.7.2.2 Peanut oil based extruded filling

The procedure for creating an extruded filling was then repeated with peanut oil replacing HOSO. Table 7.12 shows that the volume fraction of air incorporated into the mixture after 60 minutes of whipping was significant. It is clear that more air was incorporated into the extruded filling produced with peanut oil (0.32) than with HOSO (0.28). This large amount of foam may be due to a favourable viscosity of the mixture.

**Table 7.12.** Volume fraction of air incorporated into the whipped peanut oil extruded filling as whipping time increased with a Hobart mixer at  $20 \pm 1$  °C.

| Whipping time/ min. | Volume fraction of air<br>$\pm 0.02$ |
|---------------------|--------------------------------------|
| 5                   | 0.05                                 |
| 10                  | 0.13                                 |
| 15                  | 0.19                                 |
| 20                  | 0.27                                 |
| 30                  | 0.3                                  |
| 60                  | 0.32                                 |

Once the whipped product was produced with both peanut oil and HOSO it was then extruded into a chocolate cereal tube (see Figure 7.47) with the use of a piping bag. The average weight of the cereal tubes was  $1 \pm 0.1$  g. The average amount of the peanut oil based filling added to the cereal tubes was  $0.7 \pm 0.05$  g, with the HOSO based filling  $0.8 \pm 0.05$  g was added.

**Figure 7.47.** Photographs of (a), and (b), a whipped HOSO based filling in a chocolate cereal tube. (c) is an overview of the extruded products at  $20 \pm 1$  °C. Scale bar is 1 cm.

(a) (b)



(c)



### 7.7.3 Biscuit filling

An aerated biscuit filling was also created with 10 wt.% Dimodan HR kosher in HOSO which was heated to 90 °C, then white sugar and white chocolate was added. The white chocolate was chosen to investigate if it, like milk chocolate, could be aerated and then used for this concept. The mixture was stirred by hand at 45 °C, then cooled to 18.7 °C at approximately 1 °C/min. The mixture was then whipped with a Hobart mixer with speed setting 2 at  $20 \pm 1$  °C for 20 minutes. Table 7.13 shows that a large amount of air was incorporated into the mixture (0.31 after 20 minutes of whipping). The whipped product was then placed between two oreo biscuits to demonstrate the application of the whipping technique to biscuit fillings (shown in Figure 7.48). It was found that the oreo biscuits had a filling of 3 g, whereas with the whipped filling only  $2.5 \pm 0.2$  g was required to get the same appearance.

**Table 7.13.** Volume fraction of air incorporated into the whipped biscuit filling as whipping time increased with a Hobart mixer at  $20 \pm 1$  °C.

| Whipping time/ min. | Volume fraction of air<br>$\pm 0.02$ |
|---------------------|--------------------------------------|
| 5                   | 0.16                                 |
| 10                  | 0.28                                 |
| 15                  | 0.30                                 |
| 20                  | 0.31                                 |

**Figure 7.48.** Whipped biscuit filling between 2 oreo biscuits at  $20 \pm 1$  °C. Scale bar 1 cm.



#### 7.7.4 Whipped spread

To create a whipped spread 10 wt.% Dimodan HR kosher in hazelnut oil was heated to 90 °C, then milk chocolate and white sugar was added (to ensure that a paste like texture was produced). The homogeneous fluid-like paste (at 50 °C) was cooled to 21.0 °C at approximately 1 °C/min. The sample was then whipped for 30 minutes with a Hobart mixer with speed setting 2 at  $20 \pm 1$  °C as can be seen in Table 7.14. It is clear that after 30 minutes of whipping there was a volume fraction of 0.28 of air in the mixture. The resulting whipped hazelnut oil paste is shown in Figure 7.49. It is not clear if the addition of white sugar had an effect on the amount of air incorporated into the mixture. This is stated because the volume fraction of air present after 20 minutes of whipping is the same (0.21) as that seen with the indulgent chocolate filling (where white sugar was not added). The indulgent chocolate filling needs to be whipped for 30 minutes to determine if sugar addition had a significant effect on foam formation.

**Table 7.14.** Volume fraction of air incorporated into the hazelnut oil based chocolate spread as whipping time increased with a Hobart mixer at  $20 \pm 1$  °C.

| Whipping time/ min. | Volume fraction of air<br>$\pm 0.02$ |
|---------------------|--------------------------------------|
| 5                   | 0.12                                 |
| 10                  | 0.18                                 |
| 15                  | 0.21                                 |
| 20                  | 0.21                                 |
| 30                  | 0.28                                 |

**Figure 7.49.** Photograph of a whipped hazelnut oil based chocolate spread at  $20 \pm 1$  °C. Scale bar 1 cm.



#### 7.7.5 Wafer filling

The ability to create an aerated wafer filling was also investigated. The wafer filling was the same as that used to create the whipped spread. The aerated mixture was placed between wafers (4 wafer layers and 3 whipped filling layers) with a ratio of 60 % filling, 40 % wafer as shown in Figure 7.50. The wafer and filling was then cut into 10 cm x 2 cm pieces.

**Figure 7.50.** Photograph of the whipped wafer filling which was produced with the use of a Hobart mixer at  $20 \pm 1$  °C. Scale bar 1 cm.



It is impressive that cooling a mixture and then whipping it with a Hobart mixer to create aerated products can be applicable to many different oils and edible ingredients used for making confectionary. It is clear that the technique has a lot of potential for use with Nestlé products.

## 7.8 Conclusions

It was found that a foam could be produced with numerous oils and surfactants. A significant amount of air was incorporated into a foam produced with FHR-B in HOSO (volume fraction of 0.43) where the foam was stable for over 18 months. A foam could also be produced with cetostearyl alcohol in both HOSO and dodecane, the foamability in dodecane was higher, but foam stability was lower than that observed in HOSO. A large amount of foam was produced with Dimodan HR kosher in HOSO after whipping with both a Hobart mixer and a hand held double beater electric whisk. It was found that the temperature Dimodan HR kosher in HOSO was cooled to prior to aeration was important for the production of a foam. It is likely to be due to an optimum viscosity and/or solid content being necessary for foam formation. The foam produced with Dimodan HR kosher in HOSO was stable for over 18 months.

It was found that a foam was produced with stearic acid in HOSO and that the foamability reached a maximum with 5-8 wt.%. It was also found that the foam collapsed when temperature was increased 1 °C/min. Aeration temperature was important to create a foam, foamability decreased as temperature increased. It was clear that a gel was necessary for foam formation.

It was also found that a foam could be created with palmitic, arachidic and behenic acid in HOSO. It was found that foamability with palmitic acid was higher than that observed with the other fatty acids. The foams produced with the fatty acids in HOSO were stable for at least 9 months (with myristic and stearic acid the foam was stable for over 18 months).

A foam could be produced by whipping 1-hexadecanol, 1-octadecanol, 1-eicosanol and 1-docosanol in HOSO (but not with 1-tetradecanol in HOSO). There appeared to be an optimum foamability with 1-octadecanol and a maximum foam stability with 1-eicosanol. It was found that the foams produced were stable for over 9 months. The volume of foam produced with the fatty alcohols was lower than that produced with the fatty acids.

Finally, it was found that the technique is applicable to edible, commonly used confectionary ingredients for the creation of confectionary products with an aerated aspect.

## 7.9 References

1. K. Higaki, Y. Sasakura, T.Koyano, I. Hachiya and K. Sato, *J. Am. Oil Chem. Soc.*, **80**, 263 (2003).
2. K. Higaki, T. Koyano, I. Hachiya, K. Sato and K. Suzuki, *Food Res. Int.*, **37**, 799 (2004).
3. K. Higaki, T. Koyano, I. Hachiya and K. Sato, *Food Res. Int.*, **37**, 2 (2004).
4. J. Daniel and R. Rajasekharan, *J. Am. Oil Chem. Soc.*, **80**, 417 (2003).
5. F. G. Gandolfo, A. Bot and E. Floter, *J. Am. Oil Chem. Soc.*, **81**, 1 (2004).
6. H. M. Schaink, K. F. van Malssen, S. Morgado-Alves, D. Kalnin and E. van der Linden, *Food Res. Int.*, **40**, 1185 (2007).
7. M. Perneti, K. F. van Malssen, E. Floter and A. Bot, *Curr. Opin. Colloid Interface Sci.*, **12**, 221 (2007).
8. *Rheology for chemists an introduction*, J.W. Goodwin and R.W. Hughes, Royal Society of Chemistry, U.K. 2000.
9. S. Da Pieve, S. Calligaris, A. Panozzo, G. Arrighetti and M.C. Nicoli, *Food Res. Int.*, **44**, 2978 (2011).
10. E. Tarabukina, F. Jago, J-M. Haudin, P. Navard and E. Peuvrel-Disdier, *J. Food Sci.*, **74**, 405 (2009).
11. N.K.O. Ojijo, I. Neeman, S. Eger and E. Shimoni, *J. Sci. Food Agric.*, **84**, 1585 (2004).
12. K.P.A.M. van Putte and J. van den Enden, *J. Phys. E Sci. Instrum.*, **6**, 910 (1973).
13. K. van Putte and J. van den Enden, *J. Am. Oil Chem. Soc.*, **51**, 316 (1974)
14. M.A.J.S. van Boekel, *J. Am. Oil Chem. Soc.*, **58**, 768 (1981).
15. A.K. Chesterton, G.D. Moggridge, P.A. Sadd and D.I. Wilson, *J. Food Eng.*, **105**, 343 (2011).
16. *Handbook of Chemistry and Physics*, D. R. Lide, CRC Press, Boca Raton, 1997.

## 8 SUMMARY OF CONCLUSIONS AND FUTURE WORK

### 8.1 Conclusions

This thesis significantly furthers knowledge in the area of non-aqueous foams as numerous oils, edible surfactants, aeration methods and gas types along with the effect of temperature and time on foamability and foam stability has been investigated. It was clear that viscosity played an important role in the generation of foams as well as the stability of foams. It was found that a larger volume of foam was more likely to be produced with a viscous mixture aerated with the whipping technique than with the foaming column or soda siphon and the reverse is the case when the mixture was fluid-like. The stability of the foam produced with the whipping technique was considerably higher than that observed with the foaming column and soda siphon. The foam produced with a relatively fluid-like mixture was found to increase in stability as viscosity increased (the increase in viscosity reduced the rate of liquid drainage). It was clear that as the viscosity increased significantly there was an adverse effect on foamability-there was little or no foam formation with the foaming column and soda siphon as it was difficult for gas to be incorporated into the continuous phase due to the high viscosity. Viscosity was also very important for the generation of foam with the whipping technique. It was clear that once a gel was formed a foam could be produced, although the amount was dependent on the mixture viscosity (as viscosity further increased the amount of foam reduced). It was thought that as the mixture became more solid-like the air could not be incorporated into the continuous phase.

It was found that, in general, with the foaming column and soda siphon foamability was not effected by aeration temperature, however foam stability was (foams produced when the aeration was above the surfactant solubility temperature were only stable for several minutes). This was thought to be due to foams being able to be produced when the surfactant was present both as a molecular solution and a particular dispersion (both above and below the surfactant solubility temperature); however the particular dispersion (below the surfactant solubility temperature) was necessary for foam stability.

It was clear that the temperature a mixture was cooled to prior to aeration at 22 °C with the whipping technique with some systems was very important. This, along with many

other measurements, indicated that the crystal size and viscosity of the mixture prior to aeration was extremely important for foam formation. The foams produced with myristic acid in HOSO via the whipping technique were found to be highly stable. This was thought to be due to the myristic acid being present at the bubble surface causing a resistance to foam collapse. The foam produced collapsed once temperature increased (when the myristic acid melted) indicating the necessity of the myristic acid for stability. The oil the myristic acid was added to had a large effect on foamability as a foam was not produced with all of the non-edible oils investigated. However, a foam was produced with all of the edible vegetable oils studied (10 in total). This is thought to be because the triglyceride content of the vegetable oil aided favourable packing with the fatty acid to then generate a foam. The stability of the foam differed significantly with oil type; the reason for this is unclear.

## 8.2 Future work

Due to there being a lack of knowledge in the area of non-aqueous foams stabilised by edible surfactants there is many areas that have, as yet, not been investigated. Factors that could be studied include fatty acid and fatty alcohol combinations in various oils, also the effect of unsaturated and branch chained fatty acids and fatty alcohols, on the generation of foams and the subsequent stabilities of the foams. The effect of these parameters would be extremely interesting particularly because it will bring a further understanding to the phenomena. Factors such as the chain length of the oil continuous phase and the saturation of these chains would also be able to provide a lot of information which may lead to the understanding of the different foam stabilities observed with the different oils. It would be interesting to investigate the effect of the temperature fatty alcohols and fatty acids are cooled to, prior to whipping at 22 °C with various vegetable oils. Viscosity measurements determined through rheology could give some valuable information for understanding the behaviour of a mixture when it is being whipped. Repeated viscosity measurements with 5 minute rest intervals to simulate the whipping protocol can identify the extent of any disruption to the gelled network as the whipping time increased to 45 minutes.

An alternative area that would be of interest both academically and to industry would be to investigate the effect of sugar content on foam formation and stability, both with and without the presence of surfactants in edible oils. Sugar is a commonly used ingredient

in the food industry but the behaviour in the presence of surfactants within aerated edible oils is unknown. Therefore, it would be interesting to study the effect of surfactant type used in combination with sugar, along with parameters such as aeration method, sugar particle size, gas type, temperature and surfactant concentration, on the foamability and subsequent foam stability of a vegetable oil.

Industrially, areas that could be investigated include the aeration of other oils or even emulsions (which would be of interest to the food, cosmetic and paint industry) as it is clear from this work that oils with edible surfactants, whether fluid-like or viscous, can be aerated. It would also be interesting to investigate the foamability of various fat mixtures, and the effect of an ingredient such as milk powder when added to edible oils and surfactants, with the whipping technique for the applicability of the method to areas other than confectionary such as dairy products.

The aeration of products can create a huge cost saving to industry and may also lead to the creation of innovative new products for consumers. The aeration of products can also lead to a different product texture which can be beneficial to companies in the areas of food and cosmetics.

## **APPENDIX**

This section contains Figures discussed in Chapter 5.

**Figure A1.1** Simulated 1-D pattern of neat myristic acid with a copper wavelength of 1.54 Å as stated by A. Bond<sup>10</sup> with the prominent d-spacings labelled in Å.

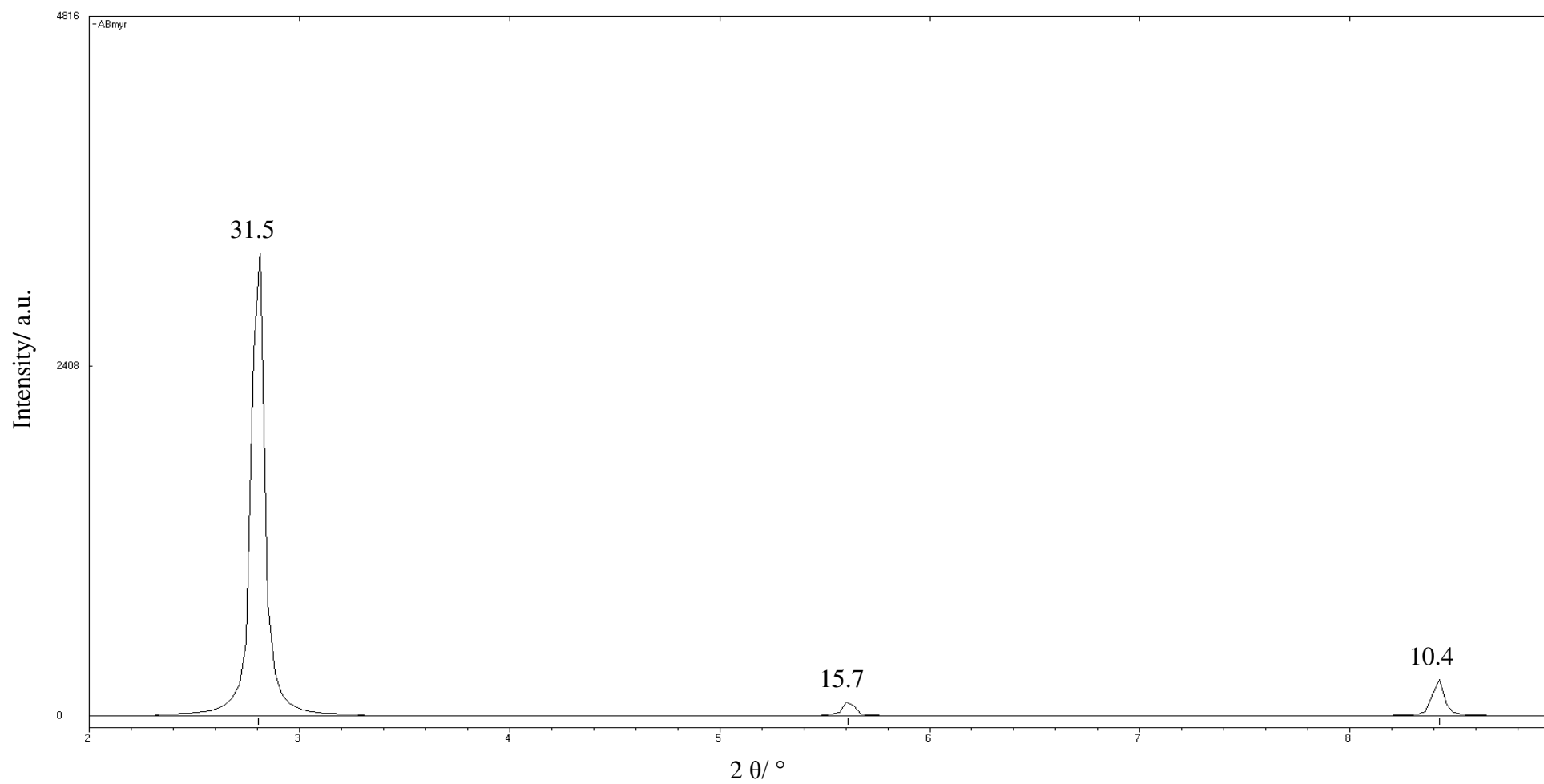


**Figure A1.2** Simulated 1-D powder pattern of neat myristic acid with a molybdenum wavelength of 0.71 Å as stated by A.Bond<sup>10</sup> with the prominent d-spacings labelled in Å.

